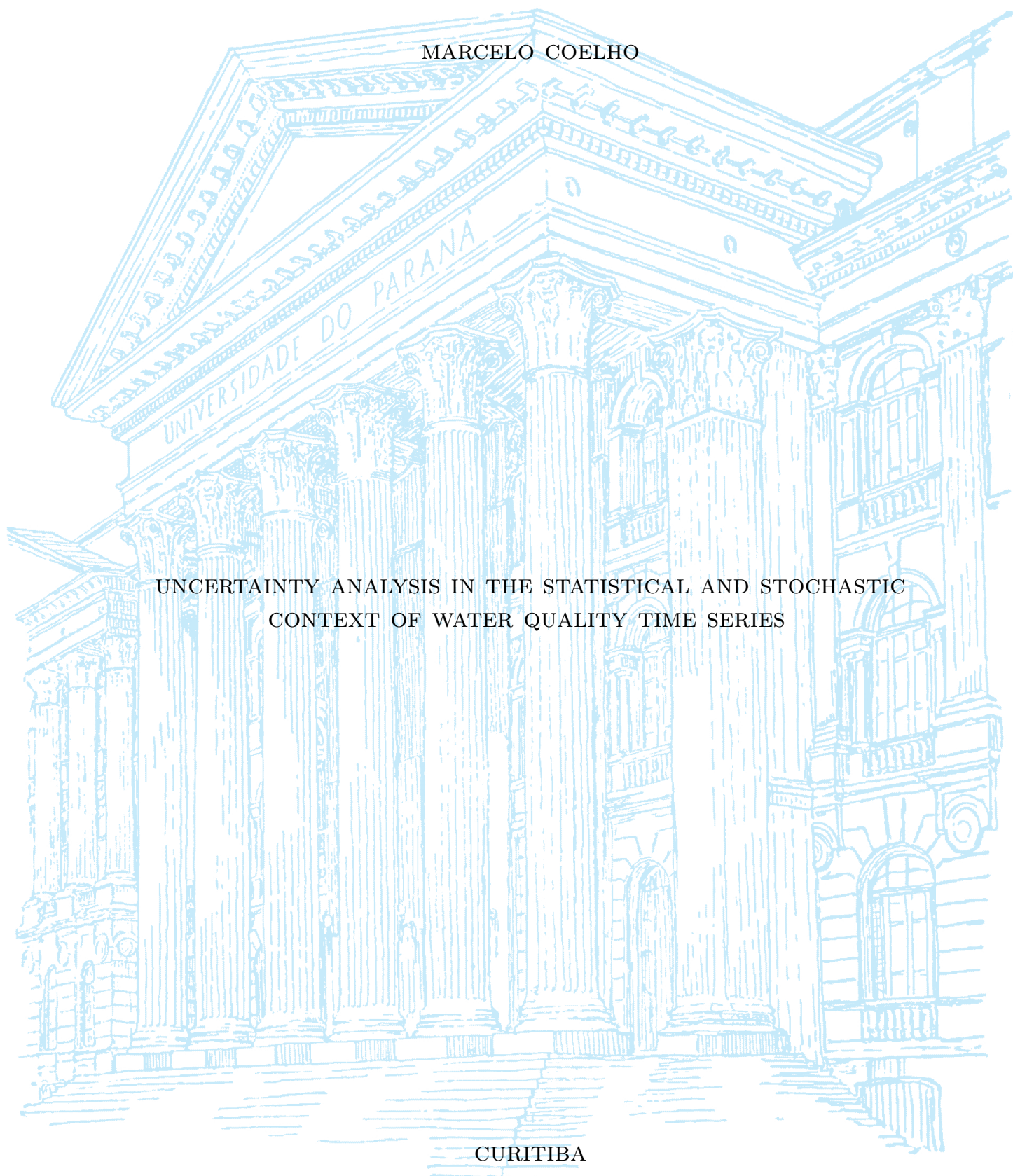UNIVERSIDADE FEDERAL DO PARANÁ

MARCELO COELHO

UNCERTAINTY ANALYSIS IN THE STATISTICAL AND STOCHASTIC
CONTEXT OF WATER QUALITY TIME SERIES

CURITIBA

2019

MARCELO COELHO

UNCERTAINTY ANALYSIS IN THE STATISTICAL AND STOCHASTIC
CONTEXT OF WATER QUALITY TIME SERIES

Tese apresentada ao Programa de Pós-Graduação em Engenharia de Recursos Hídricos e Ambiental, **Setor de Tecnologia da Universidade Federal do Paraná**, como um requisito par-cial para a obtenção do título de Doutor em Engenharia de Recursos Hídricos e Ambien-tal.

Orientador: Prof. PhD Cristovão Vicente Scapulatempo Fernandes
Co-orientador: Prof. D.Eng. Daniel Henrique Marco Detzel

CURITIBA

2019
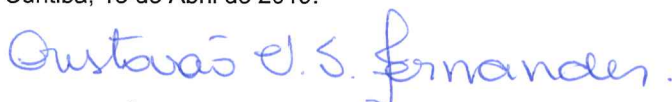
TERMO DE APROVAÇÃO

Os membros da Banca Examinadora designada pelo Colegiado do Programa de Pós-Graduação em ENGENHARIA DE RECURSOS HÍDRICOS E AMBIENTAL da Universidade Federal do Paraná foram convocados para realizar a arguição da Tese de Doutorado de **MARCELO COELHO**, intitulada: **UNCERTAINTY ANALYSIS IN THE STATISTICAL AND STOCHASTIC CONTEXT OF WATER RESOURCES TIME SERIES**, após terem inquirido o aluno e realizado a avaliação do trabalho, são de parecer pela sua _aprovação_ no rito de defesa.

A outorga do título de Doutor está sujeita à homologação pelo colegiado, ao atendimento de todas as indicações e correções solicitadas pela banca e ao pleno atendimento das demandas regimentais do Programa de Pós-Graduação.

Curitiba, 18 de Abril de 2019.

CRISTOVÃO VICENTE SCAPULATEMPO FERNANDES
Presidente da Banca Examinadora

JULIO CESAR RODRIGUES DE AZEVEDO
Avaliador Interno ()

ADILSON PINHEIRO
Avaliador Externo (FURB)

WALTER COLLISCHONN
Avaliador Externo (UFRGS)

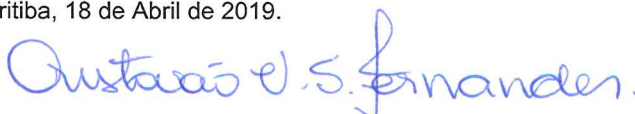DANIEL HENRIQUE MARCO DETZEL
Coorientador - Avaliador Interno (UFPR)

ELOY KAVISKI
Avaliador Interno (UFPR)

MINISTÉRIO DA EDUCAÇÃO
SETOR SETOR DE TECNOLOGIA
UNIVERSIDADE FEDERAL DO PARANÁ
PRÓ-REITORIA DE PESQUISA E PÓS-GRADUAÇÃO
PROGRAMA DE PÓS-GRADUAÇÃO ENGENHARIA DE
RECURSOS HÍDRICOS E AMBIENTAL - 40001016021P0

ATA N° 46

ATA DE SESSÃO PÚBLICA DE DEFESA TESE PARA OBTENÇÃO DO GRAU DE DOUTOR EM ENGENHARIA DE RECURSOS HÍDRICOS E AMBIENTAL.

No dia dezoito de abril de dois mil e dezenove às 12:30 horas, na sala Auditório,CESEC do Setor de SETOR DE TECNOLOGIA da Universidade Federal do Paraná, foram instalados os trabalhos de arguição do Doutorando **MARCELO COELHO** para a Defesa Pública de sua Tese de Doutorado intitulada: **UNCERTAINTY ANALYSIS IN THE STATISTICAL AND STOCHASTIC CONTEXT OF WATER RESOURCES TIME SERIES**. A Banca Examinadora, designada pelo Colegiado do Programa de PósGraduação em ENGENHARIA DE RECURSOS HÍDRICOS E AMBIENTAL da Universidade Federal do Paraná, foi constituída pelos seguintes Membros: CRISTOVÃO VICENTE SCAPULATEMPO FERNANDES (UFPR), WALTER COLLISCHONN (UFRGS), JULIO CESAR RODRIGUES DE AZEVEDO (), DANIEL HENRIQUE MARCO DETZEL (UFPR), ADILSON PINHEIRO (FURB), ELOY KAVISKI (UFPR). Dando início à sessão, a presidência passou a palavra a(o) discente, para que o mesmo expusesse seu trabalho aos presentes. Em seguida, a presidência passou a palavra a cada um dos Examinadores, para suas respectivas arguições. O aluno respondeu a cada um dos arguidores. A presidência retomou a palavra para suas considerações finais. A Banca Examinadora, então, e, após a discussão de suas avaliações, decidiu-se pela _aprovação_ do aluno. O Doutorando foi convidado a ingressar novamente na sala, bem como os demais assistentes, após o que a presidência fez a leitura do Parecer da Banca Examinadora. A aprovação no rito de defesa deverá ser homologada pelo Colegiado do programa, mediante o atendimento de todas as indicações e correções solicitadas pela banca dentro dos prazos regimentais do programa. A outorga do título de Doutor está condicionada ao atendimento de todos os requisitos e prazos determinados no regimento do Programa de Pós-Graduação. Nada mais havendo a tratar a presidência deu por encerrada a sessão, da qual eu, **CRISTOVÃO VICENTE SCAPULATEMPO FERNANDES**, lavrei a presente ata, que vai assinada por mim e pelos membros da Comissão Examinadora.

Observações: _a pedido da banca o titulo da tese passe a ser: Uncertainty Analysis in the Statistical and Stochastic context of water Quality time series._

Curitiba, 18 de Abril de 2019.

CRISTOVÃO VICENTE SCAPULATEMPO FERNANDES
Presidente da Banca Examinadora

WALTER COLLISCHONN
Avaliador Externo (UFRGS)

JULIO CESAR RODRIGUES DE AZEVEDO
Avaliador Interno ()

DANIEL HENRIQUE MARCO DETZEL
Coorientador - Avaliador Interno (UFPR)

ADILSON PINHEIRO
Avaliador Externo (FURB)

ELOY KAVISKI
Avaliador Interno (UFPR)

Dedicated to the water and all the living communities

Acknowledgements

"Free fall flow river flow, on and on it goes. Breath under water 'till the end. Yes, the river knows.
Jim Morrison"

RESUMO

A análise de incertezas é um tópico de pesquisa desafiador em gestão de recursos hídricos. A aplicação de métodos estatísticos para as pesquisas em recursos hídricos requer que as séries temporais estejam de acordo com as hipóteses de aleatoriedade, homogeneidade, independência e estacionariedade (RHIS). O não atendimento a estes pré-requisitos pode ocorrer quando tendências, ciclos e/ou deslocamentos estão presentes. No entanto, as incertezas e a subjetividade associada à sua avaliação e a expressão podem dificultar a detecção desses padrões de variabilidade. Uma abordagem tradicional para lidar com incertezas em estudos hidrológicos é a aplicação de modelos autoregressivos (ARIMA). No entanto, sua aplicação em estudos de qualidade da água é dificultada devido às características de séries temporais típicas, como frequência curta e frequência irregular. Uma maneira de superar esses problemas é o uso de técnicas de regressão entre vazões e concentrações. No entanto, a variabilidade das concentrações não depende apenas da variabilidade de vazões, especialmente em bacias hidrográficas urbanas. Uma análise de incerteza integrada, envolvendo incertezas de medição, métodos e de representatividade faz-se necessária para validar a aplicação de abordagens estocásticas em estudos de qualidade da água. Nesta pesquisa, uma avaliação das incertezas relacionadas à identificação e avaliação padrões de variabilidade em dados de frequência irregular foi realizada através da geração de séries temporais sintéticas (STS) a partir das incertezas de medição das vazões e da qualidade da água. Três cenários de incerteza foram definidos, nível baixo (LL: 10–30%), nível médio (ML: 30–50%) e nível alto (LH: 50–70%). O método de Monte Carlo (MCM) foi aplicado com as distribuições de probabilidade uniforme, normal e lognormal. Em cada cenário, as médias e os desvios padrão (std) foram calculados como uma medida da incerteza dos p-valores. A significância das tendências, ciclos e/ou deslocamentos foi avaliada testando-se as hipóteses de RHIS com os testes Single-Sample runs, de Mann-Whitney, de Wald e Wolfowitz e de Mann-Kendall, respectivamente. Os testes foram aplicados com um número crescente de elementos (N). As incertezas relacionadas ao uso de modelos auto-regressivos para séries temporais de qualidade de água foram avaliadas pela aplicação de um modelo auto-regressivo (modelo de Markov) para as vazões, concepção de um modelo de regressão entre vazões e concentrações, e estimativa de concentrações e cargas diárias a partir das vazões diárias. Os resultados indicam que no atual contexto de incertezas na gestão dos recursos hídricos, a representatividade desempenha o papel mais importante. O problema da representatividade não está no passado, mas no futuro, pois, apesar das dificuldades na detecção de tendências, ciclos e/ou deslocamentos, esses padrões podem levar vários anos para causar mudanças significativas nas estatísticas. A modelagem estocástica da qualidade da água a partir de vazões diárias e séries temporais de frequência irregular parece ser uma opção razoável pois, os principais obstáculos causados por frequências irregulares e períodos curtos, podem ser superados através de técnicas de regressão sem comprometimento das características estatísticas. As séries temporais de qualidade da água de estratégias tradicionais de monitoramento podem ser utilizadas para o planejamento sem grandes incertezas relacionadas a padrões e medições de variabilidade. No entanto, a estatística descritiva terá incertezas relacionadas à representatividade temporal.

Palavras-chave: Incertezas. Séries históricas de qualidade da água. Gestão de recursos hídricos.

ABSTRACT

Uncertainty analysis is a recent research topic in water resources management. The application of statistical methods for water resources research requires time series to be compliant with the hypotheses of randomness, homogeneity, independence, and stationarity (RHIS). Noncompliance may occur when trends, cycles, and/or shifts are present. However, the uncertainties and associated subjectivity in assessment and expression may make it difficult to detect these patterns of variability. A traditional approach for dealing with uncertainties in hydrological studies is the application autoregressive models (ARIMA). However, its application in water quality studies is hampered by short and irregular-frequency time series. One way to overcome these problems is the use of regression techniques between flows and concentrations. However, the concentrations variability is not only dependent on the flows variability, especially in urban watershed. An integrated uncertainty analysis, involving measurement, methods, and representativeness uncertainties is needed to validate the application of stochastic approaches in water quality studies. In this research, an assessment of the uncertainties related to identification and evaluation of variability patterns in irregular-frequency data was performed through the generation of synthetic time series (STS) from the uncertainties of flows and water quality measurements. Three uncertainty scenarios were defined, the low level (LL: 10–30%), mid level (ML: 30–50%) and high level (HL: 50–70%). The Monte Carlo Method (MCM) was applied with uniform, normal and lognormal probability distributions. In each scenario, averages and standard deviations (std) were calculated as a measure of the p-values uncertainty. The significance of trends, cycles and/or shifts was evaluated by testing the RHIS hypotheses with the Single-Sample Runs, Mann-Whitney, Wald and Wolfowitz, and Mann-Kendall tests, respectively. The tests were applied with an increasing number of elements (N). The uncertainty related to the use of autoregressive models for typical water quality time series was assessed by application of an autoregressive model (Markov model) for the flows, conception of a regression model between flows and concentration, and estimation of daily concentrations and loads from daily flows. The results indicate that in the current context of uncertainty concerns in water resources management, the representativeness plays the most important role. The problem of representativeness is not in the past, but in the future, since despite the difficulties in detection of trends, cycles and/or shifts in typical water quality time series, these patterns may probably take a several years to cause significant changes in statistics. The stochastic water quality modeling from daily flows and irregular-frequency times series seems to be a reasonable option since the main obstacles, caused by irregular frequency and short periods, can be overcome by using regression techniques without compromising statistical characteristics. The water quality time series from traditional monitoring strategies can be used for the planning without high uncertainties related to variability patterns and measurements. However, the descriptive statistics will have uncertainties related to temporal representativeness.

Key-words: Uncertainties. Water Resources Management. Time Series. Statistical Analysis.

List of Figures

List of Tables

List of abbreviations and acronyms

C	Concentration
ISO	International Standards Organization
GUM	Guide to Expression of Uncertainty in Measurements
HL	High level
LL	Low level
MCM	Monte Carlo Method
ML	Mid level
OTS	Original Time Series
Pdf	Probability density function
PPGERHA	Water Resources and Environmental Engineering Graduate Program
Q	Flows
QA/QC	Quality Assurance/Quality control
RHIS	Randomness, Homogeneity, Independence and Stationarity
RM	Regression model
RMSE	Root Mean Square Error
std	Standard deviation
STS	Synthetic Time Series
TSGENUIN	Time Series Generator in Uncertainty Intervals
UFPR	Federal University of Paraná
UM	Uncertainty Model
W	Loads
WFD	Water Framework Directive
WRM	Water Resources Management
WMO	World Meteorological Organization

Contents

1 Introduction

"Reject any final form that can not express the internal reality"

Bruce Lee

The growing concern about uncertainties in water resources management is not only a scientific issue (POLASKY et al., 2011; WALKER; HAASNOOT; KWAKKEL, 2013; BEVEN, 2016; MCMILLAN et al., 2017; PREIN; GOBIET, 2017; TENG et al., 2017; JUNG; NIEMANN; GREIMANN, 2018; TIAN et al., 2018), but also a worldwide concern regarding the water resources availability. It requires strategical policies towards sustainable decisions (ASCOUGH et al., 2008; BRADY et al., 2015; UNESCO, 2015). The Global Risks 2015 report from the World Economic Forum (BRADY et al., 2015) highlights inter-state conflicts with regional consequences as the main overall risk, mainly due to water supply crises, with high impacts by 2025. Between 2000 and 2050, it is expected an increase of 400% in global water demand by the manufacturing industry, affecting all other sectors, with most of this increase occurring in emerging economies and developing countries (UNESCO, 2015). In addition, uncertainties about climate change have increased the need to better understand uncertainties, specially those related to the representativeness of current time series (MILLY et al., 2008; MONTANARI; KOUT-SOYIANNIS, 2014).

This concern became evident in the European Union (EU) policy basis for water resources management, the Water Framework Directive 2000/60/EC (EC, 2000). The more specific guidance documents (e.g., Wateco (2003) and Proclan (2003)) emphasize that uncertainty analysis should be performed for appropriate and consistent water resources planning and management. However, there is no recommendation of the best approach to be applied (REFSGAARD et al., 2005; SIGEL; KLAUER; PAHL-WOSTL, 2010). It may require actions that extend from improvements of data to reframing of problems and solutions, or changing the structural governance context (BEVEN, 2016; WARMINK et al., 2017). Additionally, most of the important strategic planning problems are characterized by uncertainties about the future that are not statistical in nature (WALKER; HAASNOOT; KWAKKEL, 2013). According to Ben-Haim e Demertzis (2015), a distinction between risk and uncertainty was proposed by Frank Knight, that defined the uncertainties that can be handled with probabilities as "risk", and the ones that cannot by uncertainty or Knightian uncertainty.

Uncertainty assessment, expression and propagation should follow the international Guide to the Expression of Uncertainty in Measurements, known as GUM 2008 (JCGM/WG1, 2008a). Based on probability theory, it defines uncertainty in measure-

ment as a non-negative parameter, associated with the result of a measurement, that characterizes the dispersion of values that could reasonably be attributed to the measurand. When possible, uncertainty should be expressed as a probability density function (pdf) (BICH; COX; HARRIS, 2006; BICH et al., 2012; JCGM/WG1, 2008a; JCGM/WG1, 2009). Uncertainty can be assessed from repeated measurements or other non-statistical methods, e.g., expert judgment. Propagation can be performed by analytical methods or Monte Carlo Method (MCM), but also by a simplified scheme, i.e. the GUM uncertainty framework, which might not be satisfactory when: (i) distributions for the input and output quantities are asymmetric, or not a Gaussian or t-distribution; (ii) the measurement function is non-linear; (iii) uncertainty contributions are not of approximately the same magnitude (JCGM/WG1, 2009).

However, the application of probability theory in water resources management is not trivial, since water quality and hydrological data have been typically reported without uncertainty information and the complexity of water resources monitoring imposes considerable difficulties to repetition of measurements or measurement steps in the same flow, weather and quality conditions (GROVES, 2006; ASCOUGH et al., 2008; POLASKY et al., 2011; MCMILLAN et al., 2017; TIAN et al., 2018). Although recent efforts have been directed towards identification and quantification of the main sources of uncertainties and impacts on water resources management, there are a number of challenges for the successful application of uncertainty analysis (REFSGAARD et al., 2005; HARMEL et al., 2006; GROVES, 2006; BROWN; HEUVELINK, 2007; RODE; SUHR, 2007; HARMEL et al., 2009; SIGEL; KLAUER; PAHL-WOSTL, 2010; COZ, 2012; BEVEN, 2016; WARMINK et al., 2017; COELHO et al., 2017; MCMILLAN et al., 2017). For example, the uncertainty assessment in time series data, would involve high level of subjectivity with respect to past environmental and measurement conditions.

Harmel et al. (2006) estimated the cumulative uncertainty of discharges, water quality constituents and storm loads in typical monitoring conditions, which includes discharge measurement by stage-discharge method, moderate errors associated with single-grab flow or time-interval sampling, refrigerated sample storage for 54 h prior to analysis and moderate errors for low constituent concentrations. The authors found that uncertainty can range from 6% to 19% in discharge measurement, from 4% to 48% in sample collection, from 2% to 16% in sample preservation/storage, and from 5% to 21% in laboratory analysis. Uncertainty in storm loads ranged from 8% to 104% for dissolved nutrients, from 8% to 110% for total phosphorous and nitrogen, and from 7% to 53% for total suspended solids. McMillan, Krueger e Freer (2012) provide an overview of uncertainty sources and their typical magnitudes in flow data. Typical confidence bounds for flow uncertainties when using the rating curve method were found to be ±50–100% for low flows, ±10–20% for medium or high (in-bank) flows, and ±40% for out of bank flows. Although these estimates can give insight about the magnitude of uncertainties, the use

of this information on time series data would be subjective and uncertain, due to the lack of knowledge about the conditions in which each measurement was performed.

Furthermore, the difficulties of uncertainty analysis in environmental data should be investigated in the statistical/stochastic and modeling context, in which information is generated. It involves uncertainties beyond the measurements, e.g. those related to spatial and temporal representativeness and choice of appropriate methods and models. Representativeness of water quality and hydrological time series is achieved by monitoring strategies with sampling frequencies, locations, techniques and methods adjusted to capture the influence of diverse sources of variability and to meet the objectives of the program, including the needs of statistical methods (RODE; SUHR, 2007; ANTTILA et al., 2012; COELHO et al., 2017; NDIONE; SAMBOU; KANE, 2017).

Although the time series can be considered representative due to well-developed monitoring strategies, it may not be to application of statistical methods. Fundamentally, prior to statistical analysis, compliance with basic assumptions of randomness, homogeneity, independence and stationarity (RHIS) should be verified to confirm that the data stem from an unique random population (DURRANS; TOMIC, 1996; MERZ; THIEKEN, 2005; HULLEY; CLARK; WATT, 2015; COELHO et al., 2017; NDIONE; SAMBOU; KANE, 2017). Time series may not be compliant when trends, cycles and/or shifts are present. The high dynamic variety of land and water uses, specially in urban watersheds, associated with complex dynamics of environmental variability, i.e. daily variations, seasonality, atypical phenomena and long-term changes, gives rise to these patterns and variability structures in data (HULLEY; CLARK; WATT, 2015; COELHO et al., 2017; NDIONE; SAMBOU; KANE, 2017). Additionally, these long-term structures of variability can appear due to measurement errors and changes in techniques and methods (WAHLIN; GRIMVALL, 2008; HULLEY; CLARK; WATT, 2015). Under these conditions, the statistical results may lose meaning (GILBERT, 1987; MCBRIDE, 2005). These statistical properties of the time series are conditioning for the application of stochastic approaches which are important tools for dealing with ontological uncertainties, i.e. those associated with the inherent variability of the system. Although widely known in hydrological studies, stochastic approaches are rarely applied for water quality management purposes due the typical low and irregular frequency data, that challenges a reliable identification of trends, cycles and/or shifts and autocorrelations (KURUNç; YüREKLI; ÇEVIK, 2005; KOUTSOYIANNIS, 2006; YAN; ZOU, 2013; HIRSCH; ARCHFIELD; CICCO, 2015; BEVEN, 2016; NDIONE; SAMBOU; KANE, 2017).

In this context, Anttila et al. (2012) assessed these characteristics using high frequency data in a temperate, meso-eutrophic lake and Ndione, Sambou e Kane (2017) in rainfall time series from 6 monitoring stations in Senegal. High errors in seasonal statistics (±10% (mean), ±23% (std)) and low probability (12.8%) of observing concentrations in

the upper 75th percentile were found from monthly sampling. Ndione, Sambou e Kane (2017), additionally applied different statistical tests for the same purpose in two different periods (1960-2010 and 1970-2010), i.e. the Kendall and Spearman's rank correlation tests for independence (autocorrelation), Hubert and Lee-Heghinian procedures, Pettitt test, Buishand's U Statistic and Bois's Ellipse for homogeneity and Mann-Kendall (M-K) and Seasonal M-K (seasonal and monthly scales) tests for trend assessment. Different results were found depending on station, statistical tests, period of analysis and scales involved. These results highlight the importance of uncertainties related to representativeness and choice of methods to the final information for water resources management.

Recent researchers have focused in identifying, understanding, typifying (ontological, epistemic, ambiguity, etc.) and quantifying sources of uncertainty in water resources management. Difficulties with probability theory and intrinsic subjectivity of uncertainty analysis have been often mentioned (PAPPENBERGER; BEVEN, 2006; GROVES, 2006; SIGEL; KLAUER; PAHL-WOSTL, 2010; BEVEN; BINLEY, 2014; WARMINK et al., 2017). However, the knowledge about the implications of these characteristics to uncertainty analysis and information for water resources management is still incipient. In order to contribute for a better understanding of these relations, the present research investigates the effects of different types of uncertainties and intrinsic subjectivity in the statistical/stochastic context of water resources management. The identification of trends, cycles and/shifts was performed on uncertain hydrological and water quality/quantity data. The significance of the variability patterns was assessed by testing the hypothesis of randomness, homogeneity, independence ans stationarity (RHIS). An algorithm was developed to generate synthetic time series (STS) from uncertainty intervals with Monte Carlo Method (MCM) and apply the statistical tests. The subjectivity of uncertainty assessment, propagation and expression was also investigated by performing the analysis in different uncertainty scenarios and with different probability density functions (pdf's). An autoregressive model was used to generate synthetic daily flows, and a regression model was used to estimate daily concentration from daily flows. The irregular-frequency and daily time series were tested for RHIS and the results compared.

1.1   Hypothesis and Objectives

The hypothesis is that the stochastic approach for water quality assessment can provide more consistent and reliable information for the planning than the deterministic approach, once the latter is subjected to uncertainties from input data (epistemic and ontological) and errors from simplified representations of the biological, physical, and chemical system, and the former, only from the input data (epistemic and ontological). In other words, the hypothesis is that stochastic approaches can be a reliable tool for dealing with uncertainties in water quality management.

The objective of the present research is to evaluate the limitations and possible benefits from stochastic approaches in water quality analysis in a context of diverse sources/types of uncertainties, e.g., knightian, spatial/temporal representativeness, measurements, techniques and methods uncertainties. In a broader sense, it is the investigation of an alternative method for the deterministic approaches commonly used for water quality assessment. The specific goals are:

(i) Definition of uncertainty scenarios;

(ii) Understanding of the impact of uncertainties in the statistical context of water resources analysis through the verification of compliance with the basic assumptions (RHIS) for application of statistical methods;

(iii) Stochastic modeling of flows;

(iv) Application of a regression model for estimation of concentrations from flows;

(v) Stochastic modeling of water quality from synthetic flows.

1.2   Motivation

This research is motivated by the current growing concern about uncertainties, expressed in diverse references around the world. Most of the recent researches are focused in measurement uncertainties and their impact on modeling results. Until the publication of the present research, no researches about the combined impact of the different sources of uncertainties on information were found. For example, Coelho et al. (2017), called attention for the uncertainties related to non-compliance with the basic assumptions for the application of statistical methods (RHIS). The tests were applied in time series of concentration, loads and other units of 34 water quality variables from 12 monitoring sites in a predominantly urban watershed in south Brazil, the Upper Iguassu Watershed. There were rejection in 15%, 26%, 51% and 31% of the time series for randomness, homogeneity,

independence and stationarity, respectively. The research reveled that, although this verification is rarely performed, there is evidence that statistical results of water quality time series can be subject to an uncertainty due to non-compliance with basic assumptions.

A second reason was the advances in regression techniques for estimation of concentrations from flows. Hirsch, Moyer e Archfield (2010) presented a regression model that takes into account other factors beyond discharge to estimate a missing concentration in a chronological sequence. It considers the seasonal and time effect on the structure of data, making the estimates much more realistic. This type of tools can make the use of stochastic water quality modeling more feasible and reliable.

A third reason is the perception of the existent interrelation amongst the current need for better understanding of uncertainties, the challenges for uncertainty assessment in hydrological and water quality/quantity data, e.g subjectivity, the impact of uncertainties in identification of major variabilities (trends, cycles and shifts), and the increased power of regression models. All these issues are put together in the stochastic process, which is in essence a WRM tool to deal with ontological uncertainties, but is typically applied only in hydrological studies.

1.3   Guidance for the reader

In the next chapters the theoretical background, methods, study area, results and conclusions are presented. In chapter 2, the sections 2.1, 2.2, 2.3, 2.4, 2.5, and 2.6 present discussions about: (i) uncertainties in the water resources management; (ii) current basis for measurement assessment and expression; (iii) sources of uncertainty in hydrological measurements; (iv) advances in water quality assessment and expression; (v) uncertainties related to time series analysis, and finally; (vi) a synthesis of the chapter, respectively. In chapter 3, the section 3.1 present an overview and the philosophical/scientific background of the method. Sections 3.2 and 3.3 present the Upper Iguassu Watershed and monitoring sites of this research, and a description of the monitoring practices and time series, respectively. Sections 3.4, 3.5, 3.6, 3.7, 3.8 present the methods for: (i) for definition of uncertainty scenarios; (ii) generation of synthetic time series; (iii) significance assessment of variability patterns; (iv) regression among flows, and among flows and concentrations; (v) stochastic flow and water quality/quantity modeling, respectively. In chapter 4, the sections 4.1, 4.2 present the results from irregular-frequency time series; and from the joint analysis of irregular-frequency and continuous time series, respectively. Finally, the conclusions are presented in chapter 5.

2 Theoretical Background

"Stone river
Water ain't runnin' no more
What used to be a stream
Is now just a dream"
JJ Cale

2.1 Uncertainties in water resources management

The main uncertainty in water resources management is associated to the future availability of water for the many different water uses in a watershed. Diverse types of information are required to guide the decision-making processes to the consistent identification of pressures and solutions to meet future goals of quantity and quality. The planning of water resources is typically performed in the scale of decades being large enough to include significant changes in the environment, economy, water uses and needs or even war and peace. Consequently, the actual statistics are subject to significant changes in the planning period, being expected to be at least non-stationary, specially in the actual context of high uncertainties about climate change and sustainable development. The success depends on the ideas about what to expect in relation to these issues and to how water resources will respond to a given set of management actions and policies. A large part of these information is provided by statistical analysis of monitoring data and mathematical/statistical models.

The decision-making processes typically occur in a context of deep uncertainties, i.e., unknown uncertainties, not described by probabilities (SIGEL; KLAUER; PAHL-WOSTL, 2008). Climate change today is the most discussed source of uncertainty. Recently, this topic has received increasing attention. Particularly, it appears in the last version of the EU Water Framework Directive (WFD) (COMMISSION, 2000) as one of the "Key issues" that remain to be explored. According to the document, the pressing methodological questions are: "How to deal with uncertainty: which approaches can be proposed to water managers for integrating uncertainty into decision-making and for developing adequate communication on uncertainty towards the public and stakeholders?". According to Refsgaard et al. (2005), Sigel, Klauer e Pahl-Wostl (2008), the guidance documents of the WFD, as the Wateco (WATECO, 2003) and Proclan (PROCLAN, 2003) mention uncertainty several times and emphasize that uncertainty analysis should be performed. However, in spite of strong recommendations, these guidance documents do not include recommendations on how to do so. The water scarcity that could affect some re-

gions would probably impact others through migratory movements and increasing water conflicts.

These challenges are giving rise to the development of methods and practices as the robust decision-making (RDM) (GROVES, 2006) and adaptive management (BRUG-NACH et al., 2008; WARMINK et al., 2017). Briefly, RDM is a technique that prioritize the solutions that will work well in most of the scenarios considered for future conditions, and the adaptive management prioritize flexible solutions that are able to adapt to changing conditions and unexpected developments (GROVES, 2006; BRUGNACH et al., 2008; WARMINK et al., 2017). Even though these methods can lead to more consistent decisions, the scenarios are still generated from data and models, thus being subject to uncertainties about representativeness, measurements and parameters/structure of the models. Nowadays, these uncertainties are typically not taken into account, especially in water quality studies, for diverse reasons (HARMEL et al., 2006; REFSGAARD et al., 2006; LINDENSCHMIDT; FLEISCHBEIN, 2007). In hydrological and hydraulic modeling, uncertainties are typically not considered due to seven reasons: (i) uncertainty analysis is not necessary given physically realistic models; (ii) uncertainty analysis is not useful in understanding hydrological and hydraulic processes; (iii) uncertainty distributions can not be understood by policy makers and the public; (iv) uncertainty analysis can not be incorporated into the decision making process; (v) uncertainty analysis is too subjective; (vi) uncertainty analysis is too difficult to perform; and (vii) uncertainty does not really matter in making the final decision. Pappenberger e Beven (2006) provides a detailed discussion on each topic and argue that these reasons do not apply, and instead of not considering uncertainties, there is a need for the development of a code of practice that makes uncertainty an integral part of the modeling process.

Probabilities are the standard scientific approach to deal with uncertainties. However, there are considerable difficulties for application in environmental studies, once the events can not be repeated. As an example, the uncertainty of a water quality measurement, which involves sampling, sample storage and preservation, laboratory analysis, preparing of a team and transporting through long distances, would be a laborious and costly task. The most relevant and recent advances were presented by Refsgaard et al. (2005), Harmel et al. (2006), Brown e Heuvelink (2007), Harmel et al. (2009). The researches are evolving towards the development of softwares for measurement uncertainty assessment in water quality and hydrological data. The approach for building the software consists in a database with uncertainty information on water resources measurements (e.g., Harmel et al. (2006)), calculation of a combined uncertainty and expression of uncertainty by pdf's. However, the available uncertainty information on water quality and hydrological data is rarely sufficient for the calculation of empirical probabilities and fitting of pdf's, leaving a large part for subjectivity and professional judgment. Furthermore, common approaches for uncertainty analysis, as Monte Carlo Method, rely on confidence

intervals and empirical probability distributions, and thus, fail when uncertainties can not be captured in terms of probabilities (GROVES, 2006; BRUGNACH et al., 2008; SIGEL; KLAUER; PAHL-WOSTL, 2008).

Uncertainties, in a general way, can be understood as lack of confidence, which is mainly caused by lack of information (epistemic uncertainty), inherent random variation of the systems (ontological uncertainty), and a recently identified source of uncertainty in the social context of the water resources management, when the stakeholders must come to consensus which is called ambiguity. There are often many valid ways of framing a problem, which may result in ambiguities and conflicts about the problem domain and its solution. Any attempt to deal with uncertainty in natural resources management should also include the plurality of perspectives with respect to issue at hand. For example, a situation of water shortage can be framed as a problem of "insufficient water supply" by one actor and of "excessive water consumption" by another. In each frame for the same problem there will be different considerations about which uncertainties are more relevant. When a problem is framed as insufficient water supply, the most relevant uncertainties will be those associated with the amount of water available, and technical solutions that help avoiding water shortage can be favored (e.g., adopt a more efficient irrigation technology). On the other hand, when the problem is framed as an excessive water consumption issue, other solutions can be considered, such as changing the way in which water is used and consumed (e.g., diversification of crops). In this case, uncertainties associated with how society will react to a change in land use, or policies that stimulate the change (e.g., Common Agricultural Policy) will be the most important (BRUGNACH et al., 2008; WARMINK et al., 2017). Epistemic uncertainty can be reduced by gathering more information about the system, through investments in research and monitoring strategy for example. Ontological uncertainty can not be reduced, generally it can only be elucidated by statistical analysis. It should be noticed that being confident or not is a subjective perception. Hence, there will always be a subjective part of the uncertainty. This implies that an adequate assessment of uncertainty always requires an attitude of openness and a person's ability to assess the reliability of their knowledge (BROWN, 2004; SIGEL; KLAUER; PAHL-WOSTL, 2008; WARMINK et al., 2017).

Currently there is no established method or guidance document on how to perform the integrated uncertainty analysis, i.e., integrating uncertainties in measurements, statistics, modeling and social context of water resources management, and the knowledge related to these individual components of integrated uncertainty analysis is incipient (REFSGAARD et al., 2005; BROWN; HEUVELINK, 2007; SIGEL; KLAUER; PAHL-WOSTL, 2008; COZ, 2012; WARMINK et al., 2017; COELHO et al., 2017).

2.2   Measurement uncertainty

According to JCGM/WG1 (2008b), a guidance document (GUM 2008) providing rules on the expression of measurement uncertainty for use within standardization, calibration, laboratory accreditation, and metrology services was developed to attend the recommendation of the Bureau International des Poids et Mesures (BIPM) Working Group on the Statement of Uncertainties. The objectives were to promote full information on how uncertainty statements are arrived at, and to provide a basis for the international comparison of measurement results.

The document was developed in order to attend the following recommendations in the document **Recommendation INC-1 (1980)** - Expression of experimental uncertainties:

1. "The uncertainty in the result of a measurement generally consists of several components which may be grouped into two categories according to the way in which their numerical value is estimated:

A. those which are evaluated by statistical methods,

B. those which are evaluated by other means.

There is not always a simple correspondence between the classification into categories A or B and the previously used classification into "random" and "systematic" uncertainties. The term "systematic uncertainty" can be misleading and should be avoided. Any detailed report of the uncertainty should consist of a complete list of the components, specifying for each the method used to obtain its numerical value.

2. The components in category A are characterized by the estimated variances s_i^2, (or the estimated "standard deviations" s_i) and the number of degrees of freedom v_i. Where appropriate, the covariances should be given.

3. The components in category B should be characterized by quantities u_j^2, which may be considered as approximations to the corresponding variances, the existence of which is assumed. The quantities u_j^2 may be treated like variances and the quantities u_j like standard deviations. Where appropriate, the covariances should be treated in a similar way.

4. The combined uncertainty should be characterized by the numerical value obtained by applying the usual method for the combination of variances. The combined uncertainty and its components should be expressed in the form of "standard deviations".

5. If, for particular applications, it is necessary to multiply the combined uncertainty by a factor to obtain an overall uncertainty, the multiplying factor used must always be stated."

Additionally, the Recommendation 1 (CI-1986) requests that the paragraph 4 of Recommendation INC-1 (1980) should be applied by all participants in giving the results of all international comparisons or other work done under the auspices of the CIPM and the Comités Consultatifs and that the combined uncertainty of type A and type B uncertainties in terms of one standard deviation should be given.

Uncertainty, error, random error and other related terms have received different interpretations throughout different areas of knowledge, being sometimes difficult to have a common understanding about what is really meant to be expressed. This was considered an obstacle to the general development of science and technologies by most of the institutes involved with metrology, and as a consequence, in 2008, the **Joint Committee for Guides in Metrology** (JCGM) published the *JCGM 100:2008: Evaluation of measurement data - Guide to the expression of uncertainty in measurement* (GUM 2008). This document establishes the definition and concept of uncertainty and provides a general method to estimate and express the uncertainty of a measured quantity.

According to JCGM/WG1 (2008b), the formal definition of the term "uncertainty of measurement" and some related terms used in the guide is as follows:

*"**uncertainty of measurement***
parameter, associated with the result of a measurement, that characterizes the dispersion of the values that could reasonably be attributed to the measurand, considering that:

(i) the parameter may be, for example, a standard deviation (or a given multiple of it), or the half-width of an interval having a stated level of confidence;

(ii) uncertainty of measurement comprises, in general, many components. Some of these components may be evaluated from the statistical distribution of the results of series of measurements and can be characterized by experimental standard deviations. The other components, which also can be characterized by standard deviations, are evaluated from assumed probability distributions based on experience or other information;

(iii) it is understood that the result of the measurement is the best estimate of the value of the measurand, and that all components of uncertainty,

including those arising from systematic effects, such as components associated with corrections and reference standards, contribute to the dispersion;

standard uncertainty
uncertainty of the result of a measurement expressed as a standard deviation

type A evaluation (of uncertainty)
method of evaluation of uncertainty by the statistical analysis of series of observations

type B evaluation (of uncertainty)
method of evaluation of uncertainty by means other than the statistical analysis of series of observations

combined standard uncertainty
standard uncertainty of the result of a measurement when that result is obtained from the values of a number of other quantities, equal to the positive square root of a sum of terms, the terms being the variances or covariances of these other quantities weighted according to how the measurement result varies with changes in these quantities

expanded uncertainty
quantity defining an interval about the result of a measurement that may be expected to encompass a large fraction of the distribution of values that could reasonably be attributed to the measurand, considering that:

(i) *the fraction may be viewed as the coverage probability or level of confidence of the interval;*

(ii) *to associate a specific level of confidence with the interval defined by the expanded uncertainty requires explicit or implicit assumptions regarding the probability distribution characterized by the measurement result and its combined standard uncertainty. The level of confidence that may be attributed to this interval can be known only to the extent to which such assumptions may be justified;*

coverage factor
numerical factor used as a multiplier of the combined standard uncertainty in order to obtain an expanded uncertainty. A coverage factor, k, is typically in the range 2 to 3.

An important discussion in GUM 2008 is about the concept of "true" value of

measurand. According to JCGM/WG1 (2008b), the "true" value is an idealized concept, as it depends on the definition of the measurand. This definition can be more or less specified, e.g., "the biochemical oxygen demand in temperature $20°C$, after 5 days'" or "the biochemical oxygen demand in temperature $20°C$, after 5 days and pressure 100 hPa". Even with very complete specifications of the measurand, there will be always a factor not accounted for, that will impose an uncertainty to the "true" value, or some specifications that can not be met exactly. This refers to the minimum uncertainty of a measurand. The more or less specified definition of the measurand gives place to many "true" values and, hence, an uncertain "true" value. Although the final result is sometimes viewed as the best estimate of the "true" value of the measurand, in reality the result is simply the best estimate of the value of the quantity intended to be measured.

The uncertainty of a measurement, as defined in GUM 2008, is a range of values that encompasses all possibilities of error in relation to the best value that is consistent with the available knowledge, not the value of the measurand, sometimes called the "true" value (impossible to be known exactly) . As it is unknown, the exact value of the error is also unknown, but the uncertainties associated with random and systematic effects that gives rise to the error can be evaluated, and so on, the uncertainty of a measurement. Its is important to notice that there is no guarantee that this range represents an indication of the likelihood that a result of a measurement is near the value of the measurand. It is just an indication of the likelihood of the nearness to the best value that is consistent with the available knowledge.

A corrected measurement result is not the value of the measurand — that is, it is in error — because of imperfect measurement of the realized quantity due to random variations of the observations (random effects), inadequate determination of the corrections for systematic effects, and incomplete knowledge of certain physical phenomena (also systematic effects). Neither the value of the realized quantity nor the value of the measurand can ever be known exactly; all that can be known is their estimated values (JCGM/WG1, 2008b).

The uncertainties evaluated from repeated measurements (Type A) or methods other than statistics, e.g., scientific judgment (Type B) must be propagated by analytical methods or Monte Carlo Method (MCM), but they can also be propagated by a simplified scheme, the *GUM uncertainty framework*, which might not be satisfactory when: (i) distributions for the input and output quantities are asymmetric, or not a Gaussian or t-distribution; (ii) the measurement function is non-linear; (iii) uncertainty contributions are not of approximately the same magnitude (JCGM/WG1, 2009).

2.3   Hydrological uncertainty

Water availability in watersheds is subjected to uncertainties related to climate change, water use and needs and effectiveness of management actions. The planning of water resources management is highly dependent on measurements of the flows. There are many different demands for open channel flow information within the broad context of water management, as water supply, pollution control, irrigation, flood control, energy generation and industrial use. None of these needs can be met without reliable open channel flow information. Although flows can be measured and a historical sequence formed, the exact flow conditions under which the discharge occurred may never happen again. The probability that the historical sequence of flow history at a given site will occur again is remote. Given the uniqueness of a historical sequence, efforts should be directed to improve the quality of the measurements and reduce uncertainties (HERSCHY, 2002).

The reliability of the information depends essentially on the quality of the monitoring program, including appropriate methods and its correct application, continuous maintenance of equipments and appropriate measurement frequencies. According to Herschy (2002), in agreement with GUM 2008, states that the result of a measurement is only an estimate of the true value of the measurement and is therefore only complete when accompanied by a statement of its uncertainty. The discrepancy between the true and measured values is the measurement error. The measurement error, which cannot be known, causes an uncertainty about the correctness of the measurement result. The measurement error is a combination of component errors that arise during the performance of various elementary operation during the measurement process. For measurements of composite quantities, that depend on several component quantities, the total error of the measurement is a combination of the errors in all component quantities. Determination of measurement uncertainty involves identification and characterization of all components of error and the quantification and combination of the corresponding uncertainties.

The flow measurement can be performed by diverse methods. The stage-discharge, the acoustic doppler current profiler (ADCP) and the velocity-area are the most applied (COZ, 2012). Literature presents many estimates of the uncertainties related to the steps of the flow measurements (DICKINSON, 1967; PELLETIER, 1988; SAUER; MEYER, 1992; SCHIMDT, 2002). However, this individual uncertainties are rarely used to estimate the cumulative uncertainty (HARMEL et al., 2006; HARMEL et al., 2009). Publications as "Call for Collaboration in World Meteorological Organization (WMO) Project for the Assesment of the Performance of Flow Measurement Instruments and Techniques" (FULFORD et al., 2007) and "A literature review of methods for estimating the uncertainty associated with stage-discharge relations" (COZ, 2012) reflect the current concern with the uncertainties in flow measurements. Coz (2012) states that the expression of the uncertainty associated to stream flow measurements or estimates is of paramount

importance in issues related to water resources, flood frequency analysis, flood control, flood and drought forecast, compensation discharges and water use conflicts. According to Goodwin (2005) it is important to study these uncertainties because they often underpin many hydrological studies at many different spatial and temporal scales, and users may include climate impact modellers, hydrologic modellers as well as national and regional analysts/planners.

The stage-discharge method is the most applied method for river flow measurement (COZ, 2012; GOODWIN, 2005). The sources of uncertainty are the cross-section hydraulic characteristics, flow regime, stage measurement, stage-discharge relation and human imperfection. According to Coz (2012), all the sources of uncertainty of this method seem to have been investigated, however future researches for development of a simple, practical, versatile and widely recognized method for a global understanding of uncertainties are needed. According to Coz (2012), some important requirements of an ideal method for the expression of uncertainty associated with discharge estimates from stage-discharge relations are:

- Expression of uncertainty should be compliant with the ISO GUM or any other standard methodology for uncertainty analysis. If possible, the best practice is to express uncertainty in the form of a probability density function.

- Hydraulic analysis of the physical stage-discharge relation at a site must be quantified, even roughly, and taken into account in the rating curve analysis. This is particularly important for low-flow and high-flow ranges where the stage-discharge relation has to be extended outside of the more intensively rated region of the rating curve.

- Uncertainty analysis of individual ratings should be performed in a rigorous and individual way, including the deviation from the reference hydraulic regime. In the rating curve analysis, the uncertainty of each individual rating should be taken into account. Thus, data uncertainty sensu Schimdt (2002) should be clearly separated from the uncertainty in the stage-discharge relation itself (knowledge uncertainty sensu Schimdt (2002)).

- Uncertainty analysis of stage-discharge relation in the reference hydraulic regime should be conducted using a sounded mathematical approach. To separate knowledge uncertainty from *natural uncertainty* sensu Schimdt (2002), the reference hydraulic regime must be elicited. Possible heteroscedasticity of the reference stage-discharge relation should be accounted for.

- Non-stationarity of stage-discharge relation due to temporary/permanent changes of the reference hydraulic regime should be quantified in the uncertainty analy-

sis, either continuously or periodically, according to the physical cause of the non-stationarity. Weighted fuzzy regression, variographic as well as Bayesian inference techniques are promising tools to assess non-stationarity of stage-discharge relations.

- Uncertainty in the instantaneous discharge Q_t derived from the rating curve should be computed taking into account the uncertainty in the water level record and the potential deviation from the reference regime at time t, due to transient flow effects or backwater effects for instance.

Most of the researches about uncertainties in flow measurements and estimates present a unique value for a given condition of measurement or estimate method. However, in many real cases the uncertainty can not be the same for all estimated flows from a given rating curve, instead, it must be greater for low and high flows since there are few data on these ranges and the rating curve must be extended. According to Goodwin (2005), the uncertainty will increase at the extremes of the stage/discharge curve where the flow estimates are outside the range for which the stage-discharge curve was established. Harmel et al. (2006) presents uncertainty estimates for each step of the storm load determination process, i.e., stream flow measurement, sample collection, storage/preservation and laboratory analysis, and also for the combined (or cumulative) uncertainty on the final results. The author presents uncertainty estimates for discharge measurements and estimates for best, typical and worst case scenarios, as shown in Table 1. A unique value was presented, without differentiation according to the region of the stage-discharge relation. The typical and best case scenarios estimates are consistent with the acceptable uncertainty of ±15% to ±20% recommended by the WMO when sources of uncertainty cannot be reduced (GOODWIN, 2005).

Table 1 – Uncertainty estimates for stream flow by Harmel et al. (2006)

Scenarios	Description	Uncertainty
Worst case	stream flow estimation with manning's equation with a stage-discharge relationship for an unstable, mobile bed and shifting channel	±42%
Typical	A range of individual stream flow measurement techniques, channel types, and channel conditions	±6% to ±19%
Best case	flow measurement under ideal hydrologic conditions, specifically a pre-calibrated flow control structure (stable bed and channel) and a stilling well for stage measurement	±3%

Stage-Discharge Method

The method consists in building a fluviometric station at an appropriate cross-section of a river and establishing a relation between water level and flow direct measurements, that provides estimates of discharges from stage records. The direct measurements of flow are usually performed by velocity-area method. The relation is obtained by setting the discharge measurements at the abscissa and stage at the ordinates and applying the minimum squares or finite differences methods. The obtained relation can vary in time depending on the hydraulic conditions of the cross-section. The higher the number of measurements in different flow conditions, the better the quality of the relation. Typically, there are measurements in all but high flow conditions, and thus the relation for this condition is extrapolated by different techniques (PINTO et al., 1976; SANTOS et al., 2001). The uncertainties can be related to a number of factors (GOODWIN, 2005):

- Uncertainty in stage measurements;

- Uncertainty due to the stage-discharge relationship no longer being valid;

- Uncertainty due to the method used to derive the stage-discharge relationship, and the range of flows for which it is valid.

The method also imposes a problem of representativeness, since the two stage records of each day, typically at 7:00 h and 17:00 h, may not be representative of the average daily situation. This problem is important in rivers with operating hydro power plants, small watersheds and urban watersheds, where fast water level variations can be observed in a day. In addition, not always the stage discharge relation is unequivocal. In some cases, the presence of a flood wave (transient regime) or water retention downstream can cause significantly different discharges with the same water level. Theoretically, very few rivers satisfy the conditions for an unequivocal relation. However, in many cases, the error associated with incorrect use of unequivocal relation is negligible compared to the imprecision of measurements, being acceptable its use (PINTO et al., 1976; SANTOS et al., 2001).

According to Goodwin (2005), within most hydrological models where flow measurements are required, average daily flows are used, and for the purpose of most studies daily values are sufficient. Holmes, Round e Young (2000) *apud* Goodwin (2005) investigated the uncertainty associated with assuming that a flow value taken at any point within a day will reflect the daily average. The study indicated that, within the UK, the within day variability is controlled by the permeability and size of the catchment. Whilst the variability of flows within a permeable catchment is generally the same for high and low flows, for an impermeable catchment the within variability of flows is far greater for higher flows than low flows. The uncertainty with estimating high flow events using low

resolution data will therefore be greater within impermeable catchments hence, the time support will be of most important when extreme values are being assessed. The effect will be further emphasized within urban catchments which have artificial drainage networks which will tend to result in the response of the catchment being accelerated, indicated by a steeper rising limb, with the time to peak reduced.

According to Goodwin (2005), the WMO recommends that for detailed experimental catchments (in which process based models will be set up) 15 minute or hourly data is required. For small pristine catchments up to 1000 km², hourly to mean daily data is necessary, and for national and regional runoff studies mean daily to monthly data is necessary.

Cross-Section

The characteristics of the cross-section as river bed nature, existence of dams up and/or downstream, vegetation of river bank and water level variation, have fundamental importance on the constancy of the stage-discharge relation and precision of the estimated flows. Stations can be more or less sensitive in relation to water level variations depending on the types of controls at the cross-section. The controls are a combination of the physical characteristics of the river at a given cross-section, especially at the downstream reach, as nature, configuration and plant recovery at river banks and meadows. If there are high flow variations associated with small stage variations, the estimates will be more uncertain and vice-versa (PINTO et al., 1976; SANTOS et al., 2001).

Stage Measurement

The stage measurement is performed, most usually, by reading the water level on a ruler placed on the river bank. The main advantages of the method are its low cost and simplicity. The main disadvantage is the ease with which the reader can make mistakes. Typically, a person that lives close to the location, without any knowledge about hydrometry and water resources management, is paid to read and record the water level twice a day. Many materials and forms of writing the scale on the ruler has been applied to avoid misunderstandings by the reader. The chance of error occurrence is higher during floods and when the water level fluctuates too much. Among the most common errors are the error of entire meters, pure invention and wrong readings made at long distances from the ruler. Other type of error, not focused on the reader, are the systematic errors, which are differences between the real water level and the water level read on the ruler. The most frequent cause is a displacement of the zero of the ruler, i.e. a vertical displacement changing the original level of its origin. In addition, it is common for things brought by the water flow to crash against the ruler, sometimes accumulating on it and/or causing damage to it (PINTO et al., 1976; SANTOS et al., 2001).

Stage-Discharge Relationship

Often the method which is used to derive the rating curve is the non-linear least squares method (NLS). This assumes that each measurement has equal weighting in the rating curve estimation. However, this will not happen if there is heteroscedacity. This occurs when the distribution of the residual is dependent on the indicator variable. This can be detected by plotting the residuals from the estimation procedure. If there is greater variability of the residuals for large or small variables then heteroscedacity is present. Petersen-Overleir (2004) *apud* Goodwin (2005) found that out of 20 gauges within Norway for which NLS curves were used, half were found to have some indication of heteroscedacity. The impact of heteroscedacity on flow estimates is of most importance when extrapolation and extreme value analysis is used. Other methods of determining rating curves, for example, using Generalized Least Squares, or maximum likelihood tend to provide estimates for the rating curve which minimize the impact of the heteroscedacity (PETERSEN-OVERLEIR, 2004; GOODWIN, 2005).

International Standards

The uncertainty management and control can be improved mainly by carefully applying techniques and methods available on international standards. Thomas (2002) compiled the main standards related to open channel flow measurement as follows:

- ISO 748 Velocity-area methods;

- ISO 1070 Slope-area method;

- ISO 1088 Velocity-area methods: Collection and processing of data for determination of errors in measurement;

- ISO 1100-1 Establishment and operation of a gauging station;

- ISO 1100-2 Determination of the stage-discharge relation;

- ISO 4373 Water-level measuring devices;

- ISO 4375 Cableway system for stream gauging;

- ISO 6416 Measurement of discharge by the ultrasonic (acoustic) method;

- ISO 8368 Guidelines for selection of structure;

- ISO 9123 Stage-fall-discharge relationships;

- ISO 9825 Field measurement of discharge in large rivers and floods;

- ISO 14139 Compound gauging structures;

- ISO/TS 15769 Guidelines for the application of Doppler-based flow measurements;

- ISO/TR 7178 Investigation of total error;

- ISO/TR 9823 Velocity-area method using a restricted number of verticals.

2.4   Water quality uncertainty

The first source of uncertainty is related to the representativeness provided by the monitoring strategy, i.e., the choice of sites, sampling frequency, variables and techniques/methods of measurement. This is the most important step for reliable results as it is related to the accuracy of the measurement. The next steps are related to the precision of techniques, sensors and methods in field measurements and laboratory analysis, and correct execution of data management, transfer and record. These uncertainties combine themselves on the final results of monitoring programs, however being rarely estimated and reported with the final results (REFSGAARD et al., 2005; HARMEL et al., 2006; HARMEL et al., 2009).

Combined Uncertainty

Estimates of combined uncertainty of water quality data can be found in Harmel et al. (2006). The author estimated the combined (or cumulative) uncertainty of some water quality parameters and stream flow by propagating the individual uncertainties of each step of the measurement process. The individual uncertainties (Table 2) were provided by literature review and reported as standard percentages (±%) and the combined uncertainty (Table 3) calculated by the root mean square error method. The sources of uncertainty were the stream flow measurements, sampling, storage/preservation and laboratory analysis. The most relevant sources of uncertainty were the sample collection and laboratory analyses, which ranged from 1%–109% and 1%–400%, respectively. The combined uncertainty for loads reached values » 100% in the worst case scenario especially for nitrate and dissolved phosphorous. In a context of inexistent information on uncertainty, which is the current scenario, these estimates can be of great importance for the inclusion of uncertainty analysis in the planning of water resources. One should be careful with uncertainty estimates higher than 100% since it yields negative values of flows, concentration and loads. Furthermore, the uncertainty assessment of environmental measurements is a non-trivial task. Refsgaard et al. (2005), (HARMEL et al., 2006), (BROWN; HEUVELINK, 2007) and (HARMEL et al., 2009) seem to be the first and still rare published research focused on the assessment of combined uncertainty of hydrological and water quality variables.

Table 2 – Uncertainty results for individual steps of storm load measurements by Harmel et al. (2006)

Step	Worst case		Typical case		Best case	
	Description	±%	Description	±%	Description	±%
Stream flow measurement	Manning's equation with a stage-discharge relationship for an unstable, mobile bed and a shifting channel	42%	A range of individual stream flow measurement techniques, channel types, and channel conditions	6% to 19%	flow measurement under ideal hydrological conditions, specifically a pre-calibrated flow control structure (stable bed and channel) and a stilling well for stage measurement	3%
Sample collection	Liberal estimates of error associated with sample collection at a single point, infrequent time-interval sampling at a high minimum flow threshold, and disregard of conditions outside the sampling period	104% for dissolved constituents and 109% for TSS and total N and P	Moderate errors associated with frequent flow- or time-interval sample collection at a single point and estimation of conditions outside a high flow threshold	4% to 47% for dissolved constituents and from 4% to 50% for TSS and total N and P	Conservative error estimates associated with frequent flow or time-interval sample collection at a single point and estimation of conditions outside a low flow threshold	1% for dissolved and sediment-associated constituents
Sample preserv./storage	Unpreserved, unrefrigerated sample storage for 144 h and then refrigerated storage for 48 h prior to analysis	20% to 90% for dissolved constituents and from 9% to 84% for total nutrients	Refrigerated sample storage for 54 h prior to analysis	2% to 16% for dissolved nutrients and from 7% to 9% for total nutrients	Iced sample storage for 6 h prior to analysis	0% to 2% and from 1% to 3% for dissolved and total nutrients, respectively
Laboratory analysis	Liberal estimates of error for constituents present in very low concentrations	200% to 400% for dissolved constituents, 88% to 211% for total nutrients, and 10% for TSS	Moderate error estimates for low constituent concentrations	4% to 26% for dissolved nutrients, from 3% to 32% for total nutrients, and from 1% to 5% for TSS	Conservative error estimates for constituents present in moderate concentrations	Less than 2%, 4%, 1%, respectively, for dissolved nutrients, total nutrients, and TSS

Table 3 – Cumulative uncertainty estimates for storm loads by Harmel et al. (2006)

Scenarios	Streamflow	NO_3^--N	NH_4-N	Total N	Diss. P	Total P	TSS
Worst case	42%	421%	246%	168%	417%	249%	117%
Typical maximum	19%	69%	100%	70%	104%	110%	53%
Typical average	10%	17%	31%	29%	23%	30%	18%
Typical minimum	6%	8%	11%	11%	11%	8%	7%
Best case	3%	4%	3%	6%	4%	3%	3%

Software Tools

Harmel et al. (2009) presented an application of a software tool for estimating the combined uncertainty of water quality data, called Data Uncertainty Estimation Tool for Hydrology and Water Quality (DUET-H/WQ). DUET-H/WQ was developed from an existing uncertainty estimation framework for small watershed flow, sediment, and N and P data. The root mean square error propagation methodology (RMSE) is used to provide uncertainty estimates, instead of more rigorous approaches requiring detailed statistical information, rarely available (HARMEL et al., 2009). The RMSE method estimates the most probable value of the cumulative or combined error by propagating the error from each procedure (TOPPING, 1972). Whereas errors were assumed to represent the 0.68 significance level (1 standard deviation for the normal distribution) by Sauer e Meyer (1992), the 0.9999 significance level (3.9 standard deviations) was assumed based on Harmel e Smith (2007) and (HARMEL et al., 2009).

DUET-H/WQ lists published uncertainty information for data collection procedures to assist the user in assigning appropriate data-specific uncertainty estimates and then calculates the combined uncertainty for individual discharge, concentration, and load values. Results of DUET-H/WQ application in several studies indicated that substantial uncertainty can be contributed by each procedural category (discharge measurement, sample collection, sample preservation/storage, laboratory analysis, and data processing and management). Both DUET-H/WQ and its framework-basis focus on measured discharge, sediment, and N and P (dissolved and particulate) data collected at the small watershed scale (HARMEL et al., 2009).

The framework-basis presented in Harmel et al. (2006) did not accounted for errors due to malfunction of equipments or personnel mistakes, which were included in DUET-H/WQ. This allowed quantitative estimates for uncertainty contributed by missing and/or incorrect data to be included in combined uncertainty estimates. The probable error are calculated by Equation 2.1, where EP is the cumulative probable error or uncertainty for individual measured values ($\pm$%), E_Q = uncertainty in discharge measurement ($\pm$%), E_C =

uncertainty in sample collection (±%), E_{PS} = uncertainty in sample preservation/storage (±%), E_A = uncertainty in laboratory analysis (±%), and E_{DPM} = uncertainty in data processing and management (±%). The author also presents an equation (Equation 2.2) for propagation of uncertainty of aggregated data (e.g., weekly, monthly, annual or study period), also valid for determination of uncertainty in an average, where EP_{total} = cumulative probable error (±%) for the aggregated (sum or average) of n measured values, n = number of measured values with corresponding uncertainty estimates, x_i = ith measured value, and EP_i = cumulative probable error (±%) for ith measured value (HARMEL et al., 2009).

$$EP = \sqrt{E_Q^2 + E_C^2 + E_{PS}^2 + E_{DPM}^2} \tag{2.1}$$

$$EP = \frac{100}{\sum_{i=1}^n x_i} \sqrt{\sum_{i=1}^n (x_i \times \frac{EP_i}{100})^2} \tag{2.2}$$

DUET-H/WQ has the following limitations:

- Assumption of bi-directional uncertainties;

- Information for small watersheds only;

- The process by which users determine a reasonable uncertainty estimate for each procedure is quite subjective because of the considerable variability of published uncertainty information as affected by study design, collection methods, and monitoring conditions;

- Does not include all sources of uncertainty (e.g., uncertainty contributed by spatial and temporal variability). Such uncertainty sources were excluded to maintain a focus on uncertainty estimation for individual measured values;

- It's focused in storm load estimates in agricultural watersheds.

The DUET-H/WQ was applied to estimate the combined uncertainty in data from three small watersheds in Texas (Riesel, Hamilton and Austin), Indiana (Waterloo) and Ohio (Centerburg). The drainage areas ranged from 8.4 to 5,506 ha, most with agricultural land uses. Data from 8 monitoring sites were analyzed. The results and discussion were divided in a comparison of procedural categories and a comparison of constituent type. In the comparison of procedural categories the results were grouped across all sites and by constituent type with dissolved N and P and total N and P further grouped, since little difference occurred between dissolved NO_3-N and PO_4-P or between total N and P. The uncertainties in flow measurements for storm events ranged from 7 to 27%

with a median of 14%. Although uncertainty in sample collection is often ignored, it can be the dominant source in environmental investigations (RAMSEY, 1998), as it was the case for sediment and total N and P sample collection in the this study. Unlike for the dissolved constituents, the cross-sectional and vertical gradients in particulate-associated concentrations make the collection of representative sediment and total N and P samples quite difficult. The dissolved constituents are typically uniformly distributed within the channel (MARTIN; SMOOT; WHITE, 1992; GING, 1999; RODE; SUHR, 2007). This difference was exemplified by the greater sample collection uncertainties for sediment and total N and P concentrations, which ranged from 12 to 26%, than for dissolved NO_3-N and PO_4-P concentrations, which ranged from 6 to 17%. Uncertainties contributed by sample preservation/storage ranged from 6 to 22% for dissolved NO_3-N and PO_4-P concentrations and from 6 to 27% for total N and P concentrations. For storm events, laboratory analysis introduced little uncertainty ($< 8\%$) in sediment concentrations due to relatively simple analytical procedures but often introduced considerable uncertainty in N and P concentrations. Whereas little difference occurred between the uncertainty contributed by sample collection and sample preservation/storage in dissolved and total N and P concentrations, an important difference occurred for laboratory analysis. Although laboratory analysis uncertainty was typically similar for dissolved NO_3-N and PO_4-P concentrations (range = 6 - 21%) and for total N and P (range = 6 - 15%), uncertainty increased to 23% for one event with very low total P concentrations (< 0.05 mg/l). Kotlash e Chessman (1998) noted this influence on reference stream data with very low nutrient concentrations, which are sensitive to small absolute errors and result in high relative errors. Data processing and management typically introduced $< 5\%$ uncertainty, but missing and incorrect data did introduce 10–100% uncertainty in several cases.

In the comparison of constituent types the cumulative uncertainties in concentrations and loads were determined for individual storms. These results were grouped across all sites. For individual TSS values, the uncertainties in measured storm concentrations ranged from 12 to 26% with a median of 18%. Sediment load uncertainties ranged from 15 to 35% with a median of 20%. The uncertainties in NO_3-N concentrations ranged from 13 to 102% (median = 17%) and in PO_4-P concentrations ranged from 13 to 103% (median = 19%). Load uncertainties ranged from 14 to 103% (median = 22%) for NO_3-N and from 14 to 104% (median = 23%) for PO_4-P. The occasional high uncertainty estimates (100%) in the study resulted from extreme high flows and/or missing samples. Concentration uncertainties ranged from 14 to 104% (median = 23%) for total N and from 16 to 104% (median = 24%) for total P. Load uncertainties ranged from 15 to 105% (median = 25%) for total N and from 17 to 105% (median = 27%) for total P. The occasional high uncertainties again resulted from extreme high flows and/or missing samples.

Across all watersheds, the 10*th* and 90*th* percentiles for uncertainty in measured storm flows were 7–23%; in concentrations were 12–22% for TSS, 13–24% for dissolved

N and P, and 16–28% for total N and P; and in loads were 16–27% for TSS, 14–31% for dissolved N and P, and 18–36% for total N and P. Since no complete error propagation results have been previously published for real-world data, these results provide initial uncertainty estimates for field staff, modelers, stakeholders, and regulators to use in data analysis and decision-making. Results showed that even data collected with concerted quality assurance can have appreciable uncertainty, and also that uncertainty is related to constituent type (Q < TSS < dissolved N and P < total N and P). Although the RMSE method does not provide the most rigorous uncertainty estimates, it is a widely accepted and should encourage broader practical application than statistical alternatives with unsubstantiated assumptions (HARMEL et al., 2009).

Brown e Heuvelink (2007) presented a software tool for assessing uncertainties in environmental data and generating realizations of uncertain data for use in uncertainty propagation analyses: the Data Uncertainty Engine (DUE). The software is more complex than the software presented by Harmel et al. (2009) by the following main reasons: (i) it was designed for environmental data; (ii) generates an uncertainty model (UM) (pdf) for environmental data; (iii) analyzes the uncertainty of a dataset, instead of just individual values; (iv) accounts for positional uncertainty and (v) applies Monte Carlo Simulations (MCS) to generate realizations of uncertain data. The combined uncertainties are estimated by consulting in a library with uncertainty informations (as in DUET-H/WQ) and by expert judgment. A "Sources dialog" is used to identify the main sources of uncertainty in a dataset, including those that cannot be modeled reliably, and to estimate the ranked importance or percentage contribution of each source of uncertainty to the overall uncertainty about the data. It also includes a skeleton library of uncertainty sources (in XML format), which can be expanded and edited by the user. Once the combined uncertainty is defined, an uncertainty model must be defined. Currently, the available uncertainty model is a pdf.

The software treat things as objects with attributes, for example, a river object may have length and volume as constant attributes, together with nutrient concentrations, navigation pressures and fish stocks as variable attributes. The UM can be a marginal pdf or a joint pdf which accounts for correlations in space and time. Currently, a UM can be constructed from either expert judgment or sample data. In terms of the latter, a geostatistical model is used to parameterise a joint pdf for all sampled attributes and locations. Here, samples are used, first, to estimate the joint pdf, and, secondly, to improve the accuracy of the simulated output by reproducing the samples at nearby locations. Using expert judgment, a parametric distribution can be assigned by selecting individual locations, either manually or with logical operators on the attribute values (<, >, etc.), and by then entering the parameter values. Alternatively, a parameter can be assigned via a functional relationship with one or more attributes at all locations. For example, the standard deviation or "spread" of the normal distribution may be assigned to 10% of

the attribute value at each location.

In applying a geostatistical model, the underlying process, or its uncertainty, is assumed joint-normally distributed and second-order stationary, for which the mean may be known (simple Kriging) or unknown (ordinary Kriging). In this framework, the correlations or covariances between pairs of locations depend only on their separation distance in space or time. Given these assumptions, the observations may be transformed to a normal distribution in DUE and back-transformed to their original distributions after MCS. The software procedural structure can be resumed by following five stages:

1. Importing (and saving) data as objects with attributes;

2. Describing the sources of uncertainty;

3. Defining an uncertainty model, aided by the description of sources;

4. Evaluating the quality or "goodness" of the uncertainty model; and

5. Generating realisations of uncertain data for use in MCS with models.

According to Brown e Heuvelink (2007), an ongoing challenge is to balance statistical realism with practicality in applying pdfs to environmental data. DUE was developed, and is currently being used, in the project "Harmonised Techniques and Representative River Basin Data for Assessment and Use of Uncertainty Information in Integrated Water Management (HarmoniRiB)" (REFSGAARD et al., 2005). This project includes the establishment of representative river basins for generation of uncertainty information, which is currently missing in literature.

2.5 Time series analysis

When the water quality is analyzed in the perspective of time and space there are many characteristics of variability that must be taken into account in the statistical and modeling context of water resources management (GILBERT, 1987; HELSEL; HIRSCH, 2002; NAGHETTINI; PINTO, 2007; MILLY et al., 2008; DETZEL, 2015; HULLEY; CLARK; WATT, 2015; NDIONE; SAMBOU; KANE, 2017; COELHO et al., 2017). The presence of non-randomness, non-homogeneities, dependence and non-stationarities can make the statistical and modeling results little representative of the real water quality and quantity conditions (COELHO et al., 2017). The uncertainties related to climate change increases the chance of actual hydrological and water quality time series to be non-representative by influencing seasonality, trends and shifts. Hence, the information from statistical analysis of data and modeling exercises should be carefully analyzed through this new perspective of uncertainties. The typical deterministic or stochastic modeling

approaches may not provide reliable answers if the actual statistics are not representative and/or are expected to change over the planning period (HULLEY; CLARK; WATT, 2015; BEVEN, 2016; COELHO et al., 2017). The criteria for being statistically representativeness is that the time series must be compliant with the properties of randomness, homogeneity, independence and stationarity. It is met when significant shifts, trends, seasonality and autocorrelation are not present (HULLEY; CLARK; WATT, 2015; BEVEN, 2016; COELHO et al., 2017). However, the natural environment and especially urban watersheds are subjected to climate changes, seasonality, atypical meteorological phenomena and management actions, which make the quantity and quality conditions highly variable and having patterns as these ones discussed above.

The measurement uncertainties are also expected to change over space and time. For example, a ruler for stage measurement of a river may be in good reading conditions one day, but in poor conditions on the next days due to damages caused by a flood. The conditions for measurement also change from site to site, for example the distance to read the stage or the cross-section width. Thus, the uncertainty analysis in the context of time series should also consider time and space influences on variability. In this sense, uncertainty may be understood as a random variable which may be autocorrelated in space and time and subject to diverse types time and space related variabilities (BROWN; HEUVELINK, 2007; GOODWIN, 2005).

The identification of these phenomena in time series is a complex task. The variability of the flows generally introduces considerable "noise" in the variability of concentrations making it difficult to assess the presence of patterns (HIRSCH; MOYER; ARCHFIELD, 2010). Hydrological data often have higher and regular monitoring frequencies in comparison to water quality data. Although it facilitates the identification and management of variability patterns, previously to statistical analysis and modeling, any time series is just part of the whole history that will be used for the planning of another part (KOUTSOYIANNIS, 2006; BEVEN, 2016). This means that a time series may cause a distorted or incomplete impression about its variability. Typical water quality time series have few data, large intervals and irregular frequency, imposing considerable difficulties and high uncertainties to identification and management of these properties, and hence, to statistical inference and modeling (HAGGARD et al., 2003; COELHO et al., 2017). Rode e Suhr (2007) stated that the most important factors of river water quality data are sampling and measurement or analytical uncertainties, and that sampling uncertainties can be categorized between uncertainties related to the selection of a representative sampling location, representative samples at a given river cross section and the choice of an appropriate sample frequency.

Besides the limitations and uncertainties imposed by low and irregular sampling frequency, flow and water quality data reflects not only natural variability but also those

caused by malfunction of measurement equipments, changes in methods, laboratories and other sampling practices, and intrinsic uncertainty of measurements. Wahlin e Grimvall (2008) investigated the presence of trends in phosphorous and nitrogen time series from 34 rivers in Sweden and concluded that there was strong evidence that the observed long-term trends were more extensively influenced by changes in sampling practices and measurement errors than by actual changes in the state of the environment. It was recommended that the measured concentrations should be properly visualized before they were entered into a database, and that a retrospective analysis should be performed involving meteorological/hydrological adjustment of measured concentrations and joint analysis of several time series of data.

2.5.1 Regression

Regression analysis, also known as Ordinary Least Squares (OLS) has been used in water resources management to describe in some sense the behavior of a random variable of interest, called the dependent or response variable. The dependent variable changes according to changes in one or more conditions in a process, which are called independent or explanatory variables. In a regression model the dependent variable is typically represented by the letter y and the independent variables, assumed to be known constants, by the letter x with subscripts as needed to denote different independent variables (in the case of multiple regression). The model also involves constant parameters represented by Greek letters which are estimated from the data. These parameters control the model behavior. Regression models can be divided in two major groups, i.e. linear and nonlinear in the parameters. The nonlinear models can also be divided in two categories, the intrinsically linear models and those that can not be linearized (RAWLINGS; PENTULA; DICKEY, 1998; HELSEL; HIRSCH, 2002).

The simplest form of a regression model is represented in eq. 2.3. It states that the true mean ($\mathcal{E}(Y_i)$) of the dependent variable changes at a constant rate as the independent increases or decreases. The problem consists in finding the parameters that minimize $\sum_{i=1}^{n}(\hat{Y}_i - y_i)^2$, where $\hat{Y}_i$ is the estimate of observed y_i, given by eq. 2.4. It can be solved by the set of equations in Table 4, also known as normal equations. The observations y and the errors ϵ_i are assumed to be random, normally and independently distributed (NID) observations from populations of random variables with mean $\mathcal{E}(Y_i)$. The random error assumptions can be formally represented by eq. 2.5.

$$Y_i = \beta_0 + \beta_1 x_i + \epsilon_i \qquad (2.3)$$

Y_i is the ith dependent variable.

β_0 is the intercept.

Table 4 – Equations for OLS method

Equation	Name
$\bar{x} = \sum_{i=1}^{n} \frac{x_i}{n}$	mean x
$\bar{y} = \sum_{i=1}^{n} \frac{y_i}{n}$	mean y
$SS_y = \sum_{i=1}^{n} (y_i - \bar{y})^2$	sum of squares y
$SS_x = \sum_{i=1}^{n} (x_i - \bar{x})^2$	sum of squares x
$SS_{xy} = \sum_{i=1}^{n} (x_i - \bar{x})(y_i - \bar{y})$	sum of xy cross products
$\hat{\beta}_1 = \frac{SS_{xy}}{SS_x}$	the estimate of β_1 (slope)
$\hat{\beta}_0 = \bar{y} - \hat{\beta}_1 \bar{x}$	the estimate of β_0 (intercept)
$\hat{Y}_i = \hat{\beta}_0 + \hat{\beta}_1 x_i$	the estimate of y given x_i
$e_i = y_i - \hat{y}_i$	the estimated residual for observation i
$SSE = \sum_{i=1}^{n} e_i^2$	error sum of squares
$s^2 = \sum_{i=1}^{n} e_i^2 / (n-2)$	the estimate of σ^2, also called the mean square error (MSE)
$SE(\beta_1) = s / \sqrt{SS_x}$	standard error of β_1
$SE(\beta_0) = s\sqrt{\frac{1}{n} + \frac{\bar{x}^2}{SS_x}}$	standard error of β_0
$r = \beta_1 \sqrt{SS_x / SS_y}$	the correlation coefficient
$R^2 = r^2$	coefficient of determination

Adapted from Helsel e Hirsch (2002)

β_1 is the slope of the line.

x_i is the ith independent variable.

ϵ_i is the deviation of y_i from the true mean $\mathcal{E}(Y_i)$.

$$\hat{Y}_i = \hat{\beta}_0 + \hat{\beta}_1 x_i \tag{2.4}$$

$\hat{Y}_i$ is the ith estimated dependent variable.

$\hat{\beta}_0$ is the estimated intercept.

$\hat{\beta}_1$ is the estimated slope of the line.

x_i is the ith independent variable.

$$\epsilon_i \sim NID(0, \sigma^2) \tag{2.5}$$

Different applications of the OLS must be compliant to a set of assumptions as shown in Table 5. For all applications it is assumed that y is linearly related to x and that the data used to fit the model is representative of the data of interest. These are the only assumptions if the model is used only to predict y given x. The quality of fit can be evaluated by the correlation coefficient r and by the determination coefficient R_2, which, in the case of just one independent variable, is simply the square of r (see Table 4). The regression line, as a conditional mean, is sensitive to the presence of outliers in much the same way as a sample mean is sensitive to outliers (RAWLINGS; PENTULA; DICKEY, 1998; HELSEL; HIRSCH, 2002).

For data with many outliers, alternative methods as the Kendall-Theil Robust Line (KTRL) can be applied. These methods avoid the inflation of the standard error of the estimates. The main difference from OLS regression, is that the calculation of the KTRL intercept and slope is not based on the mean of response and explanatory variables, instead, it is based on the median of x and y and of the slopes that can be calculated among all x, y pairs of data. The KTRL is defined as eq. 2.6, and the intercept and slope of the KTRL can be calculated by Eqs. 2.7 and 2.8, respectively. This method is efficient in the presence of outliers and non-normal residuals (HELSEL; HIRSCH, 2002).

$$\hat{Y} = \hat{b_0} + \hat{b_1}x \tag{2.6}$$

$$\hat{b_0} = y_{med} - \hat{b_1}x_{med} \tag{2.7}$$

$y_{med} =$ the median of y

$m_{med} =$ the median of x

$$\hat{b_1} = median\frac{y_j - y_i}{x_j - x_i} \tag{2.8}$$

For all $i < j$ and $i = 1, 2, \ldots, (n-1)$ $j = 2, 3, \ldots, n$.

When the relation between response and explanatory variable does not change at a constant rate, other types of model should be investigated. An option is the polynomial model (Eq. 2.9), which is an extension of the straight-line model. The simplest extension of the straight-line model involving one independent variable is the second-order polynomial (quadratic) model (Eq. 2.10). It should be noted that the polynomial model is a special case of the multiple regression model where $x_1 = x$ and $x_2 = x^2$, hence the estimation method for multiple regression (OLS) is valid. The normal equations can be solved from writing them in matrix notation.

In the context of environmental sciences this technique had to evolve for taking into account characteristics as seasonality, trends, non-normality of the residuals among

Table 5 – Assumptions necessary for the purposes to which OLS is put.

Assumptions	Predict y given x	Predict y and a variance for the prediction	Obtain best linear unbiased estimator for y	Test hypothesis, estimate confidence or prediction intervals
(1) Model form is correct: y is linearly related to x	X	X	X	X
(2) Data used to fit the model are representative of the data of interest	X	X	X	X
(3) Variance of the residuals is constant (is homoscedastic). It does not depend on x or on anything else (e.g. time).		X	X	X
(4) The residuals are independent			X	X
(5) The residuals are normally distributed				X

Adapted from Helsel e Hirsch (2002)

others. Helsel e Hirsch (2002) present diverse alternative regression methods for situations where the assumptions of constant variance and normality of residuals required by OLS regression are not satisfied, and transformations to remedy this are either not possible, or not desirable. Some examples are the Line of Organic Correlation, Least Normal Squares, Weighted Least Squares, Iteratively Weighted Least Squares and Locally Weighted Scatterplot Smoothing (LOWESS).

Haggard et al. (2003) applied simple regression to estimate the annual loads of total phosphorous (TP) at the Illinois river in the U.S. A comparison between the simple linear regression and a seasonal approach was performed and among diverse subsets of a TP dataset. The results from the seasonal model and subsets were compared to the results from the complete dataset where the annual loads were calculated directly. It was concluded that the errors were greater for the seasonal model if the frequencies intervals were greater than semi-monthly (15 days), and that for a 19-months monitoring period, 28 water quality samples is the minimum number needed to adequately predict annual TP loads using regression models. Hirsch, Moyer e Archfield (2010) presented a new approach called Weighted Regression on Time, Discharge, and Season (WRTDS). The approach is formulated to allow for maximum flexibility in representations of the long-term trend, seasonal components, and discharge-related components of the behavior of

the water quality variable of interest. It is suitable when: (1) the number of observations is in excess of 200; (2) the period of sample collection is at least 20 years; (3) there exists a complete record of daily discharge values for the site over the entire period being analyzed; (4) all sample analyses are above the laboratory limit of detection (no "less than values"); (5) the sample is representative of the entire cross-section of the river, such that multiplying the measured concentration times discharge results in an unbiased estimate of flux; and (6) the river at the sampling point is not so "flashy" so that the daily discharge can be considerably different from the daily average. The traditional regression methods assume that: (1) the flow *vs.* concentration relation remains constant in time; (2) seasonal patterns repeat year after year, and the magnitude and timing of peaks and valleys remains constant and; (3) the trends are assumed to follow a specific functional form such as linear or quadratic.

$$\mathcal{E}(Y_i) = \beta_0 + \beta_1 x_i + \beta_2 x_i^2 + \beta_3 x_i^3 + \cdots + \beta_p x_i^p \tag{2.9}$$

$$\mathcal{E}(Y_i) = \beta_0 + \beta_1 x_i + \beta_2 x_i^2 \tag{2.10}$$

2.5.2 Stochastic processes

Stochastic modeling is an alternative to overcome some of the limitations arising from traditional deterministic approaches. A deterministic model can be defined as the one in which an input gives a unique output. The outputs of a deterministic model are subject to the assumptions for applying the model (e.g., boundary conditions, representation of physical, chemical and biological process, and representativeness of the inputs). Each assumption is a source of uncertainty for the outputs. In environmental sciences, the deterministic approaches may easily lead to wrong conclusions since most of the natural phenomena are influenced by many factors that are not taken into account in the models. The lack of knowledge and resulting uncertainties often limit the use of deterministic approaches (ROSSI et al., 2005). The stochastic approaches come from the consideration that the variables, parameters, structure and outputs (or at least one these items) of the models should be expressed in terms of probabilities. Some of these methods are based only on the characteristics of the data avoiding the uncertainty from mathematical representation of the physical, chemical and biological processes (MORETTIN; TOLOI, 2006; YAN; ZOU, 2013; DETZEL, 2015).

The traditional stochastic theory for time series was popularized by Box, Jenkins e Reinsel (2008). The definition of a stochastic process is as follows. Let T be an arbitrary set. A stochastic process is a family $Z = Z(t), t \in T$ supposedly defined in the same space of probabilities (Ω) such that for each $t \in T$, $Z(t)$ is a random variable. Since for $t \in T$, $Z(t)$ is a random variable defined on Ω, in fact, $Z(t)$ is a two-argument function, $Z(t, \omega)$,

$t \in T$, $\omega \in \Omega$ (MORETTIN; TOLOI, 2006). The stochastic process can be divided in classes:

(a) stationary or non-stationary processes, according to the independence (or not) with respect to the origin of the times;

(b) normal (Gaussian) or non-normal processes, according the pdf's that characterizes the processes;

(c) Markovian or non-Markovian processes, according to the independence of the values of the process, at a instant of time, in relation to the values at previous times.

According to Morettin e Toloi (2006) the process is stationary if the properties of $Z(t)$ are equal to the ones for $Z(t+\tau)$. It can be considered strictly or weakly stationary. The first occurs when all the finite-dimensional distributions remain the same under translations of time (Eq. 2.11). Hence, the mean and variance are constants for every $t \in T$.

$$F(z_1, \ldots, z_n; t_1 + \tau, \ldots, t_n + \tau) = F(z_1, \ldots, z_n; t_1, \ldots, t_n) \tag{2.11}$$

For any $t_1, \ldots, t_n, \tau \in T$.

The process is weakly stationary when:

(1) $E\{Z(t)\} = \mu(t) = \mu$;

(2) $E\{Z^2(t)\} < \infty$ for all $t \in T$;

(3) $Cov\{Z(t_1), Z(t_2)\}$ is a function of $|t_1 - t_2|$.

There are diverse types of stationarity, but the models for time series analysis presented by Box, Jenkins e Reinsel (2008) and Morettin e Toloi (2006) are designed for homogeneous non-stationary process, i.e., processes in which the stage or slope change over time. Such processes can become stationary by successive differences (MORETTIN; TOLOI, 2006). According to Koutsoyiannis (2006), it is typically performed by the non-stationary approach, which considers the hydrological processes as being composed of three parts:

1. A deterministic part which is periodic and results from natural physical periodicities (e.g., seasonality).

2. A deterministic part which is aperiodic. This is commonly called 'trend' and may be considered to be due to a gradual temporal change in the physical parameters of the processes controlling weather.

3. A stationary random part.

The modeling approach followed in hydrological practices often includes the "de-seasonalization" and "detrending" of the time series prior to modeling, i.e., the removing of seasonality and trends (deterministic components of variability). After the removing, the model parameters are determined from the remaining random part (KOUTSOYIAN-NIS, 2006). The time series of flows can be understood as one of the possible realization (i.e., a sample) of a stochastic process. Traditionally, the variability patterns identified in the sample are assumed to be in the population and then are removed or considered previously to the stochastic modeling. However, there are many controversies regarding this approach, since the patterns are identified in a deterministic framework and assigned to a stochastic process (YUE; PILON, 2003; BEVEN; BINLEY, 2014; DETZEL, 2015). In other words, if a 10-years flow time series shows an downward trend, it does not necessarily mean that it will continue in the next decades because maybe it is just an effect of the sample and not a real trend in the stochastic process. It also must observed that there is a physical limit to upward and downward trends in flows and concentrations. Furthermore, the interaction between deterministic trends and autoregressive models was investigated by Yue e Pilon (2003) and it was concluded that the differencing proposed in literature can remove the trend from the time series but it can also seriously damages the existing true stochastic process. In contrast to differencing, detrending (directly remove the deterministic trend) can eliminate a deterministic trend without distorting the existing stochastic process.

The models are classified in two categories:

- parametric models, for which the number of parameters is finite, and the analysis is performed in the domain of time;

- non-parametric models, for which the number of parameters is infinite, and the analysis is performed in the domain of frequencies.

Some parametric models are the error models (regression models), the auto-regressive and moving average models (ARMA), the integrated and moving average auto-regressive models (ARIMA) , the long memory models (ARFIMA), structural and non-linear models. The most used non-parametric model is the autocovariance function and its Fourier transform. Of particular interest are the ARIMA models (FARUK, 2010; YAN; ZOU, 2013; DETZEL, 2015; LOUCKS; BEEK, 2017). The ARIMA(p, d, q) are composed by three parts: the auto-regressive component AR(p) of order p, the integration factor I(d) with differentiation degree d, and moving average component MA(q) of order q. These models has been applied in many hydrological studies since the correlation structure of hydrological time series can be reproduced (DETZEL, 2015).

The ARIMA model can be represented as Eq. 2.12, where: t_y and e_t are the actual value and random error at time period t; $\phi(B) = 1 - \phi_1 B - \phi_2 B^2 - \cdots - \phi_p B^p$ and $\theta(B) =$

$1-\theta_1 B-\theta_2 B^2-\cdots-\theta_p B^p$ are autoregressive operator of order p and moving average operator of order q, respectively; $\phi_1, \phi_2, \ldots, \phi_p$ and $\theta_1, \theta_2, \ldots, \theta_p$ are unknown coefficients estimated from sample data; B and $\nabla = 1-B$ are backward shift operators; e_t is the noise component of the stochastic model and assumed to be identically distributed with a mean of zero and a constant variance. The ARIMA modeling includes model identification, parameter estimation and goodness-of-fit. The Akaike Information Criterion (AIC) and Bayesian Information Criterion (BIC) are used to select the best model. The smaller the AIC and BIC, the better the model. The final selected model can then be used for prediction purposes (MORETTIN; TOLOI, 2006; BOX; JENKINS; REINSEL, 2008; YAN; ZOU, 2013; DETZEL, 2015). According to Yan e Zou (2013), the most important disadvantage for the ARIMA modeling approach is that the time series under study are generated from linear process and therefore, no nonlinear patterns can be captured by the ARIMA model. They may be inappropriate if the underlying mechanism is nonlinear. In fact, real world systems are often nonlinear.

$$\phi(B)\nabla^d y_t = \theta(B)e_t \tag{2.12}$$

In stochastic water resources models it is often assumed that a stochastic process $X(t)$, where t is time, is a Markov process. A first-order Markov process has the property that the dependence of future values of the process on past values depends only on the current value. These is called the state of the process. A special kind of Markov process is called a Markov chain, in which the state $X(t)$ can take on only discrete values, e.g., the daily, monthly or annual streamflows (LOUCKS; BEEK, 2017). According to Loucks e Beek (2017), a common and reasonable assumption is that the annual flows are the result of a first-order Markov process. The Markov model for annual flows is a simple autoregressive model represented by Eq. 2.13, where Q_{y+1} is the next year flow, μ is the mean annual flow, ρ is the first order correlation coefficient, Q_y is the current annual flow, and V_y is the standard normal random error with mean = 0 and variance = 1. It is also assumed that the annual flows are normally distributed. Streamflows will rarely follows a normal distribution since flows are zero-bounded. For these cases transformations of the original variable Q_y can be applied. Common choices for the distribution of streamflows are the two-parameter and three-parameter lognormal distributions or a gamma distribution. If Q_y is a lognormally distributed random variable, then it can be expressed as Eq. 2.14, X_y is the normally distributed random variable, and τ is the shift parameter, which is 0 for the two-parameter lognormal.

$$Q_{y+1} = \mu + \rho(Q_y - \mu) + V_y\sigma\sqrt{1-\rho^2} \tag{2.13}$$

$$Q_y = \tau + \exp(X_y) \tag{2.14}$$

The equation for the transformed variable is represented by Eq. 2.15, where X_{y+1} is the $\mathrm{Ln}(Q_{y+1} - \tau)$, μ is the mean of $X_y = \mathrm{Ln}(Q_y - \tau)$, ρ_x is the first order correlation

coefficient of the log-transformed time series, and σ_x is the standard deviation of the log-transformed time series.

$$X_{y+1} = \mu_x + \rho_x(X_y - \mu_x) + V_y\sigma_x\sqrt{1-\rho_x^2} \qquad (2.15)$$

There are many different stochastic approaches that have been used over the last 30 years, mostly in hydrological studies, e.g., studying operation of reservoirs, drought management, alternative input into water quality studies, or design of new hydraulic structures . The main goal is to provide input data variations that are statistically likely to occur, and also more challenging to manage than the original record terms of either the magnitude of individual events or their duration. After almost 50 years of research in this field, a stochastic model that is easy to understand, use, and is widely accepted, does not exist (ILICH, 2014). Two major groups can be identified: (i) one based on the expression of model parameters and structure as random variables, and; (ii) other based on the variability characteristics of the data, known as "time series analysis'".

Some examples of group (i) are Beven e Binley (1992), Han, Kim e Bae (2001) and Rossi et al. (2005). In 1992, Beven e Binley (1992) described the Generalized Likelihood Uncertainty Estimation (GLUE) procedure, which is a method for calibration and uncertainty estimation of distributed models. The procedure is based on the premise that there are many different models and sets of model parameters and structures equally likely to be simulators of the system. Initially, ranges and a probability density function for the parameters variation, and a set of appropriate models and model structures are defined. Each model is run many times with different parameters values, randomly chosen from the specified ranges, and a likelihood is assigned to the model depending on the quality of the performance. Han, Kim e Bae (2001) used First-Order Second-Moment and Mean-Value First-Order Second-Moment to perform stochastic water quality modeling with QUAL2E model, and compare the results with the traditional approach with Monte Carlo simulations in the parameters of the model. Rossi et al. (2005) proposed a stochastic approach to simulate the amount of discharged total suspended solids (TSS) in rivers by combined sewer overflows and storm discharges. The idea was to estimate concentrations and loads of TSS by using statistical information derived from measured data (flow rates and total volumes for a given rain event, and total mass of TSS that will be mobilized during the event). The uncertainties of the model variables were taken into account by expressing them as pdf's and performing Monte Carlo Simulations.

The time series analysis are typically performed for prediction purposes and/or generation of synthetic time series. It has been applied since more than 50 years for hydrological studies (ILICH, 2014), and more recently for water quality data. In 1968, Boughton e McKerchar (1968) applied the Thomas-Fiering model for the generation of synthetic streamflow records in some New Zealand catchments and presented a discussion on the possible errors that can occur when short time series are used to estimate monthly

means, serial correlation and other statistics. Rodriguez-Iturbe, Dawdy e Garcia (1971) studied the adequacy of Markovian models with cyclic components for stochastic stream-flow simulation, and the results showed that seasonal components should always be considered and care should should be taken when using logarithmic transformations. Valipour, Banihabib e Behbahani (2012) used monthly discharges from 1960 to 2007 to forecast the inflow of Dez dam reservoir by using Auto Regressive Moving Average (ARMA) and Auto Regressive Integrated Moving Average (ARIMA) models while increasing the number of parameters in order to increase the forecast accuracy to four parameters and comparing them with the static and dynamic artificial neural networks. Pender e Patidar (2015), in order to avoid uncertainties from calibration, and deficiencies in model capability to capture extreme flow events in simulated time series, proposed a direct method for estimating daily flows as an alternative to the traditional indirect approach of stochastically model the daily rainfall and the use as inputs in rainfall runoff models (ALODAH; SEIDOU, 2018). The method involves combinations of a hidden Markov model with the generalized extreme value and generalized Pareto distributions. It was concluded that the method appropriately captures extreme events and is generically applicable across a range of hydrological regimes.

The atypical and recent research on stochastic water quality modeling has been performed by hydrid models combining an ARIMA with artificial neural networks (ANN's). This practice was adopted to overcome the problem of non-linearities of environmental time series. Kurunç, Yürekli e Çevik (2005) used a 13-year (1984–1996) monthly time series records to evaluate the forecasting performance of two modeling approaches, ARIMA and Thomas–Fiering, for selected water quality constituents and streamflow. The results indicated that the Thomas-Fiering model was better for that case study. Faruk (2010) applied a hybrid approach, which was a seasonal ARIMA model combined with a neural network model for time series prediction using 108-month observations of water quality data, including water temperature, boron and dissolved oxygen, during 1996–2004 at Büyük Menderes river, Turkey. The results showed that the hybrid approach was robust, since it was capable of capturing the nonlinear nature of the time series. Yan e Zou (2013) developed a hybrid model (ARIMA–ANN's) to predict water quality time series data and assess its performance relative to ARIMA and ANNs models. All the studies were performed with regular-frequency water quality data.

2.6 Synthesis

The knowledge about uncertainties in water quantity and quality is still incipient. In recent research, an effort towards the definition and understanding of the concept and types of uncertainty can be observed. There are few studies in which the uncertainties in analysis of water resources data and management are addressed in a integrated way, combining and quantifying/qualifying the diverse types. In general, the assessment of individual components is observed, and the uncertainty is usually expressed as percentages instead of by pdf's. It is common sense (GUM 2008 (JCGM/WG1, 2008a)) that uncertainty is a random variable correlated in space and time which, when possible, should be expressed as pdf's. The main classes of uncertainty are epistemic, deriving from lack of knowledge, ontological, from natural variability of the systems, and ambiguity, from the different ways of framing the problems in the social context of decision-making processes. Many of these uncertainties cannot be quantified or handled with statistical approach, e.g., those related to representativeness. Traditionally, the water quality monitoring practices are performed with low frequencies at few sites that should represent the non-monitored periods and locations. Since there is no data to show which is the true state and variability characteristics of the water resources, the uncertainties related to representativeness are unknown and can be called Knightian uncertainties. Furthermore, the current context of climate change increases the representativeness-related uncertainties, the longer the planning period.

The confidence in the ultimate information to the WRM starts with representative measurements, which can be partially achieved by well-developed monitoring strategies. However, the evaluation of representativeness will always be highly subjective and based on expert judgment. Representativeness can also be decreased by imprecision of sensors, techniques, methods and technologies used for measuring. The literature available estimates of measurement uncertainties may reach 100%, or even higher magnitudes. The complexity of the water quality measurement process (i.e, streamflow measurement, sampling, storage/preservation, laboratory analysis, large areas, many sites and times, etc.) imposes considerable difficulties to estimation and expression of uncertainty as pdf's, or even in percentages. The typical approach in nowadays-research is the use of literature estimates. This practice is challenging in the context of time series since it involves assumptions about time and space autocorrelation and other variability characteristics, which is not available in literature.

The results from time series analysis will also have influence from the methods and variability patterns in data, giving rise to more uncertainties in the final information for the planning. In order to avoid high levels of this type of uncertainty, the compliance with the basic assumptions (RHIS) for application of statistical methods should be verified. The basic assumptions will not be met when trends, cycles, shifts or many outliers are

present in the time series. Unlike hydrological studies, it is rarely verified in water quality times series. It seems to be an important issue for the WRM since the time series and their statistical properties are the inputs for water quality and hydrological models. However, the water quality statistical analysis and modeling are traditionally made by deterministic approaches, without considerations about the presence of trends, cycles, and/or shifts. In hydrological studies, stochastic approaches are usually applied. The presence of trends, cycles and shifts are identified and some treatment or removing technique is used.

Stochastic approaches are chosen in order to deal with ontological uncertainties. Many or maybe all natural processes have stochastic nature. The accumulated rainfall in a year is not the same every year, the annual BOD loads vary from year to year, the inflows in water reservoirs will also be different from year to year, as many other processes derived from natural phenomena. However, the application of stochastic approaches requires statistical information and assumptions about the time series, e.g., mean, variance, covariances, correlation coefficients and RHIS. These information are hardly available for water quality time series, due to short periods, irregular frequencies with large gaps, and presence of many outliers. The few stochastic water quality modeling studies were performed with regular data. Hybrid models combining ARIMA and ANN'S have been used, since water quality time series usually present non-linear variability patterns, which cannot be dealt solely by ARIMA or ANN's models.

Currently, there seems to have no available research on integrated uncertainty analysis in water quality and hydrological literature. Most of the researches are focused on identifying, typifying and quantifying the diverse individual types of uncertainties. The questions that arise are: how these uncertainties should be expressed in the final information for WRM, given that part of the uncertainty is subjective and cannot be quantified?, and which uncertainties are more critical, i.e., strategy, measurement, statistical analysis, or modeling uncertainties? Table 6 shows some of the main advances in the current context of uncertainty concerns.

Table 6 – Advances in uncertainty analysis of water resources time series

Author	Description	Contribution
Beven e Binley (1992)	The GLUE procedure. A methodology for calibration and uncertainty estimation of distributed models based on generalized likelihood measures.	Uncertain hydrological information with uncertainties of measurements and models structures taken into account by likelihood weights assigned to a given model structure/set of parameters on the basis of evidence.

Table 6 – continued

Author	Description	Contribution
Han, Kim e Bae (2001)	Development of a QUAL2E-Reliability Analysis model (QUAL2E-RA). The uncertainties of this deterministic model were estimated by sensitivity analysis, first-order error analysis and Monte Carlo Simulations. The three approaches were based on the statistics of input data. No trends, cycles and measurement uncertainties were considered.	QUAL2E-RA - A method for stochastic analysis of water quality data with less computational effort than deterministic modeling with Monte Carlo Simulations.
Kurunç, Yürekli e Çevik (2005)	Comparison of two stochastic approaches, ARIMA and Thomas Fiering (T-F) models. 13-year period of monthly data was used.	T-F model slightly better.
Harmel et al. (2006)	Estimation of combined uncertainty for discharges, concentrations and loads of nutrients and suspended solids, according scenarios of quality in monitoring practices.	Application of GUM uncertainty framework to combine uncertainties of streamflow measurement, sampling, storage/preservation and laboratory analysis. Percentage symmetric estimates of uncertainties, not assigned to probability distributions, based in literature review.
Refsgaard et al. (2005), Brown e Heuvelink (2007)	Researches in representative river basins for designing, building and populating a database containing data and associated uncertainties, and development of a software tool (DUE) to use the database to perform uncertainty analysis of data from other basins.	Data Uncertainty Engine (DUE) - Expression and propagation of uncertainties with probability distributions, considering spatial and temporal correlations, and generation of synthetic time series from uncertainty intervals of the measurements.

Table 6 – continued

Author	Description	Contribution
Harmel et al. (2009)	Development of a software tool for estimation of uncertainty in individual measurements. It combines the uncertainties in streamflow measurement, sampling, storage/preservation, laboratory analysis and data management and processing, by application of the GUM uncertainty framework. The individual uncertainty estimates are based in Harmel et al. (2006).	Data Uncertainty Estimation Tool for Hydrology and Water Quality (DUET-H/WQ). It yields percentage symmetric estimates of uncertainties, not assigned to probability distribution.
Hirsch, Moyer e Archfield (2010)	A new approach to increase the amount of information that can be extracted from typical water quality datasets, and provide consistent estimates of the actual history of concentrations and fluxes. It consists of a weighted regression between discharge and concentrations, formulated to allow for maximum flexibility in representations of trends, seasonal components and discharge-related components. The method does not provide estimates of the uncertainty related to the procedure.	Weighted Regression on Time, Discharge and Season (WRTDS) - An approach to reduce the variance in the dataset, thus improving the power of hypothesis tests, the accuracy of estimated trend slopes, and the accuracy of flux estimates.
Yan e Zou (2013)	Evaluation of the performance of a hybrid ARIMA and Artificial Neural Network model (ARIMA-ANNs). The ANNs model were applied in the residuals of the ARIMA model to deal with the nonlinear patterns and reduce potential errors	The hybrid model has greater accuracy than ARIMA and ANNs individually applied.

Table 6 – continued

Author	Description	Contribution
McMillan et al. (2017)	Discuss the need for practical uncertainty assessment tools that generate multiple flow series realizations rather than simple error bounds	Quantifications of economic losses in diverse sectors due to uncertainty in flow measurements
Teng et al. (2017)	A review of methods, recent advances and uncertainty analysis in flood inundation modeling	Identification of the current challenges, e.g., quantification of measurement uncertainties, increasing the use of stochastic approaches, ease the constraint of computational demand
Warmink et al. (2017)	Investigation of the diverse type of uncertainty in the water resources management	identification of three challenges in current river management: balancing social and technical uncertainties, being conservative and avoiding to end up a lock-in situation. A step-wise strategy and concrete actions for policymakers
Alodah e Seidou (2018)	Evaluates the usefulness of weather generators/stochastic models by assessing how the statistical properties of simulated precipitation, temperatures, and streamflow deviate from those of observations	the choice of a particular weather generator/stochastic model for water resources assessment can have an impact on key statistics of the simulated time series, hence on the estimated level of risk and the selection of management strategies
Jung, Niemann e Greimann (2018)	Model input errors represented by Gaussian distributions, with the means and standard deviations as uncertain parameters that are estimated within the Bayesian framework	prediction ranges are substantially affected by input errors. Uncertainty is better represented when input errors are considered

It can be observed from the most recent researches in Table 6 that technical uncer-

tainties seem to have considerable impacts in terms of costs for the WRM, since it affects the statistical characteristics from time series used in the planning of water resources. Furthermore, these uncertainties should be analyzed in the social context of the WRM where other types of uncertainties arise. Currently, there is no established management strategy to deal with these uncertainties (individually or jointly). However, balancing social and technical uncertainties, being conservative and avoiding to end up a lock-in situation has been recommended.

3 Methods

"The most effective way of living is like a warrior. A warrior may worry and think before making a decision, but once he has taken it, he goes on his way, free of worries or thoughts; there will be a thousand other decisions still waiting for you."

Don Juan (Carlos Castaneda)

3.1 Overview

The method follows four steps shown in Fig. 1: (i) uncertainty assessment and generation of synthetic time series (STS) from the uncertainty intervals; (ii) statistical analysis; (iii) regression analysis between flows and concentrations; (iv) stochastic water quality modeling from daily flows. It was applied in time series of flows (Q), concentrations (C) and loads (W) from monitoring stations in the Upper Iguassu Watershed in southern Brazil.

The step (i) (section 3.4) relates to the definition of uncertainty scenarios based on the uncertainties estimated by Harmel et al. (2006). The uncertainty of each value was used to generate STS (section 3.5) of Q, C and W by the Monte Carlo Method (MCM). Step (ii) (section 3.6) relates to the significance assessment of major fluctuations (e.g., trends, cycles and shifts) by the application of randomness, homogeneity, independence and stationarity (RHIS) hypothesis tests, analysis of the descriptive statistics and comparison between the photos (irregular frequency data) and movies (regular-frequency data). The step (ii) were firstly applied on a typical water quality dataset, i.e., irregular frequency data (photos), short period with few observations and outliers presence, and then on the movies generated in the stochastic water quality modeling. This first part of the method (steps (i) and (ii) on the photos) was designed to provide information on how uncertain a statistical result may be due to measurement uncertainties and non-compliance with the basic assumptions for application of statistical methods (RHIS).

The second part starts with step (iii) (section 3.7), which relates to the conception of a regression model (RM) between flows and concentrations. The simple linear regression (SLR) method was used to estimate the parameters of the model. A probability density function (pdf) was fitted to the errors and used to the expression of the RM uncertainty ("e" in the illustrative RM in Fig. 1). Regression analysis is a traditional technique for estimation of missing data. There are many methods for data analysis that require regular frequency data, e.g., the autoregressive ARIMA models presented by Box, Jenkins e Reinsel (2008) which are extensively used for hydrological modeling. Many

statistical analyses are performed in annual basis but typically, the annual statistic is estimated from few irregularly distributed data along the years including months without any measurement. Complex and more powerful techniques than the simple linear regression are available in literature, e.g., the Cascade Correlation Artificial Neural Networks (DIAMANTOPOULOU; ANTONOPOULOS; PAPAMICHAIL, 2007) and the Weighted Regression on Time, Discharge and Season (HIRSCH; MOYER; ARCHFIELD, 2010).

In this procedure the uncertainty of the estimated concentration is partially expressed by the error of the RM. The total uncertainty cannot be represented only by the error of the model, since there are other sources of uncertainty that arises from the assumptions of the method. The SLR assumes that: (a) the relation is constant in time; (b) no significant autocorrelation, trends, cycles and/or shifts are present and; (c) the distribution of the errors is constant in time and along the measurement scales of the flows and concentrations. Hence, the concentrations estimated from the flows should be random or not, depending on the variability patterns of the flows. For example, considering a case in which there are a large period with flow rates and just a few concentrations, just enough to establish a relation by regression, if there is an upward trend in the flows, it is likely to be present in the estimated concentrations. However, it may not appear in concentrations due to the randomness introduced by the error term of the RM. The use of a water quality time series generated in this way would be highly uncertain if the real water quality was significantly influenced by management actions, seasonality, persistence, atypical phenomena (e.g., El Niño), climate and land use change, and by the flows. The more intense these external influences, the more uncertain the statistics from these time series. This uncertainty cannot be quantified, only qualified, because the truth is unknown. If the external influences are low, it is possible that there is a gain in representativeness, since the flows carry information about the concentrations.

The step (iv) (section 3.8) relates to the stochastic modeling of concentrations from the stochastic modeling of the flows by applying the regression model on the synthetic flows. An autoregressive model, Markovian model MAR(1), was used for the generation of synthetic flows. This model is often applied in hydrological studies after the removing of trends and seasoanlity. In this study, the variability patterns were not removed or treated prior to the modeling.

Disregard for non-stationarity, non-homogeneity and non-randomness of the original flows is equivalent to considering the variability random, except for daily autocorrelation. In the context of STS, the practical consequence is a wider standard deviation than if for example seasonality or trends were removed, and a displaced mean. The first part of the method ((i) and (ii)) is intended to provide the basis for the discussion of this type of uncertainty, which relates to the detection of trends, cycles and/or shifts from uncertain measurements prior to the application of statistical methods. Given all the un-

certainties involved in water quality and flow measurements, and in the identification of variability patterns, the main question is: what can increase the risk for the planning of water resources more, to consider or to not consider these variability patterns previously to statistical analysis?

The stochastic modeling of water quality data is much more challenging than for hydrological data due to the typical irregular and short time series. The use of ARIMA models for example, requires at least regular frequency data to calculate the correlations in each lag. If irregular data is used, the correlations lose physical meaning. For example, the first lag correlation would be just the correlation of one observation to the next, but the time between them would not be constant. When this correlation coefficient is used in the ARIMA model, the time runs with regular frequency, thus making it non-sense or at least highly uncertain. The regular time series generated by the RM on the original daily flows can be used to calculate the correlations and fit the ARIMA model. However, in the proposed method the ARIMA model was fitted to the original flows, since the correlations are real values. Synthetic flow time series were generated and for each one the RM model was applied to generate synthetic water quality time series and by multiplication of flows and concentrations, the load time series. This is an alternative approach for the stochastic water quality modeling which inserts different types of uncertainty (measurement, RM, disregard for RHIS and ARIMA model uncertainties).

Finally, step (ii) was applied on the synthetic Q, C and W and the results from the photos and movies compared. It is expected that the results provide the arguments to answer some of the questions related to uncertainties in the statistical/stochastic context of water resources time series. How uncertain the statistic results from stochastic water quality modeling with typical water quality data would be? Is it worst for the concentrations or for the loads? Can it provide consistent information for the planning of water resources? Is there a need for high frequency monitoring?

The proposed method is equivalent to a worst case scenario, since the regression technique and ARIMA model used are the simplest available versions for these objectives. The development of a computational program was required for all the steps since it is a innovative approach and no software is available for this type of analysis. The python programming language was used. The program was entitled TSGENUIN-WQ/H which means *Time Series Generation Under Uncertainty Intervals - for Water quality/Hydrological data.*

3.2 Upper Iguassu watershed

The research was performed on Upper Iguassu Watershed (Fig. 2) in southern Brazil, state of Parana. The watershed is located between latitudes −25.23 and −25.83, and

(i) Uncertainty assessment

Q   C   W

(iii) Regression model

C

Q

C = aQ + b + e

(ii) Statistical analysis

Representativeness

1. Monitoring strategy x spacial/temporal variability
2. RHIS
3. Sensitivity to uncertainties
4. Confidence level (low, mid, high)

(iv) Stochastic modeling

Q   C   W
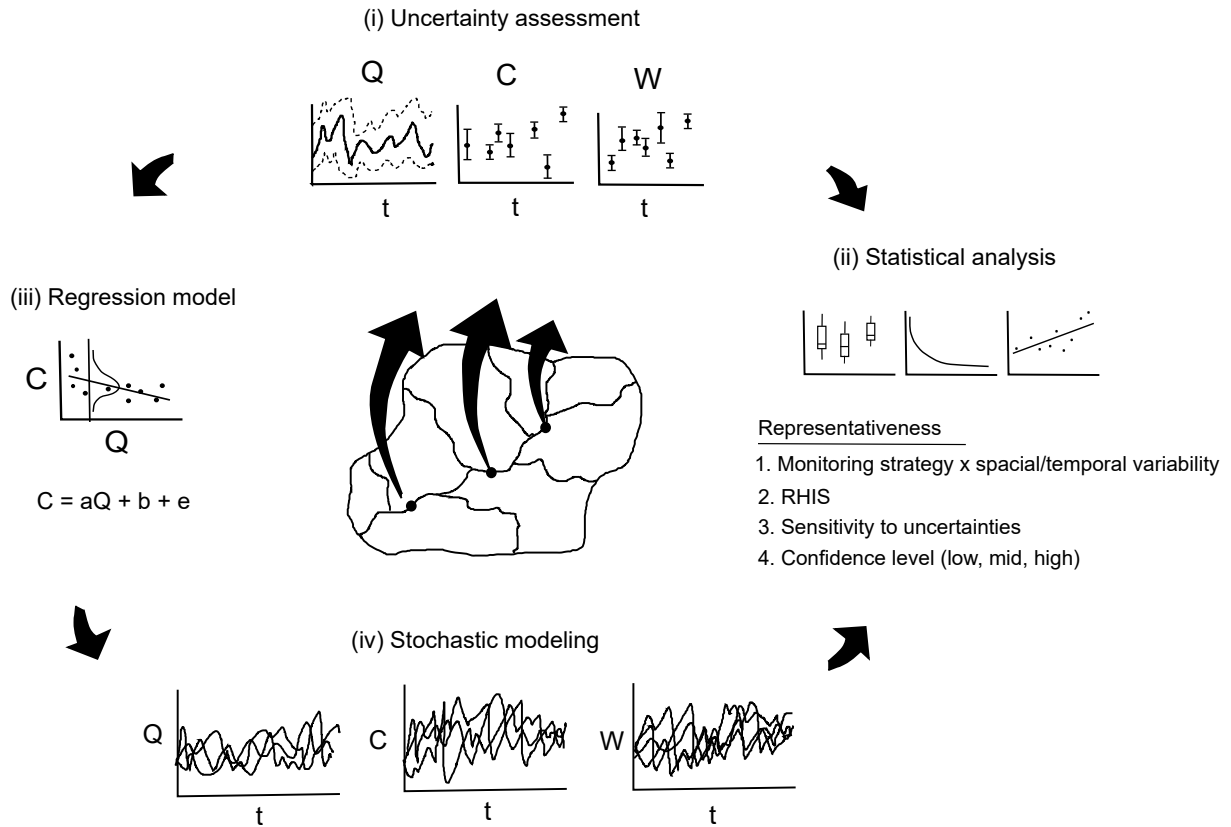
Figure 1 – Scheme of the method

longitudes -49.69 and -49.96. The total area is approximately $3,000\ km^2$ with diverse land and water uses, including intensive agricultural activities (47% of the total area), many industries (about 9000 industries) and six water supply reservoirs (one under construction) (PORRAS et al., 2016). The capital of Paraná state, Curitiba city, is totally inside the watershed area and represents the major urban spot on the map. About 3 million people live in the watershed, and from these, about 2 million are concentrated in Curitiba city. The metropolitan region has low coverage of sewage collection system due to (not only) a disordered, irregular and continuous urban sprawl over many areas around Curitiba, specially over flood plains (KNAPIK; FERNANDES; BASSANESI, 2011; FROEHNER et al., 2011; COELHO et al., 2017). The Iguassu river is highly impacted with pollution from domestic and industrial sewage, not only from waste water treatment plants, but also from the drainage system that reaches the river and tributaries at many points. Pesticides and nutrients are largely used in Brazil agricultural practices making these areas important sources of these elements to the water bodies. Curitiba and its metropolitan region have temperate climate, four well defined seasons, mean temperature of about $14°C$ on winter and $22°C$ on summer, with high variability within a day and along the year. Annual mean precipitation is around $1500\ mm$ well distributed over the year, with more frequent events and slightly higher total precipitation on summer. Two of the hottest summers were registered in 2006 and 2014, with days with maximum temperature of $35°C$. June of 2016 had the lowest mean temperature ($11.9°C$) for this month since 1990. Snow may
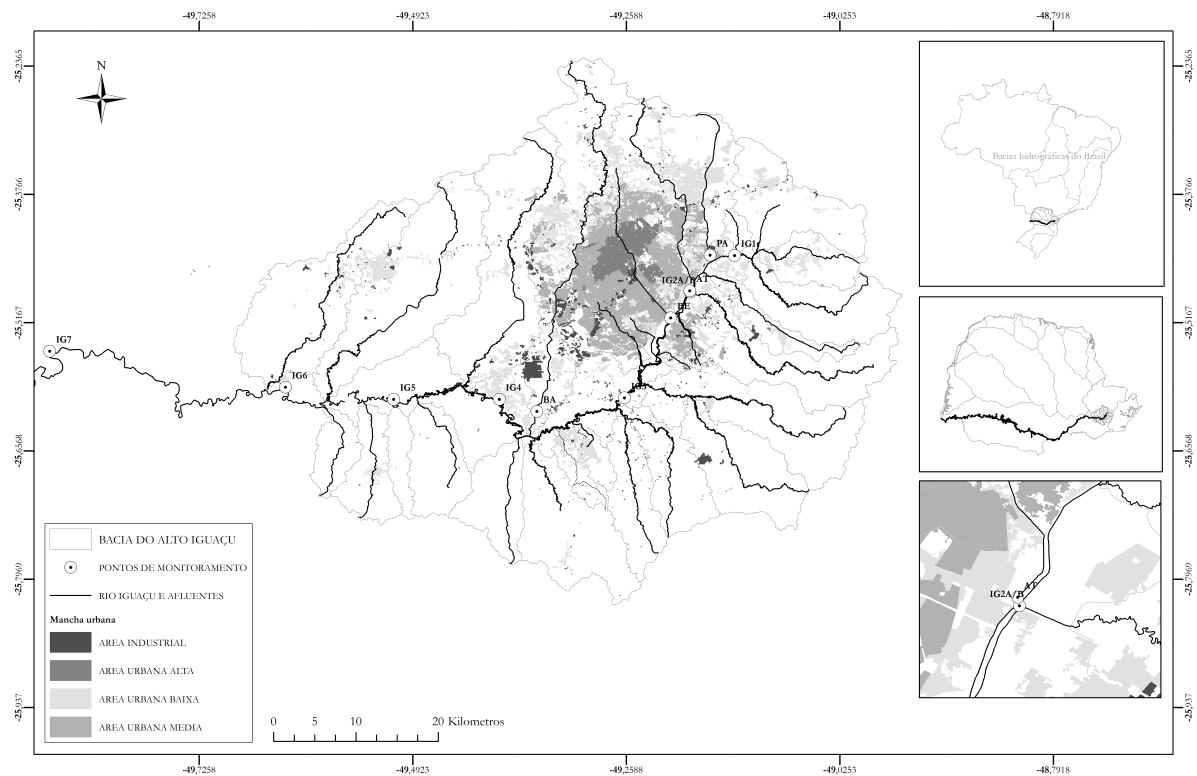
Figure 2 – Monitoring sites in the Upper Iguaçu Watershed

Table 7 – Description of monitoring stations

Station	Code	Latitude	Longitude	Area (km^2)
IG3	65017006	-25.5989	-49.2608	1,283.7
IG4	65019980	-25.6003	-49.3978	2,122.2
IG5	65025000	-25.6003	-49.5133	2,577.8
IG6	65028000	-25.5872	-49.6317	3,048.7
IG7	65035000	-25.5481	-49.8894	3,662.0
IG8	65060000	-25.8758	-50.3897	6,050.0

occur at about each 10 years, with decades without any occurrence. The last event was on July, 2013. The highest monthly accumulated precipitation volume was in January of 1995, of 473.8 mm.

3.3 Monitoring and time series

The Upper Iguassu Watershed has several official monitoring stations responsible for feeding the national system for information on water resources (HIDROWEB) with hydrological and water quality data. Fig. 2 shows the stations IG3–IG8, which has been also monitored by researchers from the Federal University of Paraná (UFPR) since 2005. In HIDROWEB, these stations are identified by codes as presented in Table 7. Both datasets were used. The UFPR dataset has irregular frequency data of water quality and

Table 8 – Water quality variables used in each dataset

Variables	Symbols	UFPR dataset	HIDROWEB dataset
Biochemical Oxygen Demand	BOD	X	X
Dissolved Oxygen	DO	X	X
Dissolved Organic Carbon	DOC	X	
Chemical Oxygen Demand	COD		X
Ammoniacal Nitrogen	NH4	X	X
Total Phosphorous	TP	X	X
Volatile Dissolved Solids	VDS	X	
Conductivity	COND		X

flows from 2005 to 2018. The HIDROWEB dataset has daily flows in diverse periods from 1930 to 2018 and irregular water quality data in the period 1981–2018. The UFPR dataset is part of the HIDROWEB dataset.

Monitoring campaigns are typically performed in business days and hours, i.e, Monday to Friday between 8 am and 6 pm. Sampling has irregular frequency, from bi-weekly to quarterly with large gaps. Water is sampled in the middle of the river cross section from a bridge at most of the stations, preserved in thermal boxes and analyzed within 24–48 hours for most water quality variables. The flows are estimated by rating curves.

The research was performed with a set of water quality variables and flows as shown in Table 8. The selected variables are related to organic matter pollution. Although the research was performed with a set of monitoring sites and water quality variables, the flow and BOD time series from station IG5 were taken as the main case.

UFPR dataset

Fig. 3 presents the flows (Q) concentrations (C), and loads (W) of BOD from station IG5. Fig. 3 shows the higher variability of the Q (m³/s) compared to C (mg/L) and W (ton/d). Although a seasonal pattern can not be identified, major fluctuations can be observed from 2005 to 2017. The significance of a longer cyclic fluctuation and of a downward trend should be tested. The high variability of discharges and the major fluctuations can be better perceived in the evolution of time series boxplot. It shows large fluctuations of the median, and data from 10 to 170 m³/s are not considered as outlier most of the time. The few outliers present are not far out from the maximum non-outlier values.

Concentration time series has lower variability than Q. Major fluctuations can also be observed, with lower concentrations in periods of higher flows (e.g., 2008-2012), with

exception of data prior to 2007. It is an indication that, in this site, the variability of C is, in part, controlled by Q. The major fluctuations do not affect the median, which is stable since the time series had 15 data (prior to 2007). There are 9 outliers (> 30 mg/L), which represent almost 20% of the data, and 4 values > 60 mg/L.

Load time series has lower variability than Q and C. Unless for the higher values, prior to 2007, which are consequence of high values of Q and C, major fluctuations and trends are not evident. As data quantity increases, higher values, prior to 2007, become outliers, and the range of the more typical variations (25th–75th percentile), gets smaller. The time series and boxplot evolution from stations IG3–IG7 can be found in the ap-
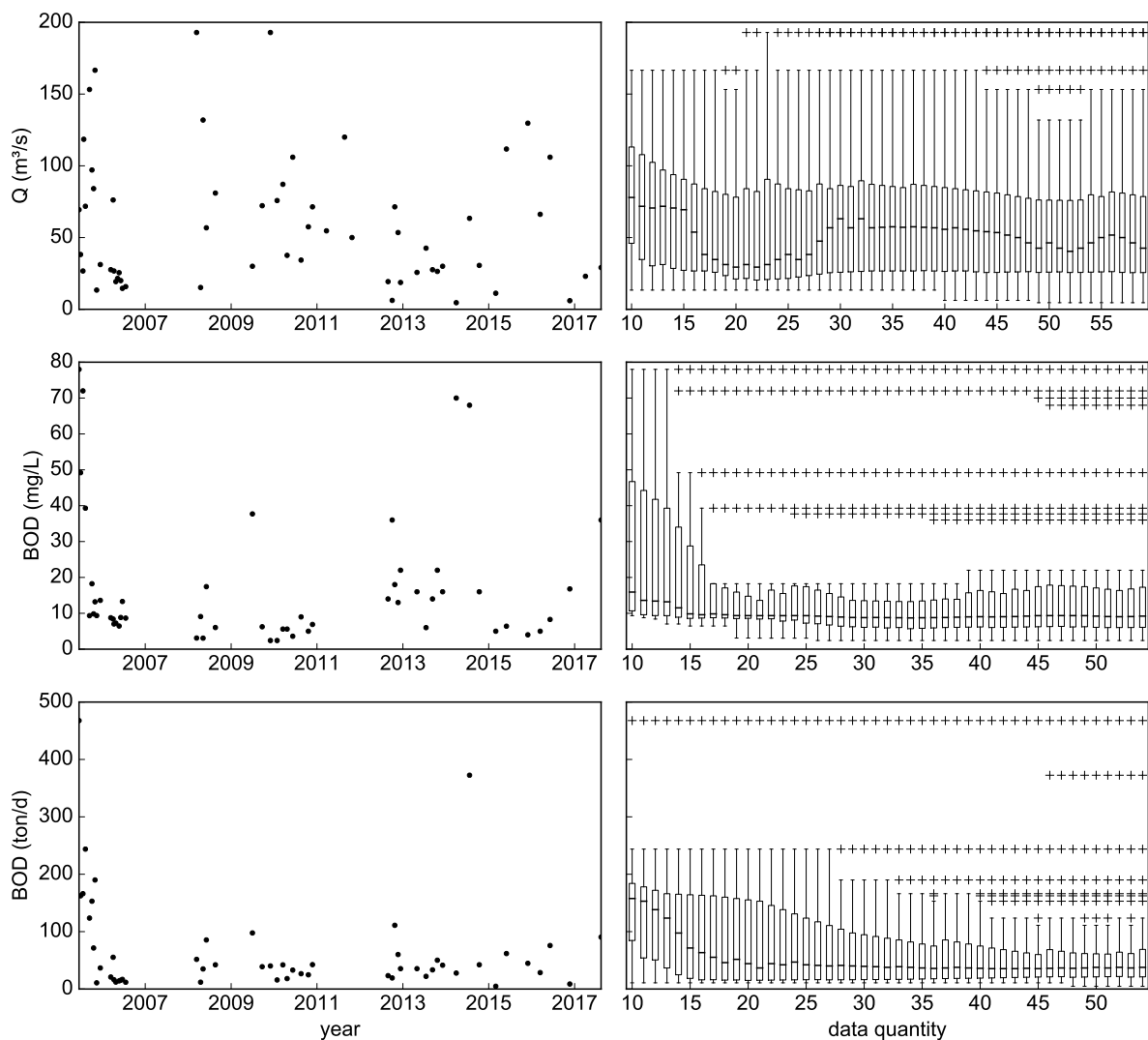
Figure 3 – Time series and boxplot evolution. Q, BOD concentrations and loads, station IG5. Updated at each data, starting with 10 elements and ending with all data. The boxes show the 25th, 50th and 75th percentiles, the whiskers are the minimum and maximum non-outlier values and the crosses are the outlier values

pendix A section A.1. From IG3 to IG7, Table 9 shows that from visual analysis there are downward trends in Q and DOC, and upward trends in BOD and TP. The up and

downward trends are also observed in terms of loads, which indicates that upward trends in concentrations are not only an effect of lower Q, instead, it is the combined effect of lower Q higher mass inputs along the river. The increase in TP indicates an increase in the supply of domestic and/or industrial sewage. The DOC should also be increasing, unless the BOD and TP increase is related to the suspended fraction in these river reaches. One should be aware that this dataset is intended to represent the period 2005–2018 with only 59 observations from irregular sampling frequency.

HIDROWEB dataset

Table 9 – Observed variability patterns in UFPR dataset

Station		Q	BOD	DO	DOC	NH4	TP	VDS
IG3	c	↓ **	↑ *	— *	↓ *	~ *	↑ *	↓ *
	w		↑ *	~ *	↓ **	↑ *	↑ *	↓ *
IG4	c	↓ *	↑ *	— **	↓ *	~ *	↑ *	— *
	w		↑ **	~ **	↓ *	~ *	— *	— *
IG5	c	↓ ~ *	~ **	— *	↓ *	~ *	↑ *	— *
	w		~ **	~ **	↓ *	~ **	↑ *	— *
IG6	c	↓ ~	~ *	— *	↓ *	— *	↑ *	— *
	w		~ *	— **	↓ *	— *	↑ *	— *
IG7	c	—	— *	↑	—	— *	— *	—
	w		— *	—	—	— *	—	— *

— no pattern, ~ cycle, ↑ upward trend, ↓ downward trend, * less than 5 outliers,
** between 5 and 10 outliers. The 1st and 2nd lines of each row are for concentration and loads, respectively

This dataset in maintained by the states and federal government. The daily flows time series presented in Fig.4 have different sizes and missing data in different dates from 1931 to 2018. The large number of data makes it difficult to visualize variability patterns. However, it can be observed through the flows and evolution of the boxplot percentiles, an increase of the high flows, especially in the more upstream stations. It has been already noticed and discussed, e.g., in (DETZEL, 2015). The author observed that the flows in the Upper Iguassu watershed started to increase more intensely in the year of 1970 due to urban expansion and consequent waterproofing of the soil.

Some of the daily flows (movies) are associated with water quality data. Fig. 5 shows the BOD concentrations with the associated Q and W at station IG5. As the UFPR dataset, this one has irregular frequency water quality data (photos), with large gaps and shorter period than the daily flows. The Q, C and W photos are apparently increasing with time and have some major fluctuations which may be real cycles, random variability or an effect of the irregular frequency. Unlike the downstream stations, the upstream
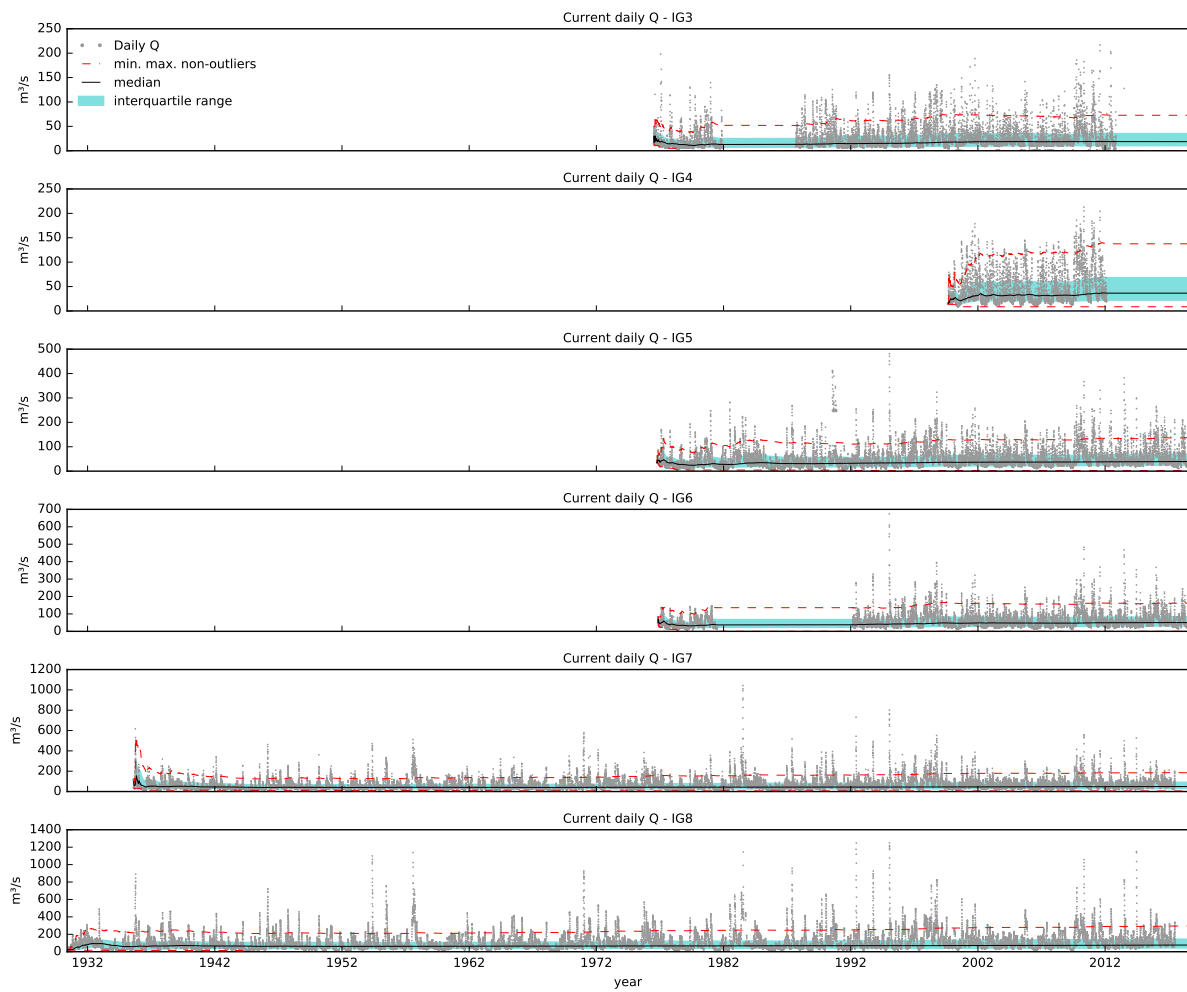
Figure 4 – Time series of daily Q for stations IG3–IG8, and evolution of the interquartile range (25th–75th percentiles), median, minimum and maximum non-outlier thresholds of the time series boxplot

photos (see appendix B section B.1) do not present the same increase as IG5. However, the number of elements in the time series and sampling frequencies are different. This difference draws attention to the influence of the window of time and sampling frequency being observed. For example, the downward trend observed in Q in the UFPR dataset is indeed an effect of the slice of time. That dataset can be observed in this one by looking to the data from 2005 to the end of 2017 in Fig. 5. The false downward trend is in fact part of major fluctuation.

3.4   Uncertainty scenarios

Considering time series of Q, C and W with N elements q_i, c_i and w_i, respectively, for $i = 1, 2, \ldots, N$, the first step, illustrated by (1) and (2) in Fig. 6, relates to the definition of 3 uncertainty scenarios for Q and C. Scenarios are ranges (a–b) defined by a minimum and maximum uncertainty that can be assigned to a measurement in the time series. Low
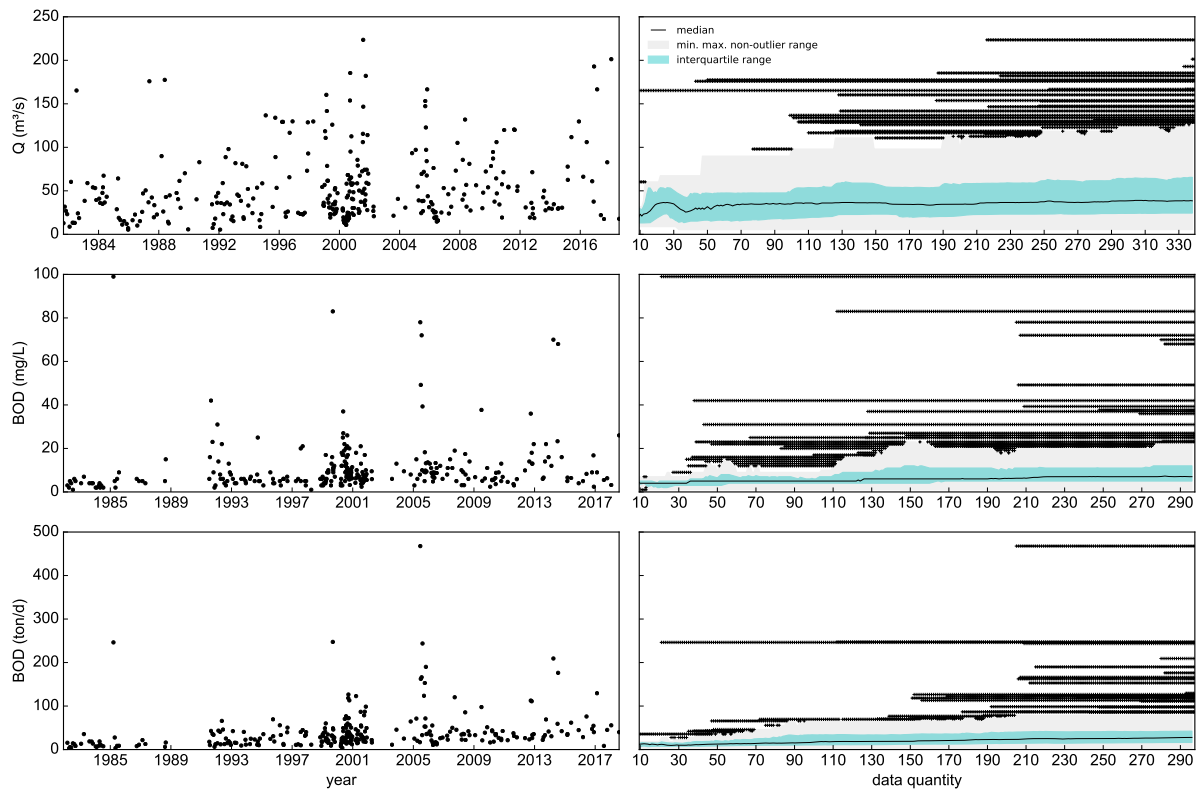
Figure 5 – Time series and boxplot evolution of Q, C and W of BOD from station IG5. Updated boxplots at each data, starting with 10 elements and ending with complete time series. The outlier values are represented by black crosses.

Table 10 – Observed variability patterns in HIDROWEB dataset, irregular frequency Q and water quality data

Station		Q	BOD	NH4	COD	TP	DO	COND
IG3	c	~ ***	—— ***	↑ *	—— **	↑	↑ *	~ *
	w		—— ***	↑ **	—— **	↑ *	~ **	
IG4	c	~ *	~ *	↑ *	~ *	↑ *	—— *	↑ *
	w		~ **	~ *	~	↑ *	—— **	
IG5	c	↑ ~ ***	↑ ~ ***	↑ **	↑ ~ **	↑ *	—— **	↑ *
	w		↑ ~ ***	↑ **	↑ **	↑ *	—— **	
IG6	c	↑ *	↑ ~ **	↑ *	~ **	↑ *	—— *	↑ *
	w		↑ ~ **	↑ **	↑ ~ **	↑ *	—— *	
IG7	c	↑	↑ **	↑ **	↑ **	↑ *	—— **	↑ *
	w		↑ **	↑ ~ **	↑ **	↑ *	—— **	
IG8	c	↑ *	↑ **	n < 20	↑ ~ *	↑ *	—— *	↑ *
	w		↑ **	n < 20	↑ **	↑ *	——*	

—— no pattern, ~ cycle, ↑ upward trend, ↓ downward trend, * less than 5 outliers,

** between 5 and 10 outliers. The 1st and 2nd lines of each row are for concentration and loads, respectively

level (LL: 10–30%), mid level (ML: 30–50%) and high level (HL: 50–70%) scenarios were defined.

$$u(w_i) = \sqrt{u^2(q_i) + u^2(c_i)} \tag{3.1}$$

An uniform pdf was assigned to each scenario and used for the generation of discharge and concentration uncertainties, $u(q_i)$ and $u(c_i)$, respectively. It was performed with the function *random.uniform(a, b)* from Python's Numpy library. The uncertainties for W, $u(w_i)$, were calculated by Eq. 3.1, which is a traditional method for propagation of variances and part of the *GUM uncertainty framework* (JCGM/WG1, 2008a). Eq. 3.1 with the minimum and maximum uncertainties from Q and C uncertainty scenarios, defines the uncertainty scenarios for W (LL: 14–42%, ML: 42–71%, HL: 71–99%).
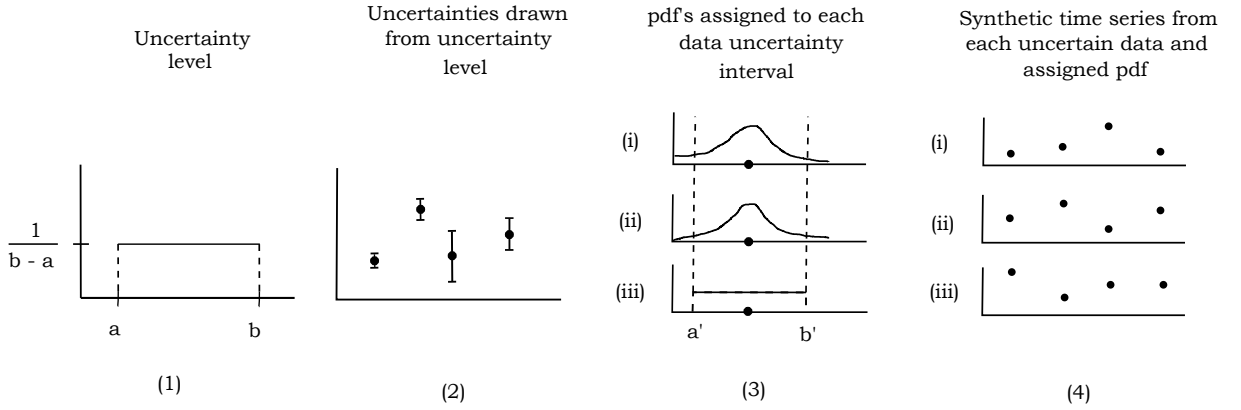
Figure 6 – Proposed method. (1) Definition of uncertainty scenarios represented by uniform probability distribution. (2) Generation of the uncertainty for each value from uncertainty scenarios. (3) Normal (i), lognormal (ii) and uniform (iii) pdf's used to uncertainty expression of each value. (4) Generation of synthetic time series from normal (i), lognormal (ii) and uniform (iii) uncertainties.

3.5 Synthetic time series (STS)

The second step, represented by (3) and (4) in Fig. 6, relates to the definition of pdf's for uncertainty expression, followed by the generation of STS using MCM. For a time series X with N elements x_i, the uncertainties $u(x_i)$, in percentage, were converted to measurement units by Eqs. 3.2. It is represented by the uncertainty bars in (2) and the a'–b' range in (3), in Fig. 6.

$$a' = x_i(1 - u(x_i))/100$$
$$b' = x_i(1 + u(x_i))/100 \tag{3.2}$$

$$\sigma^2 = \frac{(b' - a')^2}{12} \tag{3.3}$$

$$\mu = x_i$$
$$\sigma = u(x_i)/(3 * 100) \tag{3.4}$$

In events (i), (ii) and (iii), the normal pdf with parameters μ_x and σ_x given by Eqs. 3.4, lognormal pdf with parameters $\mu_{ln(x)}$ and $\sigma_{ln(x)}$ given by Eqs. 3.5 and uniform pdf with parameters $\mu = x_i$ and σ^2 given by Eq. 3.3 were, respectively, assigned to all measurements. In normal and lognormal cases the uncertainties were considered as 3 standard deviations (3σ), i.e. 99.7% of the synthetic values is inside the uncertainty range (same approach of Harmel et al. (2006), Harmel et al. (2009)). Since that the uniform and normal pdf's allow negative values, these distributions were truncated at zero, i.e. negatives were rejected and the procedure repeated until a positive value was generated. A similar procedure can be found in (TIAN et al., 2018). A thousand new values were generated from each measurement uncertainty, in LL, ML and HL scenarios, thus, generating 1000 STS.

$$\mu_x = exp\left[\mu_{ln(x)} + \frac{\sigma_{ln(x)}^2}{2}\right]$$
$$\sigma_x = \mu_x^2\left[exp(\sigma_{ln(x)}^2) - 1\right] \tag{3.5}$$

3.6 Statistical tests

The tests for RHIS were performed in OTS and STS of discharges (m³/s), BOD concentrations (mg/L) and loads (ton/d) with increasing number of elements, starting with 10 and ending with the complete time series. The tests were bilateral and, for a 5% significance level (α), H_0 was rejected when p-value < 0.05. The large sample approximation was used for all tests.

Randomness

Randomness was tested by the Single-Sample Runs Test (SIEGEL; JR., 1988; SHESKIN, 2004) with null hypothesis (H_0) that the series is random against alternative hypothesis (H_1) that it is not, due to the presence of trends, cycles and/or shifts. Let m be the number of elements of a type and n the number of elements of another type in a sequence of $N = m + n$ binary events. The test consists of counting the number of groups of equal elements in a sequence, i.e. the number of runs (r), e.g. $+ + - - -$, where $r = 2, m = 2, n = 3$, and comparison with expected values. H_0 can be rejected due to few or too many runs.

The numerical time series X were converted to a binary event by taking the median as a comparison parameter. An element x_i was considered as $+1$ if $x_i >$ median, and as -1 if $x_i <$ median. In this method, trends cycles and/or shifts can cause rejection of

randomness due to few runs, once major fluctuations will produce the runs instead of the random variability of data.

If both m and n are ≤ 20, a specific table should be used, with the expected minimum and maximum values of r as a function of m and n. If m or n is > 20, the normal distribution is used as an approximation of the distribution of r by Eqs. 3.7.

$$\mu_r = \frac{2mn}{N} + 1$$

$$\sigma_r = \sqrt{\frac{2mn(2mn - N)}{N^2(N - 1)}} \tag{3.6}$$

$$z_r = \frac{r - \mu_r}{\sigma_r} \tag{3.7}$$

Homogeneity

The null hypothesis of homogeneity was tested by the Mann-Whitney Test, available in Sheskin (2004). It is a nonparametric test employed on rank-order data for two independent samples with medians supposedly from the same population. It has the following assumptions:

1. each sample has been randomly selected from the population it represents;

2. the two samples are independent of one another;

3. the original variable, which is subsequently ranked, is continuous;

4. homogeneity of variance.

Although outliers can dramatically influence variability, and cause significant heterogeneity in variances and violation of assumption 4, the rank transformation of original data can eliminate or reduce this impact (SHESKIN, 2004).

Let n_1 be the number of cases in the sample of the group X_1 and n_2 the number of cases in the sample of the group X_2. In the context of this research, the groups X_1 and X_2 are, respectively, the first and second half of a time series with N elements. Observations were sorted and assigned to a rank, then back transformed to the original time series order, together with the ranks. The rank-order data was divided in halves, i.e. the groups X_1 and X_2, which were tested for homogeneity (SHESKIN, 2004).

The value of the test statistic U is the lower between U_1 and U_2 (Eqs. 3.8), which are, functions of the number of elements n_1 and n_2, and the sum of the ranks in each group, $\sum R_1$ and $\sum R_2$. Although sources do not agree on the value of the sample size which justifies the normal approximation, it is generally applied for sample sizes larger than 20. The normal approximation of U was applied by Eq. 3.9 (SHESKIN, 2004).

$$U_1 = n_1 n_2 + \frac{n_1(n_1 + 1)}{2} - \sum R1$$

$$U_2 = n_1 n_2 + \frac{n_2(n_2 + 1)}{2} - \sum R2 \tag{3.8}$$

$$z = \frac{U - \frac{n_1 n_2}{2}}{\sqrt{\frac{n_1 n_2 (n_1 + n_2 + 1)}{12}}} \tag{3.9}$$

It can be noted that as the test compares the halves of a time series by comparing the sum of ranks of each half (Eqs. 3.8), the shifts, major fluctuations and outliers can significantly increase/decrease the ranks of their half and cause rejection of homogeneity. Furthermore, as the time series gets longer, representing several years, the differences between groups can be related to up or downward trends and shifts.

Independence

Independence was tested using the Wald and Wolfowitz Test (WALD; WOLFOWITZ, 1943), which is, indeed, a test for randomness based on serial correlation (dependence). The test is suitable when the alternative hypothesis is the presence of an up or downward trend or a regular cyclic movement (WALD; WOLFOWITZ, 1943; NOETHER, 1950). Thus, rejection of independence, a priori, indicates the presence of a trend or regular cyclic fluctuation in data.

For a non-parametric test, observations must be sorted and assigned to a rank, then back transformed to the original time series order, together with the ranks. Considering the series of ranks $X_1, X_2, X_3, \ldots, X_N$ and the differences $X'_1, X'_2, X'_3, \ldots, X'_N$, determined between X_i and its average $\bar{X}$, Eq. 3.10 was calculated. Under an independence null hypothesis, R follows a normal distribution with mean and variance given by Eqs. 3.11. The test statistic is then determined by Eq. 3.12 (WALD; WOLFOWITZ, 1943).

$$R = X_1 X_N + \sum_{i=1}^{n-1} X'_i X'_{i+1} \tag{3.10}$$

$$E[R] = -\frac{s_2}{N-1}$$

$$VAR[R] = \frac{s_2^2 - s_4}{N-1} + \frac{s_2^2 - 2s_4}{(N-1)(N-2)} - \frac{s_2^2}{(N-1)^2}$$

$$s = N m'_r$$

$$m'_r = \frac{\sum_{i=1}^{n-1} (X'_i)^r}{N} \tag{3.11}$$

$$T = \frac{R - E[R]}{\sqrt{VAR[R]}} \tag{3.12}$$

Stationarity

Stationarity was tested by using the non-parametric Mann-Kendall Test, available in (HELSEL; HIRSCH, 2002). It is a test for linear or nonlinear monotonic trend detection. The test statistic S measures the monotonic dependence of y on x. The null hypothesis of stationarity was tested against the alternative hypothesis of an up or downward shift of data in relation with time. H_0 can be stated as Prob[1]$(y_i < y_j$ for $i < j) = 1/2$, and H_1, for a two-sided test, as $\text{Prob}(y_i < y_j$ for $i < j) \neq 1/2$.

Kendall's S is calculated by subtracting the number of "discordant pairs" M, i.e. the number of (x, y) pairs where y decreases as x increases, from the number of "concordant pairs" P, i.e. the number of (x, y) pairs where y increases with increasing x, as Eq. 3.13. There are $n(n-1)/2$ possible comparisons to be made among the n data pairs. If all y values increase along with the x values, $S = n(n-1)/2$. If all y values decrease, $S = -n(n-1)/2$.

The Kendall's correlation coefficient (τ), which varies between -1 and $+1$, is then calculated by Eq. 3.14. To test for significance of τ, S is compared to what would be expected when H_0 is true. If it is further from 0 than expected, H_0 is rejected. For $n \leq 10$ an exact test should be computed. However, the large sample approximation yields p-values very close to the exact values, even for small sample sizes. The large sample approximation was applied by Eqs. 3.15. The test is bilateral and for a 5% significance level H_0 is rejected when p-value < 0.05 (HELSEL; HIRSCH, 2002).

As this test is applied in a different transformation of data, i.e. pluses and minuses instead of ranks, the impact of outliers is even more reduced, since they will always have magnitude $+1$ or -1, as all other values.

$$S = P - M \tag{3.13}$$

P = "number of pluses", the number of times the $y's$ increase as the $x's$ increases.
M = "number of minuses", the number of times the $y's$ decrease as the $x's$ increases.

$$\tau = \frac{S}{n(n-1)/2} \tag{3.14}$$

---

[1]   Probability

$$\mu_S = 0$$

$$\sigma_S = \sqrt{(n/18)(n-1)(2n+5)}$$

$$Z_s = \begin{cases} \frac{S-1}{\sigma_S} & S < 0 \\ 0 & S = 0 \\ \frac{S+1}{\sigma_S} & S > 0 \end{cases} \qquad (3.15)$$

3.7 Regression model

Regression analysis was performed: (1) to estimate concentrations from flows and; (2) to estimate missing data in the daily flow time series from flows at neighboring stations.

Quadratic polynomial regression model (QLR) (Eq. 3.16) was used in (1), with parameters estimated from water quality and flow photos from the HIDROWEB dataset. The parameters β_0, β_1 and β_2 of the model were estimated by the OLS method (see Table 4). A 3-parameters lognormal pdf (LN3) was fitted to the errors of the model.

A simple linear parametric regression model (Eq. 3.17) (SLR) was used in (2). A list of priority stations was created for each station. When there was missing observations at one station, the algorithm searched for the observation on the same date at other station according to the priority list. The first and last station of the list are the one with the best and the worst relation (linear regression) with the one with missing data, respectively. The parameters β_0 and β_1 of these models were estimated by the OLS method and a LN3 was fitted to the errors.

The choice of a LN3 distribution derives from a preliminary investigation of the errors distribution. This procedure is allowed since if the use is the prediction of y given x, the only requirements are: (a) the model form is correct and; (b) the data used to fit the model are representative of the data of interest (see Table 5 in section 2.5.1)

$$y = \beta_0 + \beta_1 x + \beta_2 x^2 + e \qquad (3.16)$$

$$y = \beta_0 + \beta_1 x + e \qquad (3.17)$$

3.8 Stochastic approach

A first order autoregressive model (AR(1)) presented by Eq. 3.18, also known as Markov model (MAR(1)) (DETZEL, 2015; LOUCKS; BEEK, 2017), was fitted to the daily flows (HIDROWEB dataset) with the purpose of generating synthetic daily flows.

The logarithmic transformation in base e was applied to the time series prior to the fitting of the model and the synthetic daily flows were back transformed to the original form.

$$q_t = u_q + \rho_1(q_{t-1} - u_q) + \sigma_q\sqrt{1 - \rho_1^2}at' \tag{3.18}$$

Where,

$$at' \sim N(0,1)$$

q_t = daily flow at time t;

u_q = mean the daily flows;

ρ_1 = correlation coefficient of lag 1;

q_{t-1} = daily flow at $t - 1$;

σ_q = standard deviation of the daily flows;

at' = error of the model.

4 Results

"If you can't explain it simply, you don't understand it well enough"

Albert Einstein

4.1 Irregular-frequency time series (photos)

4.1.1 Uncertainty drawing

Figs. 7, 8 and 9 show the measurement uncertainties drawn in LL, ML and HL scenario for flows, BOD concentrations and loads, respectively. The graphics also present the median, the $25th$ and $75th$ percentile of the OTS. In general, it can be observed that outliers and other high values were assigned to uncertainty ranges considerably larger than other values, as a consequence of the conversion of uncertainties in percentage into parameter units. It means that this approach for uncertainty assessment gives more importance for higher values, in terms of changes in variability. Descriptive statistics, as the mean and standard deviation, may have considerable changes due to uncertainty of these values.

The high variability of the flows gives rise to the presence of many large uncertainty ranges, thus allowing considerable changes in variability. In the HL scenario, these large ranges allow the appearance of variability structures without the cyclic pattern observed in the OTS (Fig. 3). The high values of concentration and load are mostly a few outliers. It means that in this case study, loads are more affected by uncertainties in the flows than in concentrations. Furthermore, as part of the variability of concentration is controlled by variability of the flows, these results highlight the importance of of the flows to the uncertainty analysis. The same considerations are valid for the other variables and stations (see appendix A sections A.2, A.3 and A.4 for Q, C and W, respectively)

4.1.2 Synthetic time series

As a check procedure Figs. 10, 11 and 12 present the histogram of the synthetic values associated to one original measurement randomly chosen from the time series of Q, C and W, respectively. The histograms show that the uniform, normal and lognormal drawings were correctly performed in LL, ML and HL uncertainty scenarios, since the synthetic values followed the expected probability distributions. Appendix A sections A.5, A.6 and A.7 shows the Q, C and W histograms, respectively, for stations IG3–IG7.
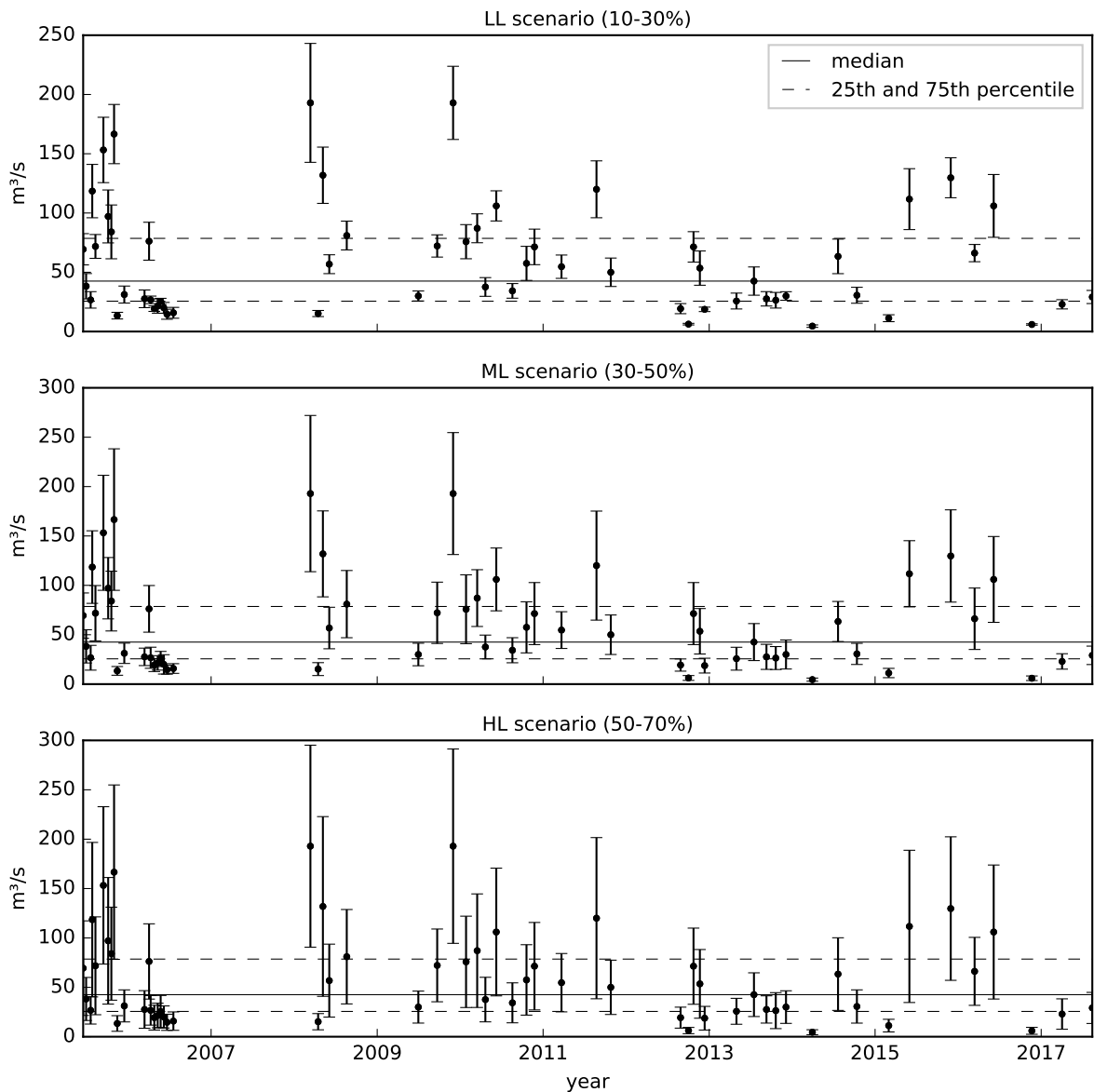
Figure 7 – LL, ML and HL uncertainty scenarios for Q time series, station IG5

4.1.3 Statistical tests

The results are presented in Figs. 13, 14 and 15, for time series of Q, C and W, respectively. A discussion is presented for each time series and a general discussion is presented at the end of the section. The results from stations IG3–IG7 can be found in appendix A sections A.8, A.9 and A.10 for Q, C and W, respectively.

Flows

The evolution of p-values in Fig. 13 shows that the decisions about RHIS may vary over time. For example, following the red lines, homogeneity and stationarity were rejected at N= 20 (p-value ≈ 0.00) but were far from rejection at N= 35 (p-value close to
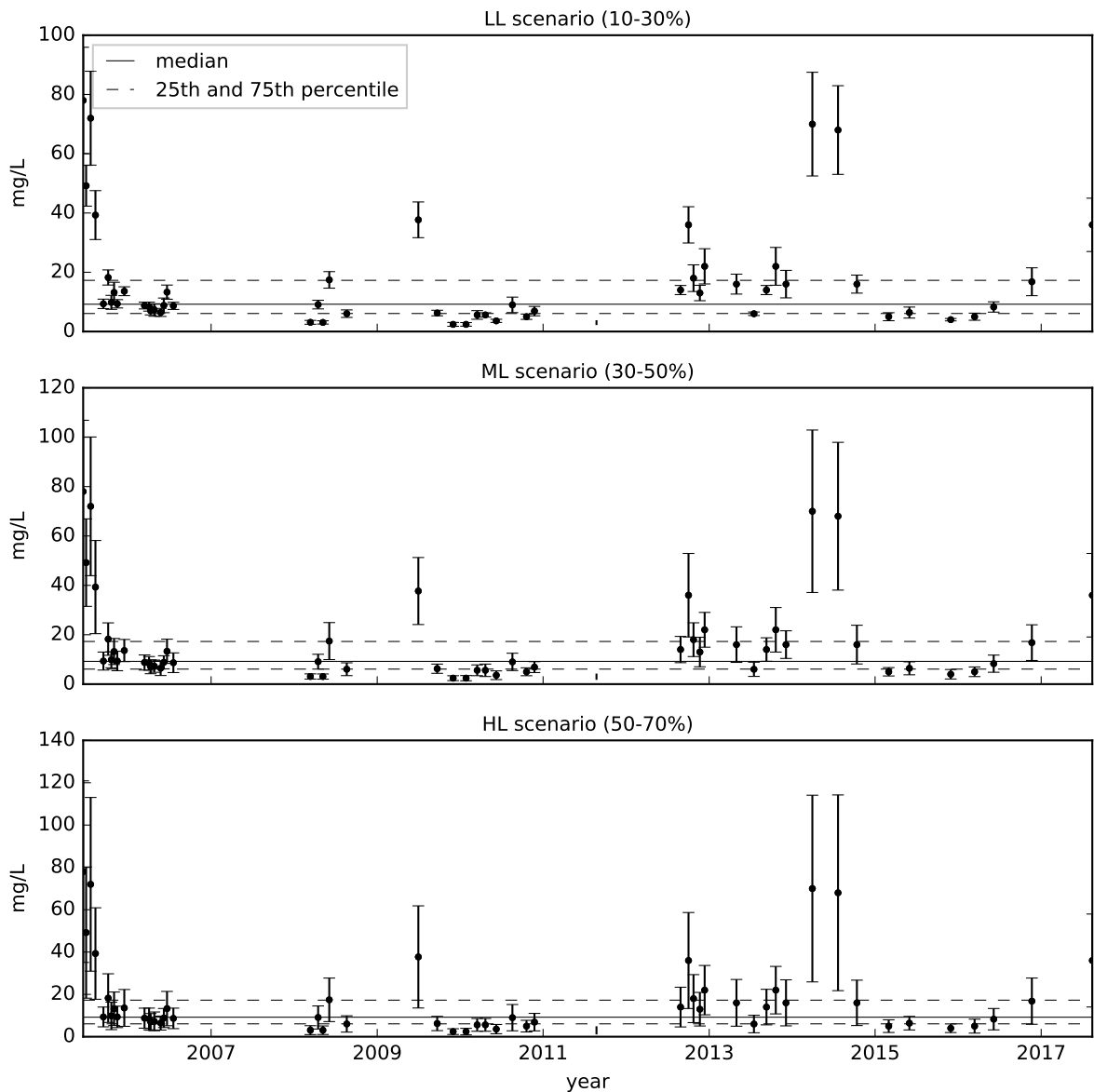
Figure 8 – LL, ML and HL uncertainty scenarios for BOD concentration time series, station IG5

1.0), and the independence p-value changed from 0.05 at N= 20 to ≈ 0.7 at N= 23, showing that the tests can be highly sensitive to small changes in N. It is true for the stations IG3–IG7.

The STS p-values from LL, ML and HL scenarios varied similarly to the OTS p-values in stations IG3–IG7. However, with differences due to measurement uncertainties. The std range (i.e., the p-value uncertainty) at each N were mostly $\ll 1.0$, while the total variability ranged from 0.0 to 1.0. It means that even with uncertainties, the same variability patterns as those from the OTS can be detected with more/less intensity (i.e., magnitude of the p-value).

At first, the observed cyclic fluctuation and downward trend in the flows from IG5
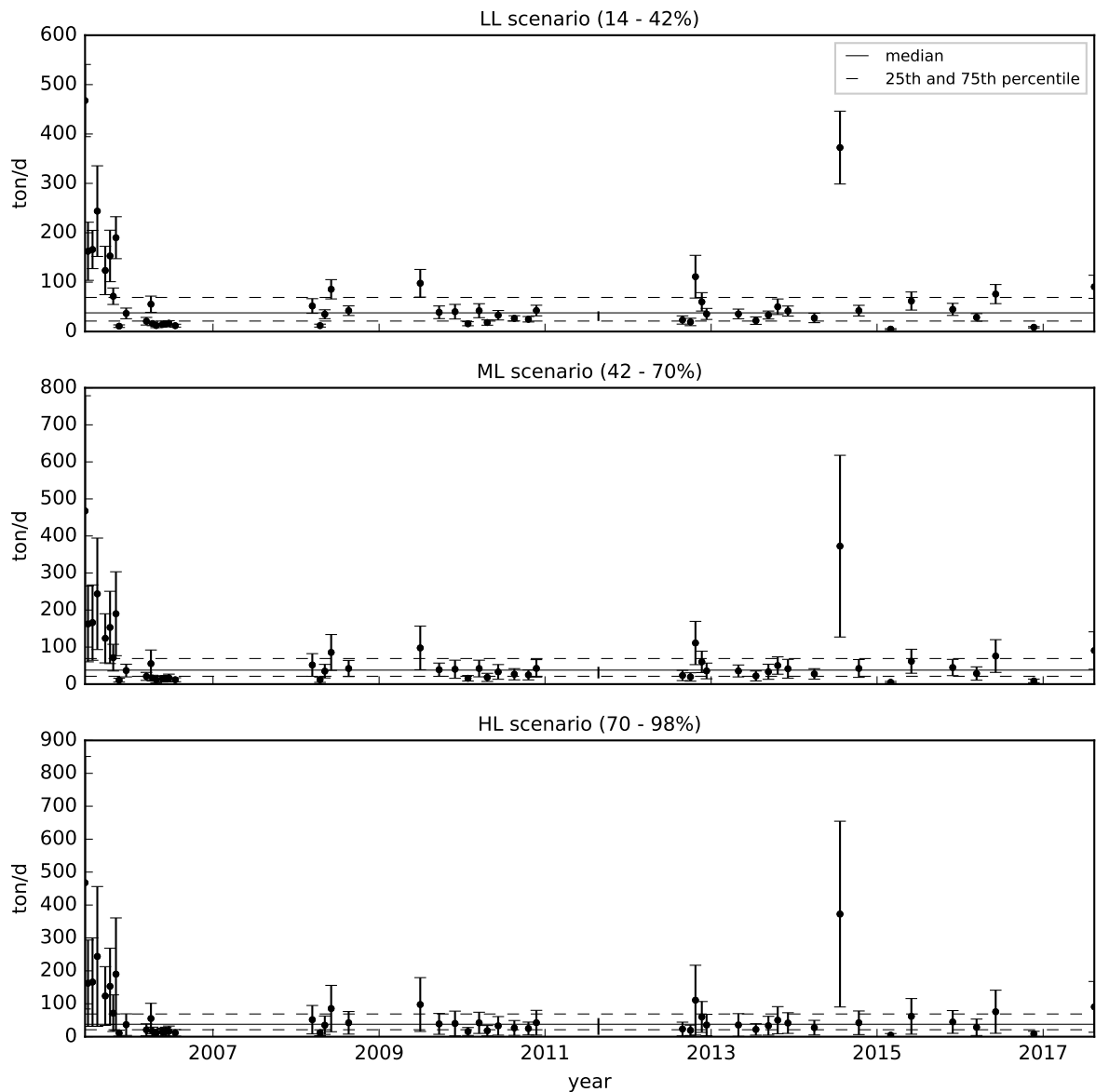
Figure 9 – LL, ML and HL uncertainty scenarios for BOD load time series, station IG5

(Fig. 3) are not significant for the complete time series, since RHIS were not rejected at N= 59. Although the randomness p-value is 0.04 for the OTS, the STS p-values are ≈ 0.05 ± 0.04 in LL, 0.09 ± 0.10 in ML and 0.18 ± 0.20 in HL scenario from uniform case. It shows that the p-value is more likely to increase in the presence of uncertainties and cause the hypothesis not to be rejected. It is also true for the normal and lognormal cases but with smaller spreads and differences from the original p-value.

Despite the non-rejection of the hypotheses at N= 59, randomness and independence p-values are in downward trends. Thus, if cycles and/or trends are present, there is a high chance that the hypotheses will be rejected later when new elements are included. Hence, the consideration or not of these patterns of variability prior to statistical analysis will depend on expert judgment about their existence and continuity. The cyclic
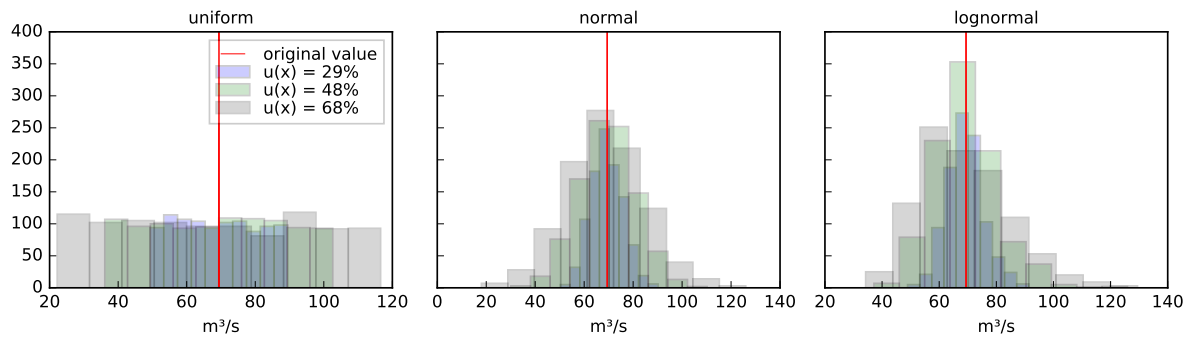
Figure 10 – Histograms of synthetic Q from one original measurement randomly chosen, station IG5
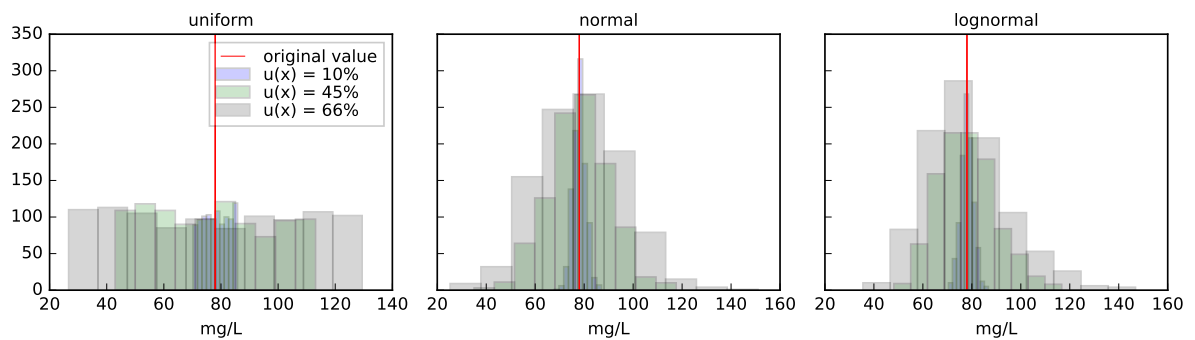
Figure 11 – Histograms of synthetic BOD concentrations from one original measurement randomly chosen, station IG5
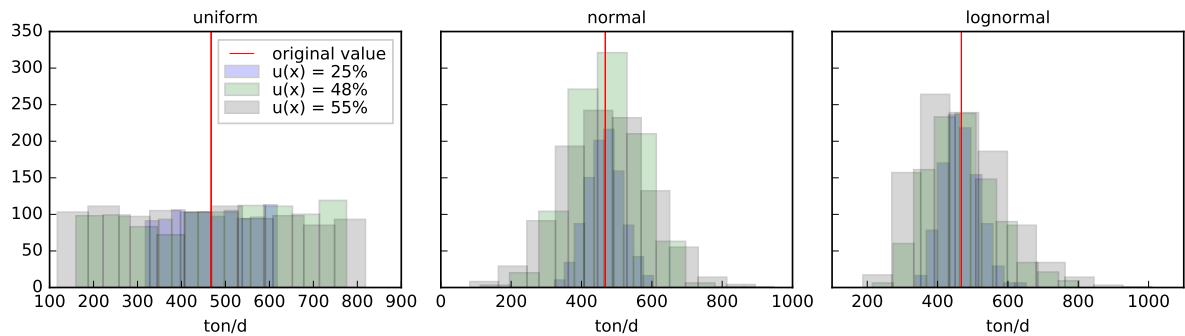
Figure 12 – Histograms of synthetic BOD loads from one original measurement randomly chosen, station IG5

fluctuation and downward trend of flows are also observed at the other stations (appendix A section A.1) and RHIS hypotheses were also not rejected for the complete time series (A section A.8), with the exception of independence. It reinforces the confidence in the presence of a significant cyclic fluctuation in the flows.

Concentrations
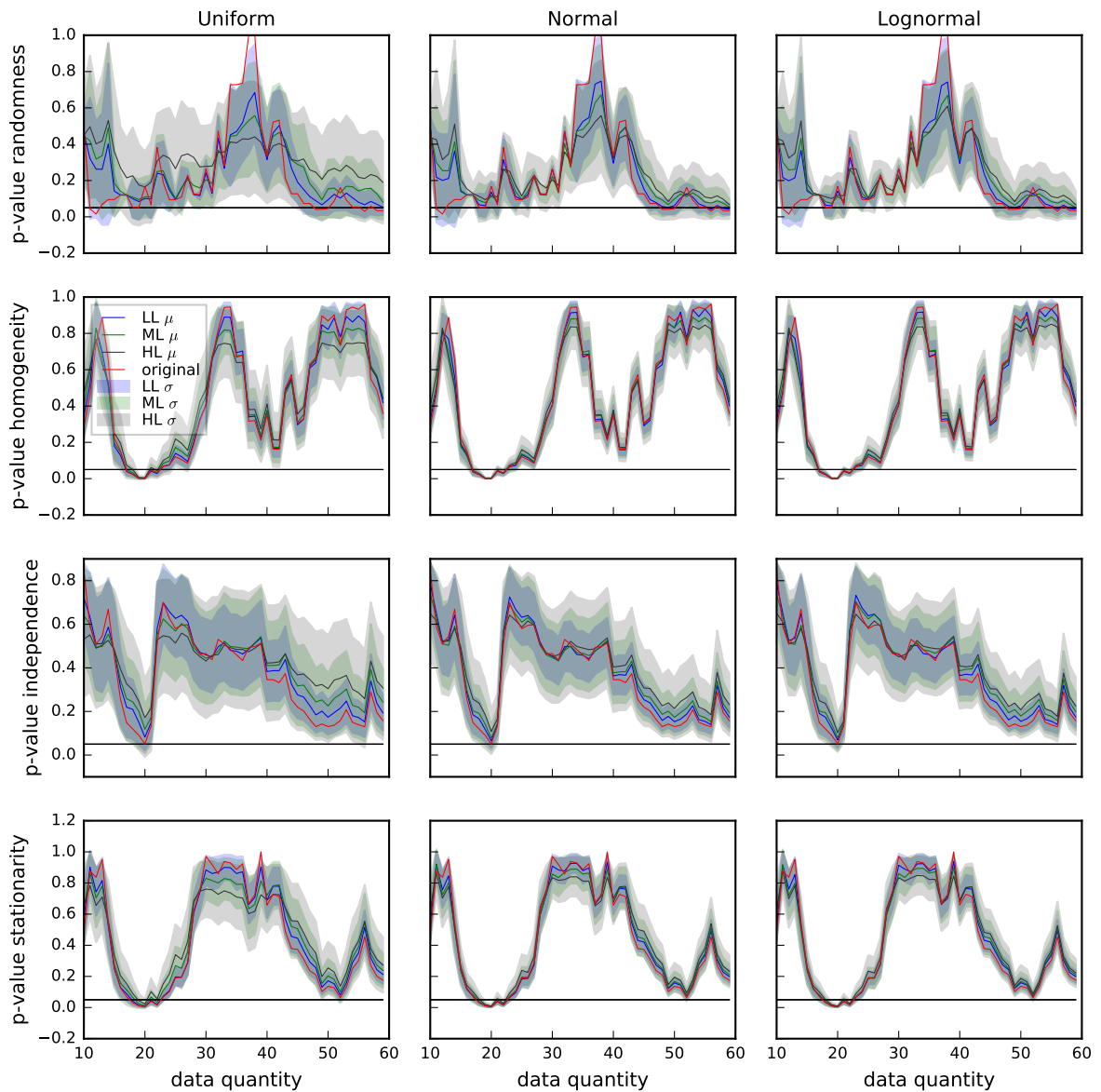
Figure 13 – Evolution of RHIS p-values from Q time series, station IG5. Red line = p-value from OTS. Blue, green, gray lines = average p-value from STS in LL, ML and HL scenarios, respectively. Blue, green, gray bands = std of p-values from STS in LL, ML and HL scenarios, respectively. Black line = significance level ($\alpha = 0.05$). Reject H_0 if p-value < 0.05

Fig. 14 shows that the high concentrations in the beginning of the BOD time series (mg/L) (4 outliers > 35 mg/L) caused rejection of homogeneity (p-value ≈ 0.00) and stationarity (p-value ≈ 0.00) until approximately N = 40. The convergence of the results from OTS and STS to the same p-values indicates a "strong" trend, i.e., a trend that is significant even in STS from HL uncertainties (50–70%).

The OTS p-values for stationarity and homogeneity increased from N= 40 varying between 0.2–1.0 and 0.0–0.1, respectively. Stationarity was no longer rejected from this point. Homogeneity is also far from rejection if uncertainties are considered, since the

p-values from LL, ML and HL scenarios varied between 0.2–1.0. The separation between OTS and STS p-values of homogeneity shows the weakening of the "trend" (false trend), which became susceptible to changes due to LL, ML and HL uncertainties. It can also be observed for BOD from IG3 to IG6 and in independence results at IG6 (appendix A section A.9). Independence was not reject at N = 43 with p-value = 1.0, but if any level of uncertainty is considered the p-value moves to the other extreme (≈ 0.0).

Although it can be concluded that there was no trend at N= 40, the decreasing variability of randomness and independence p-values, moving towards 0.00, indicates the presence of a cycle. Despite the large proportion of STS p-values of randomness > 0.05 at N = 59 ($\approx 0.04 \pm 0.11$ and 0.14 ± 0.18 in ML and HL scenarios, respectively, in the uniform case), the decreasing variability moving towards 0.00 indicates a probable rejection in the near future. Therefore, these results indicate the presence of a significant cycle, even for HL uncertainties. However, the analysis of irregular time series with large missing data gaps, few data and outliers presence leaves a high level of uncertainty about the true existence and continuity of a cycle. All the stations, except IG7 because it has only 14 observations, present the same variability patterns with similar evolution of the p-values. It does not increase the confidence in the presence of a significant cyclic fluctuation, because in this dataset all the stations are monitored in the same dates, hence, they have water quality photos of the same days at different points of the same river. It is possible that totally different results would be found if the sites had data with even 1 day-lag. It would indicate that there was no pattern related to time. The following parameters present higher similarities from IG3 to IG6: BOD (cycle), DOC (cycle and downward trend) and TP (cycle and upward trend) (appendix A section A.9). The evolution of the p-values of these water quality parameters is similar along the river reach. It indicates that the water quality condition is connected along this river reach but does not increase the confidence in the presence of variability patterns because the sites have data on the same days, with a few minutes or hours of difference. The upward trend of TP (opposite to Q) indicates that although the concentrations may be partially controlled by the flows, there are other factors that significantly influence the concentrations.

Loads

Similarly to Q and C, the p-values of BOD loads varied with N (Fig. 15). The rejection of RHIS in the OTS at approximately N= 20 indicates the presence of a significant downward trend in the period 2005–2009. Besides that, the convergence of OTS and STS p-values to 0.00 in homogeneity and stationarity tests reveals a "strong" trend, i.e., not affected by the uncertainties assumed. These rejections were caused by the initial outliers in the OTS (see Fig. 3). However, the min–max range (i.e., the minimum and maximum p-values observed in the std ranges) of homogeneity and stationarity p-values at N= 45
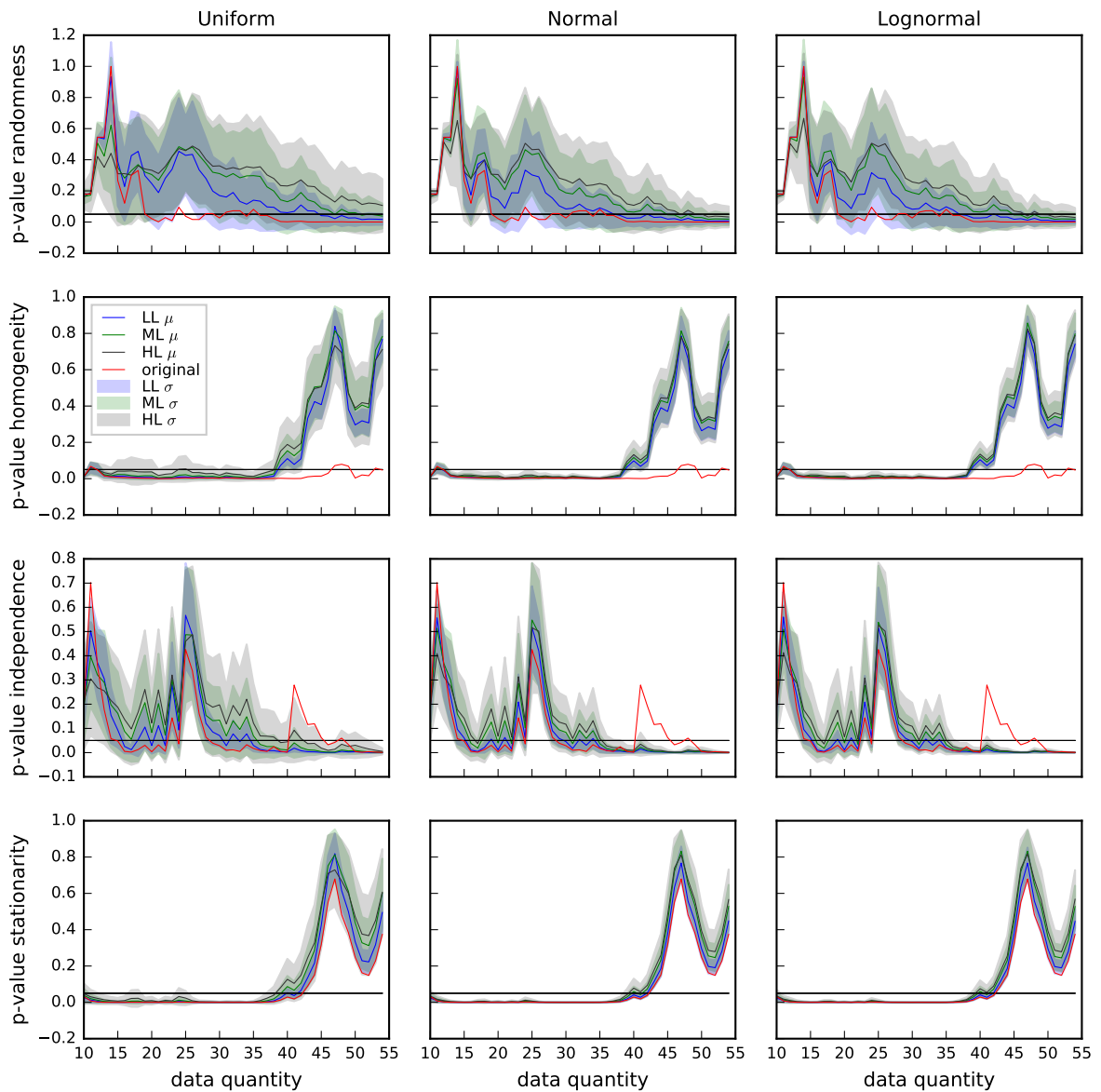
Figure 14 – Evolution of RHIS p-values from BOD concentration time series from IG5. Red line = p-value from OTS. Blue, green, gray lines = average p-value from STS in LL, ML and HL scenarios, respectively. Blue, green, gray bands = std of p-values from STS in LL, ML and HL scenarios, respectively. Black line = significance level (α = 0.05). Reject H_0 if p-value < 0.05

increased to $\approx$ 0.3–1.0 and 0.0–0.3, respectively, making the trend unlikely. The same is observed from IG3 to IG6 (appendix A section A.10).

The OTS p-values of randomness and independence showed increasing variability (between 0.0–0.2) until N= 54, changing the decision about a significant cycle many times. For the STS, the average p-values increased from 0.0 to 0.4, 0.01 to 0.4 and 0.1 to 0.4 in LL, ML and HL scenarios of randomness in uniform case. Therefore, it is more likely that the cycle is not significant if some uncertainty level is assumed. The min–max ranges of RHIS at N= 54 (0.1–0.7, 0.2–0.7, 0.0–0.5, and 0.1–0.6, respectively) indicate that the

major fluctuations are more likely to be random variability. It highlights the influence of Q in C. The product of higher Q for lower C, and vice-versa, makes the major fluctuations smoother. This effect can be better observed for TP. RHIS were rejected for TP concentrations indicating the presence of a significant cycle and upward trend. For the TP loads, randomness and independence were no longer rejected in most of the stations, indicating the smoothing of the cyclic fluctuation.
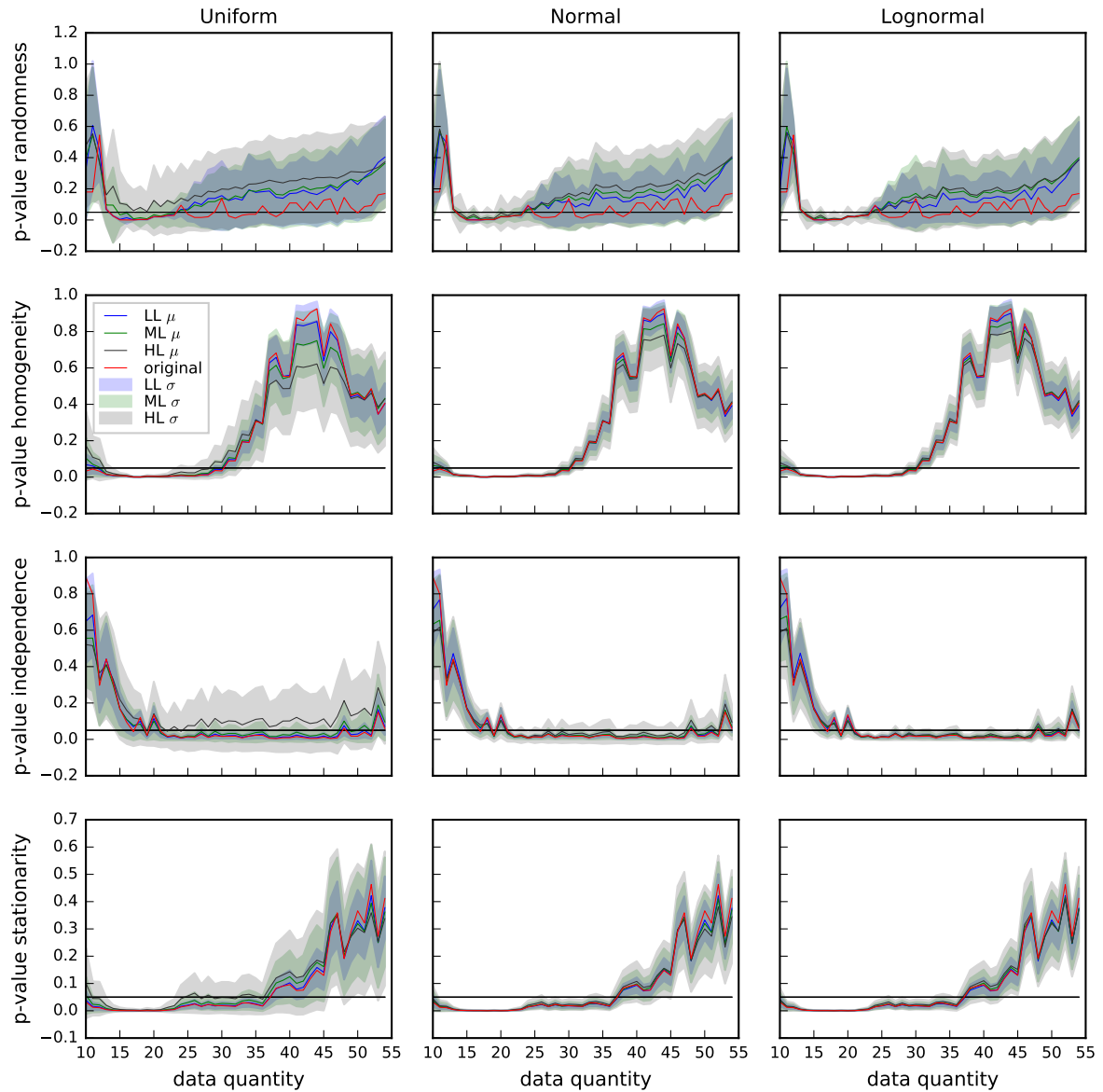
Figure 15 – Evolution of RHIS p-values from BOD load time series from IG5. Red line = p-value from OTS. Blue, green, gray lines = average p-value from STS in LL, ML and HL scenarios, respectively. Blue, green, gray bands = std of p-values from STS in LL, ML and HL scenarios, respectively. Black line = significance level ($\alpha = 0.05$). Reject H_0 if p-value < 0.05

4.1.4 Synthesis

The high variability of the p-values along the monitoring period was highlighted by applying the tests with an increasing number of elements. It reflects the uncertainty related to the representativeness of the time series, which will be greater the shorter the monitoring period. Outliers and incomplete cycles can be mistakenly understood as trends or shifts (see rejection of homogeneity and stationarity in Figs. 14 and 15). Irregular and low-frequency data, e.g., 59 measurements (59 days) in 13 years ($\approx 4,745$ days), can take a long time to provide a high level of confidence in the existence and continuity of the variability patterns. This uncertainty will become even greater with the increase in outliers quantity and magnitude.

Although trends and shifts can be detected mainly by the homogeneity and/or stationarity tests, and cycles by the randomness and/or independence tests, the results may differ between methods. For example, in Fig. 15 between N= 30 and N= 40, the OTS p-values increased from ≈ 0.0 to 0.2 for homogeneity, and varied below 0.05 for stationarity. These divergences exemplify the uncertainty related to the choice of appropriate methods. Although some tests may be more sensitive to a certain type of variability pattern, e.g., the Mann-Kendall test for trends, they may also be affected by the other types (WALD; WOLFOWITZ, 1943; DURRANS; TOMIC, 1996). This uncertainty may be reduced by the joint application of different methods for the same purpose and by understanding how the outliers can affect the results. The impact of outliers on statistical results can be eliminated or reduced by applying non-parametric tests. However, these values can still cause significant heterogeneity in variances (HELSEL; HIRSCH, 2002; SHESKIN, 2004).

Another type of uncertainty was introduced by the use of uncertain data. When the variability pattern is "weak", e.g., a smooth cyclic fluctuation, the p-value will fluctuate near the rejection limit and the decision can be changed due to uncertainties. It can be observed in Fig. 15. While the OTS p-values of independence varied between 0.0–0.05, rejecting H_0, those from STS in HL scenario (71–99%) reached more than 0.3 in the uniform case and ≈ 0.1 in the normal and lognormal cases (not rejecting H_0). Otherwise, when there is only random variability or a well-defined pattern, the p-value will be far from the rejection limit (close to 1.0 or 0.0) making measurement uncertainties and associated subjectivity irrelevant to the decision. This becomes clear in the results of homogeneity in Fig. 15. From N= 15 to N= 20, the OTS and STS p-values converged to 0.0 ("strong" trend) and at N= 45 the OTS was ≈ 0.9 and STS ranged between 0.3 and 1.0 (random variability). The uncertainty bands are irrelevant in these cases since they cannot change the decision, especially in the lognormal cases.

The differences between the normal and lognormal cases are imperceptible but can be expressive between these and the uniform case. For example, in the stationarity test for loads (Fig. 15) the min–max ranges of the p-values at N= 54 were ≈ 0.08–0.6, 0.2–0.57

and 0.22–0.55 for the uniform, normal and lognormal cases, respectively.

The consideration of diverse variables from diverse locations along the same river reach can increase the confidence in existence and continuity of the observed patterns. However, patterns can be an effect of irregular sampling frequencies. In this case study the different sites were monitored in the same dates, with a few minutes or hours from one to another. Hence, the similarities in their patterns may be coming from the similar irregular sampling frequencies instead of real variability patterns in time.

4.2 Irregular and regular-frequency time series (photos and movies)

4.2.1 Regressions

In this analysis of photos and movies, daily concentrations were generated from daily flows. First, synthetic daily flows time series were generated from an autoregressive Markov model and then, the regression model (RM) was applied on the synthetic daily flows to generate the concentrations. However, the original daily flows time series had missing data that were estimated also from a RM.

RM for the missing Q

Fig. 16 shows the results of the regressions among the flows from stations IG3–IG8. Each column present the results for one station as the response variable (vertical axis) and the others as explanatory (horizontal axis). The longer the distance between the stations in the river, the higher the standard error (stderr) of the regression and the lower the R^2. The stderr ranged from 8.22–83.32 m³/s. The higher stderr's are related to the use of upstream stations to estimate Q at IG8, where there are much higher flows. Most of the stderr's are between 10–30 m³/s (about 10–20% of the maximum flows). It must be observed that the spread of the points around the curve is not homogeneous. Although the stderr is a single value, in practice it can be observed that the error is higher for higher flows. The estimated flows from the year 1931 to 2018 can be observed in Fig. 17. Although the stderr's (right vertical axis) are relatively high compared to the flows at each station (left vertical axis), the estimated flows show an acceptable variability, since the peaks and valleys are synchronized among stations and the magnitudes of estimated and original flows are similar. Between 2005–2018 (period of the stochastic approach with the autoregressive model), there are few estimated flows at IG5, IG6, IG7, and IG8, and about half of the data at IG3 and IG4. The ranges of estimated flow and the stderr's between 2005–2018 are respectively 0–200 m³/s and 15 m³/s at IG3, 0-300 m³/s and 8 m³/s at IG4, 100–150 m³/s and 12 m³/s at IG6, 0–300 m³/s and 18 m³/s at IG7, and 0–400 m³/s and 65 m³/s at IG8. The station IG5 does not have estimated flows from regression in this period.
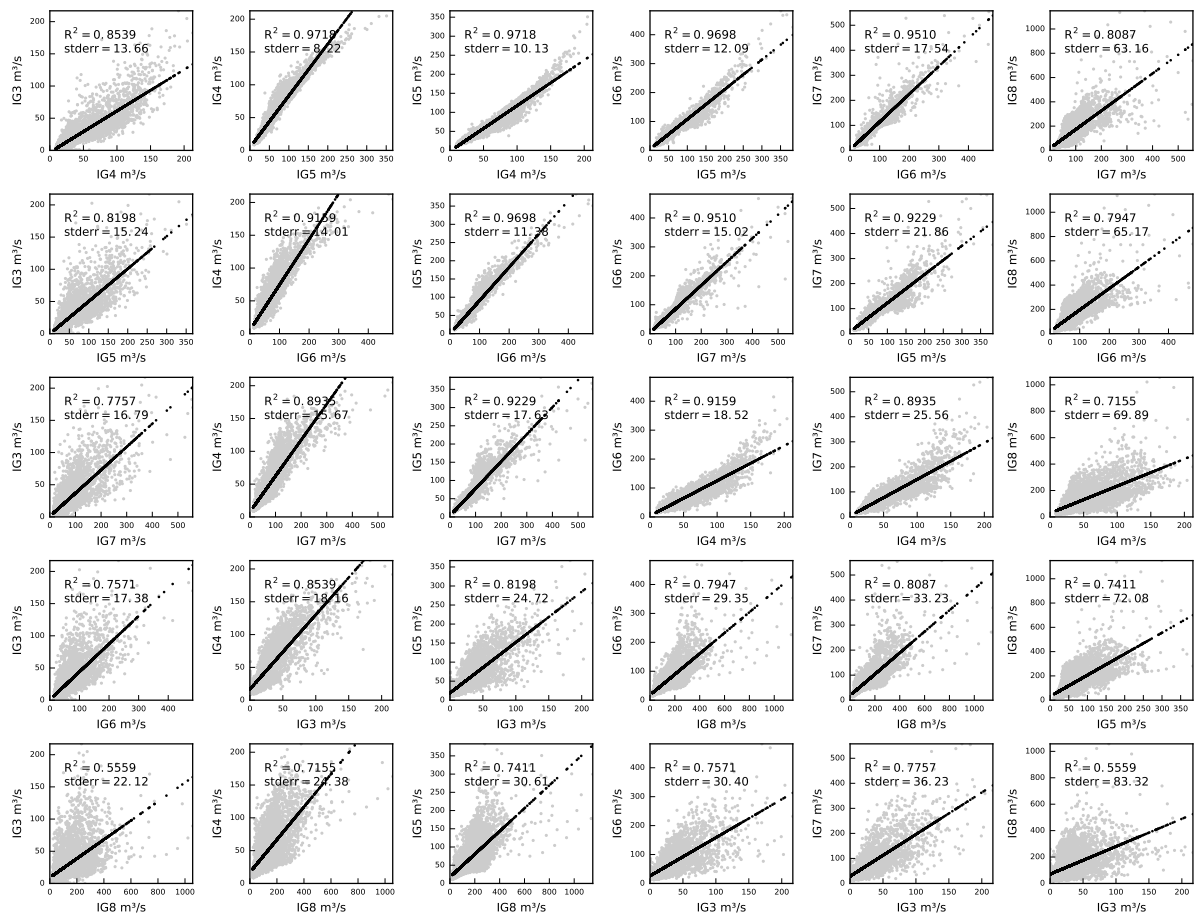
Figure 16 – Results from simple linear regression of each station to the others

RM for the concentrations

The polynomial RM for BOD concentrations is shown in Fig. 18. In all the stations there are much more observations related to low flow conditions. Furthermore, the few high flows with concentration data are not the highest flows of the daily time series of flows. They are just the highest flow in which water was sampled for water quality analysis. Hence, there will be higher uncertainty for the concentrations in the higher flows. Fig. 19 shows that the LN3 distribution is appropriate to represent the error of the RM. As a check procedure the RM was used to estimate the original photos used in the regression. Fig. 20 shows the original and estimated concentration photos. The spread of the results is similar but high errors, as at station IG5 before 1989, can occur. The regression for DO, NH4, and TP can be found in appendix B section B.2.

4.2.2 RHIS

The time series of Q, C, and W, the results for RHIS, and the percentile evolution of photos and movies are shown in Fig. 21 for BOD at station IG5, and in appendix
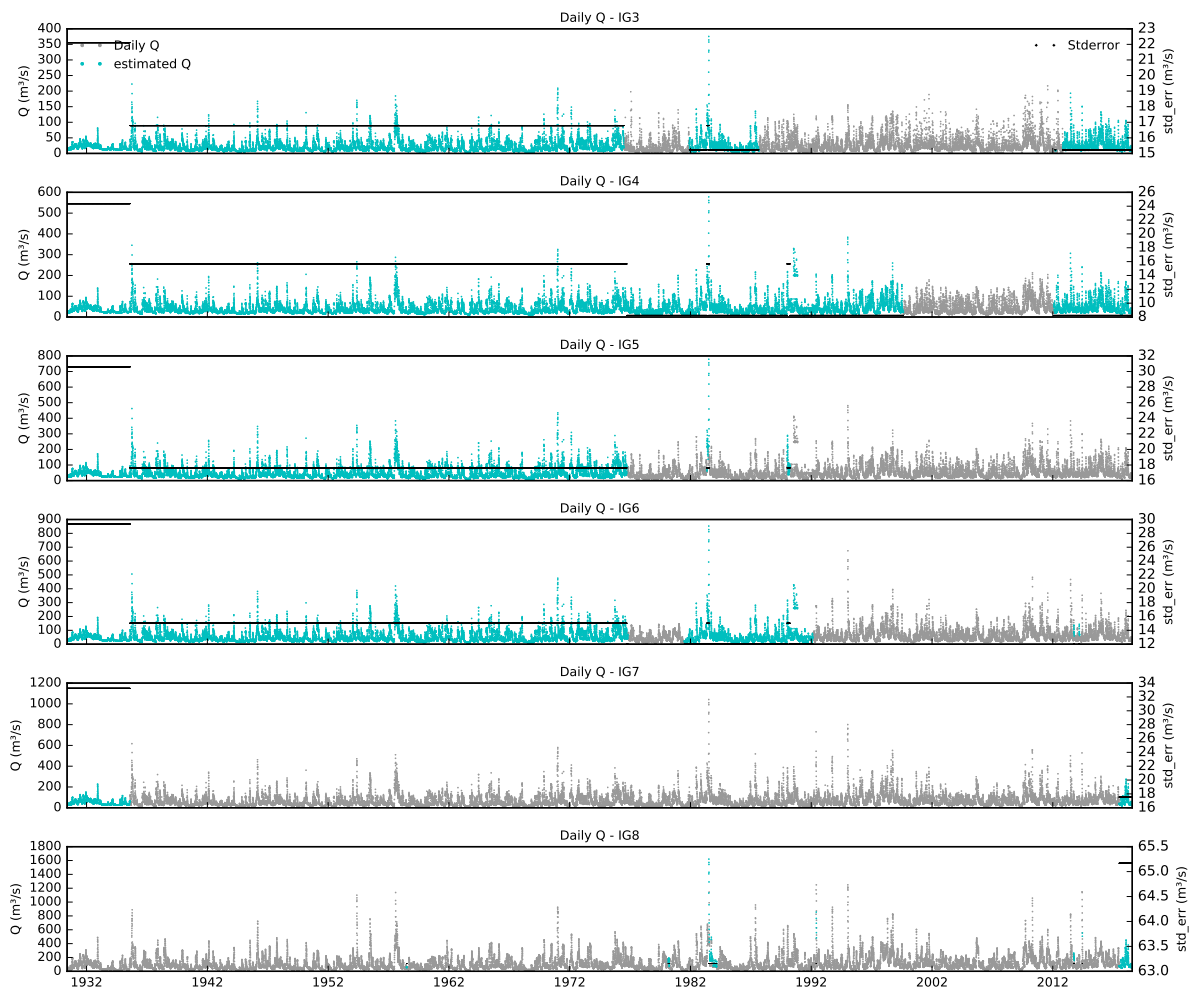
Figure 17 – Complete time series with estimated flows for stations IG3–IG8

B section B.3 for other variables and stations. The graphics in the 1st row show the time series, in the rows 2–5 are the evolution of RHIS tests, and in the 6th row are the percentile evolutions. No variability patterns can be visually identified in the photos and movies (original and synthetic) of Q, C, and W. In part, because of the small figure size for the daily time series ($\approx$ 14 years $\times$ 365 days of data). Variability patterns are not expected to be present in the synthetic movies, except the 1st order/lag autocorrelation, since no consideration was made in the autoregressive modeling process, e.g., regarding seasonality and/or trends. It is also valid for C and W since these synthetic movies were generated by combination of a Markov model (Mar(1)) for Q, and a linear RM to estimate C from Q. Stationarity and homogeneity are basic assumptions of these models.

Despite some fluctuations, the autocorrelation is indeed significant for most of the complete time series of photos and movies of Q, C, and W from IG3 to IG8, as indicated by the many null randomness, and especially independence p-values over the monitoring periods. Exceptions can be observed, for example, in Figs. 257, 258, and 260 in appendix B, section B.3. Randomness and/or independence were not rejected most of the times
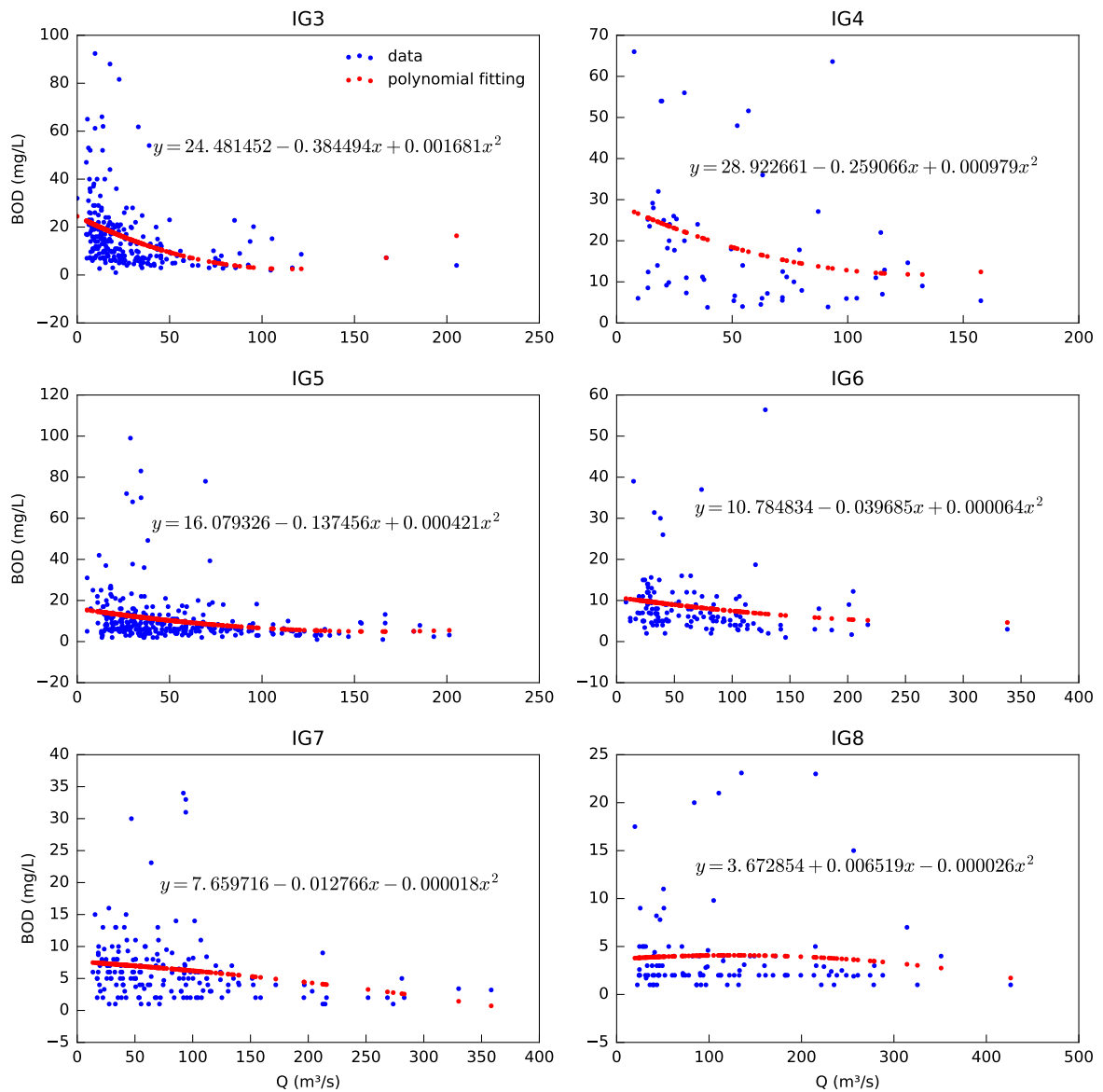
Figure 18 – Estimated flows and standard errors of regression models for stations IG3–IG8

for Q, C , and W, possibly due to fewer observations and larger gaps than in other time series, or also due to a real more random nature of the variables TP and DO at stations IG7 and IG8. The increase of randomness at more downstream stations can be justified by the increase of the watershed area and the quantity and diversity of processes that influence water quality. Indeed, it can be observed that there is higher randomness and independence p-values at more downstream stations as IG7 and IG8, not only for TP or DO, but also for BOD and NH4. At IG5, the randomness p-values are equal to 0.00 in almost the entire period, except before 2006 and between 2011–2014 for the photos (p-values ranging between 0.05–0.25). The greater randomness of the photos is expected due to the larger gaps of time between measurements. Regarding autocorrelation, the photos and movies of Q had similar behaviors, and this is also valid for stations IG3–IG8. The
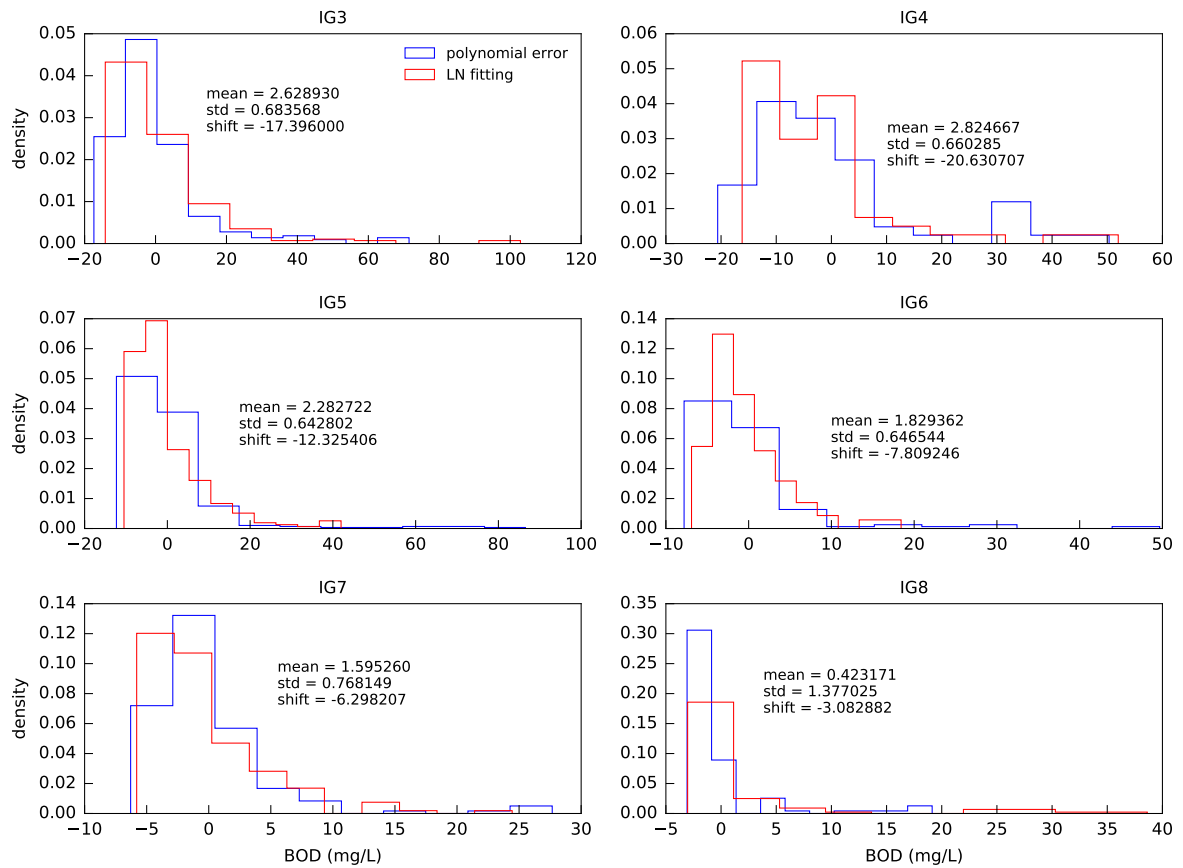
Figure 19 – Fitting of a 3 parameter-lognormal distribution to the errors of the regression models for BOD at stations IG3–IG8

p-values of original and synthetic movies were 0.00 in all the times as a result of the daily time scale and high 1st lag correlation coefficient of the Mar(1) model. The rejections in the Q photos indicate that the flows from IG3 to IG8 have seasonal behavior or other cyclic fluctuations with period higher than a day. However, the p-values from Q photos are higher than for the Q movies (> 0.05 many times), showing that these higher-period cyclic fluctuations are smoother than in the daily scale.

The results from the Q photos and movies regarding homogeneity and stationarity varied differently over time. The photos are expected to behave similarly to the original daily flows since they came from the movie. However, the results were different most of time. For example, the homogeneity and stationarity p-values of Q original movie were 0.00 from 2010 to 2017 while for the photos varied between 0.00–1.0 and 0.2–1.0 for homogeneity and stationarity respectively. It highlights the sensibility of these statistical tests to the number of observations and the lack of representativity in the irregular-frequency data regarding time series properties (RHIS). The original Q movie and the photos (1st row/column in Fig.21) varied similarly over time, but many peaks are missing in the photos. Clearly, there is considerable loss of information in the irregular-frequency data, leading to false conclusions about the presence of trends and/or shifts. The Q photos
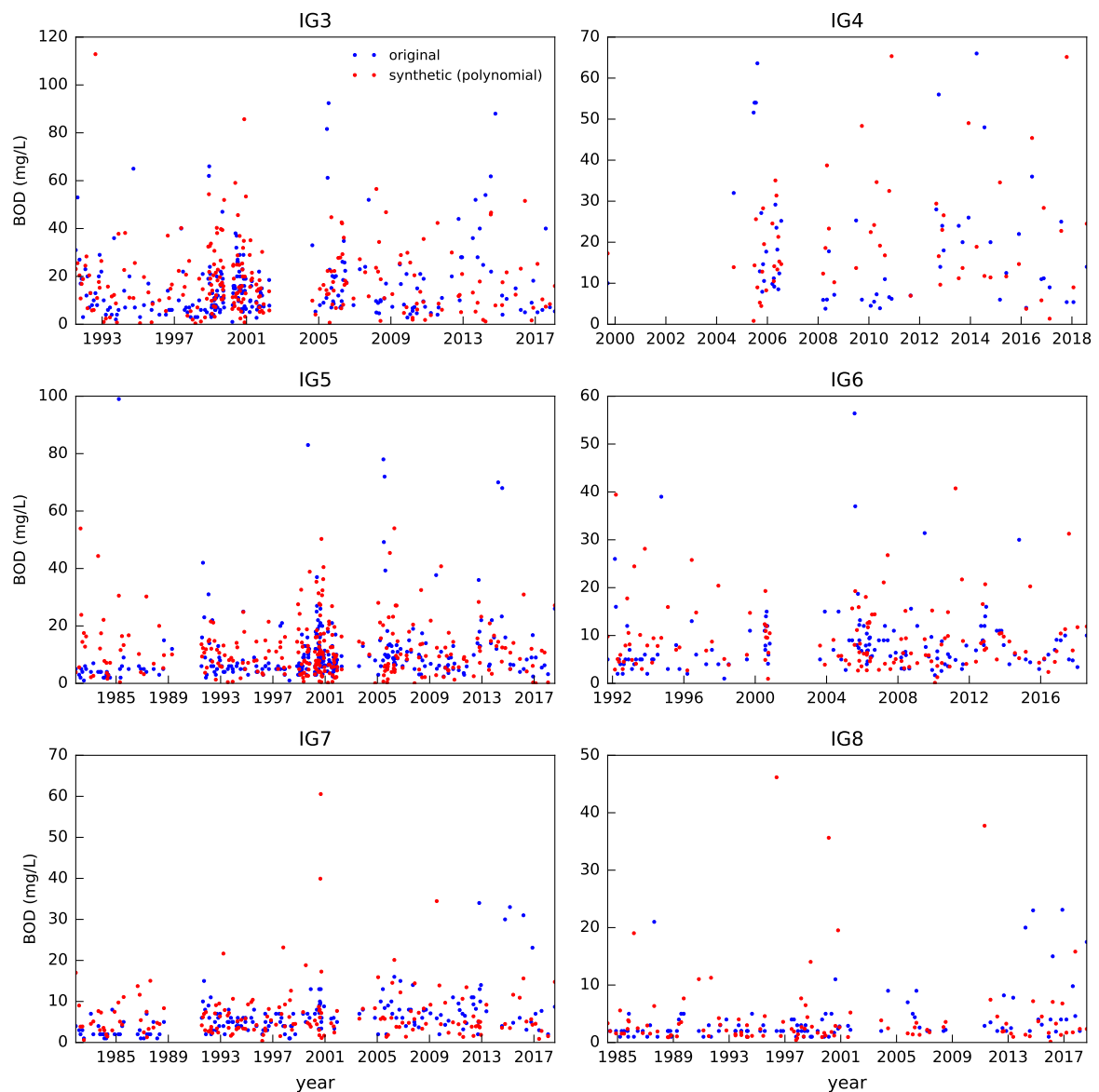
Figure 20 – Original and estimated concentrations from the regression model for BOD at stations IG3–IG8

associated to the other variables (NH4, TP, and DO) reinforce this findings working as different samples from the same daily flows, since not all variables were monitored on the same dates. In the appendix B section B.3, it can be observed, for example, in the randomness test results in Figs. 249 and 255. Randomness started to be rejected around 2011 for the NH4-associated Q photos, and in 2009 for the TP-associated Q photos.

The results from the complete time series of BOD, NH4, TP, and DO-associated Q photos at IG5 indicate that cyclic fluctuations are present (p-value $\approx$ 0.00 in randomness and independence tests), but not trends or shifts (p-value = 0.75 in homogeneity and stationarity tests for BOD-associated Q and different values for the NH4, TP, and DO-associated Q photos). From the complete original and synthetic Q movies, cyclic fluc-

tuations (p-value = 0.00 in randomness and independence) were detected. In relation to the synthetic Q movies is important to remember that a different synthetic Q movie was generated for each variable. For example, there is a different Q movie in each one of the Figs. 243, 249, 255, and 261. Hence, while the results from homogeneity and stationarity tests in the original Q movies is unique (the same in the 4 figures from each station), each station is related to 4 different synthetic Q movies. Interestingly, trends were detected many times over the monitoring period in the synthetic Q movies of stations IG3–IG8. The synthetic movies are expected to be stationary and homogeneous due to the first-order Markov model assumptions. This realizations of the stochastic process represented by the Markov model show that stationary/homogeneous time series that can take a long time until reach a constant stationarity/homogeneous status. For the complete time series, trends and/or shifts were detected only in the original Q movie (p-value = 0.00 in stationarity), also in the other stations.

The behavior of the RHIS tests from C and W is similar to the one from Q, i.e., rejection of randomness and independence, and high variability of homogeneity and stationarity. At station IG5 for BOD, the main difference is that the rejections started later, especially for C (2014). On the photos, it reflects the more random nature of C since each point is a direct measurement of the water quality. On the original C movie, it reflects the autocorrelation of the original daily flows (inputs of the regression) and the randomness introduced by the error of the regression model (RM). The autocorrelations of the original flows were transfered to the original daily concentrations through the Mar(1) model, but with less intensity due to the randomness introduced by the RM. This lagged rejection of randomness and independence for C can be observed for all other stations and variables. Regarding homogeneity and stationarity on C, it must be noticed that rejections occurred many times for the synthetic movie, as for the flows, showing that an even more random process, jointly represented by a first-order autoregressive model and a RM, can be considered non-homogeneous and/or non-stationary. This is the case, for example between 2009–2011 when the synthetic movie p-values of homogeneity and stationarity were 0.00, indicating the presence of a trend and/or shift. The multiplication of the synthetic Q movie by the synthetic C movie to produce the synthetic W movie gave rise to a highly non-random, non-homogeneous, dependent, and non-stationary time series in the case of BOD at IG5. The W synthetic movie p-values converged to 0.00 for RHIS since 2006, with an exception for homogeneity between 2012–2014. This constant convergence to 0.00 indicate "strong" variability patterns, according to the results of previous analyses on water quality photos, in section 4.1. However, it seems more like an exception than a rule since it cannot be observed at other stations and variables. It indicates that this multiplication process of a synthetic Q movie by a synthetic C movie may give rise to synthetic W movies with "strong" variability patterns. The original W movie reflects the variability patterns of the original Q movie (cyclic fluctuations, trend

and/or shifts), i.e., few p-value peaks (= 1.00) in the beginning and between 2008–2010, and with p-values constantly equal to 0.00 since 2010 indicating a "strong" trend.

The next step in this discussion is about the divergences among photos and movies in relation to the presence of different variability patterns, and how it justifies or not the use of autoregressive and regression models to generate regular-frequency time series of C and W. Can non-stationary and/or non-homogeneous time series be represented by stationary/homogeneous stochastic processes, as the first-order Markov model or another autoregressive model AR(p)? Or can the uncertainties and difficulties related to identification and quantification of variability patterns, and "poor" Q x C RM make the generation of continuous C and W time series unfeasible?

Despite the differences related to RHIS, the percentile evolution of the photos, original, and synthetic movies of Q, C, and W remained the same, except for the 95th percentile. For Q, the 5th percentile converged on $\approx$ 20 m³/s, the 50th on $\approx$ 50 m³/s, and the 95th on $\approx$ 160 m³/s. However, the synthetic 95th percentile had influence of the synthetic outliers generated by the Mar(1) model in the beginning of the period (see 1st row/column in Fig. 21), and took the entire period ($\approx$ 14 years) to converge to $\approx$ 160 m³/s. For C, the 5th, 50th, and 95th percentiles converged on $\approx$ 2, $\approx$ 10, and $\approx$ 30 mg/L, respectively. Although, the 95th percentile of the photos of C is higher than the synthetic 95th percentile, the decreasing pattern indicates that it will also converge to $\approx$ 30. It shows there may be a gain in terms of statistics through the use of regression techniques. Possibly, the information about C in the RM, which is dependent on Q, reaches the "true" 95th percentile before the photos due to the much higher number of elements in the daily scale ($\approx$ 14×365). For W, the 5th, 50th, and 95th percentiles converged on $\approx$ 20, $\approx$ 30, and $\approx$ 200 ton/d, respectively.

The convergence of the percentiles can be observed for all stations and variables including even the 95th percentile. An exception can be observed in Fig. 251 in appendix B, section B.3. The 95th percentile of the original and synthetic W movies of NH4 converged to 60 ton/d while the one from the photos to 20 ton/d. Some characteristics that contributed to this divergence are fewer observations than other time series, only one NH4 W photo in the region of higher loads (> 100 ton/d). In general, it can be observed that the 1st-order Markov model can generate time series with much higher flows than the ones in the photos or original movie, which will combine with high concentrations generated by the RM yielding much higher loads than those from the W photos. The most important information is that, even with considerable differences related the presence of trends, cycles, and/or shifts, the photos and movies have the same descriptive statistics, e.g., boxplots, mean, median, duration curves, with higher uncertainty for the higher flows, concentration, and especially loads. One way to avoid the higher uncertainty in the higher loads may be the conception of RM's directly between Q and W. These synthetic

time series should not be used for statistical inference purposes, e.g., trend analysis, since their real variability properties (RHIS) are unknown.

4.2.3 Synthesis

An autoregressive model was used to generate synthetic daily flows from the original time series of daily flows. A regression model (RM) was designed from photos of Q and C to estimate daily C from original and synthetic daily Q, generating original and synthetic daily C. Although not expected on the synthetic movies due to stationarity/homogeneity assumptions of the stochastic processes (Markov and simple linear RM's), "strong" trends, cycles, and/or shifts were detected on these time series. The presence of these patterns indicates that even stationary/homogeneous models can generate time series temporarily non-compliant with RHIS. It is clear that compliance/non-compliance with RHIS is a temporary status.

Despite the differences among photos, in terms of variability properties, original and synthetic movies of Q, C, and W, the results showed that, in a 13-year period, for diverse stations and water quality variables, patterns were not sufficient to produce significant changes in terms of statistical results. The percentiles converged even in the presence of "strong" trends and/or shifts, autocorrelation, and cyclic fluctuations, especially for Q and W. However, these synthetic time series could not be used for statistical inferences as trend analysis because their RHIS status does not represent the reality.

Possibly, if more sophisticated autoregressive and regression models were used, the variability patterns of flows and concentrations could be better represented in the synthetic time series. It could allow the use of statistical inferences. However, it was shown that it would not influence the descriptive statistics observed in the photos.
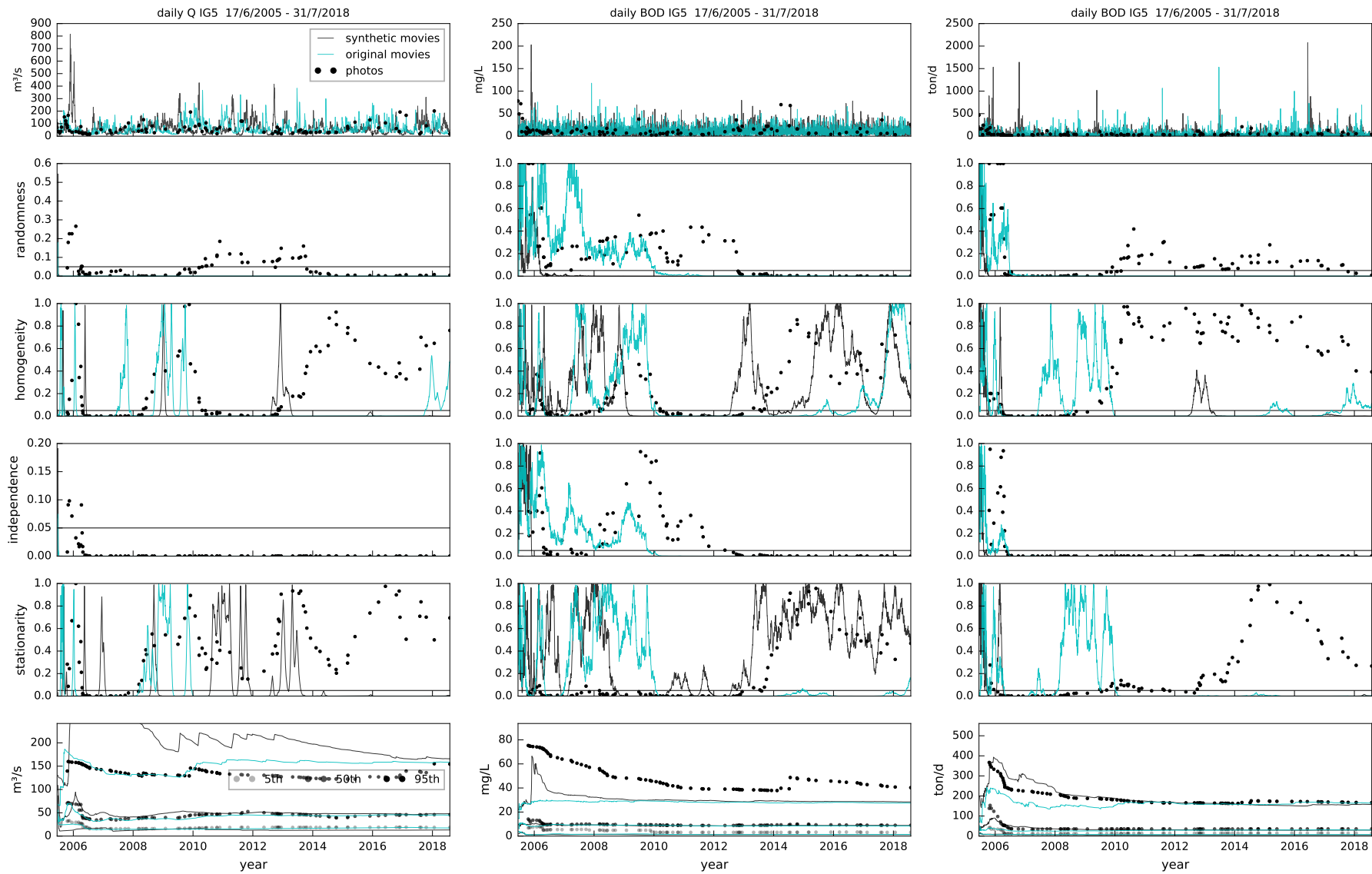
Figure 21 – Evolution of the RHIS p-values and percentiles of Q, C and W, BOD station IG5, photos and daily movies

5 Conclusions

*"Don't make a plan of fighting. That's a very good way to loose your teeth. If
you try to remember you will lose! Empty your mind. Be formless, shapeless,
like water. Put water into a cup, it becomes the cup. Put the water into a
teacup, it becomes the teacup. Water can flow or creep or drip or crash. Be
water, my friend."*

Bruce Lee

The uncertainty related to the representativeness of water resources time series is
the most important for the detection of patterns of variability. Confidence in the existence
and continuity of the observed (or not observed) patterns is affected by this type of
uncertainty. Its reduction can be achieved not only by the increase in sampling frequencies,
which would be costly but also by the analysis of external evidence, e.g., longer and/or
higher frequency time series in the watershed. The joint analysis of Q, C, and W can
improve the analysis of the variabilities since much of the variability of C may be controlled
by Q. Adequate interpretation of data variability and statistical results is essential to avoid
wrong decisions, based only on p-values. As an example, the rejection of RHIS in favor of
a "strong" trend (OTS and STS p-values = 0.0) in the homogeneity and stationarity tests
for W (Fig. 15) was caused by the presence of outliers (see Fig. 3).

The use of GUM uncertainty framework (JCGM/WG1, 2008a) and estimates of
uncertainties described in the literature (e.g., Harmel et al. (2006) and McMillan, Krueger
e Freer (2012)) seems to be reasonable in this context. The subjectivity associated to
uncertainty assessment, expression and propagation has little influence on decisions. The
different levels of measurement uncertainty ($\approx$ 10–100%) and different pdf's (uniform,
normal and lognormal) did not change the decisions about significance of trends, cycles
and/or shifts. The efforts to reduce uncertainties in the detection of variability patterns
should be directed towards the development of robust monitoring strategies and adequate
analysis/interpretation of data, instead of more precise measurements.

Fig. 22 summarizes these conclusions. Prior to significance tests, one should ques-
tion the confidence in the existence and continuity of the observed patterns of variability.
If it is low, the reasons and possible actions should be investigated. If it is high, appro-
priate methods should be applied to test for significance. If confidence in methods is low,
one should investigate the existence or need for development of more appropriate ones.
If it is high, the tests should be applied observing the temporal evolution of the results,
as they may also exhibit variability patterns. The closer to 0.0 or 1.0, the less important
are the measurement uncertainties and subjectivity. If the p-values are varying close to
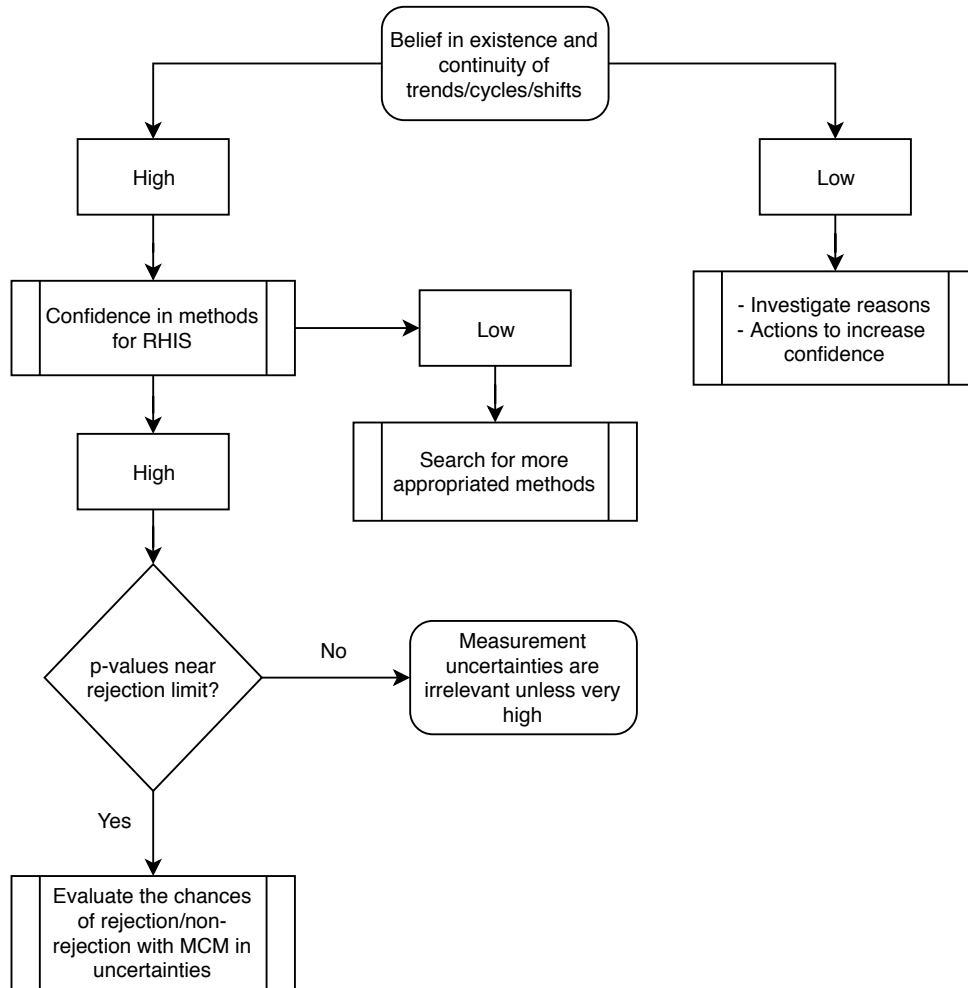
Figure 22 – Summary of conclusions

the rejection limit, the measurement uncertainties may be relevant to the decision. The probabilities of rejecting or not the hypotheses can be evaluated by application of MCM.

In the light of the hypothesis formulated, the stochastic water quality/quantity modeling from daily flows and irregular-frequency times series seems to be a reasonable and reliable option since the main obstacles, caused by irregular frequency and short periods, can be overcome by using regression techniques without compromising statistical characteristics. The stochastic approach used in this research for water quality/quantity analysis, i.e., (1) use of a 1st order autoregressive model (Markov) for the generation of synthetic daily flows; (2) estimation of daily concentrations with a regression model (simple linear polynomial regression) established from irregular flows and concentrations (≈ 200 observation in 13 years) and; (3) multiplication of the synthetic flows and concentrations to determination of daily loads, is the simplest of many possible ways to perform. This approach is expected to introduce the highest errors to the generated daily time series. More appropriate autoregressive and regression models are available in literature. These errors, which are comparable to measurement uncertainties, had no impact on the

BOD, NH4, TP, and DO statistics of stations IG3–IG8, except for the 95th percentiles, and when there was a much smaller period available in the data. The use of more appropriate models would probably reduce this uncertainty in the higher values. It was also demonstrated that the variability patterns of the daily flows will be transferred to the estimated daily concentrations and loads since they can hardly be overcome by measurement and/or regression model uncertainties.

The main reasons for concluding that stochastic water quality/quantity modeling is a more reliable option than deterministic approaches for the planning of water resources are:

- The precipitation, flows, and water quality conditions depend on many diverse factors that cannot be exactly predicted. Thus, it is a stochastic problem;

- Despite the typical poor relation between flows and concentrations (since concentrations depends on many factors beyond the flows), the large number of estimated concentrations, due to the longer periods of the daily flows, makes the concentration and load percentiles to converge to the "true values" (i.e., those from the original photos);

- The identification/qualification/quantification of variability patterns (trends, cycles, and/or shifts) from irregular-frequency and/or short period time series is a highly uncertain task, with high risk of leading to errors. Thus, in these conditions the consideration in both deterministic and stochastic modeling is not recommended;

- If variability patterns are present in the flows and are considered in the stochastic modeling of the flows, they will reflect in the synthetic concentrations (as it should be) despite the error introduced by the regression model;

- The deterministic modeling approaches although highly uncertain due to simplified representations of physical, chemical, and biological systems, usually do not have an established procedure for expressing these uncertainties. However, it could be done in water quality studies through the use of synthetic time series.

5.1 Final reflections

It was demonstrated that the identification, qualification, and quantification of variability patterns in typical water quality time series is a complex task. The short periods, irregular frequency, high variability, and outliers make it highly uncertain. The traditional significance tests are sensitive to small changes in data variability. In Fig. 21, high fluctuations of the p-values, changing from 0.0 to 1.0 with the increase of few

observations, could be observed. The consideration of trends, cycles and/or shifts in statistical/stochastic modeling practices for the planning of water resources requires careful analysis of the time series in the watershed. The decision about significance should be based on diverse factors beyond the p-value of a statistical test, e.g., visual impressions of variability patterns, the presence in other time series in the watershed, expert judgment. Water quality conditions cannot be evaluated by one parameter, but by a set of parameters typically included in water quality indexes. The parameters that represent organic matter inputs, e.g., BOD, NH4, DOC, DO, TP and VDS are expected to present similar temporal and spatial variabilities since they are generally affect by the same factors. The joint analysis of sets of water quality parameters can provide more reliable results regarding the presence of variability patterns in the time series.

Assuming that the existence/presence of variability patterns can be diagnosed with high confidence in the available time series, a high level of subjectivity/expert judgment would still be needed due to representativeness issues. The actual context of climate change and the uncertainty related to the use of present time series for the future has been extensively discussed in literature (KOUTSOYIANNIS, 2006; MILLY et al., 2008; MONTANARI; KOUTSOYIANNIS, 2014; BEVEN, 2016). The longer the planning period, the less representative the time series may be. Depending on the level of confidence in existence and continuity, ignoring patterns and working with the "raw" variability may be the best practice.

The traditional methods for non-randomness (Runs test), non-homogeneities (Mann-Whitney), non-independence (Wald & Wolfowitz), and non-stationarity (Mann-Kendall) evaluation seem to be highly sensitive to patterns that in fact do not produce significant changes in the statistics, and thus could be ignored. Despite the "strong" variability patterns that were detected in continuous time series but not in the irregular, and vice-versa, the percentiles of both time series converged to the same values. For example, in Fig. 21, the stationarity p-value of the daily loads is constantly 0.00 from 2010 to 2018, while the one from the irregular time series varied between 0.05–1.0 most of the time. Even with considerable differences in variability, the 5th, 50th, and 90th percentiles converged to the same values since around 2006, 2008, and 2010 respectively. It can also be observed in the randomness and homogeneity results. Hence, it can be concluded that the application of traditional tests for RHIS is not sufficient to decide when a variability pattern should be considered in statistical/stochastic analysis. Although patterns may be "strong", it may take several years to make changes in statistical results.

The results from the present research demonstrated that a 13-years period is still short, especially for the percentiles below the 95th which had greater convergence. It means that for water resources planning periods shorter than around 20 years, the disregard for variability patterns leads to small differences in statistical terms. This statements

could fail due to a limitation of the assessment made exclusively by the p-values. The p-value can only classify a pattern as statistically significant, but the intensity evaluation is limited by the scale range (0.0–1.0), i.e., a high slope trend and a higher slope trend may yield the same 0.0 p-values. However, the higher slope of a trend, sooner it will cause significant changes in statistics.

The time series of this research represent the influence of typical processes of urban areas in water quality. Possibly, higher seasonality and trends may be found in other regions of the world, e.g., in developed countries where there is a higher financial support for the implementation of water resources management actions and significant statistical changes could occur in shorter periods. In the other hand, in typical urban watershed from developing countries the changes are expected to occur in a slower time step, similar to the Upper Iguassu Watershed. The Upper Iguassu Watershed is located in latitudes of well marked seasonality. Therefore, these are the regions where statistical results should be more influenced by seasonality. However, it could be observed, for example in Figs. 247, 245, that the randomness and independence results for the loads are different among irregular and daily time series. The p-values are 0.00 for the daily BOD time series and varied between 0.05–1.0 for the irregular BOD in almost the entire period, but small differences can be observed in the percentiles.

The results indicate that in the current context of uncertainty concerns in water resources management, the representativeness plays the most important role. The problem of representativeness is not in the past, but in the future, since despite the difficulties in detection of trends, cycles and/or shifts in typical water quality time series, these patterns may probably take a very long time to cause significant changes in statistics. Although it provides more confidence for the use of past-present statistics in the planning of water resources, the current climate change context introduces unknown uncertainties that demand adaptive management actions, as discussed by Groves (2006) and Warmink et al. (2017). The measurement uncertainties associated to the traditional monitoring practices have little importance in the statistical context since they can introduce less impact than trends, shifts, and/or cycles in the variability of time series. Much of the impact will be "dissolved" with the increase of the number of measurements. The water quality time series from traditional monitoring strategies with irregular data usually from sunny working days/hours (8am–6pm), with no data from night time, stormy days, weekends, holidays, and holiday seasons can be used for the planning without high uncertainties related to variability patterns and measurements. However, the descriptive statistics will have uncertainties related to temporal representativeness.

The impact of this research on recent and current studies related to uncertainties, e.g., the DUE (REFSGAARD et al., 2005; BROWN; HEUVELINK, 2007) and the DUET-H/WQ (HARMEL et al., 2006; HARMEL et al., 2009) software tool for mea-

surement uncertainties estimation, is that the subjectivity of uncertainty assessment and expression does not seem to cause significant impacts in the variability of water resources time series. These studies represent a joint effort from the European nations to meet the uncertainty-related requirements in the last version of Water Framework Directive. The present findings allows that literature estimates can be used and expressed by probability density functions defined by expert judgment. The fact is that when these measurement uncertainties are put into a statistical context, they are rapidly merged with the time series variability. In order to develop a code of practice for uncertainty analysis in datasets and modeling outputs, as discussed in (REFSGAARD et al., 2005) and (PAPPENBERGER; BEVEN, 2006), the results indicate that it should start by a qualitative uncertainty assessment of the monitoring strategies and spacial/temporal representativeness of the time series, followed by a quali-quantitative uncertainty assessment of the methods and models, and finally, by the quali-quantitative measurement uncertainty assessment.

The conclusions and final reflections are limited by the assumptions of the proposed method, which are: (i) uncorrelated uncertainties in space and time; (ii) symmetric uncertainties; (iii) no differences related to the uncertainty in different regions of the measurement scales; (iv) 2nd-order polynomial regression between flows and concentrations; (v) representation of daily flows by 1st-order autoregressive Markov model and; (vi) disregard for spacial correlations among flows, concentration and loads. As an example, more realistic approaches could assign higher uncertainties to the extreme regions of the rating curves, since the estimates of flows are more susceptible to errors, as discussed by Coz (2012) and McMillan, Krueger e Freer (2012). An important limitation that may arise when the stochastic approaches are used is the computational power. In these research the water quali-quantitative stochastic analysis with daily times series was performed through the generation of one synthetic time series for each water quality variable, at each station. It was done due to the long time required for the application of RHIS tests with increasing number of observations in the time series.

Future research is needed on spatial and temporal correlations, asymmetric uncertainties, more appropriate autoregressive and regression models to reduce the uncertainty of the higher percentiles, and more appropriate statistical tests (e.g., non-linear trend detection). Also, on means of qualifying variability patterns additionally to the p-value-based decisions since null-p-value patterns can take several years, possibly more than the planning period, to produce significant changes in statistics.

Bibliography

ALODAH, A.; SEIDOU, O. The adequacy of stochastically generated climate time series for water resources systems risk and performance assessment. *Stochastic Environmental Research and Risk Assessment*, 2018. Cited 2 on pages 63 and 68.

ANTTILA, S. et al. Assessing temporal representativeness of water quality monitoring data. *Journal of Environmental Monitoring*, v. 14, p. 589–595, 2012. Cited on pages 29.

ASCOUGH, J. C. I. et al. Future research challenges for incorporation of uncertainties in environmental and ecological decision-making. *Ecological Modelling*, v. 219, p. 383–399, 2008. Cited 2 on pages 27 and 28.

BEN-HAIM, Y.; DEMERTZIS, M. Decision-Making in Times of Knightian Uncertainty: An Info-Gap Perspective. *Economic Discussion Papers*, n. 2015–42, 2015. Cited on pages 27.

BEVEN, K. Facets of uncertainty: epistemic uncertainty, non-stationarity, likelihood, hypothesis, and communication. *Hydrological Sciences Journal*, v. 61, n. 9, p. 1652–1665, 2016. Cited 5 on pages 27, 28, 29, 53, and 110.

BEVEN, K.; BINLEY, A. The future of distributed models: model calibration and uncertainty prediction. *Hydrological Processes*, v. 6, p. 279–298, 1992. Cited 2 on pages 62 and 65.

BEVEN, K.; BINLEY, A. GLUE: 20 years on. *Hydrological Processes*, v. 28, p. 5897–5918, 2014. Cited 2 on pages 30 and 60.

BICH, W. et al. Revision of the 'Guide to the Expression of Uncertainty in Measurement'. *Metrologia*, v. 49, p. 702–705, 2012. Cited on pages 28.

BICH, W.; COX, M. G.; HARRIS, P. M. Evolution of the 'Guide to the Expression of Uncertainty in Measurement'. *Metrologia*, v. 43, p. 161–166, 2006. S. Cited on pages 28.

BOUGHTON, W. C.; MCKERCHAR, A. Generating synthetic stream-flow records for new zealand rivers. *Journal of Hydrology*, v. 7, n. 2, p. 112–123, 1968. Cited on pages 62.

BOX, G. E. P.; JENKINS, G. M.; REINSEL, G. C. *Time Series Analysis Forecasting and Control*. New Jersey: John Wiley & Sons, 2008. Cited 4 on pages 58, 59, 61, and 70.

BRADY, A. et al. *Global Risks 2015*. [S.l.], 2015. Disponível em: <http://reports-.weforum.org/global-risks-2015/>. Cited on pages 27.

BROWN, J. D. Knowledge, uncertainty and physical geography: towards the development of methodologies for questioning belief. *Transactions of the Institute of British Geographers*, v. 29, p. 367–381, 2004. ISSN 0020-2754. Cited on pages 35.

BROWN, J. D.; HEUVELINK, G. B. M. The data uncertainty engine (due): A software tool for assessing and simulating uncertain environmental variables. *Computers & Geosciences*, v. 33, p. 172–190, 2007. Cited 9 on pages 28, 34, 35, 46, 51, 52, 53, 66, and 111.

BRUGNACH, M. et al. Toward a relational concept of uncertainty: about knowing too little, knowing too differently, and accepting not to know. *Ecology and Society*, v. 13, n. 2:30, 2008. Disponível em: <http://www.ecologyandsociety.org/vol13/iss2/art30>. Cited 2 on pages 34 and 35.

COELHO, M. et al. Statistical validity of water quality time series in urban watersheds. *Brazilian Journal of Water Resources*, v. 22, n. 51, 2017. ISSN 2318-0331. Cited 7 on pages 28, 29, 31, 35, 52, 53, and 73.

COMMISSION, E. (Ed.). *Directive 2000/60/EC of the European Parliament and of the Council of 23 October 2000 establishing a framework for community action in the field of water policy.* [S.l.]: European Commission, 2000. Cited on pages 33.

COZ, J. L. *A literature review of methods for estimating the uncertainty associated with stage-discharge relations.* Cemagref, Hydrology-Hydraulics, Lyon, France: [s.n.], 2012. Draft version. Disponível em: <https://pdfs.semanticscholar.org/b685-/243d91acd17a64c3e31ecff08ea39d5b279d.pdf>. Cited 5 on pages 28, 35, 40, 41, and 112.

DETZEL, D. H. M. *Modelagem de Séries Hidrológicas: uma abordagem de múltiplas escalas temporais.* Tese (Doutorado) — F, 2015. Cited 6 on pages 52, 58, 60, 61, 77, and 85.

DIAMANTOPOULOU, M. J.; ANTONOPOULOS, V. Z.; PAPAMICHAIL, D. M. Cascade Correlation Artificial Neural Networks. *Water Resources Management*, v. 21, n. 3, p. 649–662, 2007. Cited on pages 71.

DICKINSON, W. T. *Accuracy of discharge determinations.* Fort Collins, 1967. Cited on pages 40.

DURRANS, S. R.; TOMIC, S. Regionalization of low-flow frequency estimates: an Alabama case study. *Water Resources Bulletin*, v. 32, n. 1, 1996. American Water Resources Association. Cited 2 on pages 29 and 96.

EC. *Water Framework Directive 2000/60/EC.* 2000. European Commission. Cited on pages 27.

FARUK, D. Ömer. A hybrid neural network and ARIMA model for water quality time series prediction. *Engineering Applications of Artificial Intelligence*, v. 23, p. 586–594, 2010. Cited 2 on pages 60 and 63.

FROEHNER, S. et al. Inputs of domestic and industrial sewage in Upper Iguassu, Brazil identified by emerging compounds. *Water, Air & Soil Pollution*, v. 1, n. 4, p. 251–259, 2011. Cited on pages 73.

FULFORD, J. M. et al. Call for collaboration in wmo project for the assesment of the performance of flow measurement instruments and techniques. *Journal of Hydraulic Engineering*, p. 1439–1440, 2007. Cited on pages 40.

GILBERT, R. O. *Statistical Methods for Enviromental Pollution Monitoring.* New York: Willey, 1987. Cited 2 on pages 29 and 52.

GING, P. *Water assessment of south-central Texas: comparison of water quality in suface-water samples collected manually and by automated samplers.* Washington, D.C., 1999. USGS Fact Sheet FS-172-99. Cited on pages 50.

GOODWIN, T. Discharge data. In: LOON, E. V.; REFSGAARD, J. C. (Ed.). *Guidelines for assessing data uncertainty in river management studies.* [S.l.: s.n.], 2005. Cited 6 on pages 41, 42, 43, 44, 45, and 53.

GROVES, D. G. *New methods for identifying robust long-term water resources management strategies for California.* Tese (Doutorado) — Pardee RAND Graduate School, 2006. Disponível em: <http://www.rand.org/pubs/rgs_dissertations/RGSD196-.html>. Cited 5 on pages 28, 30, 34, 35, and 111.

HAGGARD, B. E. et al. Using regression methods to estimate stream phosphorous loads at Illinois river, Arkansas. *Applied Engineering in Agriculture*, v. 19, n. 2, p. 187–194, 2003. Cited 2 on pages 53 and 57.

HAN, K.-Y.; KIM, S.-H.; BAE, D.-H. Stochastic water quality analysis using reliability method. *Journal of the American Water Resources Association*, v. 37, n. 3, 2001. Cited 2 on pages 62 and 66.

HARMEL, R. D. et al. Cumulative uncertainty in measured streamflow and water quality data for small watersheds. *American Society of Agricultural and Biological Engineers*, v. 49, n. 3, p. 689–701, 2006. ISSN 0001-2351. Cited 14 on pages 23, 28, 34, 40, 42, 46, 47, 48, 66, 67, 70, 81, 107, and 111.

HARMEL, R. D. et al. Estimating storm discharge and water quality data uncertainty: A software tool for monitoring and modeling applications. *Environmental Modelling & Software*, v. 24, p. 832–842, 2009. Cited 10 on pages 28, 34, 40, 46, 48, 49, 51, 67, 81, and 111.

HARMEL, R. D.; SMITH, P. K. Consideration of measurement uncertainty in the evaluation of goodness-of-fit in hydrologic and water quality modelling. *Journal of Hydrology*, v. 337, p. 326–336, 2007. Cited on pages 48.

HELSEL, D. R.; HIRSCH, R. M. *Statistical Methods for Water Resources.* 2002. In Techniques of water resources investigation of the United States Geological Survey, Book 4, Hydrologic analysis and interpretation. Disponível em: <http://pubs.usgs.gov/twri-/twri4a3/>. Cited 7 on pages 52, 54, 55, 56, 57, 84, and 96.

HERSCHY, R. W. Editorial to: Open channel flow measurement. *Flow Measurement and Instrumentation*, v. 13, p. 189–190, 2002. Cited on pages 40.

HIRSCH, R. M.; ARCHFIELD, S. A.; CICCO, L. A. D. A bootstrap method for estimating uncertainty of water quality trends. *Environmental Modelling & Software*, v. 73, p. 148–166, 2015. Cited on pages 29.

HIRSCH, R. M.; MOYER, D. L.; ARCHFIELD, S. A. Weighted regressions on time, dischargea nd season (wrtds) with an application to Chesapeake bay river inputs. *Journal of the American Water Resources Association*, v. 46, n. 5, p. 857–880, 2010. Cited 5 on pages 32, 53, 57, 67, and 71.

HOLMES, M. G. R. H.; ROUND, C.; YOUNG. *Sampling errors in the estimation of mean flow and flow duration statistics from gauged records in the UK. Enhaced Low Flow Estimation Project.* [S.l.], 2000. Cited on pages 43.

HULLEY, M.; CLARK, C.; WATT, E. Low flow frequency analysis for stream with mixed populations. *Canadian Journal of Civil Engineering*, v. 42, n. 8, p. 503–509, 2015. Cited 3 on pages 29, 52, and 53.

ILICH, N. An effective three-step algorithm for multi-site generation of stochastic weekly hydrological time series. *Hydrological Sciences Journal*, v. 59, n. 1, p. 85–98, 2014. Cited on pages 62.

JCGM/WG1. *JCGM 100:2008 GUM 1995 with minor corrections - Evaluation of measurement data - Guide to the expression of uncertainty in measurement.* First. [S.l.], 2008. Cited 5 on pages 27, 28, 64, 80, and 107.

JCGM/WG1. *JCGM 100:2008 GUM 1995 with minor corrections - Evaluation of measurement data - Guide to the expression of uncertainty in measurement.* [S.l.], 2008. Disponível em: <http://www.bipm.org/en/publications/guides/gum.html>. Cited 3 on pages 36, 37, and 39.

JCGM/WG1. *JCGM 104:2009 - Evaluation of measurement data - An introduction to the "Guide to the expression of uncertainty in measurement" and related documents.* First. [S.l.], 2009. Cited 2 on pages 28 and 39.

JUNG, J. Y.; NIEMANN, J. D.; GREIMANN, B. P. Modeling input errors to improve uncertainty estimates for onedimensional sediment transport models. *Stochastic Environmental Research and Risk Assessment*, v. 32, p. 1817–1832, 2018. Cited 2 on pages 27 and 68.

KNAPIK, H. G.; FERNANDES, C. V. S.; BASSANESI, K. Qualidade da água na Bacia do Alto Iguaçu: diferenças conceituais entre os modelos QUAL2E e QUAL2K. *RBRH - Revista Brasileira de Recursos Hídricos*, v. 16, n. 2, p. 75–88, 2011. Cited on pages 73.

KOTLASH, A. R.; CHESSMAN, B. C. Effects of water sample preservation and storage on nitrogen and phosphorus determinations: implications for the use of automated sampling equipment. *Water Resources*, v. 32, n. 12, p. 3731–3737, 1998. Cited on pages 50.

KOUTSOYIANNIS, D. Nonstationarity versus scaling in hydrology. *Journal of Hydrology*, v. 324, p. 239–254, 2006. Cited 5 on pages 29, 53, 59, 60, and 110.

KURUNç, A.; YüREKLI, K.; ÇEVIK, O. Performance of two stochastic approaches for forecasting water quality and streamflow data from Yesilirmak River. *Environmental Modelling & Software*, v. 20, p. 1195–1200, 2005. Cited 3 on pages 29, 63, and 66.

LINDENSCHMIDT, K.-E.; FLEISCHBEIN, K. Structural uncertainty in river water quality modelling system. *Ecological Modelling*, v. 204, p. 289–300, 2007. Cited on pages 34.

LOUCKS, D. P.; BEEK, E. van. *Water Resources Systems Planning and Management.* [S.l.]: Springer, 2017. Cited 3 on pages 60, 61, and 85.

MARTIN, G. R.; SMOOT, J. L.; WHITE, K. D. A comparison of surface-grab and cross-sectionally integrated stream-water-quality sampling methods. *Water Environment Research*, v. 64, n. 7, p. 866–876, 1992. Cited on pages 50.

MCBRIDE, G. B. *Using Statistical Methods for Water Quality Management*. New Jersey: Wiley & Sons, 2005. Cited on pages 29.

MCMILLAN, H.; KRUEGER, T.; FREER, J. Benchmarking observational uncertainties for hydrology: rainfall, river discharge and water quality. *Hydrological Process*, v. 26, p. 4078–4111, 2012. Cited 3 on pages 28, 107, and 112.

MCMILLAN, H. et al. How uncertainty analysis of streamflow data can reduce costs and promote robust decisions in water management applications. *Water Resources Research*, v. 53, p. 5220–5228, 2017. Cited 3 on pages 27, 28, and 68.

MERZ, B.; THIEKEN, A. H. Separating natural and epistemic uncertainty in flood frequency analysis. *Journal of Hydrology*, v. 309, p. 114–132, 2005. Cited on pages 29.

MILLY, P. C. D. et al. Stationarity is dead: Whither water management? *Science*, v. 319, n. 1, 2008. Published by AAAS. Cited 3 on pages 27, 52, and 110.

MONTANARI, A.; KOUTSOYIANNIS, D. Modeling and mitigating natural hazards: stationarity is immortal! *Water Resources Research*, v. 50, p. 9748–9756, 2014. Cited 2 on pages 27 and 110.

MORETTIN, P. A.; TOLOI, C. M. C. *Análise de Séries Temporais*. [S.l.]: Blucher, 2006. Cited 3 on pages 58, 59, and 61.

NAGHETTINI, M.; PINTO, E. J. A. *Hidrologia e Estatística*. Belo Horizonte, MG: Serviço Geológico do Brasil - CPRM, 2007. Cited on pages 52.

NDIONE, D. M.; SAMBOU, S.; KANE, M. L. S. S. Statistical Analysis for Assessing Randomness, Shift and Trend in Rainfall Time Series under Climate Variability and Change: Case of Senegal. *Journal of Geoscience and Environmental Protection*, v. 5, p. 31–53, 2017. Cited 3 on pages 29, 30, and 52.

NOETHER, G. E. Asymtotic properties of the Wald - Wolfowitz test of randomness. *The Annals of Mathematical Statistics*, v. 21, n. 2, p. 231–246, 1950. Cited on pages 83.

PAPPENBERGER, F.; BEVEN, K. J. Ignorance is bliss: or seven reason not to use uncertainty analysis. *Water Resources Research*, v. 42, n. W05302, 2006. Cited 3 on pages 30, 34, and 112.

PELLETIER, P. M. Uncertainties in the single determination of river discharge: A literature review. *Canadian J. Civil Eng.*, v. 15, n. 5, p. 834–850, 1988. Cited on pages 40.

PENDER, D.; PATIDAR, S. Stochastic simulation of daily streamflow sequences using a hidden Markov model. *Hydrology Research*, v. 47, n. 1, p. 75–88, 2015. Cited on pages 63.

PETERSEN-OVERLEIR, A. Accounting for heteroscedacity in rating curve estimates. *Journal of Hydrology*, v. 292, n. 1-4, p. 173–181, 2004. Cited on pages 45.

PINTO, N. L. de S. et al. *Hidrologia basica.* [S.l.]: Edgard Blucher, 1976. Cited 2 on pages 43 and 44.

POLASKY, S. et al. Decision-making under great uncertainty: environmental management in an era of global change. *Trends in Ecology and Evolution*, v. 26, n. 8, 2011. Cited 2 on pages 27 and 28.

PORRAS, E. A. A. et al. Estimation of phosporous emissions in the Upper Iguazu Basin (Brazil) using GIS and the MORE model. *The International Archives of the Photogrammetry, Remote Sensing and Spacial Information Sciences*, XLI-B8, 2016. Cited on pages 73.

PREIN, A. F.; GOBIET, A. Impacts of uncertainties in European gridded precipitation observations on regional climate analysis. *International Journal of Climatology*, v. 37, p. 305–327, 2017. Cited on pages 27.

PROCLAN (Ed.). *Planning process. Commom implementation strategy for the Water Framework Directive, guidance document No. 11.* [S.l.: s.n.], 2003. Cited 2 on pages 27 and 33.

RAMSEY, M. H. Sampling as a source of measurement uncertainty: techniques for quantification and comparison with analytical sources. *Journal of ANalytical Atomic Spectrometry*, v. 13, p. 97–104, 1998. Cited on pages 50.

RAWLINGS, J. O.; PENTULA, S. G.; DICKEY, D. A. *Applied regression analysis: a research tool.* Second. New York: Springer-Verlag, 1998. Cited 2 on pages 54 and 56.

REFSGAARD, J. C. et al. Harmonised techniques and representative river basin data for assessment and use of uncertainty information in integrated water management. *Environmental Science & Policy*, v. 8, p. 267–277, 2005. Cited 10 on pages 27, 28, 33, 34, 35, 46, 52, 66, 111, and 112.

REFSGAARD, J. C. et al. A framework for dealing with uncertainty due to model structure error. *Advances in water resources*, v. 29, p. 1586–1597, 2006. Cited on pages 34.

RODE, M.; SUHR, U. Uncertainties in selected river water quality data. *Hydrology and Earth System Sciences*, n. 11, p. 863–874, 2007. Cited 4 on pages 28, 29, 50, and 53.

RODRIGUEZ-ITURBE, I.; DAWDY, D. R.; GARCIA, L. E. Adequacy of Markovian models with cyclic components for stochastic streamflow simulation. *Water Resources Research*, v. 7, n. 5, p. 1127–1143, 1971. Cited on pages 63.

ROSSI, L. et al. Stochastic modeling of total suspend solids (TSS) in urban areas during rain events. *Water Research*, v. 39, p. 4188–4196, 2005. Cited 2 on pages 58 and 62.

SANTOS, I. dos et al. *Hidrometria aplicada.* [S.l.]: LACTEC - Instituto de Tecnologia para o Desenvolvimento, 2001. Cited 2 on pages 43 and 44.

SAUER, V. B.; MEYER, R. W. *Determination of error in individual discharge measurements.* Washington, D. C.: USGS, 1992. Cited 2 on pages 40 and 48.

SCHIMDT, A. R. *Analysis of stage-discharges relations for open channel flows and their associated uncertainties*. Tese (phdthesis) — University of Illinois, Urbana-Champaign, Ill., 2002. Cited 2 on pages 40 and 41.

SHESKIN, D. J. *Parametric and Nonparametric Statistical Procedures*. Third. [S.l.]: CHAPMAN & HALL/CRC, 2004. Cited 3 on pages 81, 82, and 96.

SIEGEL, S.; JR., N. J. C. *Nonparametric statistics for the behavioral sciences*. [S.l.]: McGraw-Hill, 1988. Cited on pages 81.

SIGEL, K.; KLAUER, B.; PAHL-WOSTL, C. Conceptualising uncertainty in environmental decision-making: The example of the eu water framework directive. *UFZ-Diskussionspapiere*, n. 8, 2008. Cited 2 on pages 33 and 35.

SIGEL, K.; KLAUER, B.; PAHL-WOSTL, C. Conceptualising uncertainty in environmental decision-making: The example of EU Water Framework Directive. *Ecological Economics*, v. 69, n. 3, p. 502–510, 2010. Cited 3 on pages 27, 28, and 30.

TENG, J. et al. Flood inundation modelling: A review of methods, recent advances and uncertainty analysis. *Environmental Modelling & Software*, v. 90, p. 201–216, 2017. Cited 2 on pages 27 and 68.

THOMAS, F. Open channel flow measurement using international standards: introducing a standards programme and selecting a standard. *Flow Measurement and Instrumentation*, v. 13, p. 303–307, 2002. Cited on pages 45.

TIAN, W. et al. A review of uncertainty analysis in building energy assessment. *Renewable and Sustainable Energy Reviews*, v. 93, p. 285–301, 2018. Cited 3 on pages 27, 28, and 81.

TOPPING, J. *Errors of observation and their treatment*. 4th. ed. London, UK: Chapman and Hall, 1972. Cited on pages 48.

UNESCO. *Relatório Mundial das Nações Unidas sobre Desenvolvimento dos Recursos Hídricos: Água para um Mundo Sustentável*. Italy, 2015. Executive summary. Cited on pages 27.

VALIPOUR, M.; BANIHABIB, M. E.; BEHBAHANI, S. M. R. Comparison of the ARMA, ARIMA, and the autoregressive artificial neural network models in forecasting the monthly inflow of Dez dam reservoir. *Journal of Hydrology*, v. 476, n. 2013, p. 433–441, 2012. Cited on pages 63.

WAHLIN, K.; GRIMVALL, A. Uncertainty in water quality data and its implication for trend detection: lessons from Swedish environmental data. *Environmental Science & Policy*, p. 115–124, 2008. Cited 2 on pages 29 and 54.

WALD, A.; WOLFOWITZ, J. An exact test for randomness in the non-parametric case based on serial correlation. *Presented to the Institute of Mathematical Statistics and the American Mathematical Society at a joint meeting at News Brunswick, New Jersey*, 1943. Cited 2 on pages 83 and 96.

WALKER, W. E.; HAASNOOT, M.; KWAKKEL, J. H. Adapt or Perish: A Review of Planning Approaches for Adaptation under Deep Uncertainty. *Sustainability*, v. 5, n. 3, p. 955–979, 2013. Cited on pages 27.

WARMINK, J. J. et al. Coping with uncertainty in river management: Challenges and ways forward. *Water Resources Management*, v. 31, p. 4587–4600, 2017. Cited 7 on pages 27, 28, 30, 34, 35, 68, and 111.

WATECO (Ed.). *Economics and the Environment - The Implementation Challenge of the Water Framework Directive. Commom Implementation Strategy for the Water Framework Directive, Guidance Document No. 1*. [S.l.: s.n.], 2003. Cited 2 on pages 27 and 33.

YAN, H.; ZOU, Z. Application of hybrid ARIMA and neural network model to water quality time series forecasting. *Journal of Convergence Information Technology (JCIT)*, v. 8, n. 4, 2013. Cited 6 on pages 29, 58, 60, 61, 63, and 67.

YUE, S.; PILON, P. Interation between deterministic trend and autoregressive process. *Water Resources Research*, v. 39, n. 4, p. 1077, 2003. Cited on pages 60.

Appendix

APPENDIX A – Data and results from photos

A.1 Time series and boxplots

BOD - IG3
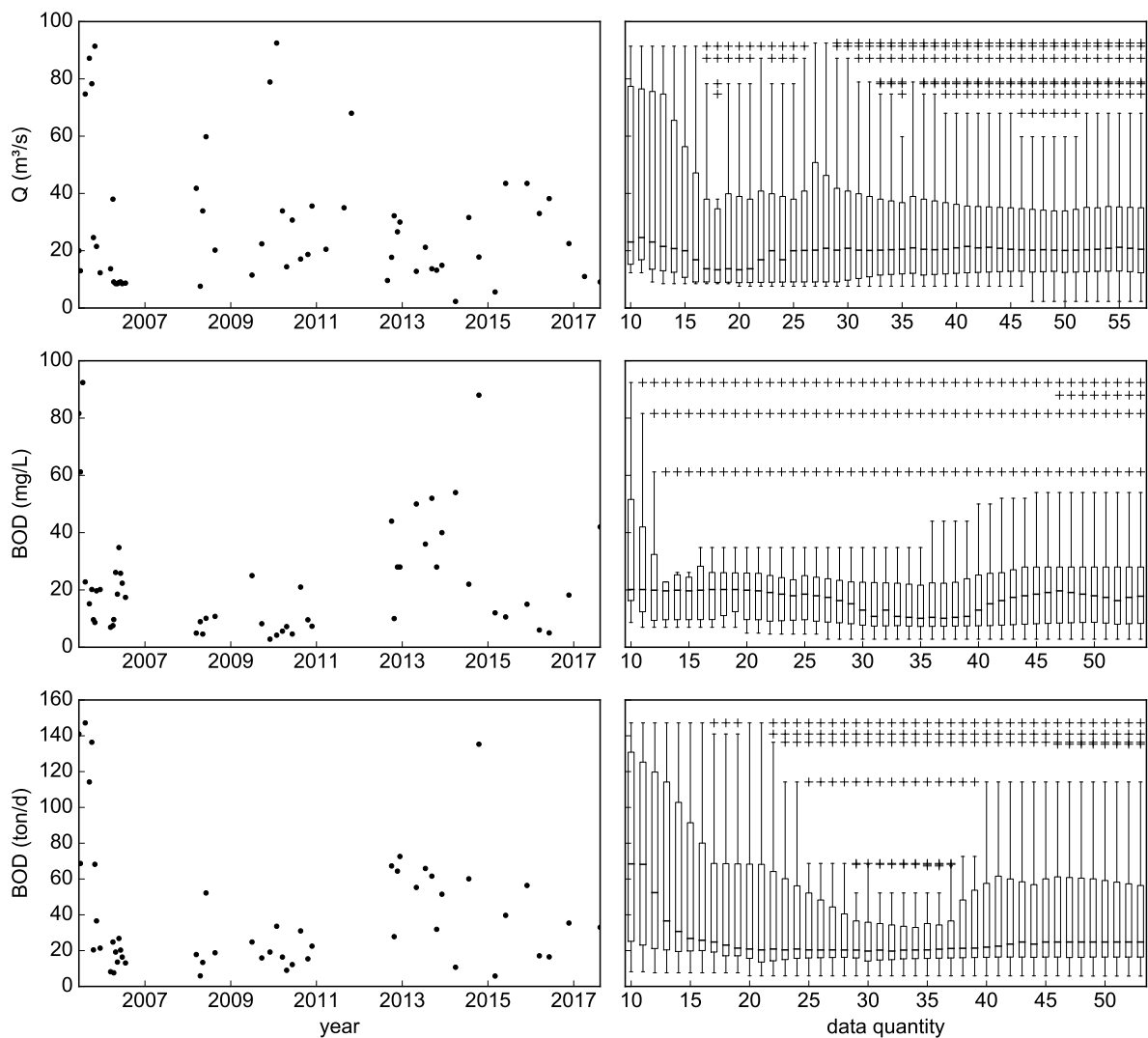
Figure 23 – Time series and boxplot evolution. Q, BOD concentrations and loads, station IG3. Updated boxplots at each data, starting with 10 elements and ending with all data. The boxes show the 25th, 50th and 75th percentiles, the whiskers are the minimum and maximum non-outlier values and the crosses are the outlier values

BOD - IG4
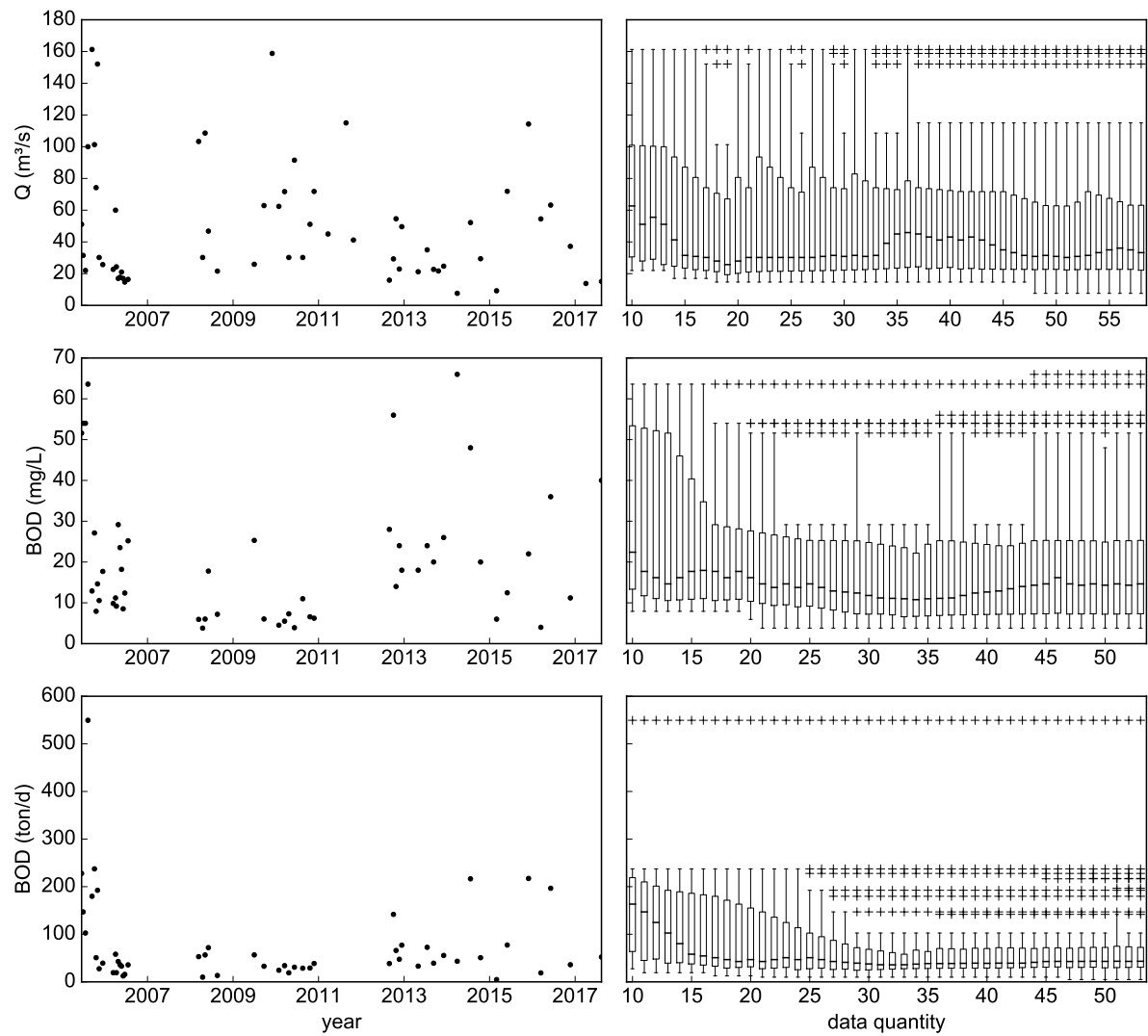
Figure 24 – Time series and boxplot evolution. Q, BOD concentrations and loads, station IG4. Updated boxplots at each data, starting with 10 elements and ending with all data. The boxes show the 25th, 50th and 75th percentiles, the whiskers are the minimum and maximum non-outlier values and the crosses are the outlier values

BOD - IG5
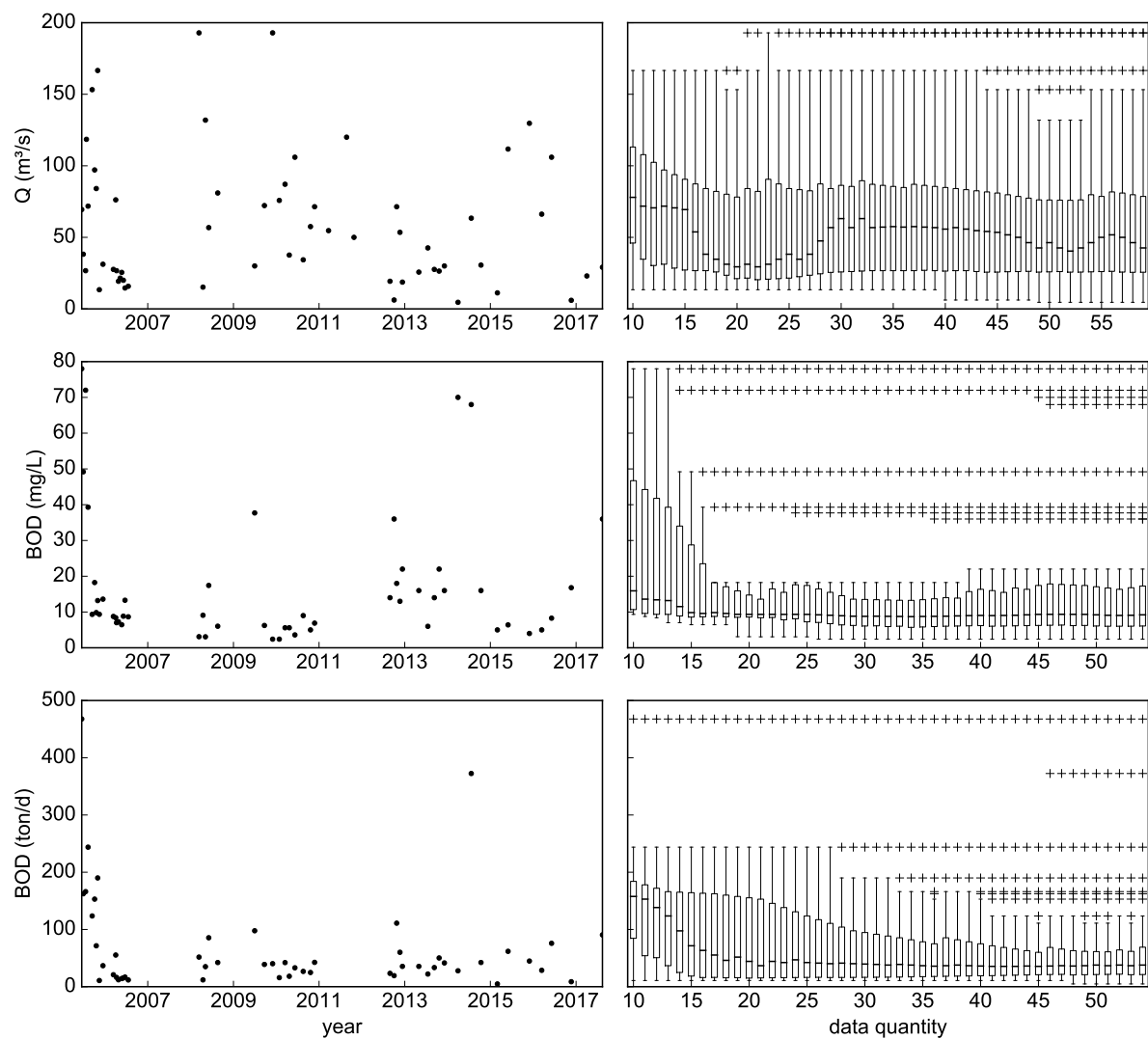
Figure 25 – Time series and boxplot evolution. Q, BOD concentrations and loads, station IG5. Updated boxplots at each data, starting with 10 elements and ending with all data. The boxes show the 25th, 50th and 75th percentiles, the whiskers are the minimum and maximum non-outlier values and the crosses are the outlier values

BOD - IG6
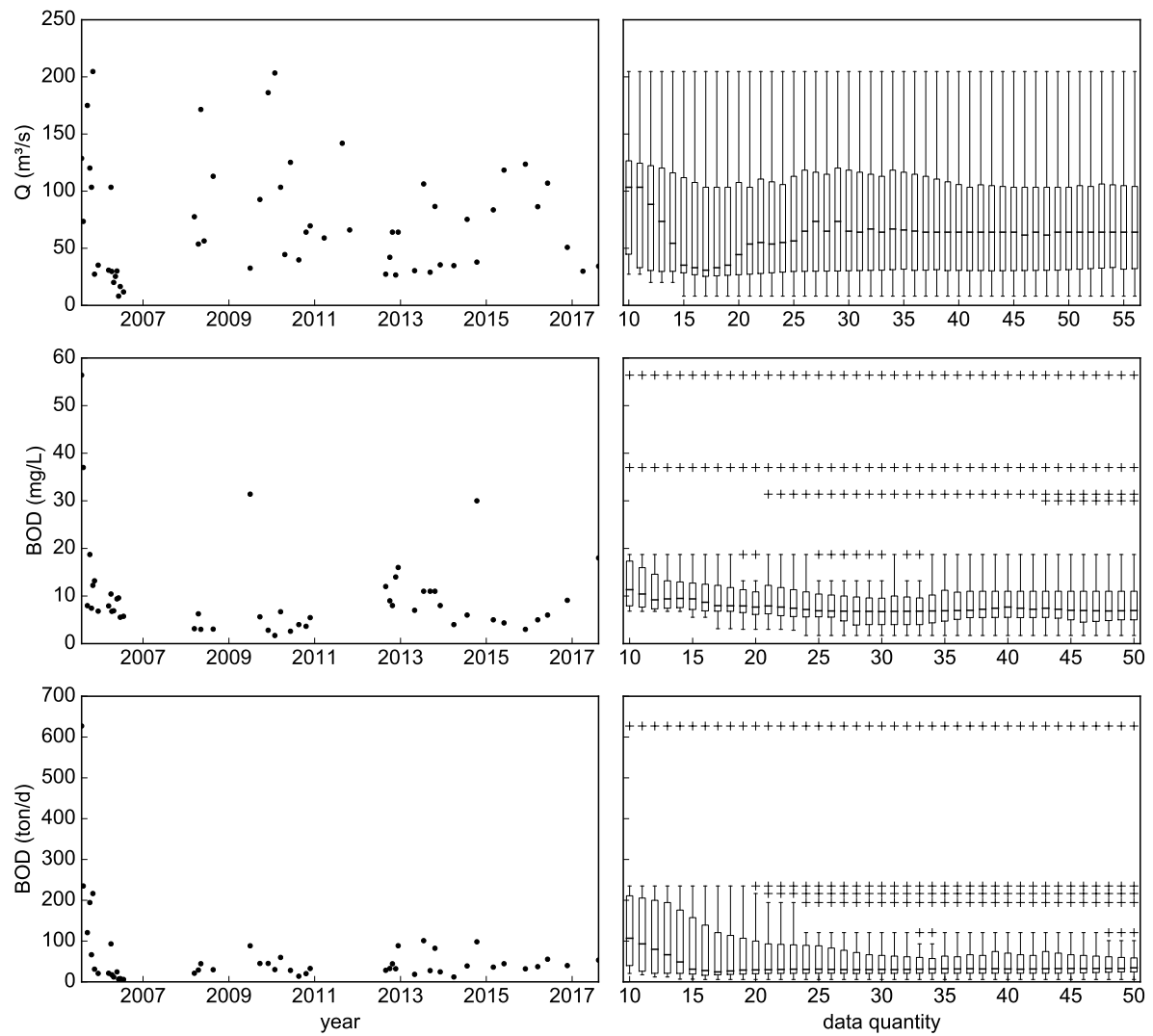
Figure 26 – Time series and boxplot evolution. Q, BOD concentrations and loads, station IG6. Updated boxplots at each data, starting with 10 elements and ending with all data. The boxes show the 25th, 50th and 75th percentiles, the whiskers are the minimum and maximum non-outlier values and the crosses are the outlier values

BOD - IG7
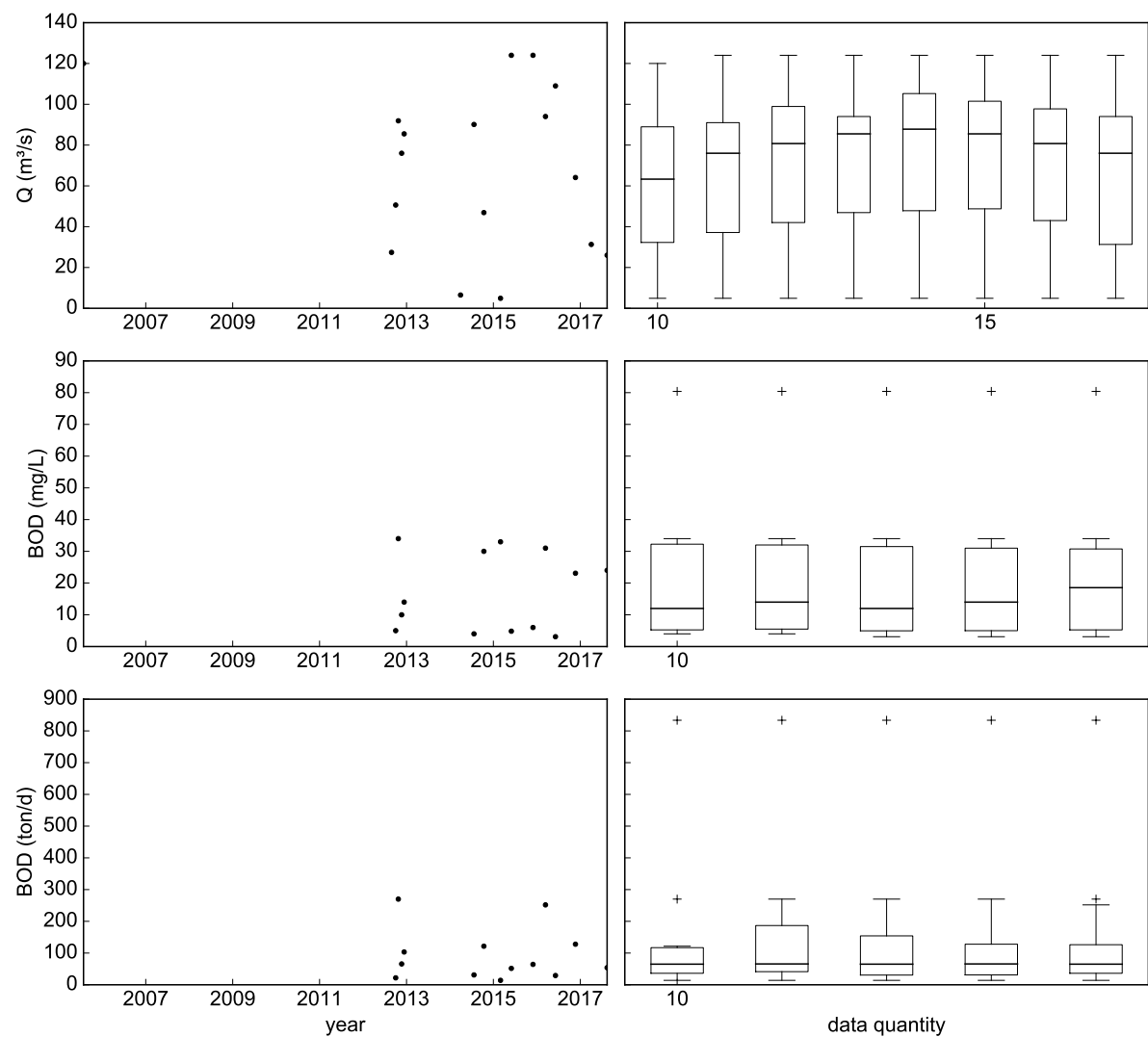
Figure 27 – Time series and boxplot evolution. Q, BOD concentrations and loads, station IG7. Updated boxplots at each data, starting with 10 elements and ending with all data. The boxes show the 25th, 50th and 75th percentiles, the whiskers are the minimum and maximum non-outlier values and the crosses are the outlier values

DO - IG3
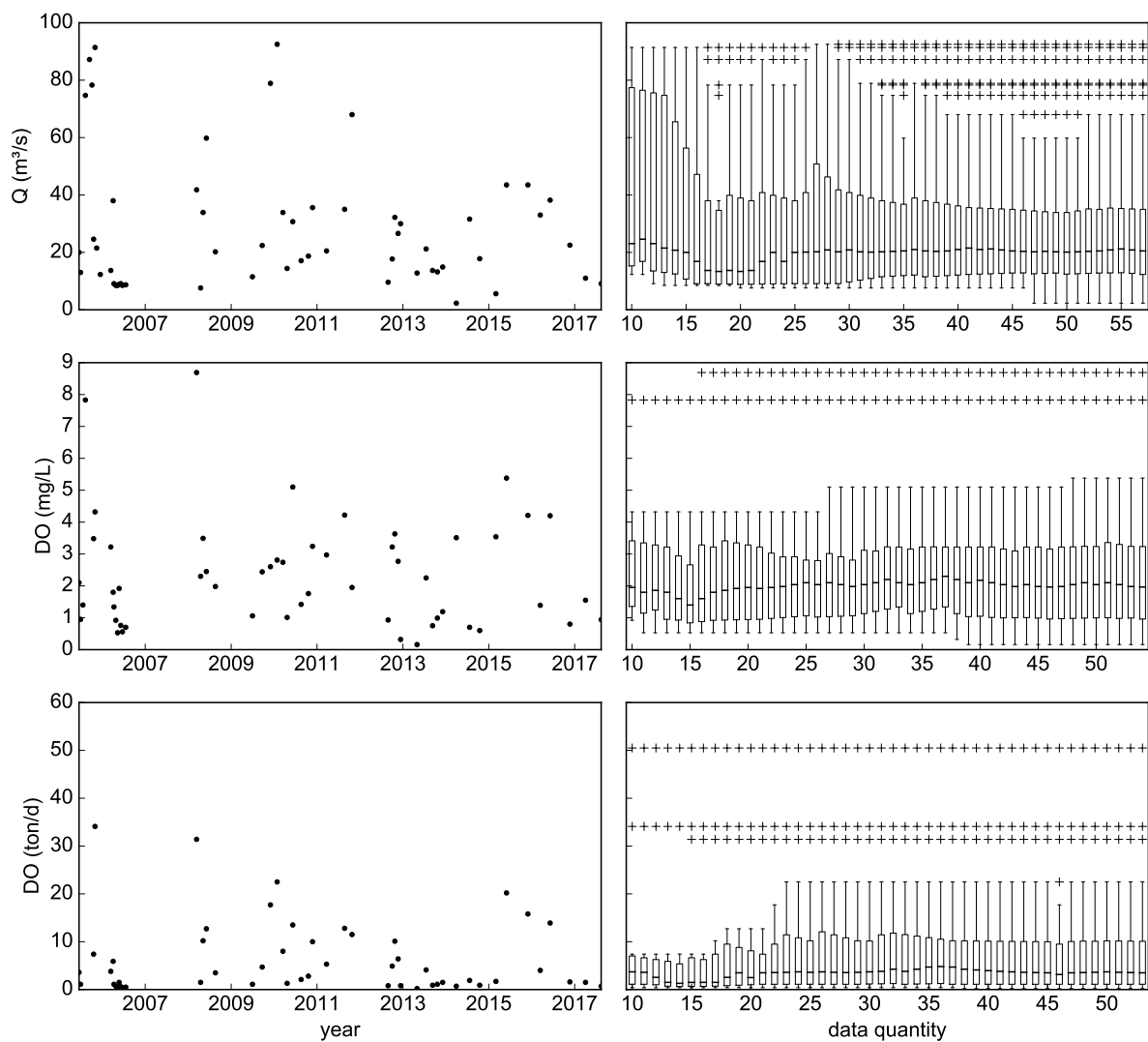
Figure 28 – Time series and boxplot evolution. Q, DO concentrations and loads, station IG3. Updated boxplots at each data, starting with 10 elements and ending with all data. The boxes show the 25th, 50th and 75th percentiles, the whiskers are the minimum and maximum non-outlier values and the crosses are the outlier values

DO - IG4
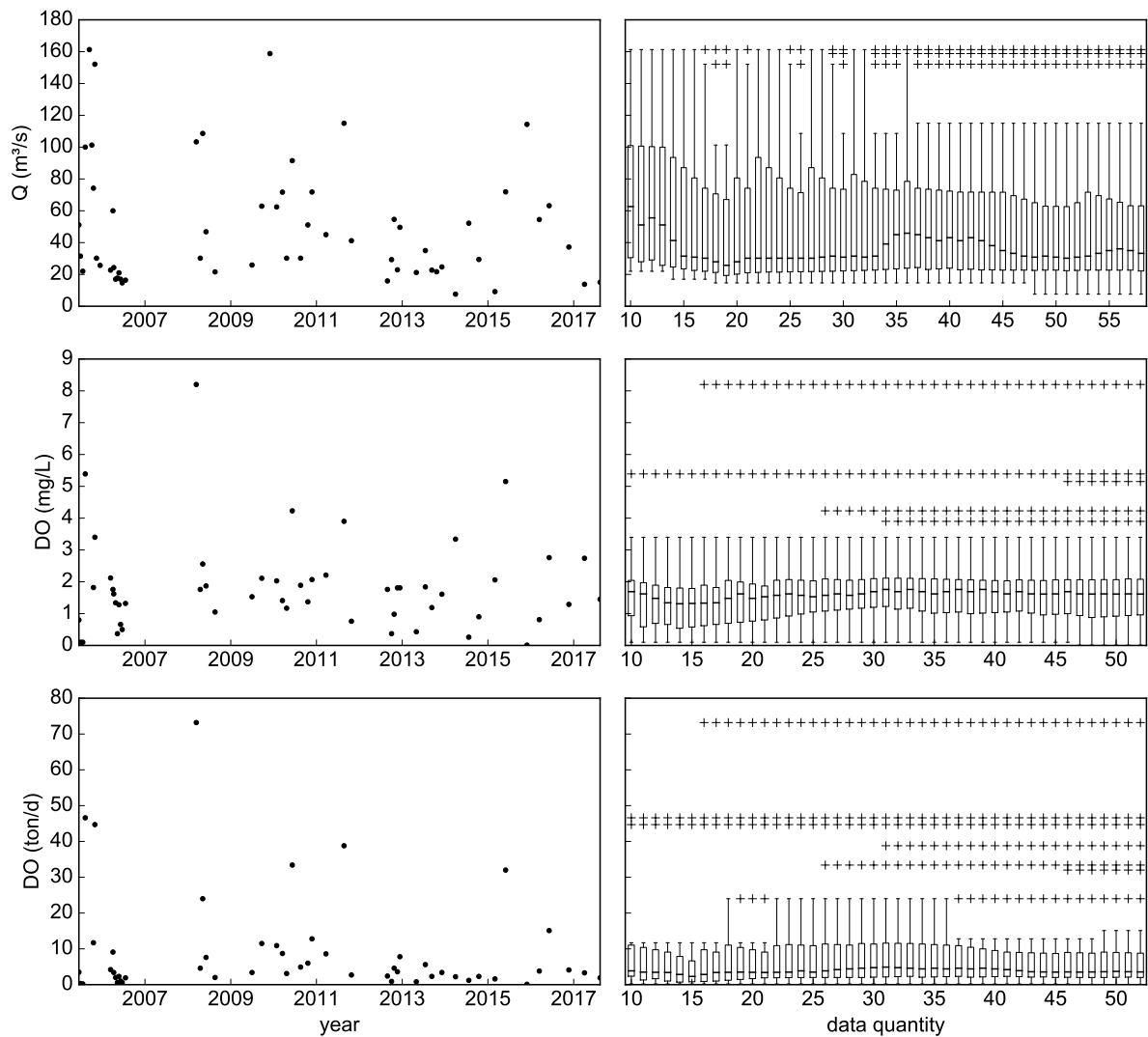
Figure 29 – Time series and boxplot evolution. Q, DO concentrations and loads, station IG4. Updated boxplots at each data, starting with 10 elements and ending with all data. The boxes show the 25th, 50th and 75th percentiles, the whiskers are the minimum and maximum non-outlier values and the crosses are the outlier values

DO - IG5
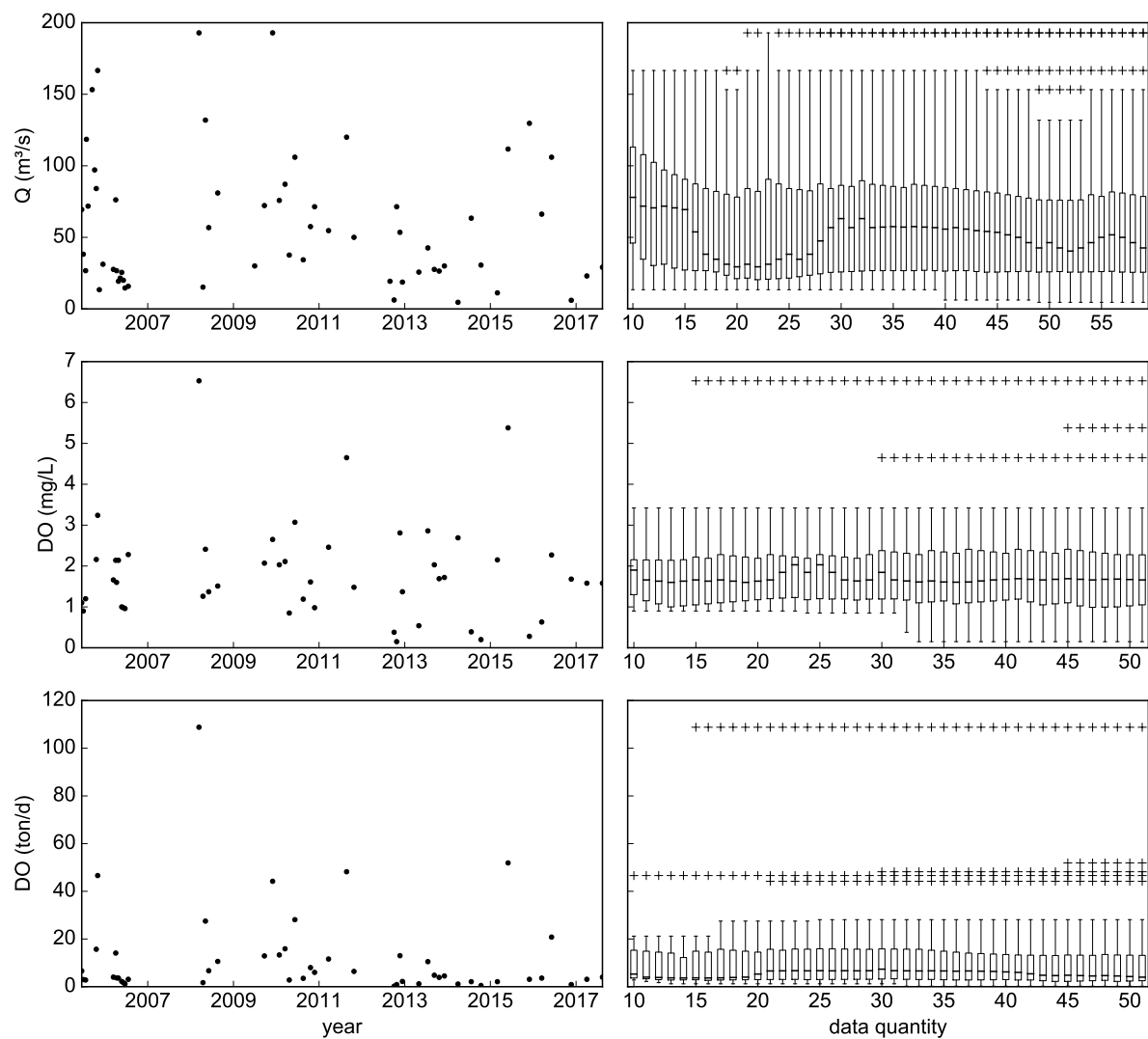
Figure 30 – Time series and boxplot evolution. Q, DO concentrations and loads, station IG5. Updated boxplots at each data, starting with 10 elements and ending with all data. The boxes show the 25th, 50th and 75th percentiles, the whiskers are the minimum and maximum non-outlier values and the crosses are the outlier values

DO - IG6
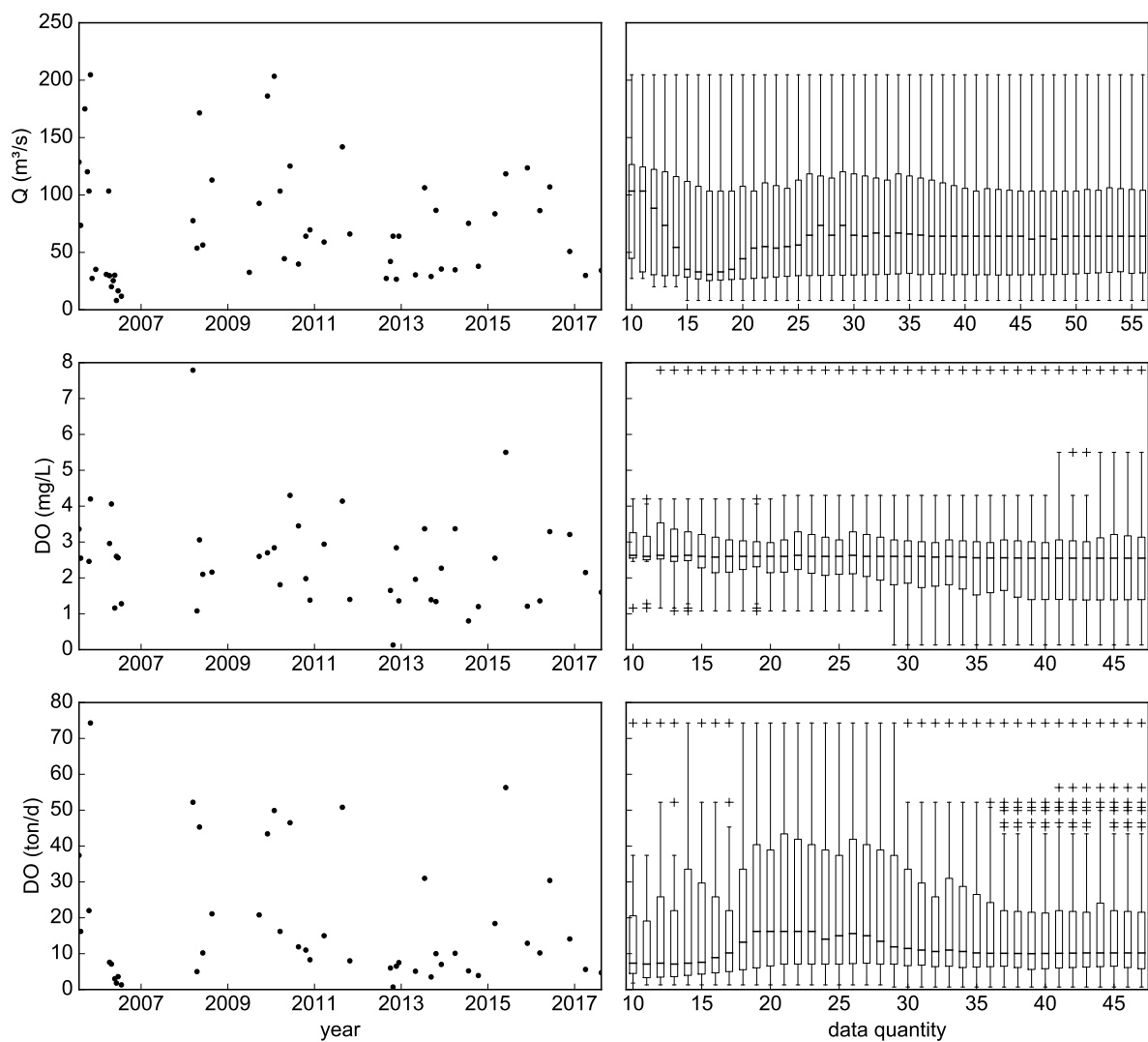
Figure 31 – Time series and boxplot evolution. Q, DO concentrations and loads, station IG6. Updated boxplots at each data, starting with 10 elements and ending with all data. The boxes show the 25th, 50th and 75th percentiles, the whiskers are the minimum and maximum non-outlier values and the crosses are the outlier values

DO - IG7
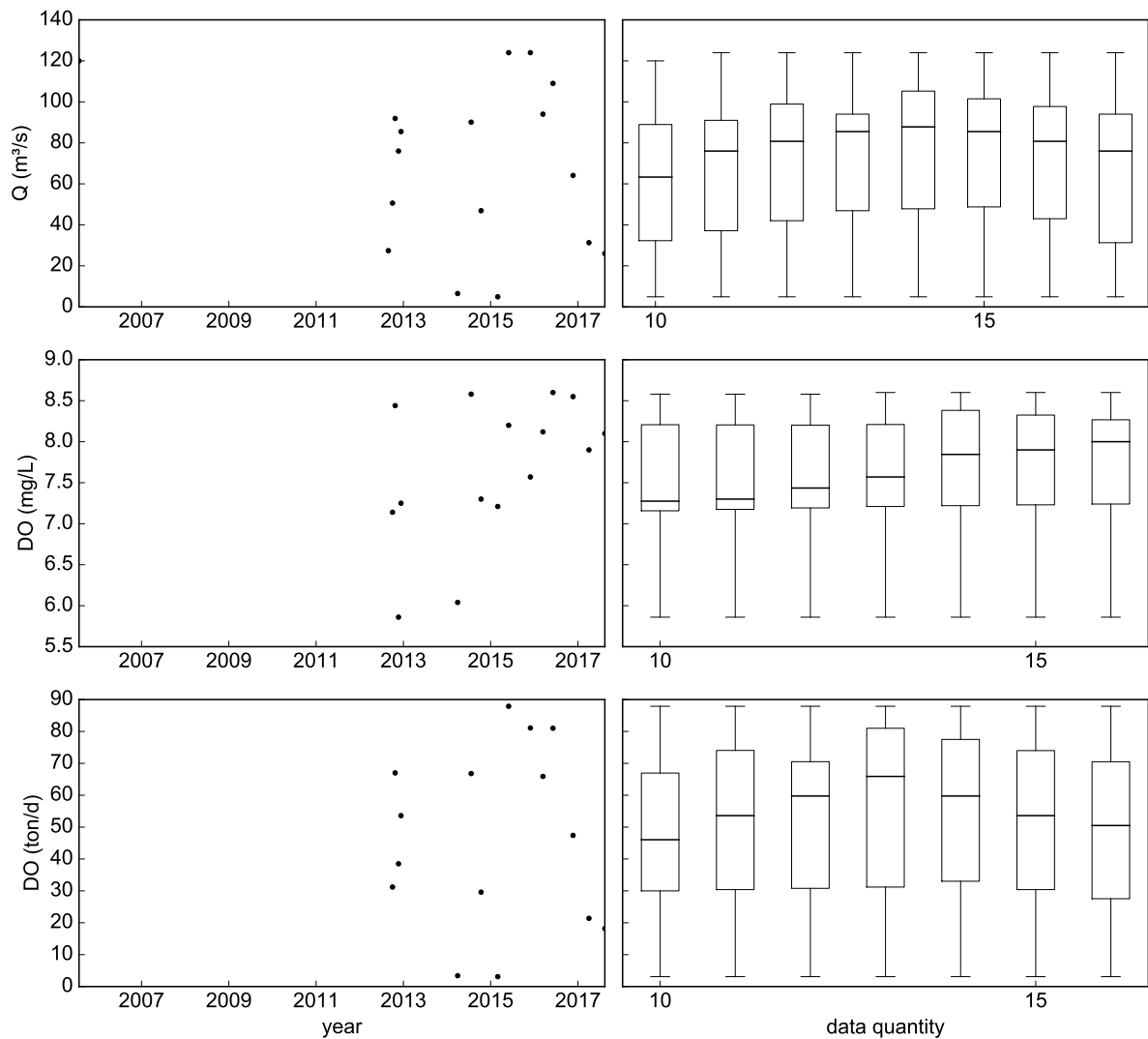
Figure 32 – Time series and boxplot evolution. Q, DO concentrations and loads, station IG7. Updated boxplots at each data, starting with 10 elements and ending with all data. The boxes show the 25th, 50th and 75th percentiles, the whiskers are the minimum and maximum non-outlier values and the crosses are the outlier values

DOC - IG3
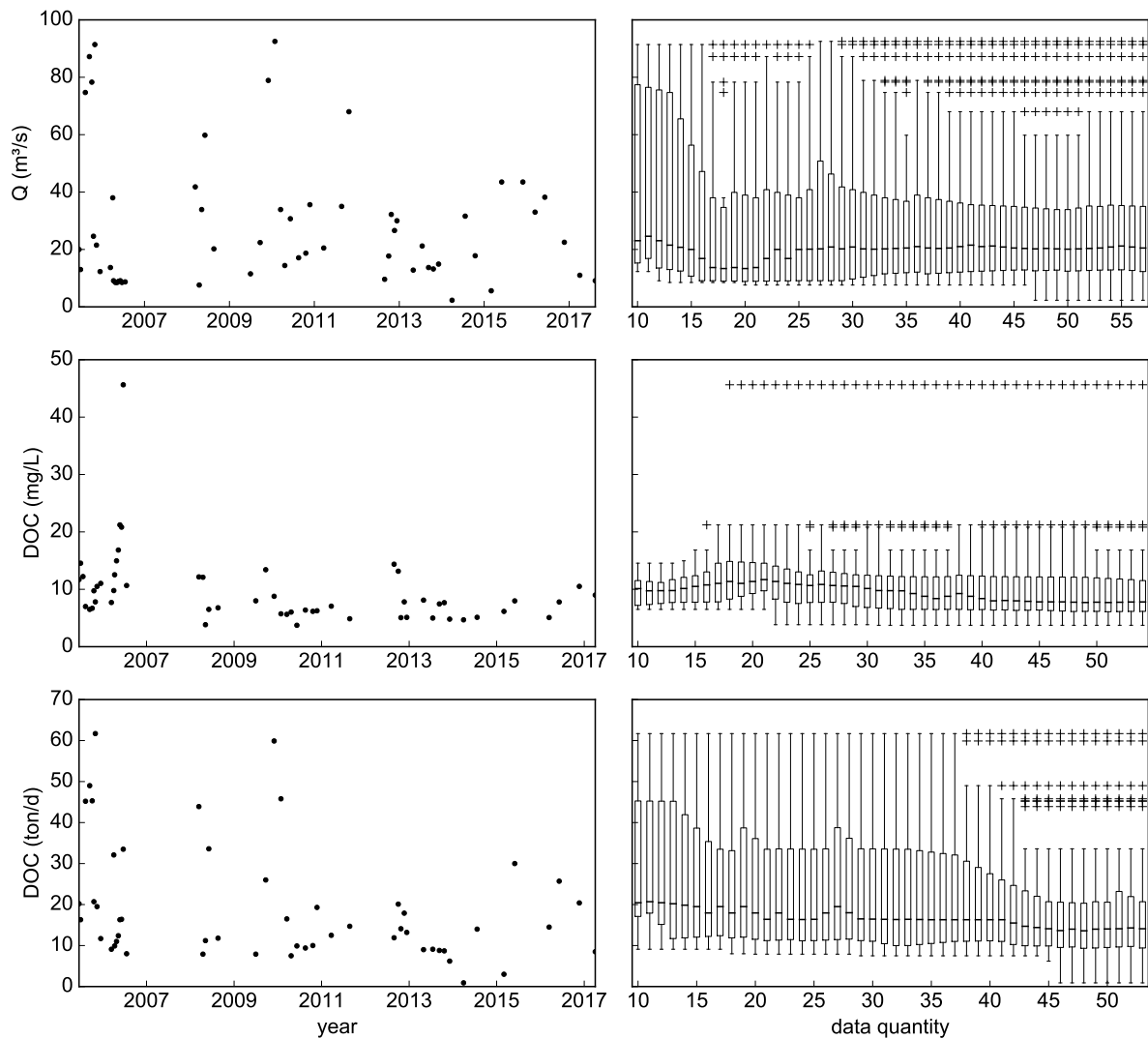
Figure 33 – Time series and boxplot evolution. Q, DOC concentrations and loads, station IG3. Updated boxplots at each data, starting with 10 elements and ending with all data. The boxes show the 25th, 50th and 75th percentiles, the whiskers are the minimum and maximum non-outlier values and the crosses are the outlier values

DOC - IG4
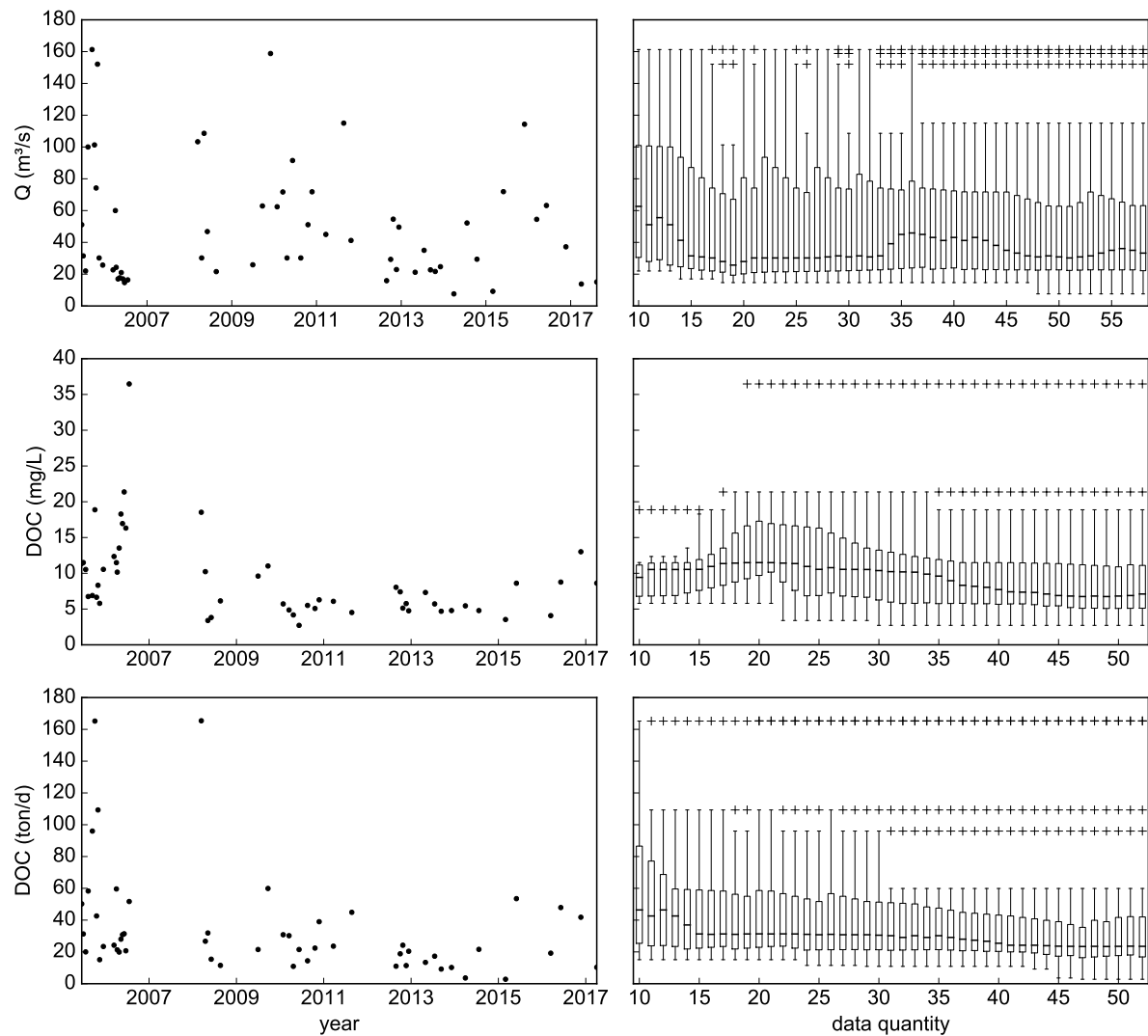
Figure 34 – Time series and boxplot evolution. Q, DOC concentrations and loads, station IG4. Updated boxplots at each data, starting with 10 elements and ending with all data. The boxes show the 25th, 50th and 75th percentiles, the whiskers are the minimum and maximum non-outlier values and the crosses are the outlier values

DOC - IG5
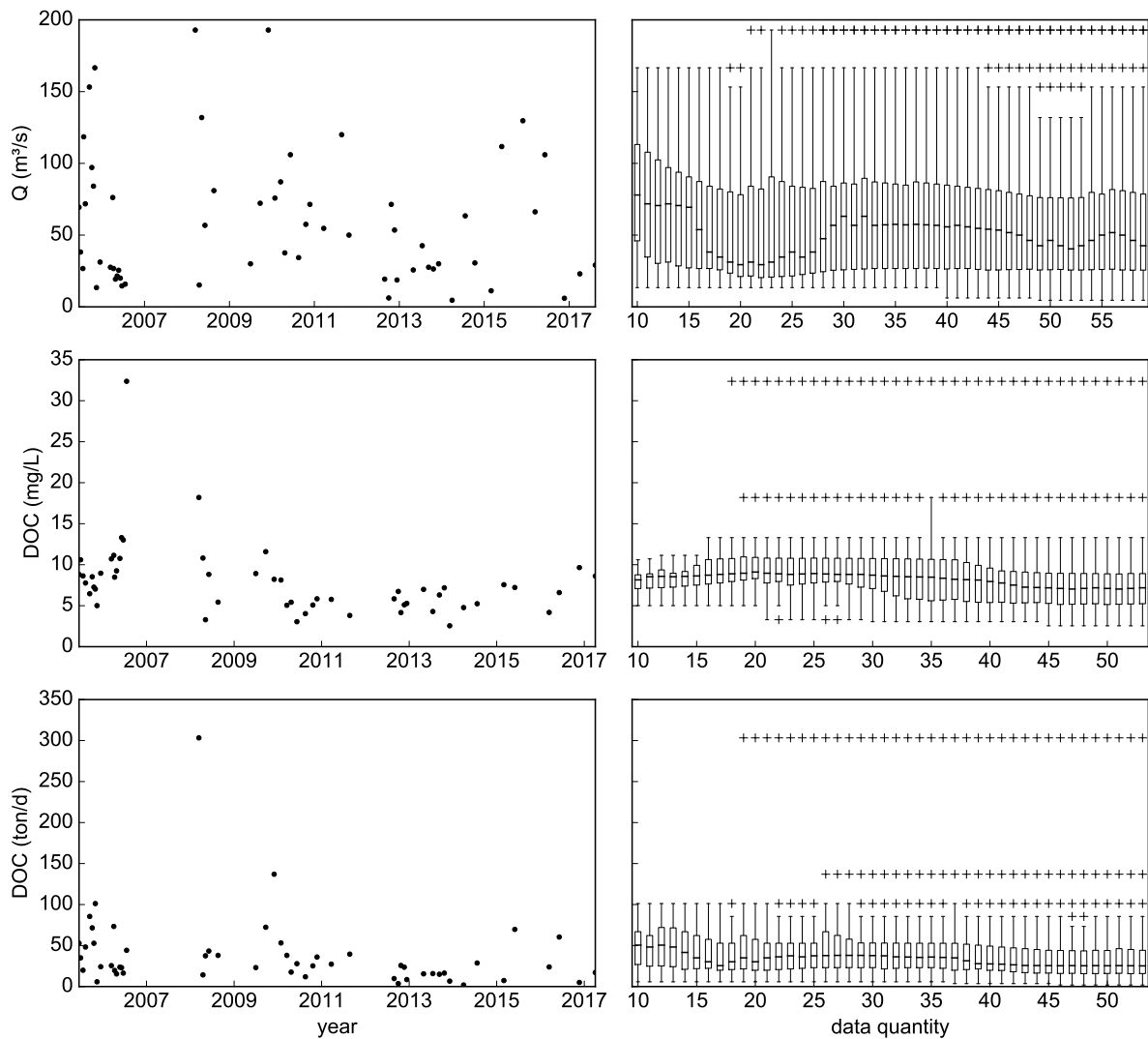
Figure 35 – Time series and boxplot evolution. Q, DOC concentrations and loads, station IG5. Updated boxplots at each data, starting with 10 elements and ending with all data. The boxes show the 25th, 50th and 75th percentiles, the whiskers are the minimum and maximum non-outlier values and the crosses are the outlier values

DOC - IG6
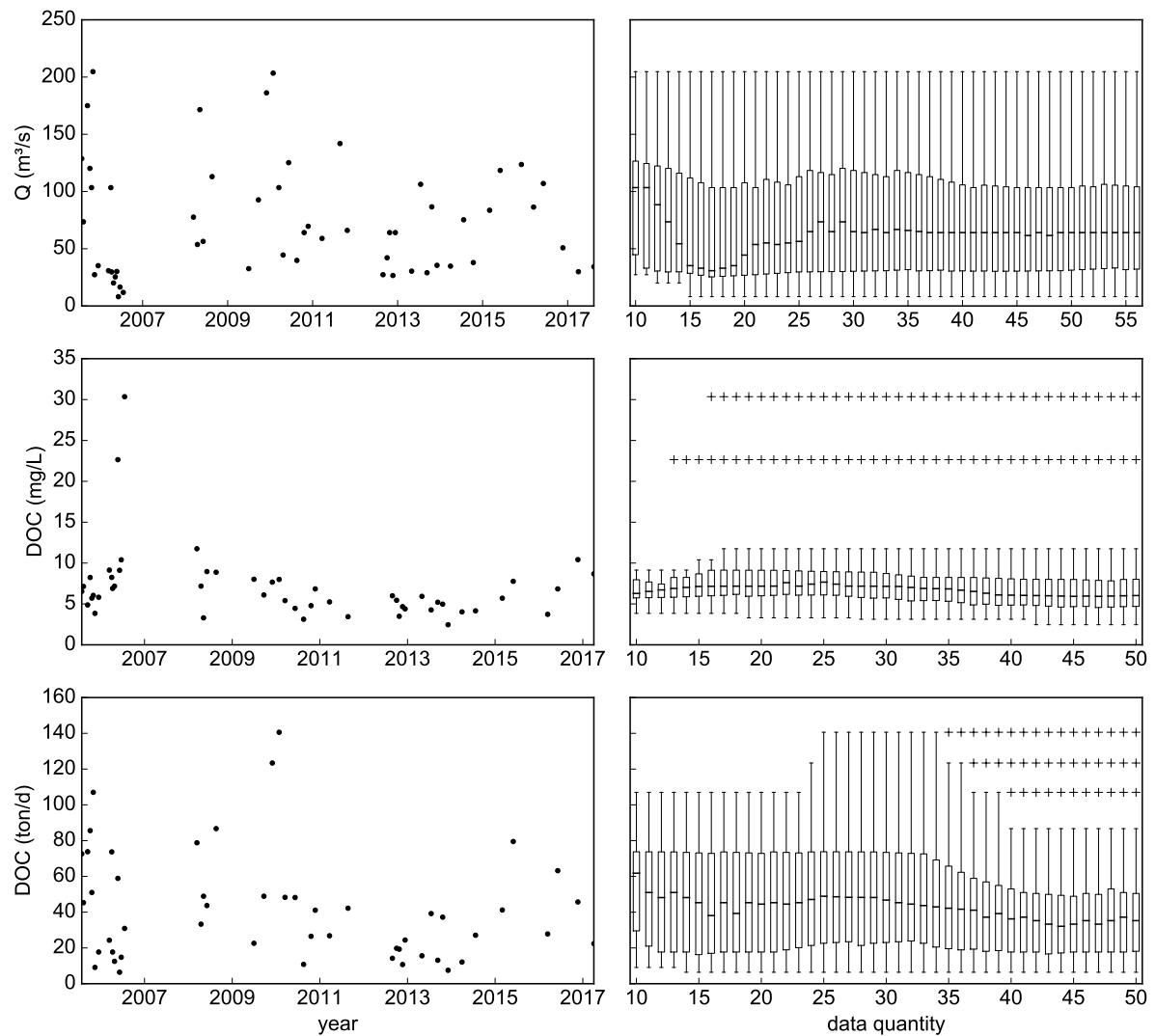
Figure 36 – Time series and boxplot evolution. Q, DOC concentrations and loads, station IG6. Updated boxplots at each data, starting with 10 elements and ending with all data. The boxes show the 25th, 50th and 75th percentiles, the whiskers are the minimum and maximum non-outlier values and the crosses are the outlier values

DOC - IG7
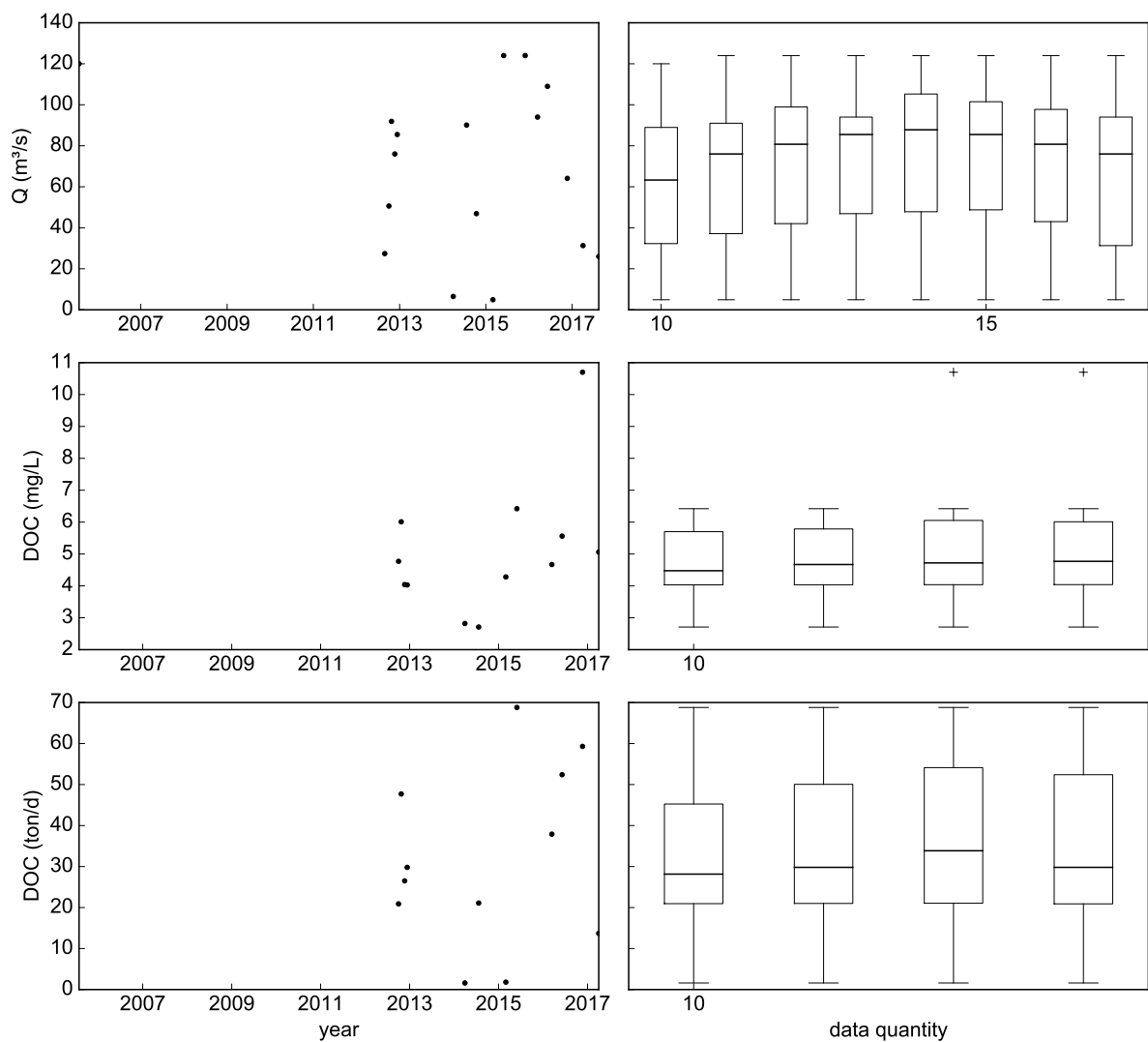
Figure 37 – Time series and boxplot evolution. Q, DOC concentrations and loads, station IG7. Updated boxplots at each data, starting with 10 elements and ending with all data. The boxes show the 25th, 50th and 75th percentiles, the whiskers are the minimum and maximum non-outlier values and the crosses are the outlier values

NH4 - IG3
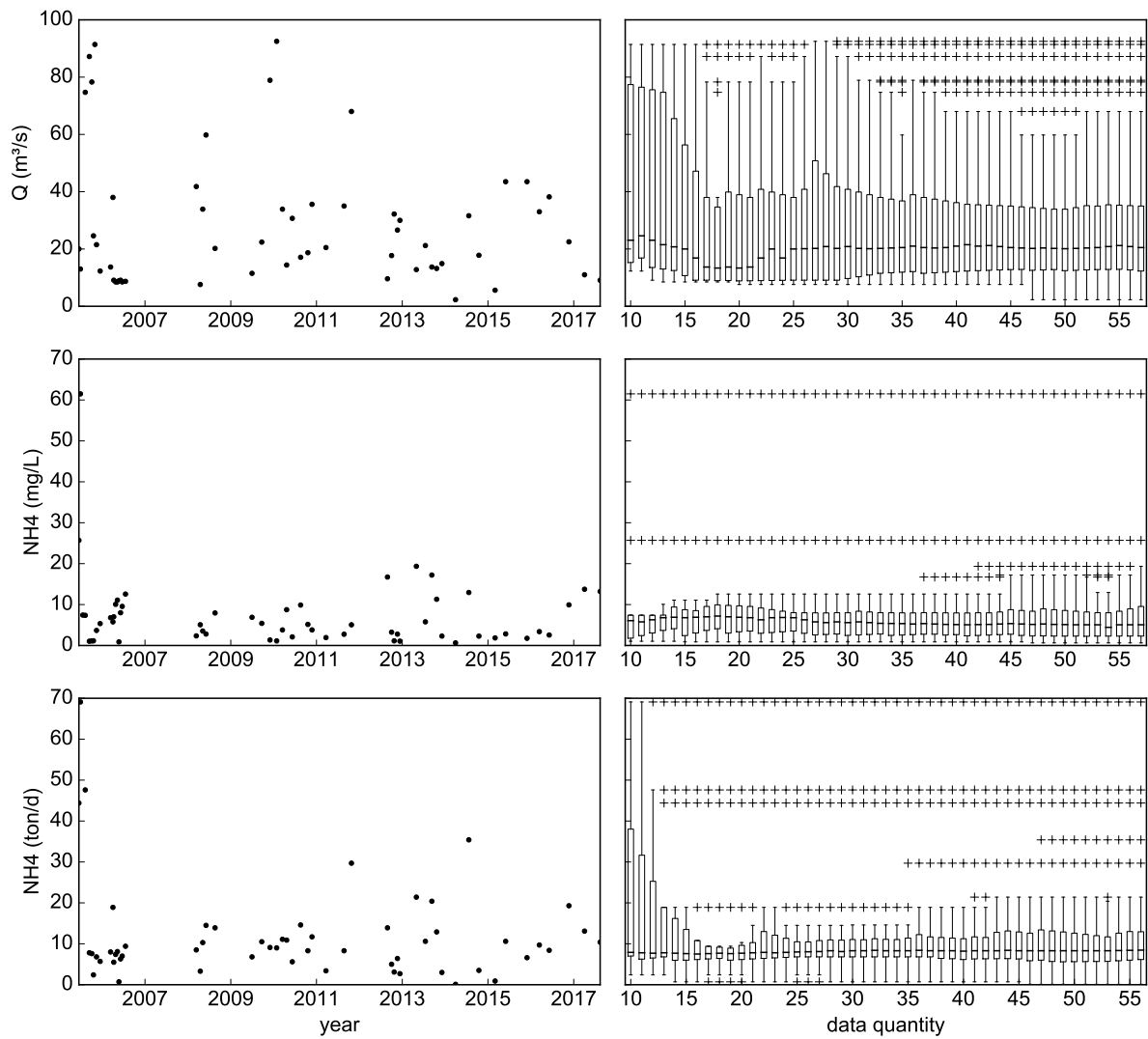
Figure 38 – Time series and boxplot evolution. Q, NH4 concentrations and loads, station IG3. Updated boxplots at each data, starting with 10 elements and ending with all data. The boxes show the 25th, 50th and 75th percentiles, the whiskers are the minimum and maximum non-outlier values and the crosses are the outlier values

NH4 - IG4
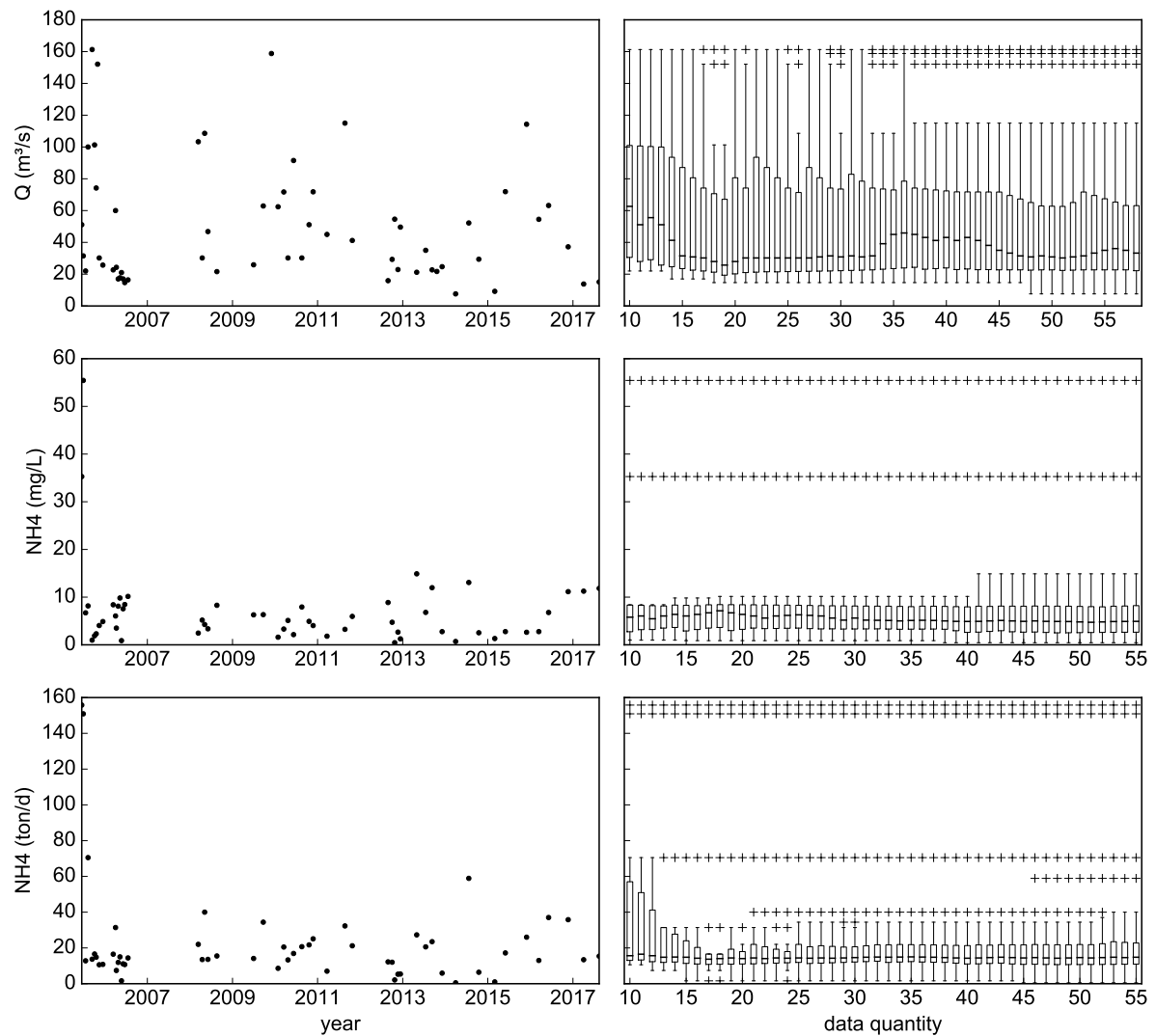
Figure 39 – Time series and boxplot evolution. Q, NH4 concentrations and loads, station IG4. Updated boxplots at each data, starting with 10 elements and ending with all data. The boxes show the 25th, 50th and 75th percentiles, the whiskers are the minimum and maximum non-outlier values and the crosses are the outlier values

NH4 - IG5
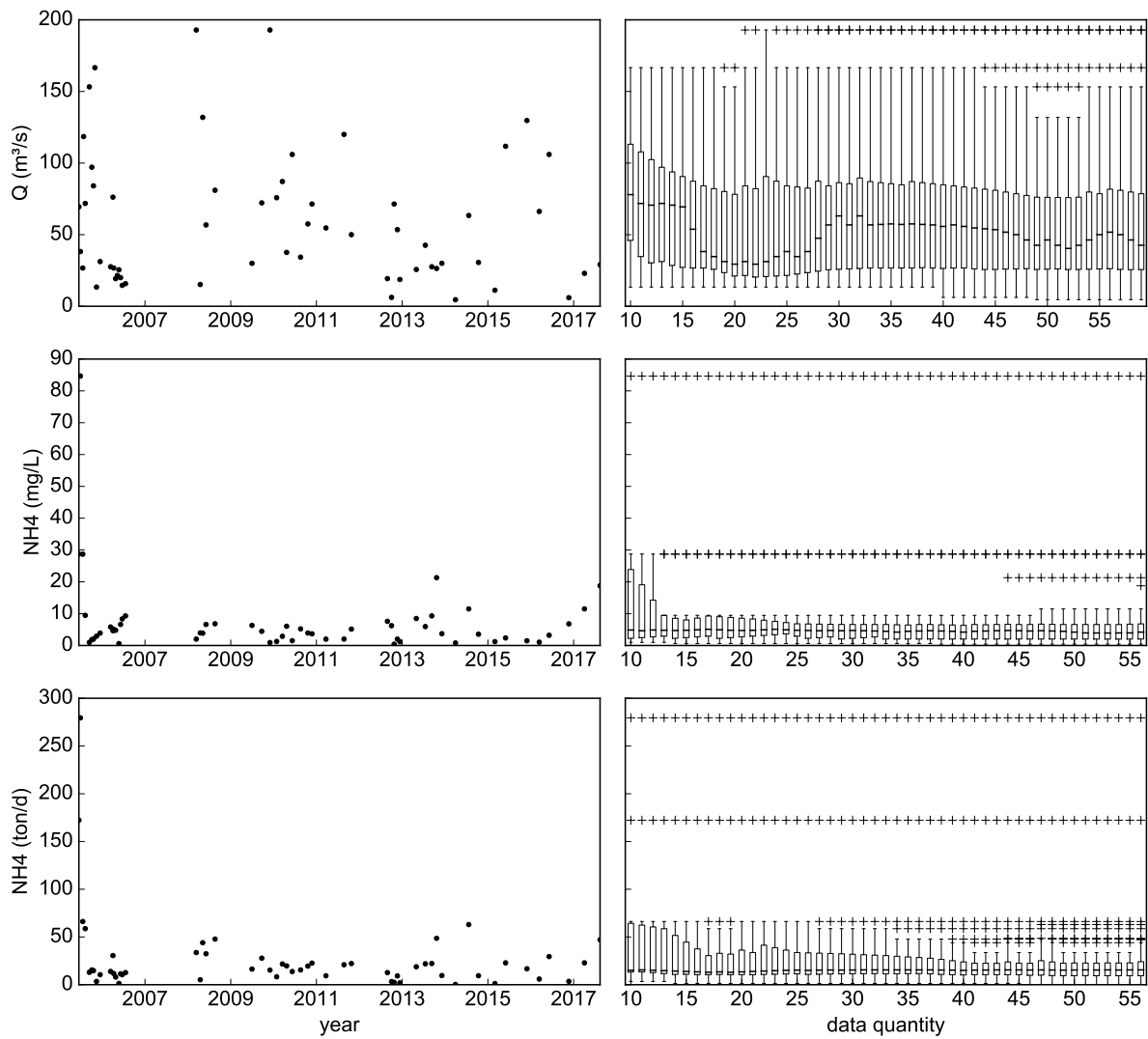
Figure 40 – Time series and boxplot evolution. Q, NH4 concentrations and loads, station IG5. Updated boxplots at each data, starting with 10 elements and ending with all data. The boxes show the 25th, 50th and 75th percentiles, the whiskers are the minimum and maximum non-outlier values and the crosses are the outlier values

NH4 - IG6
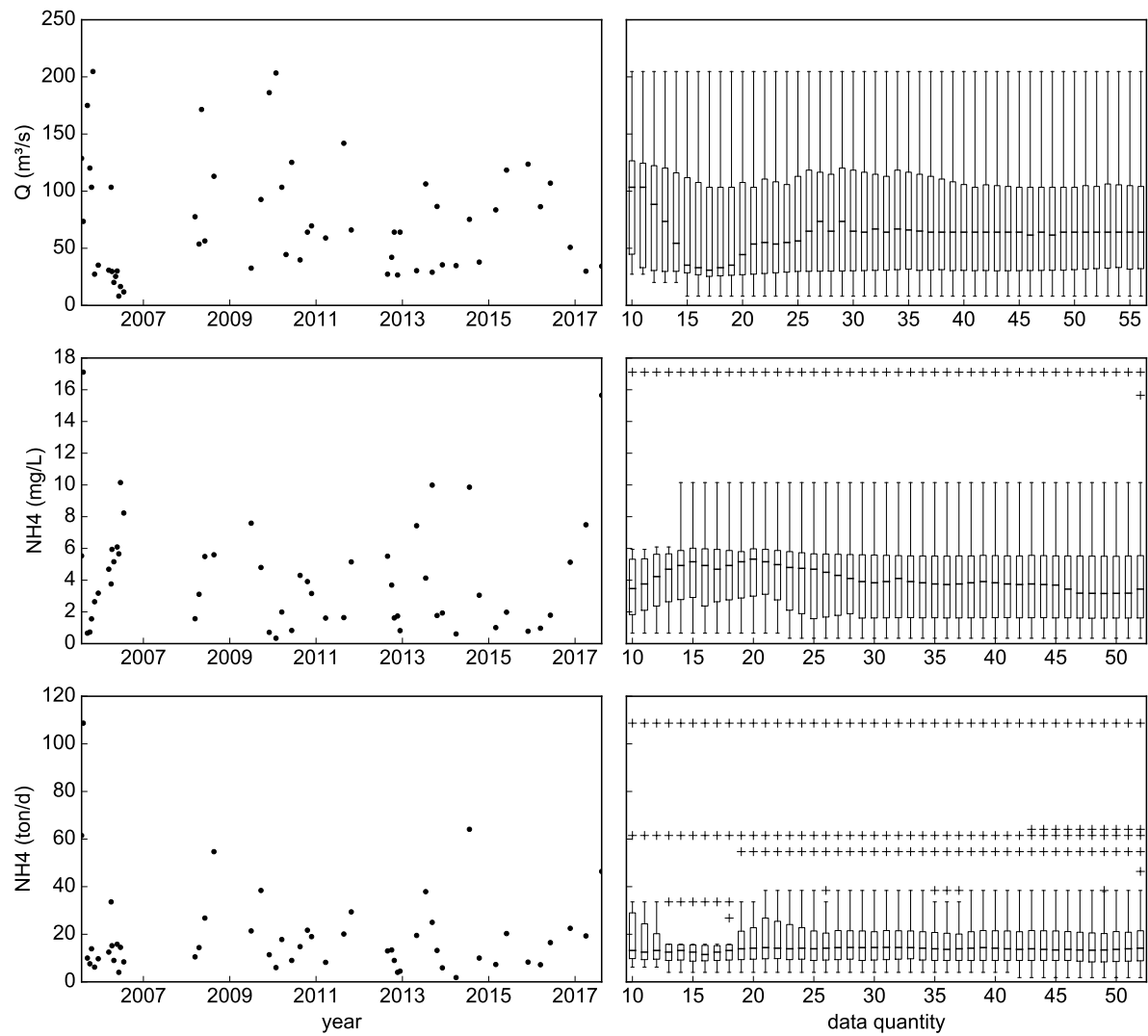
Figure 41 – Time series and boxplot evolution. Q, NH4 concentrations and loads, station IG6. Updated boxplots at each data, starting with 10 elements and ending with all data. The boxes show the 25th, 50th and 75th percentiles, the whiskers are the minimum and maximum non-outlier values and the crosses are the outlier values

NH4 - IG7
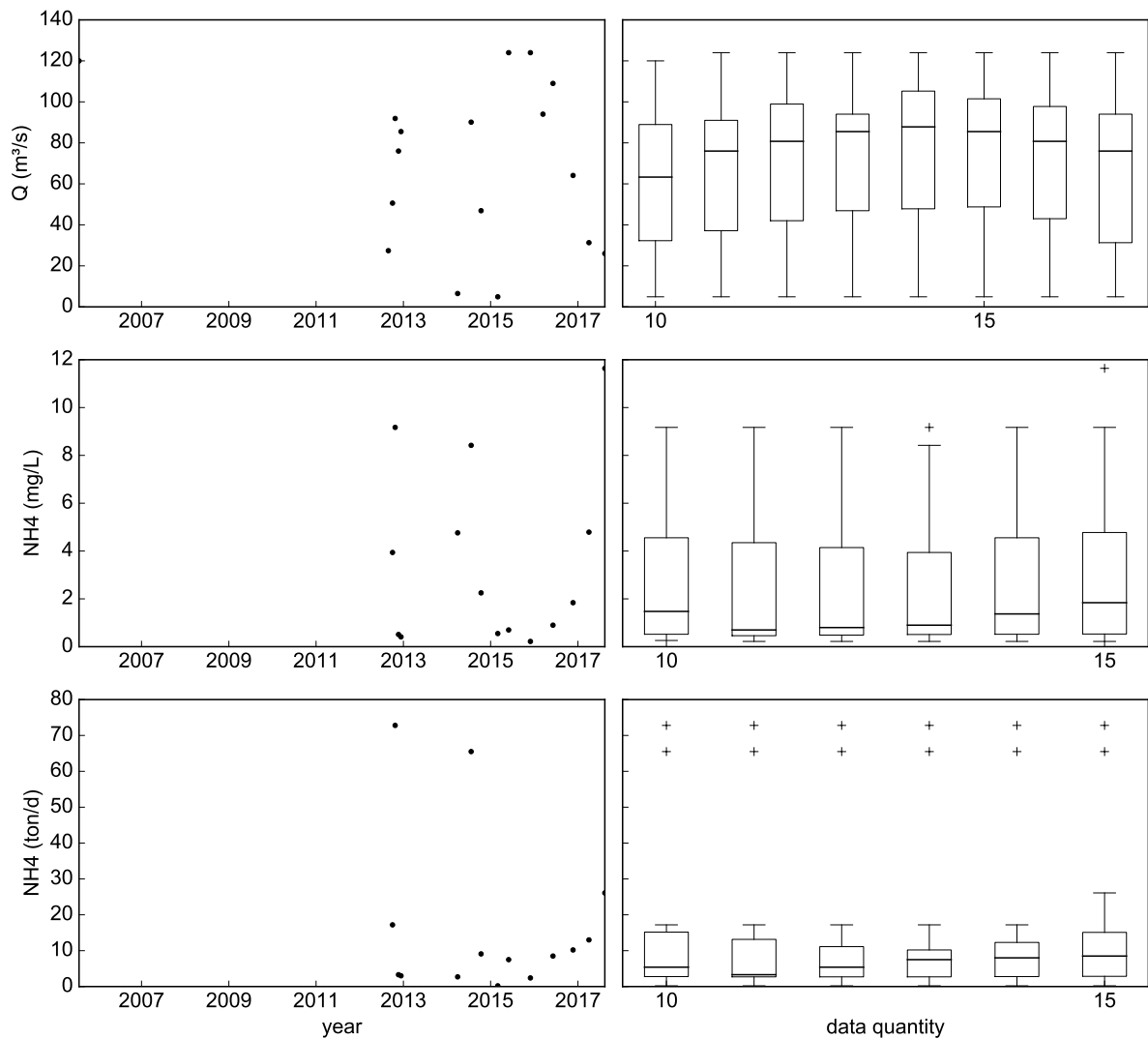
Figure 42 – Time series and boxplot evolution. Q, NH4 concentrations and loads, station IG7. Updated boxplots at each data, starting with 10 elements and ending with all data. The boxes show the 25th, 50th and 75th percentiles, the whiskers are the minimum and maximum non-outlier values and the crosses are the outlier values

TP - IG3
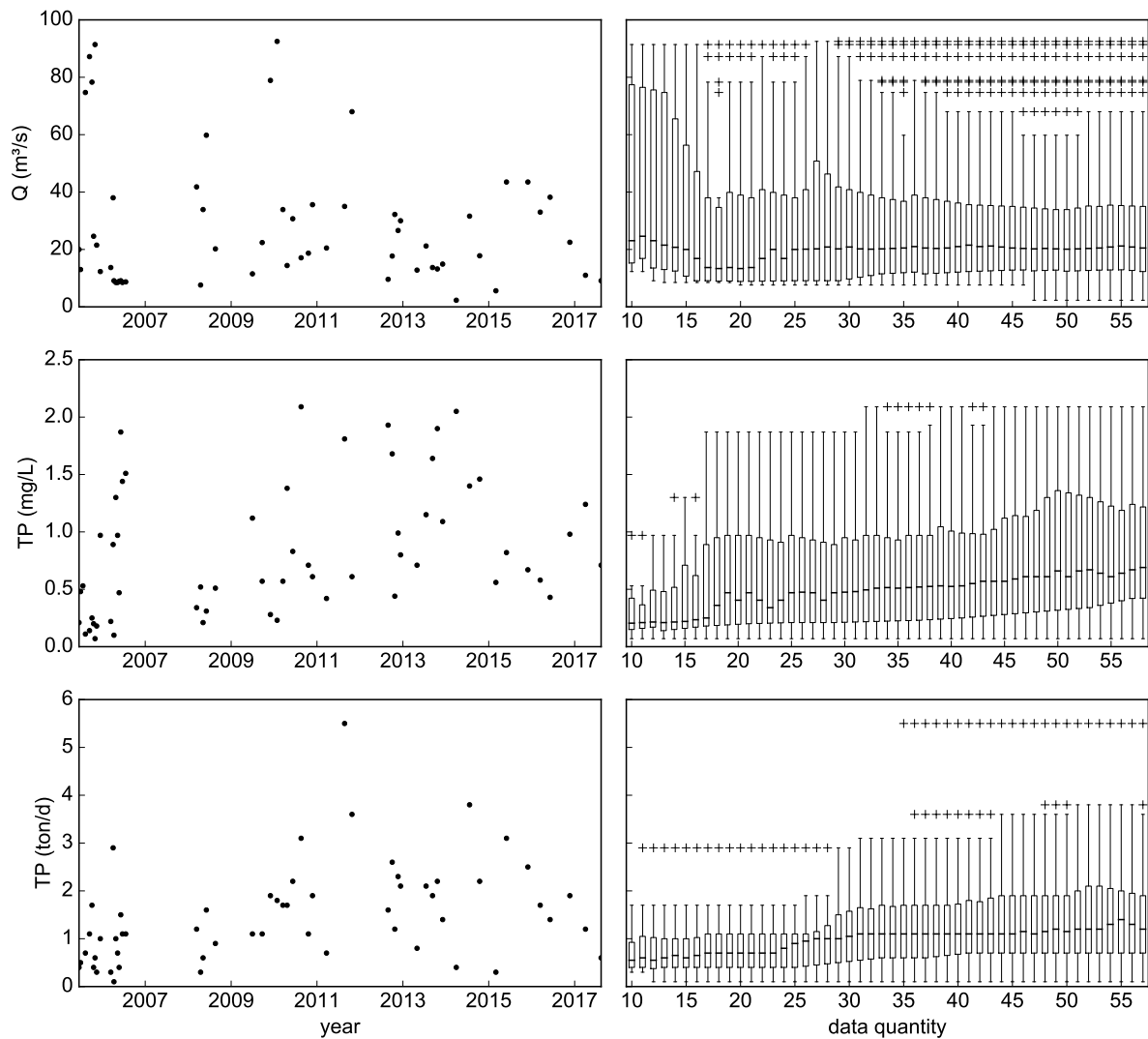
Figure 43 – Time series and boxplot evolution. Q, TP concentrations and loads, station IG3. Updated boxplots at each data, starting with 10 elements and ending with all data. The boxes show the 25th, 50th and 75th percentiles, the whiskers are the minimum and maximum non-outlier values and the crosses are the outlier values

TP - IG4
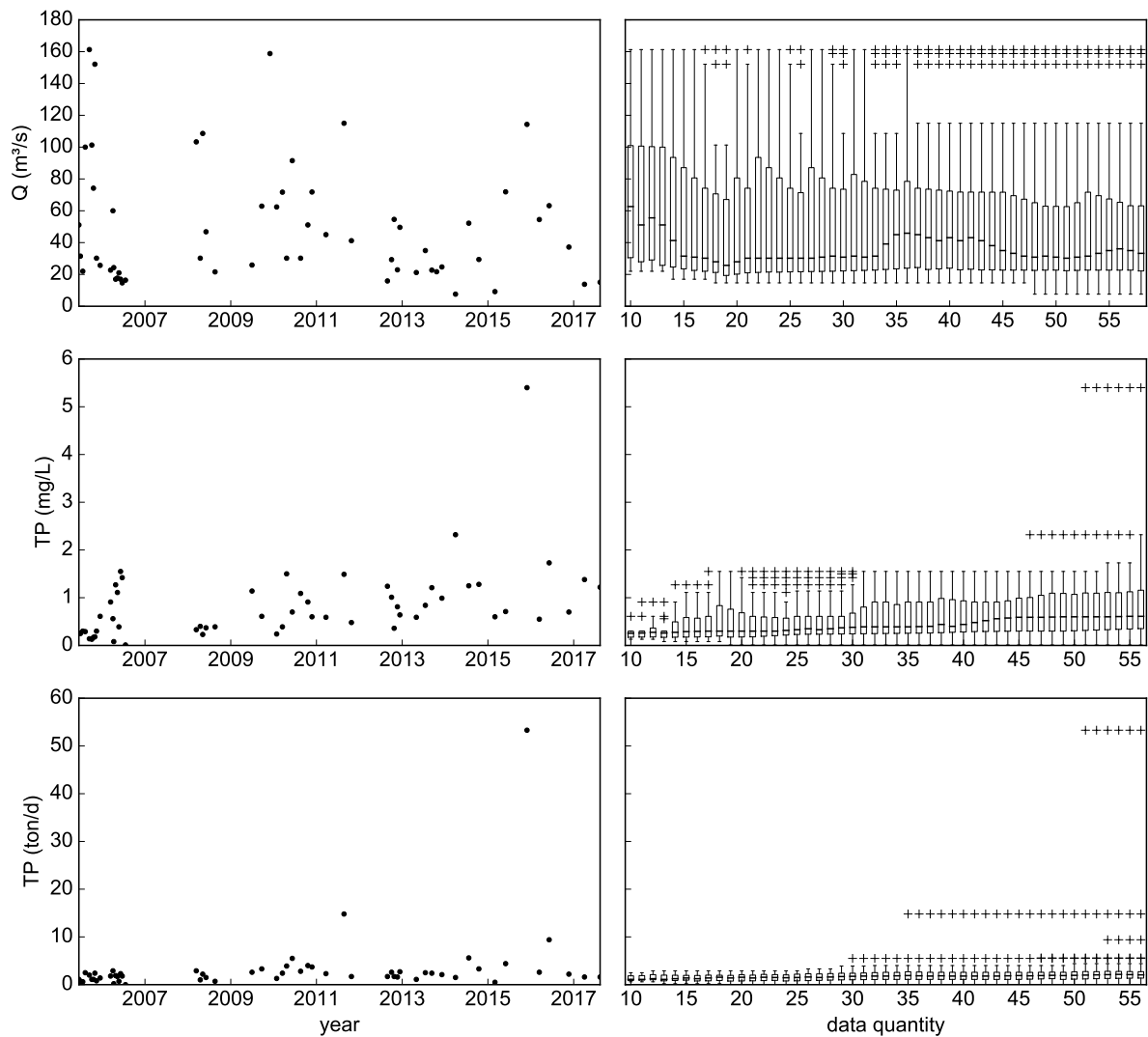
Figure 44 – Time series and boxplot evolution. Q, TP concentrations and loads, station IG4. Updated boxplots at each data, starting with 10 elements and ending with all data. The boxes show the 25th, 50th and 75th percentiles, the whiskers are the minimum and maximum non-outlier values and the crosses are the outlier values

TP - IG5
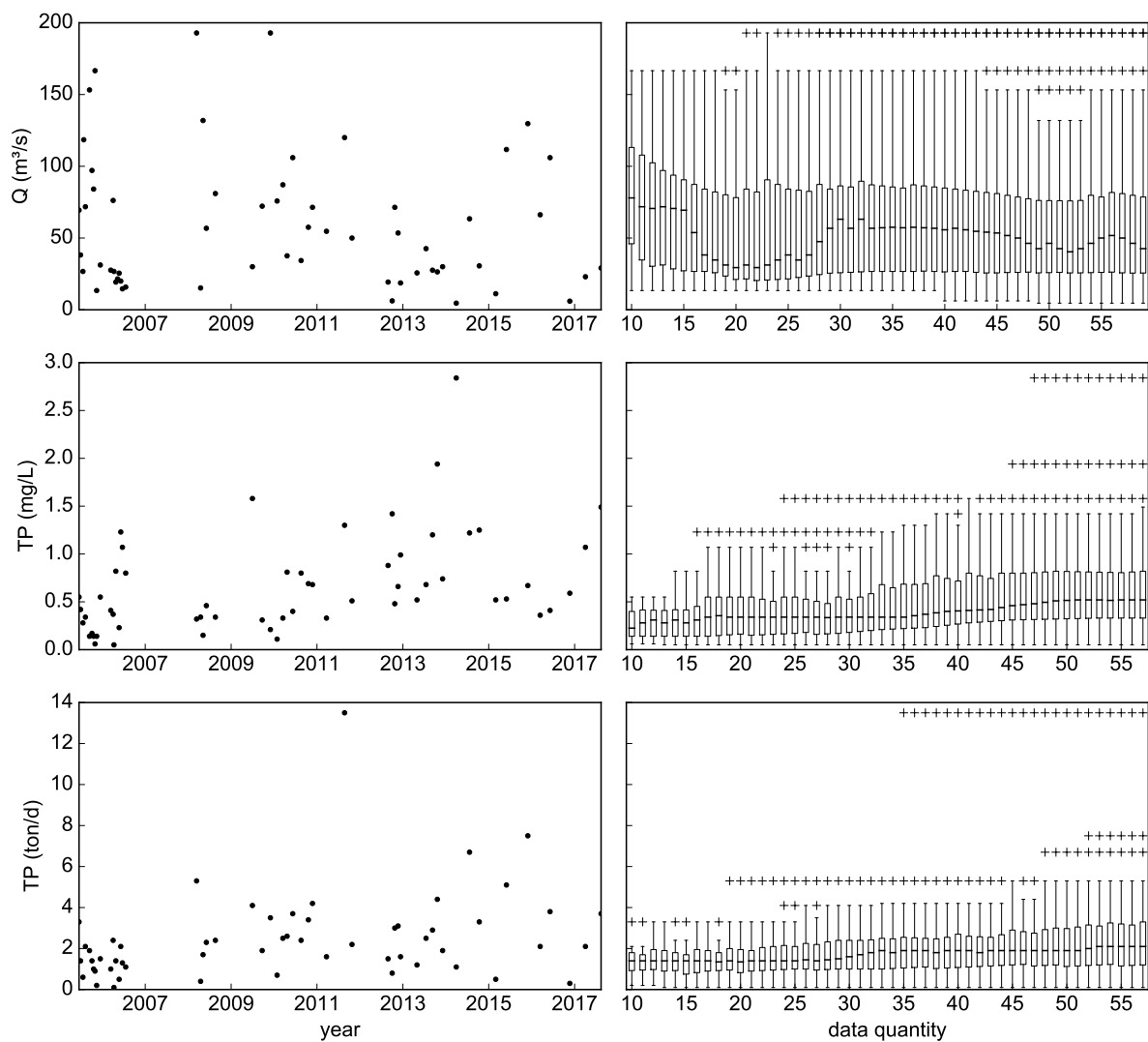
Figure 45 – Time series and boxplot evolution. Q, TP concentrations and loads, station IG5. Updated boxplots at each data, starting with 10 elements and ending with all data. The boxes show the 25th, 50th and 75th percentiles, the whiskers are the minimum and maximum non-outlier values and the crosses are the outlier values

TP - IG6
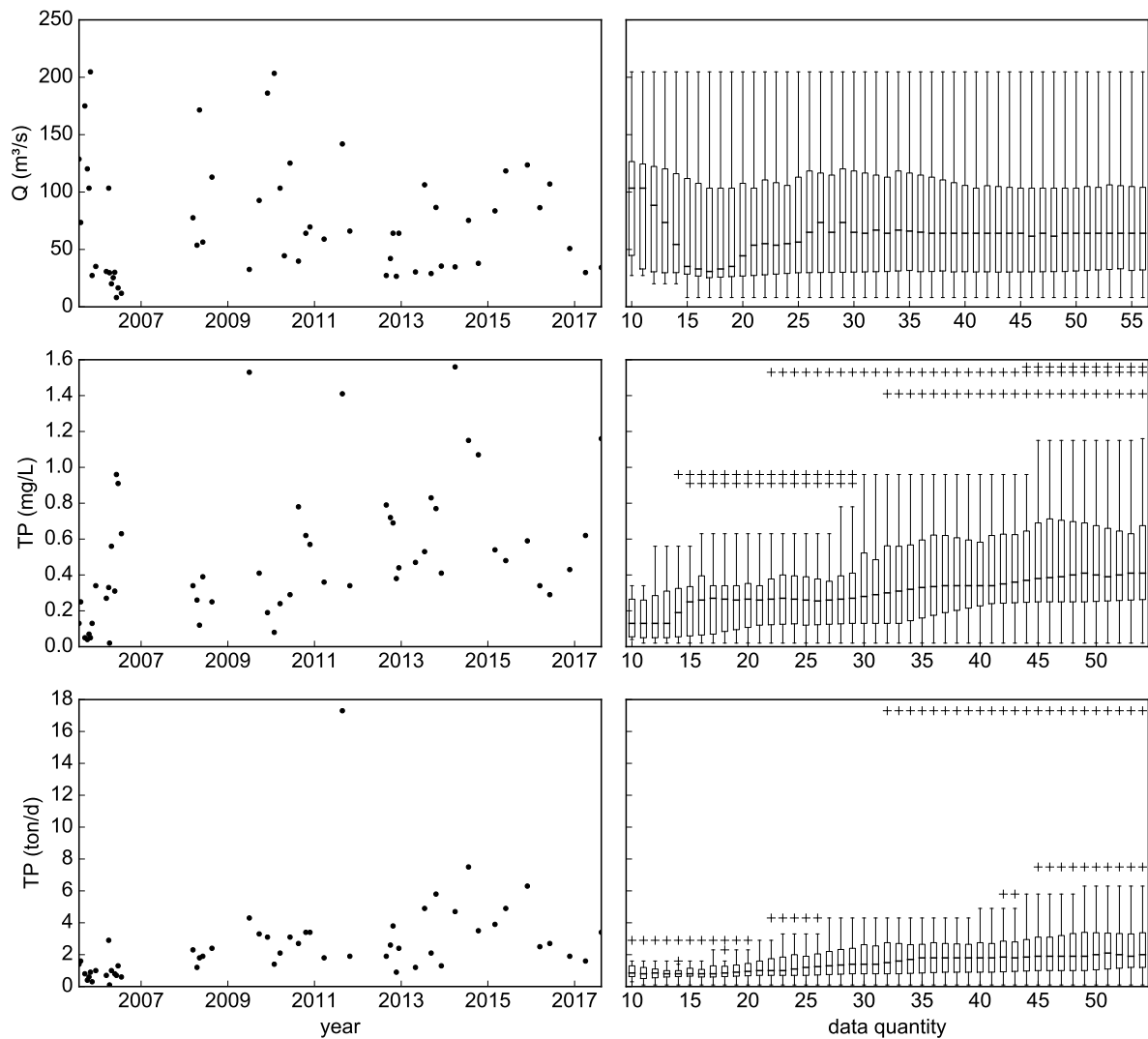
Figure 46 – Time series and boxplot evolution. Q, TP concentrations and loads, station IG6. Updated boxplots at each data, starting with 10 elements and ending with all data. The boxes show the 25th, 50th and 75th percentiles, the whiskers are the minimum and maximum non-outlier values and the crosses are the outlier values

TP - IG7
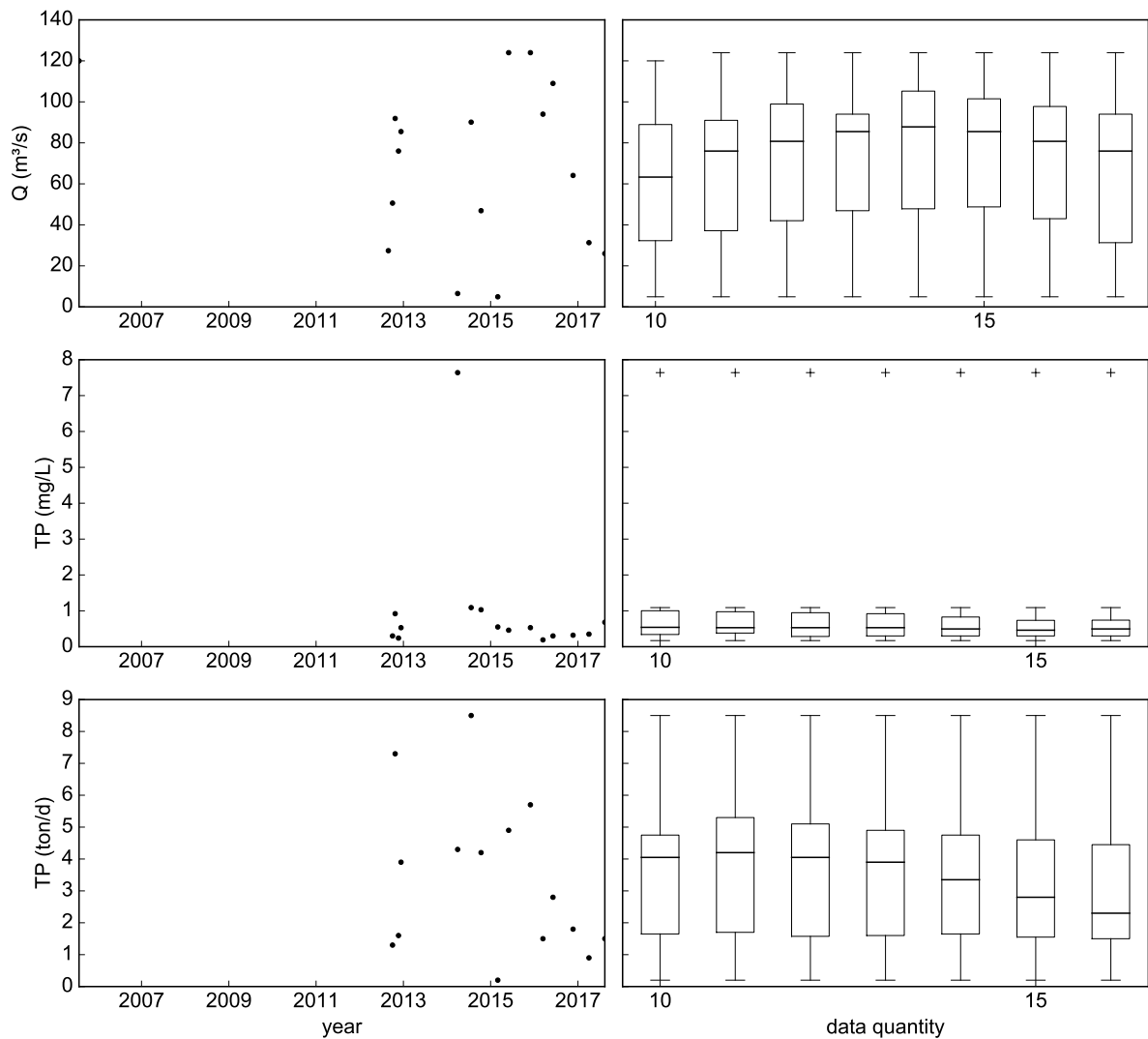
Figure 47 – Time series and boxplot evolution. Q, TP concentrations and loads, station IG7. Updated boxplots at each data, starting with 10 elements and ending with all data. The boxes show the 25th, 50th and 75th percentiles, the whiskers are the minimum and maximum non-outlier values and the crosses are the outlier values

VDS - IG3
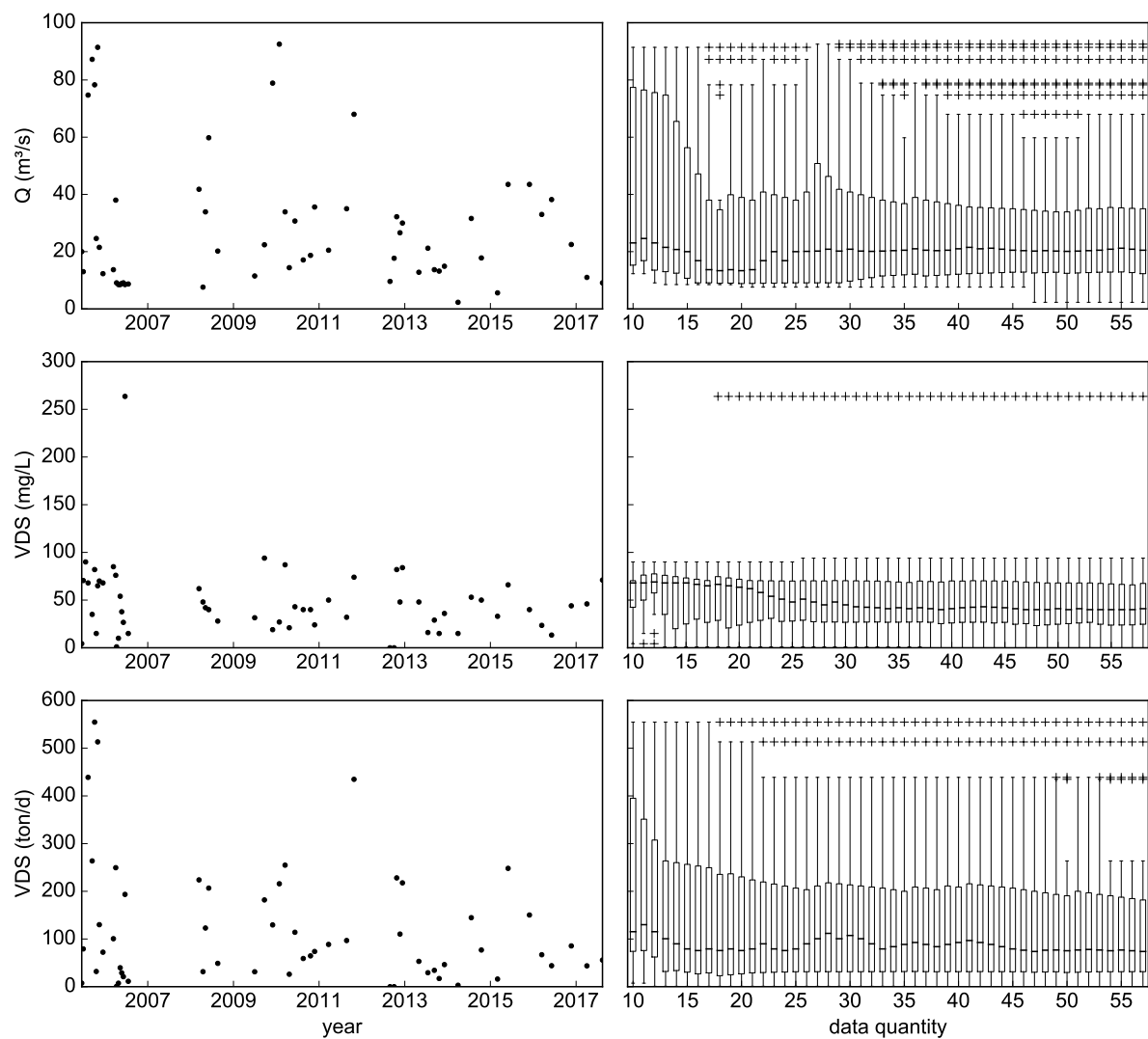
Figure 48 – Time series and boxplot evolution. Q, VDS concentrations and loads, station IG3. Updated boxplots at each data, starting with 10 elements and ending with all data. The boxes show the 25th, 50th and 75th percentiles, the whiskers are the minimum and maximum non-outlier values and the crosses are the outlier values

VDS - IG4
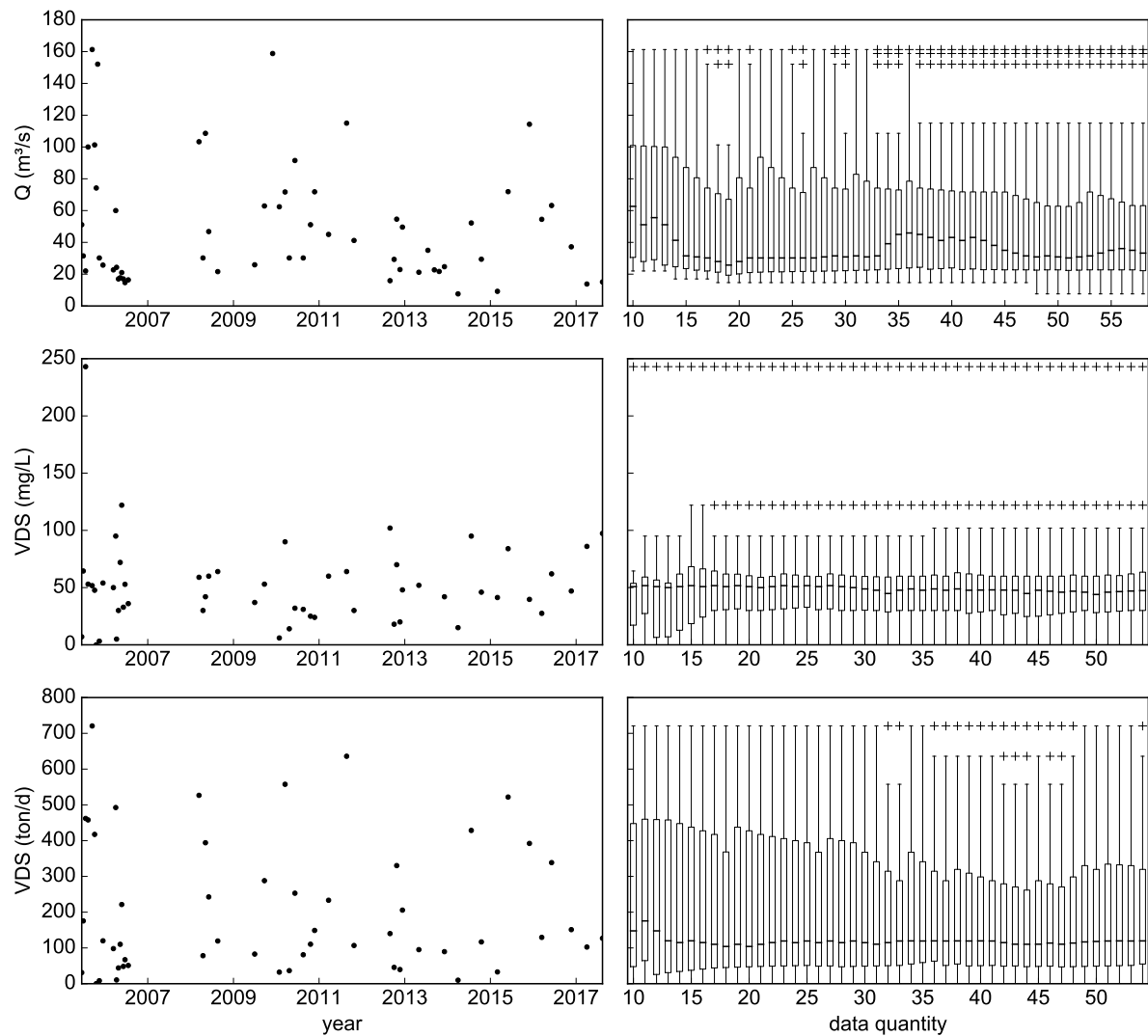
Figure 49 – Time series and boxplot evolution. Q, VDS concentrations and loads, station IG4. Updated boxplots at each data, starting with 10 elements and ending with all data. The boxes show the 25th, 50th and 75th percentiles, the whiskers are the minimum and maximum non-outlier values and the crosses are the outlier values

VDS - IG5
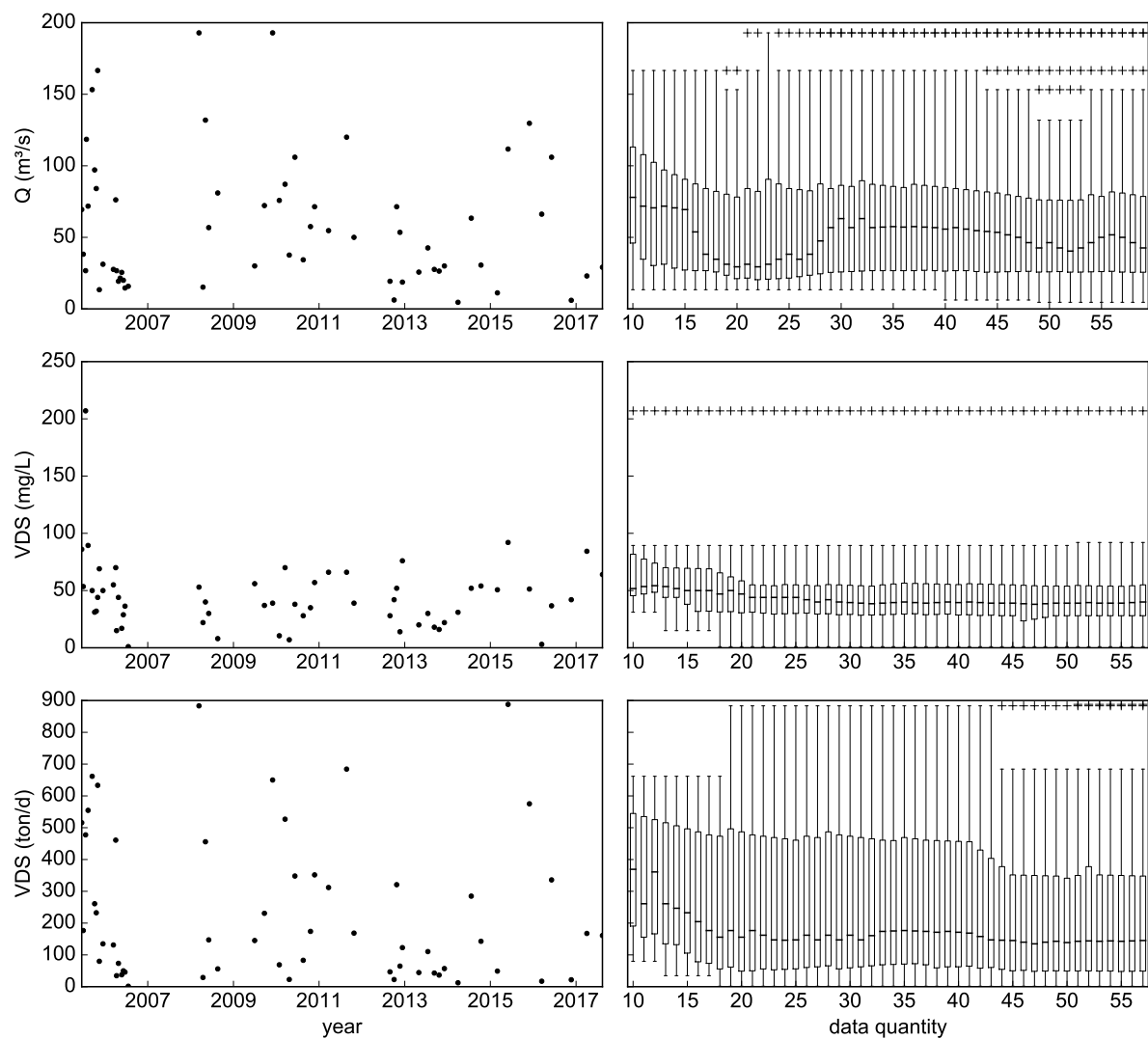
Figure 50 – Time series and boxplot evolution. Q, VDS concentrations and loads, station IG5. Updated boxplots at each data, starting with 10 elements and ending with all data. The boxes show the 25th, 50th and 75th percentiles, the whiskers are the minimum and maximum non-outlier values and the crosses are the outlier values

VDS - IG6
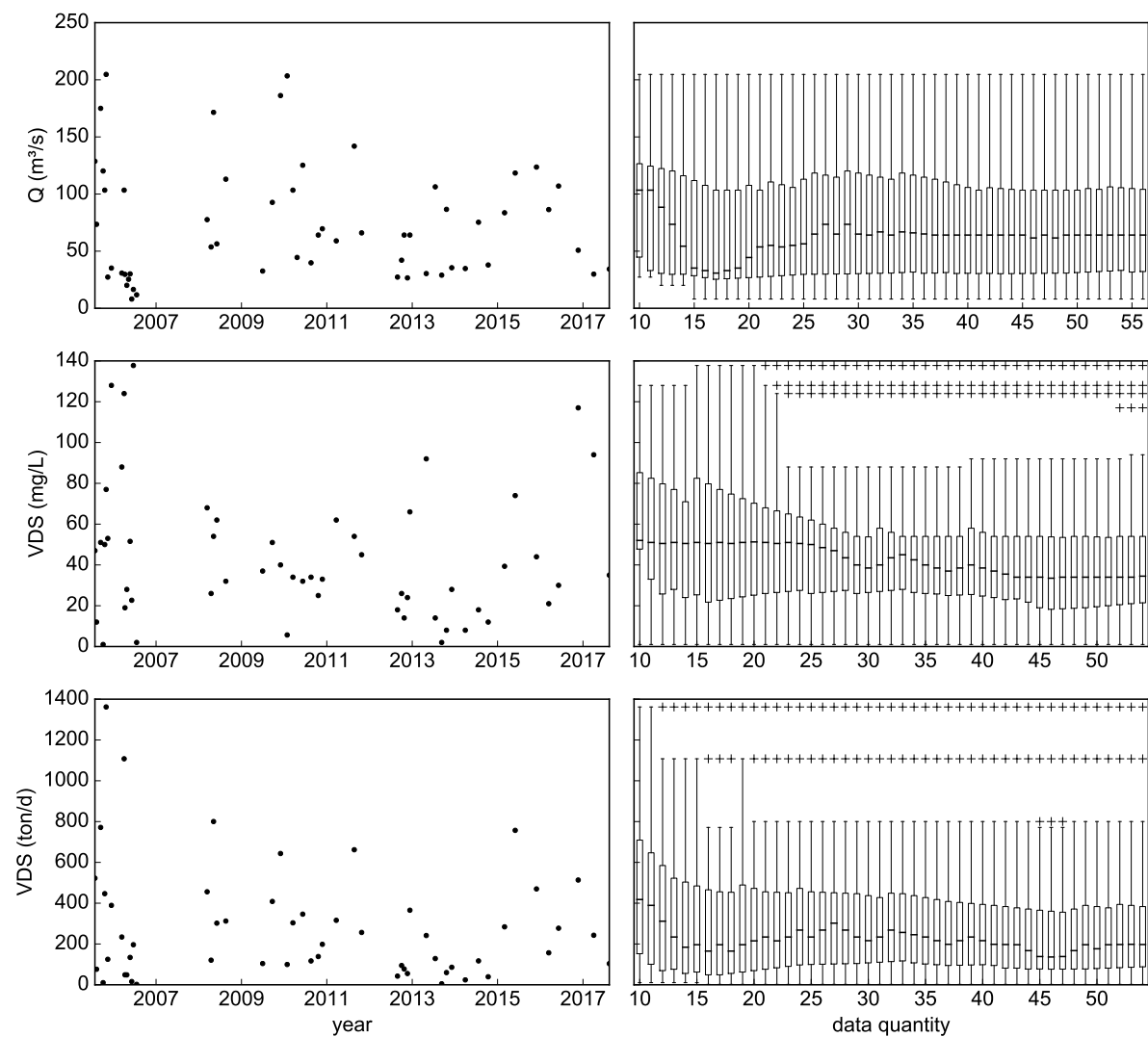
Figure 51 – Time series and boxplot evolution. Q, VDS concentrations and loads, station IG6. Updated boxplots at each data, starting with 10 elements and ending with all data. The boxes show the 25th, 50th and 75th percentiles, the whiskers are the minimum and maximum non-outlier values and the crosses are the outlier values

VDS - IG7
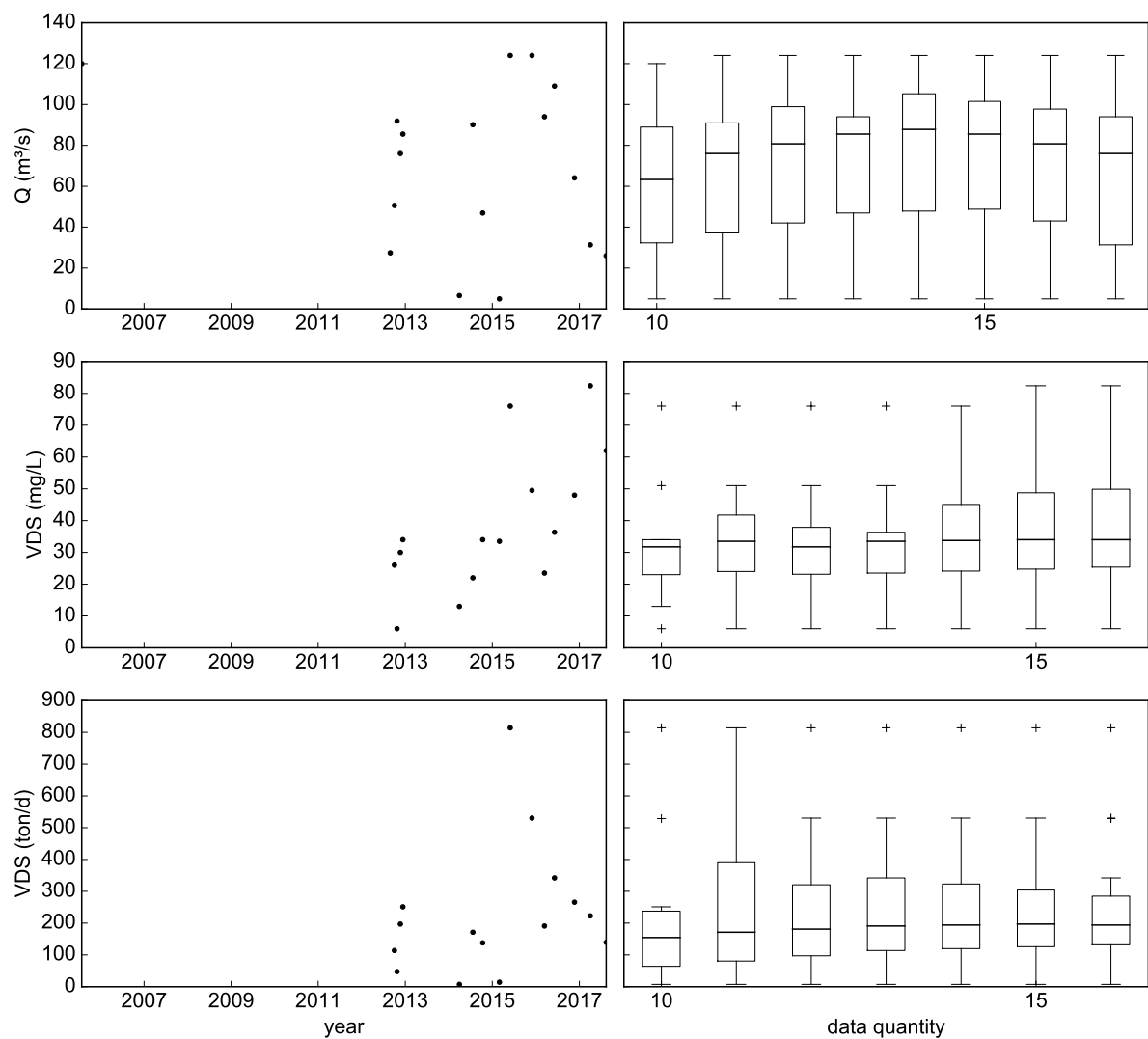
Figure 52 – Time series and boxplot evolution. Q, VDS concentrations and loads, station IG7. Updated boxplots at each data, starting with 10 elements and ending with all data. The boxes show the 25th, 50th and 75th percentiles, the whiskers are the minimum and maximum non-outlier values and the crosses are the outlier values

A.2 Uncertainty scenarios of (m³/s)

$$Q - IG3$$
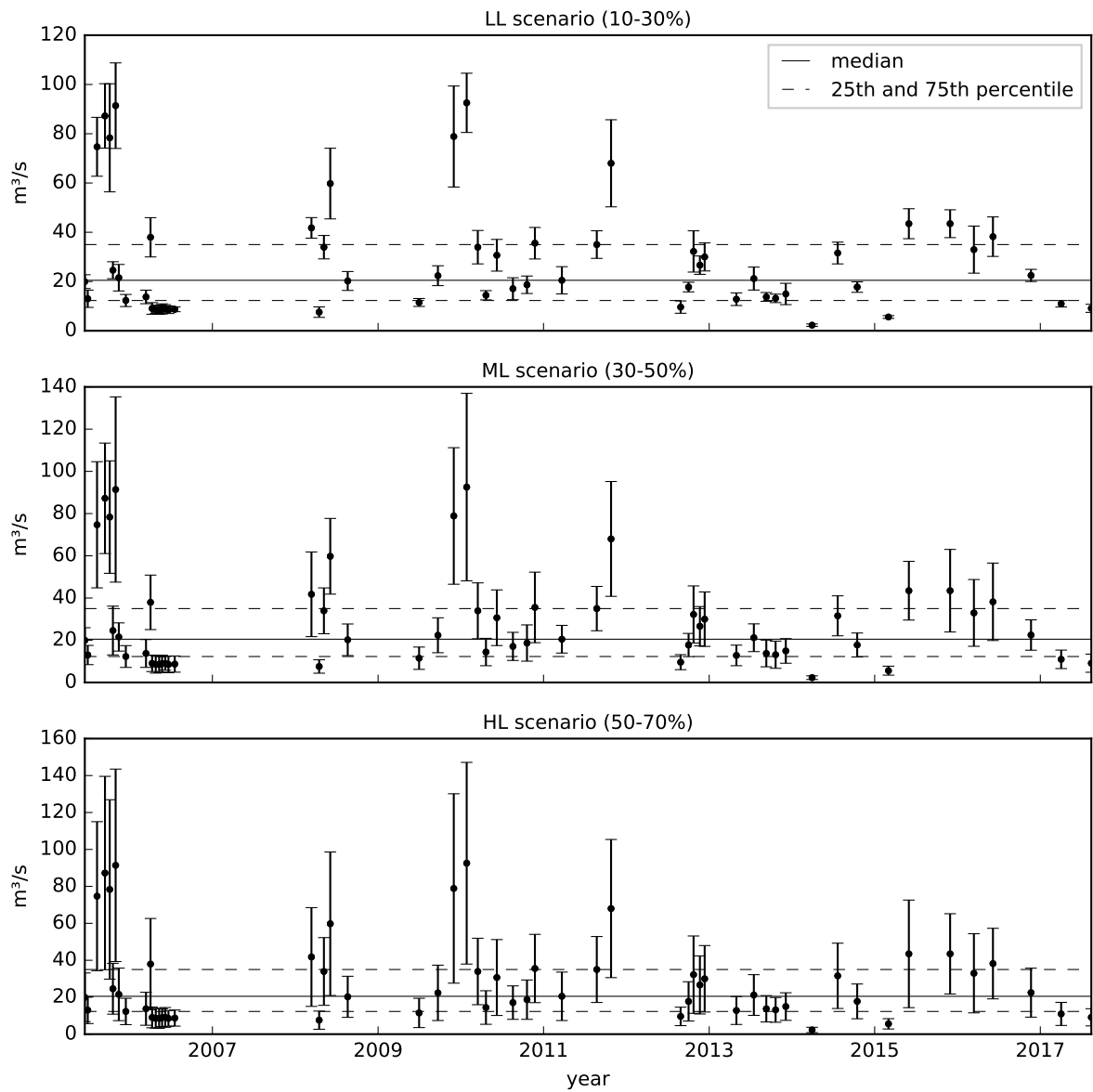
Figure 53 – LL, ML and HL uncertainty scenarios for Q time series, station IG3

Q - IG4
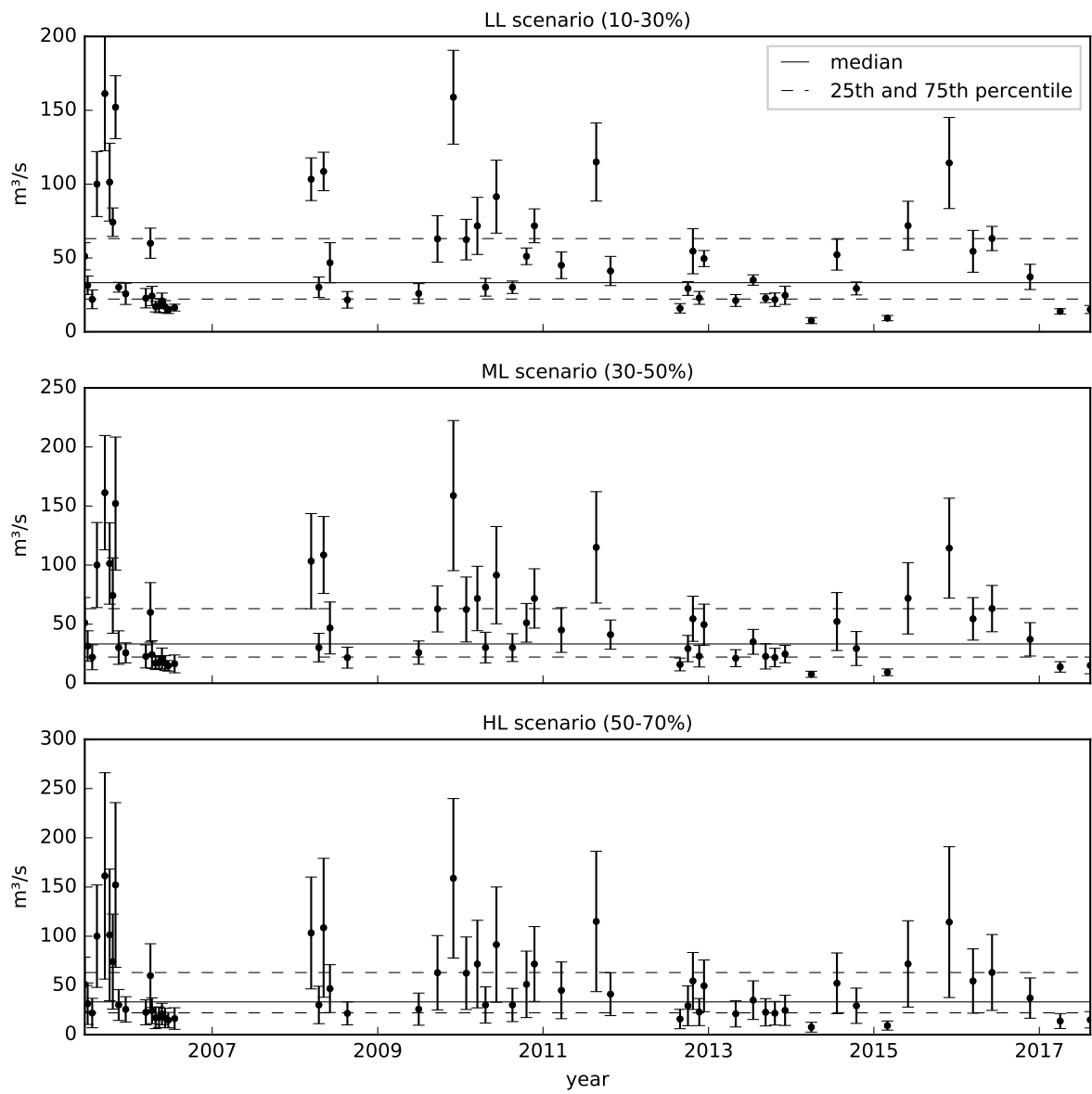
Figure 54 – LL, ML and HL uncertainty scenarios for Q time series, station IG4
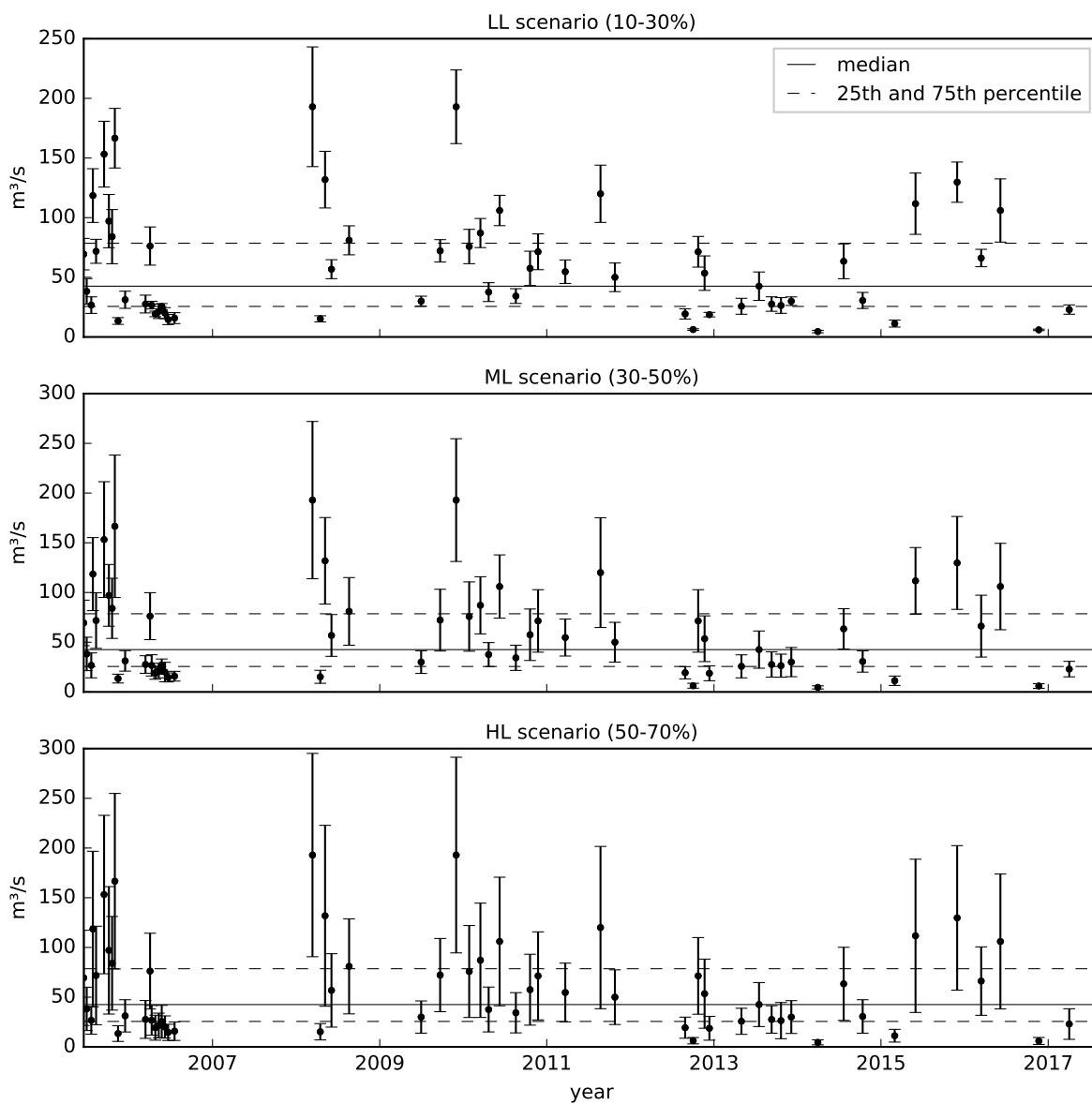
Figure 55 – LL, ML and HL uncertainty scenarios for Q time series, station IG5

Q - IG6
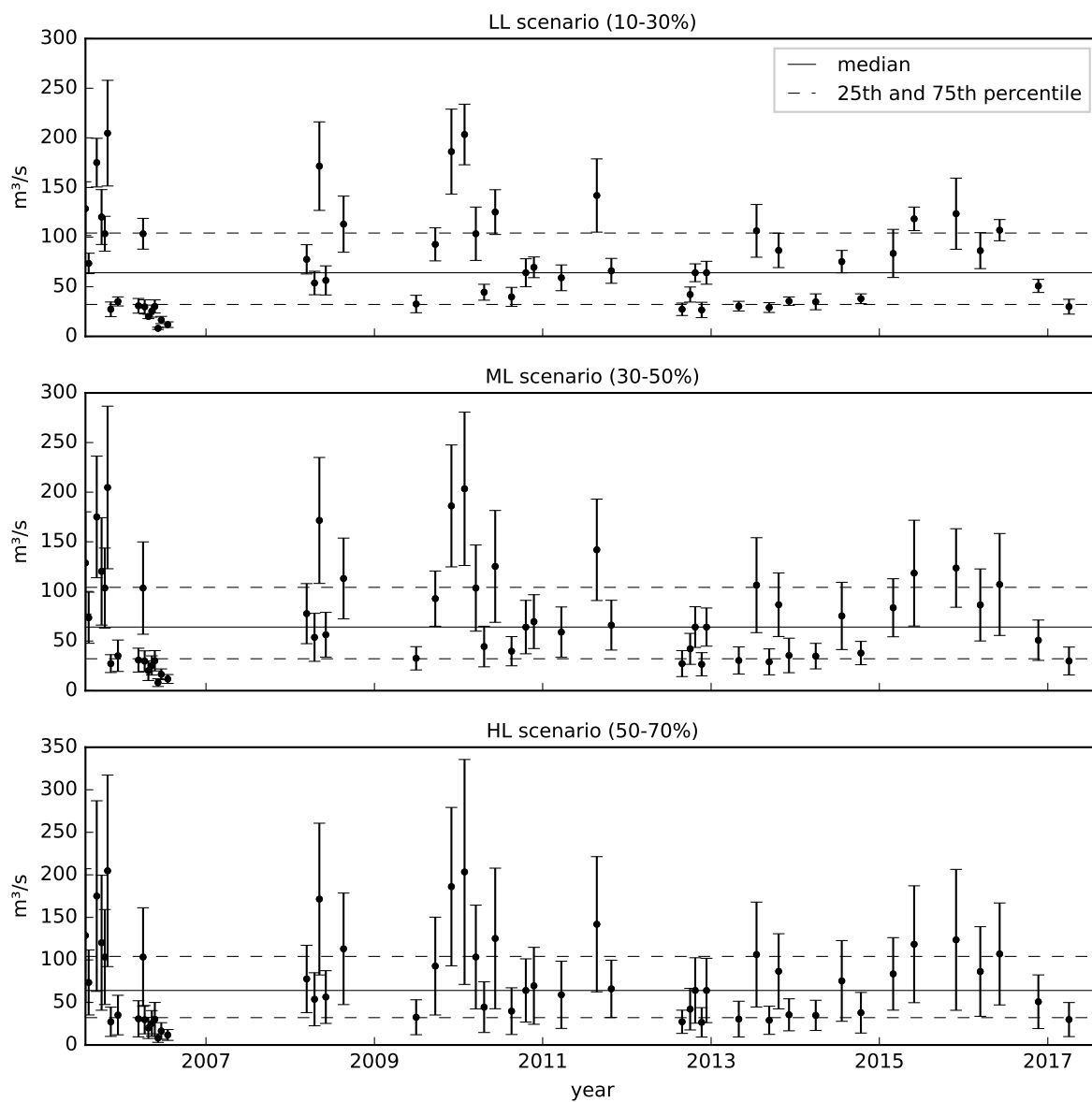
Figure 56 – LL, ML and HL uncertainty scenarios for Q time series, station IG6

Q - IG7
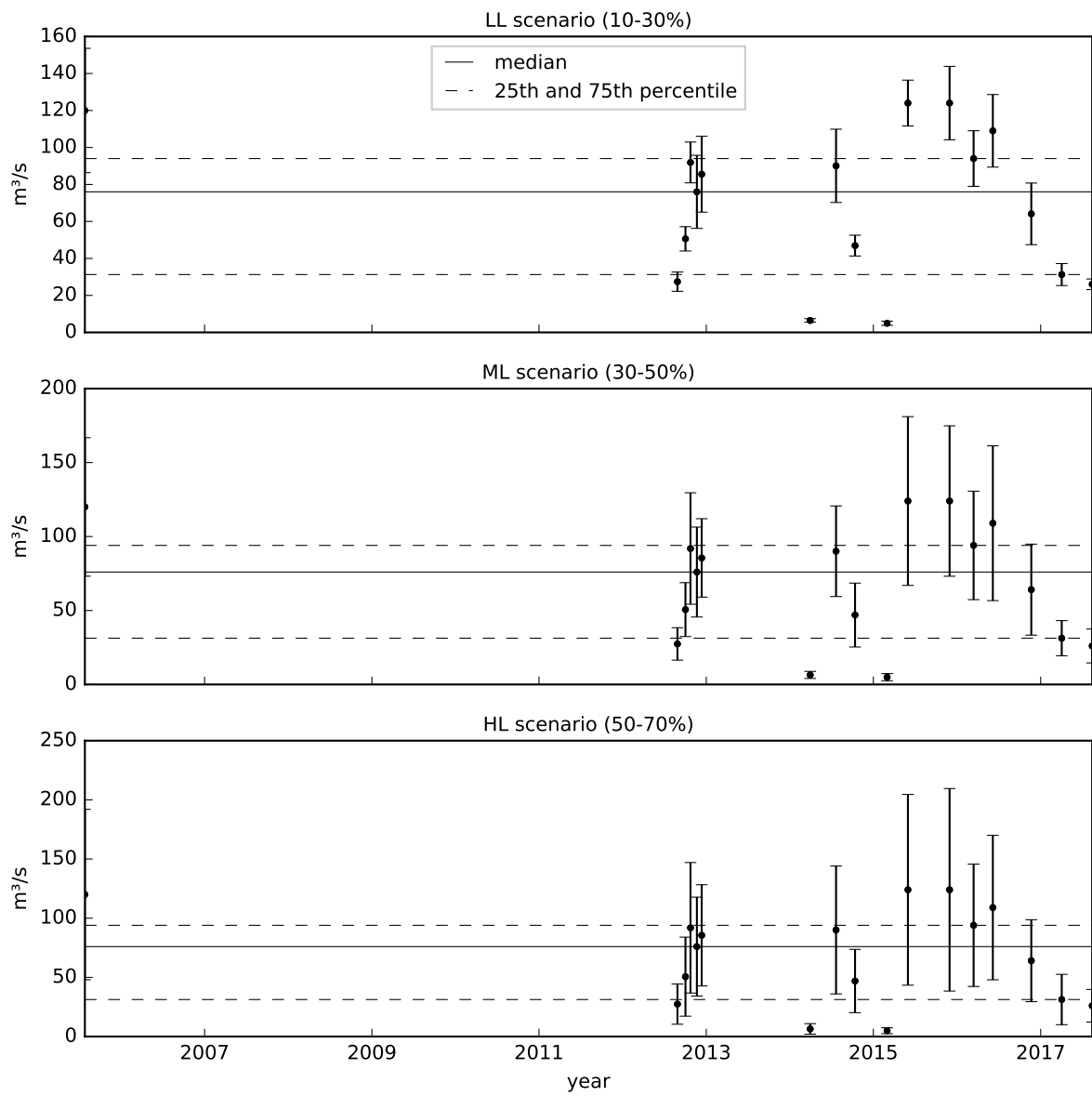
Figure 57 – LL, ML and HL uncertainty scenarios for Q time series, station IG7

A.3 Uncertainty scenarios (mg/L)
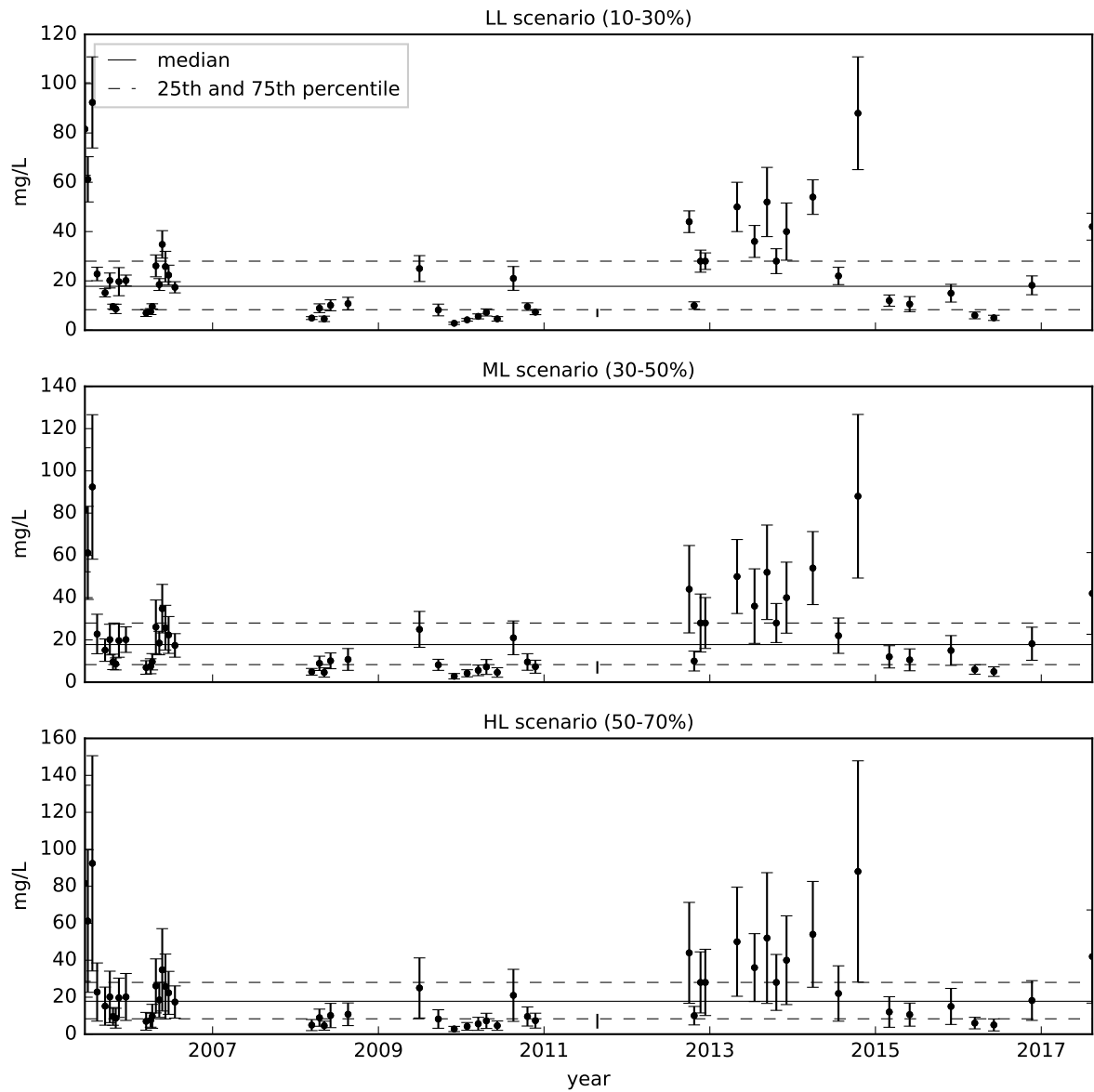
Figure 58 – LL, ML and HL uncertainty scenarios for BOD concentration time series, station IG3
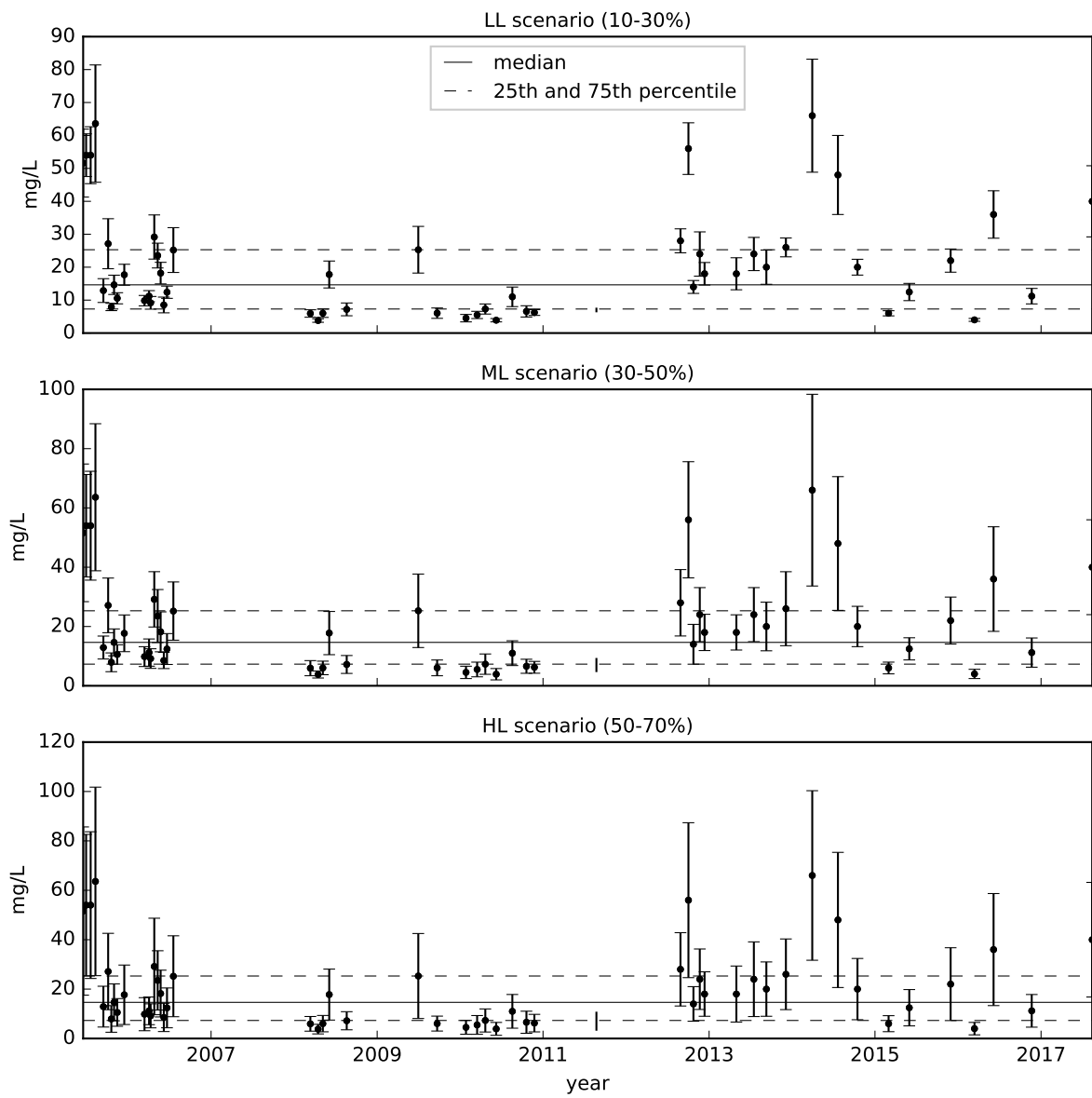
BOD - IG4

Figure 59 – LL, ML and HL uncertainty scenarios for BOD concentration time series from IG4
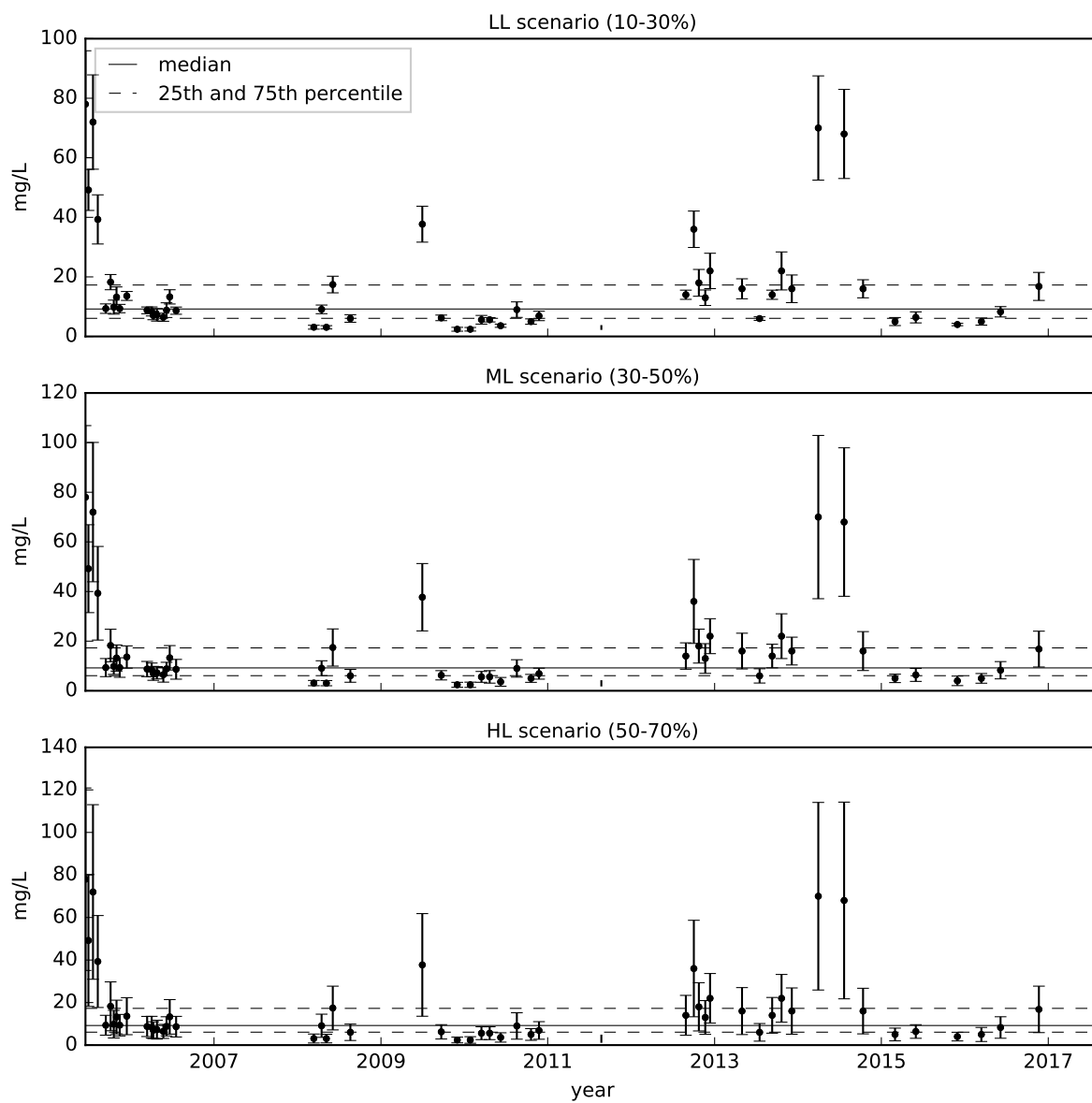
BOD - IG5

Figure 60 – LL, ML and HL uncertainty scenarios for BOD concentration time series, station IG5
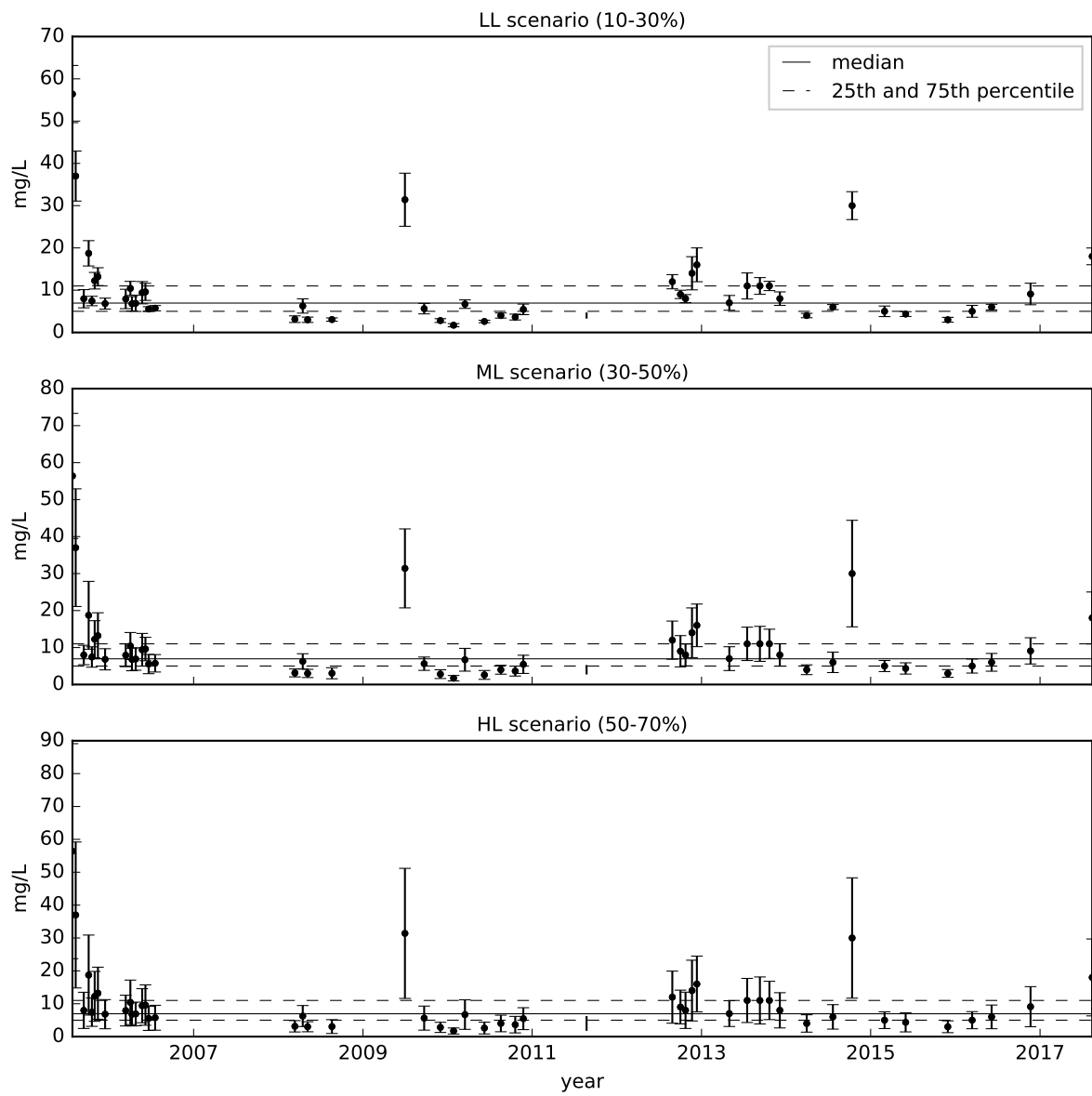
BOD - IG6

Figure 61 – LL, ML and HL uncertainty scenarios for BOD concentration time series, station IG6

BOD - IG7
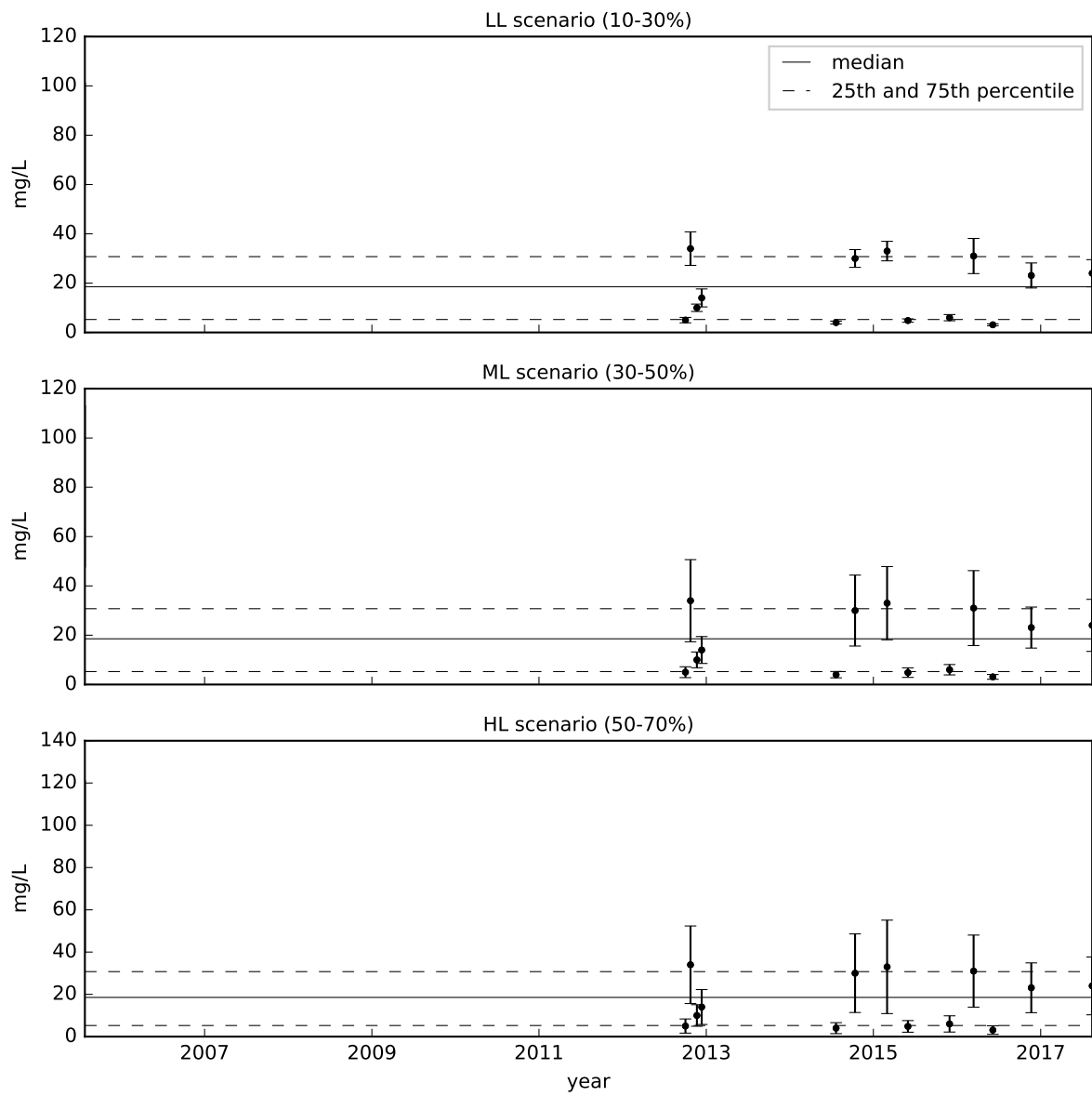
Figure 62 – LL, ML and HL uncertainty scenarios for BOD concentration time series, station IG7

DO - IG3
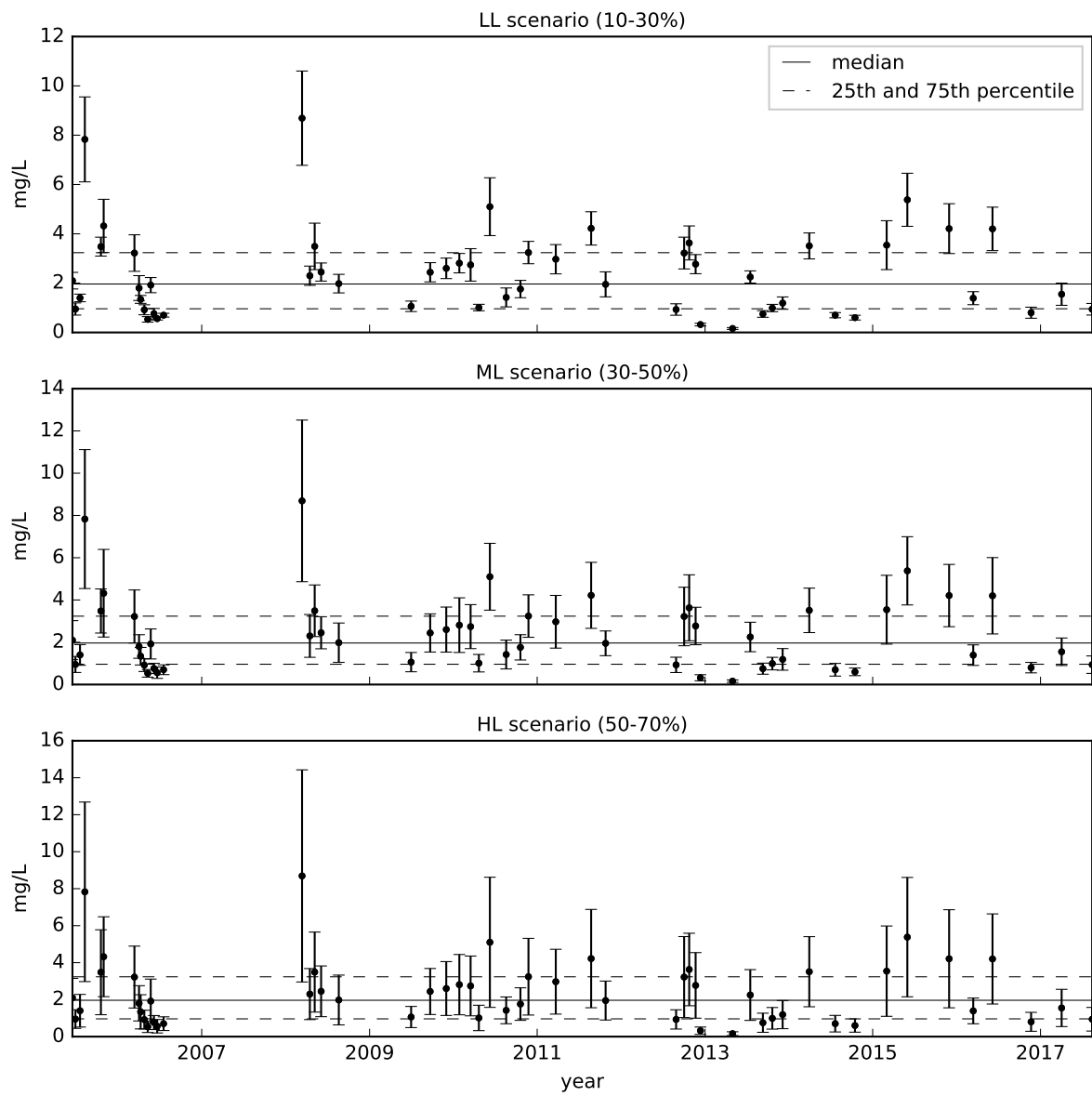
Figure 63 – LL, ML and HL uncertainty scenarios for DO concentration time series, station IG3

DO - IG4
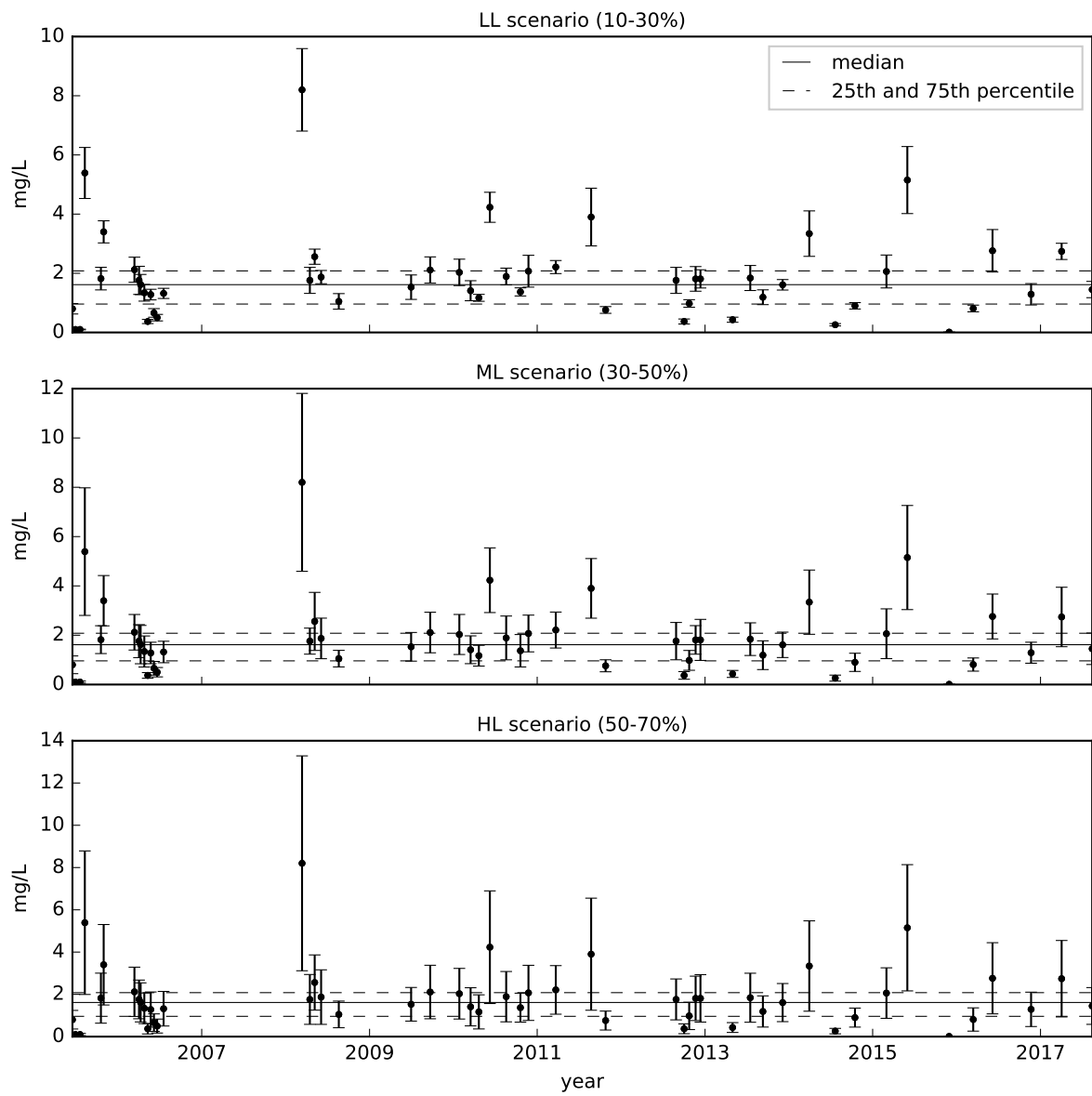
Figure 64 – LL, ML and HL uncertainty scenarios for DO concentration time series from IG4

DO - IG5
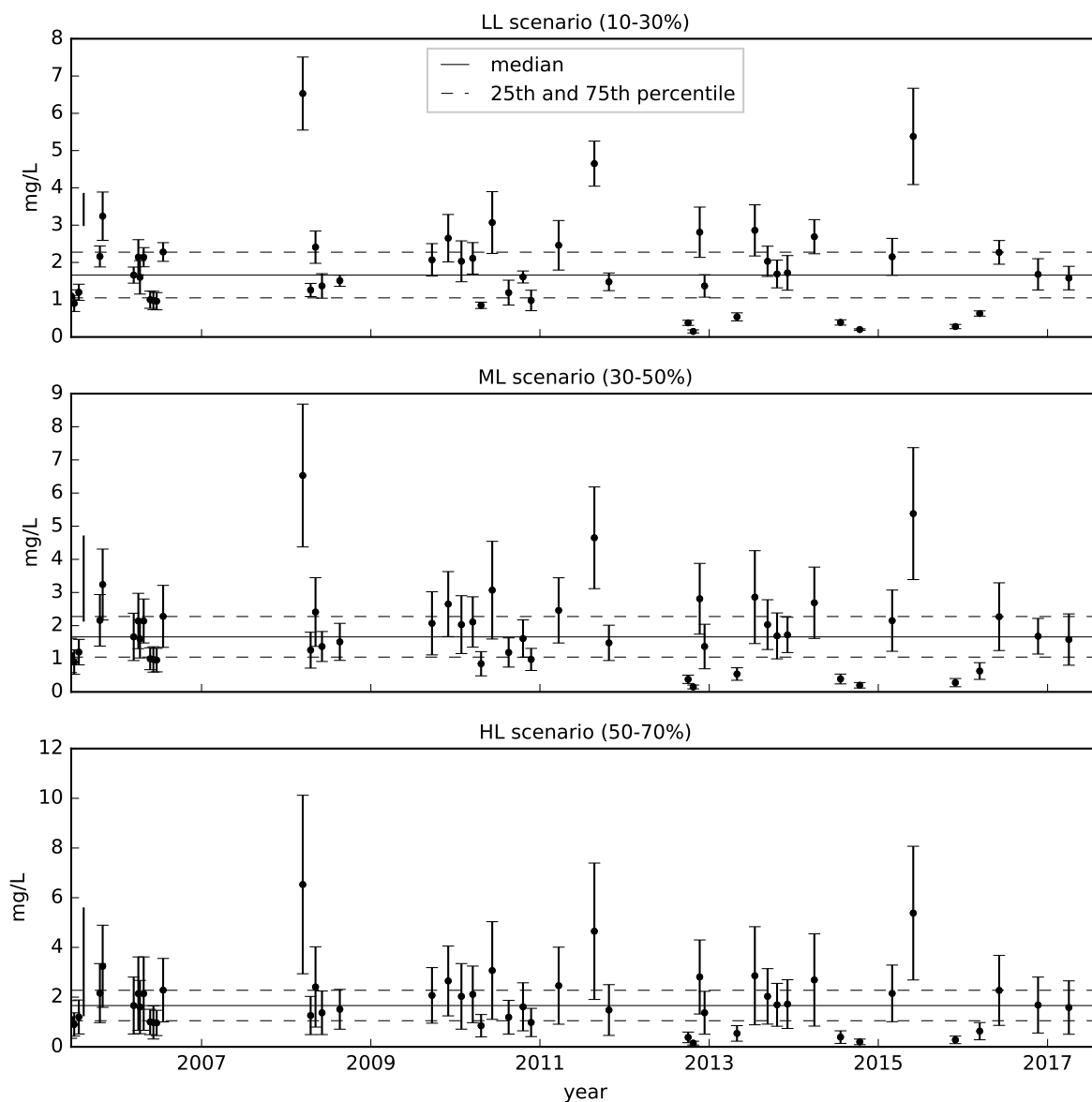
Figure 65 – LL, ML and HL uncertainty scenarios for DO concentration time series, station IG5

DO - IG6
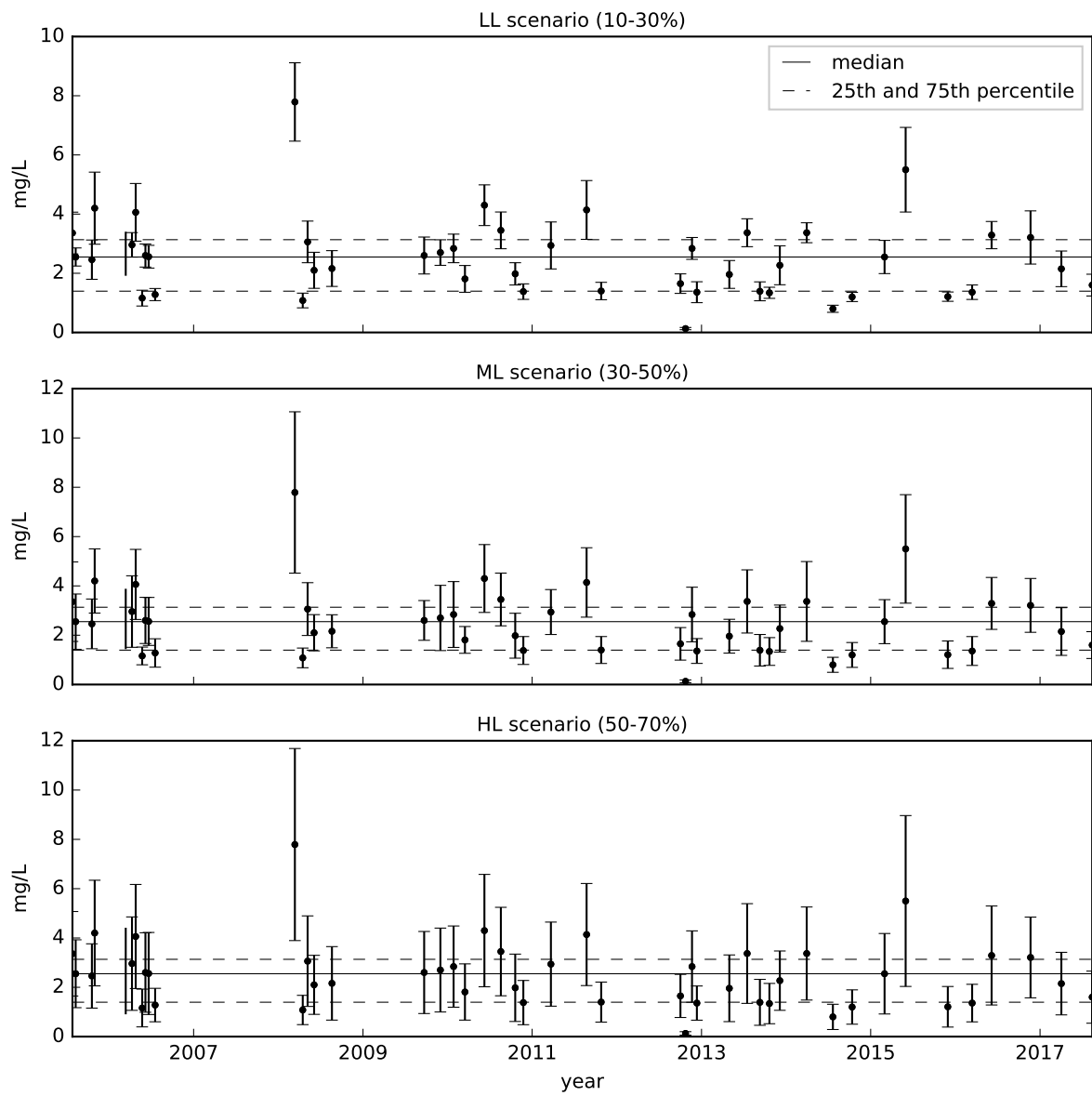
Figure 66 – LL, ML and HL uncertainty scenarios for DO concentration time series, station IG6

DO - IG7
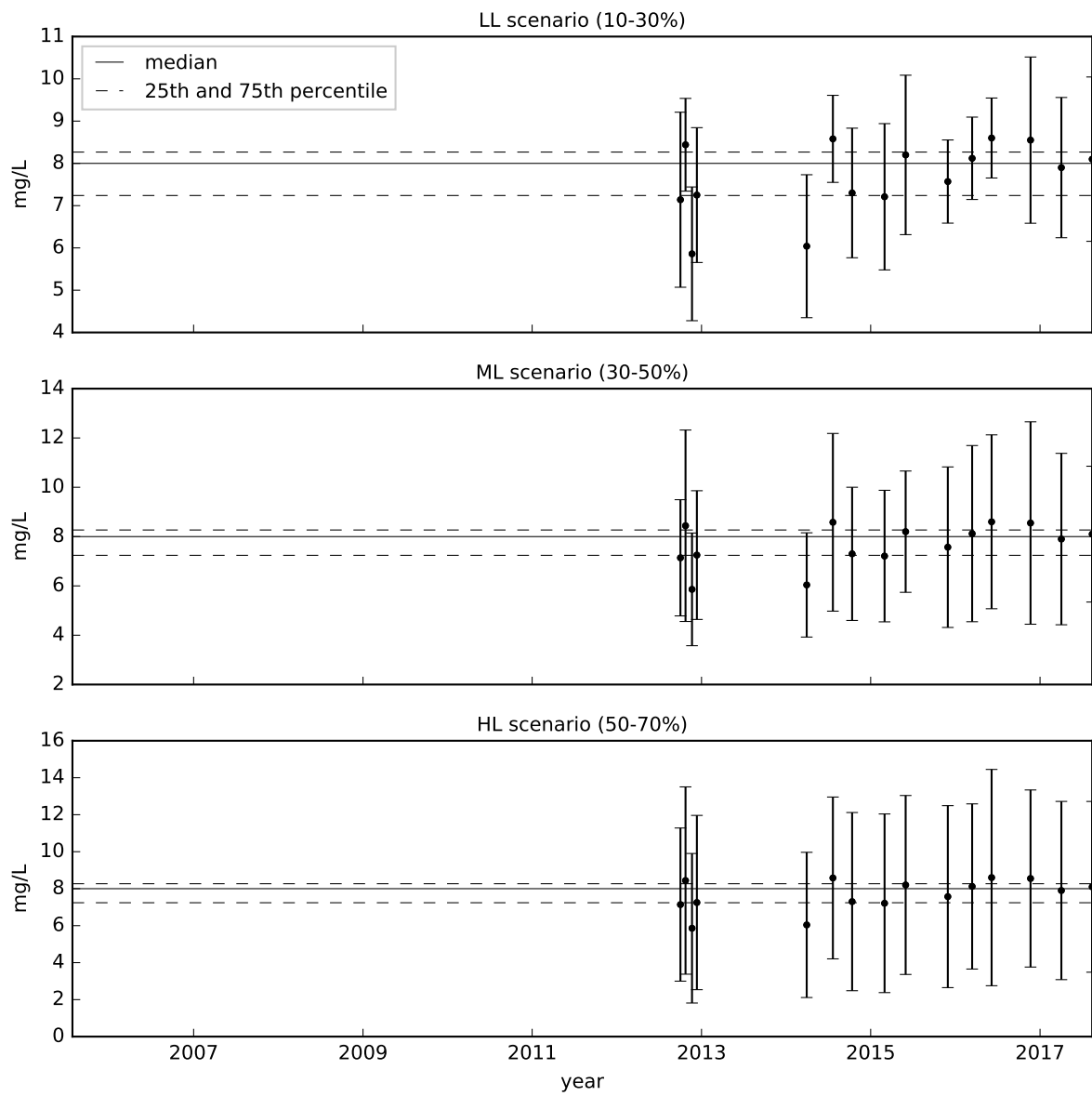
Figure 67 – LL, ML and HL uncertainty scenarios for DO concentration time series, station IG7
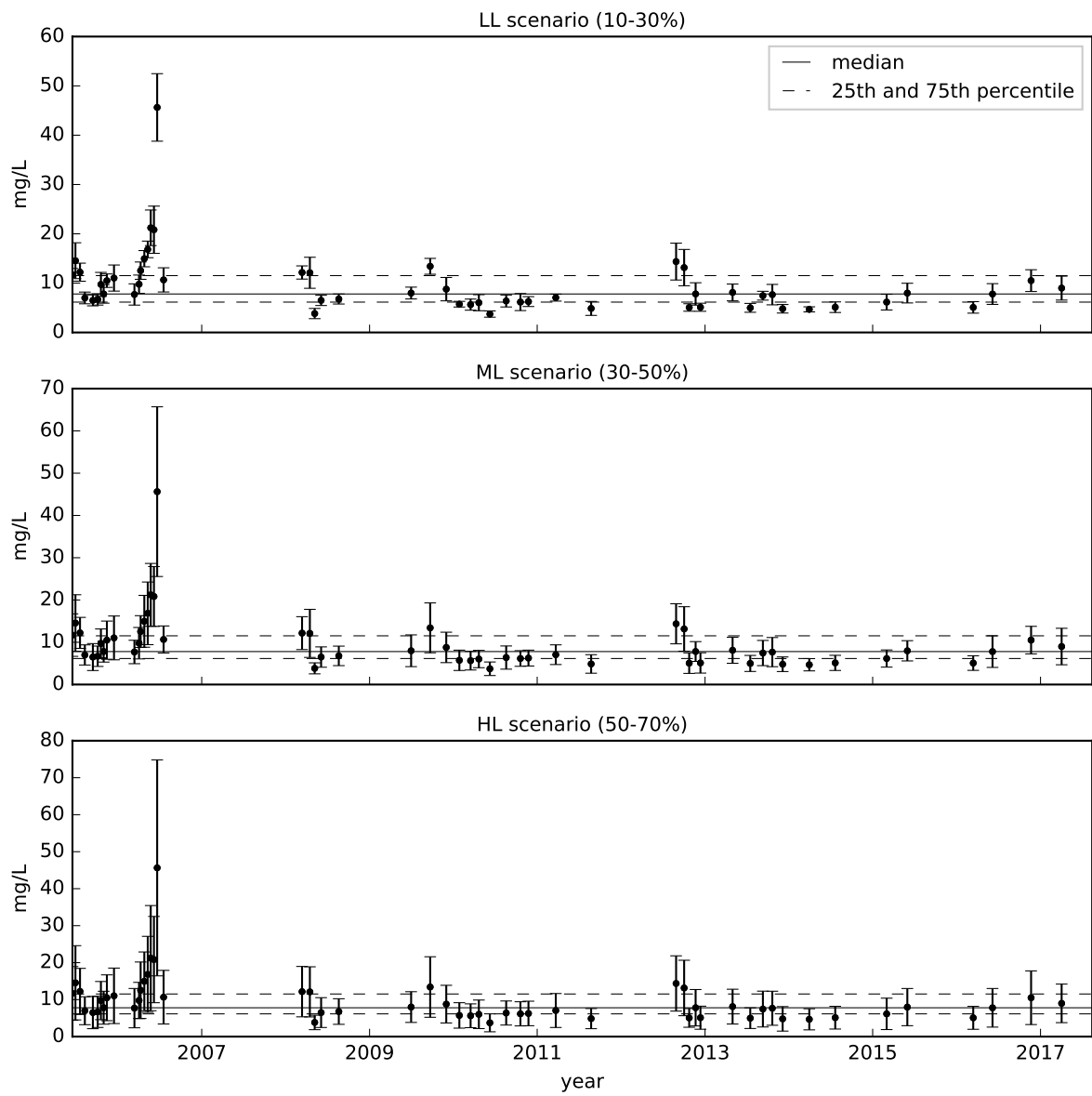
DOC - IG3

Figure 68 – LL, ML and HL uncertainty scenarios for DOC concentration time series, station IG3
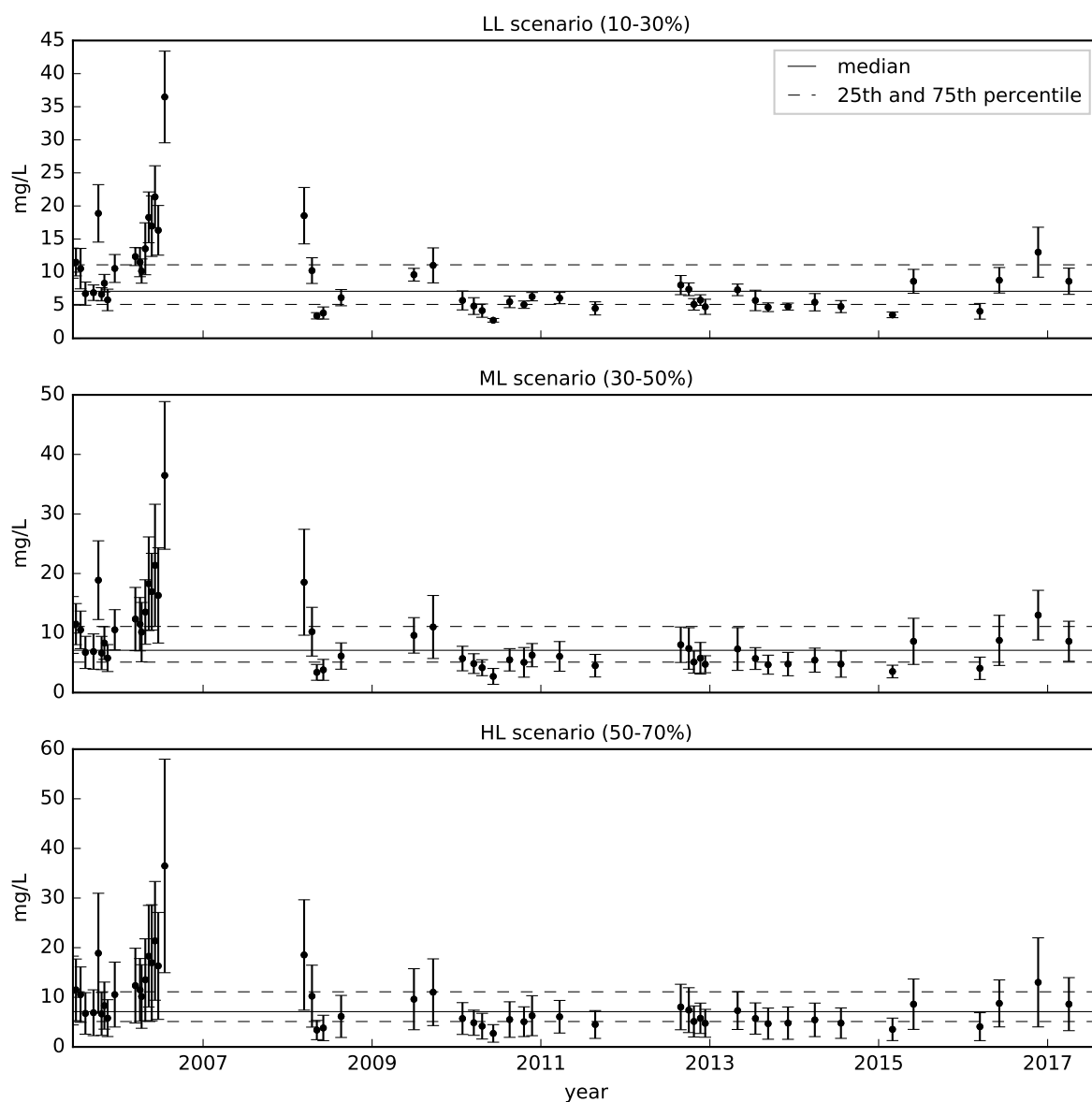
DOC - IG4

Figure 69 – LL, ML and HL uncertainty scenarios for DOC concentration time series from IG4
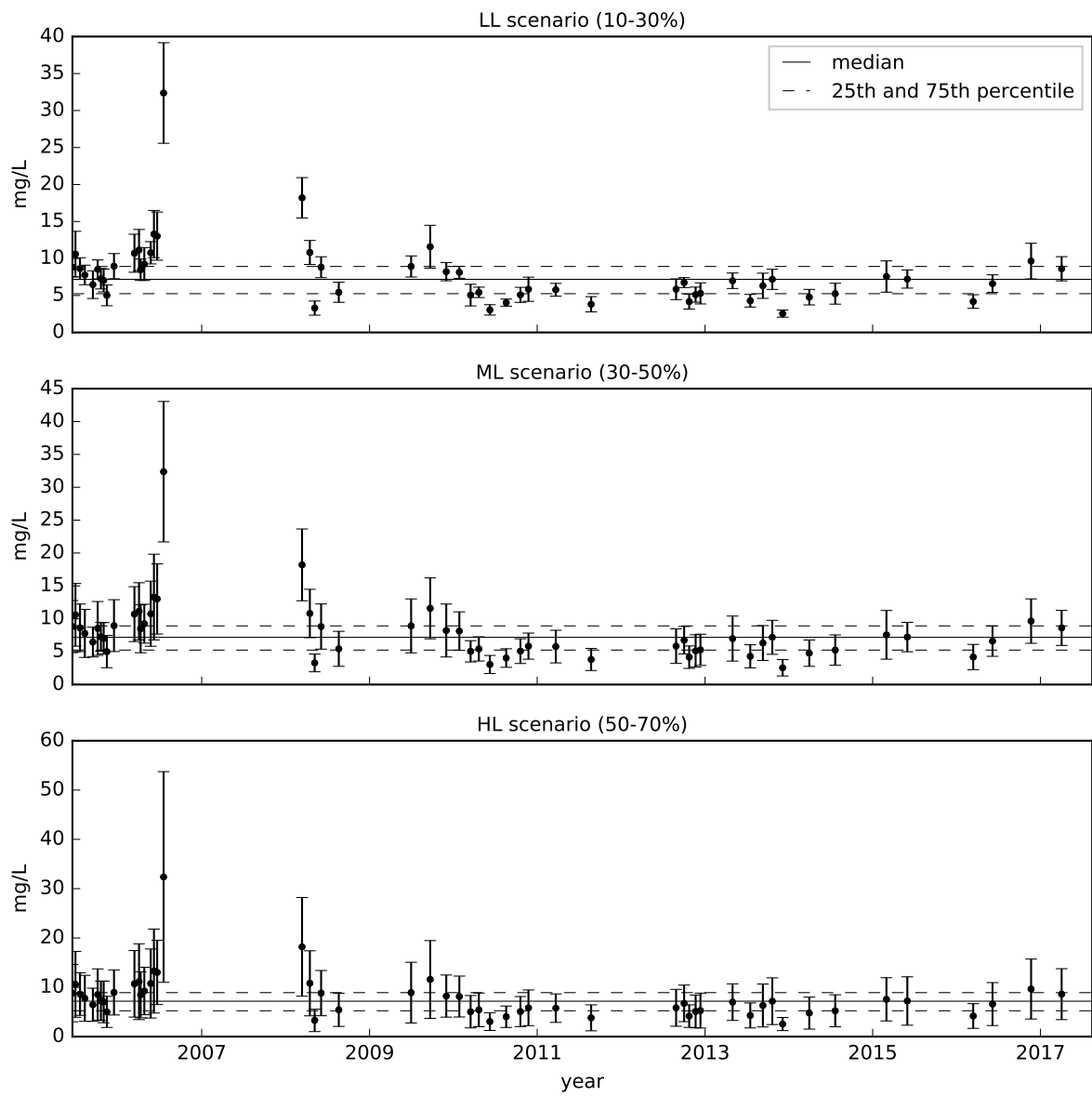
DOC - IG5

Figure 70 – LL, ML and HL uncertainty scenarios for DOC concentration time series, station IG5
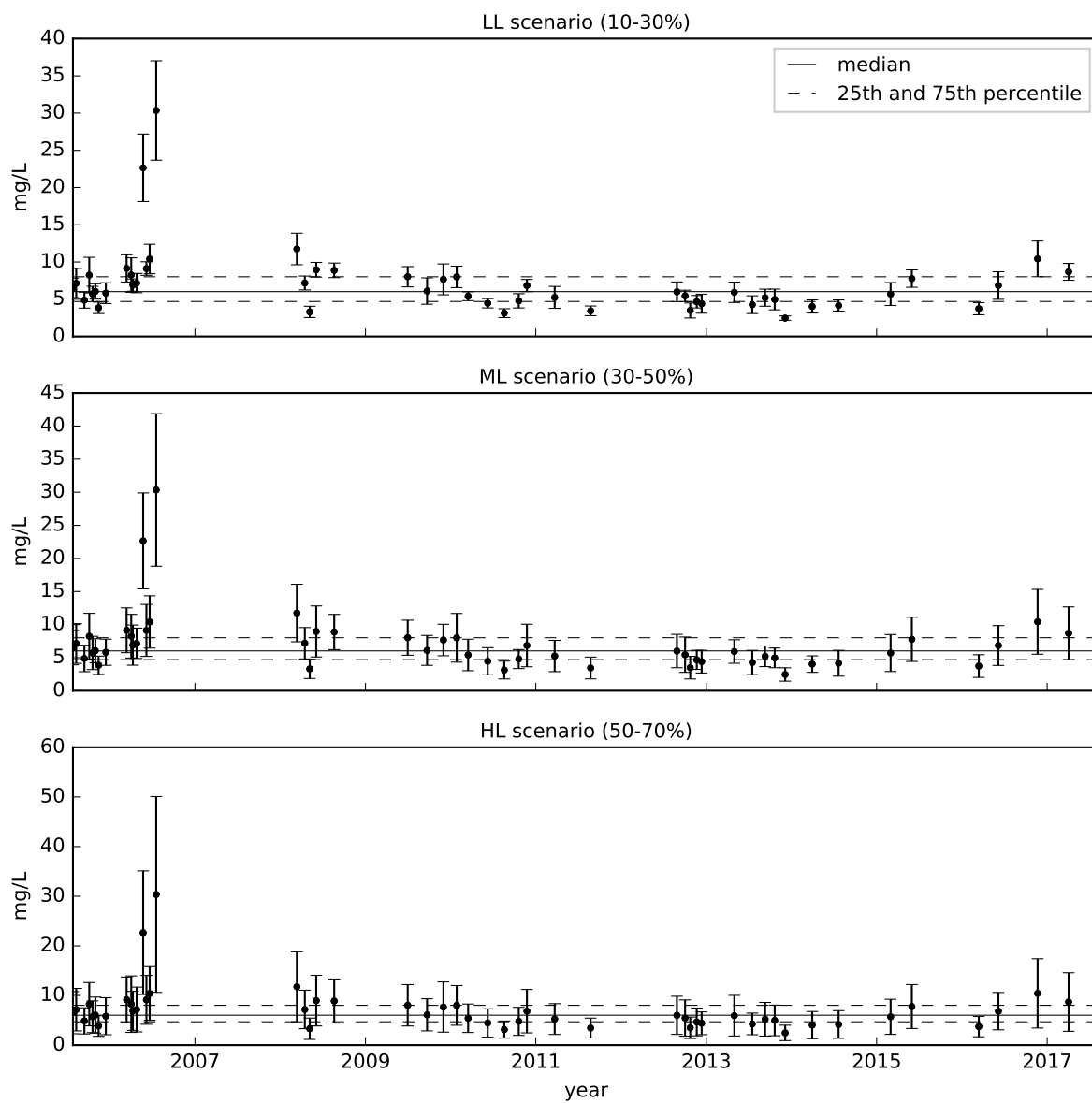
DOC - IG6

Figure 71 – LL, ML and HL uncertainty scenarios for DOC concentration time series, station IG6

DOC - IG7
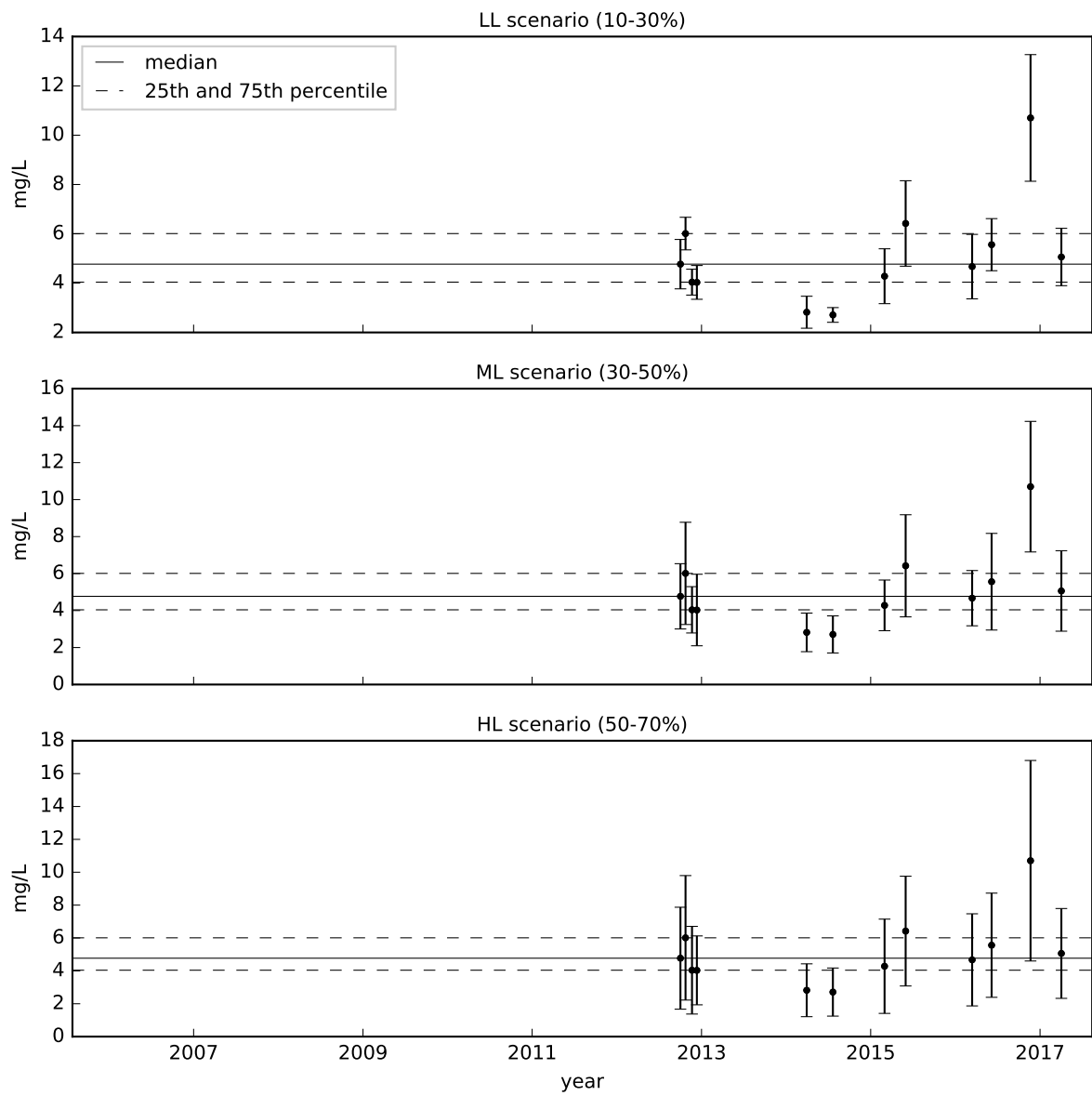
Figure 72 – LL, ML and HL uncertainty scenarios for DOC concentration time series, station IG7
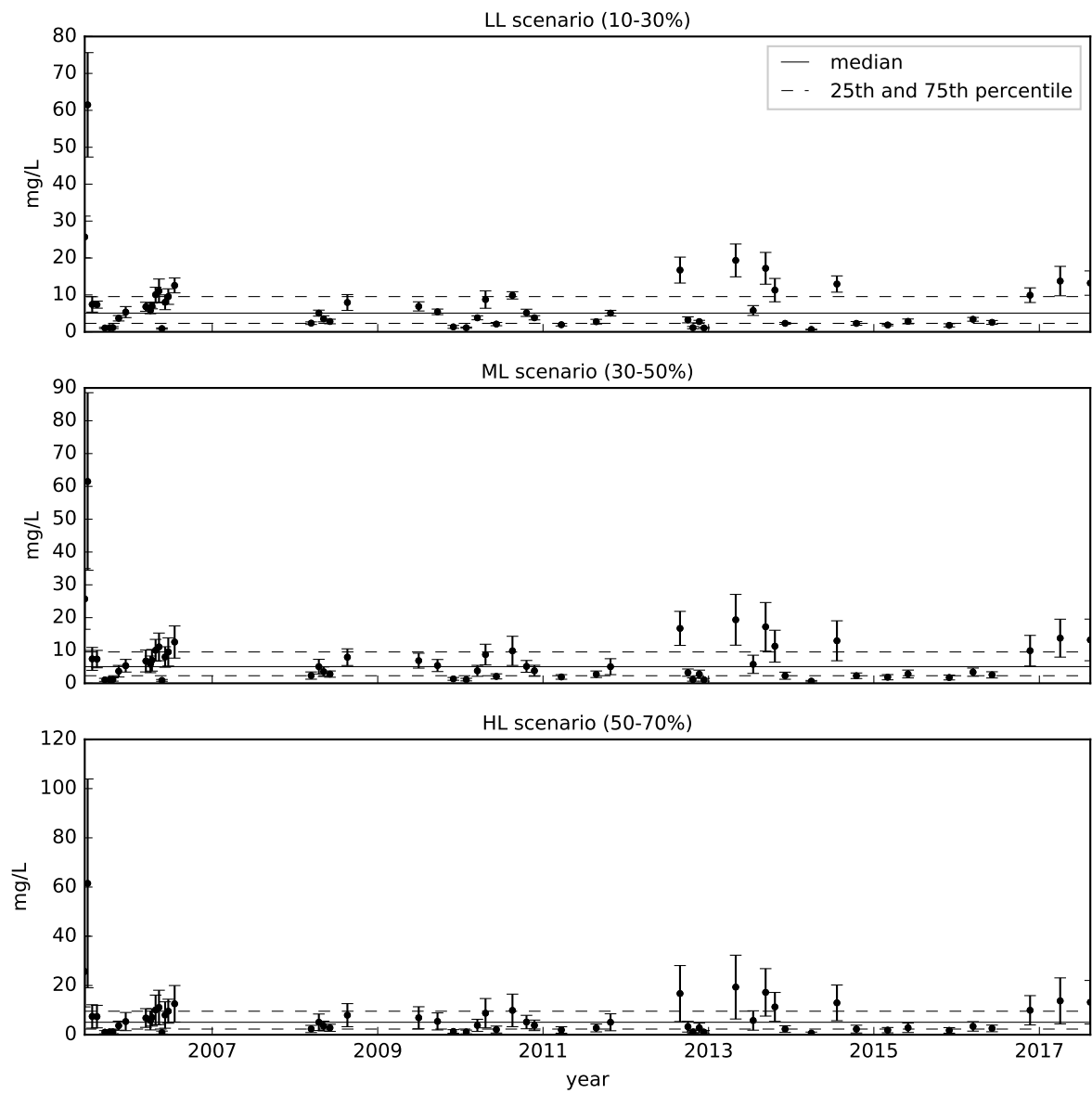
NH4 - IG3

Figure 73 – LL, ML and HL uncertainty scenarios for NH4 concentration time series, station IG3
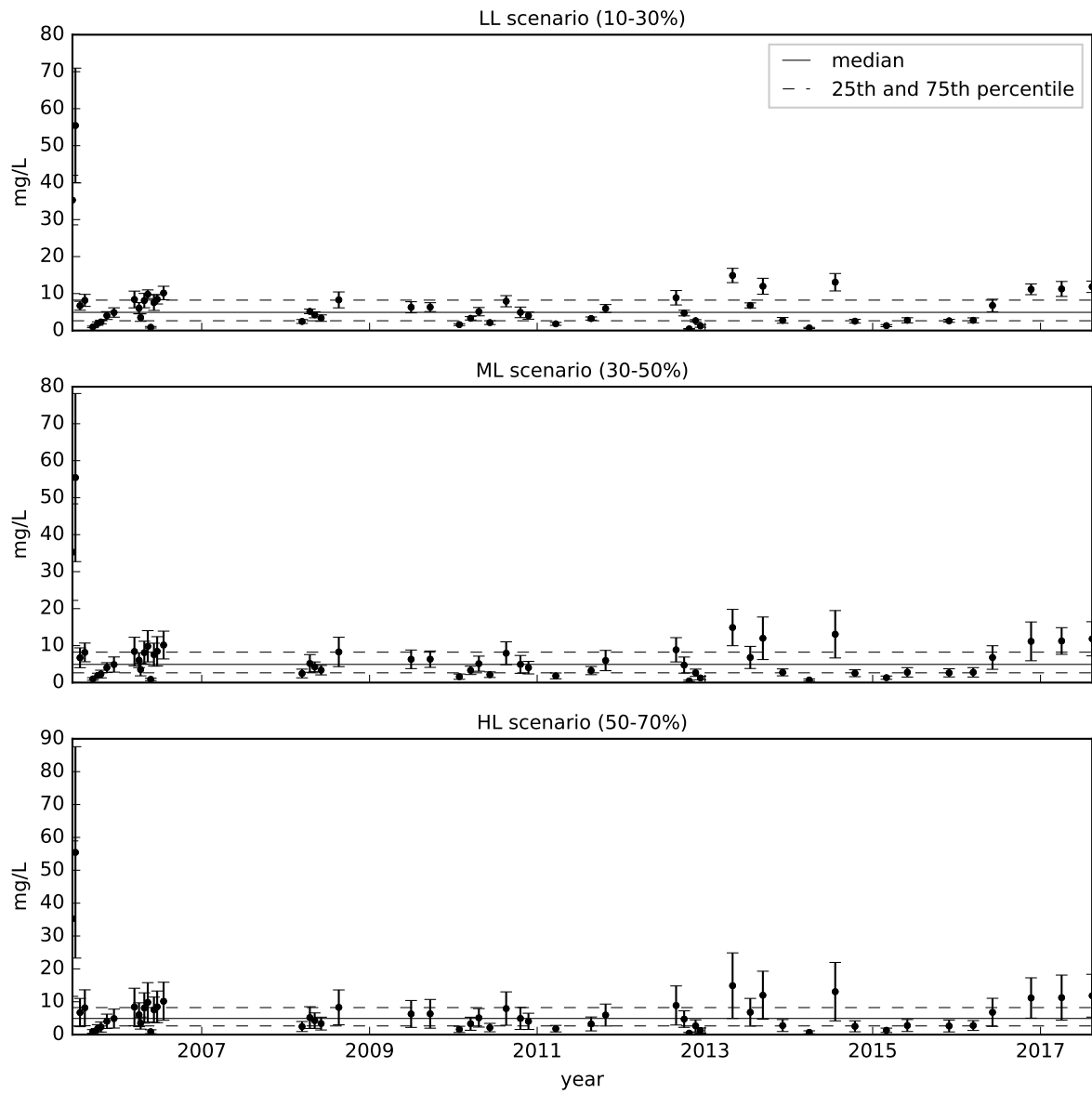
NH4 - IG4

Figure 74 – LL, ML and HL uncertainty scenarios for NH4 concentration time series from IG4
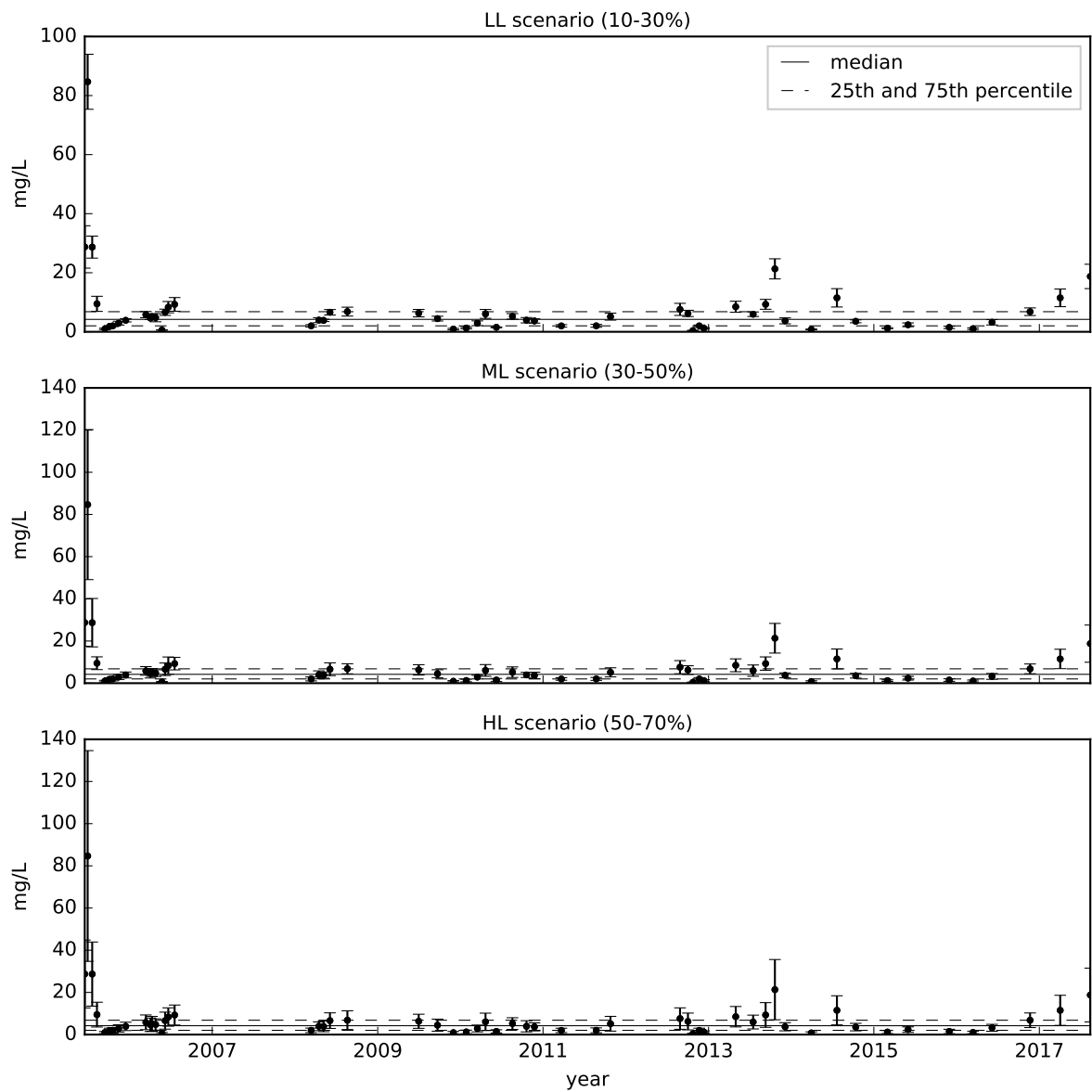
NH4 - IG5

Figure 75 – LL, ML and HL uncertainty scenarios for NH4 concentration time series, station IG5
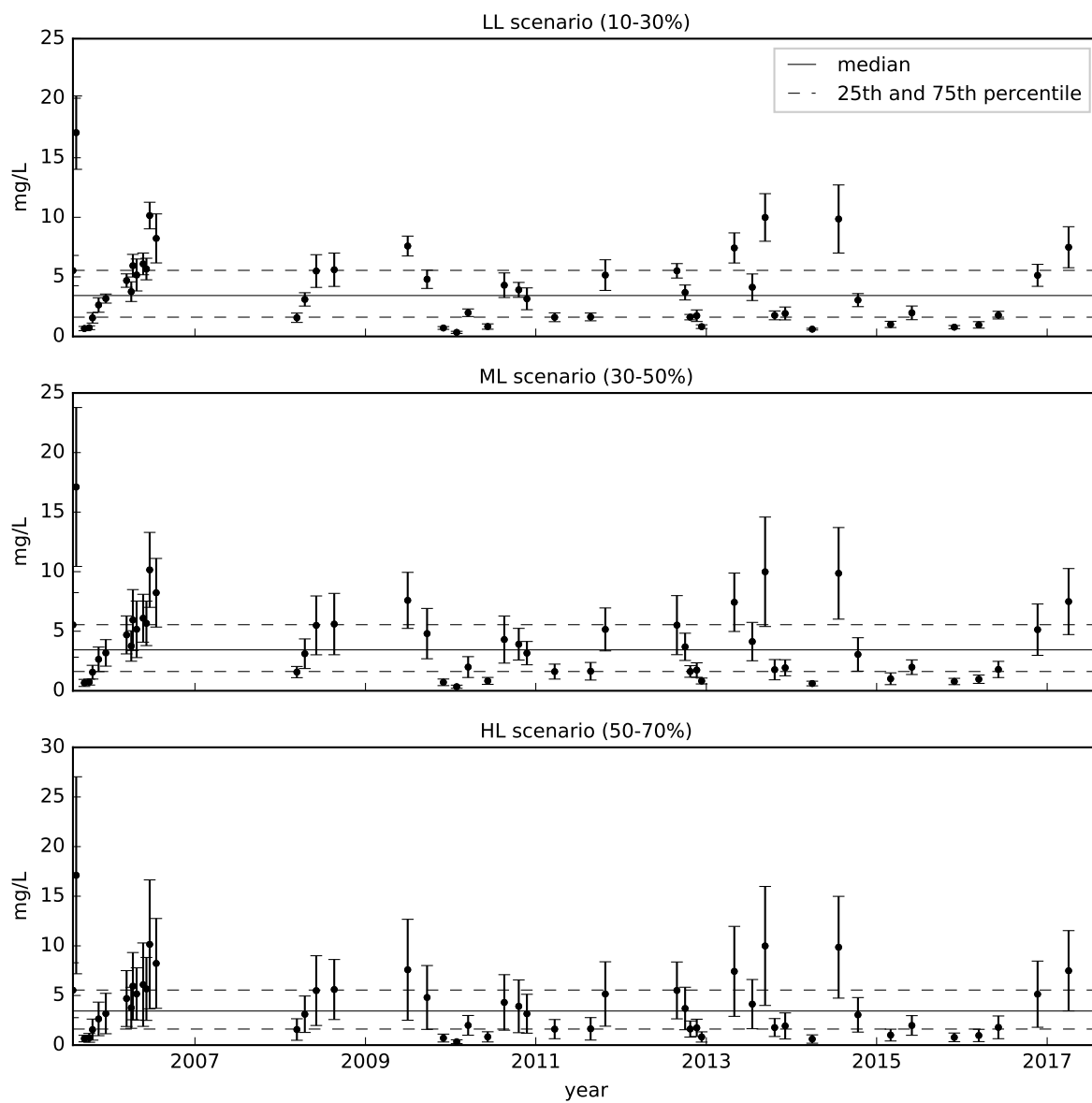
NH4 - IG6

Figure 76 – LL, ML and HL uncertainty scenarios for NH4 concentration time series, station IG6

NH4 - IG7
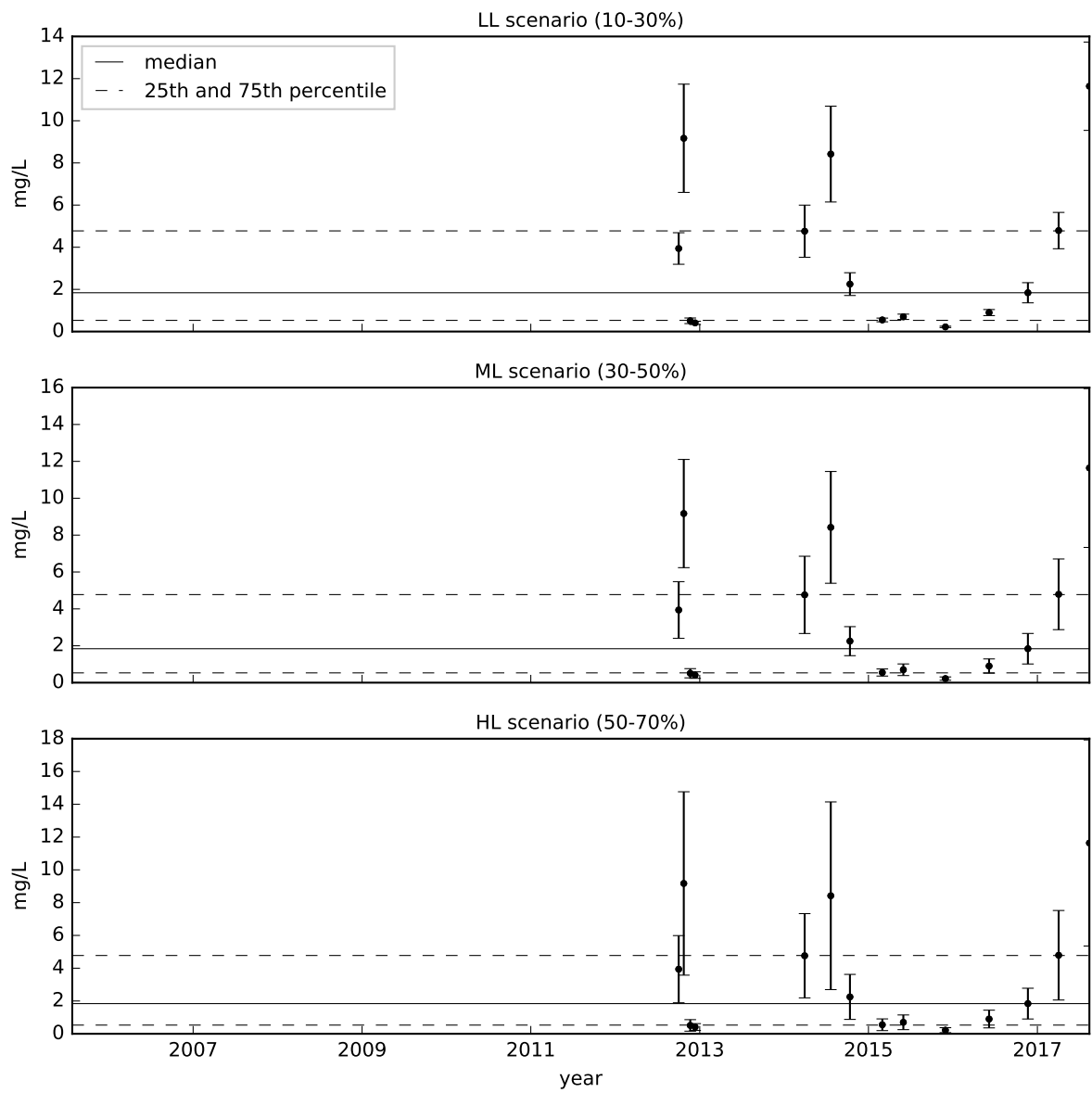
Figure 77 – LL, ML and HL uncertainty scenarios for NH4 concentration time series, station IG7

TP - IG3
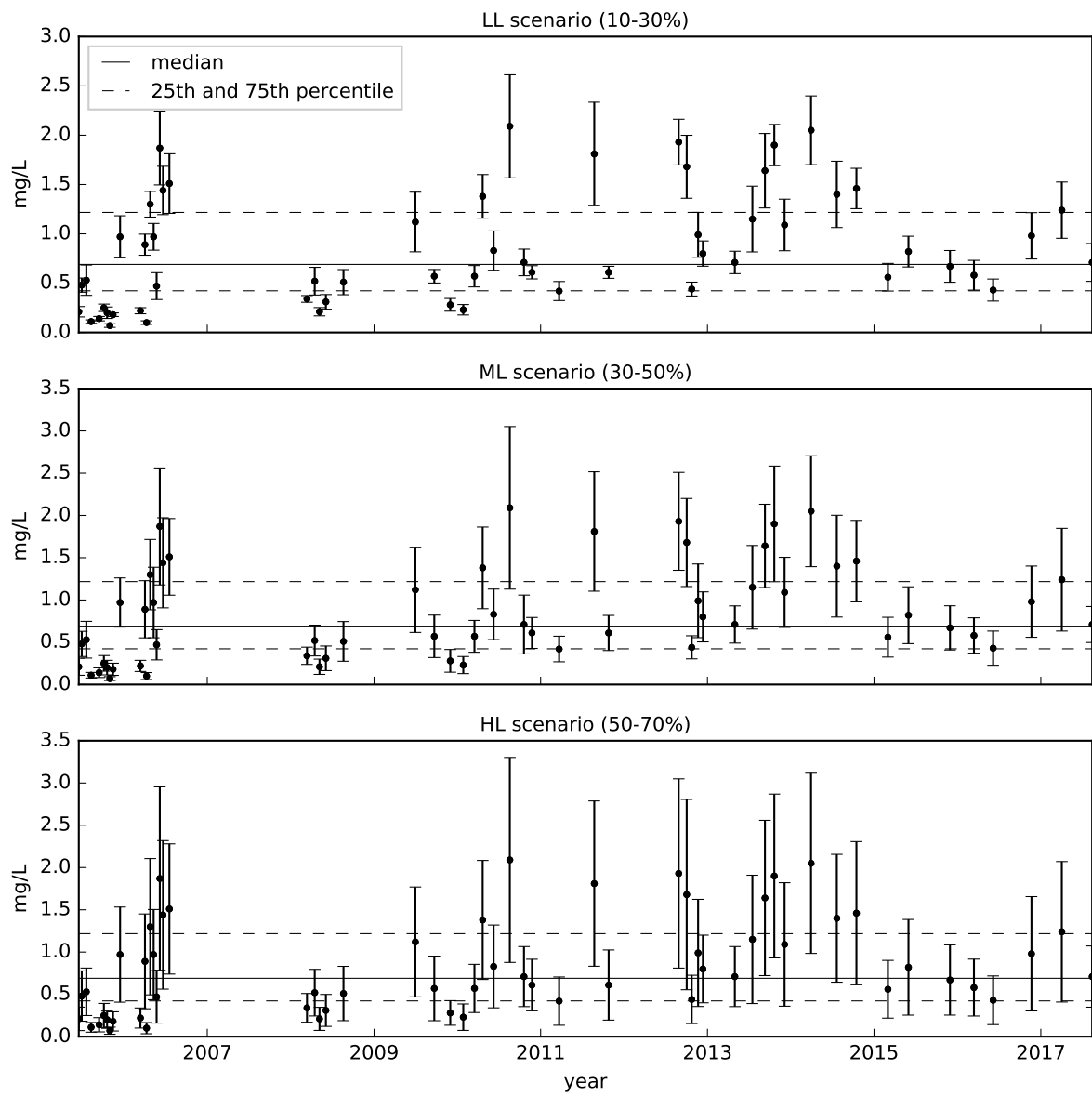
Figure 78 – LL, ML and HL uncertainty scenarios for TP concentration time series, station IG3

TP - IG4
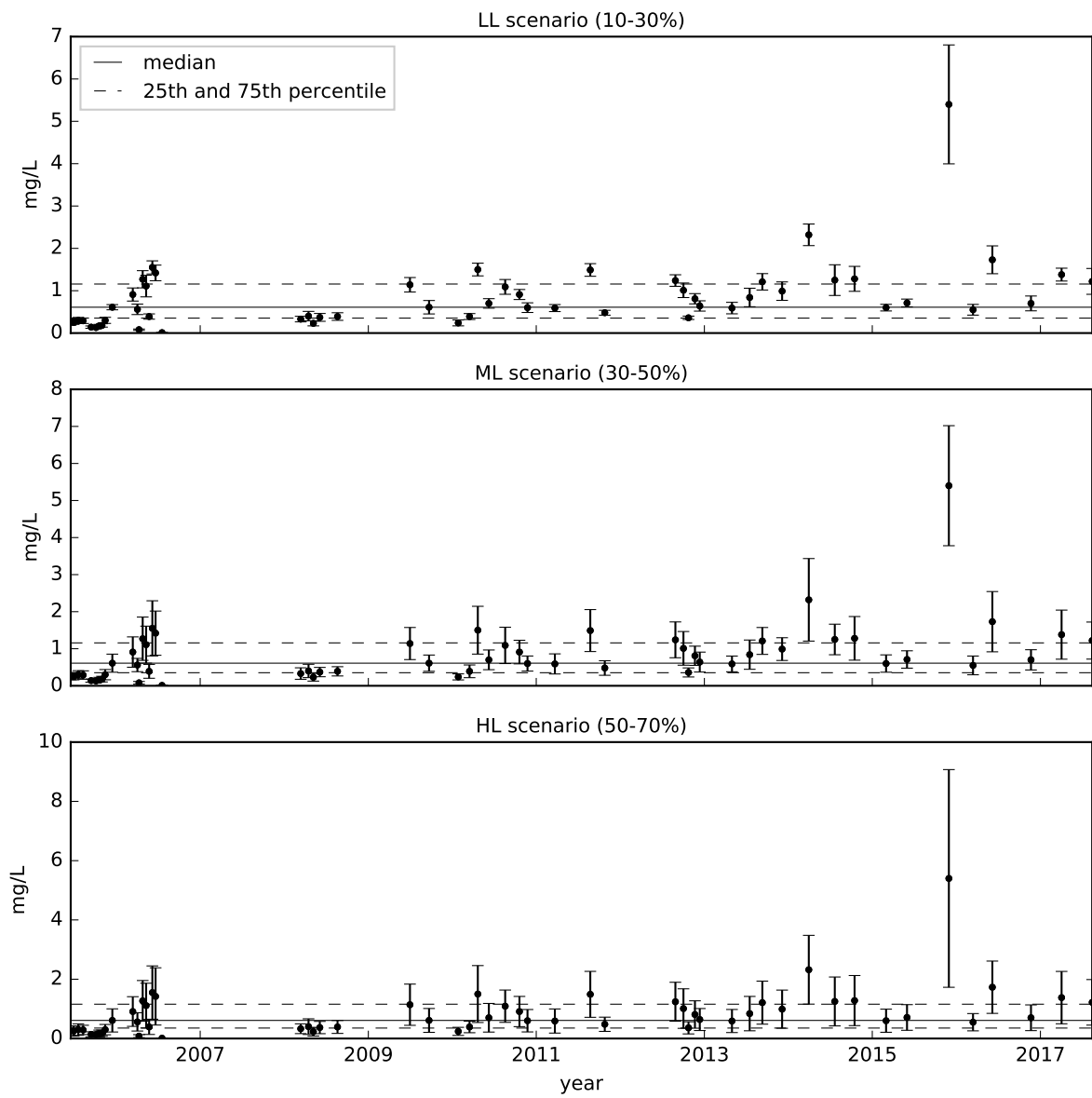
Figure 79 – LL, ML and HL uncertainty scenarios for TP concentration time series from IG4

TP - IG5
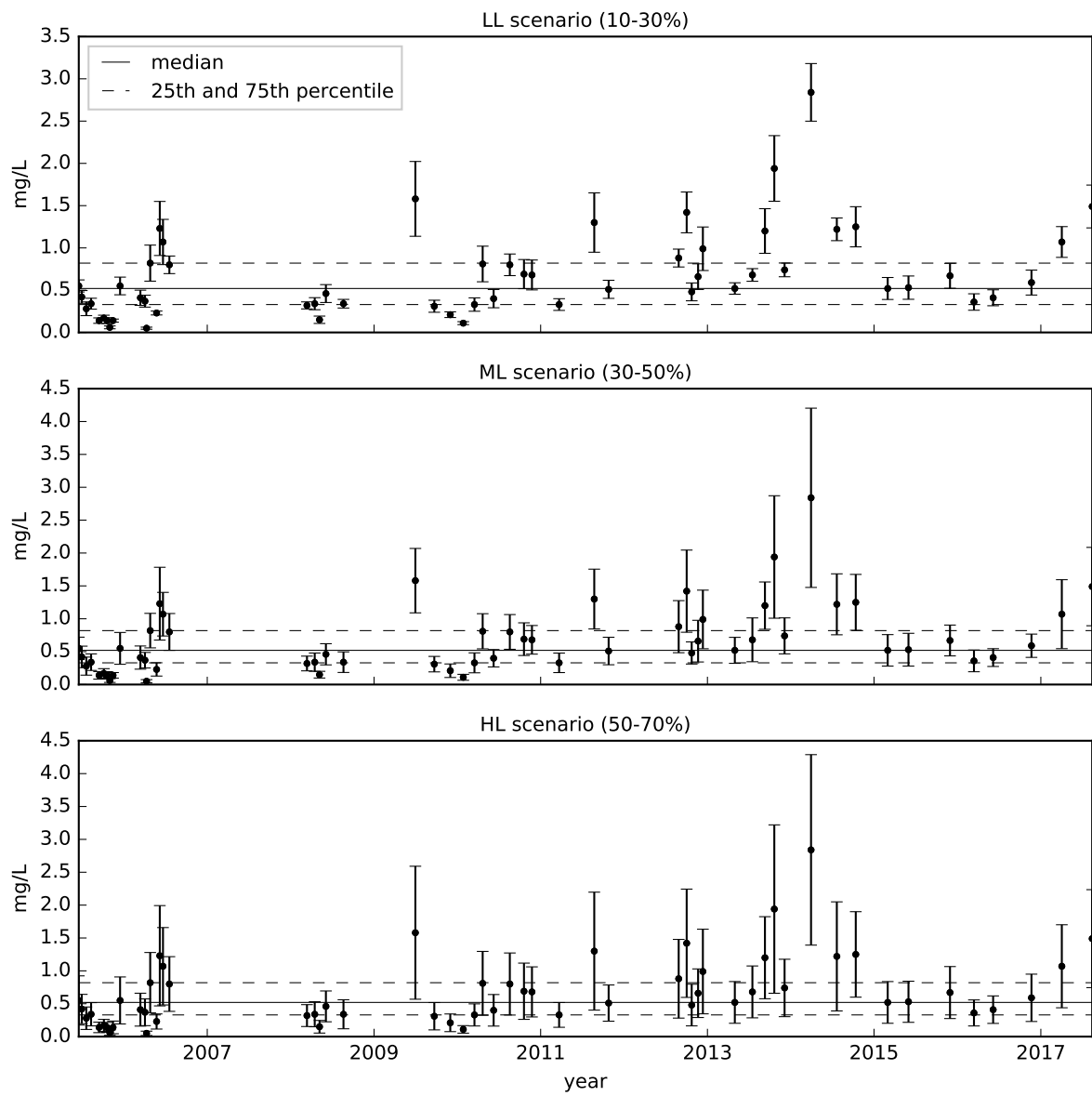
Figure 80 – LL, ML and HL uncertainty scenarios for TP concentration time series, station IG5

TP - IG6
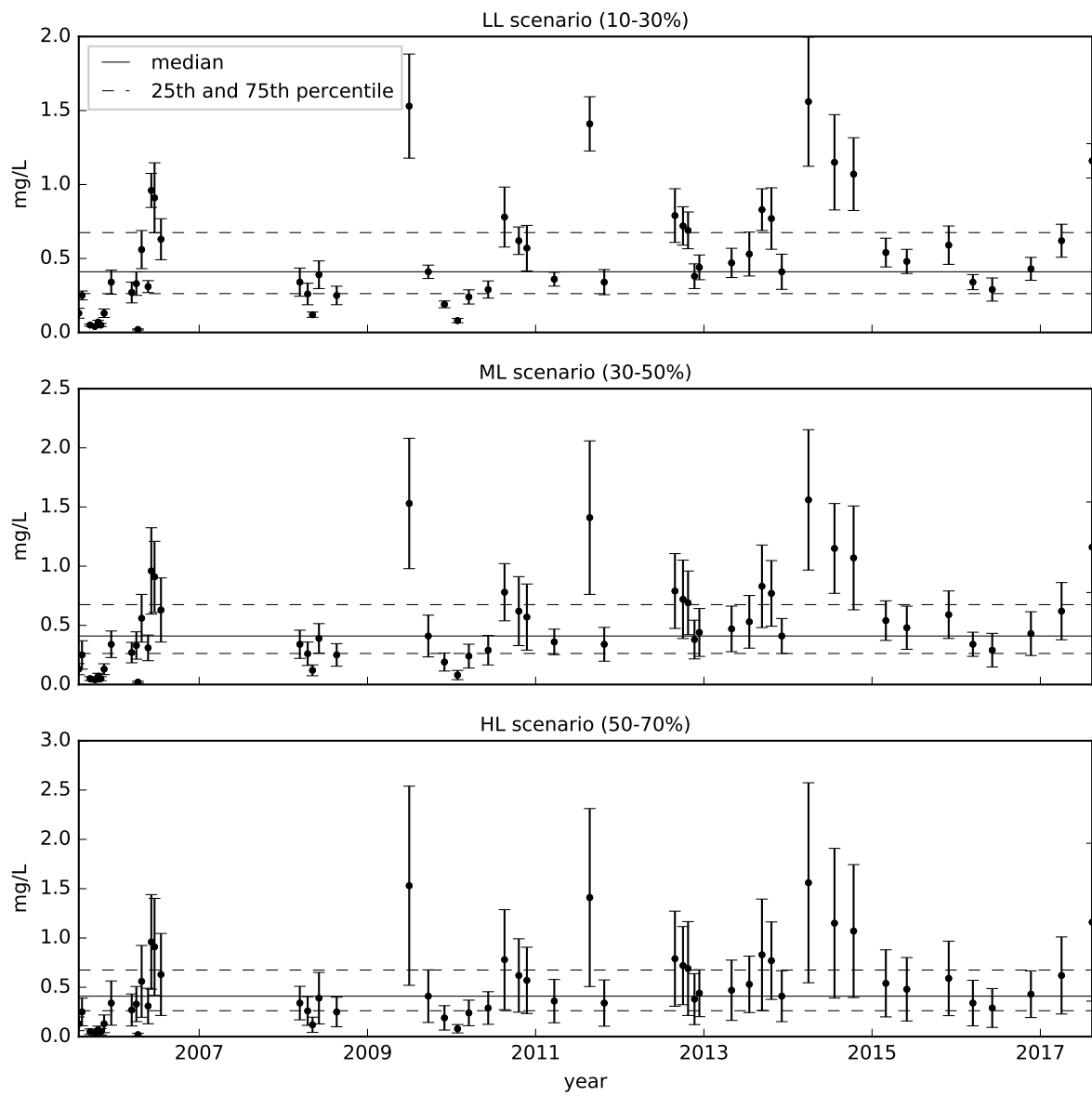
Figure 81 – LL, ML and HL uncertainty scenarios for TP concentration time series, station IG6

TP - IG7
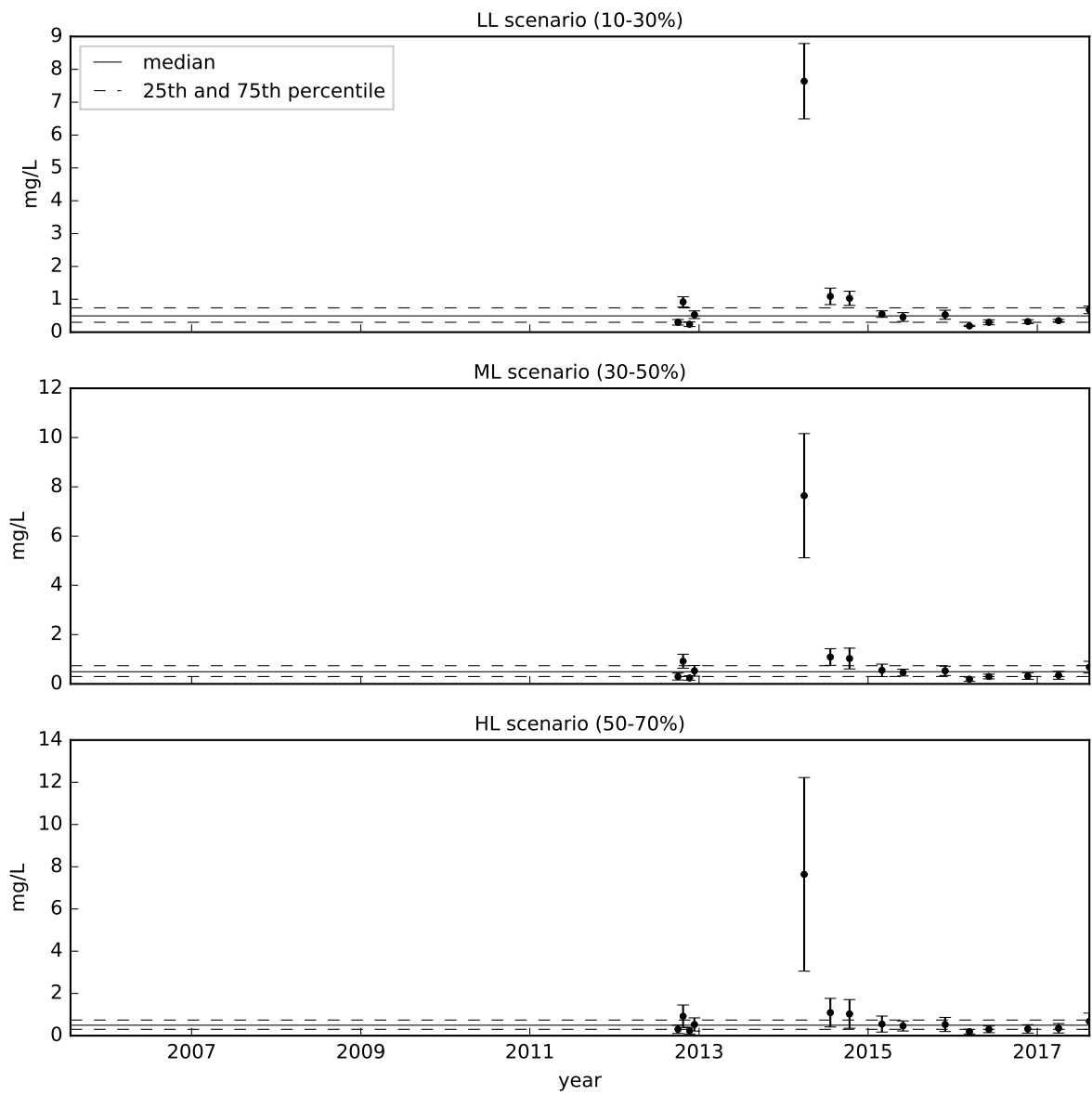
Figure 82 – LL, ML and HL uncertainty scenarios for TP concentration time series, station IG7
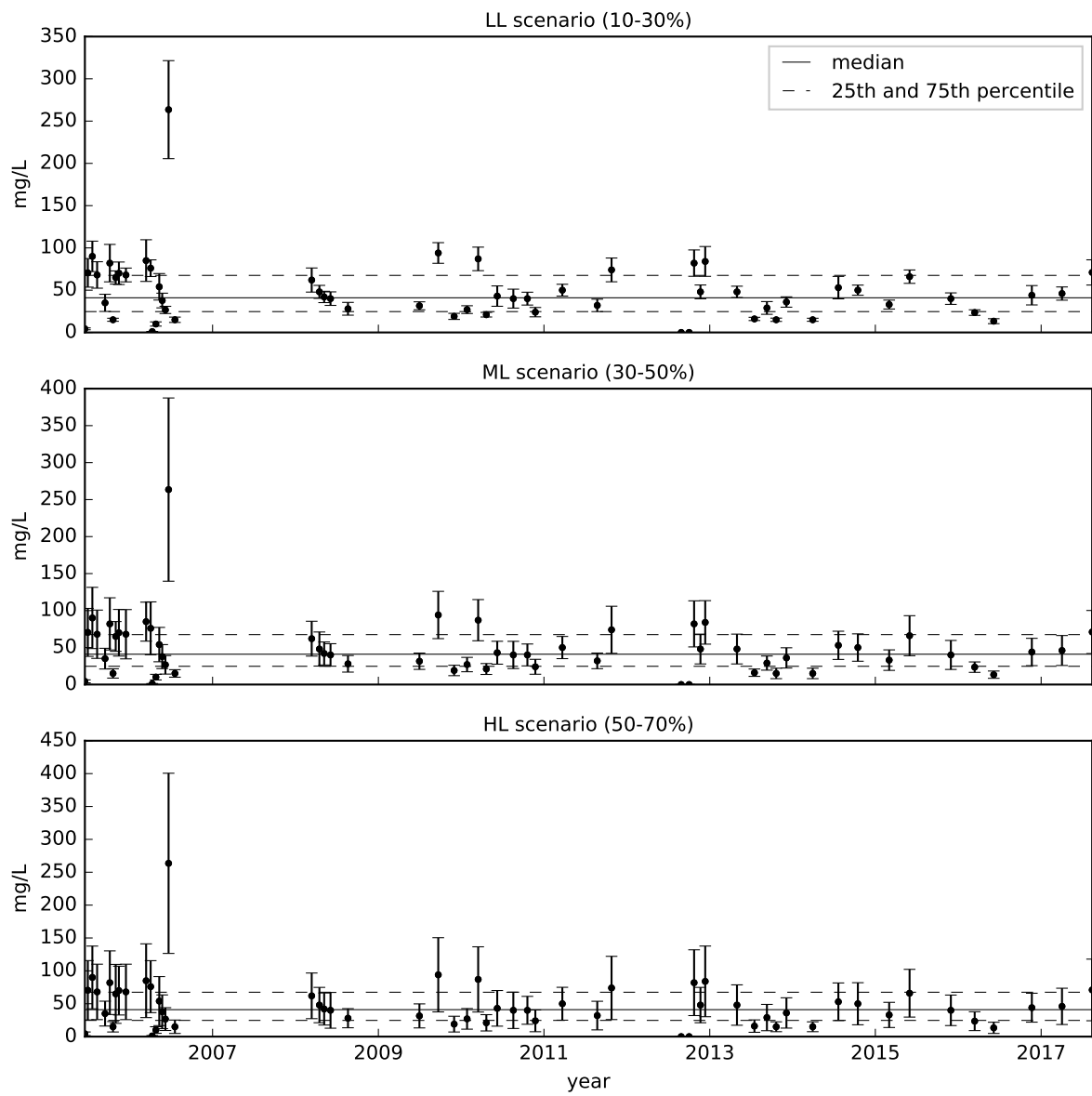
VDS - IG3

Figure 83 – LL, ML and HL uncertainty scenarios for VDS concentration time series, station IG3
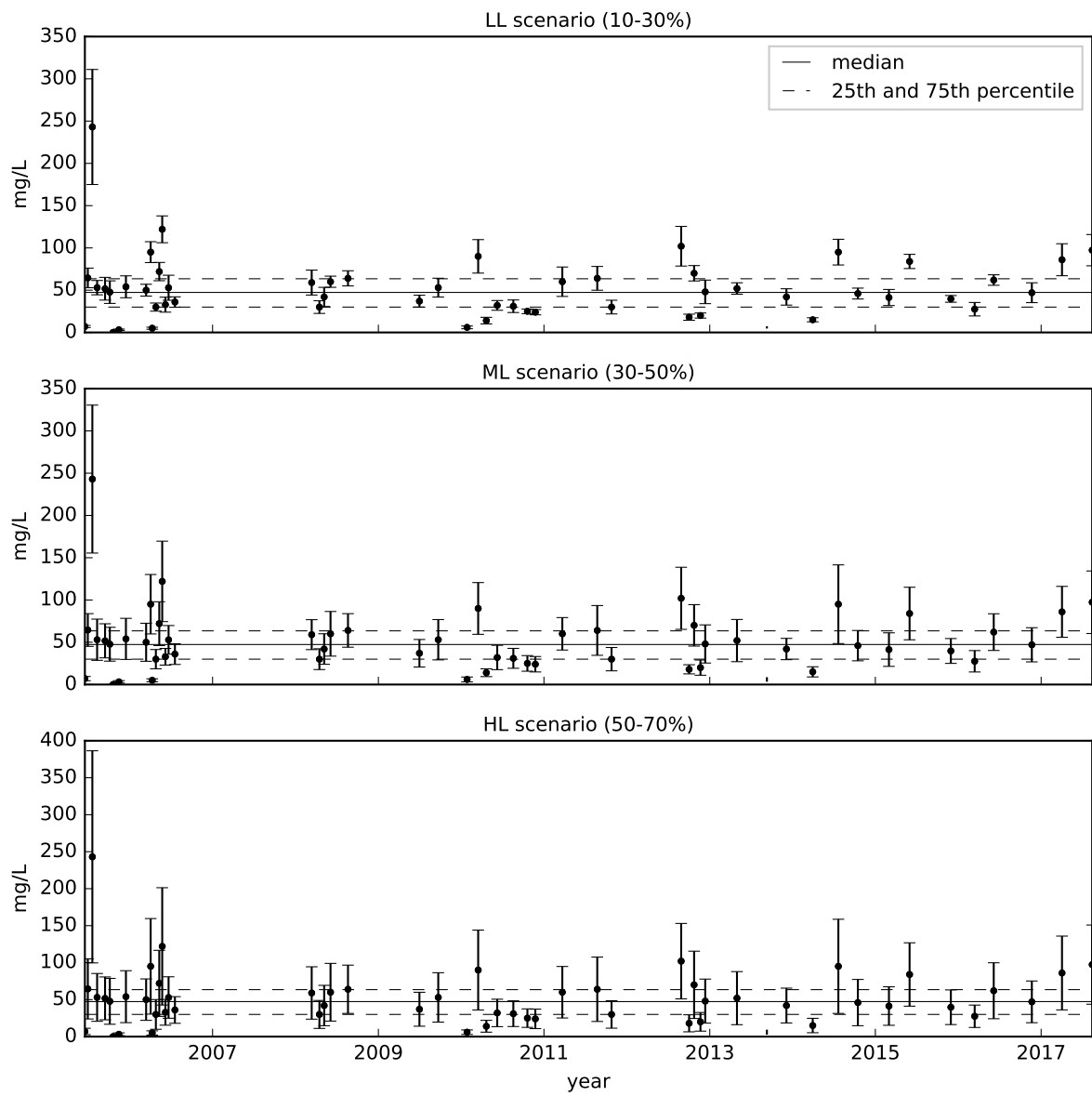
VDS - IG4

Figure 84 – LL, ML and HL uncertainty scenarios for VDS concentration time series from IG4
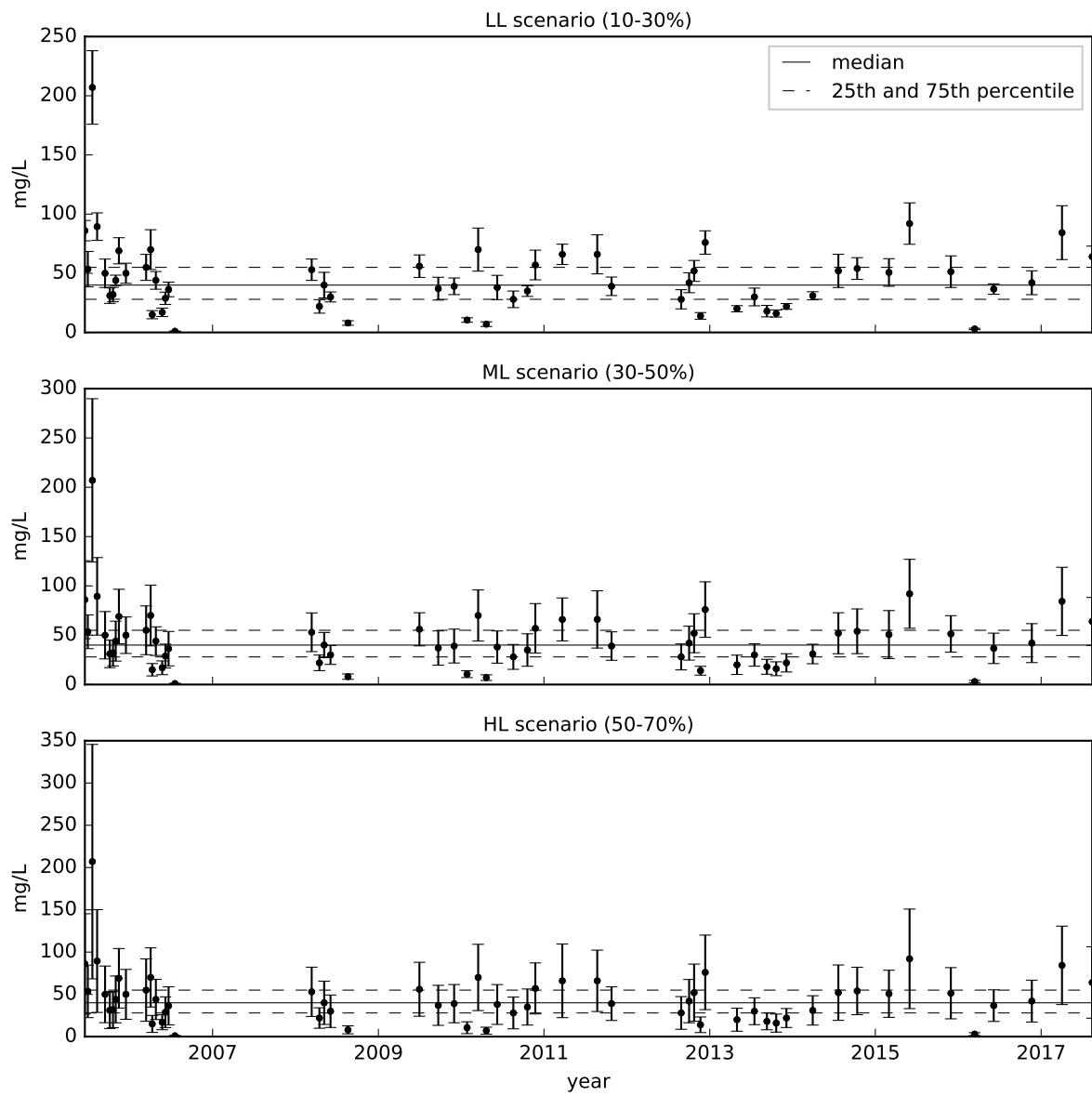
VDS - IG5

Figure 85 – LL, ML and HL uncertainty scenarios for VDS concentration time series, station IG5
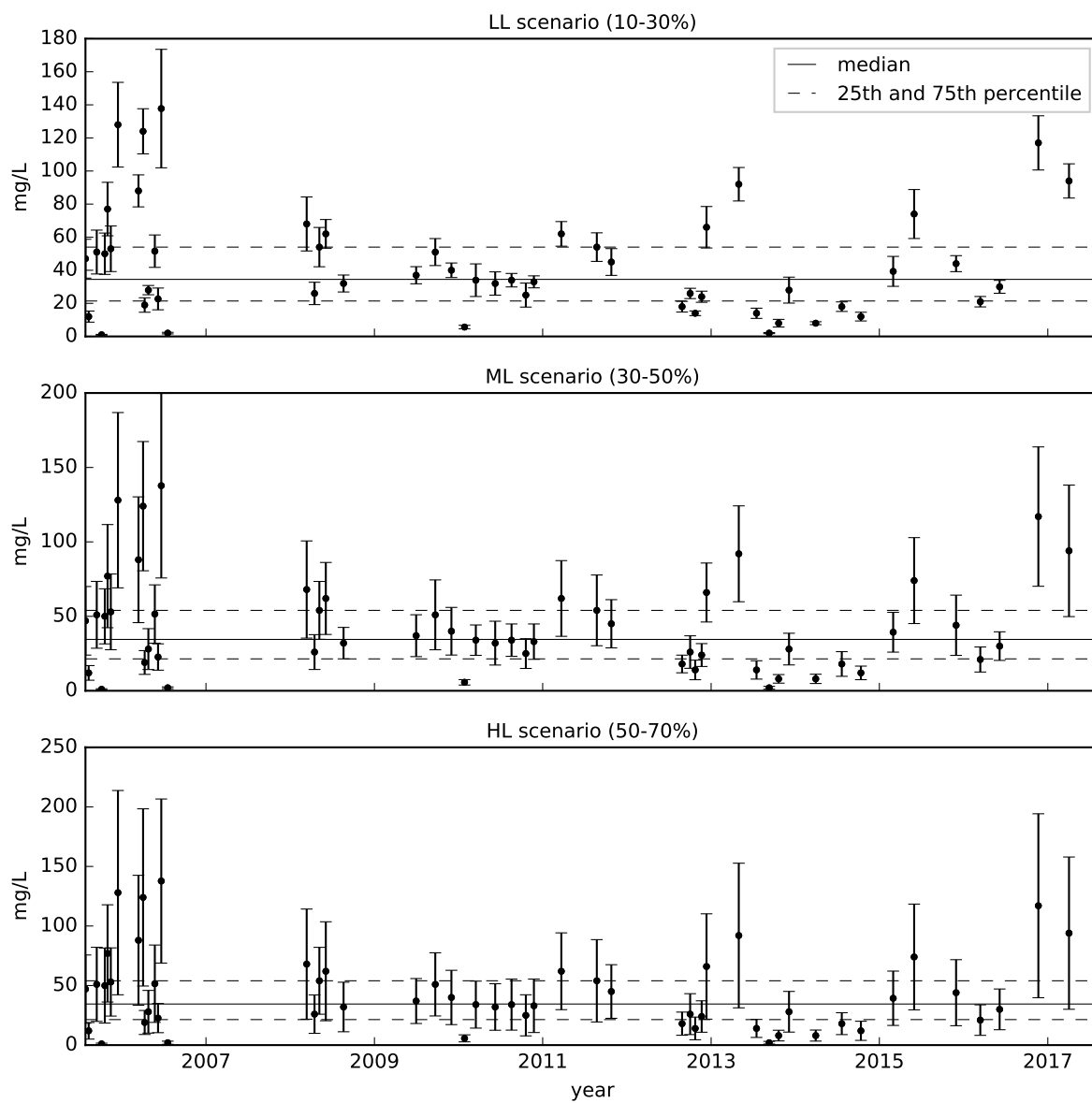
VDS - IG6

Figure 86 – LL, ML and HL uncertainty scenarios for VDS concentration time series, station IG6

VDS - IG7
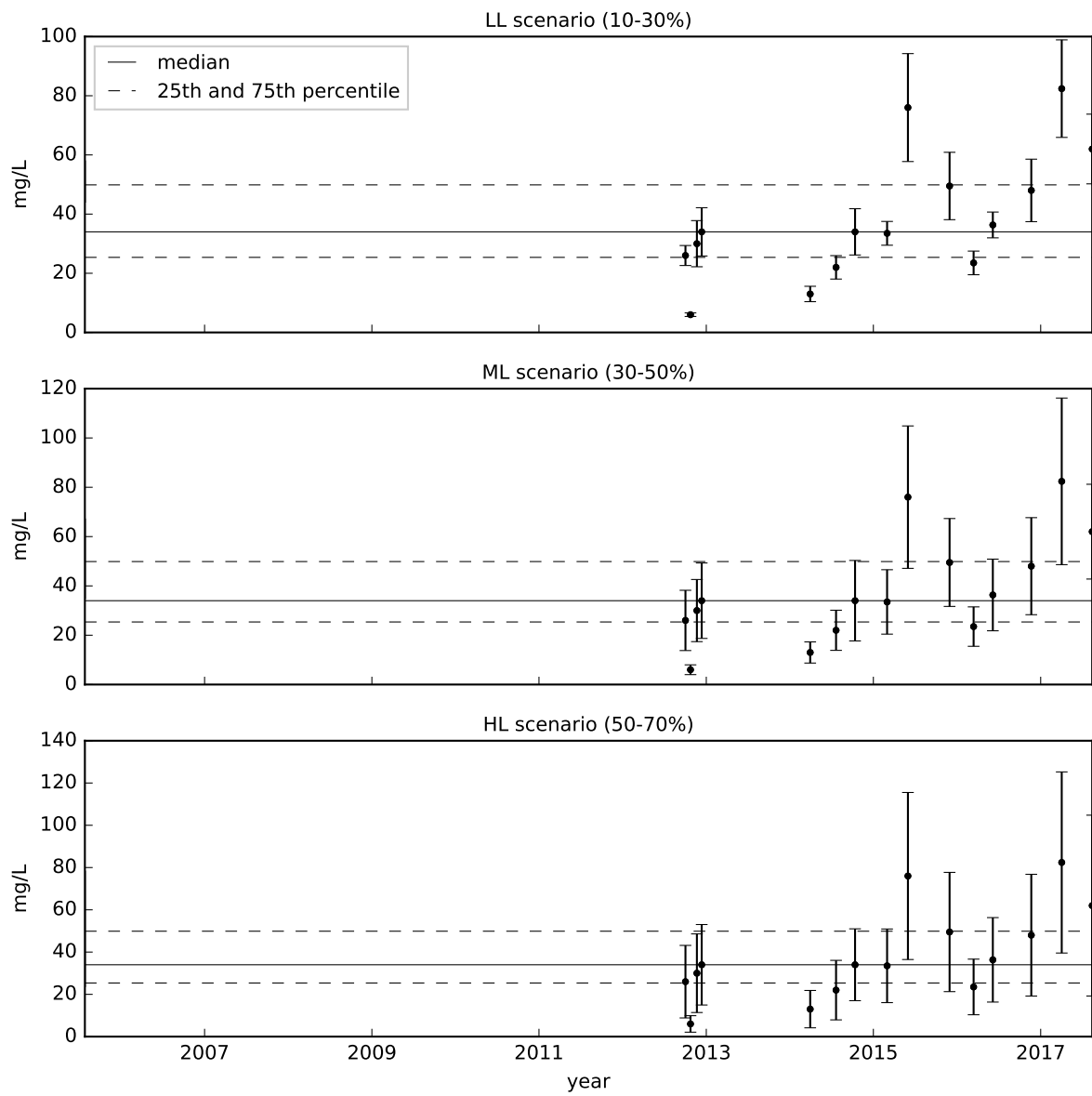
Figure 87 – LL, ML and HL uncertainty scenarios for VDS concentration time series, station IG7

A.4 Uncertainty scenarios (ton/d)

BOD - IG3
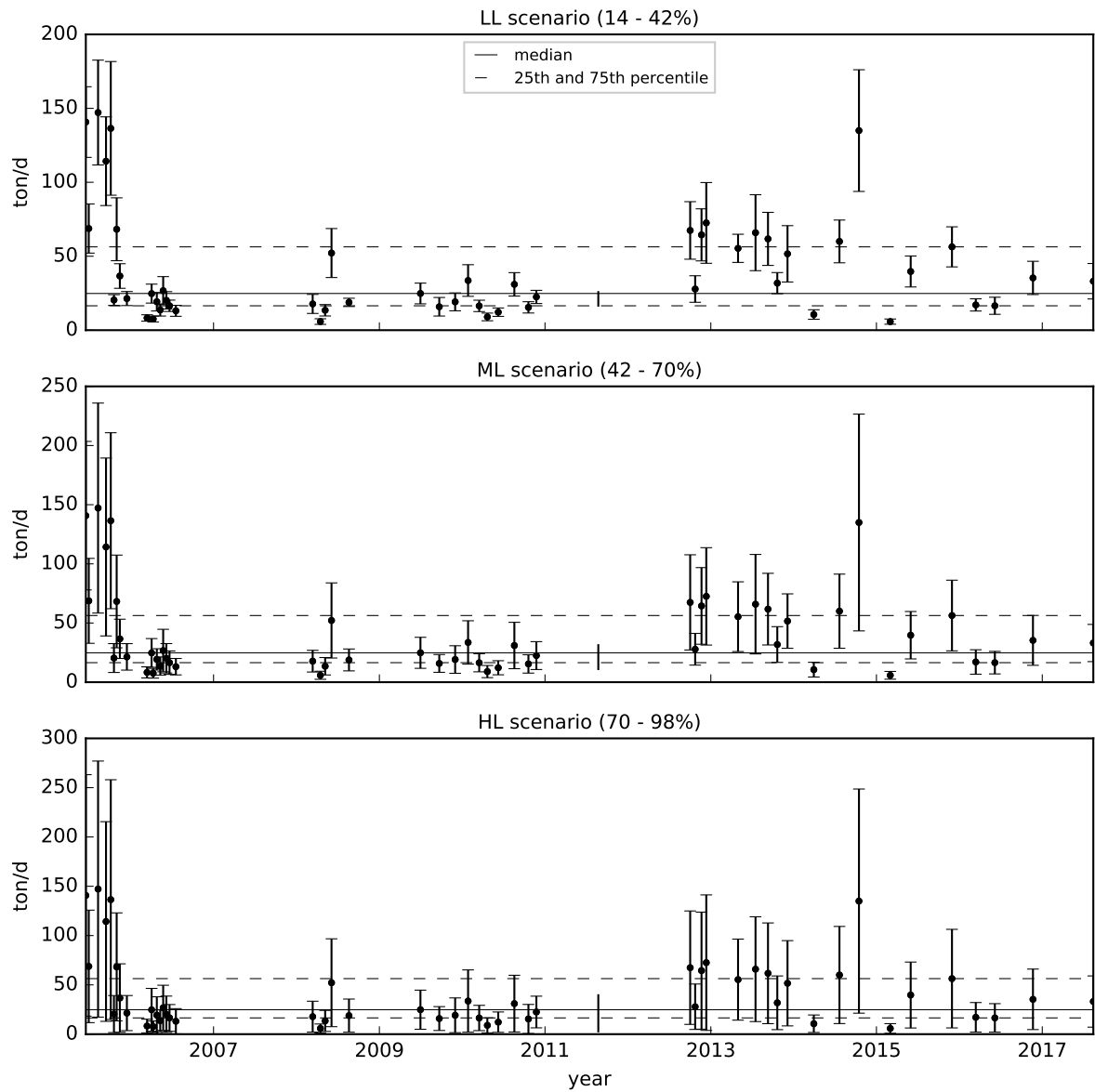
Figure 88 – LL, ML and HL uncertainty scenarios for BOD load time series, station IG3
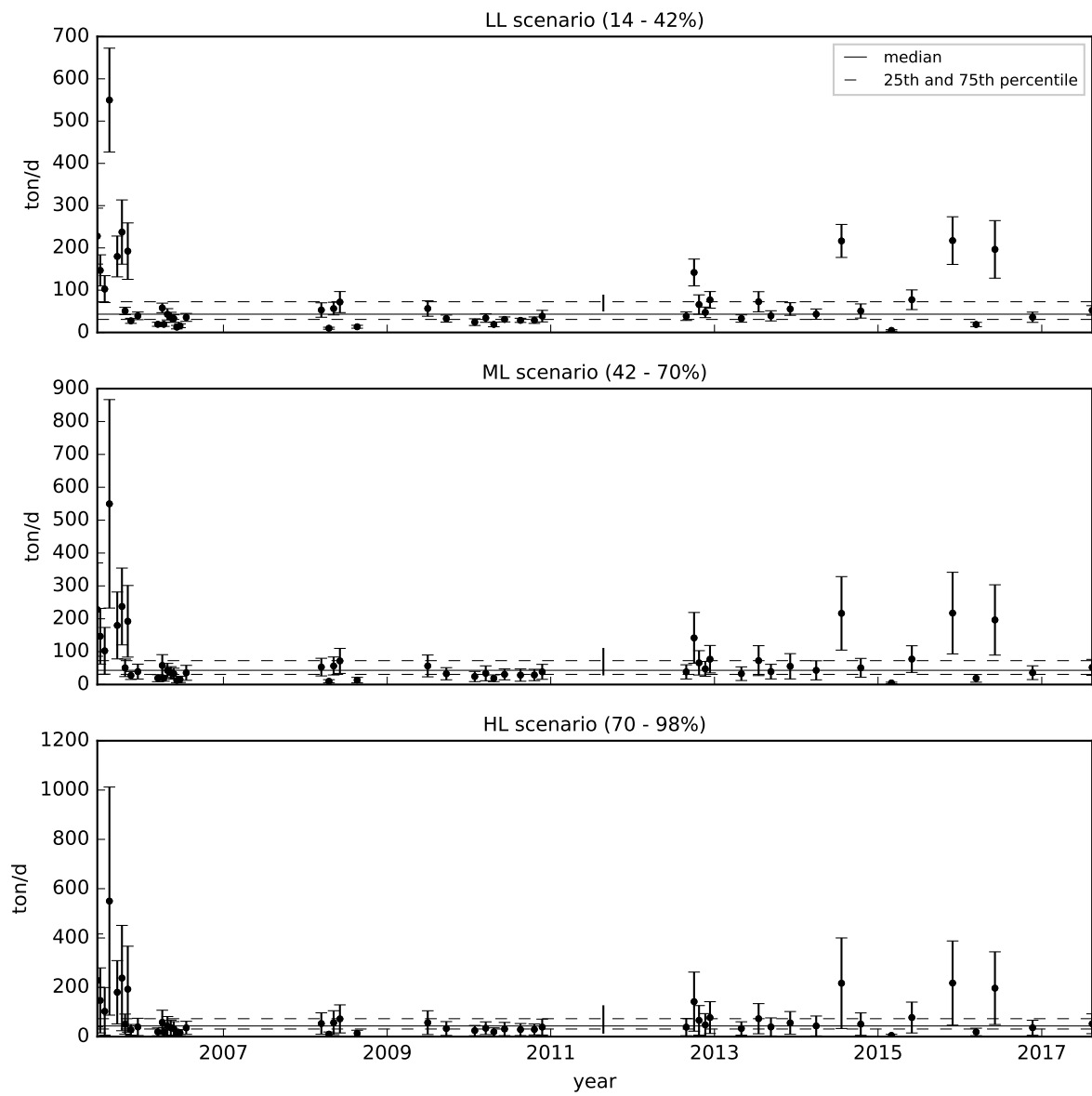
BOD - IG4

Figure 89 – LL, ML and HL uncertainty scenarios for BOD load time series from IG4
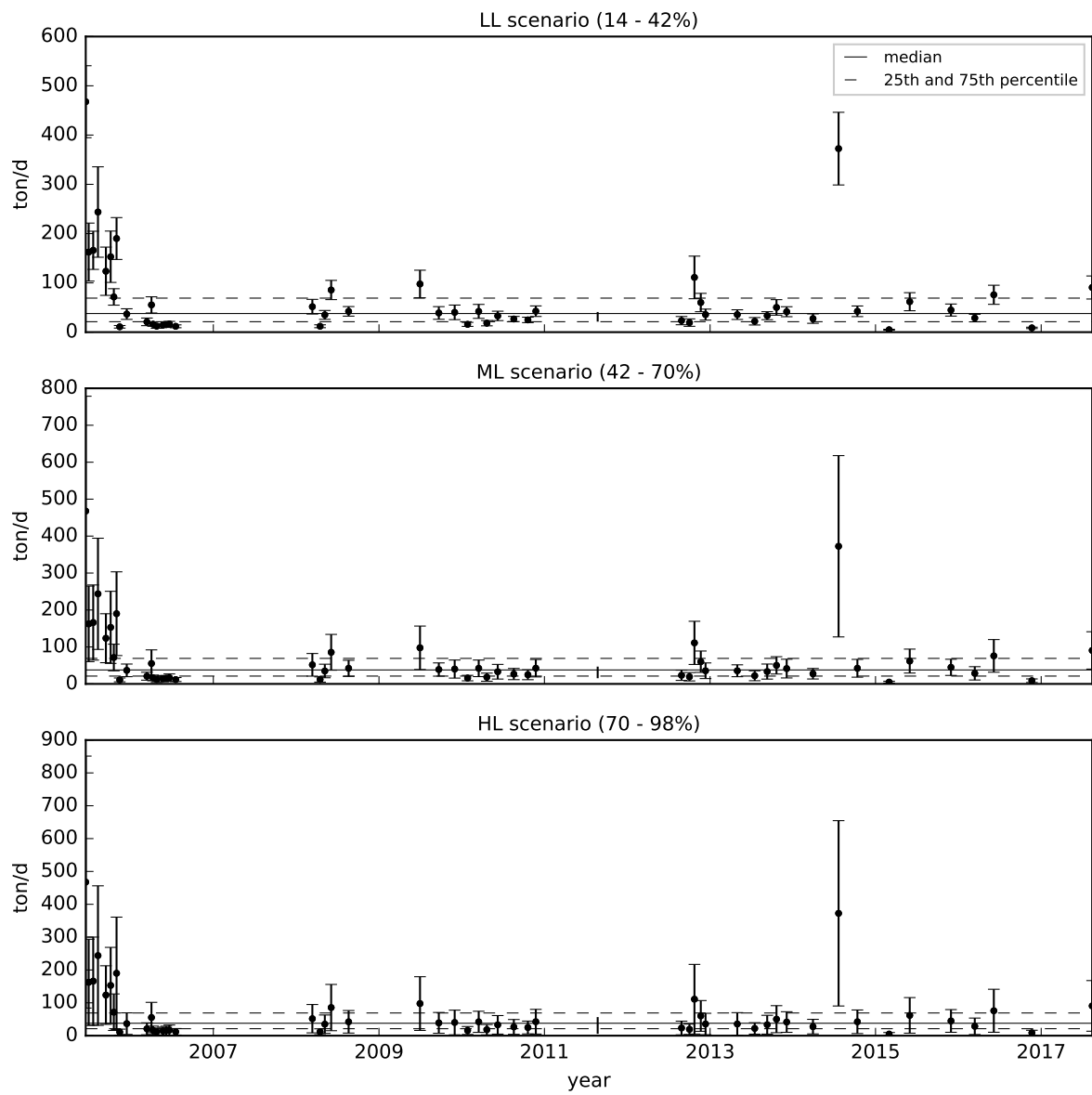
BOD - IG5

Figure 90 – LL, ML and HL uncertainty scenarios for BOD load time series, station IG5
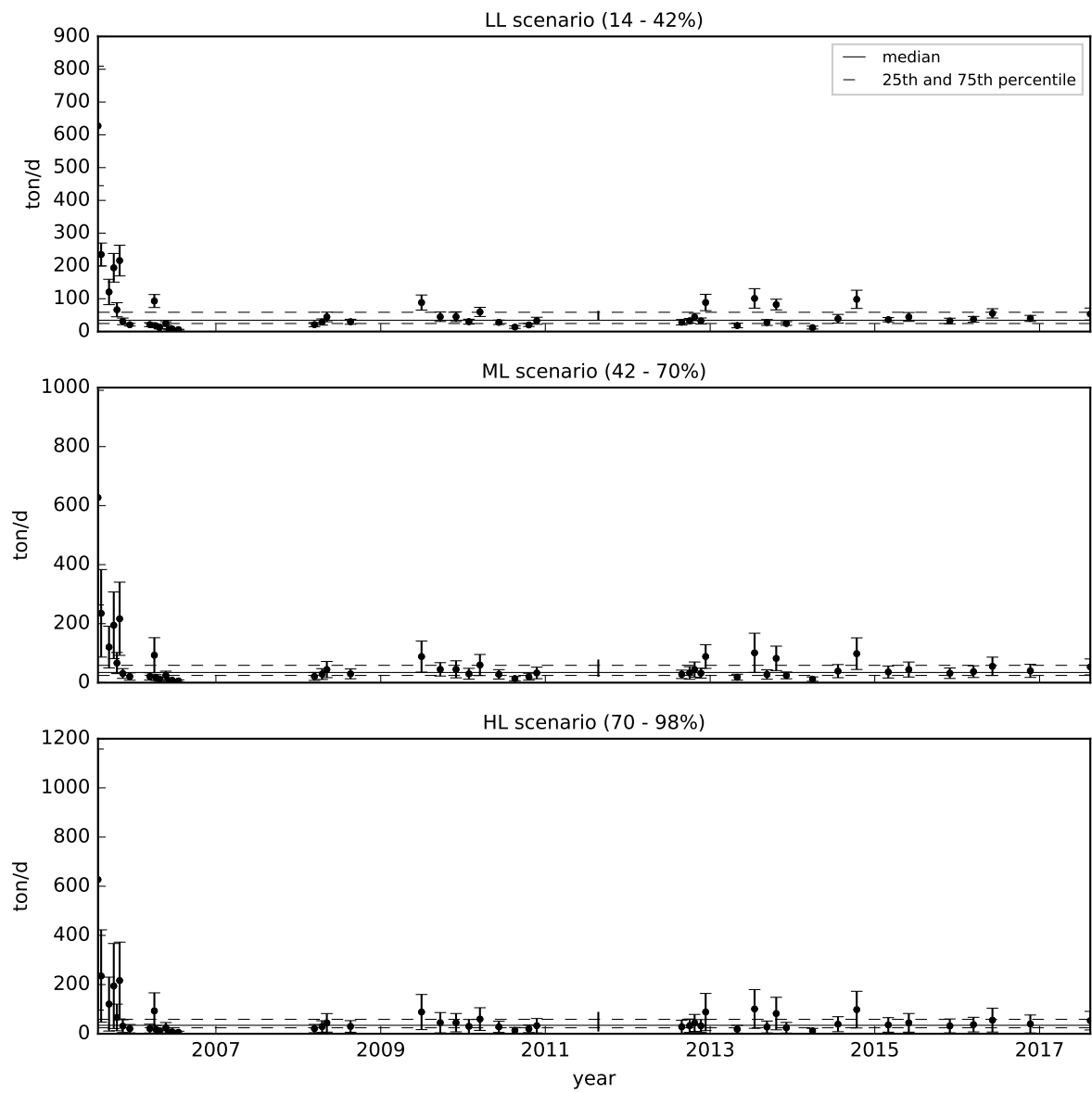
BOD - IG6

Figure 91 – LL, ML and HL uncertainty scenarios for BOD load time series, station IG6

BOD - IG7
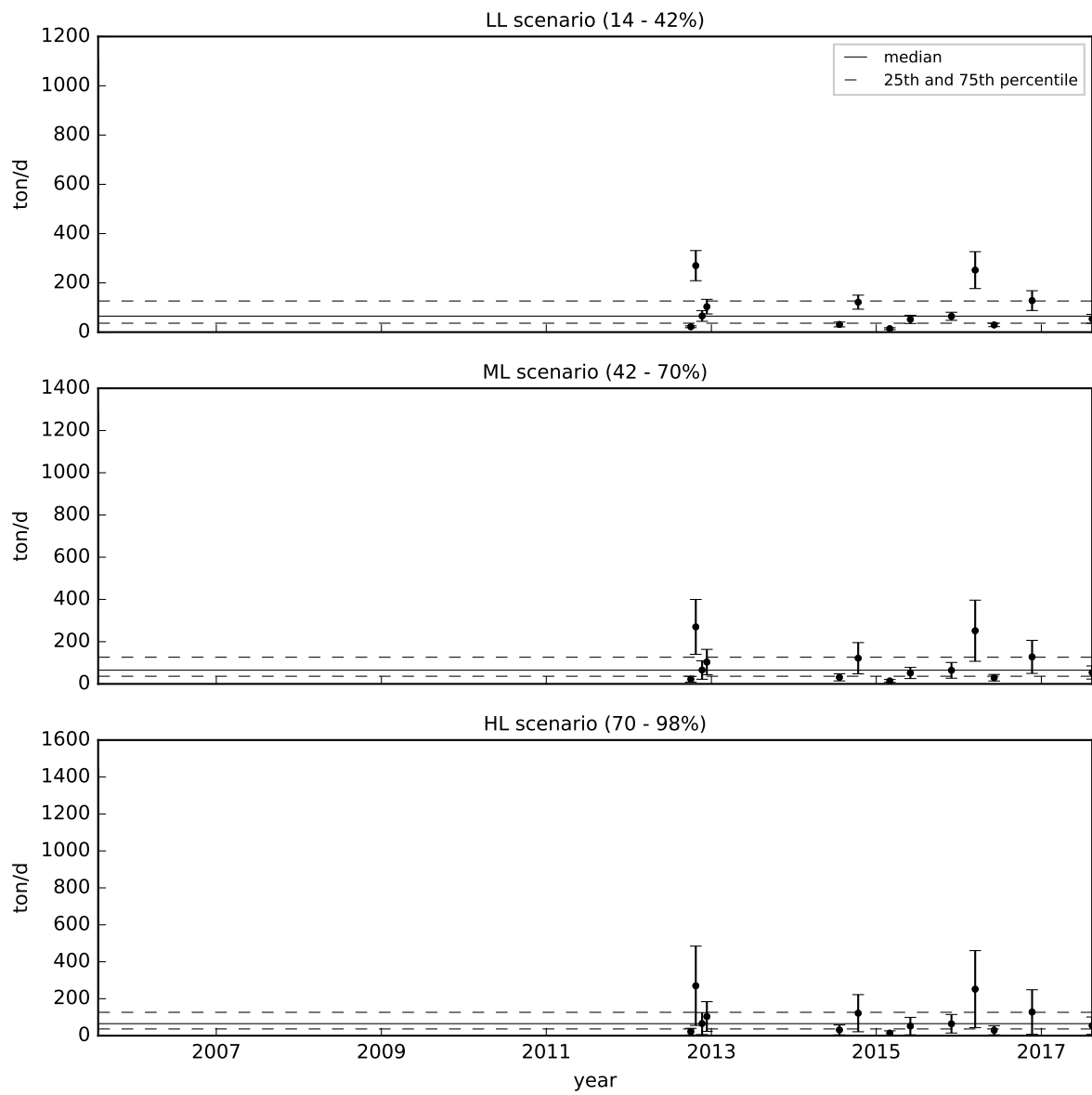
Figure 92 – LL, ML and HL uncertainty scenarios for BOD load time series, station IG7

DO - IG3
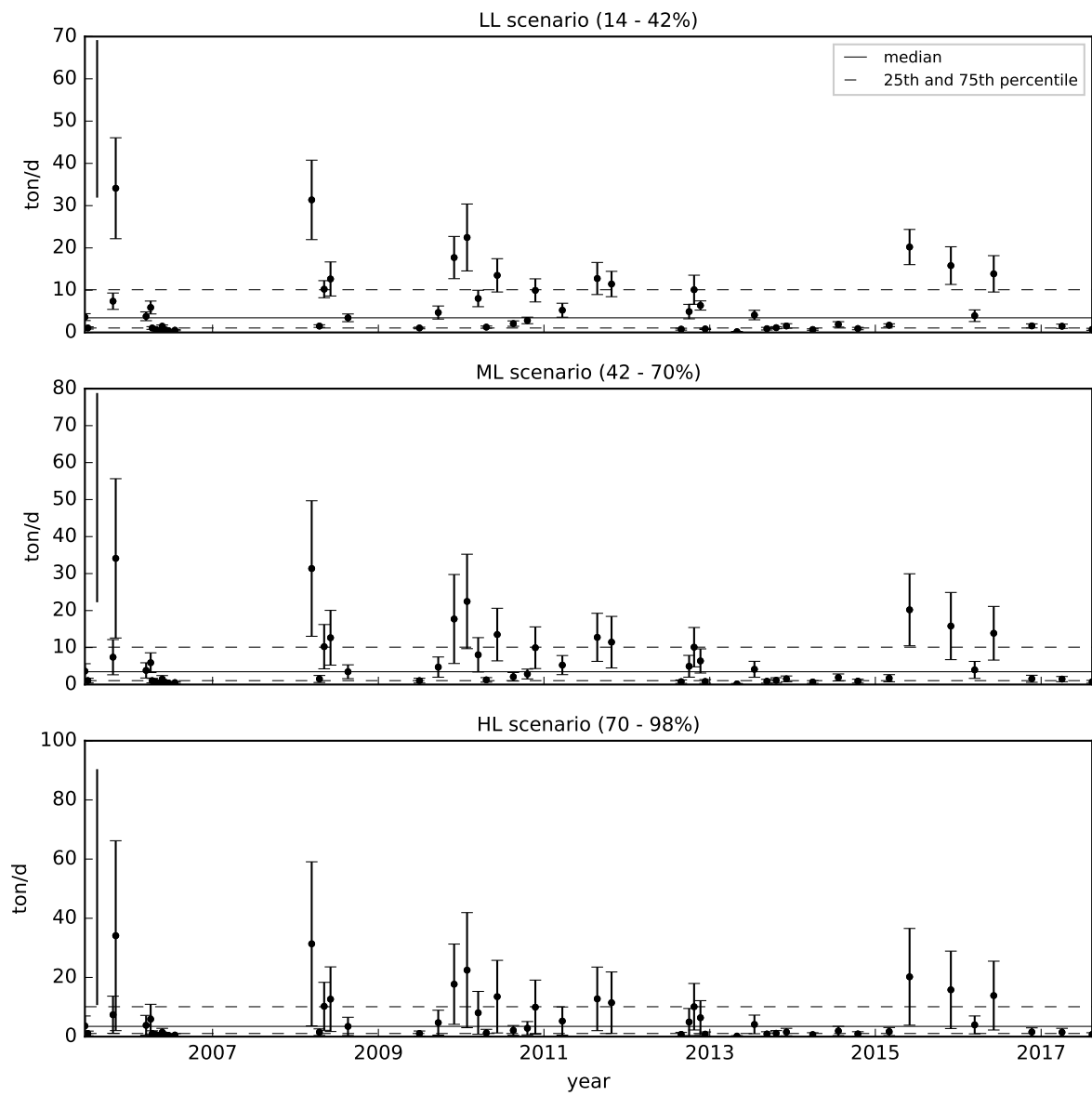
Figure 93 – LL, ML and HL uncertainty scenarios for DO load time series, station IG3

DO - IG4
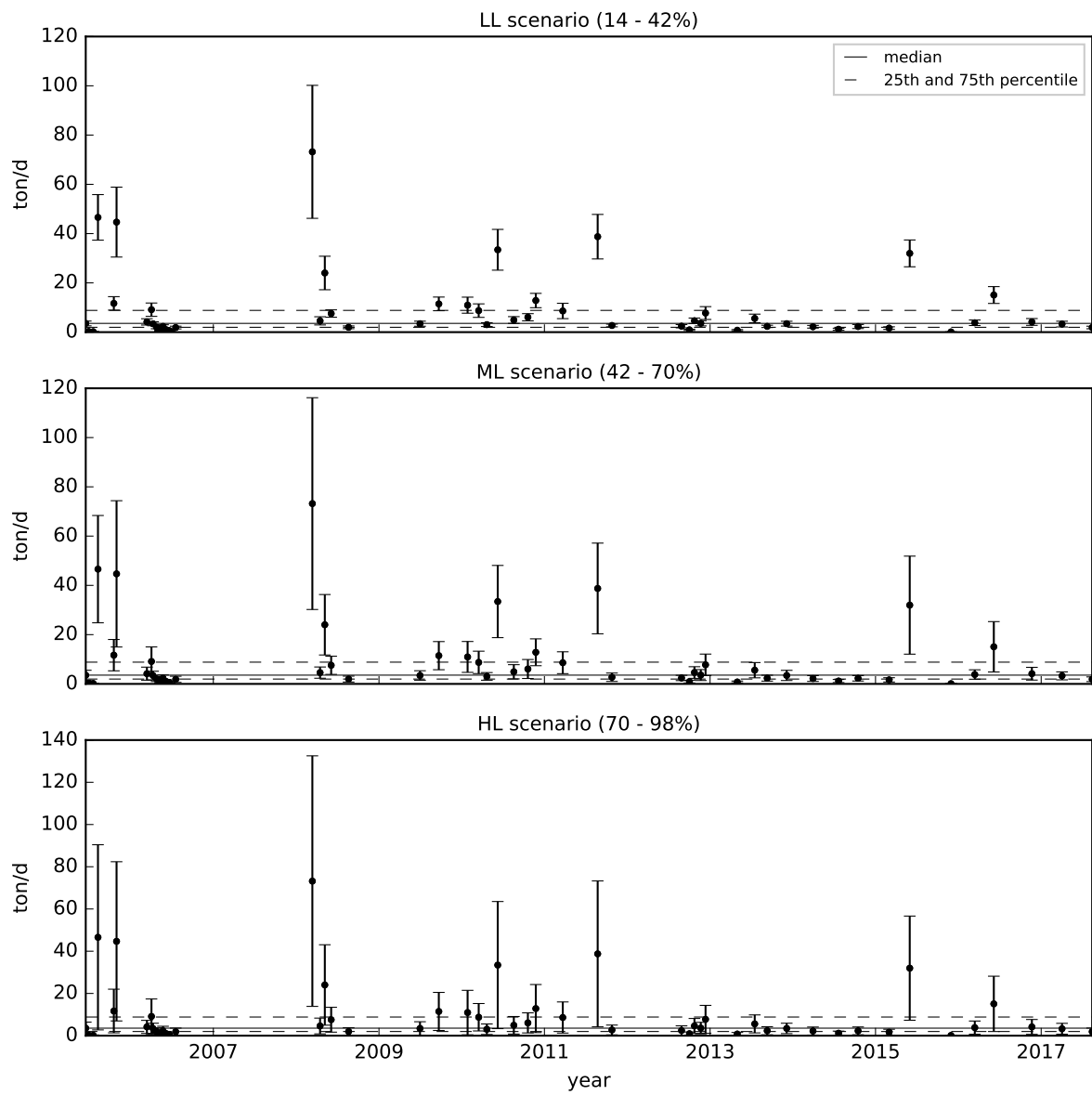
Figure 94 – LL, ML and HL uncertainty scenarios for DO load time series from IG4

DO - IG5
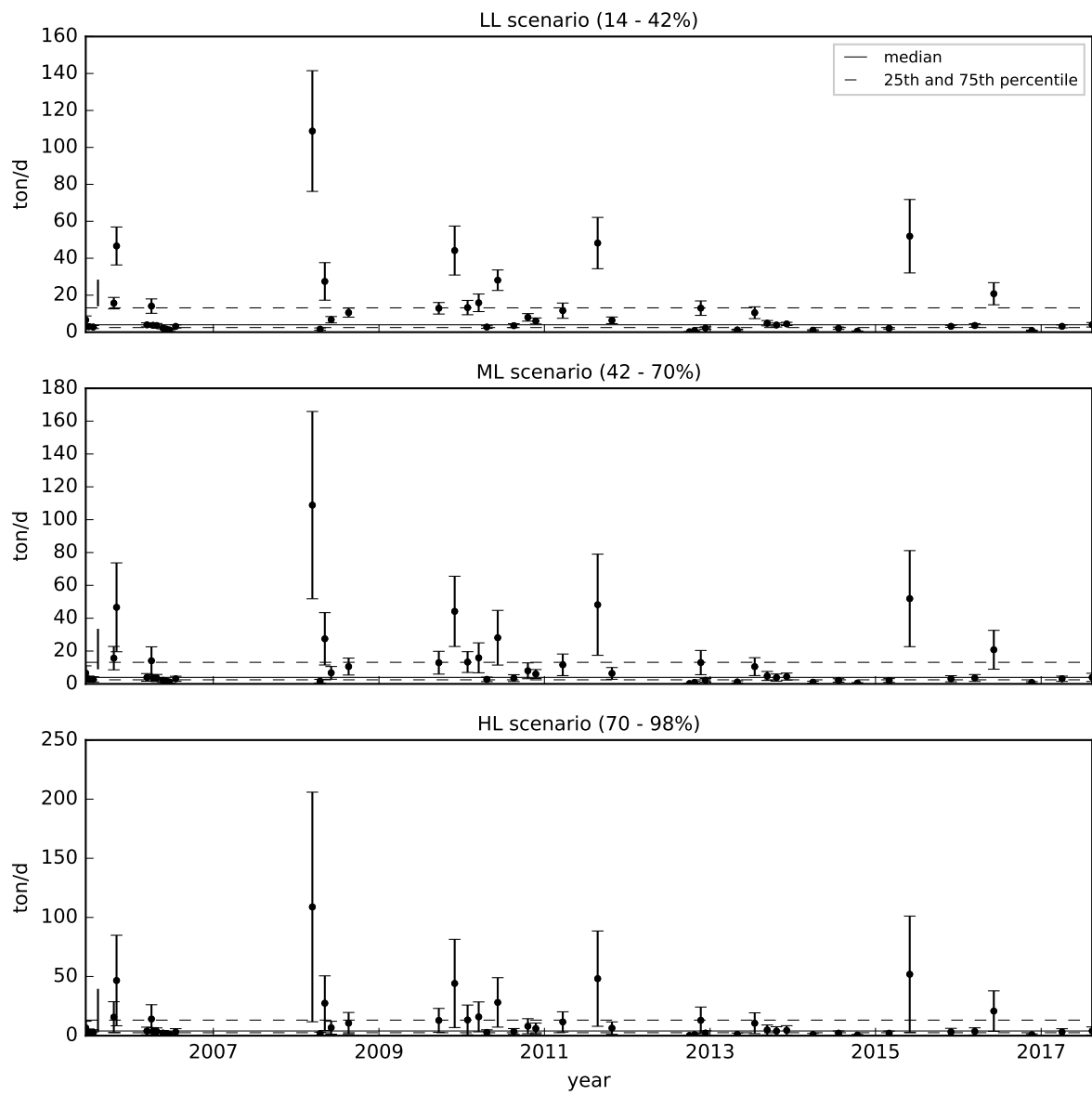
Figure 95 – LL, ML and HL uncertainty scenarios for DO load time series, station IG5

DO - IG6
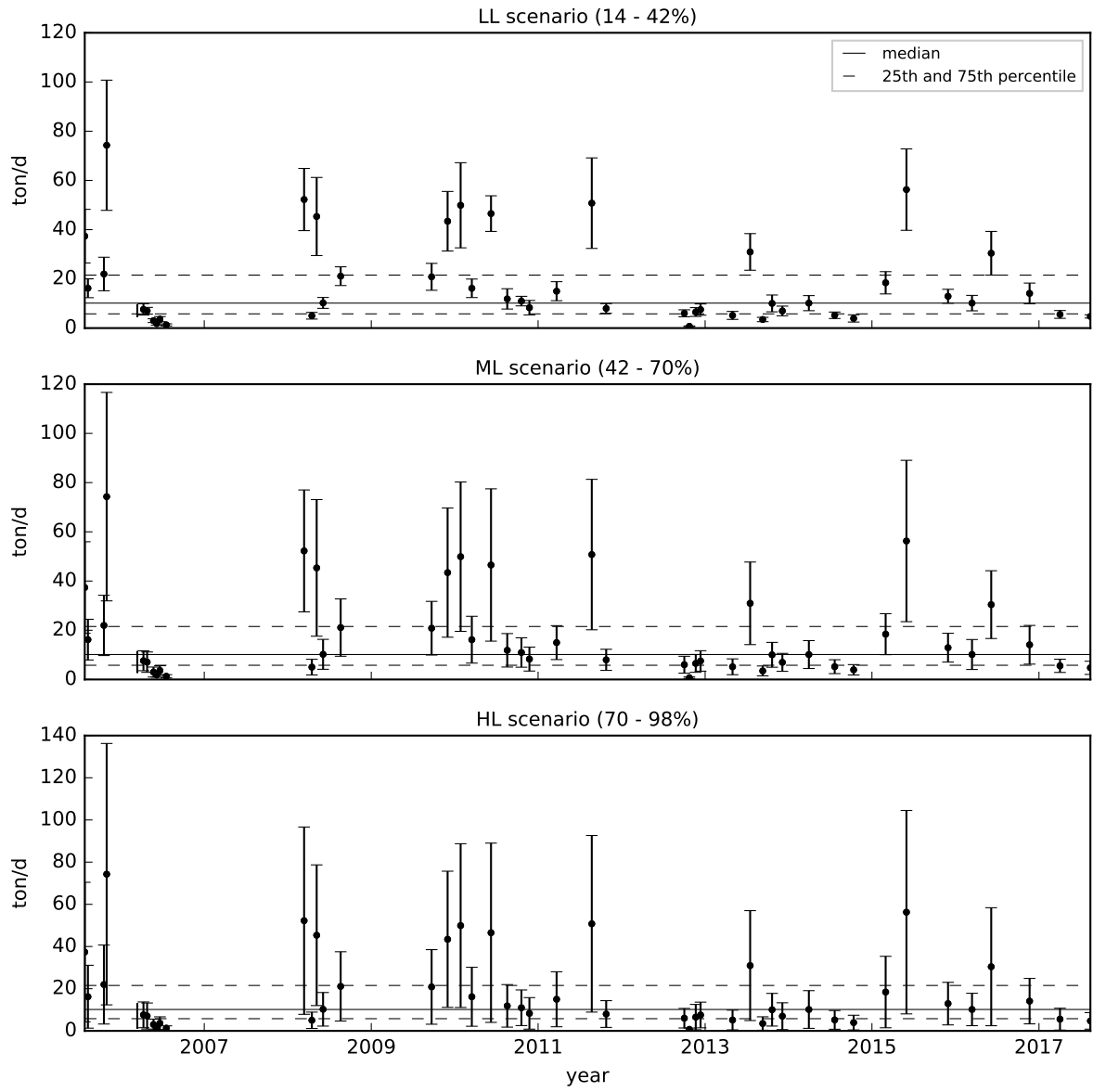
Figure 96 – LL, ML and HL uncertainty scenarios for DO load time series, station IG6

DO - IG7
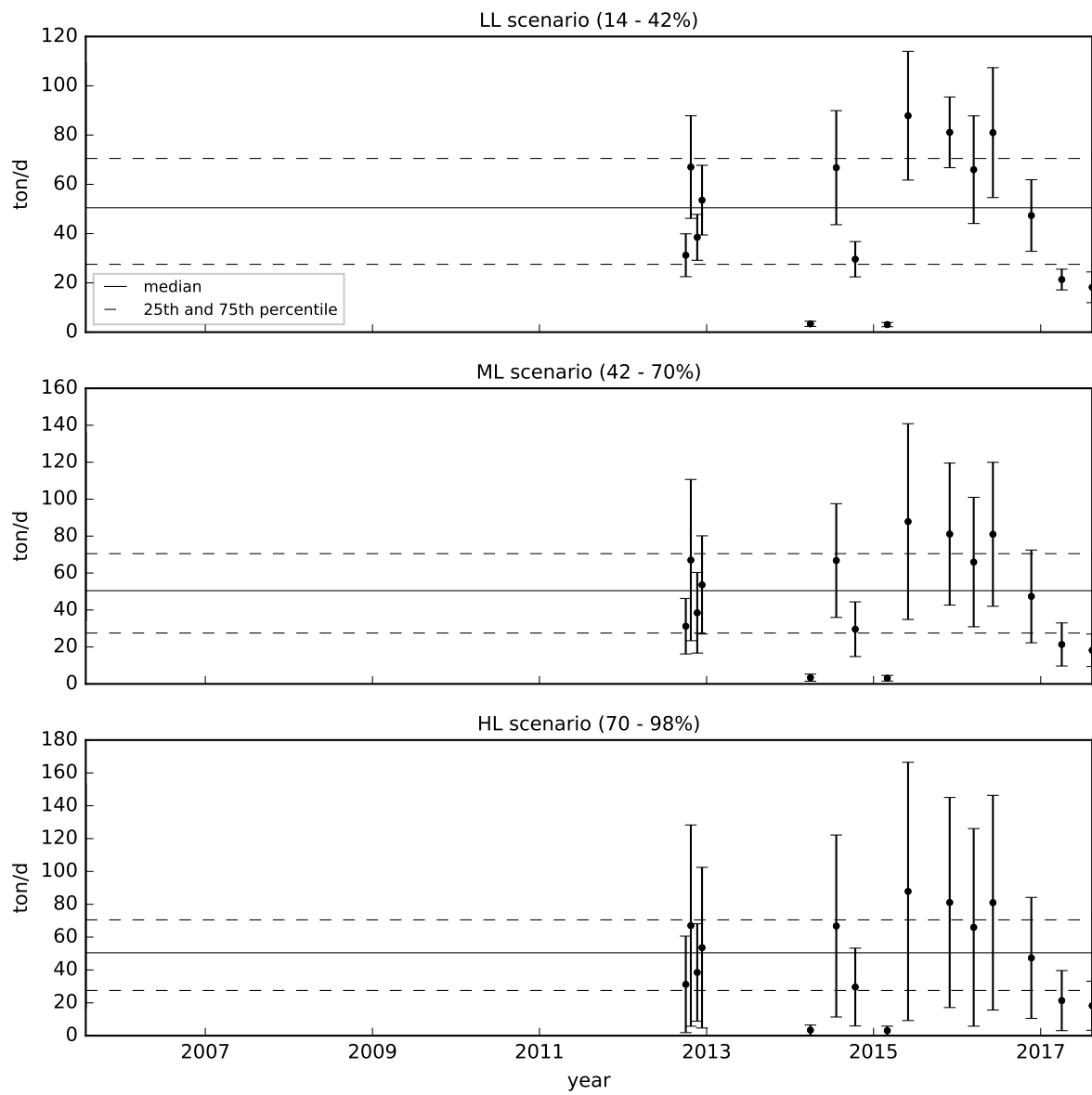
Figure 97 – LL, ML and HL uncertainty scenarios for DO load time series, station IG7
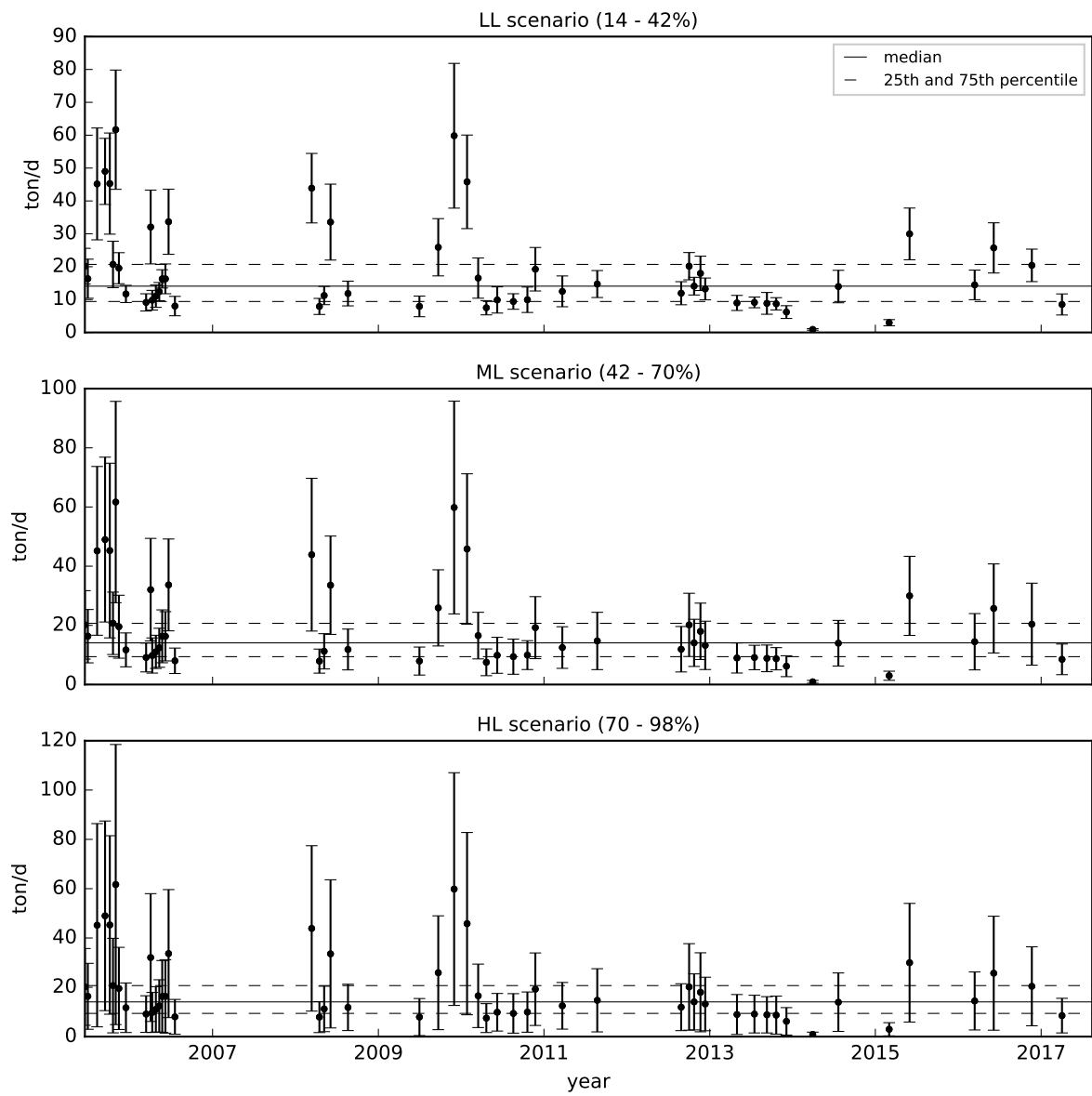
DOC - IG3

Figure 98 – LL, ML and HL uncertainty scenarios for DOC load time series, station IG3
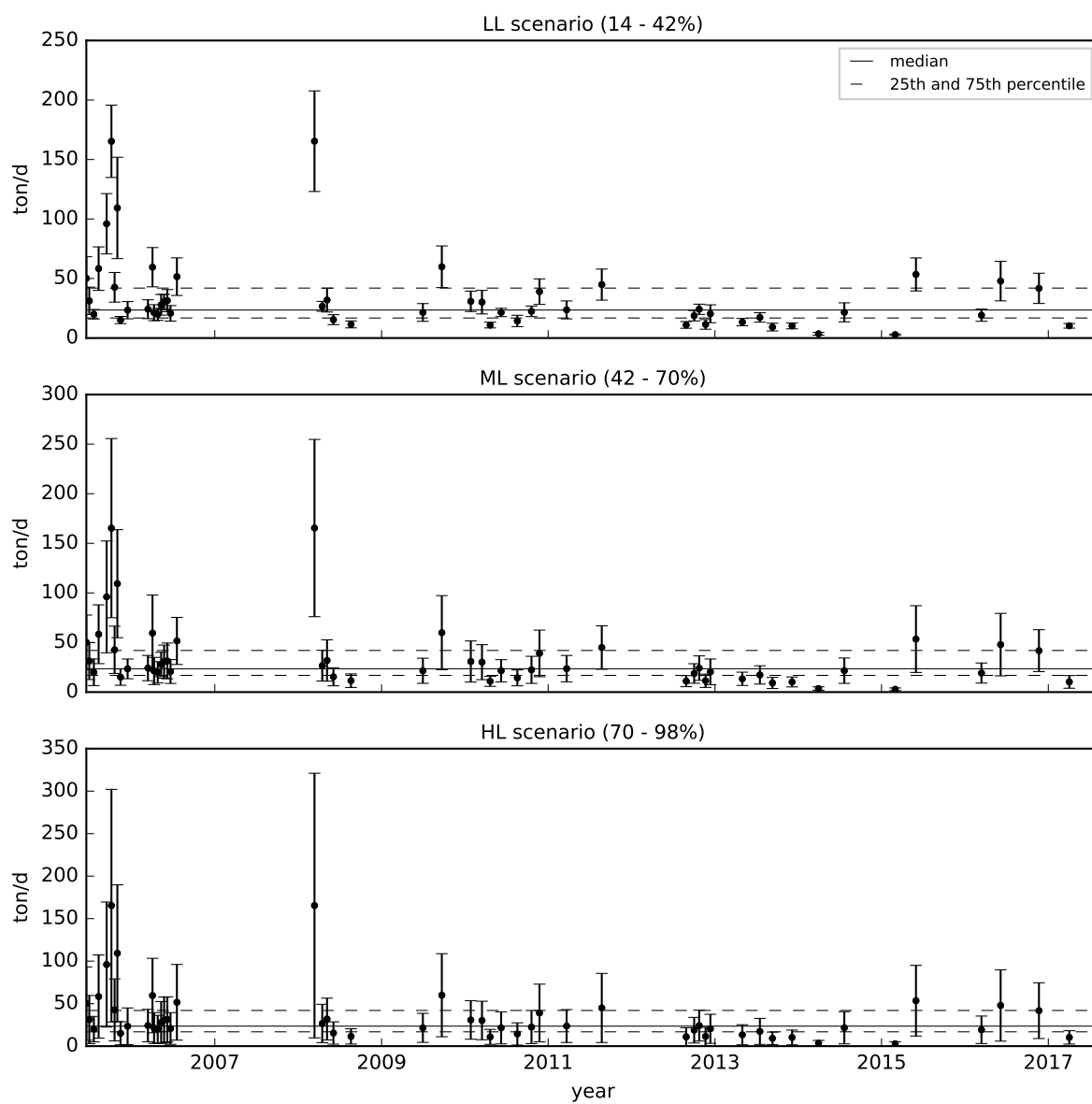
DOC - IG4

Figure 99 – LL, ML and HL uncertainty scenarios for DOC load time series from IG4
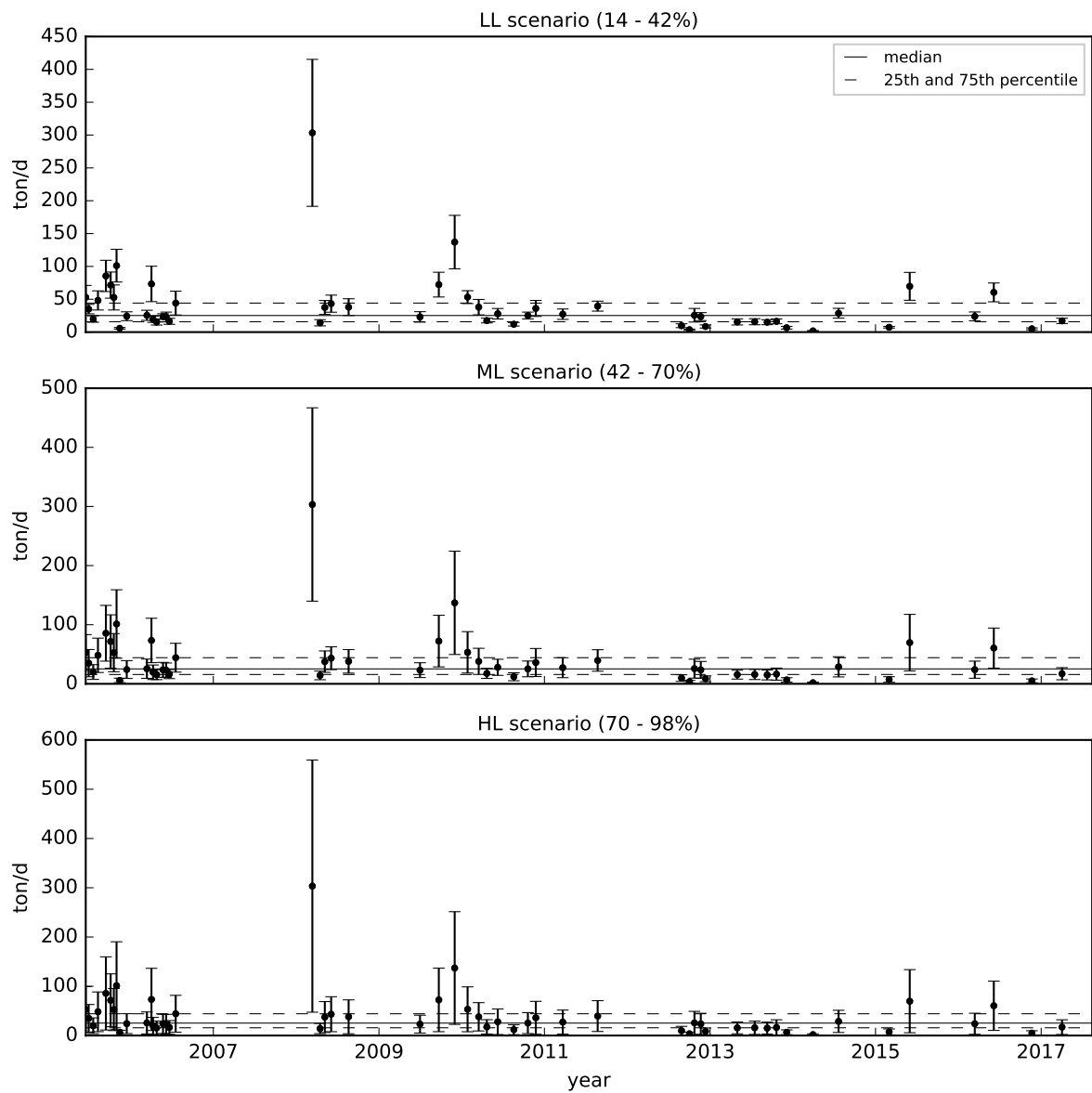
DOC - IG5

Figure 100 – LL, ML and HL uncertainty scenarios for DOC load time series, station IG5
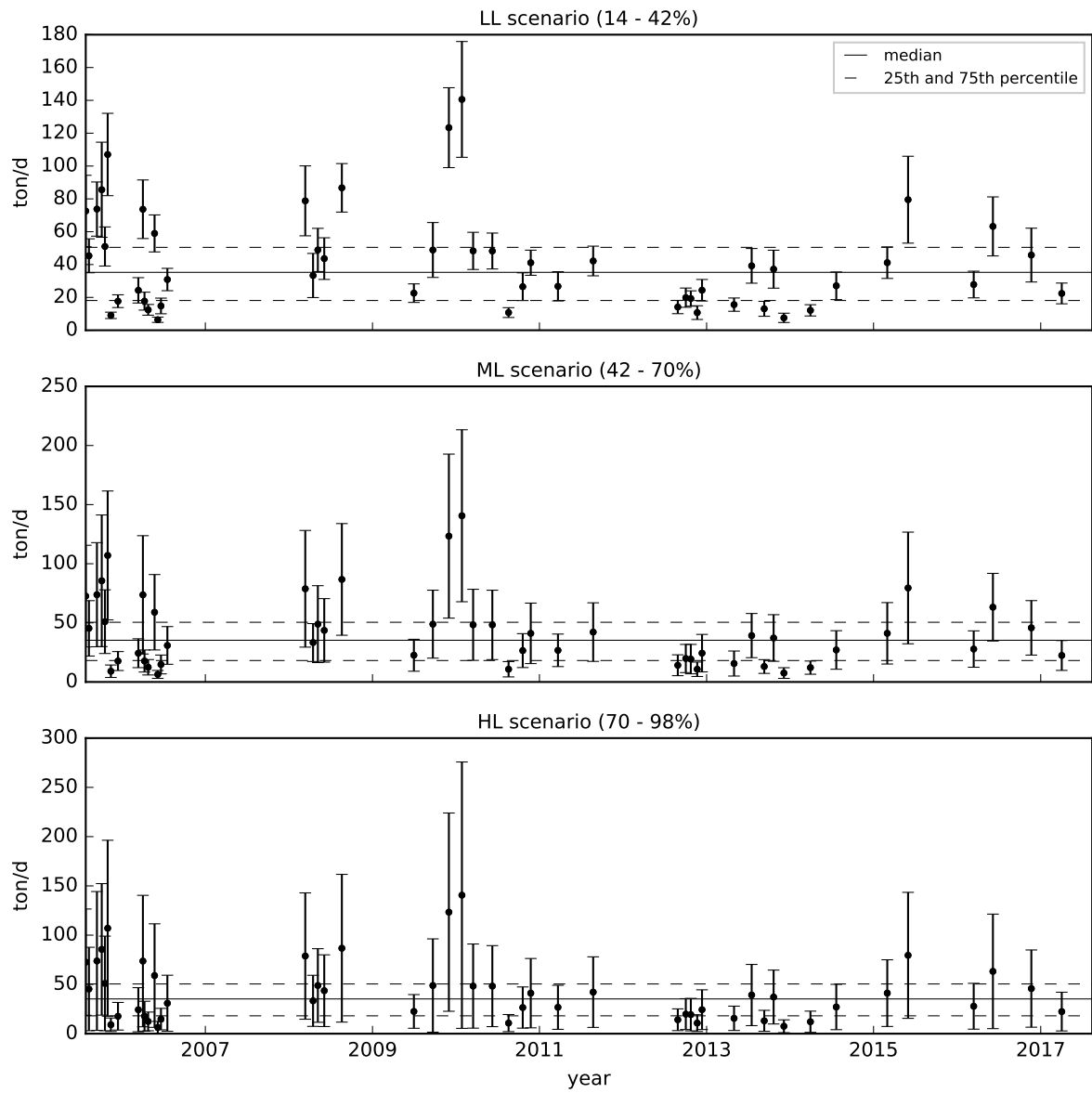
DOC - IG6

Figure 101 – LL, ML and HL uncertainty scenarios for DOC load time series, station IG6

DOC - IG7
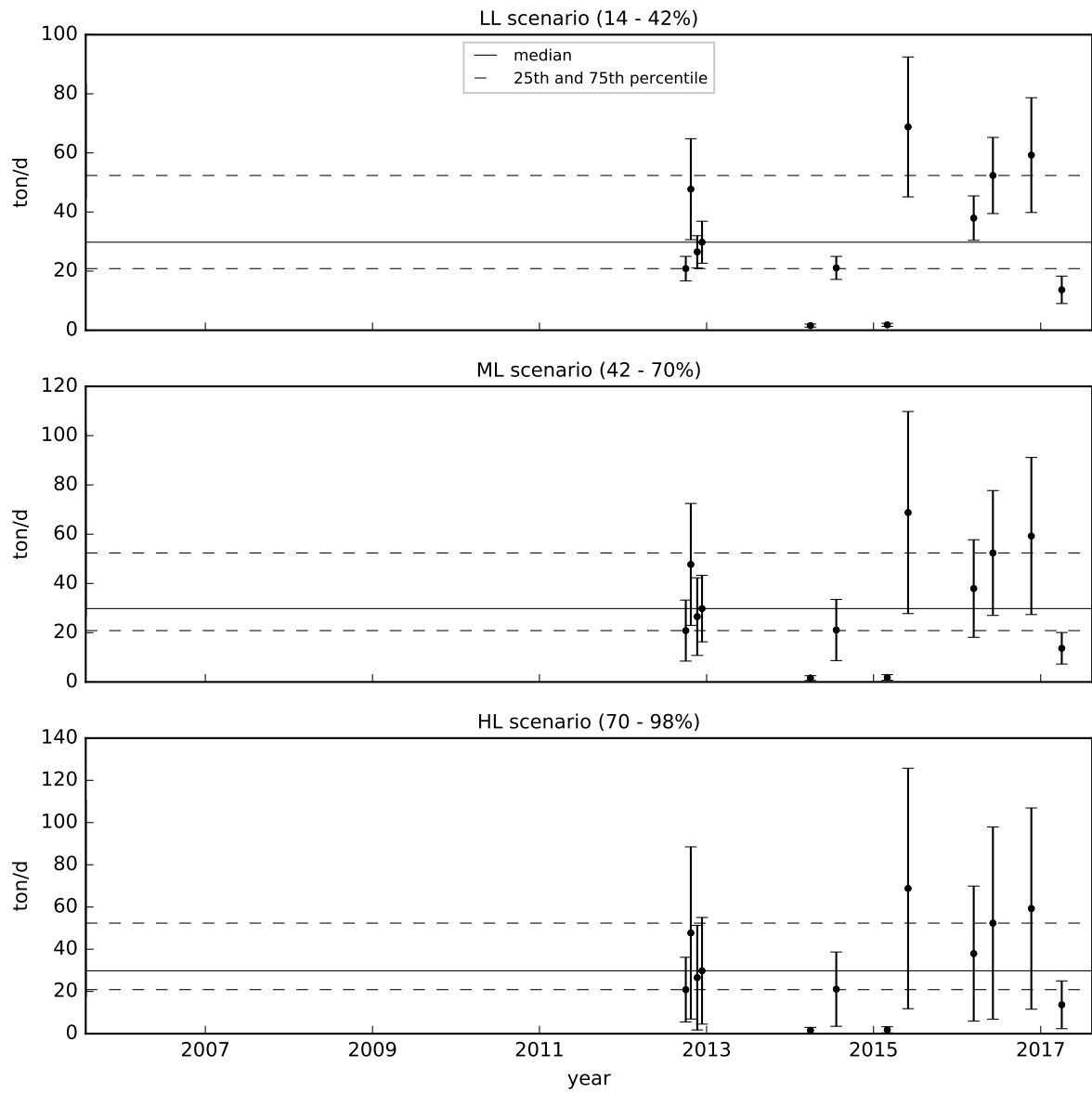
Figure 102 – LL, ML and HL uncertainty scenarios for DOC load time series, station IG7
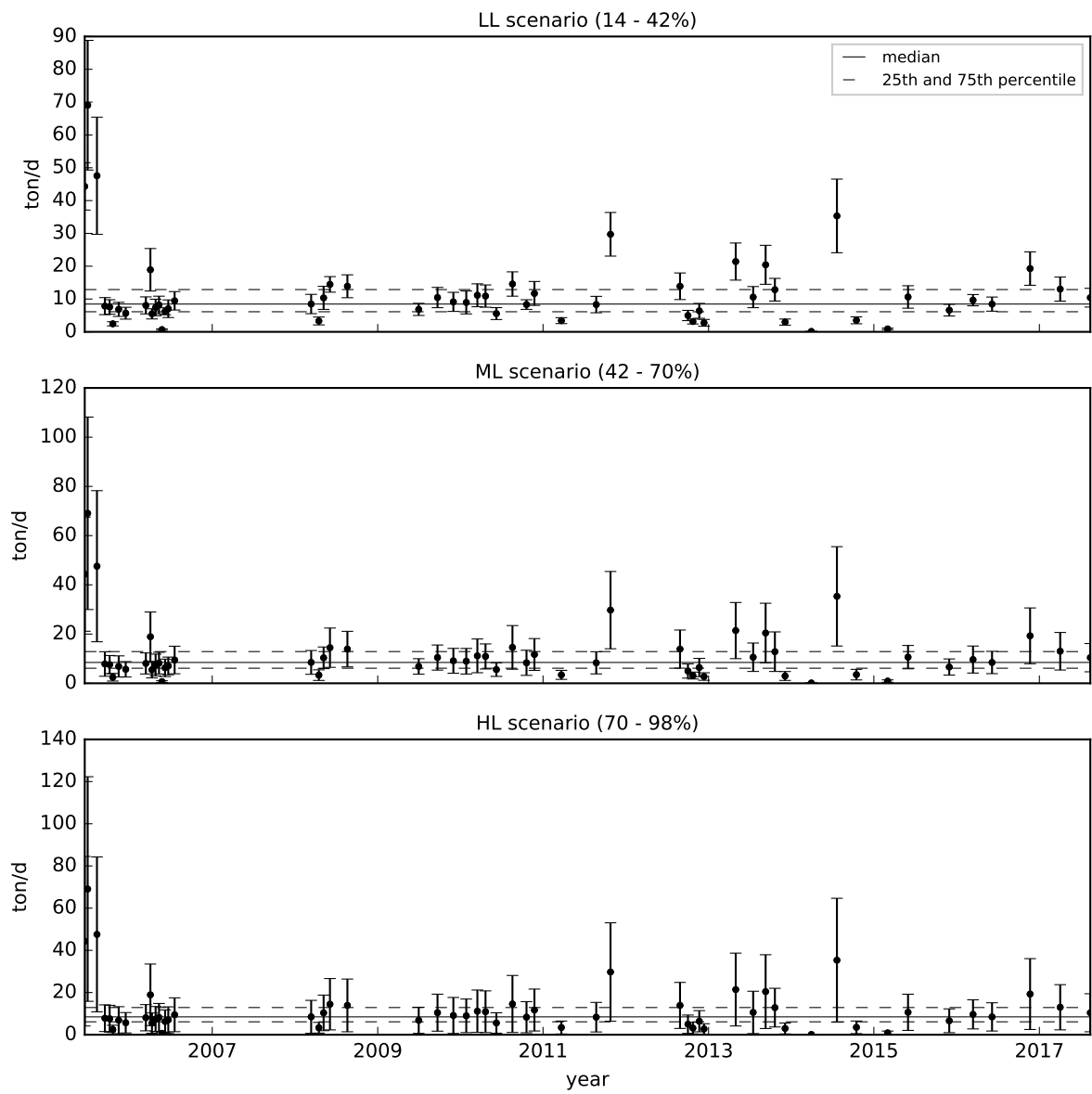
NH4 - IG3

Figure 103 – LL, ML and HL uncertainty scenarios for NH4 load time series, station IG3
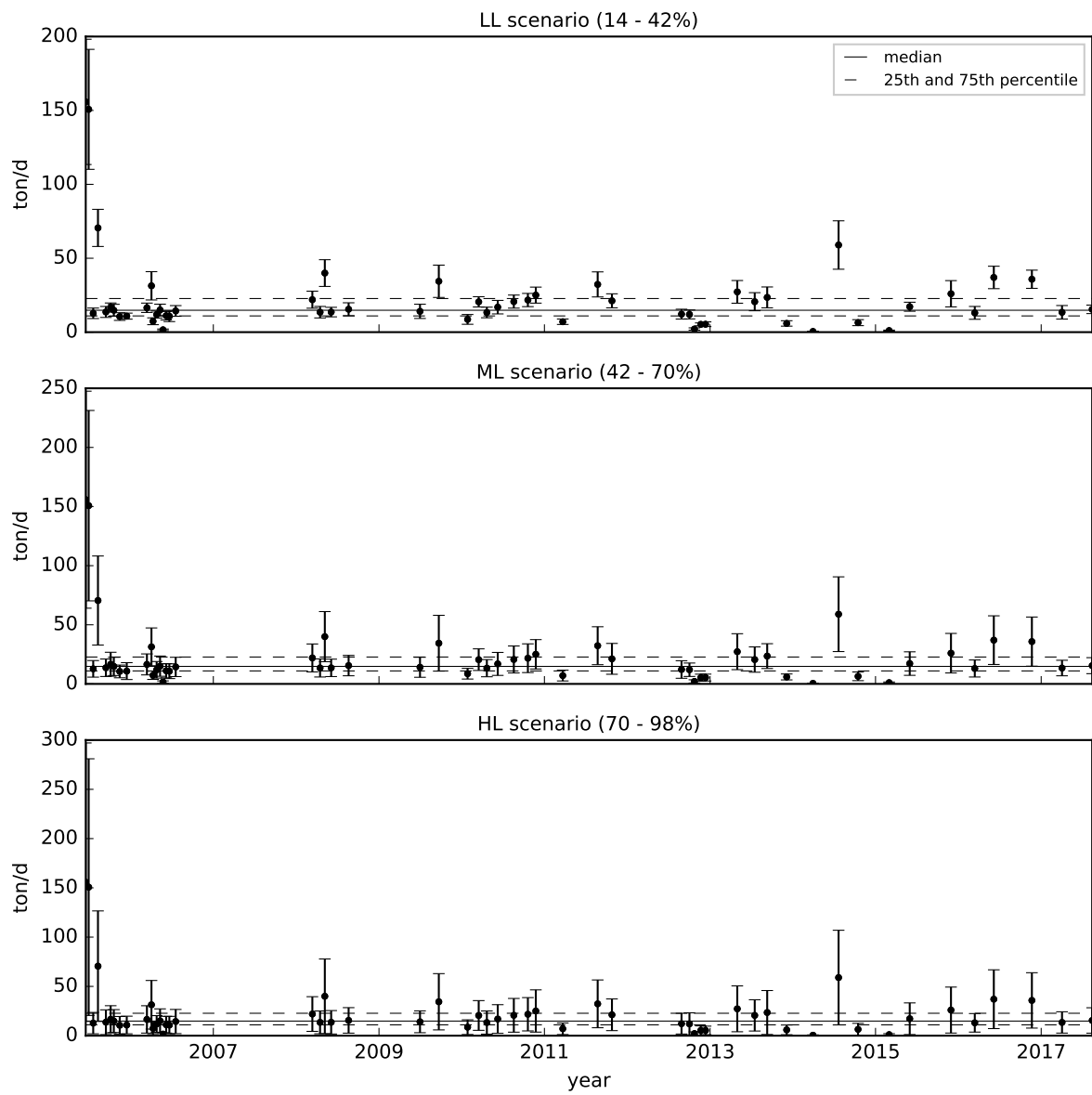
NH4 - IG4

Figure 104 – LL, ML and HL uncertainty scenarios for NH4 load time series from IG4
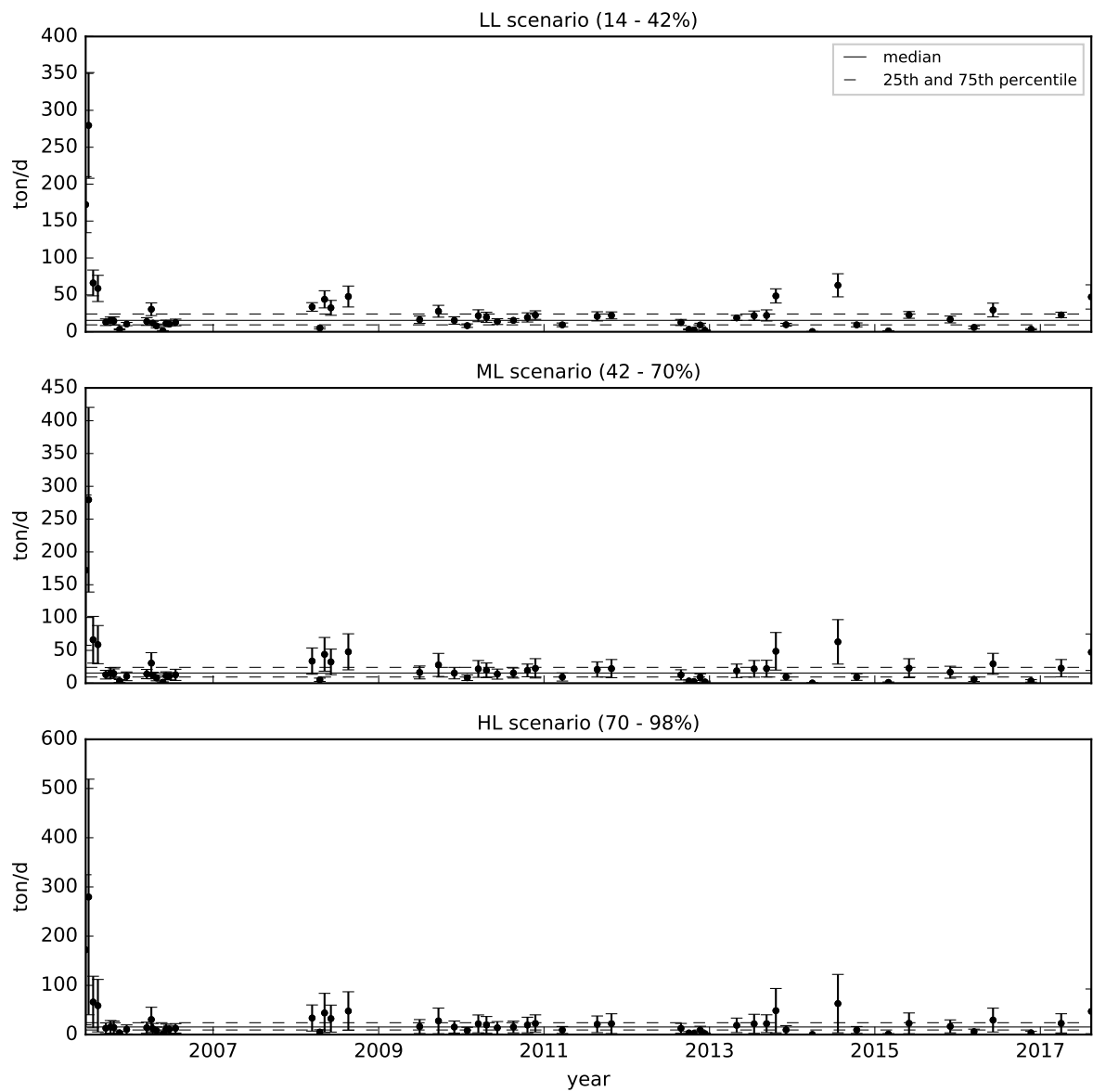
NH4 - IG5

Figure 105 – LL, ML and HL uncertainty scenarios for NH4 load time series, station IG5
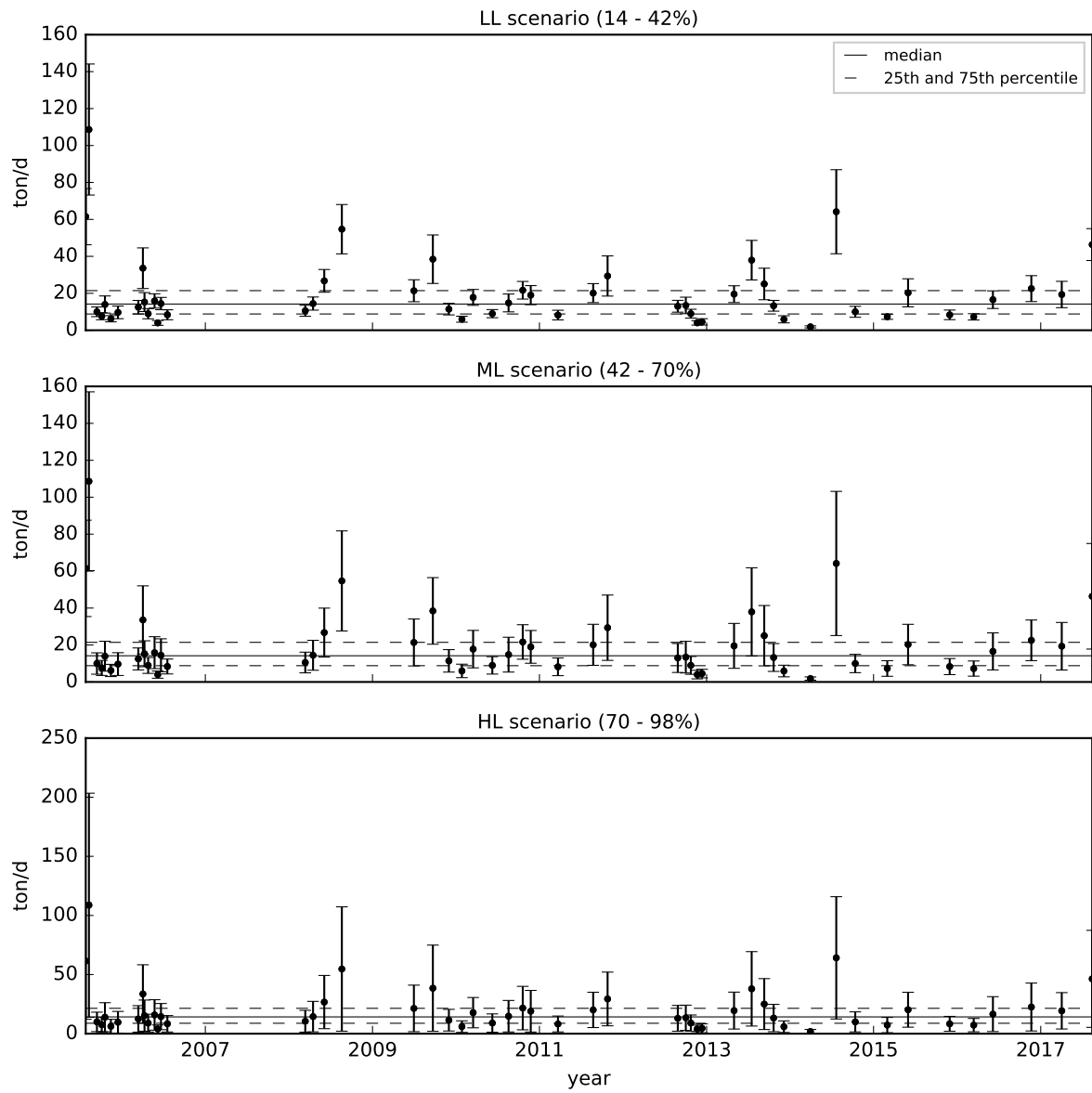
NH4 - IG6

Figure 106 – LL, ML and HL uncertainty scenarios for NH4 load time series, station IG6

NH4 - IG7
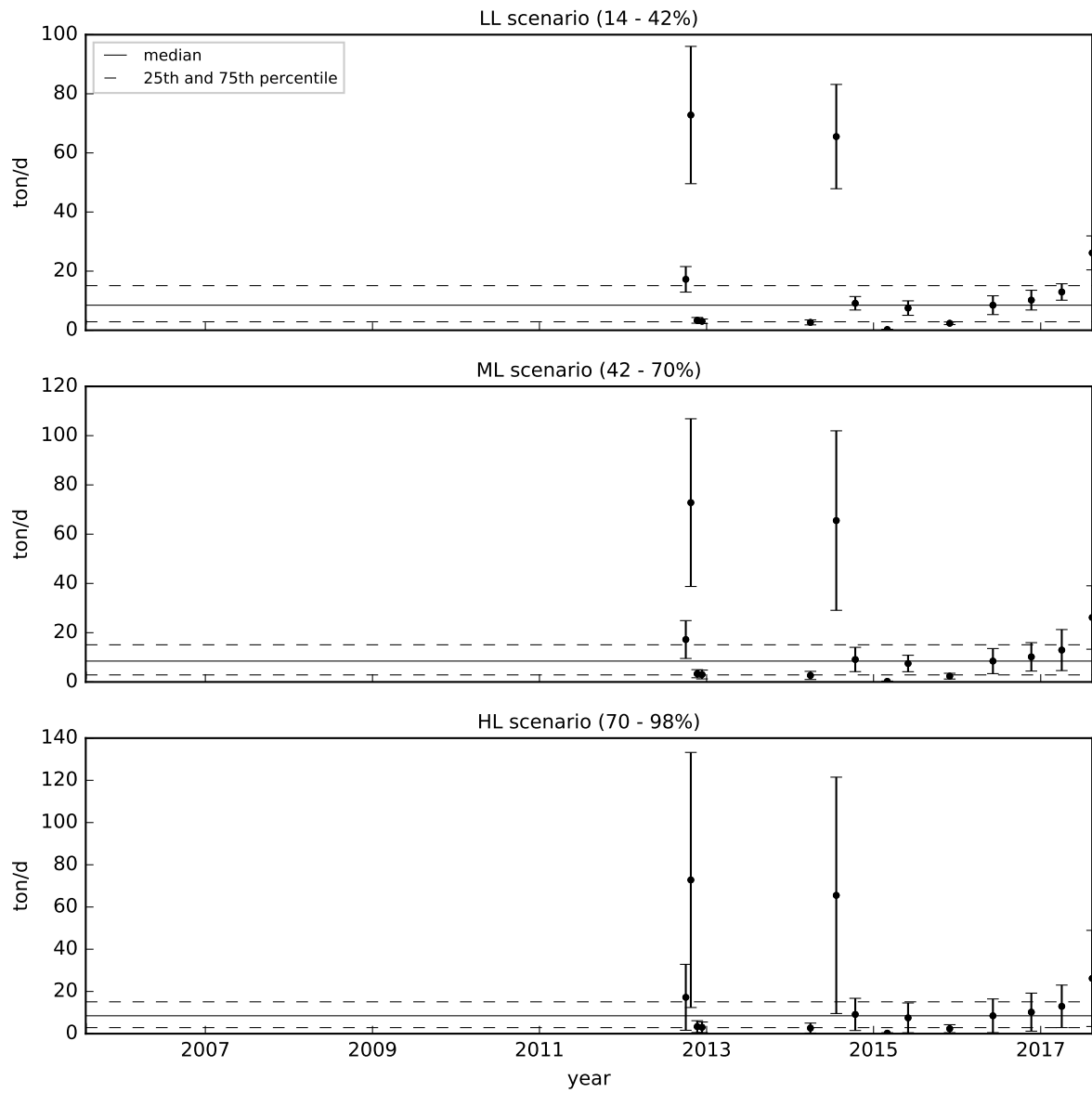
Figure 107 – LL, ML and HL uncertainty scenarios for NH4 load time series, station IG7

TP - IG3
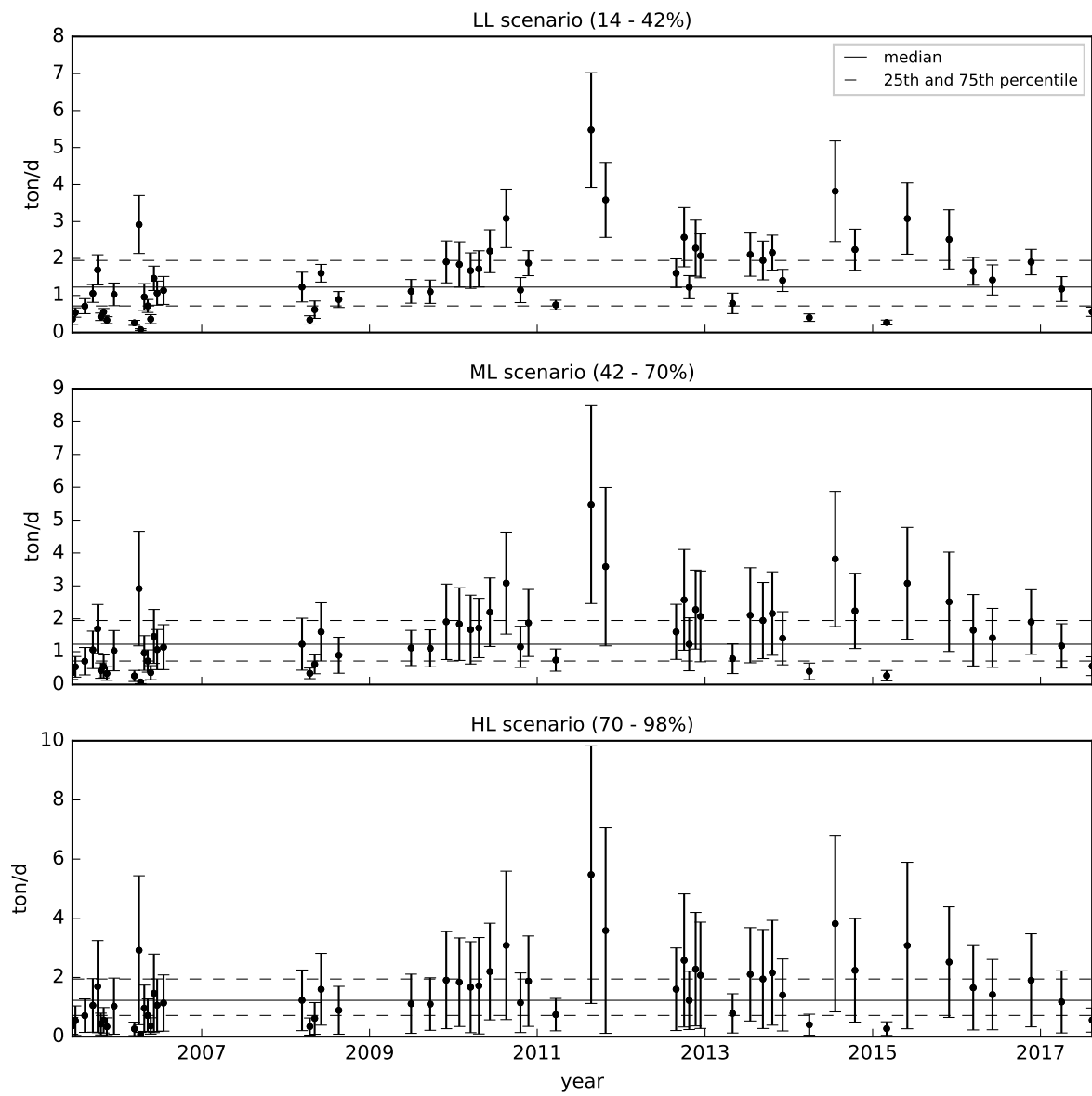
Figure 108 – LL, ML and HL uncertainty scenarios for TP load time series, station IG3

TP - IG4
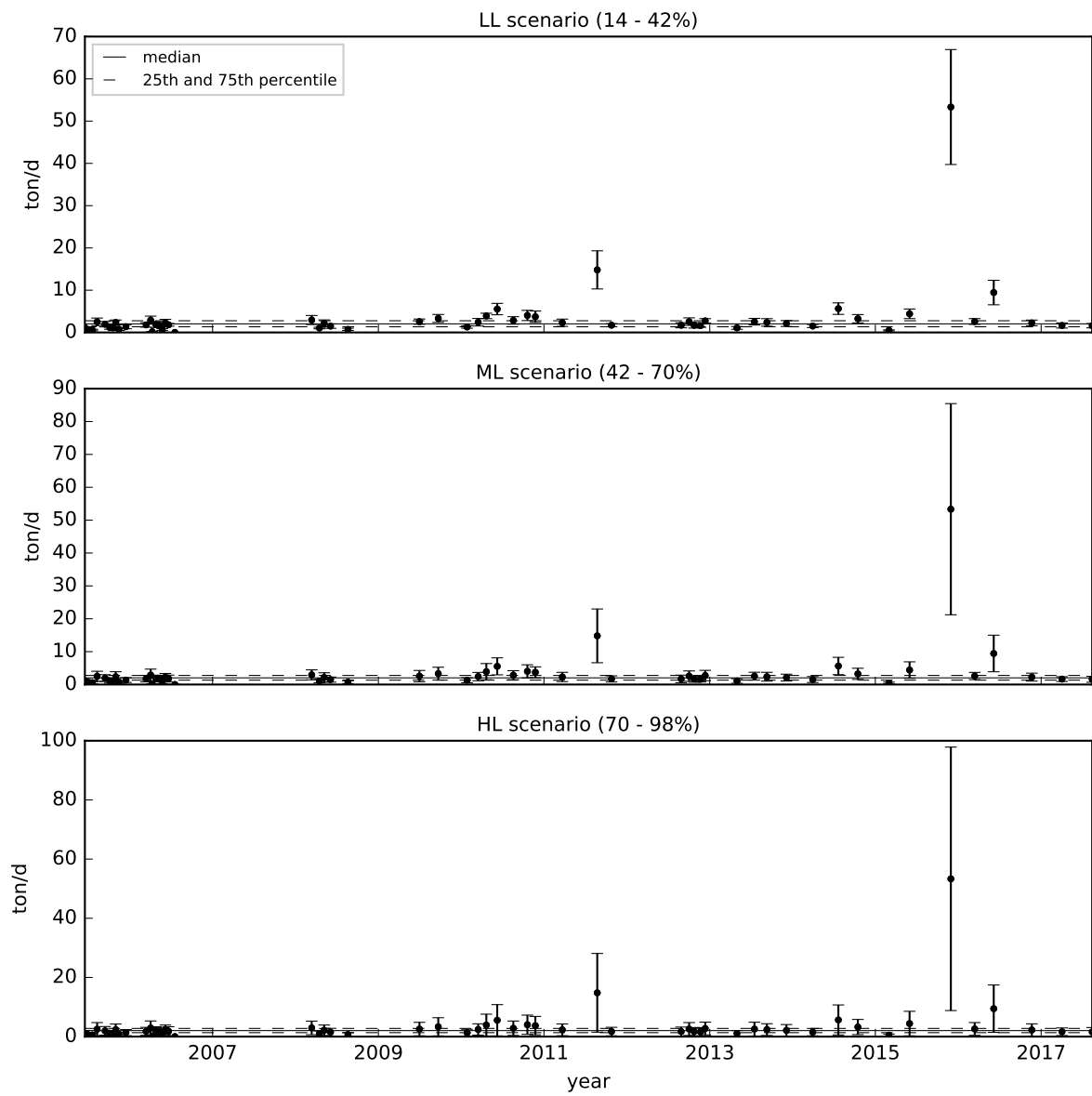
Figure 109 – LL, ML and HL uncertainty scenarios for TP load time series from IG4

TP - IG5
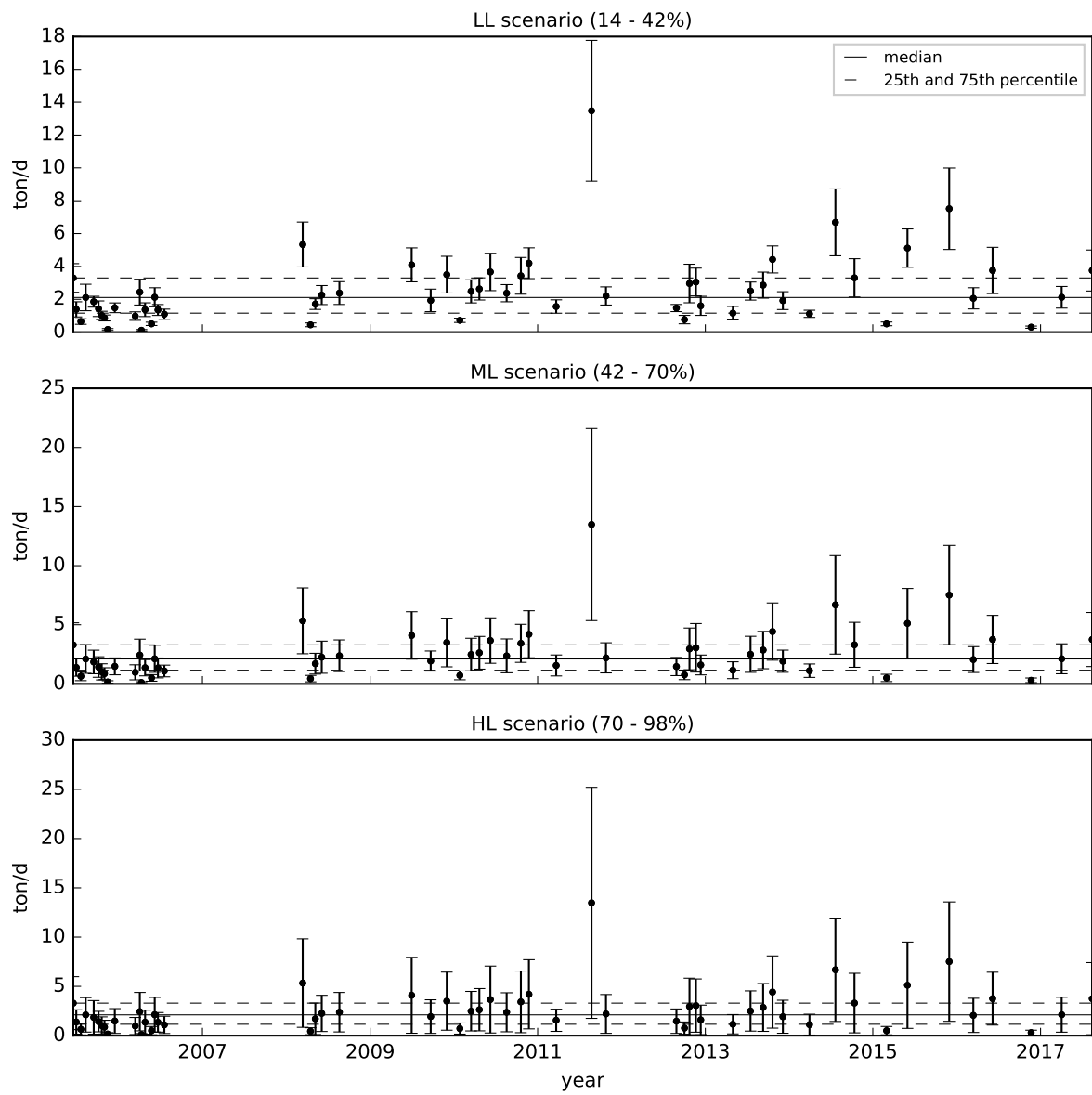
Figure 110 – LL, ML and HL uncertainty scenarios for TP load time series, station IG5

TP - IG6
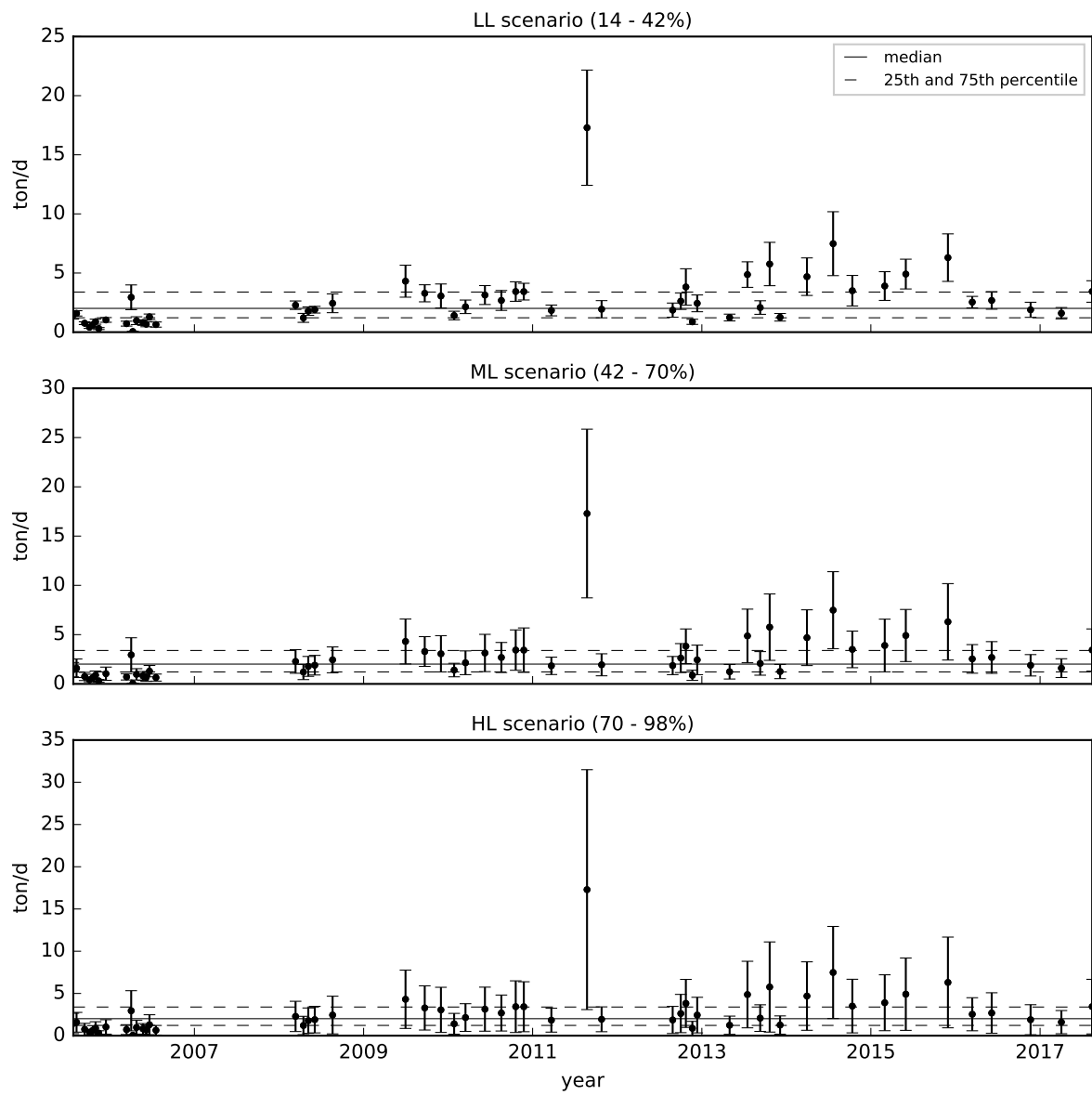
Figure 111 – LL, ML and HL uncertainty scenarios for TP load time series, station IG6

TP - IG7
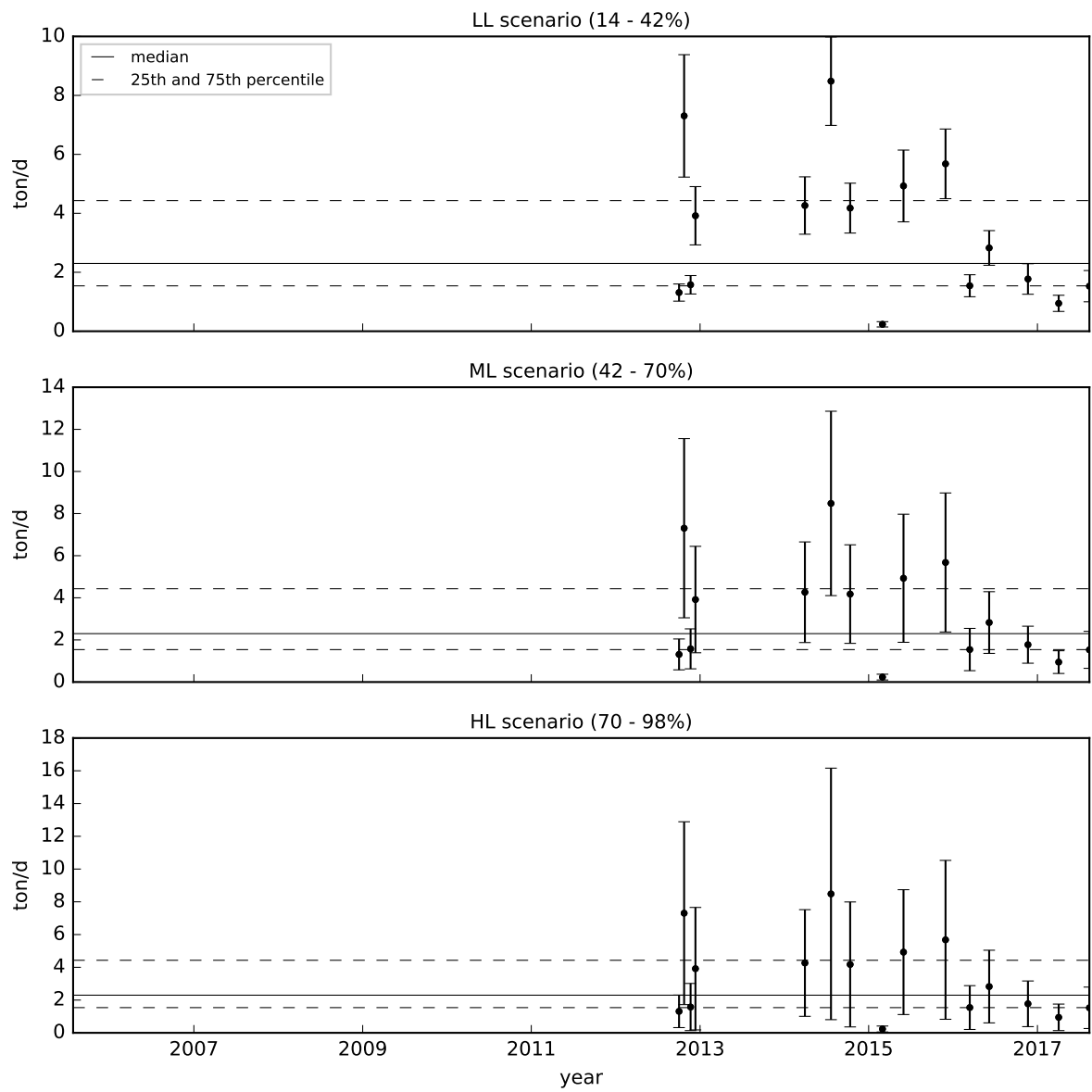
Figure 112 – LL, ML and HL uncertainty scenarios for TP load time series, station IG7
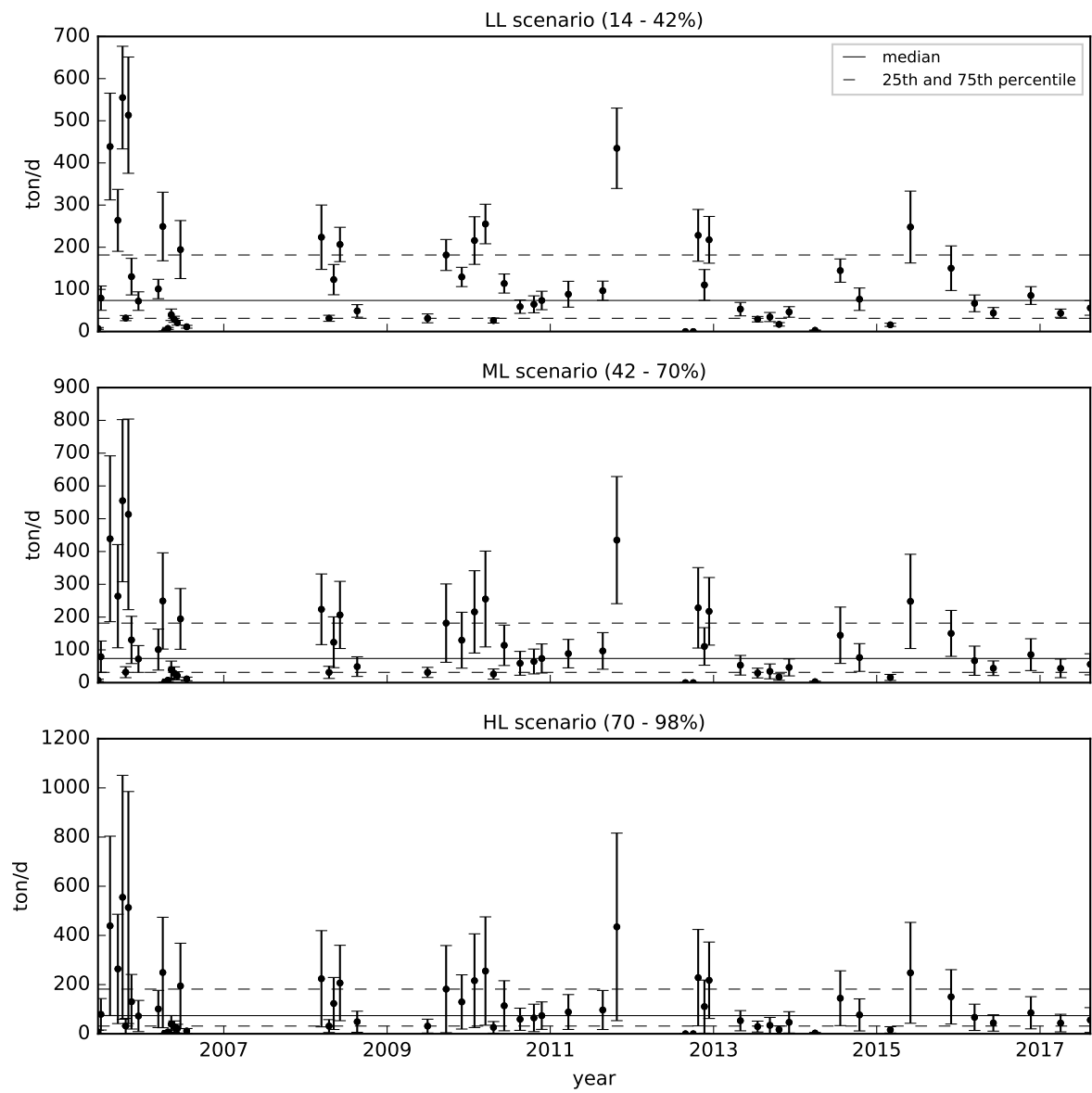
VDS - IG3

Figure 113 – LL, ML and HL uncertainty scenarios for VDS load time series, station IG3
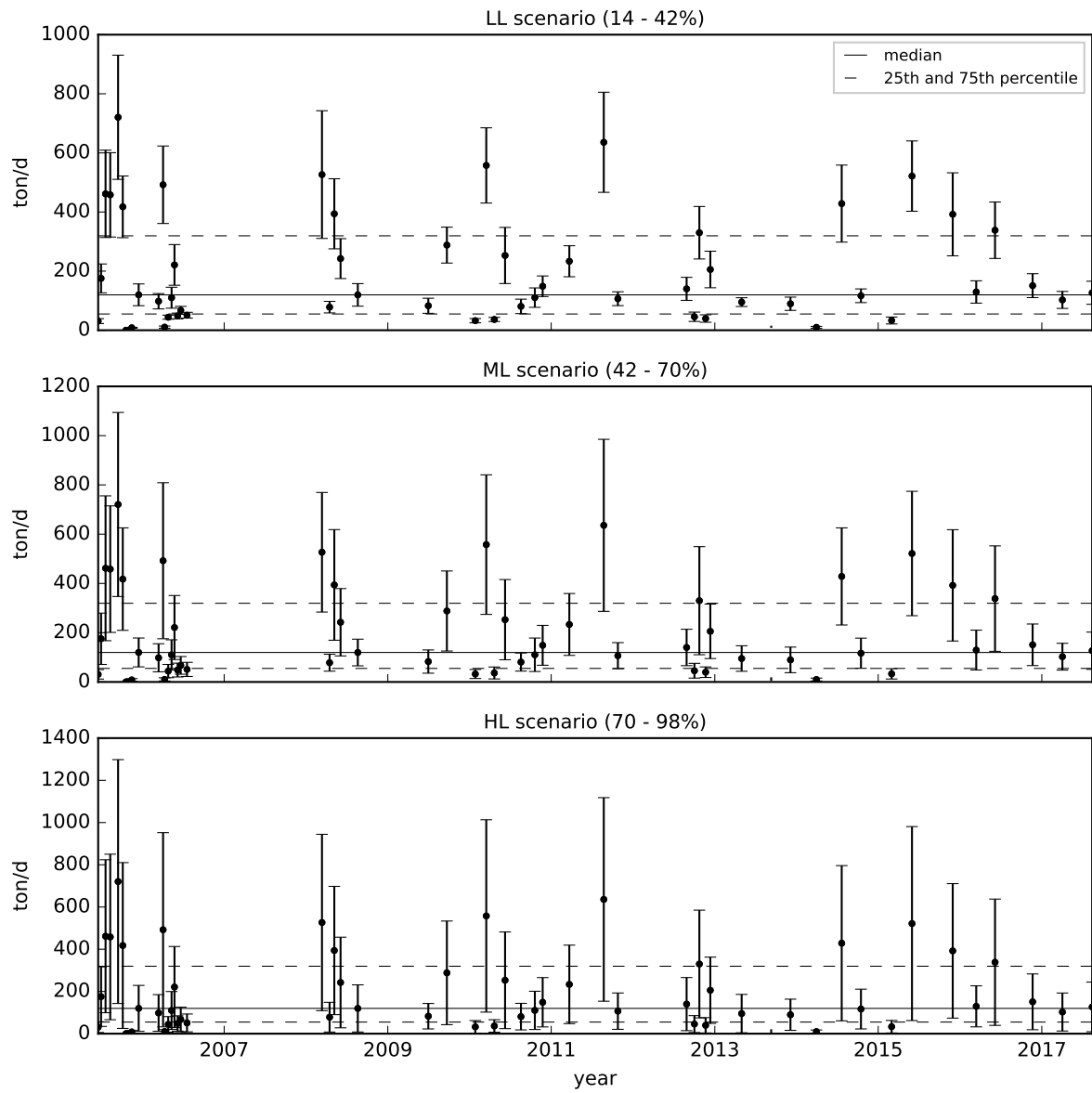
VDS - IG4

Figure 114 – LL, ML and HL uncertainty scenarios for VDS load time series from IG4
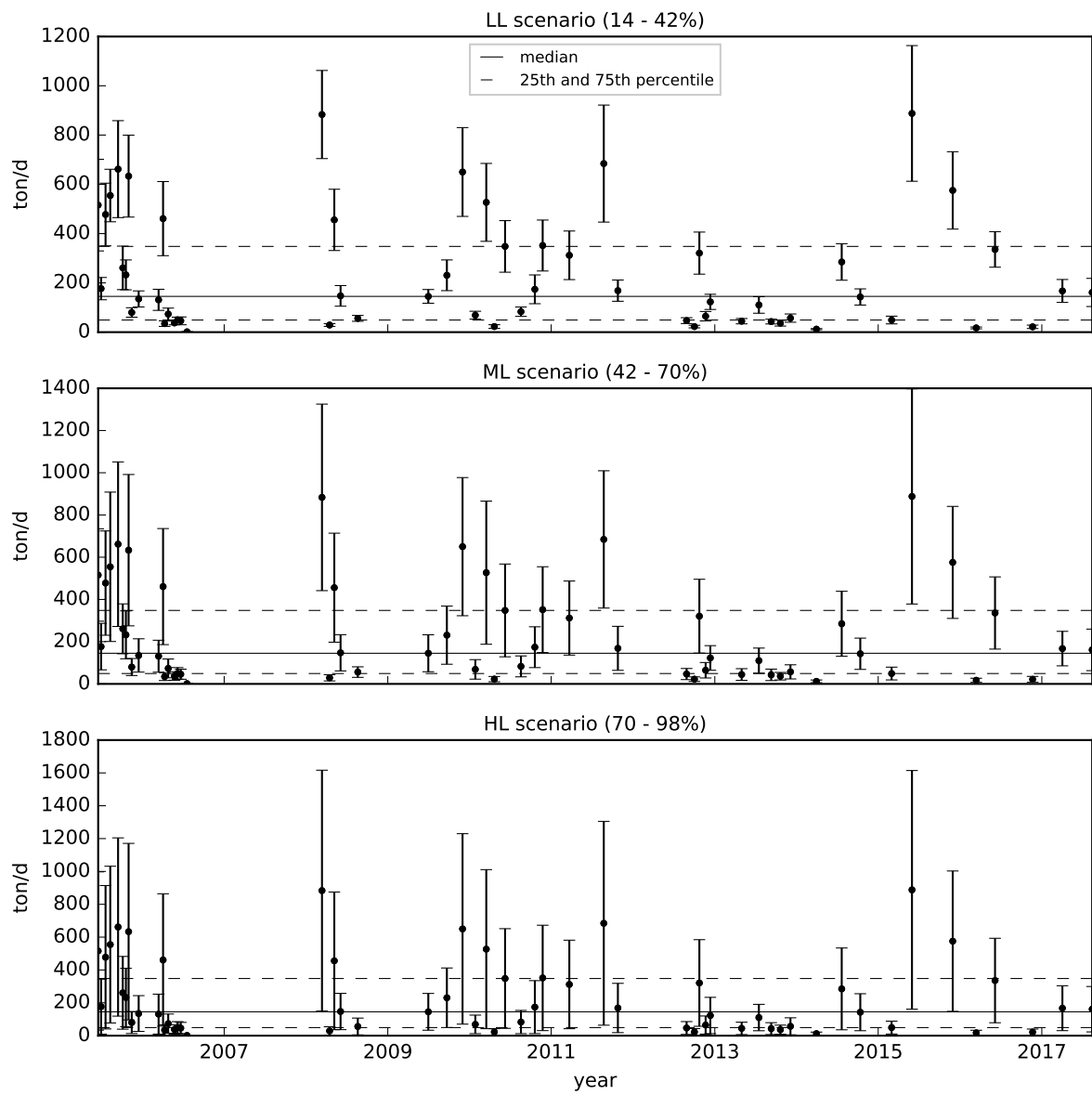
VDS - IG5

Figure 115 – LL, ML and HL uncertainty scenarios for VDS load time series, station IG5
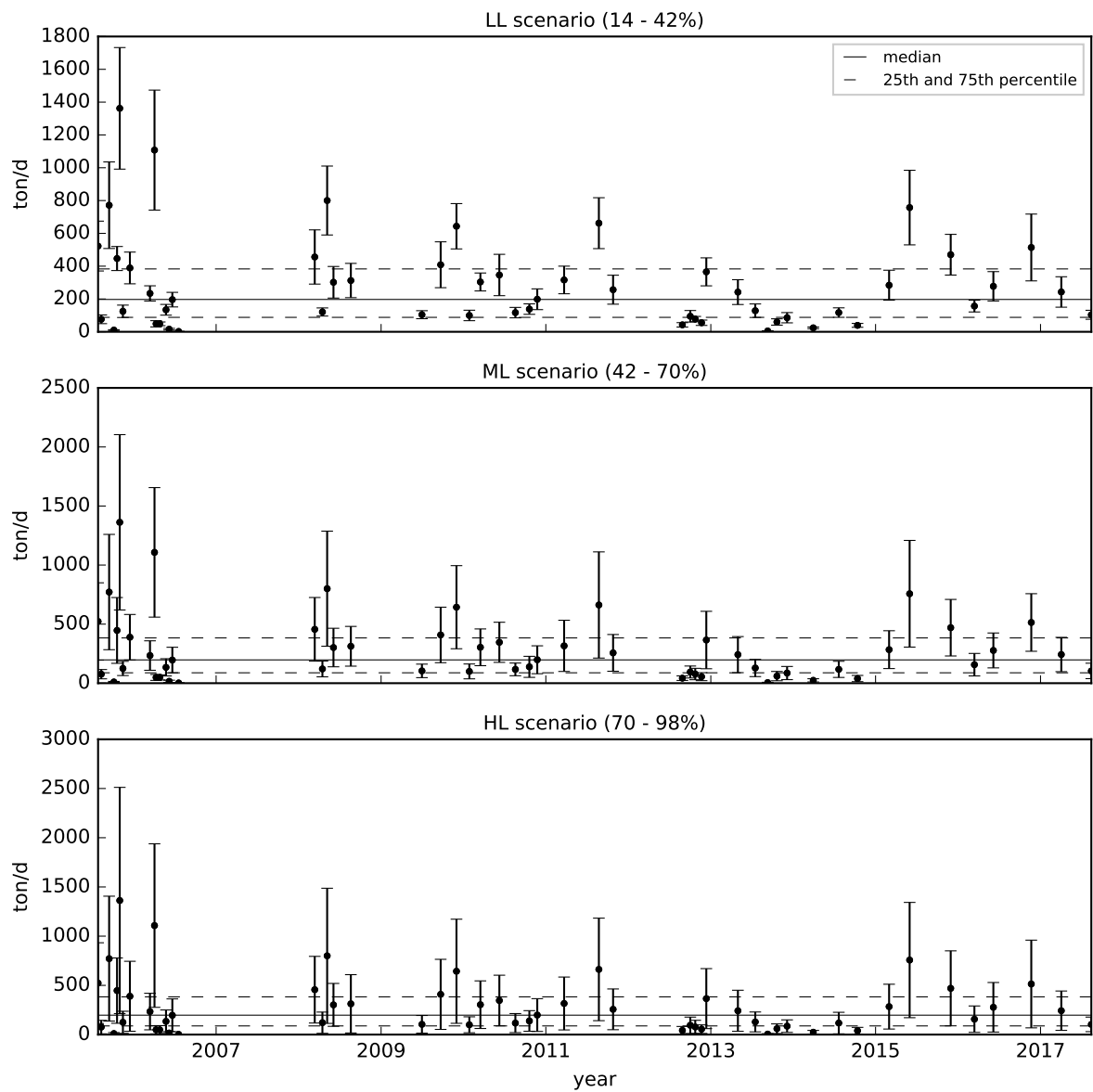
VDS - IG6

Figure 116 – LL, ML and HL uncertainty scenarios for VDS load time series, station IG6

VDS - IG7
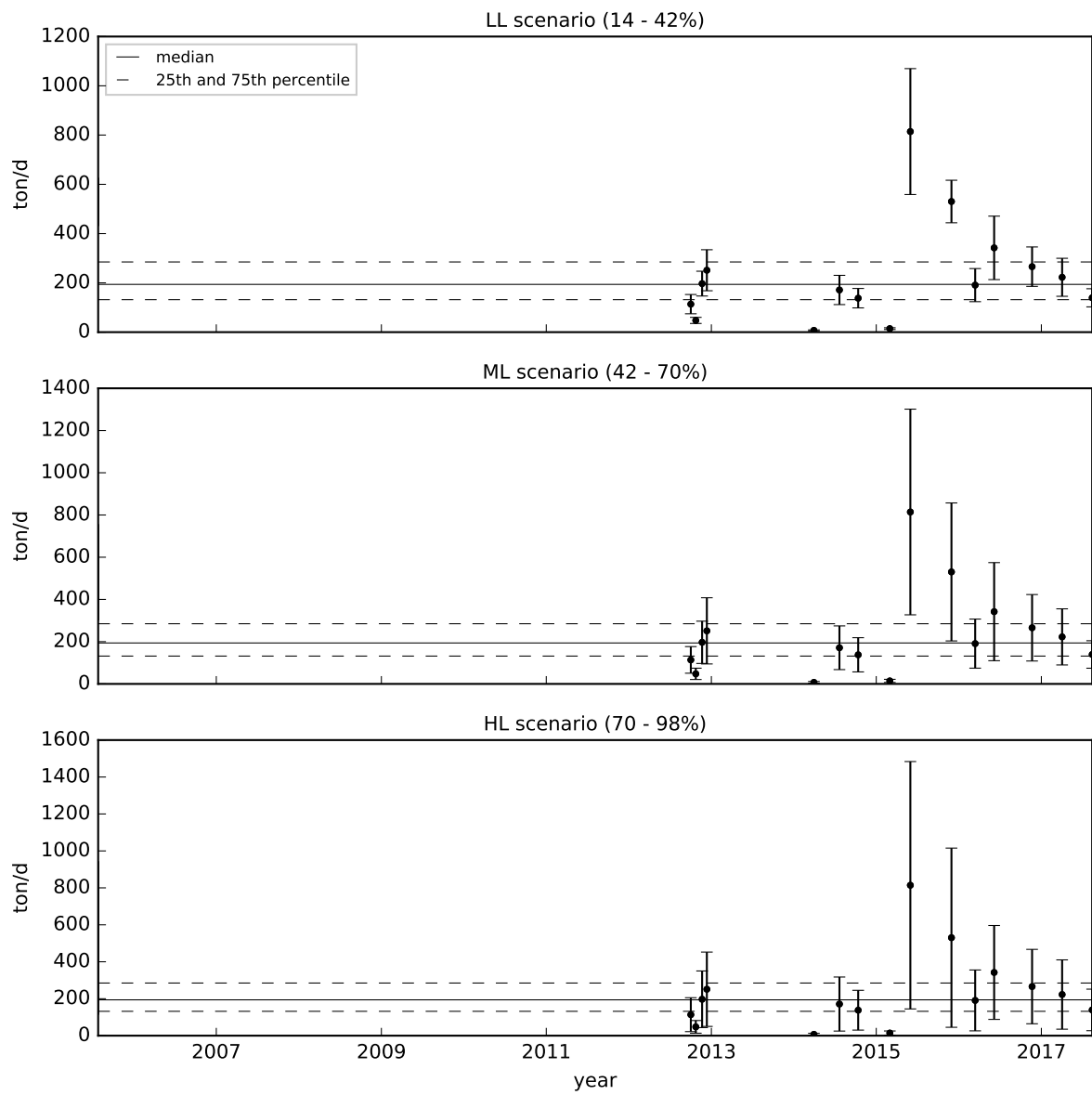
Figure 117 – LL, ML and HL uncertainty scenarios for VDS load time series, station IG7

A.5   Histograms of synthetic values (m³/s)
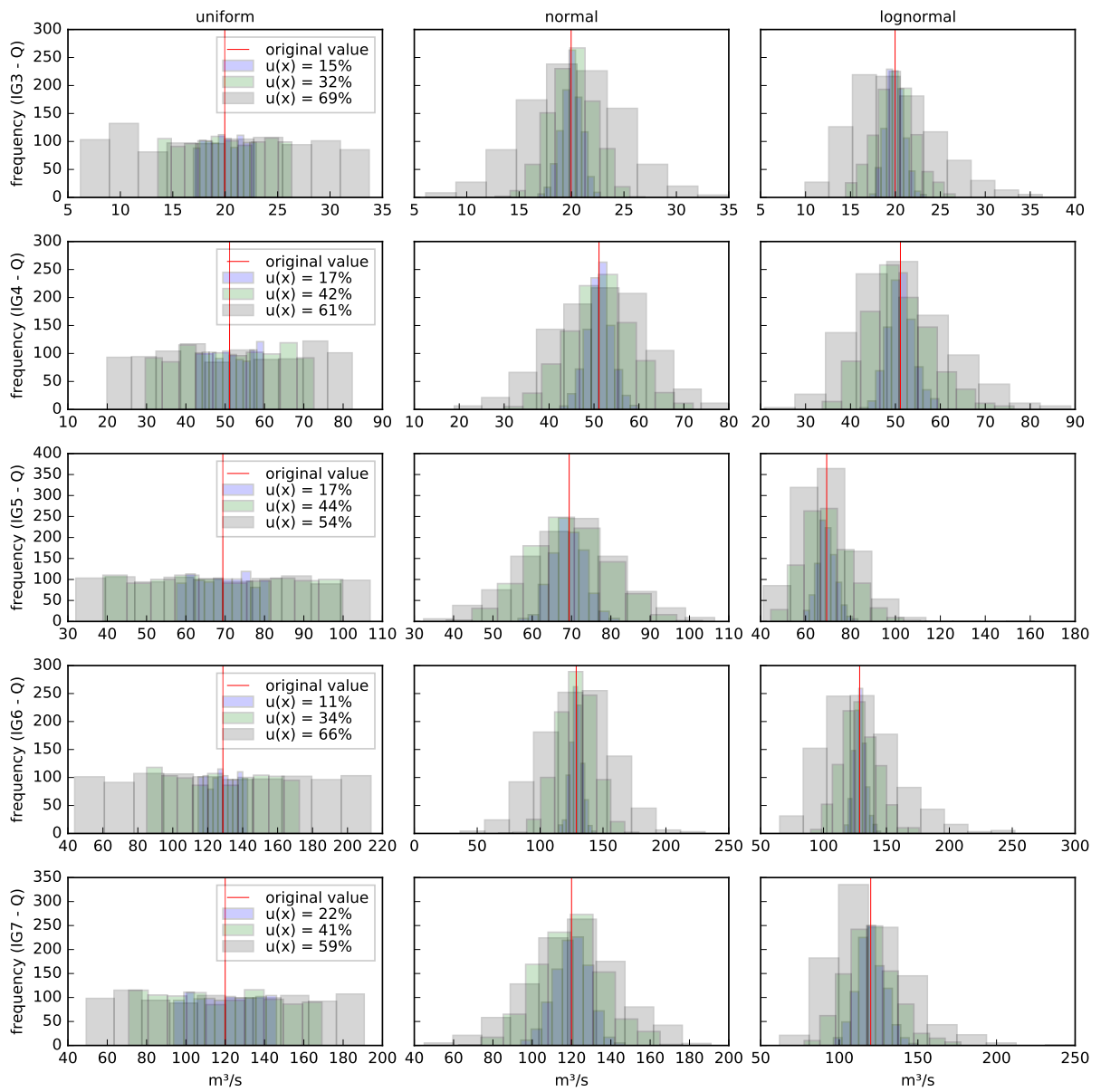
Figure 118 – Histograms of synthetic Q from one original measurement randomly chosen, station IG3–IG7

A.6   Histograms of synthetic values (mg/L)

BOD
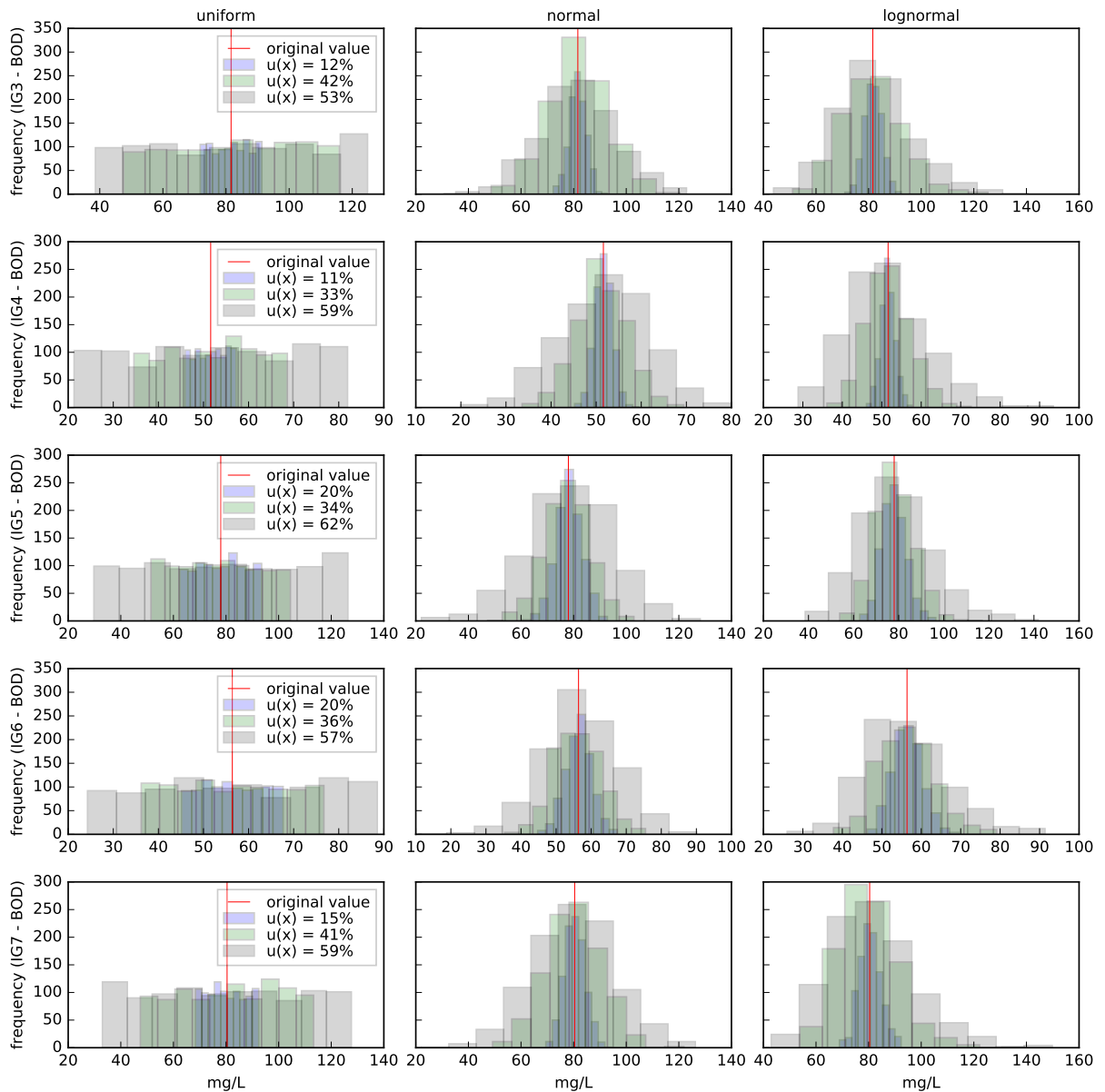
Figure 119 – Histograms of synthetic BOD concentrations from one original measurement randomly chosen, station IG3–IG7

DO
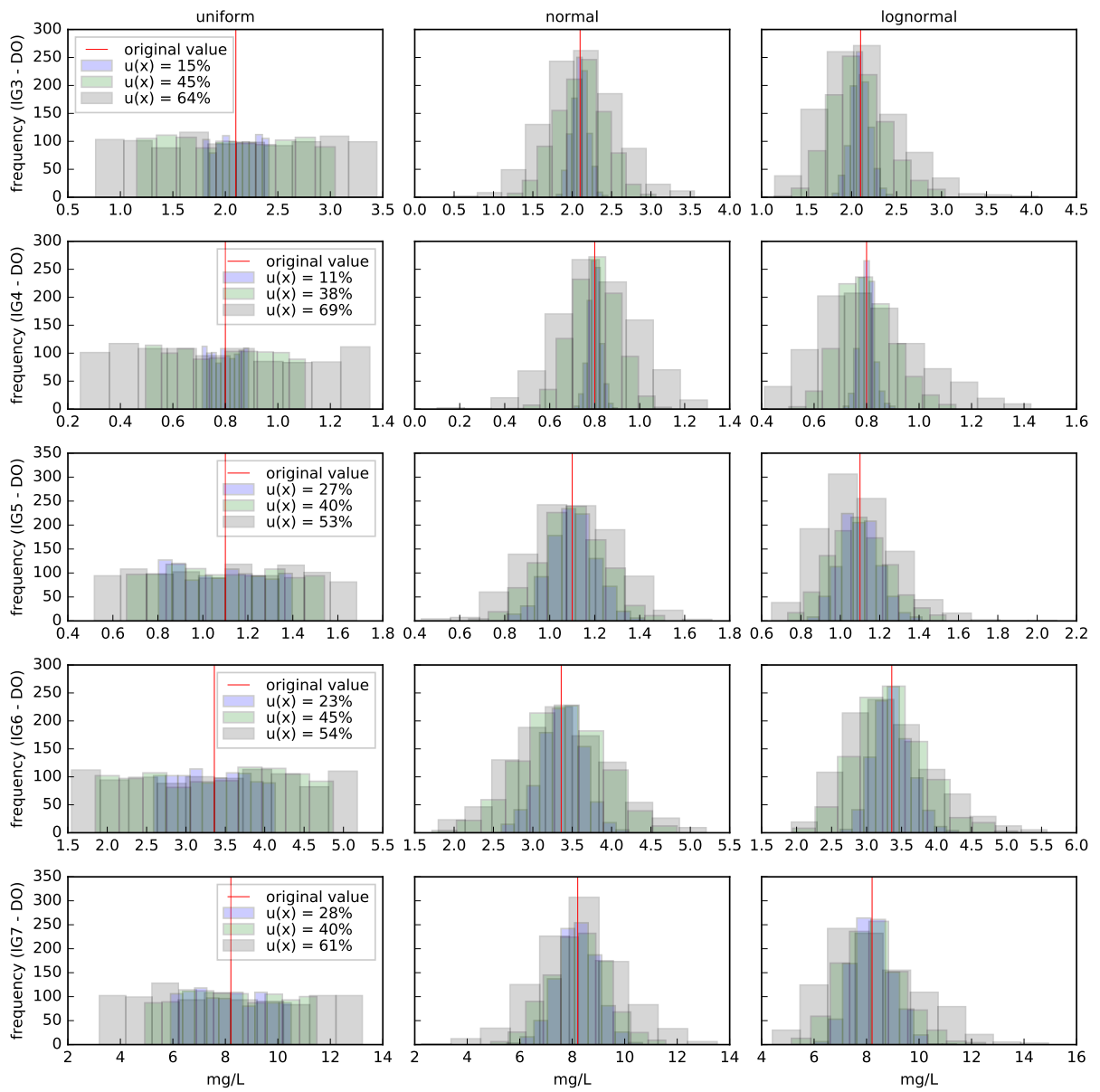
Figure 120 – Histograms of synthetic DO concentrations from one original measurement randomly chosen, station IG3–IG7

DOC
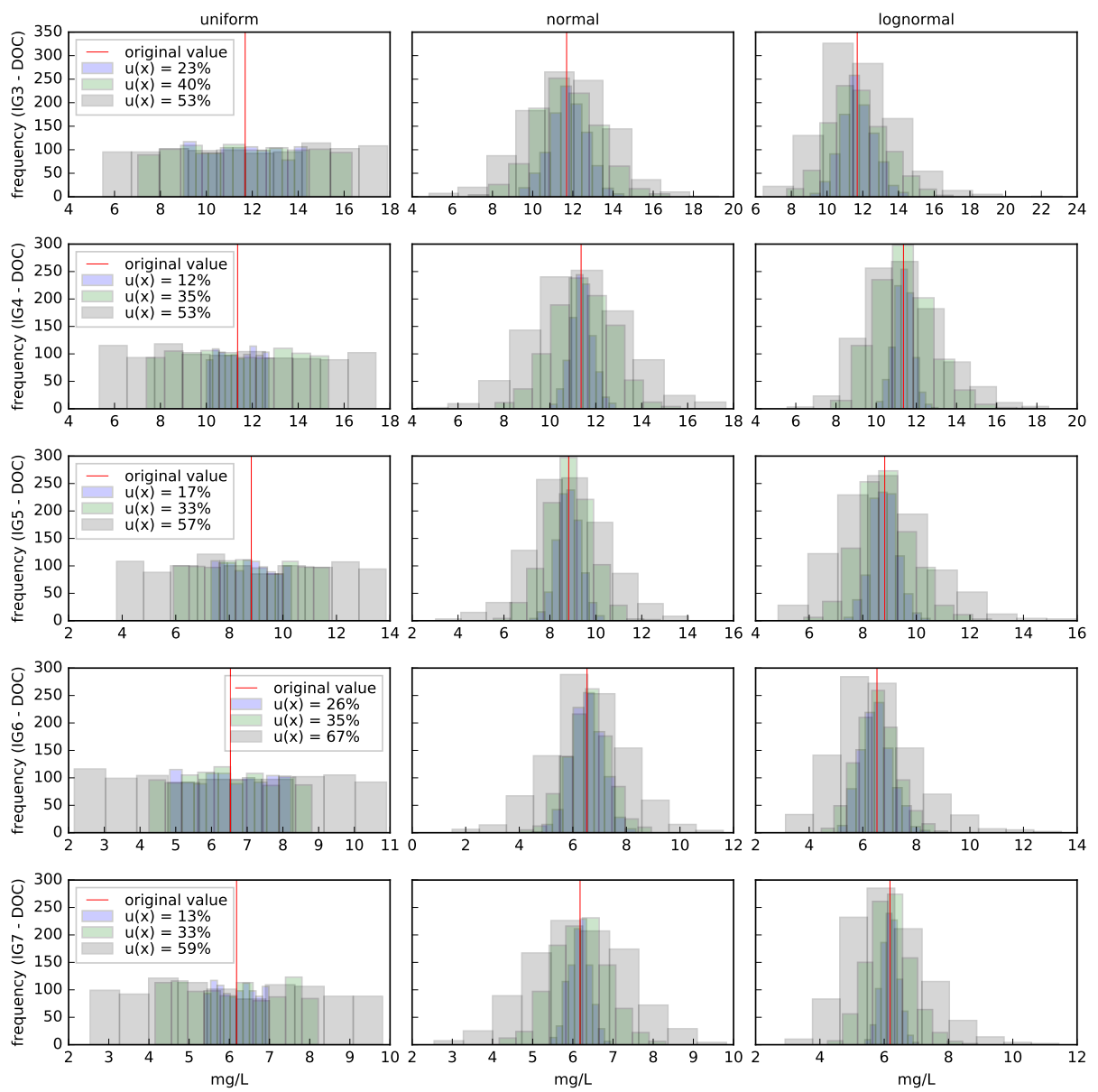
Figure 121 – Histograms of synthetic DOC concentrations from one original measurement randomly chosen, station IG3–IG7

NH4
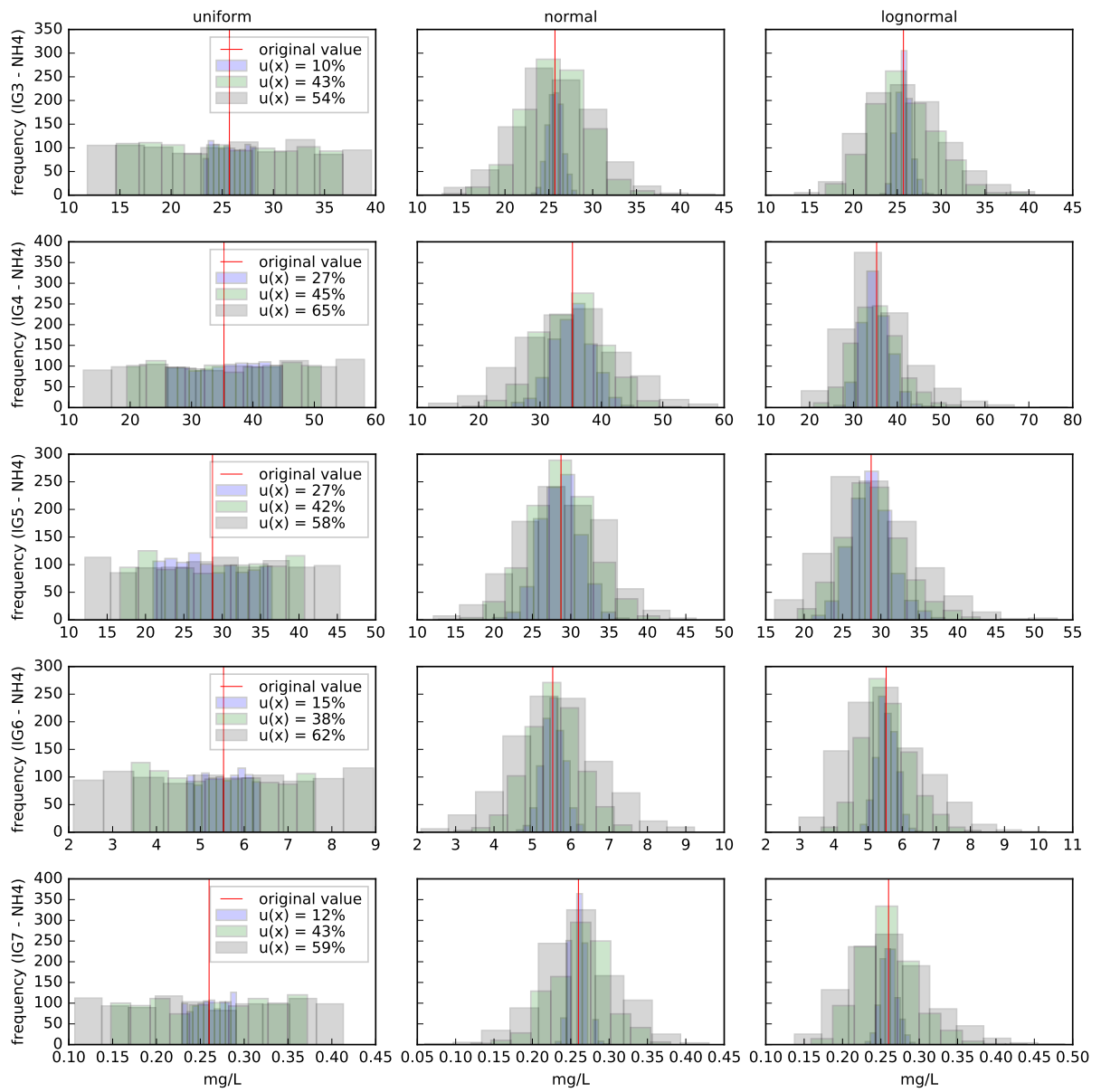
Figure 122 – Histograms of synthetic NH4 concentrations from one original measurement randomly chosen, station IG3–IG7

TP
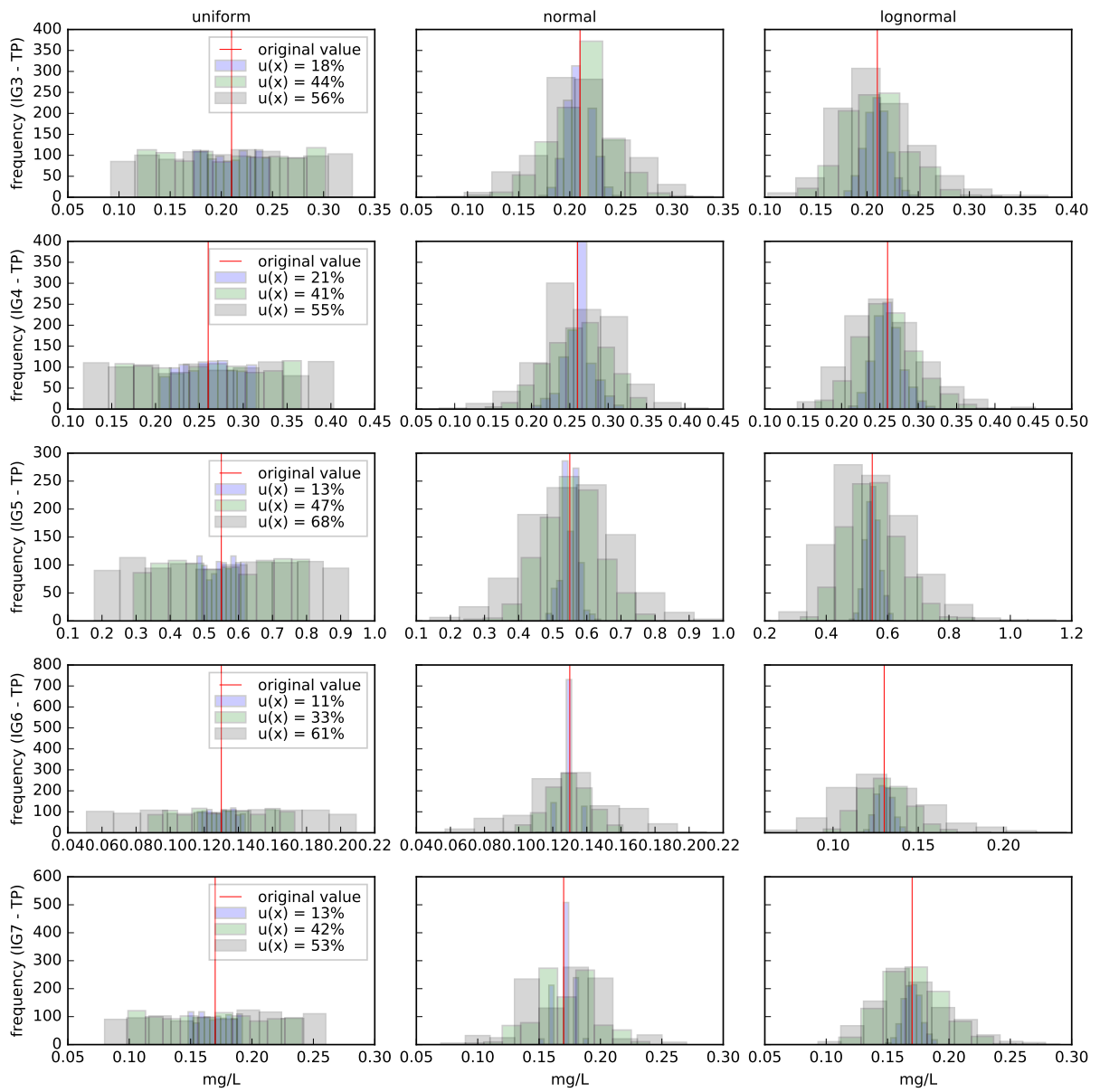
Figure 123 – Histograms of synthetic TP concentrations from one original measurement randomly chosen, station IG3–IG7

VDS
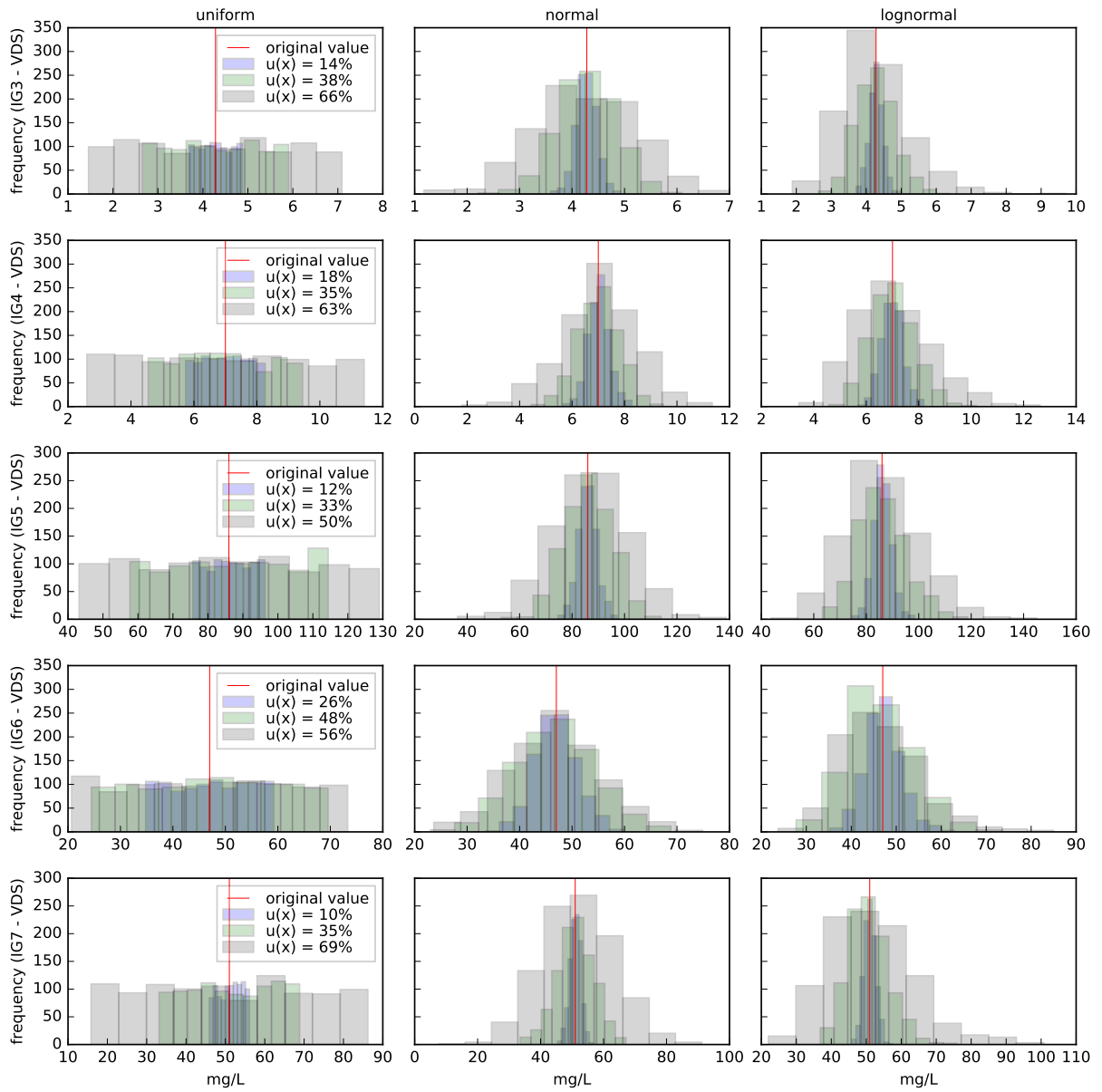
Figure 124 – Histograms of synthetic VDS concentrations from one original measurement randomly chosen, station IG3–IG7

A.7 Histograms of synthetic values (ton/d)

BOD
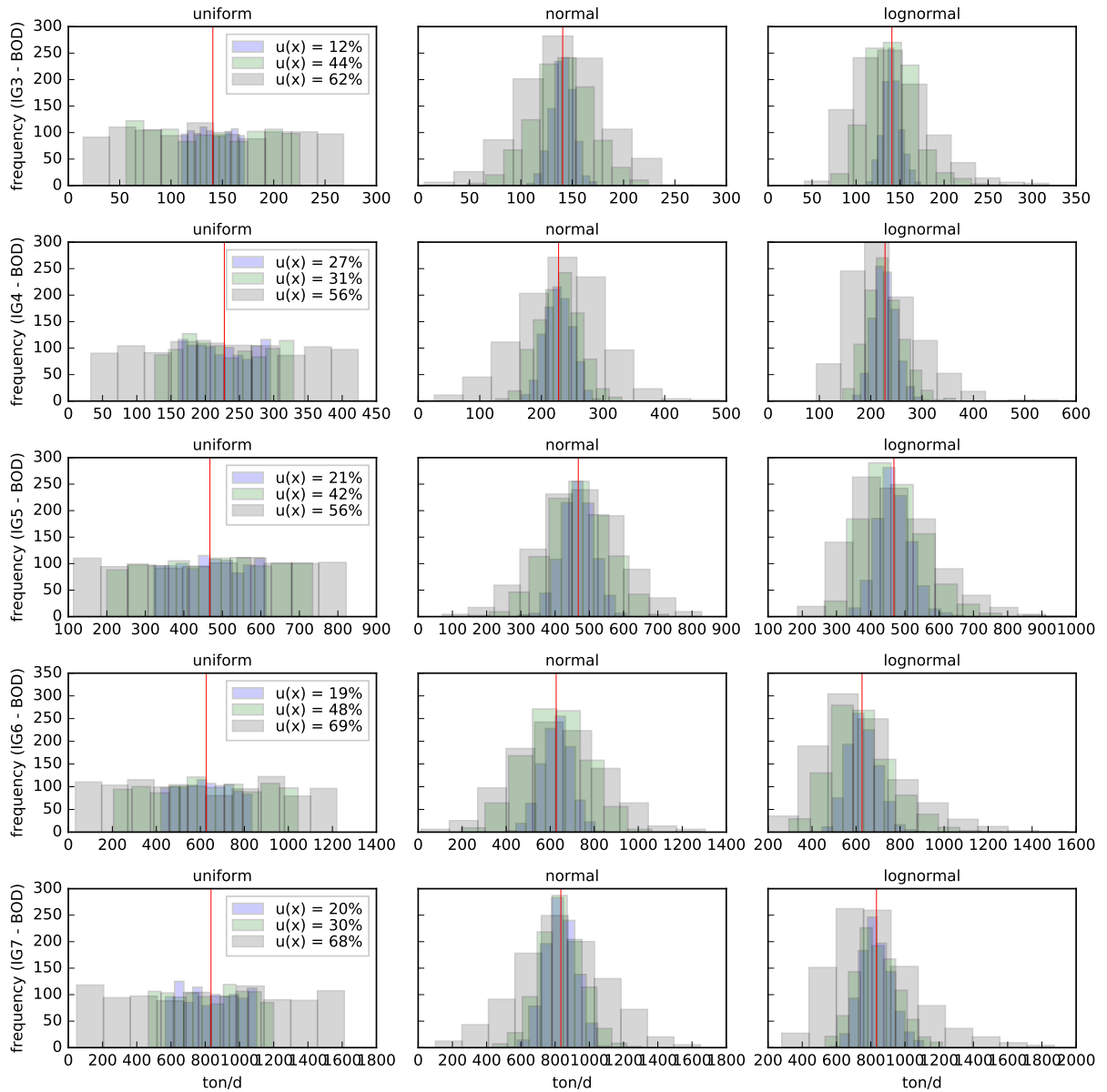
Figure 125 – Histograms of synthetic BOD loads from one original measurement randomly chosen, station IG3–IG7

DO
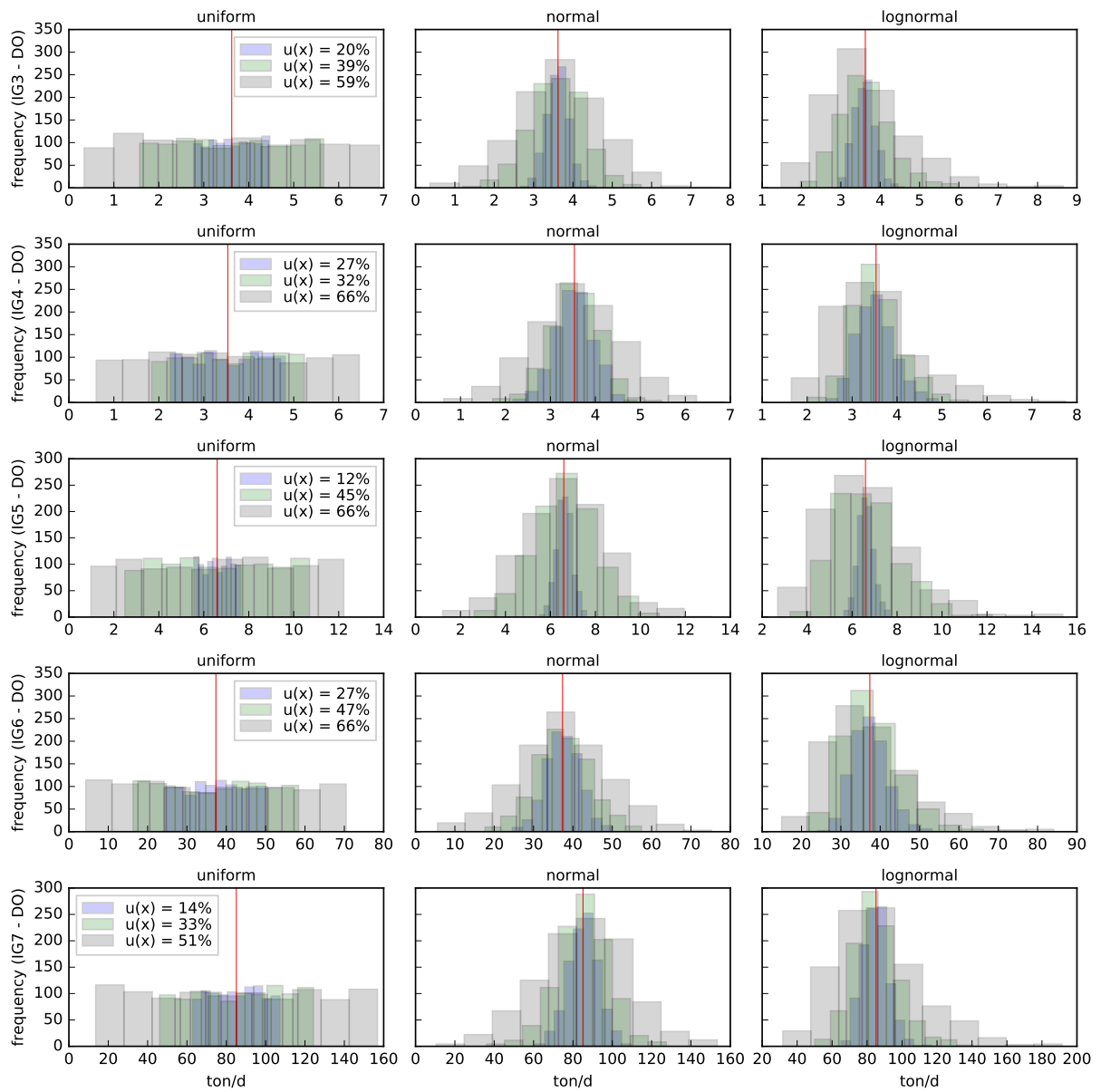
Figure 126 – Histograms of synthetic DO loads from one original measurement randomly chosen, station IG3–IG7

DOC
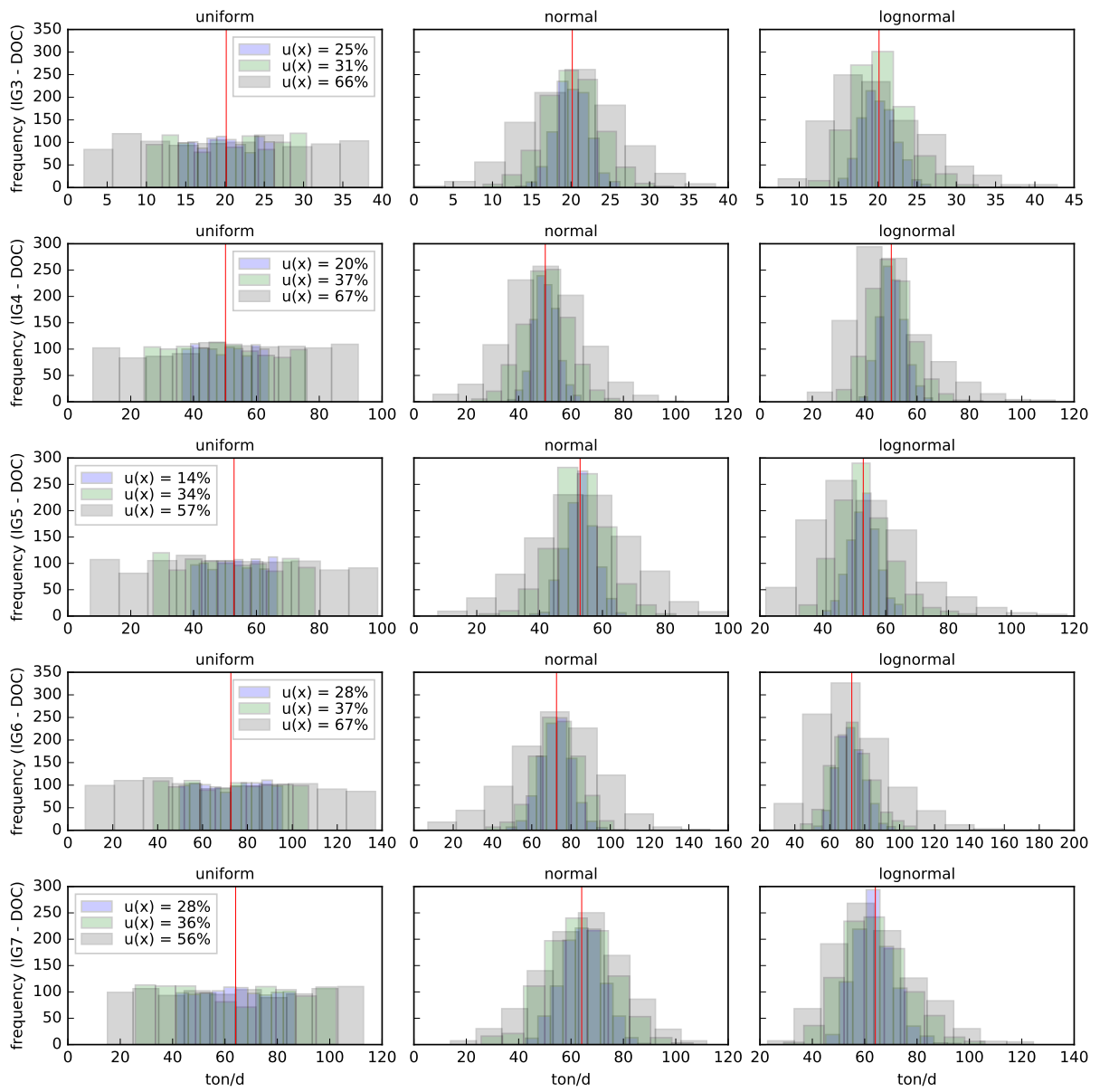
Figure 127 – Histograms of synthetic DOC loads from one original measurement randomly chosen, station IG3–IG7

NH4
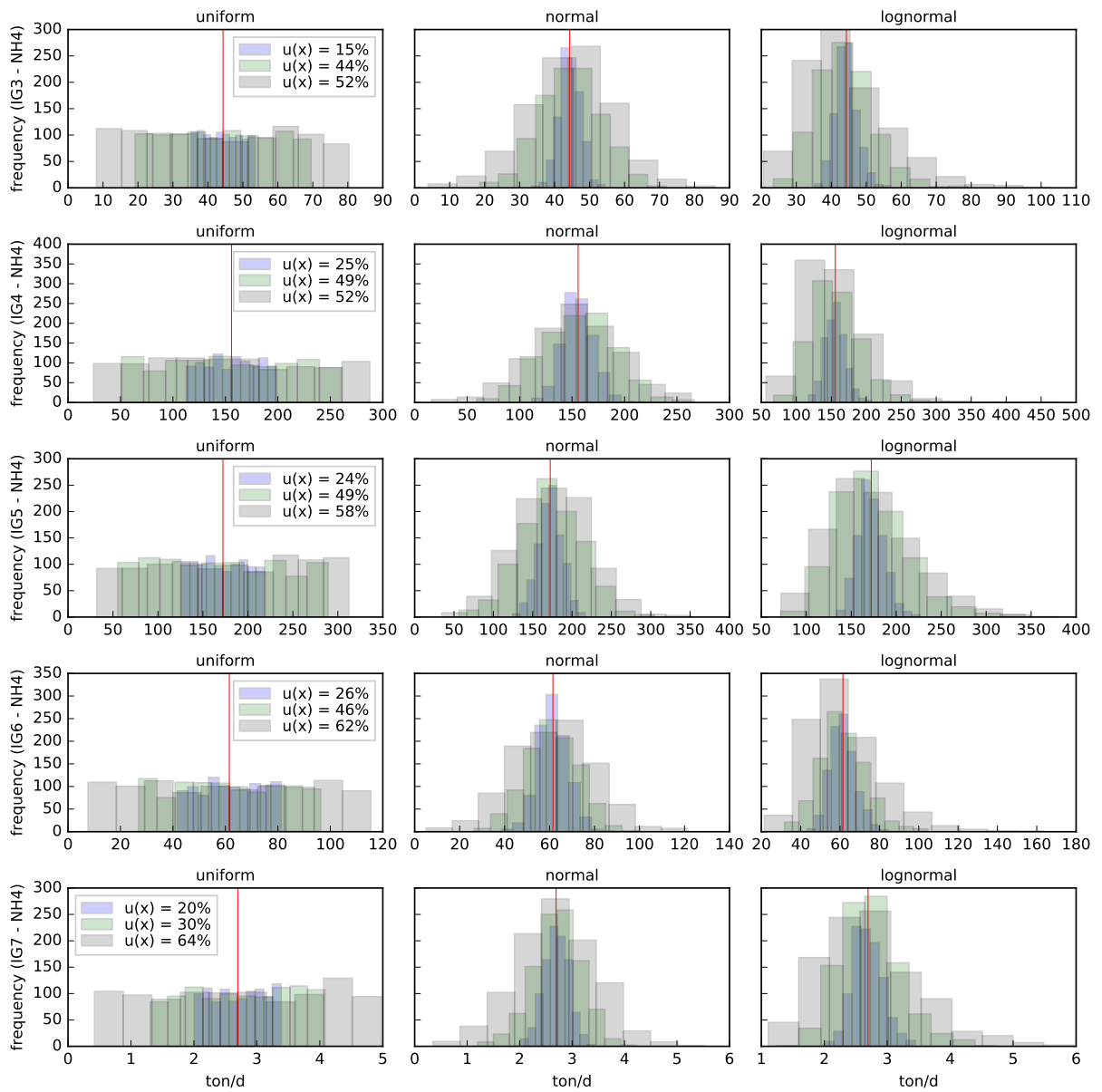
Figure 128 – Histograms of synthetic NH4 loads from one original measurement randomly chosen, station IG3–IG7

TP
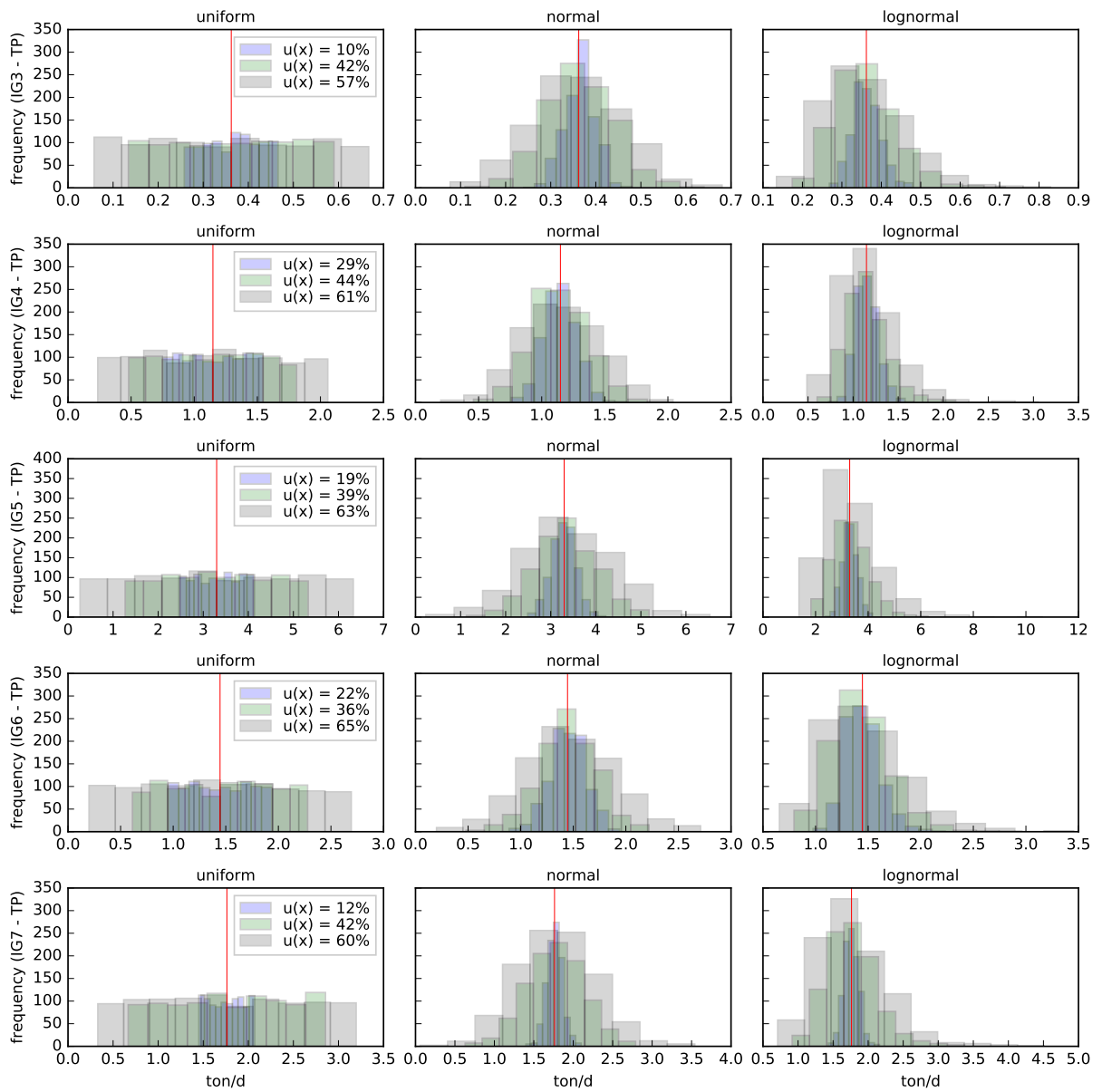
Figure 129 – Histograms of synthetic TP loads from one original measurement randomly chosen, station IG3–IG7

VDS
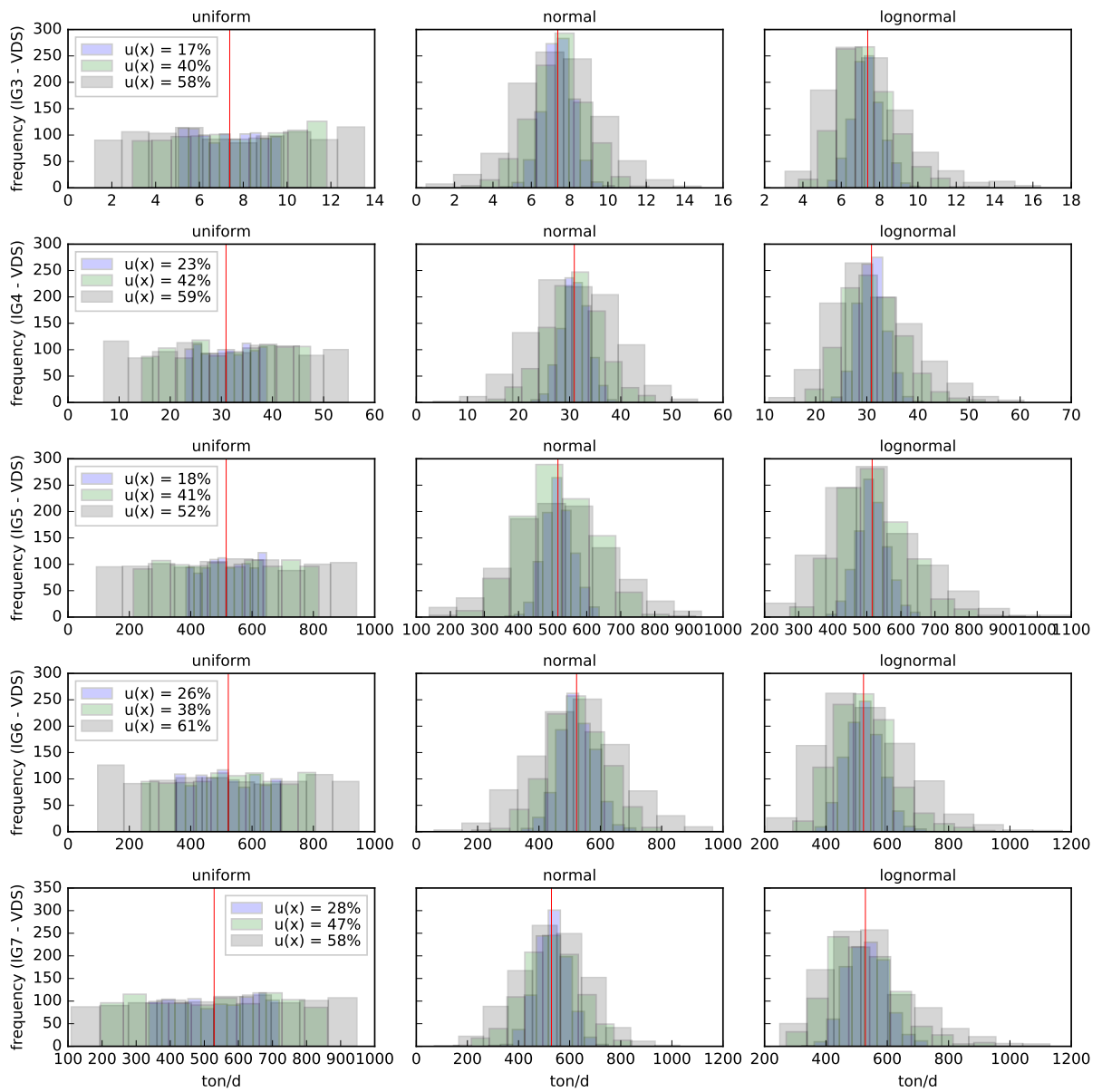
Figure 130 – Histograms of synthetic VDS loads from one original measurement randomly chosen, station IG3–IG7

A.8 RHIS (m³/s)

Q - IG3
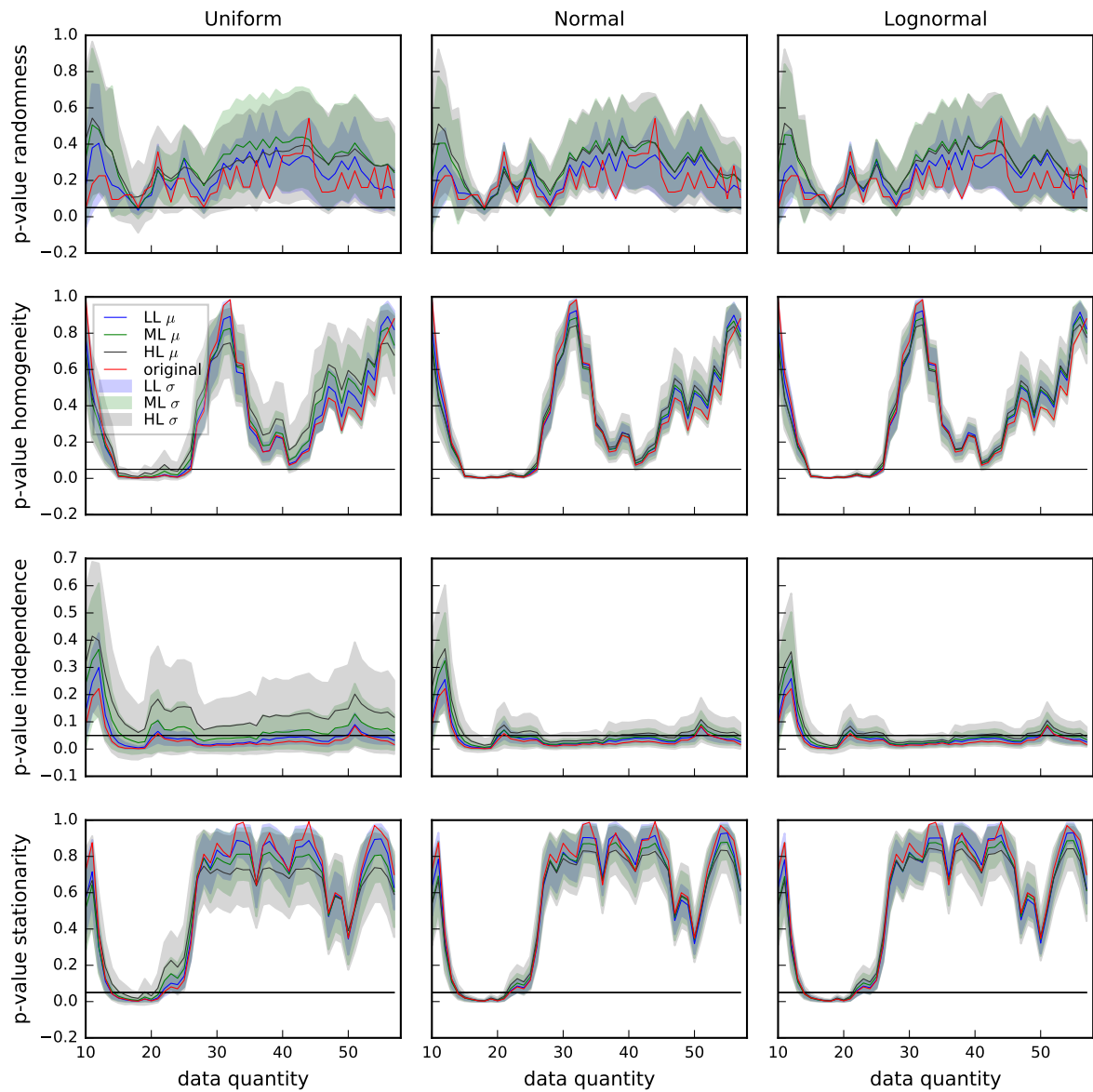
Figure 131 – Evolution of RHIS p-values from Q time series from IG3. Red line = p-value from OTS. Blue, green, gray lines = average p-value from STS in LL, ML and HL scenarios, respectively. Blue, green, gray bands = std of p-values from STS in LL, ML and HL scenarios, respectively. Black line = significance level ($\alpha = 0.05$). Reject H_0 if p-value < 0.05
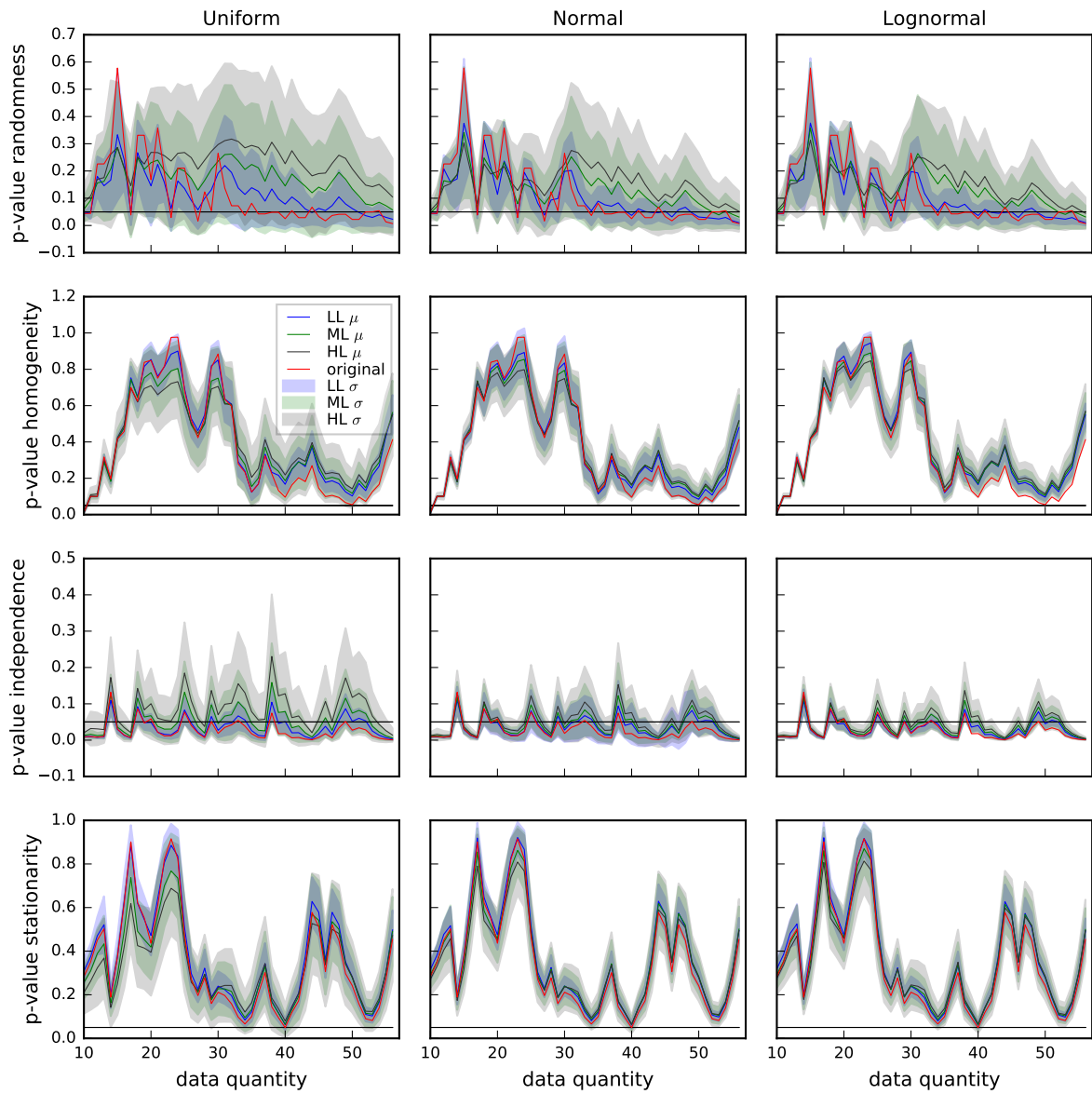
Q - IG4
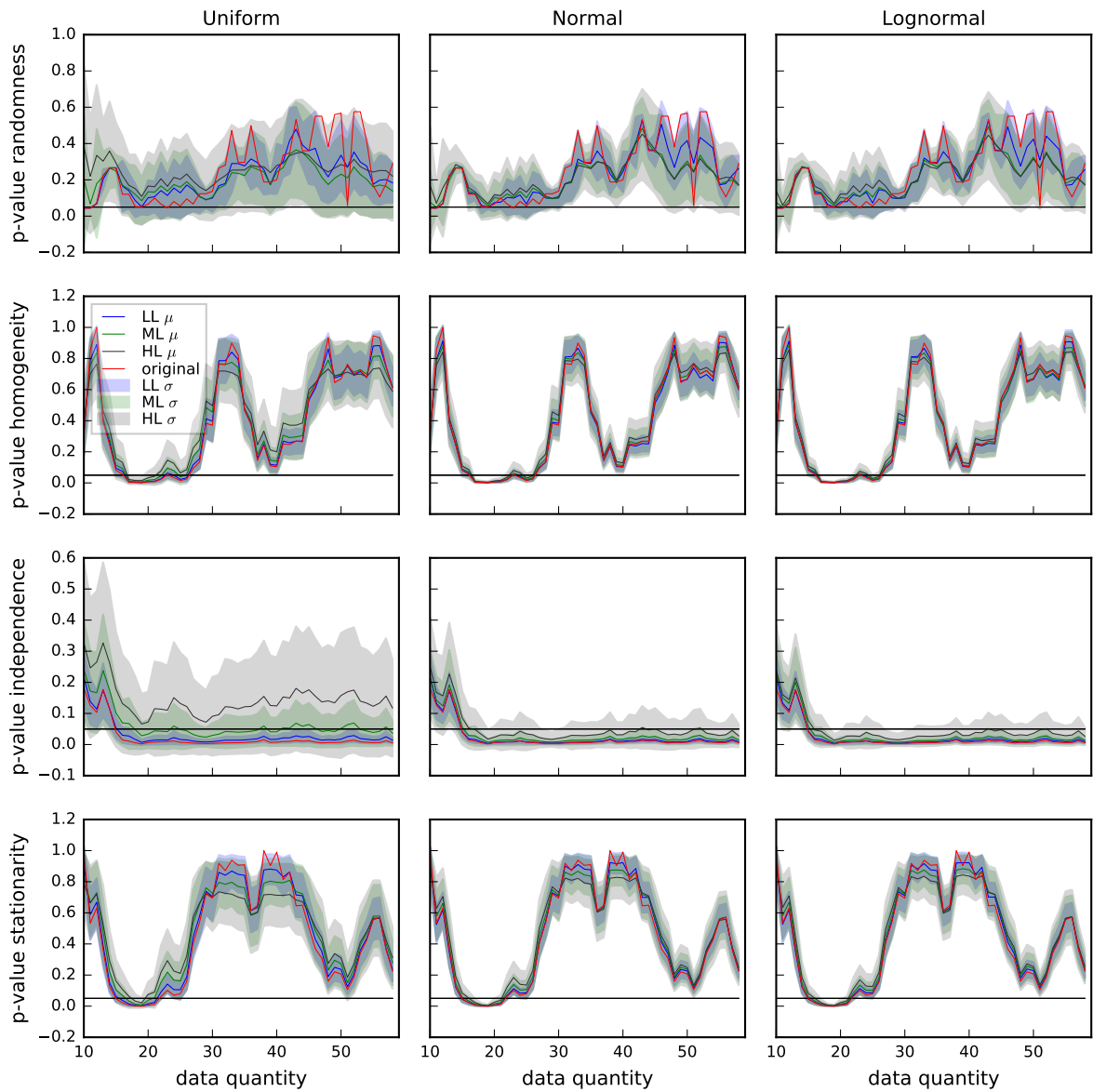
Figure 132 – Evolution of RHIS p-values fromQ time series from IG4. Red line = p-value from OTS. Blue, green, gray lines = average p-value from STS in LL, ML and HL scenarios, respectively. Blue, green, gray bands = std of p-values from STS in LL, ML and HL scenarios, respectively. Black line = significance level ($\alpha = 0.05$). Reject H_0 if p-value < 0.05
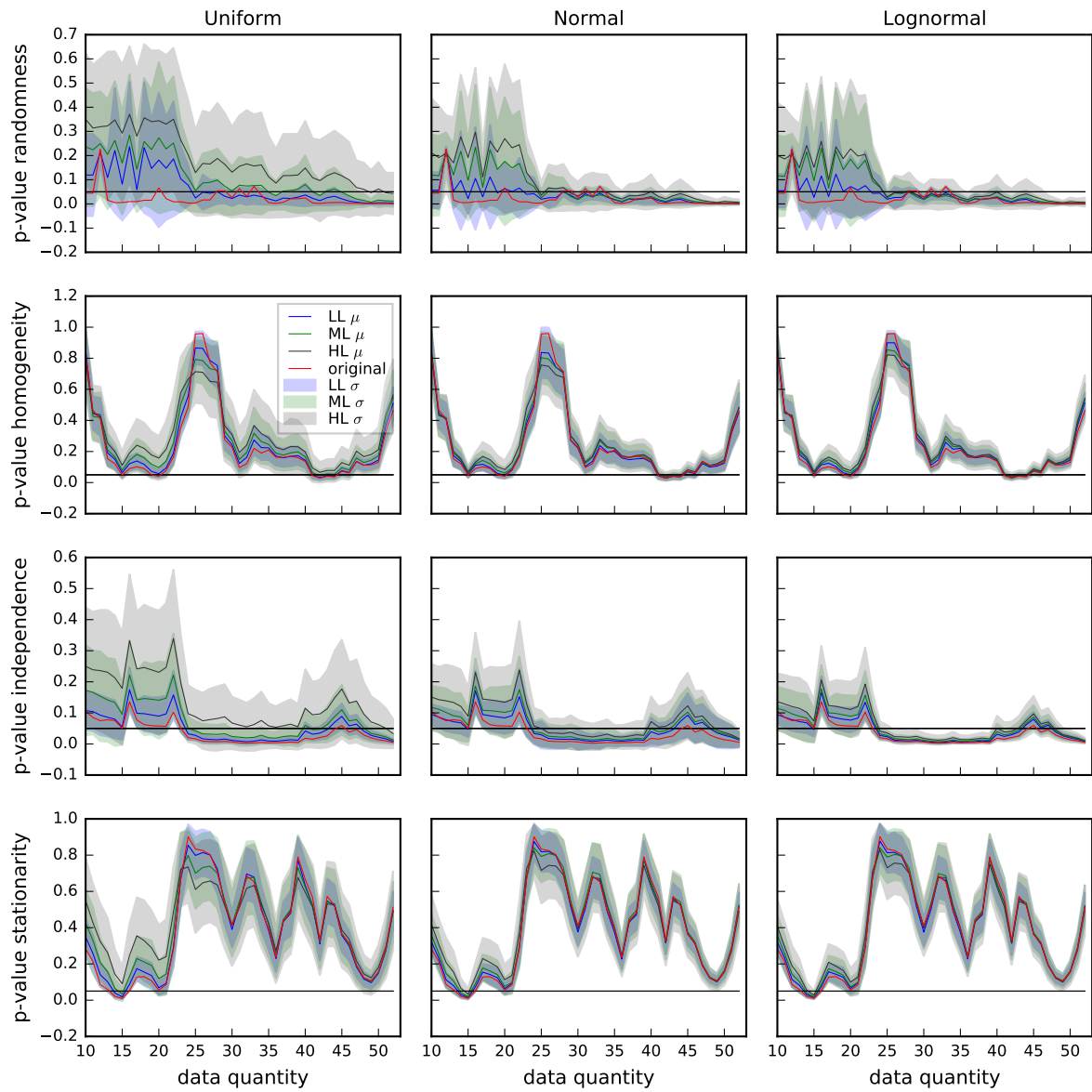
Q - IG5
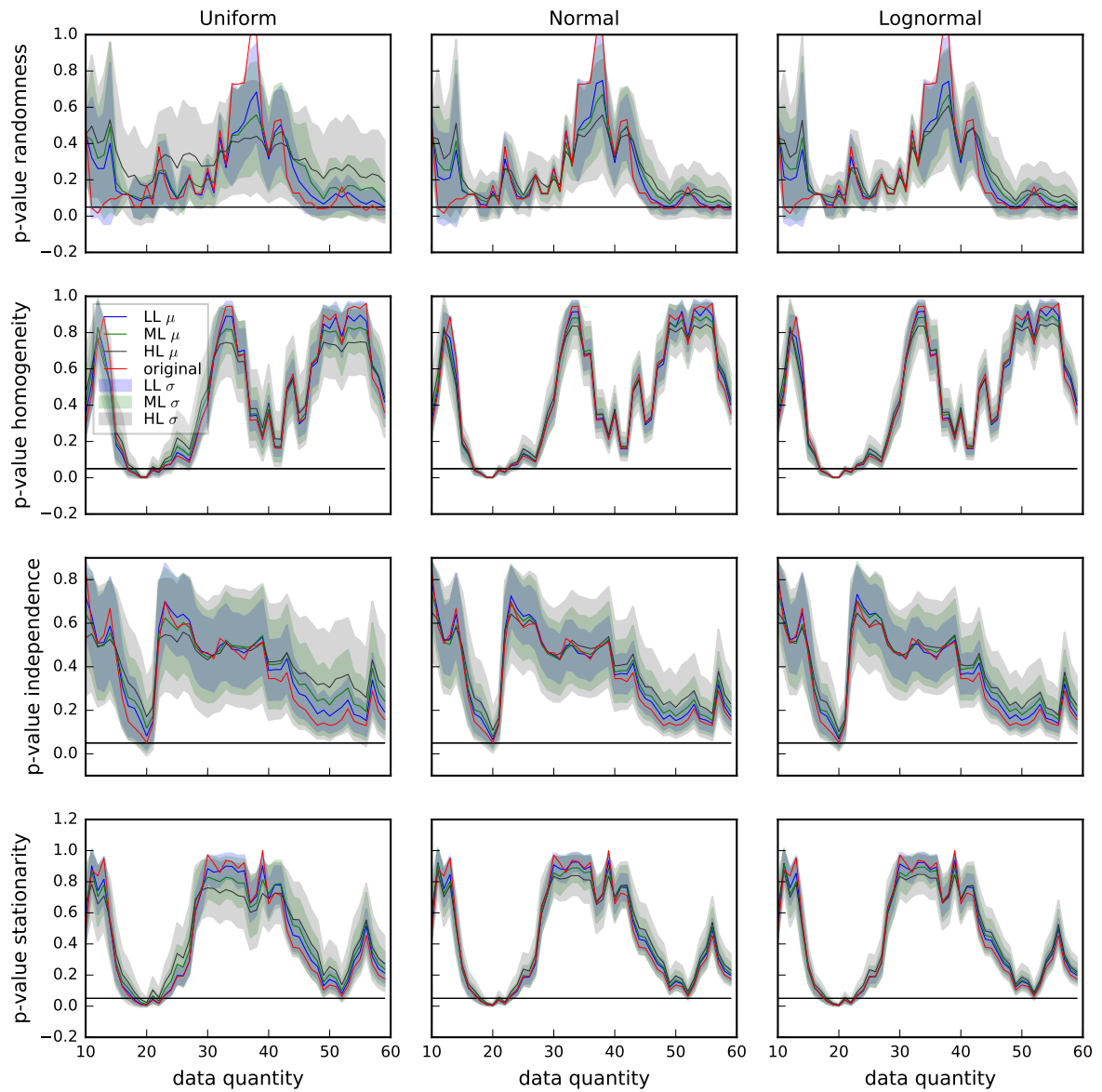
Figure 133 – Evolution of RHIS p-values from Q time series from IG5. Red line = p-value from OTS. Blue, green, gray lines = average p-value from STS in LL, ML and HL scenarios, respectively. Blue, green, gray bands = std of p-values from STS in LL, ML and HL scenarios, respectively. Black line = significance level ($\alpha = 0.05$). Reject H_0 if p-value < 0.05
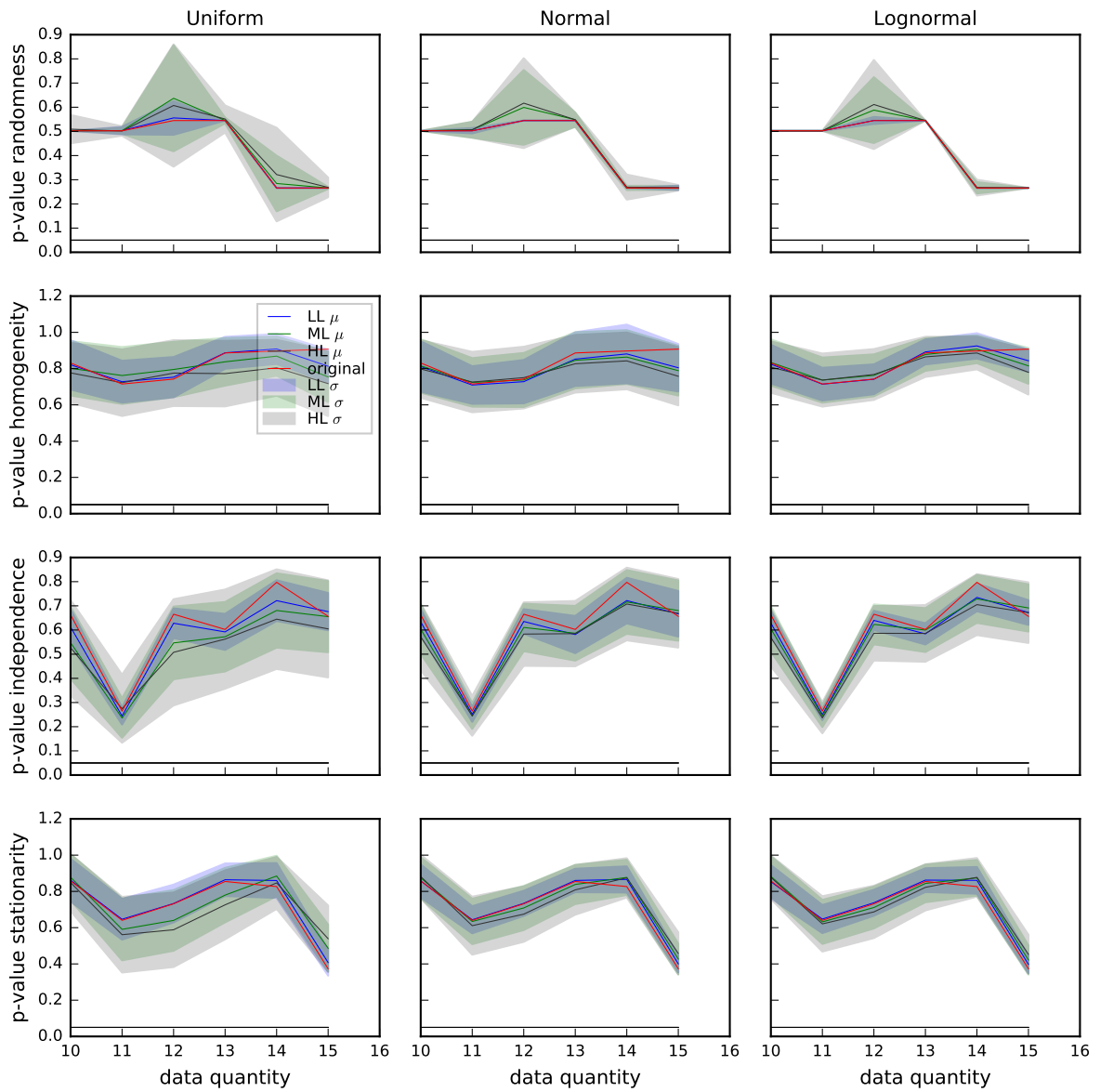
Q - IG6
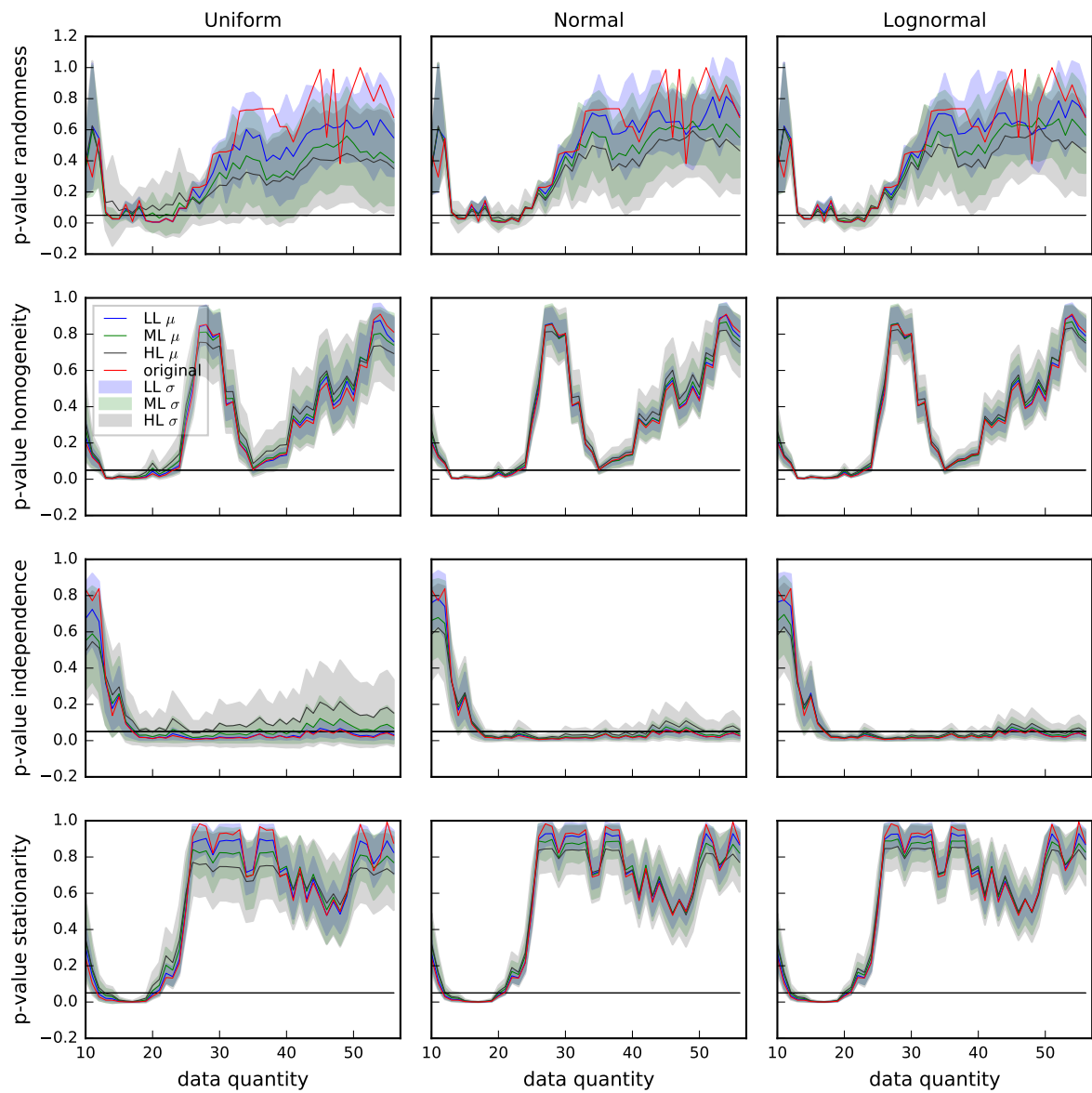
Figure 134 – Evolution of RHIS p-values from Q time series from IG6. Red line = p-value from OTS. Blue, green, gray lines = average p-value from STS in LL, ML and HL scenarios, respectively. Blue, green, gray bands = std of p-values from STS in LL, ML and HL scenarios, respectively. Black line = significance level ($\alpha = 0.05$). Reject H_0 if p-value < 0.05
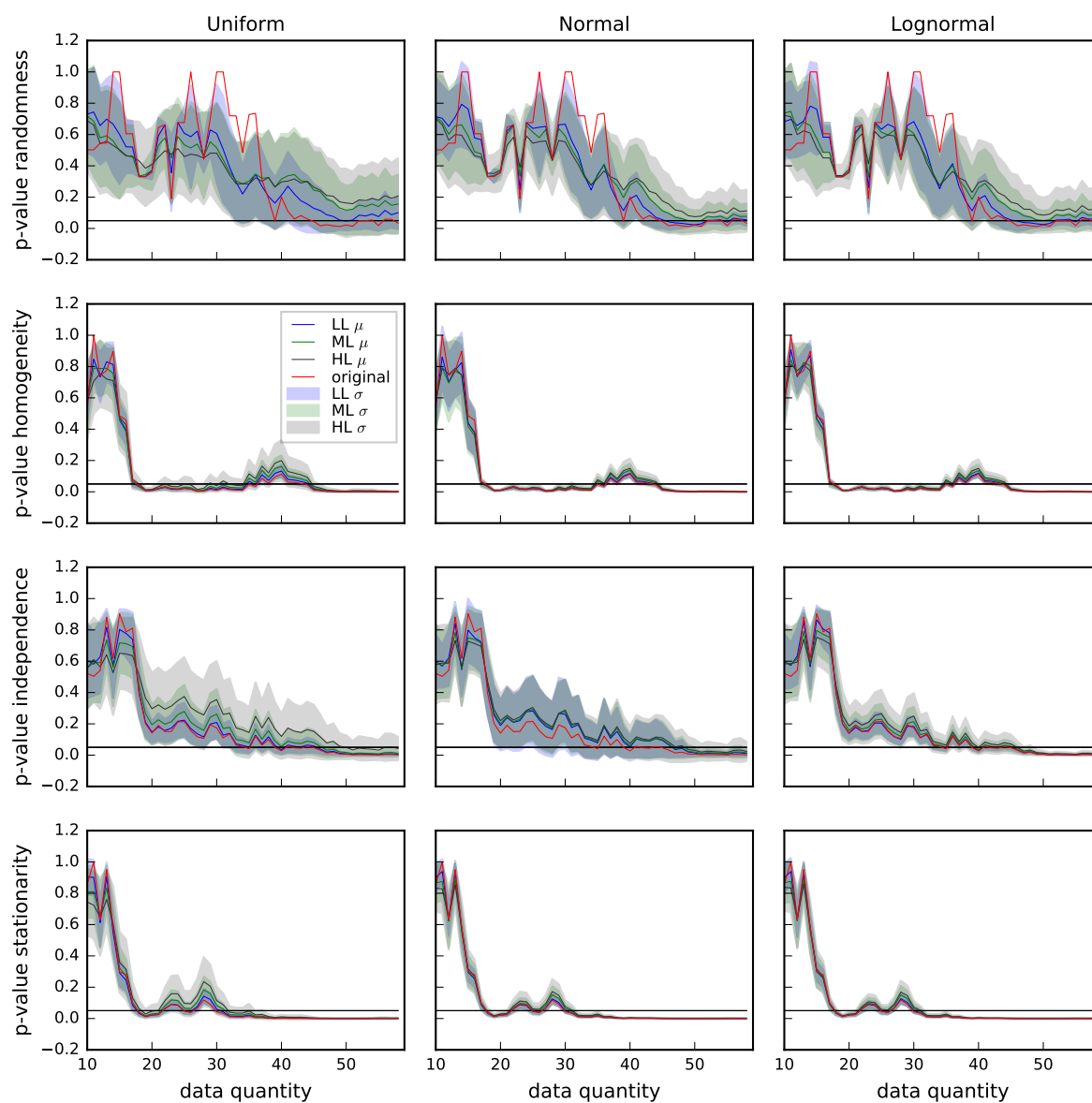
Q - IG7
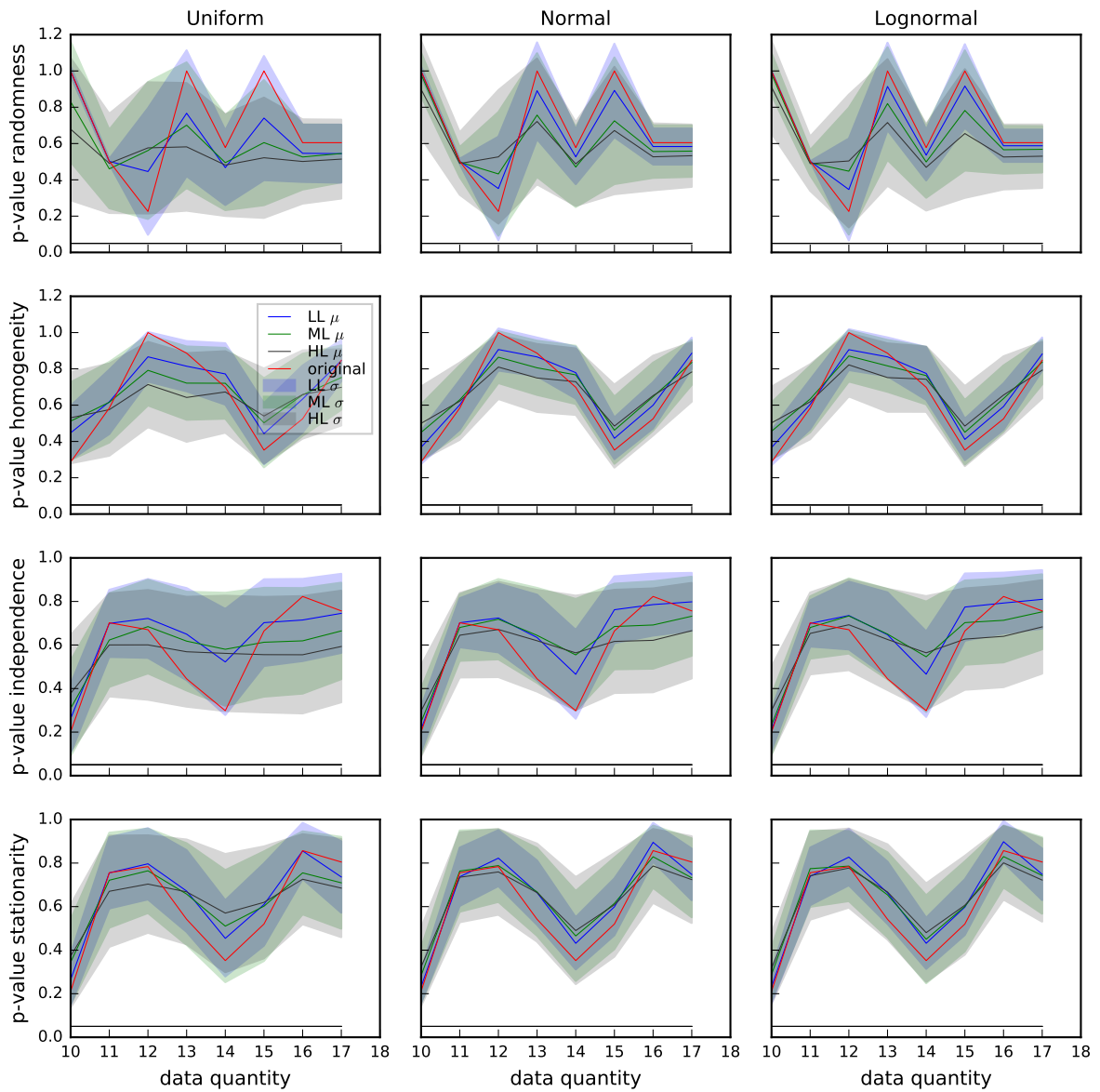
Figure 135 – Evolution of RHIS p-values from Q time series from IG7. Red line = p-value from OTS. Blue, green, gray lines = average p-value from STS in LL, ML and HL scenarios, respectively. Blue, green, gray bands = std of p-values from STS in LL, ML and HL scenarios, respectively. Black line = significance level (α = 0.05). Reject H_0 if p-value < 0.05

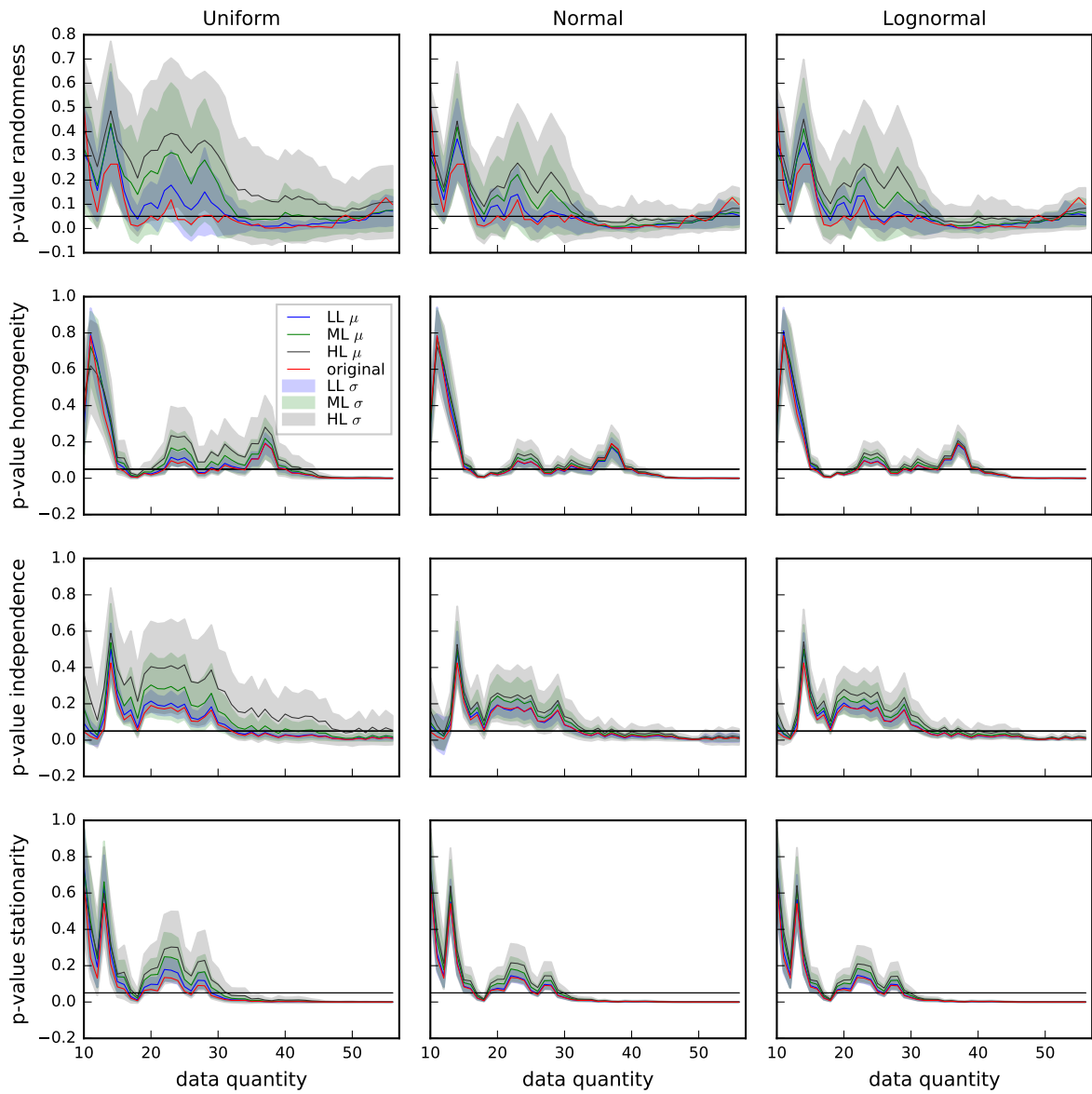## A.9   RHIS (mg/L)

BOD - IG3
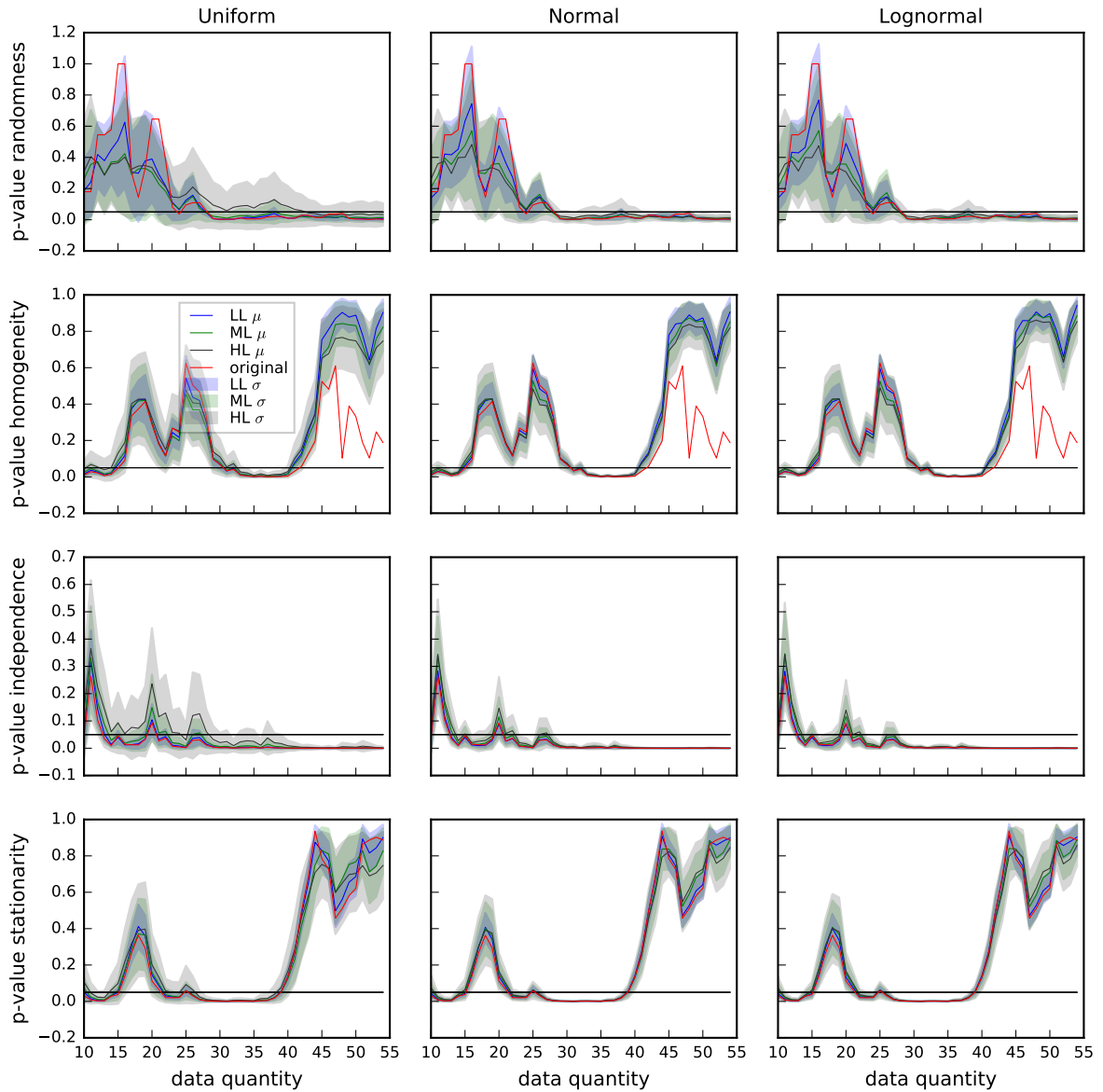
Figure 136 – Evolution of RHIS p-values from BOD concentration time series from IG3. Red line = p-value from OTS. Blue, green, gray lines = average p-value from STS in LL, ML and HL scenarios, respectively. Blue, green, gray bands = std of p-values from STS in LL, ML and HL scenarios, respectively. Black line = significance level ($\alpha = 0.05$). Reject H_0 if p-value < 0.05
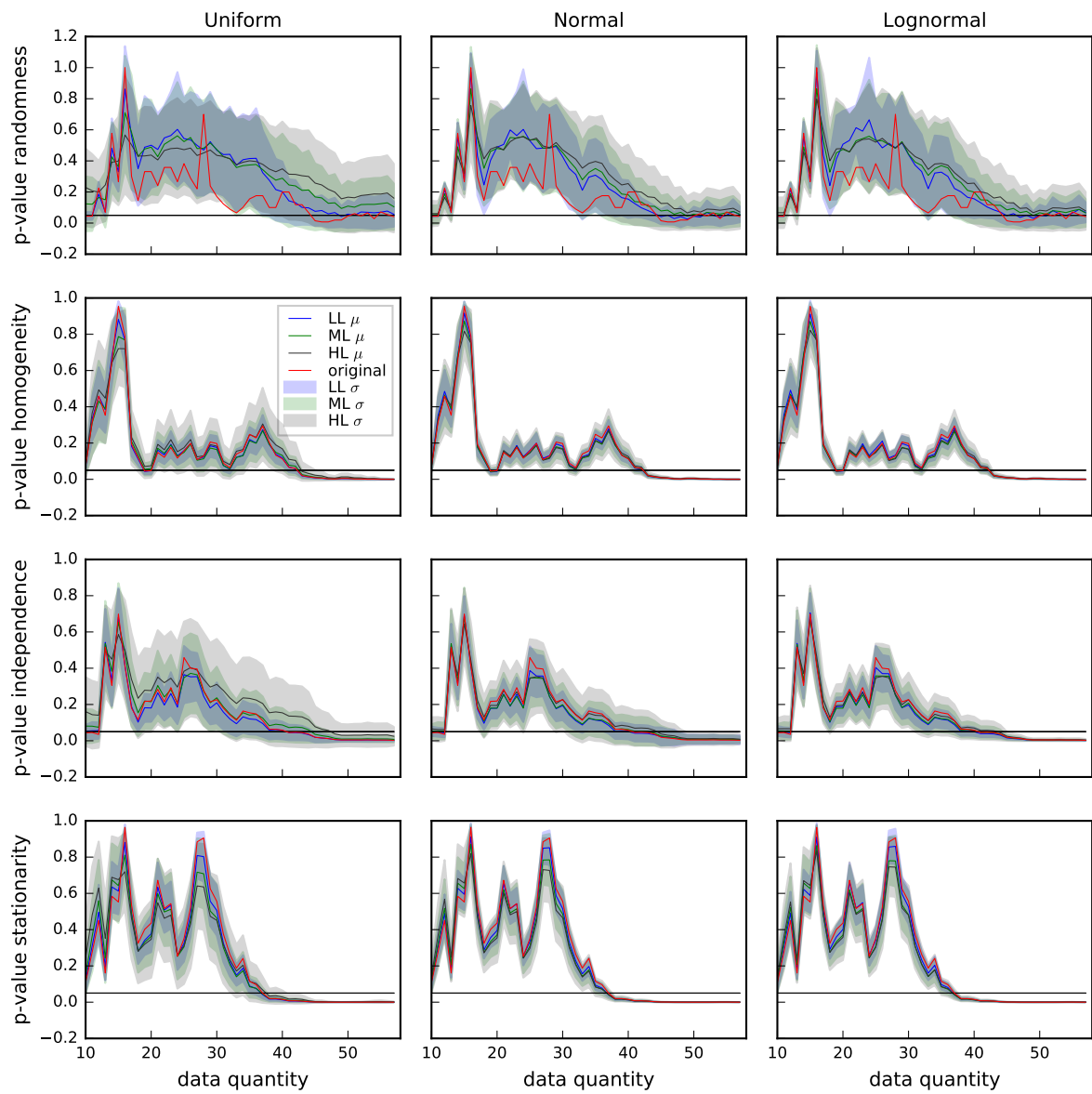
BOD - IG4
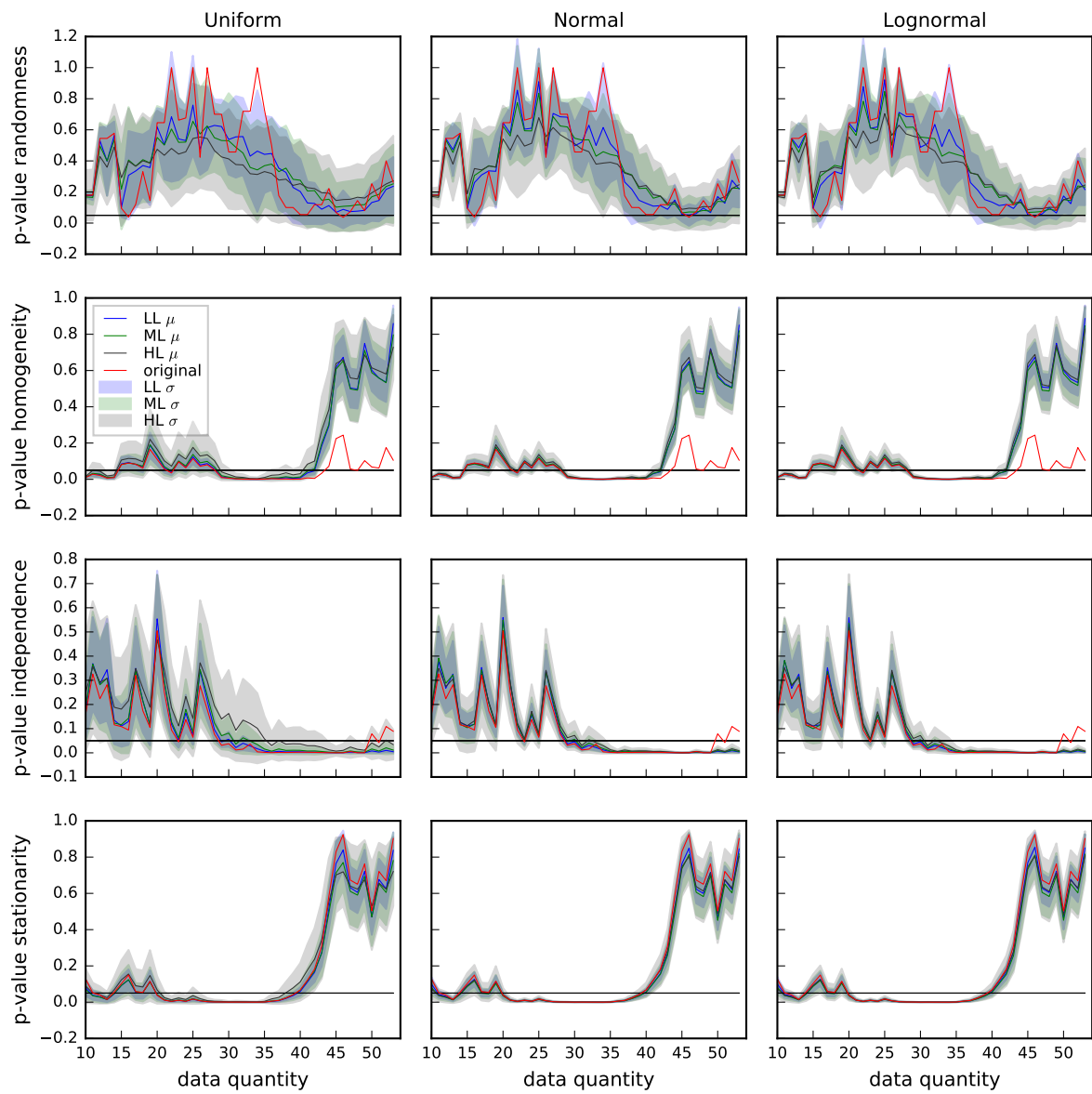
Figure 137 – Evolution of RHIS p-values from BOD concentration time series from IG4. Red line = p-value from OTS. Blue, green, gray lines = average p-value from STS in LL, ML and HL scenarios, respectively. Blue, green, gray bands = std of p-values from STS in LL, ML and HL scenarios, respectively. Black line = significance level ($\alpha = 0.05$). Reject H_0 if p-value < 0.05
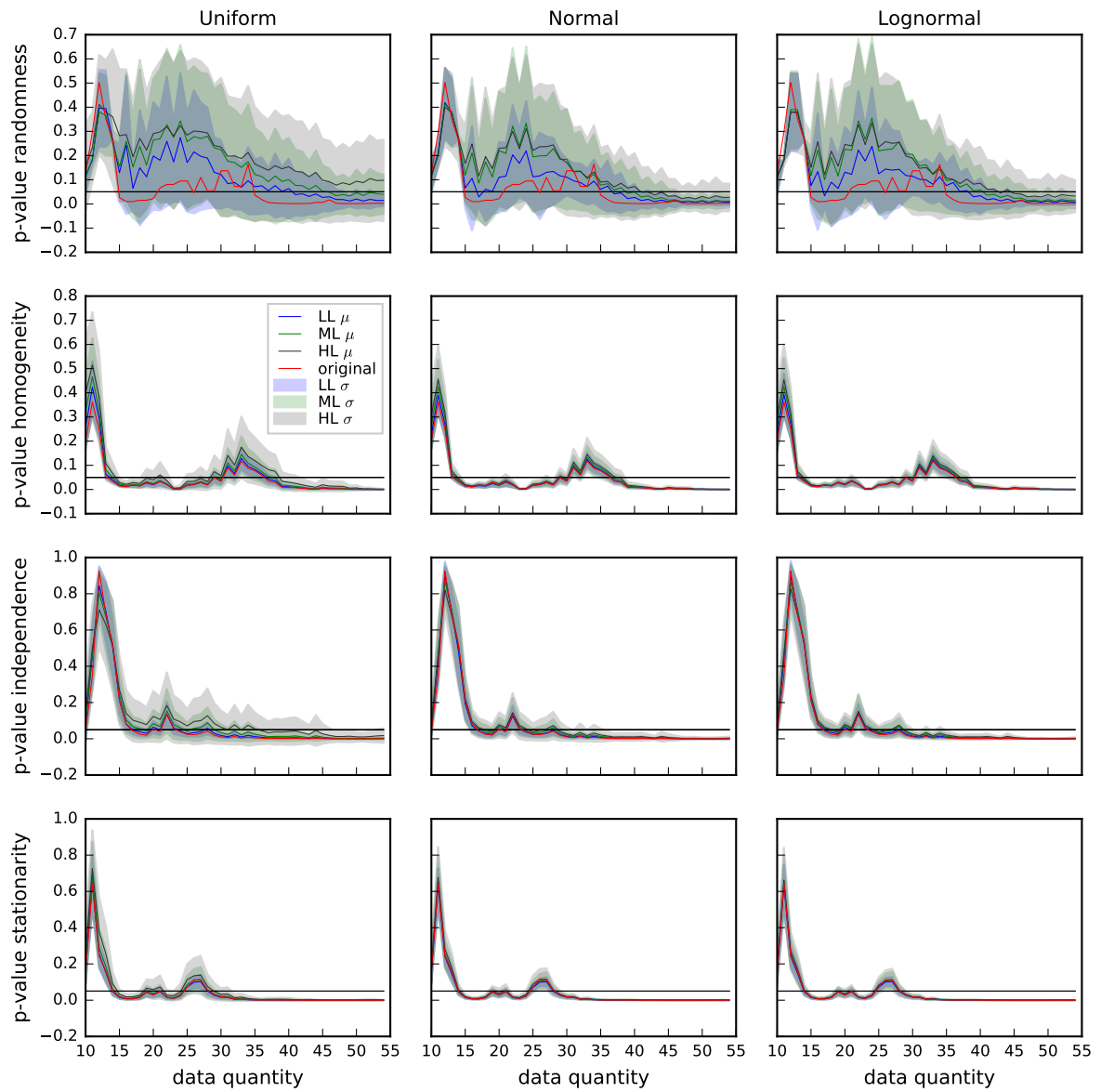
BOD - IG5
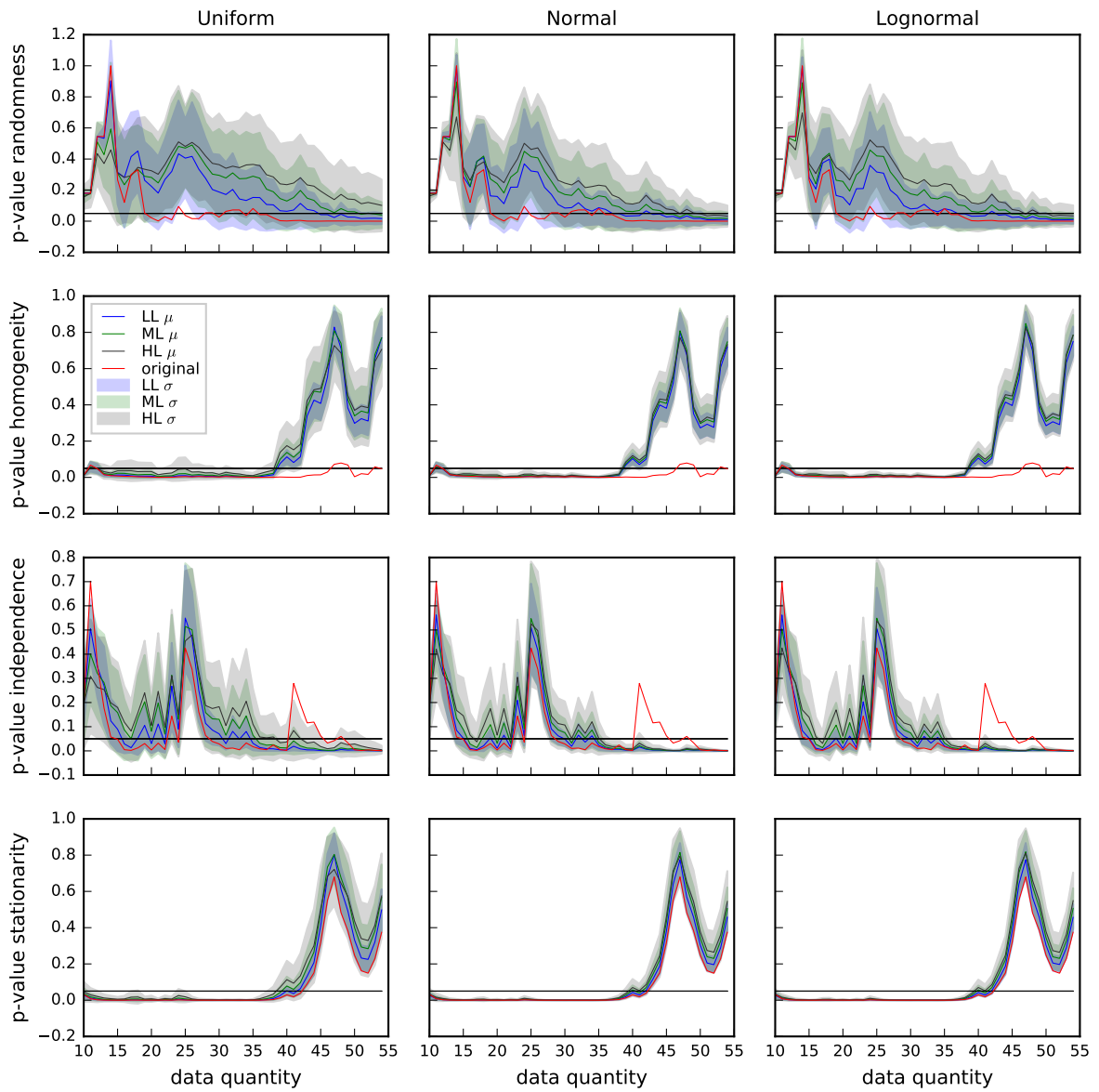
Figure 138 – Evolution of RHIS p-values from BOD concentration time series from IG5. Red line = p-value from OTS. Blue, green, gray lines = average p-value from STS in LL, ML and HL scenarios, respectively. Blue, green, gray bands = std of p-values from STS in LL, ML and HL scenarios, respectively. Black line = significance level (α = 0.05). Reject H_0 if p-value < 0.05
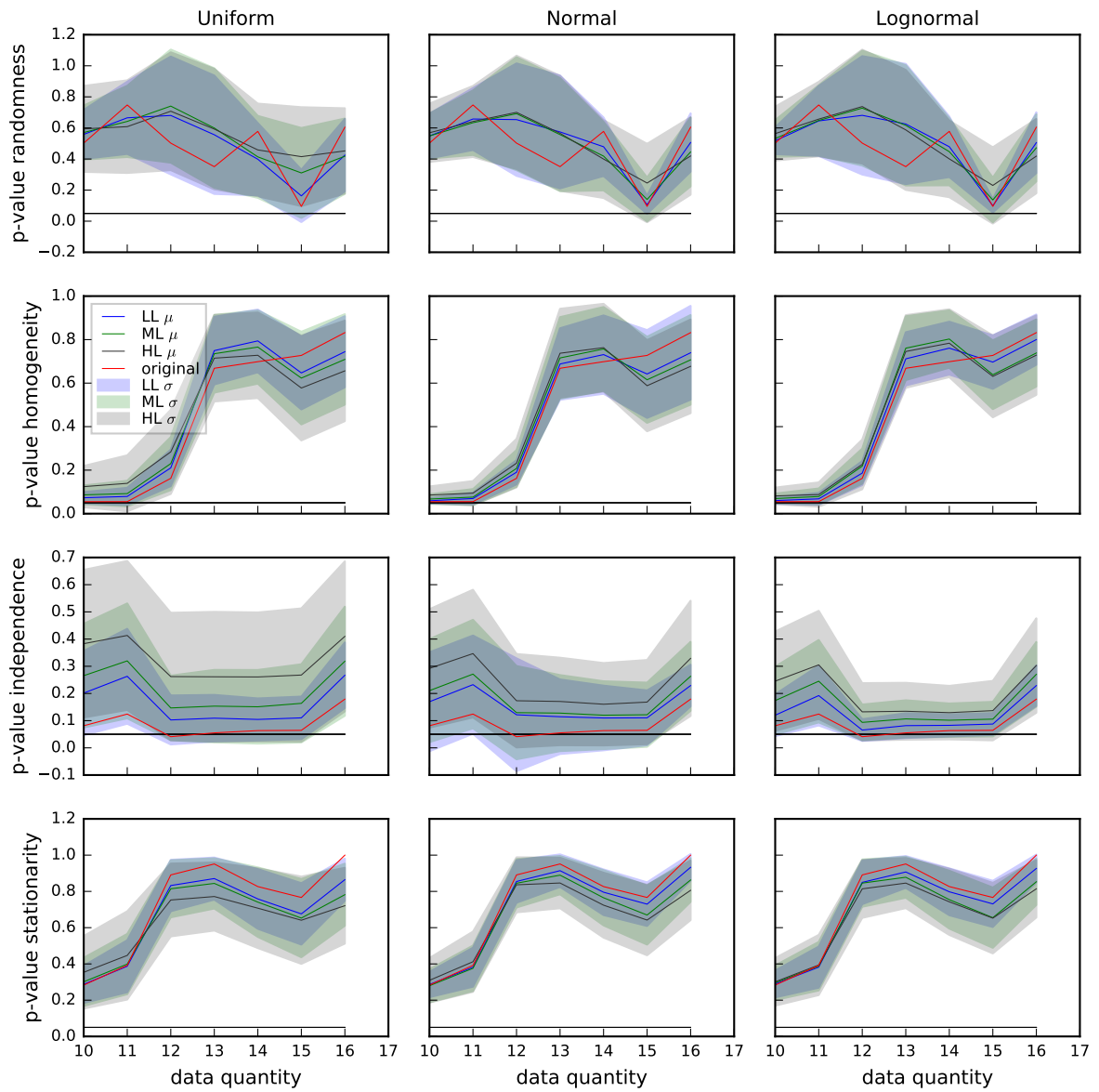
BOD - IG6
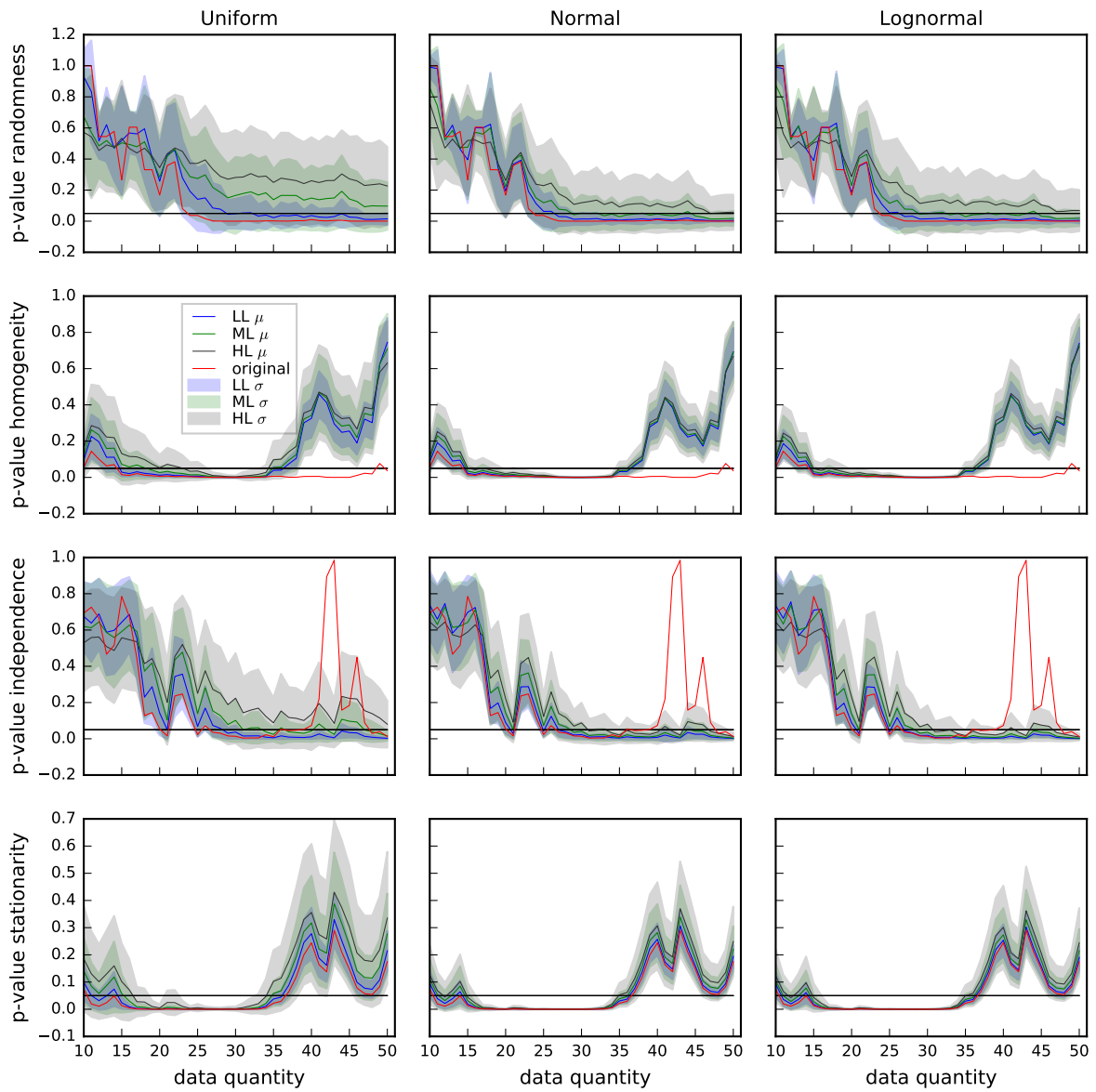
Figure 139 – Evolution of RHIS p-values from BOD concentration time series from IG6. Red line = p-value from OTS. Blue, green, gray lines = average p-value from STS in LL, ML and HL scenarios, respectively. Blue, green, gray bands = std of p-values from STS in LL, ML and HL scenarios, respectively. Black line = significance level (α = 0.05). Reject H_0 if p-value < 0.05
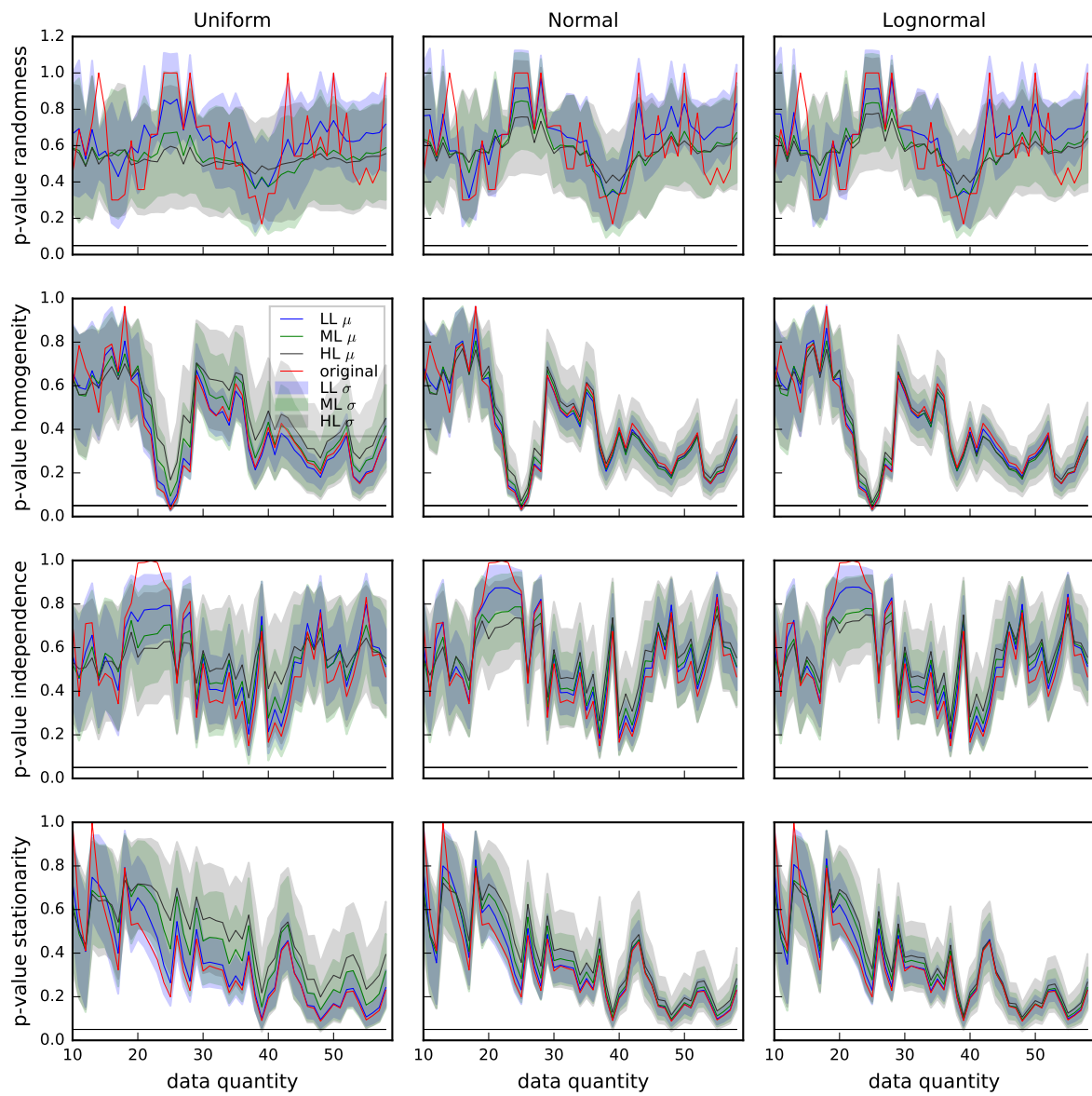
BOD - IG7
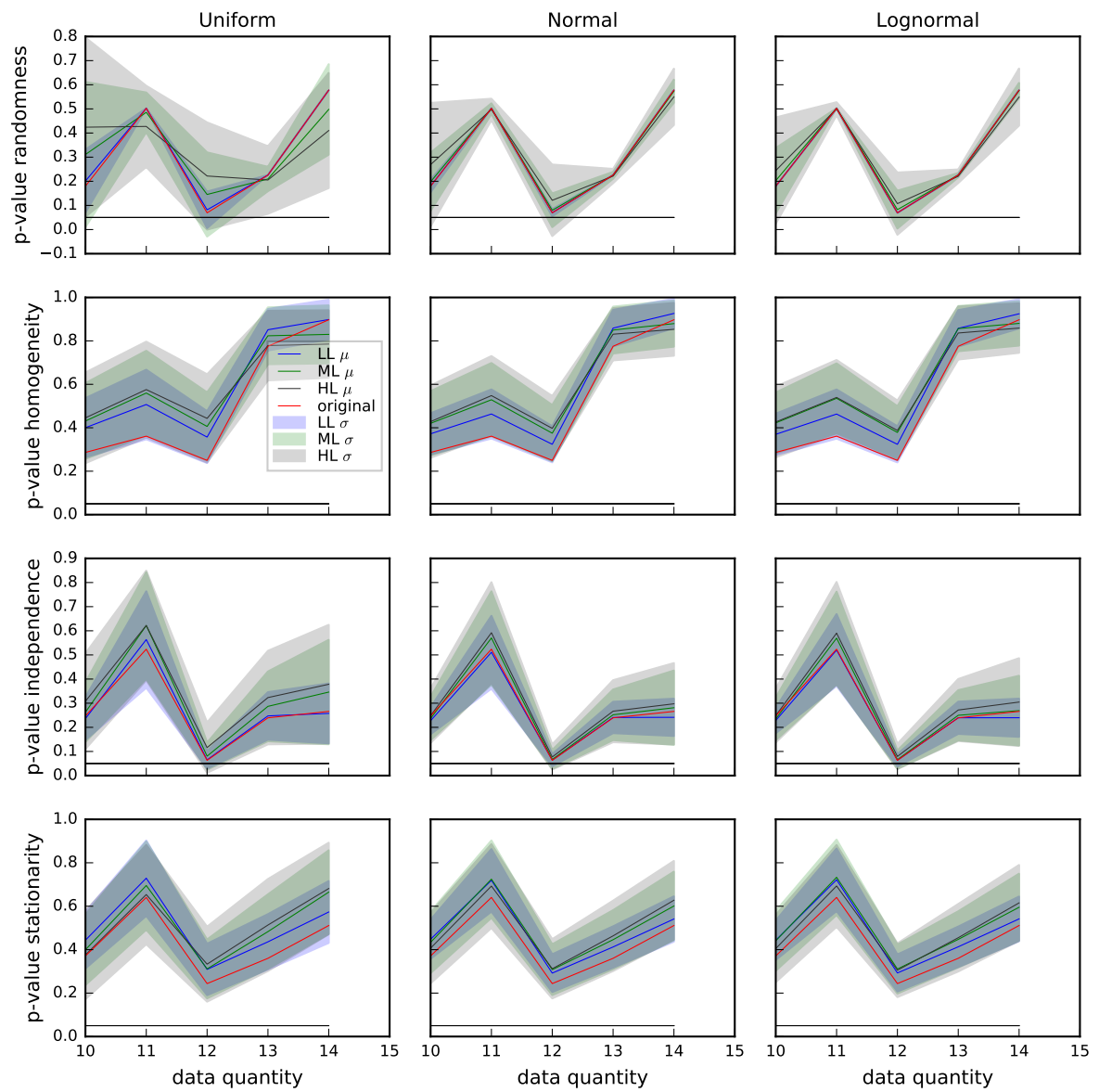
Figure 140 – Evolution of RHIS p-values from BOD concentration time series from IG7. Red line = p-value from OTS. Blue, green, gray lines = average p-value from STS in LL, ML and HL scenarios, respectively. Blue, green, gray bands = std of p-values from STS in LL, ML and HL scenarios, respectively. Black line = significance level ($\alpha = 0.05$). Reject H_0 if p-value < 0.05
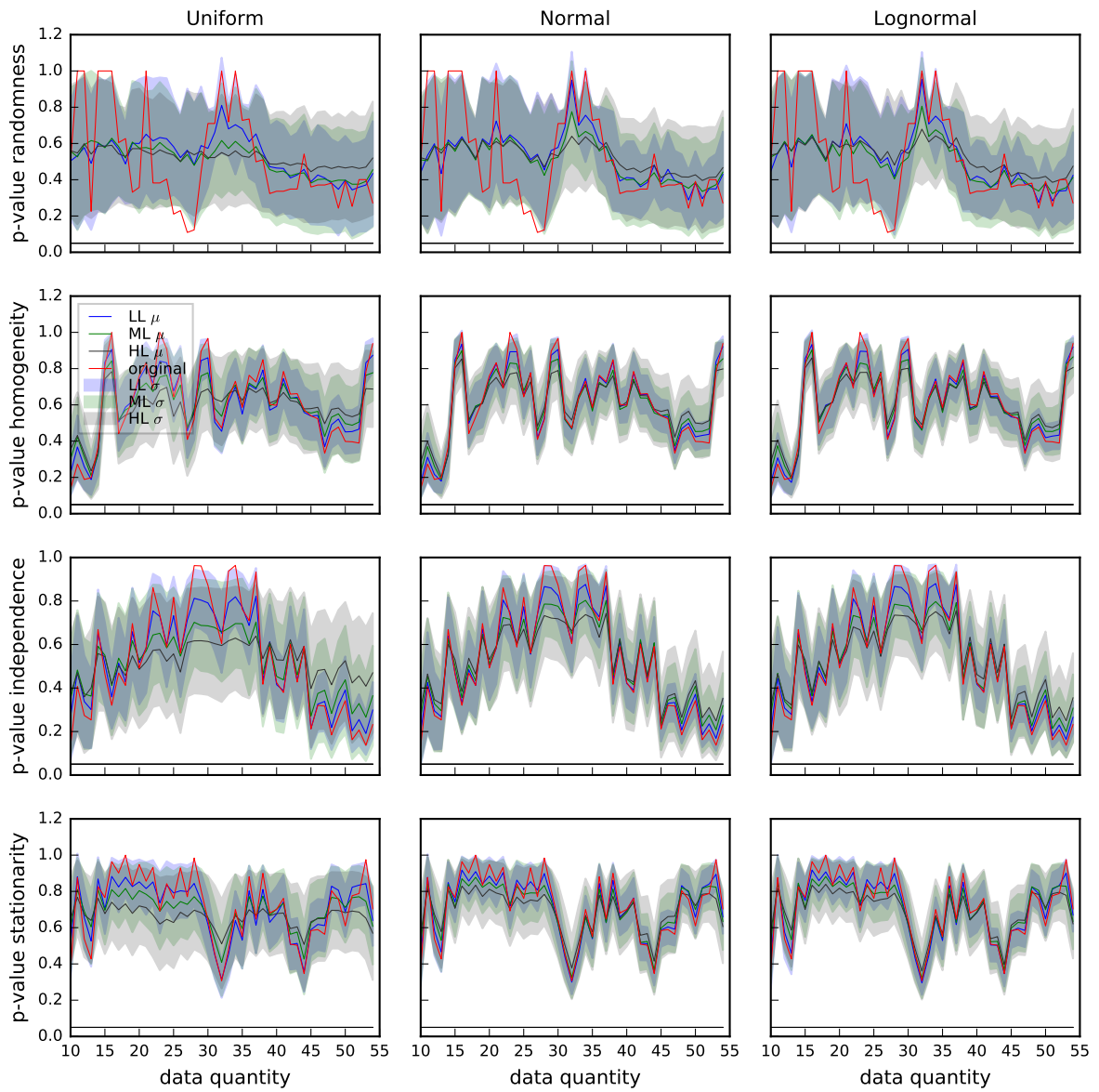
DO - IG3
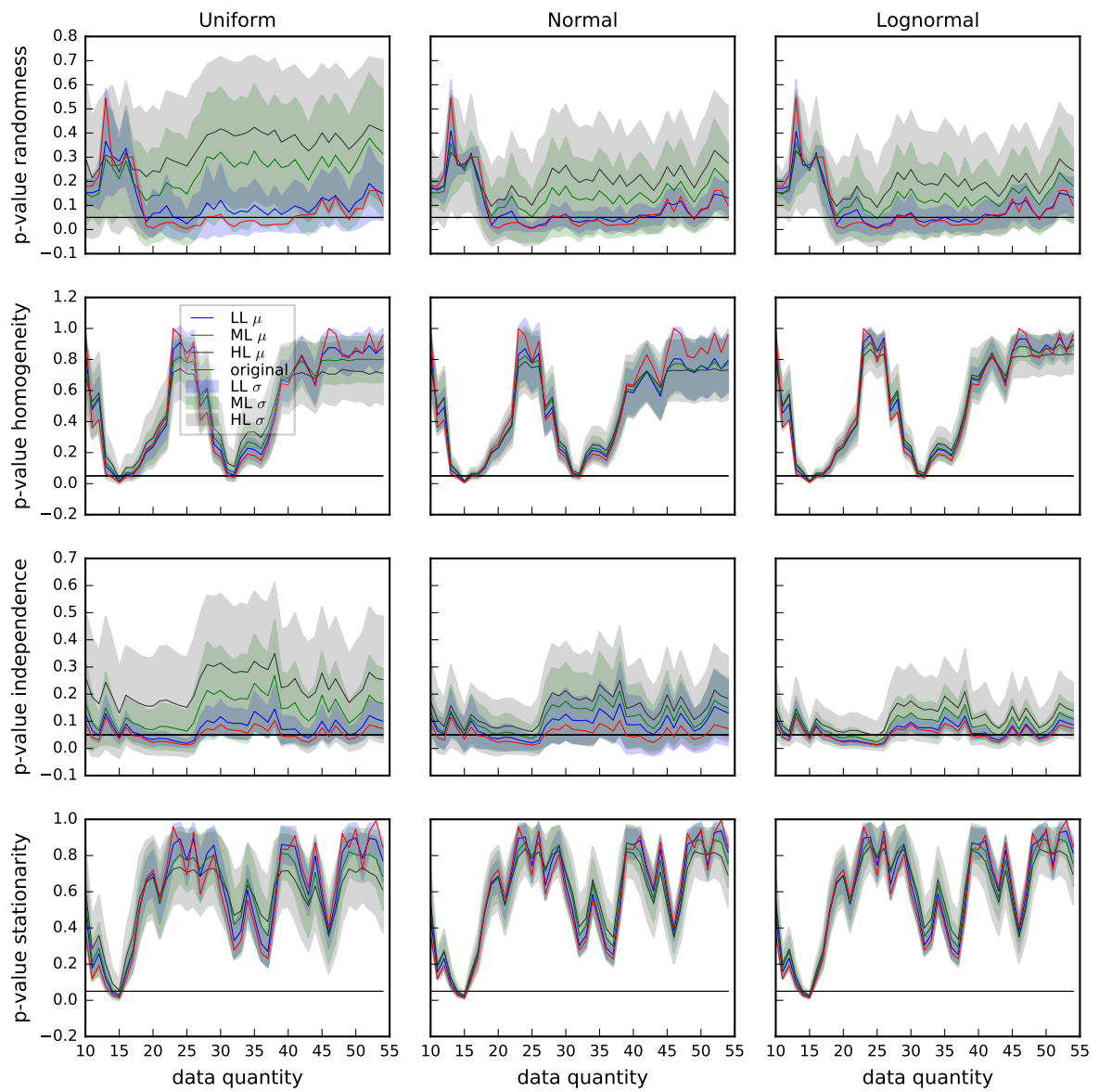
Figure 141 – Evolution of RHIS p-values from DO concentration time series from IG3. Red line = p-value from OTS. Blue, green, gray lines = average p-value from STS in LL, ML and HL scenarios, respectively. Blue, green, gray bands = std of p-values from STS in LL, ML and HL scenarios, respectively. Black line = significance level ($\alpha = 0.05$). Reject H_0 if p-value < 0.05
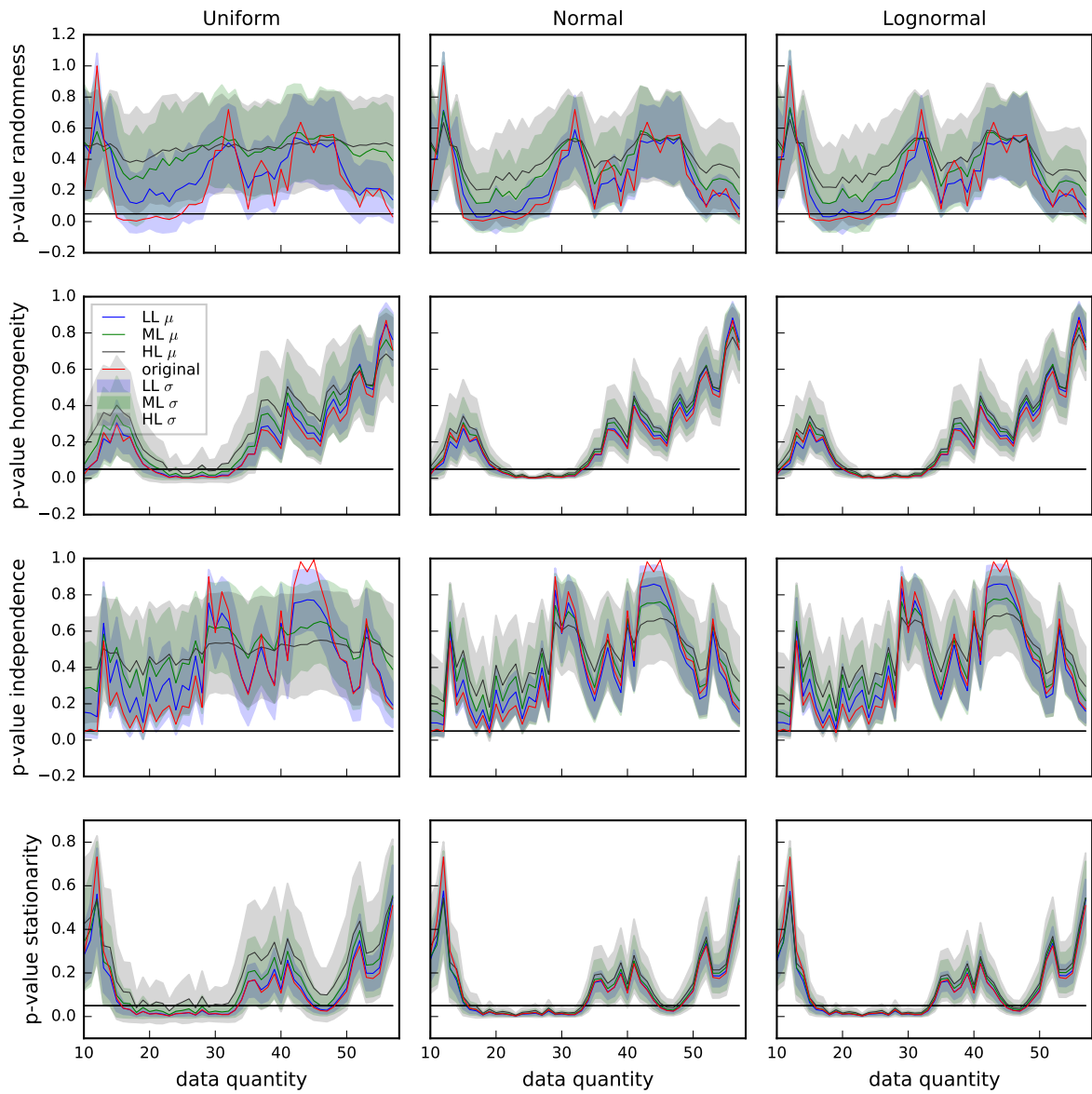
DO - IG4
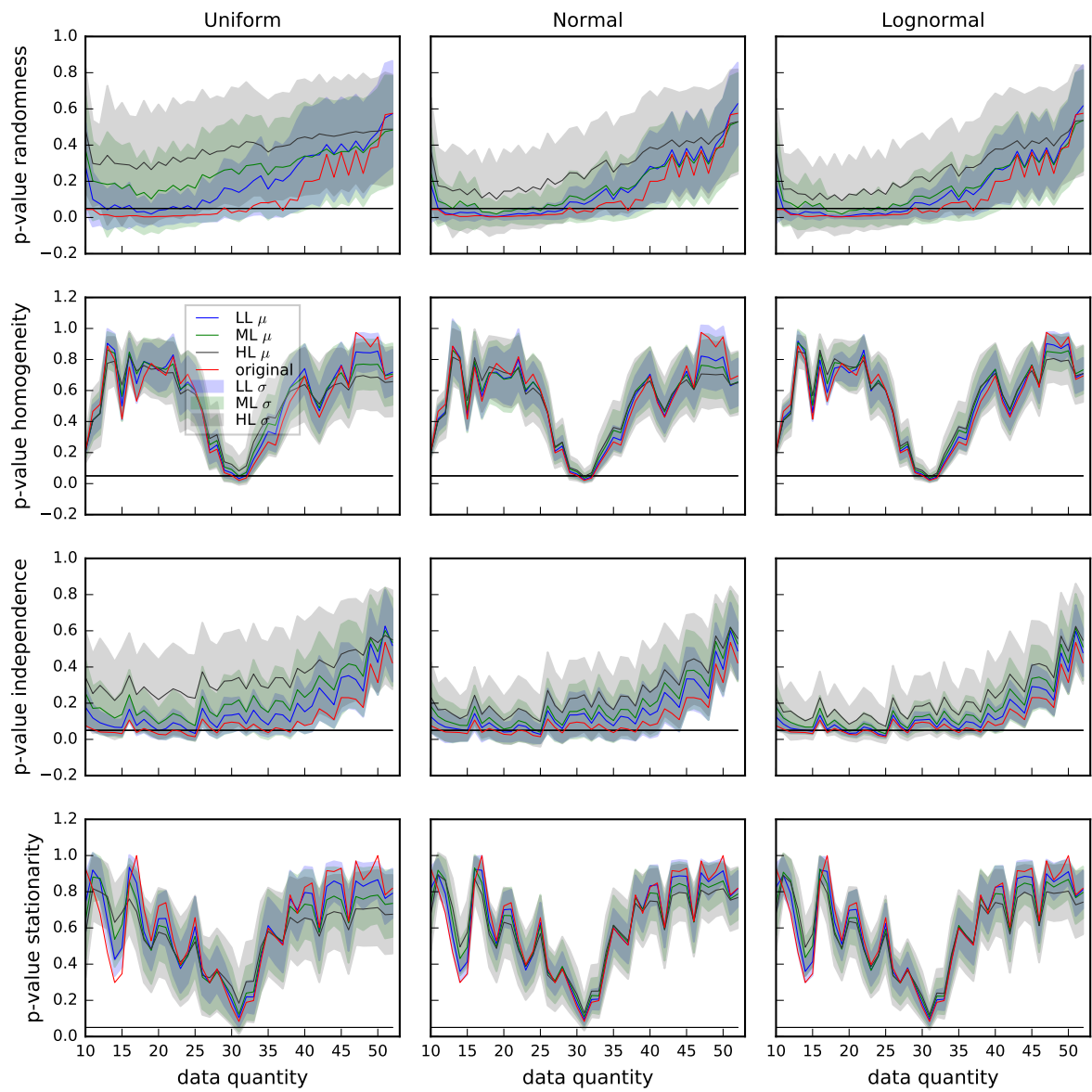
Figure 142 – Evolution of RHIS p-values from DO concentration time series from IG4. Red line = p-value from OTS. Blue, green, gray lines = average p-value from STS in LL, ML and HL scenarios, respectively. Blue, green, gray bands = std of p-values from STS in LL, ML and HL scenarios, respectively. Black line = significance level ($\alpha = 0.05$). Reject H_0 if p-value < 0.05

DO - IG5
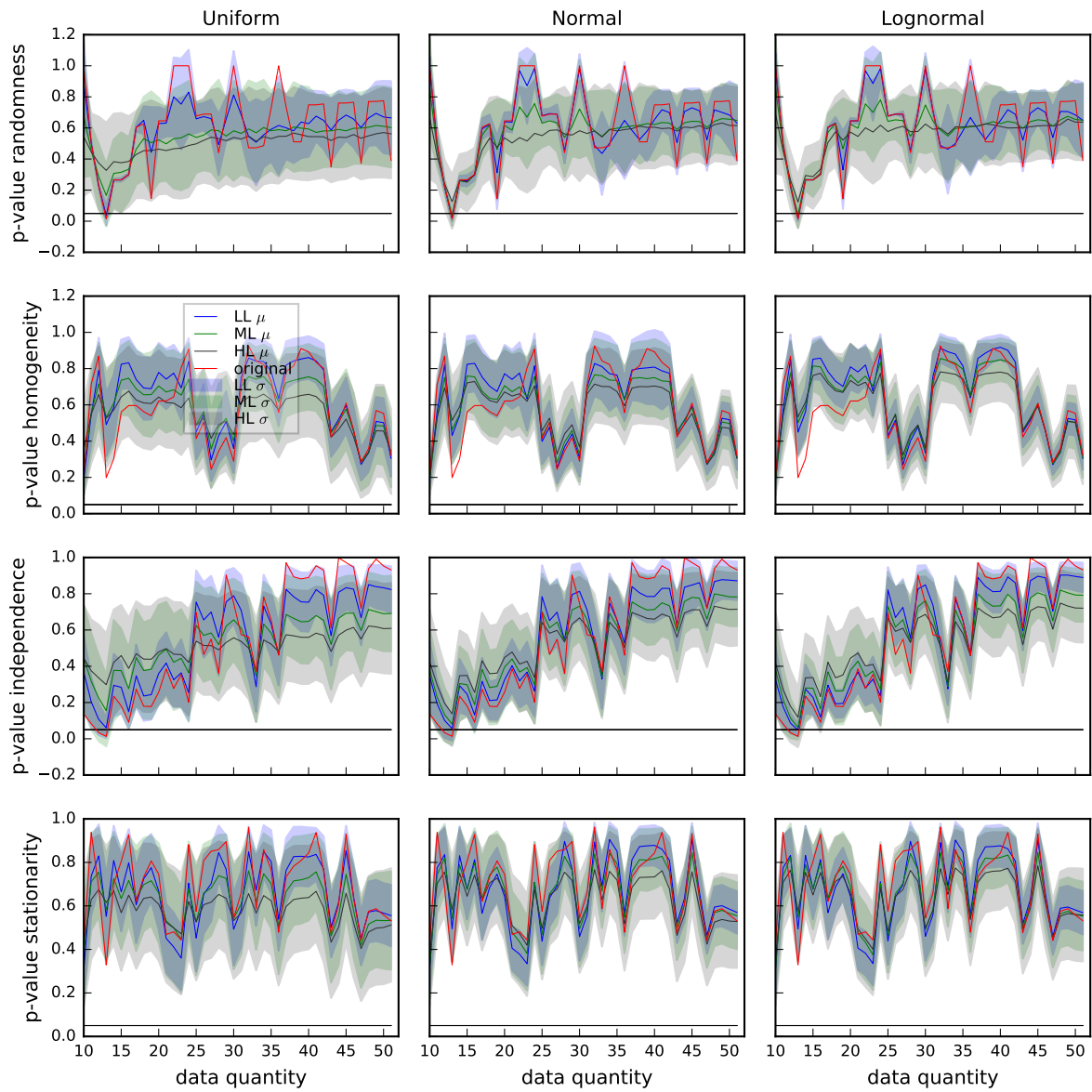
Figure 143 – Evolution of RHIS p-values from DO concentration time series from IG5. Red line = p-value from OTS. Blue, green, gray lines = average p-value from STS in LL, ML and HL scenarios, respectively. Blue, green, gray bands = std of p-values from STS in LL, ML and HL scenarios, respectively. Black line = significance level ($\alpha = 0.05$). Reject H_0 if p-value < 0.05

DO - IG6
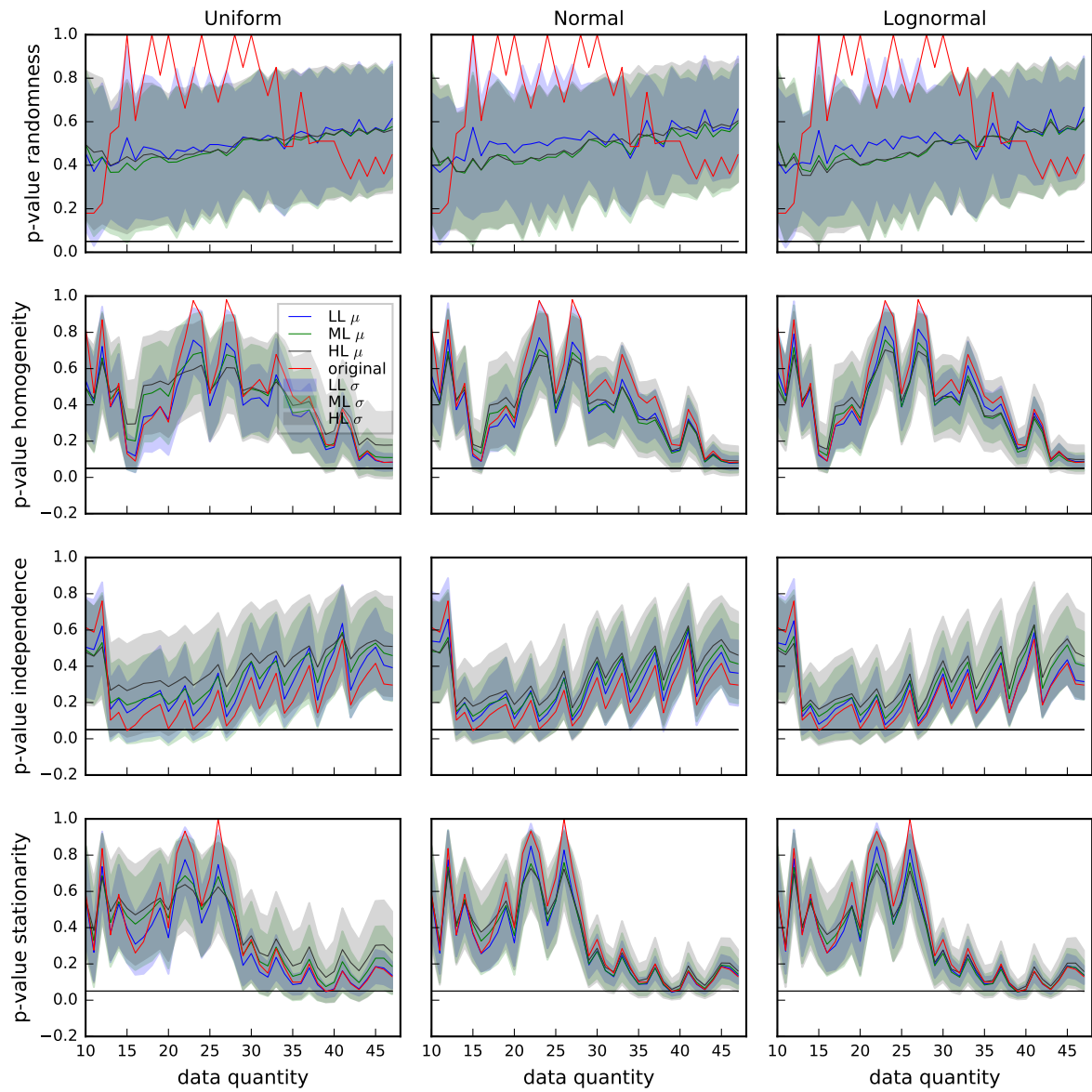
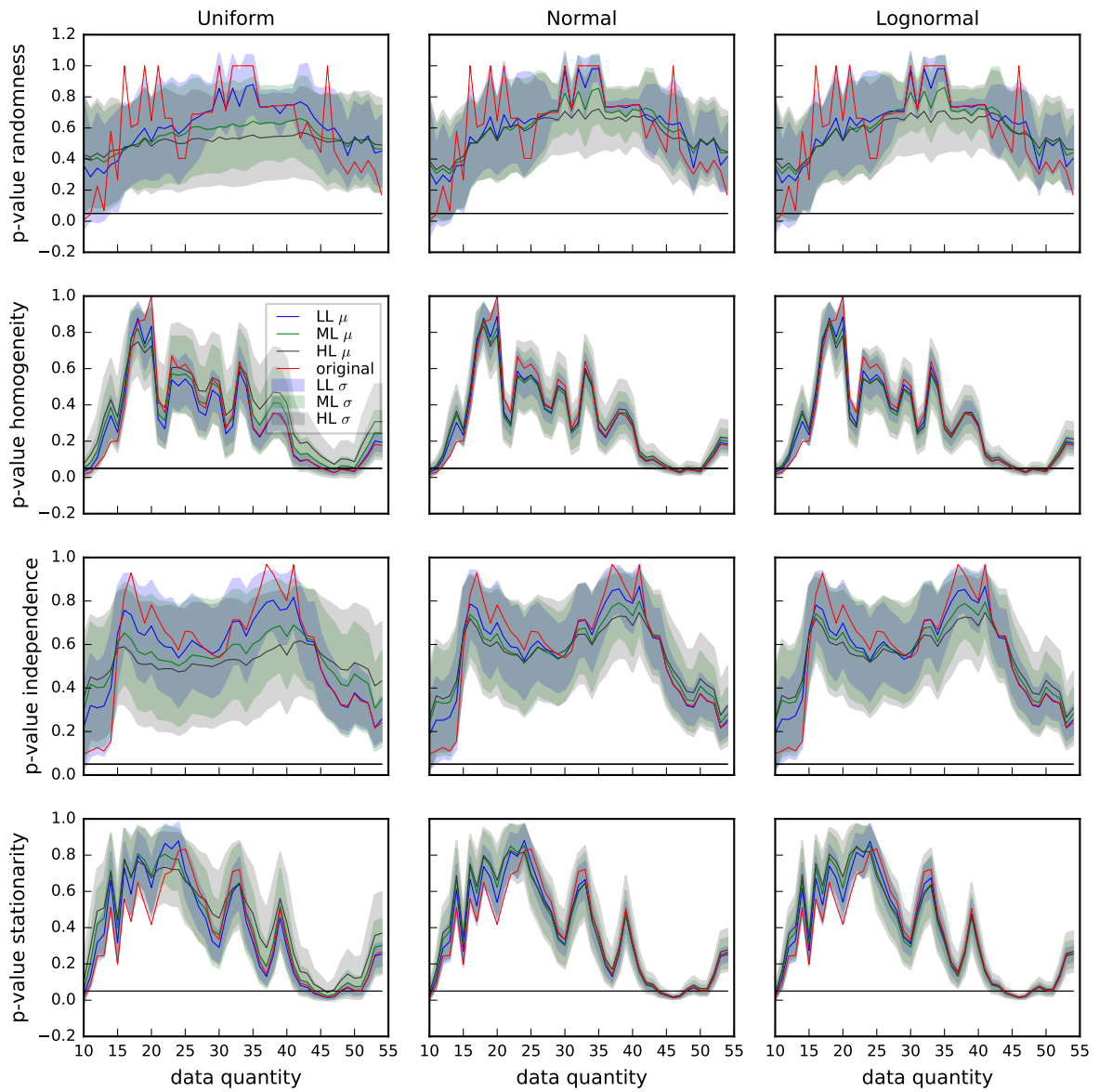Figure 144 – Evolution of RHIS p-values from DO concentration time series from IG6. Red line = p-value from OTS. Blue, green, gray lines = average p-value from STS in LL, ML and HL scenarios, respectively. Blue, green, gray bands = std of p-values from STS in LL, ML and HL scenarios, respectively. Black line = significance level (α = 0.05). Reject H_0 if p-value < 0.05

DO - IG7
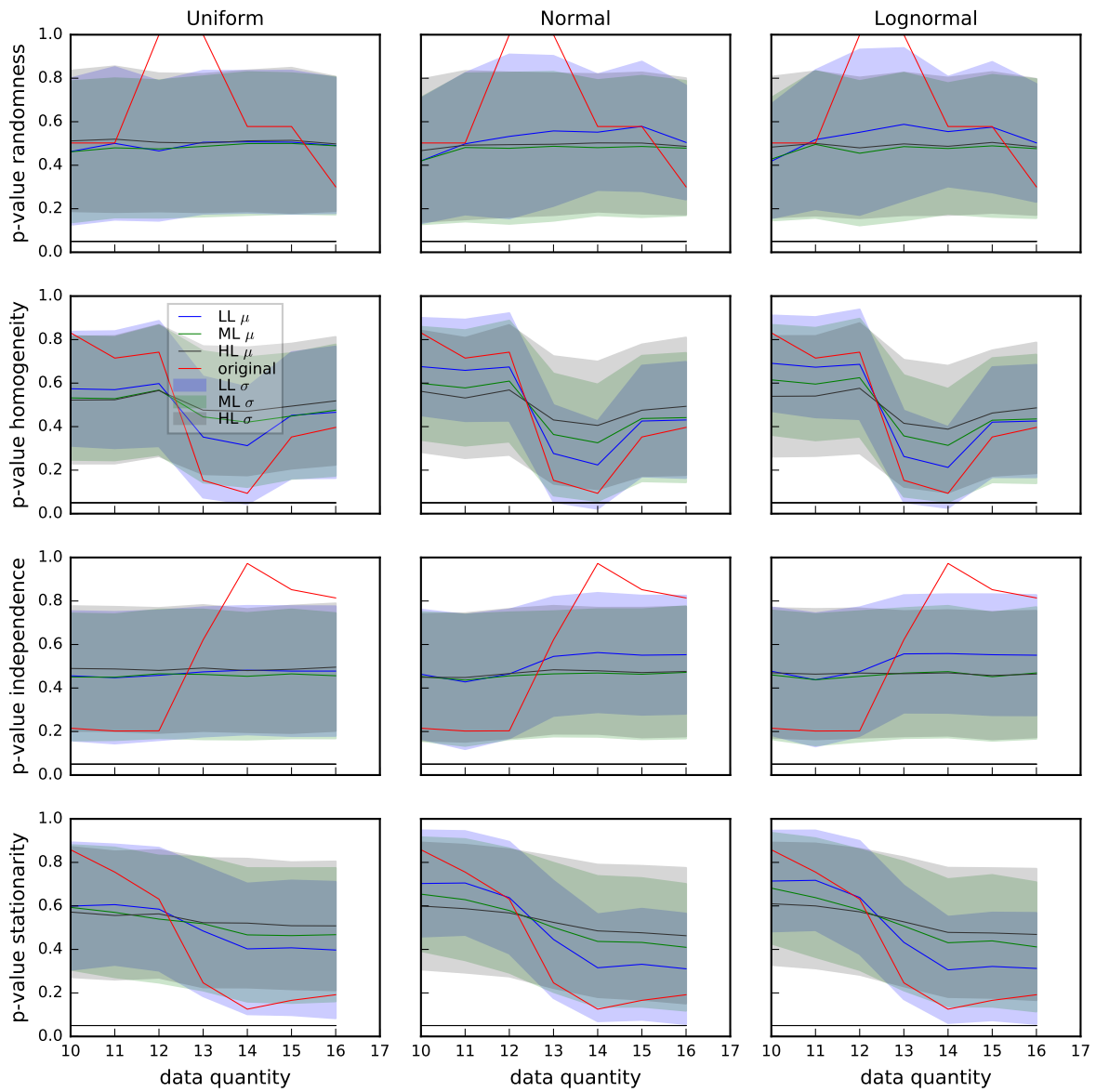
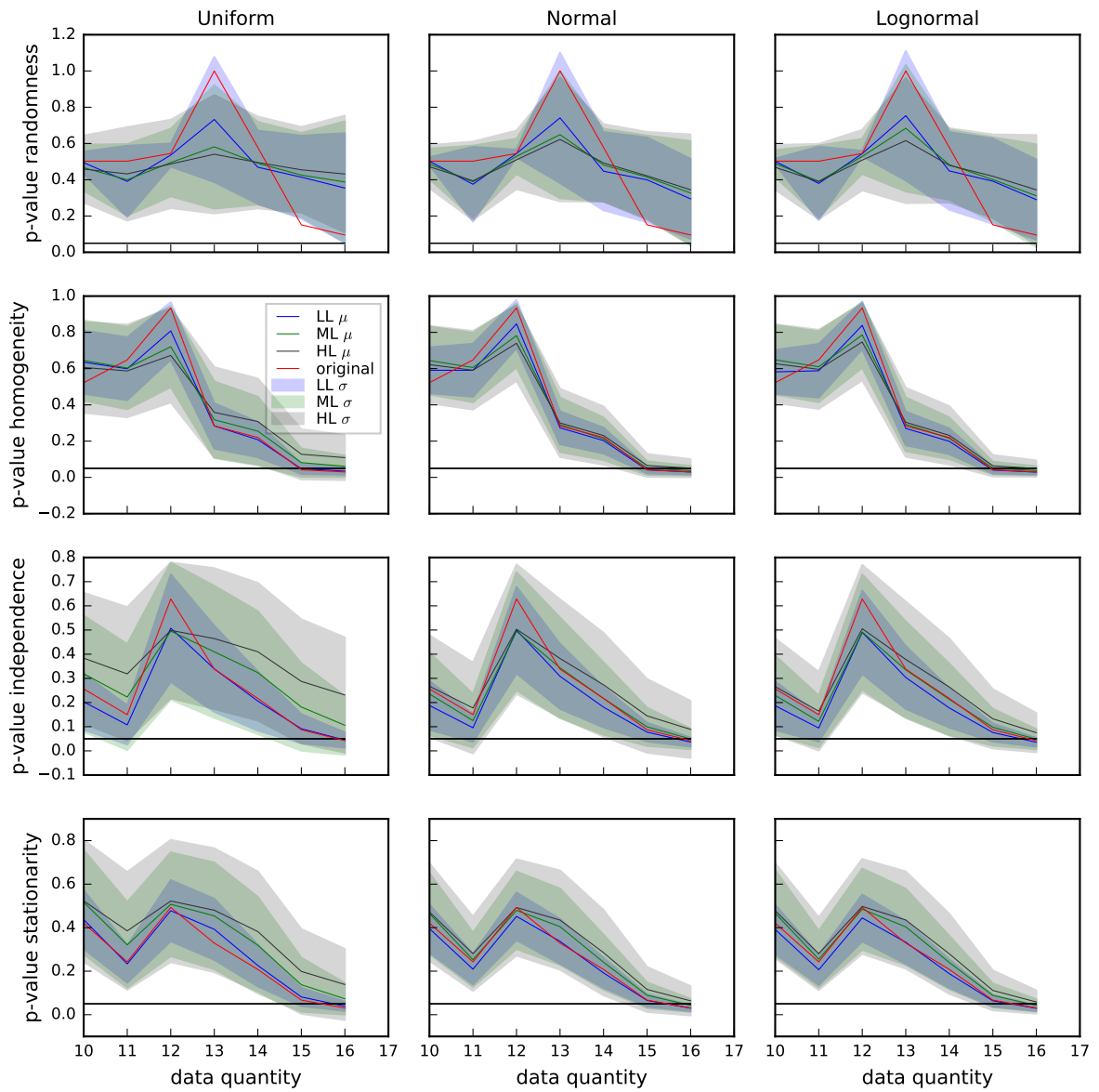Figure 145 – Evolution of RHIS p-values from DO concentration time series from IG7. Red line = p-value from OTS. Blue, green, gray lines = average p-value from STS in LL, ML and HL scenarios, respectively. Blue, green, gray bands = std of p-values from STS in LL, ML and HL scenarios, respectively. Black line = significance level ($\alpha = 0.05$). Reject H_0 if p-value < 0.05
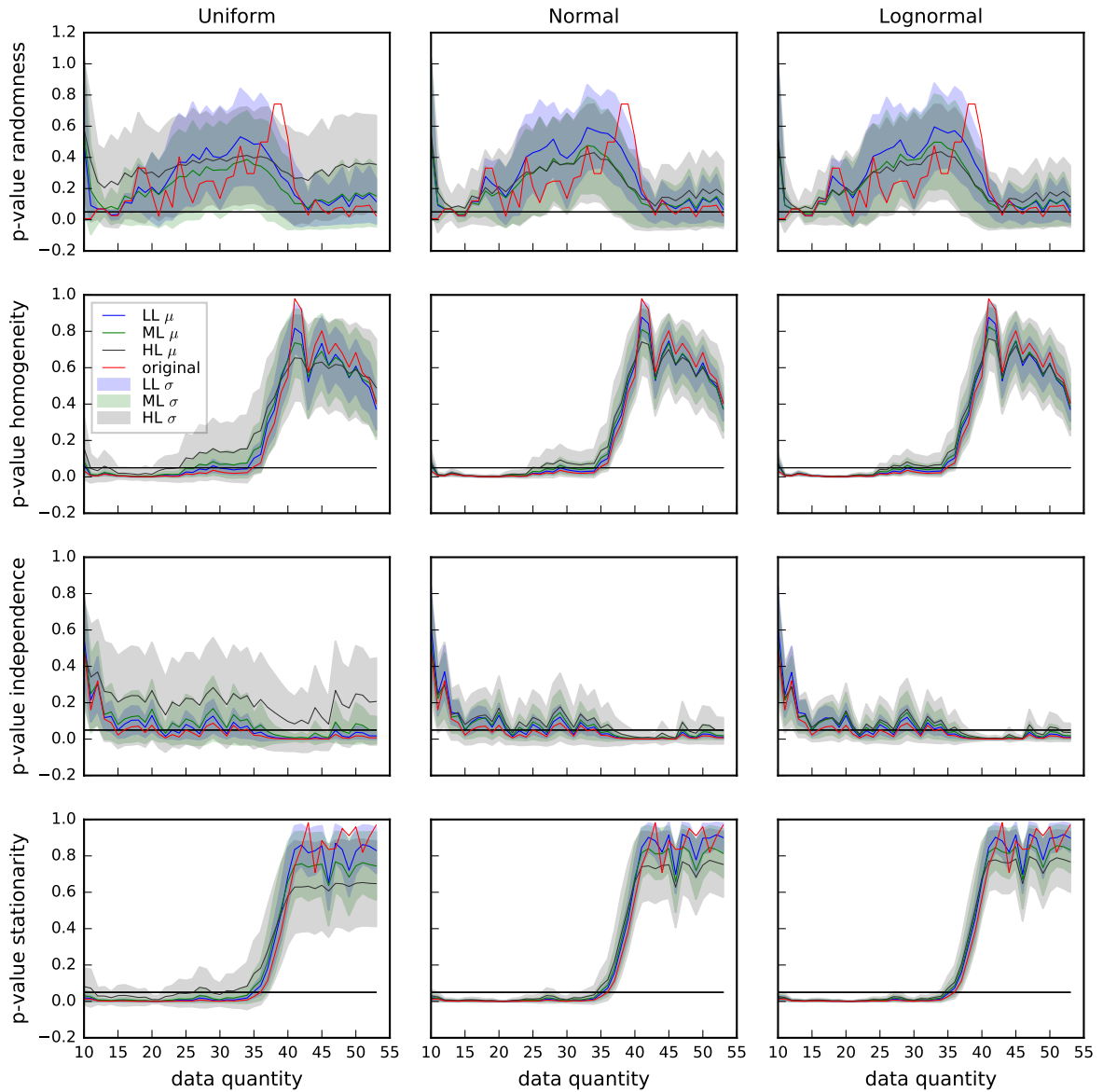
DOC - IG3
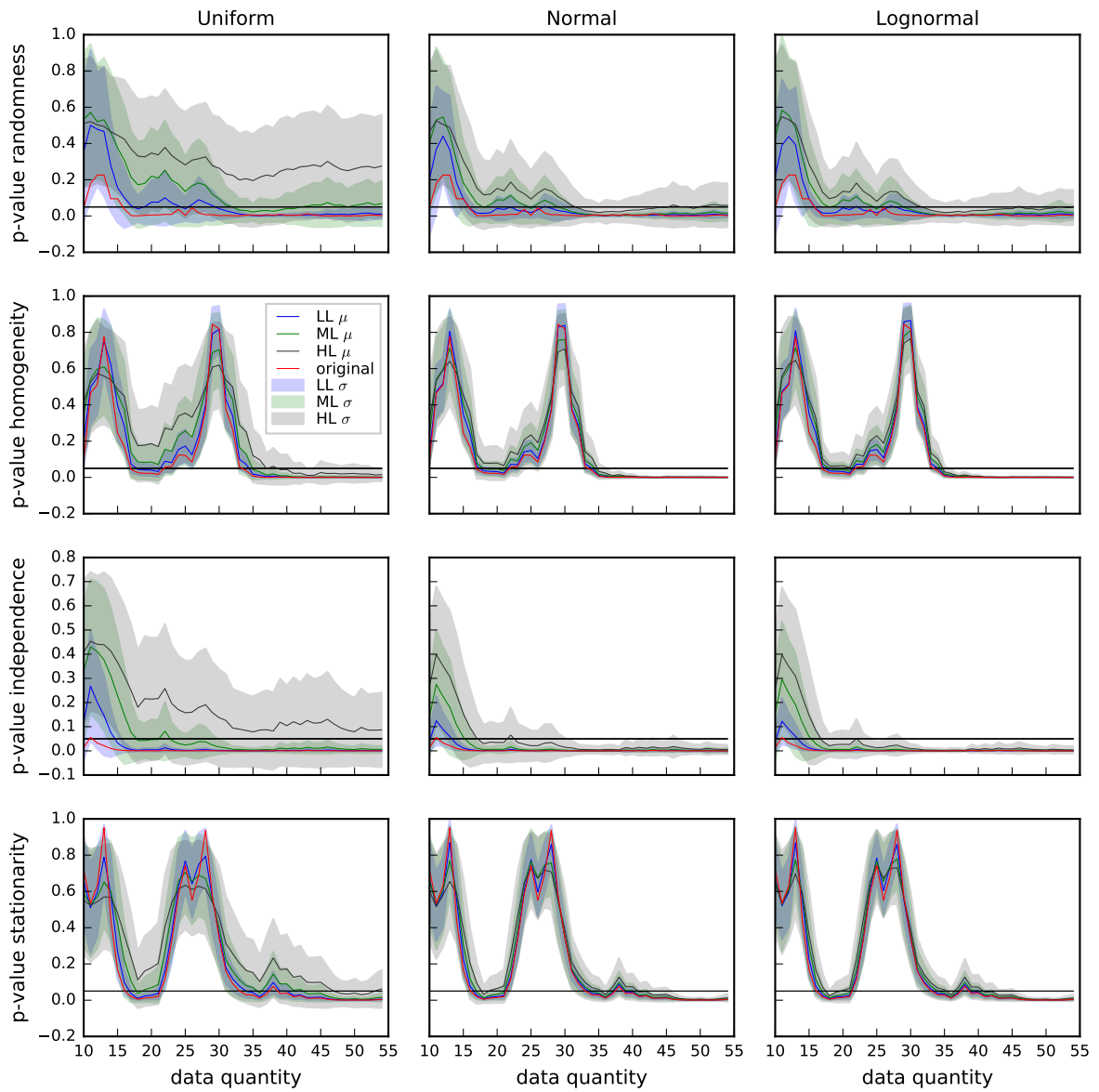
Figure 146 – Evolution of RHIS p-values from DOC concentration time series from IG3. Red line = p-value from OTS. Blue, green, gray lines = average p-value from STS in LL, ML and HL scenarios, respectively. Blue, green, gray bands = std of p-values from STS in LL, ML and HL scenarios, respectively. Black line = significance level ($\alpha = 0.05$). Reject H_0 if p-value < 0.05

DOC - IG4
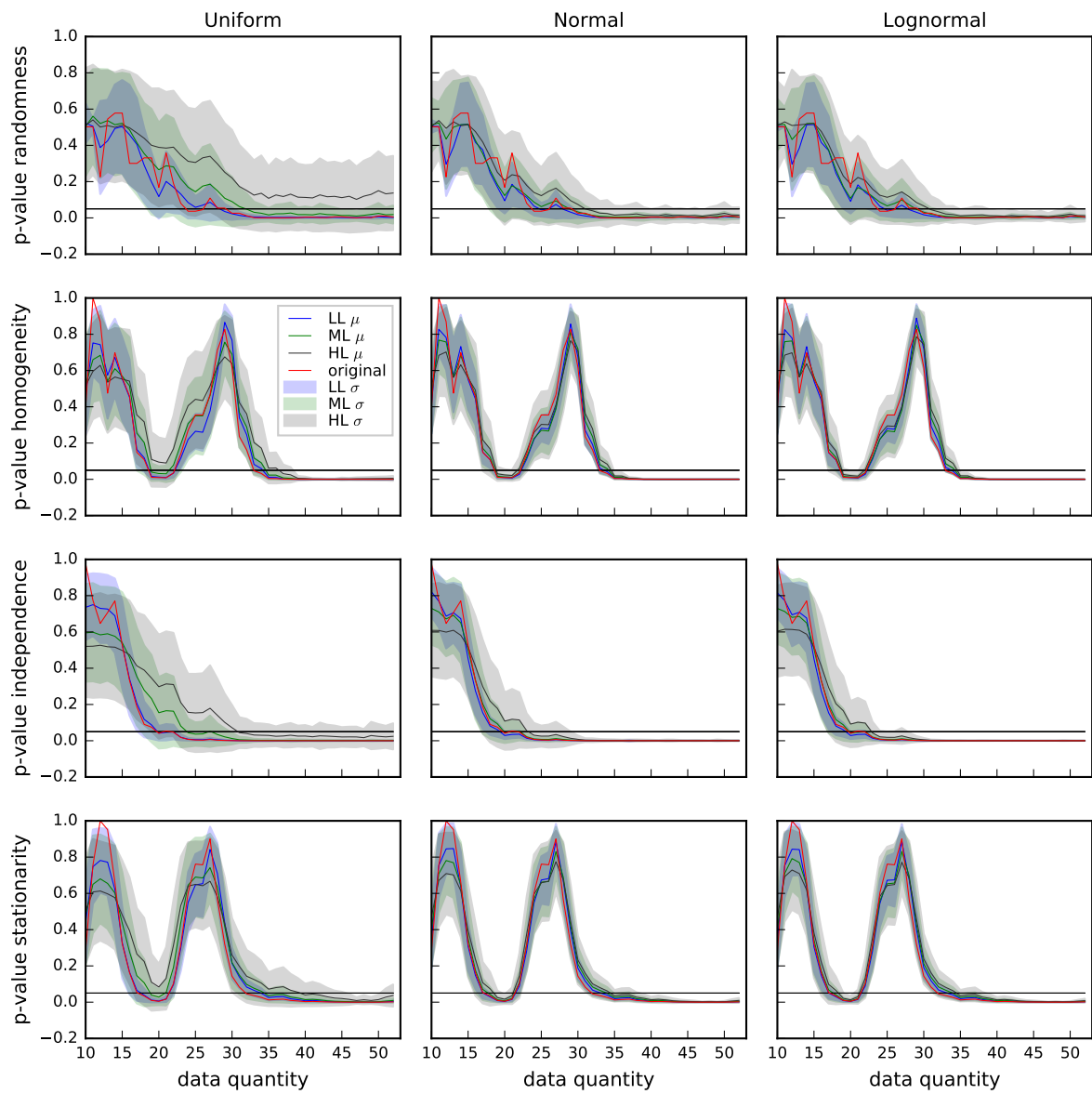
Figure 147 – Evolution of RHIS p-values from DOC concentration time series from IG4. Red line = p-value from OTS. Blue, green, gray lines = average p-value from STS in LL, ML and HL scenarios, respectively. Blue, green, gray bands = std of p-values from STS in LL, ML and HL scenarios, respectively. Black line = significance level ($\alpha = 0.05$). Reject H_0 if p-value < 0.05
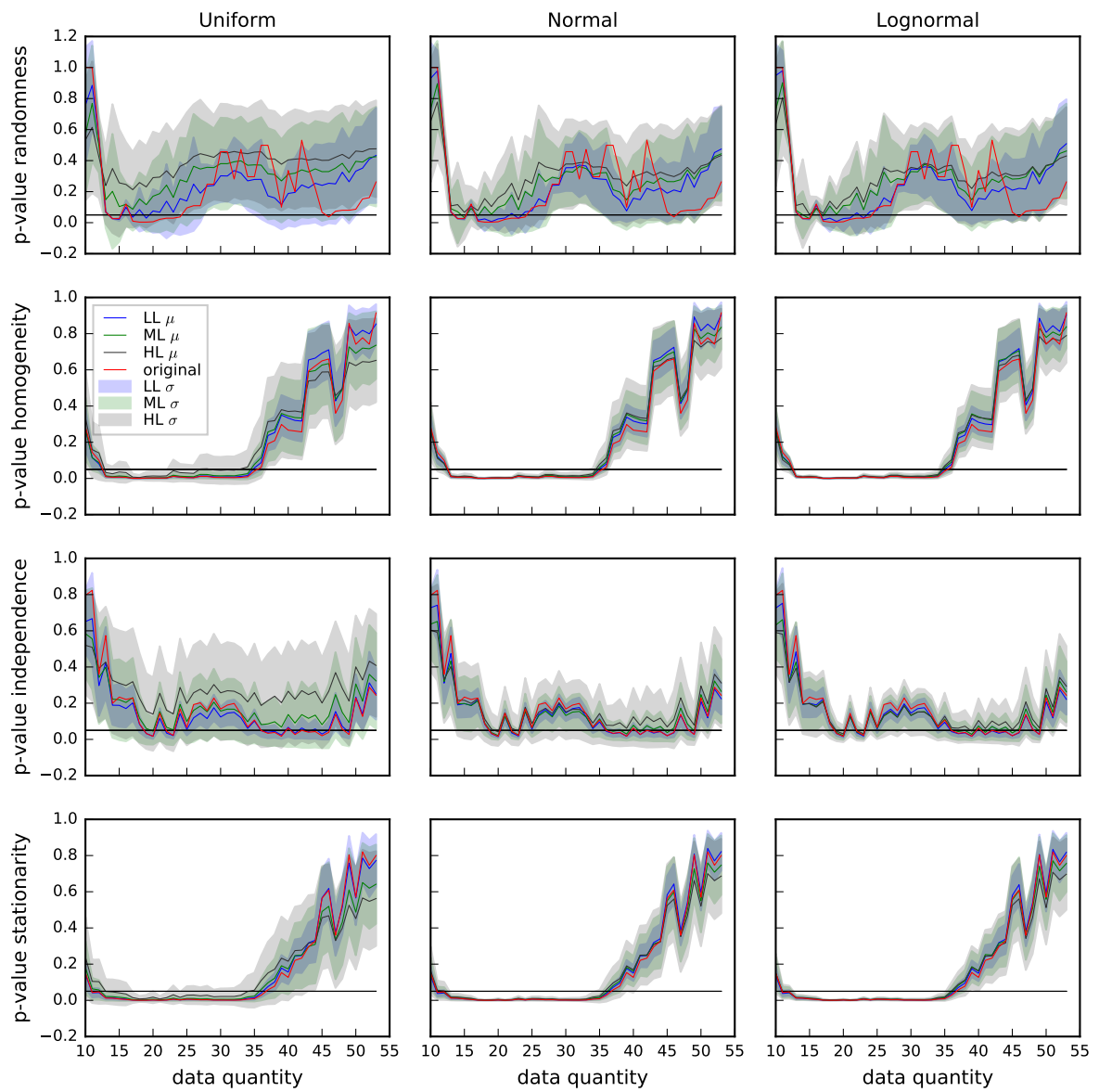
DOC - IG5
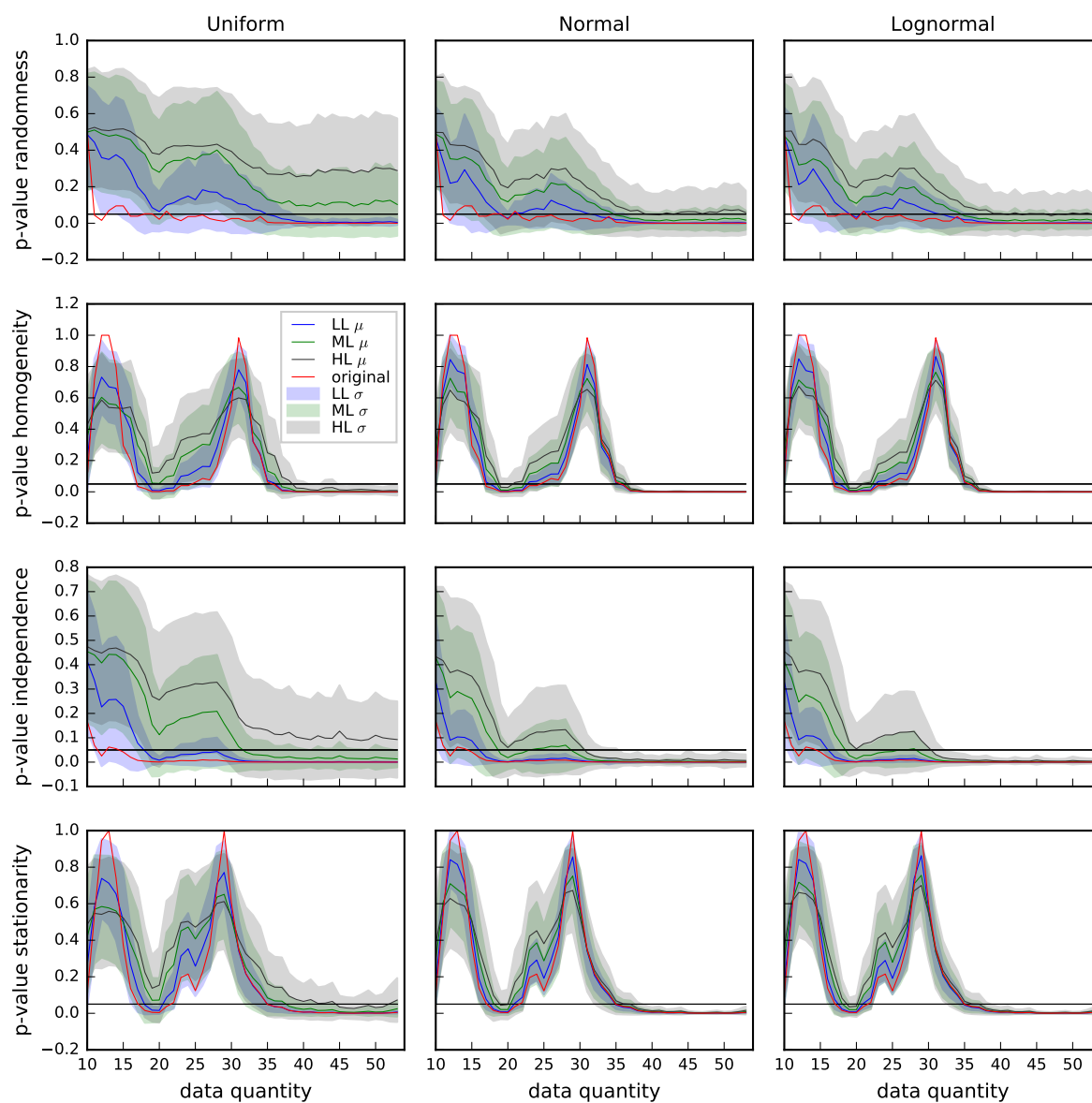
Figure 148 – Evolution of RHIS p-values from DOC concentration time series from IG5. Red line = p-value from OTS. Blue, green, gray lines = average p-value from STS in LL, ML and HL scenarios, respectively. Blue, green, gray bands = std of p-values from STS in LL, ML and HL scenarios, respectively. Black line = significance level ($\alpha = 0.05$). Reject H_0 if p-value < 0.05
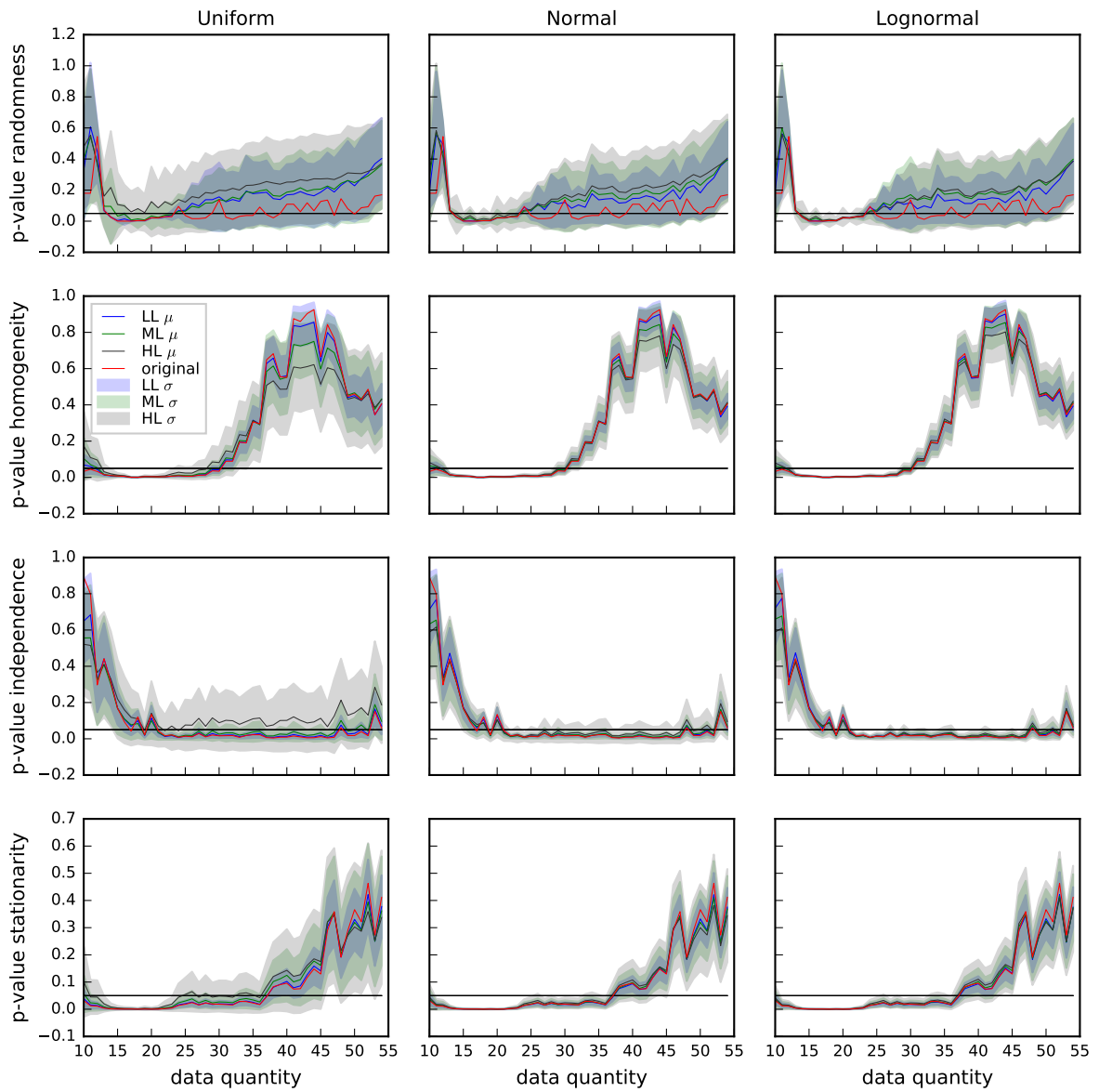
DOC - IG6
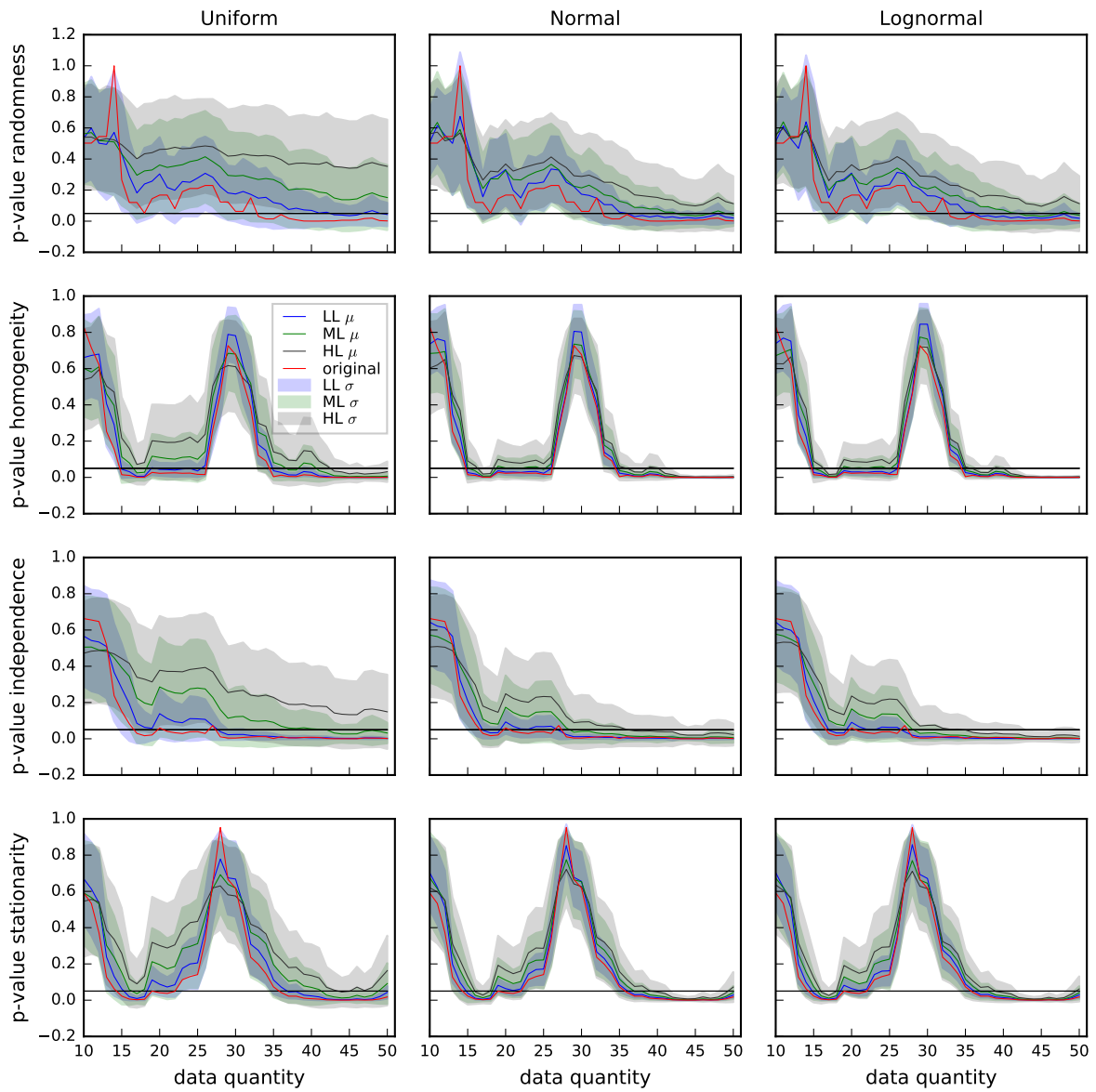
Figure 149 – Evolution of RHIS p-values from DOC concentration time series from IG6. Red line = p-value from OTS. Blue, green, gray lines = average p-value from STS in LL, ML and HL scenarios, respectively. Blue, green, gray bands = std of p-values from STS in LL, ML and HL scenarios, respectively. Black line = significance level ($\alpha = 0.05$). Reject H_0 if p-value < 0.05
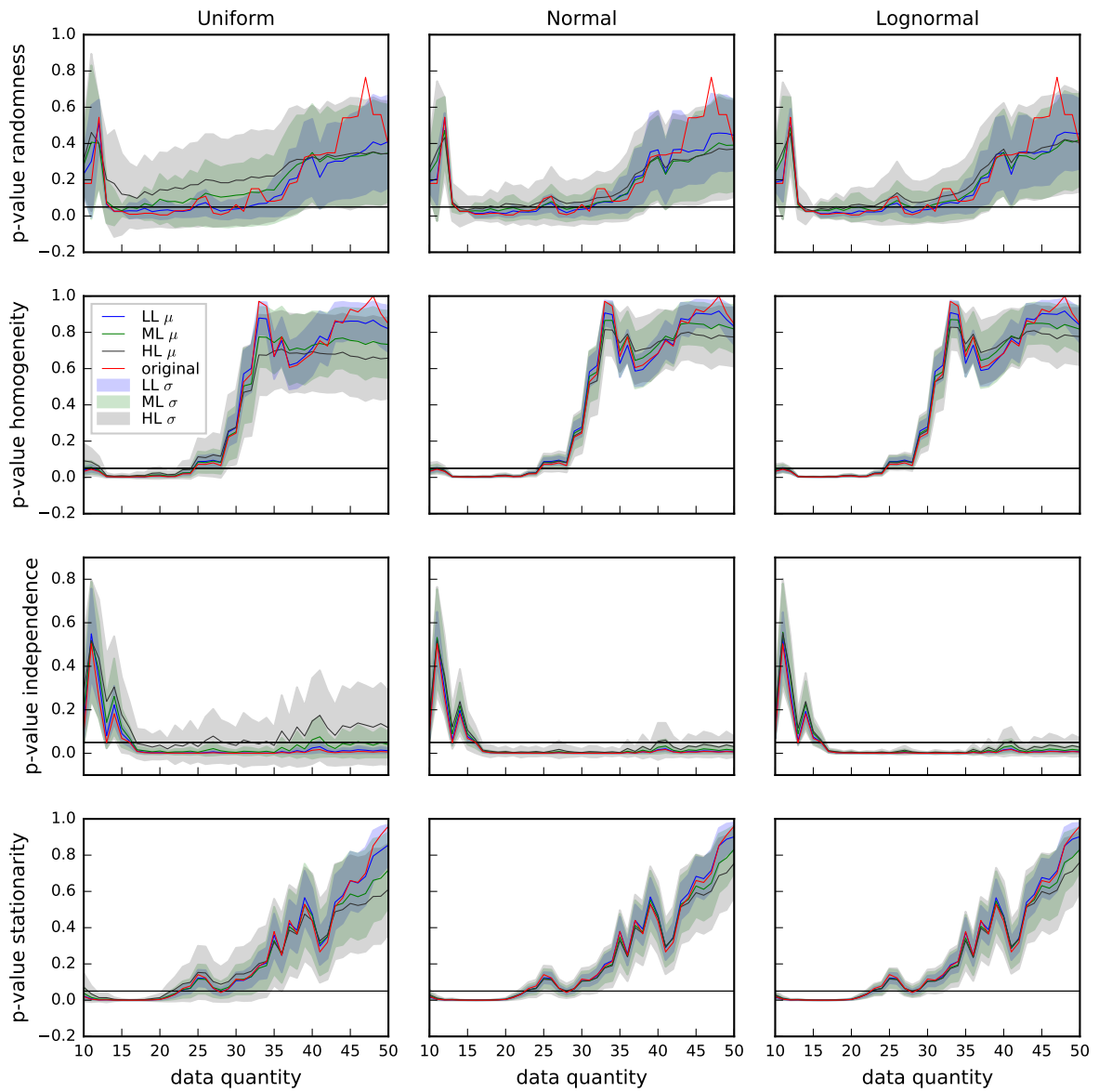
DOC - IG7
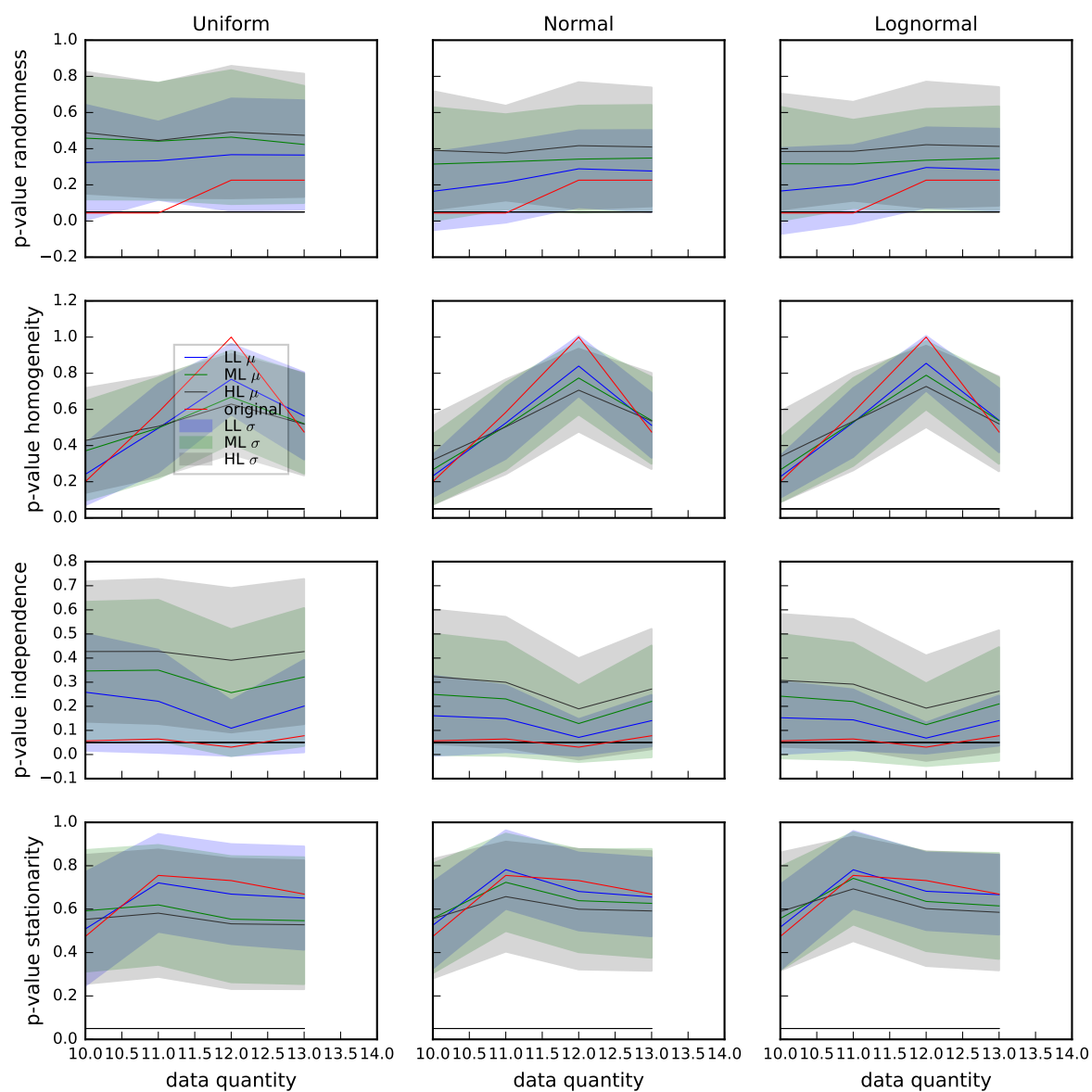
Figure 150 – Evolution of RHIS p-values from DOC concentration time series from IG7. Red line = p-value from OTS. Blue, green, gray lines = average p-value from STS in LL, ML and HL scenarios, respectively. Blue, green, gray bands = std of p-values from STS in LL, ML and HL scenarios, respectively. Black line = significance level ($\alpha = 0.05$). Reject H_0 if p-value < 0.05
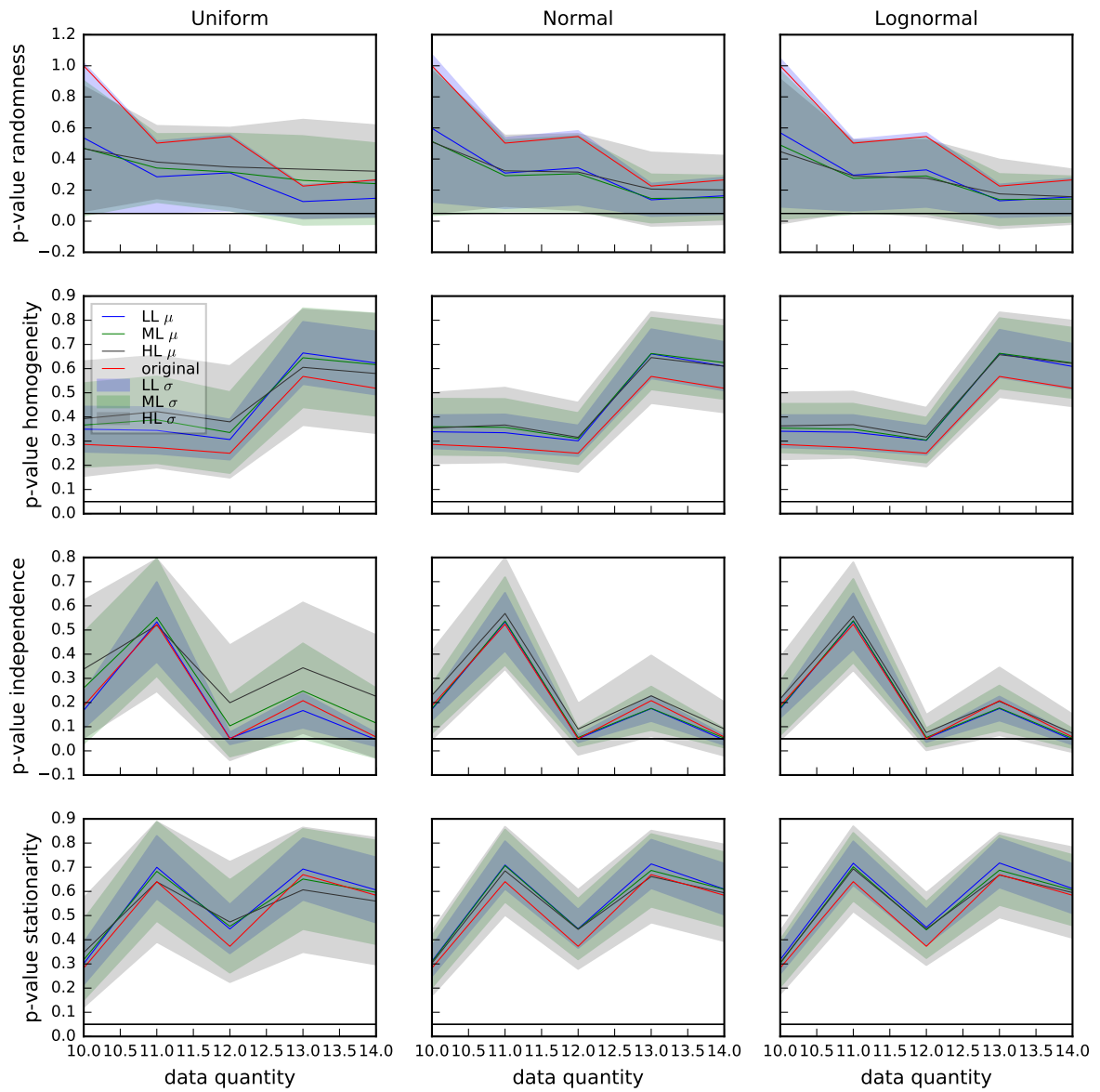
NH4 - IG3
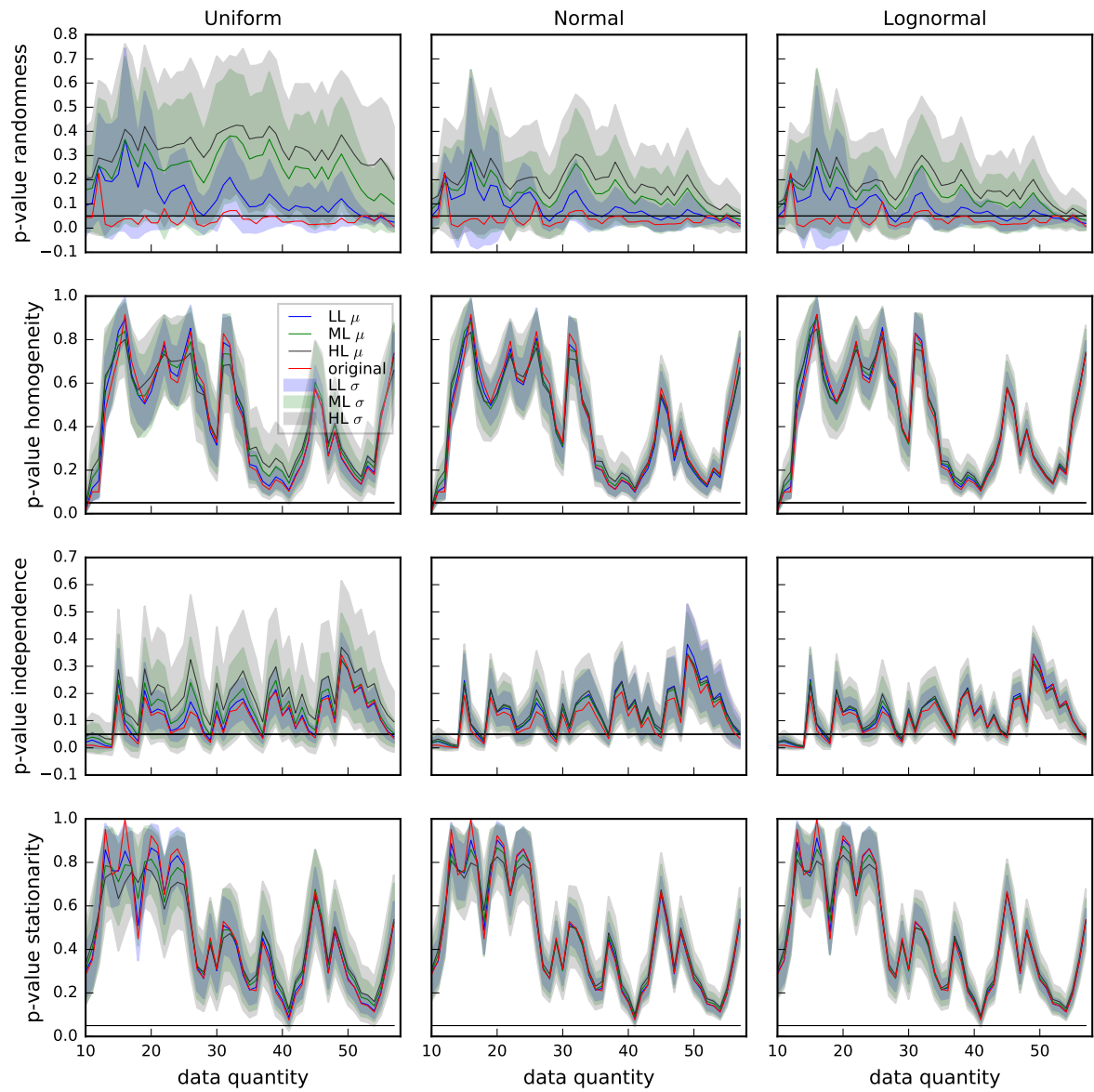
Figure 151 – Evolution of RHIS p-values from NH4 concentration time series from IG3. Red line = p-value from OTS. Blue, green, gray lines = average p-value from STS in LL, ML and HL scenarios, respectively. Blue, green, gray bands = std of p-values from STS in LL, ML and HL scenarios, respectively. Black line = significance level (α = 0.05). Reject H_0 if p-value < 0.05
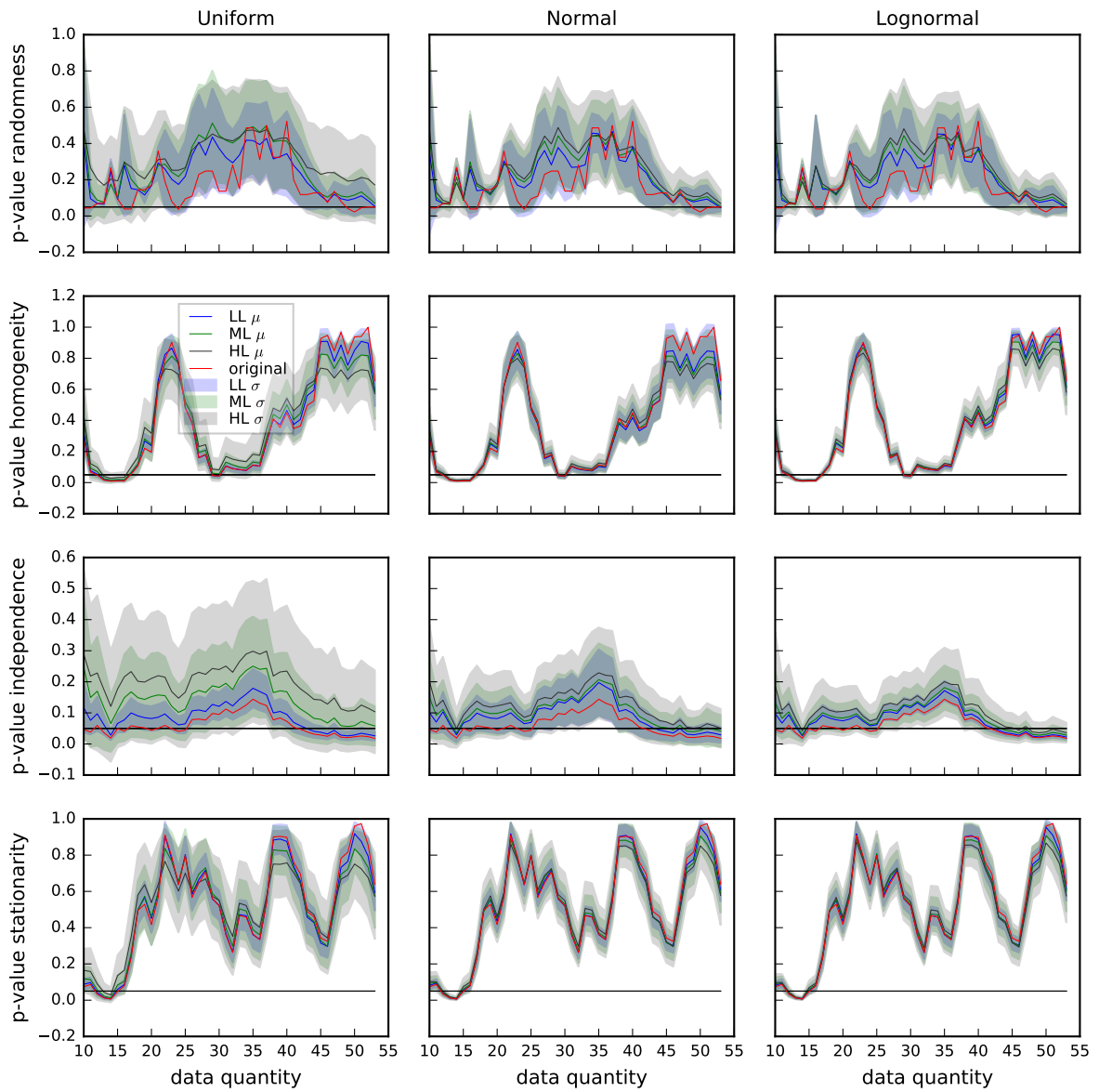
NH4 - IG4
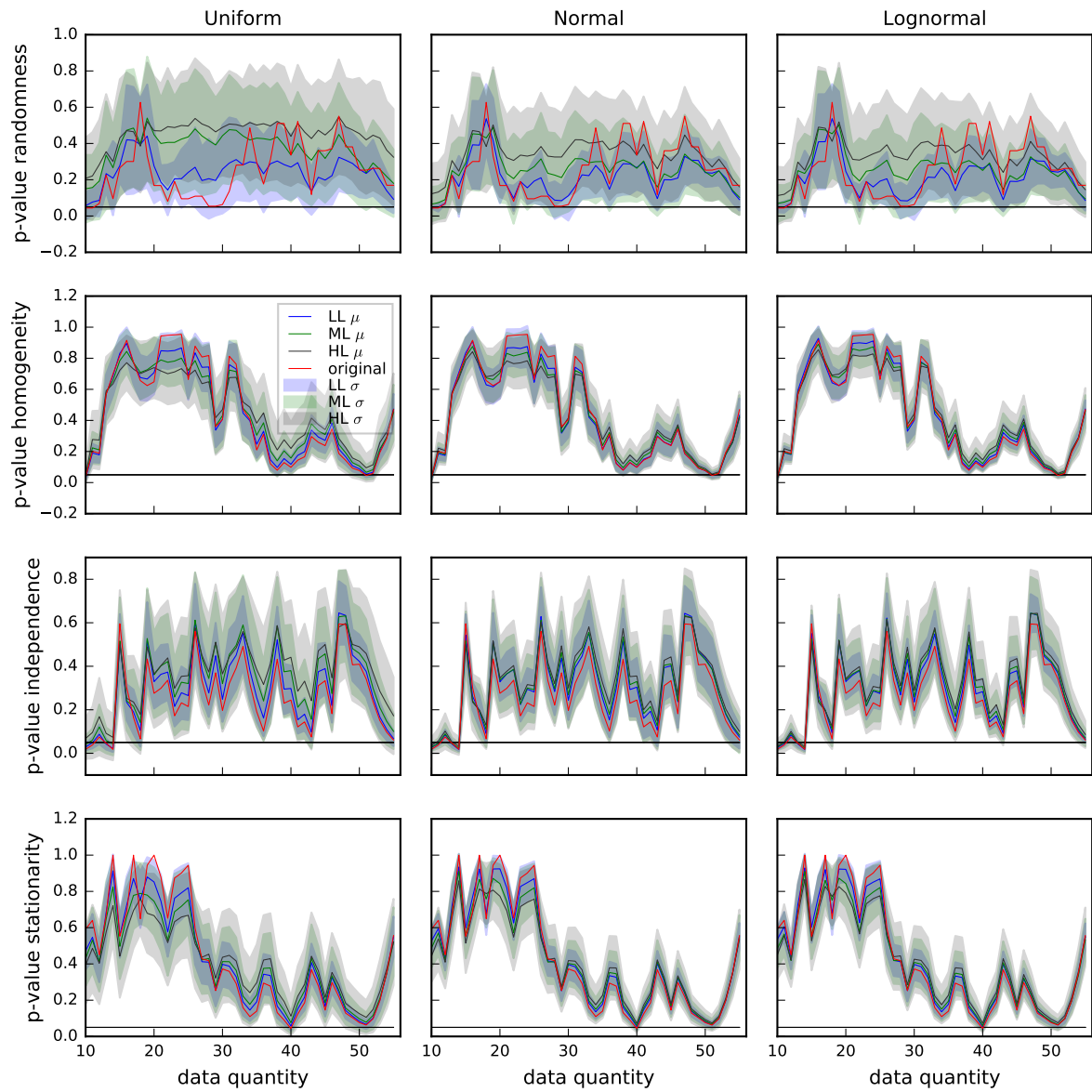
Figure 152 – Evolution of RHIS p-values from NH4 concentration time series from IG4. Red line = p-value from OTS. Blue, green, gray lines = average p-value from STS in LL, ML and HL scenarios, respectively. Blue, green, gray bands = std of p-values from STS in LL, ML and HL scenarios, respectively. Black line = significance level ($\alpha = 0.05$). Reject H_0 if p-value < 0.05
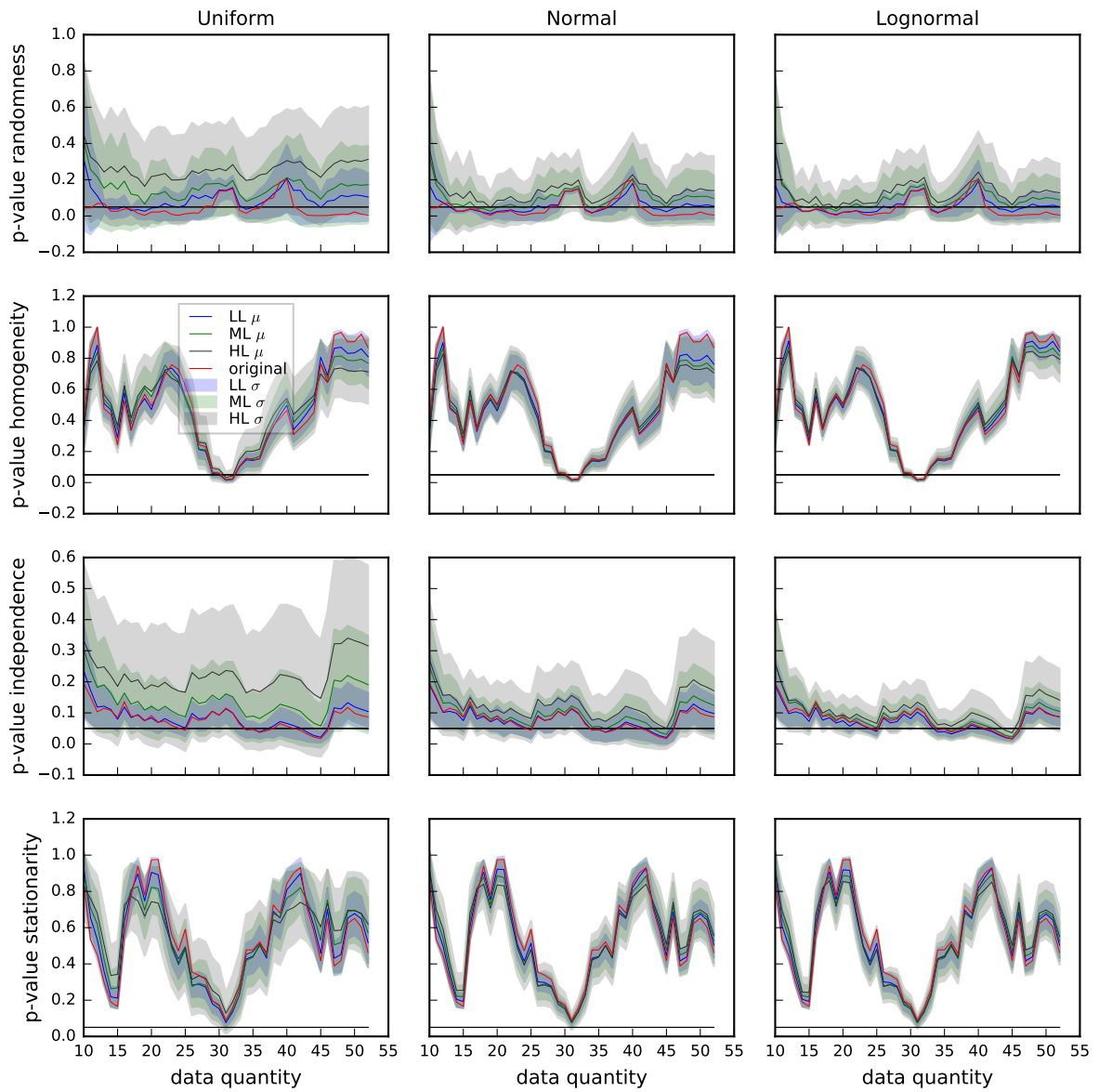
NH4 - IG5

Figure 153 – Evolution of RHIS p-values from NH4 concentration time series from IG5. Red line = p-value from OTS. Blue, green, gray lines = average p-value from STS in LL, ML and HL scenarios, respectively. Blue, green, gray bands = std of p-values from STS in LL, ML and HL scenarios, respectively. Black line = significance level ($\alpha = 0.05$). Reject H_0 if p-value < 0.05
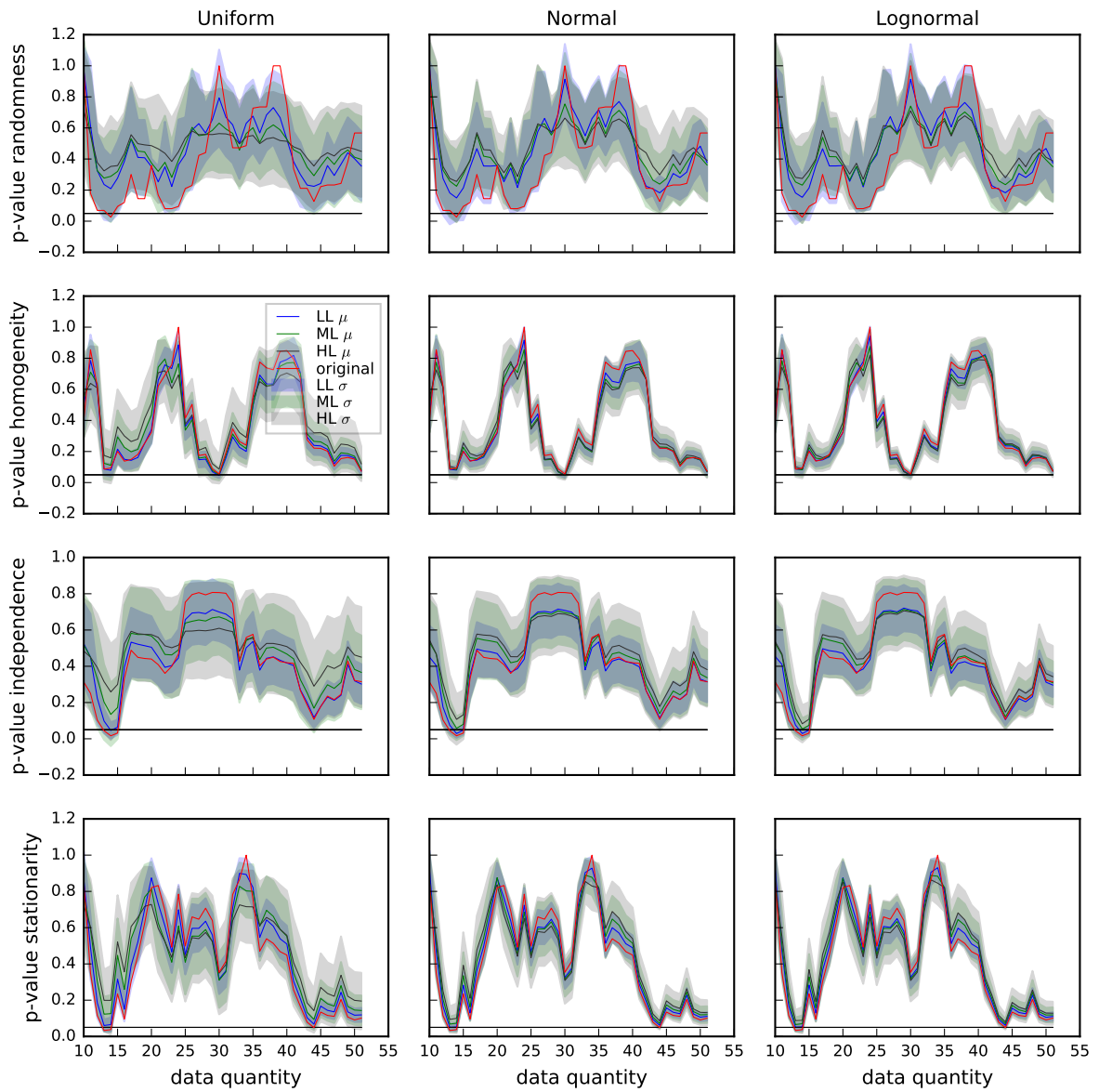
NH4 - IG6

Figure 154 – Evolution of RHIS p-values from NH4 concentration time series from IG6. Red line = p-value from OTS. Blue, green, gray lines = average p-value from STS in LL, ML and HL scenarios, respectively. Blue, green, gray bands = std of p-values from STS in LL, ML and HL scenarios, respectively. Black line = significance level ($\alpha = 0.05$). Reject H_0 if p-value < 0.05
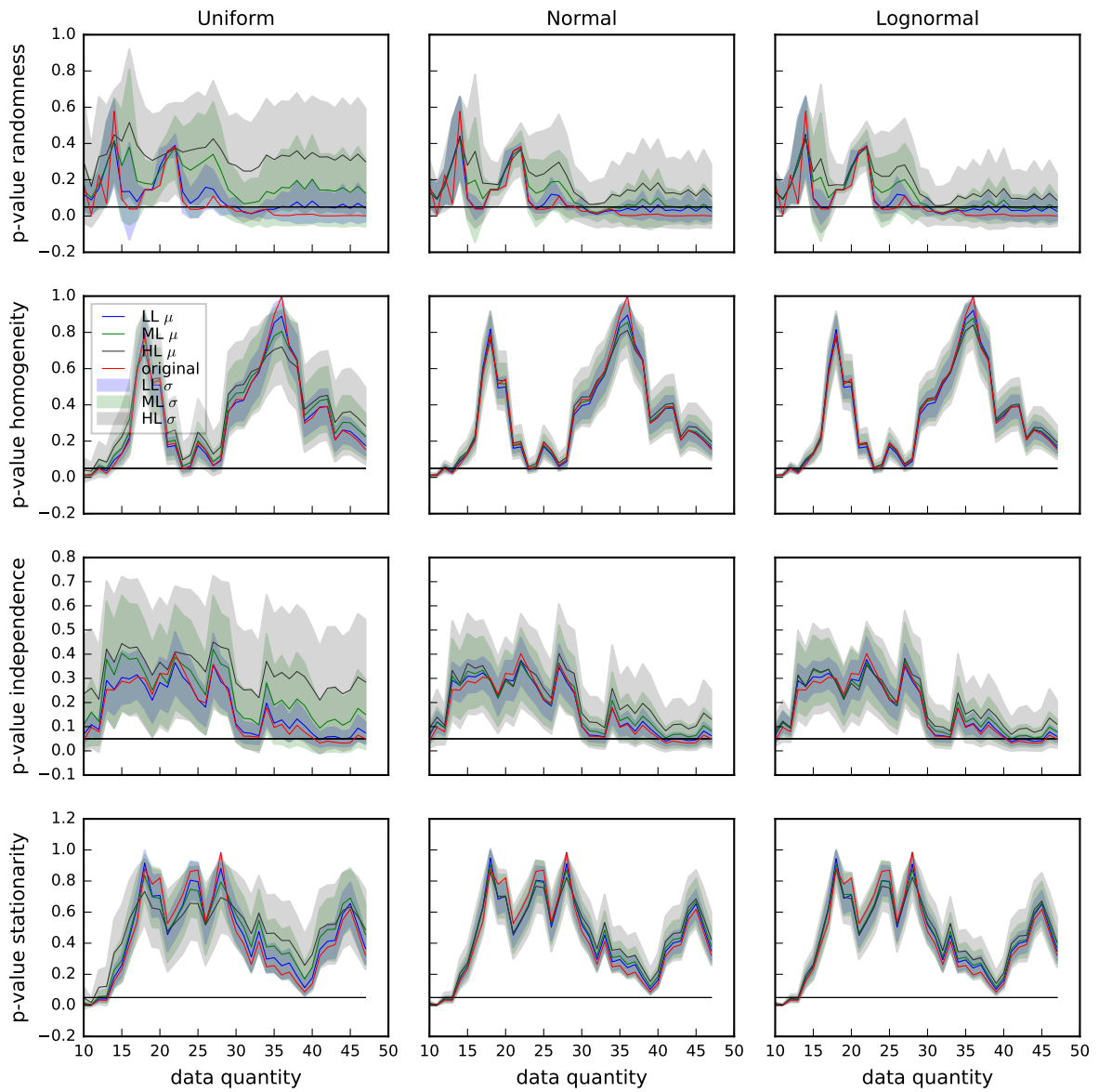
NH4 - IG7

Figure 155 – Evolution of RHIS p-values from NH4 concentration time series from IG7. Red line = p-value from OTS. Blue, green, gray lines = average p-value from STS in LL, ML and HL scenarios, respectively. Blue, green, gray bands = std of p-values from STS in LL, ML and HL scenarios, respectively. Black line = significance level (α = 0.05). Reject H_0 if p-value < 0.05
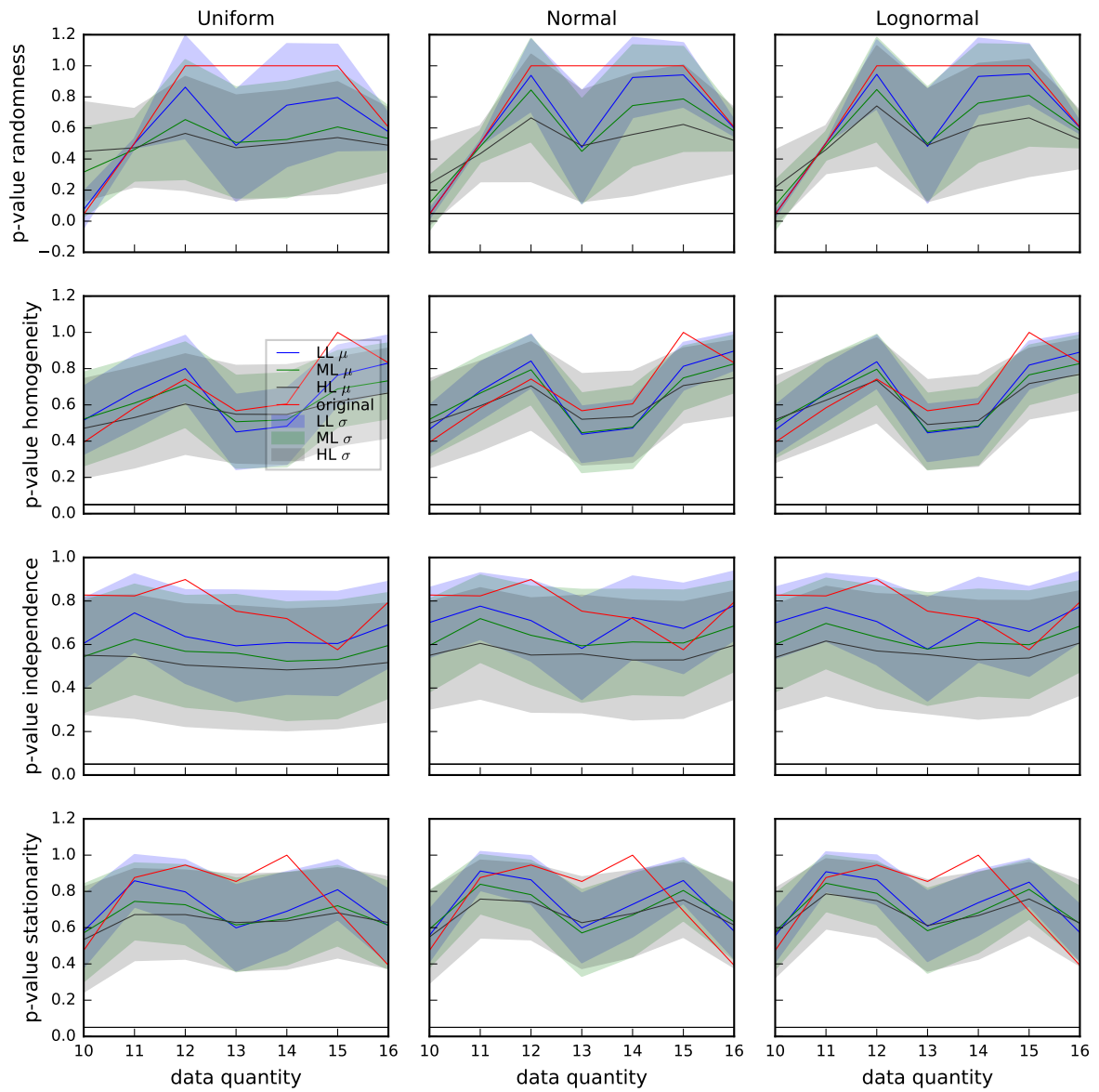
TP - IG3

Figure 156 – Evolution of RHIS p-values from TP concentration time series from IG3. Red line = p-value from OTS. Blue, green, gray lines = average p-value from STS in LL, ML and HL scenarios, respectively. Blue, green, gray bands = std of p-values from STS in LL, ML and HL scenarios, respectively. Black line = significance level ($\alpha = 0.05$). Reject H_0 if p-value < 0.05

TP - IG4

Figure 157 – Evolution of RHIS p-values from TP concentration time series from IG4. Red line = p-value from OTS. Blue, green, gray lines = average p-value from STS in LL, ML and HL scenarios, respectively. Blue, green, gray bands = std of p-values from STS in LL, ML and HL scenarios, respectively. Black line = significance level ($\alpha = 0.05$). Reject H_0 if p-value < 0.05
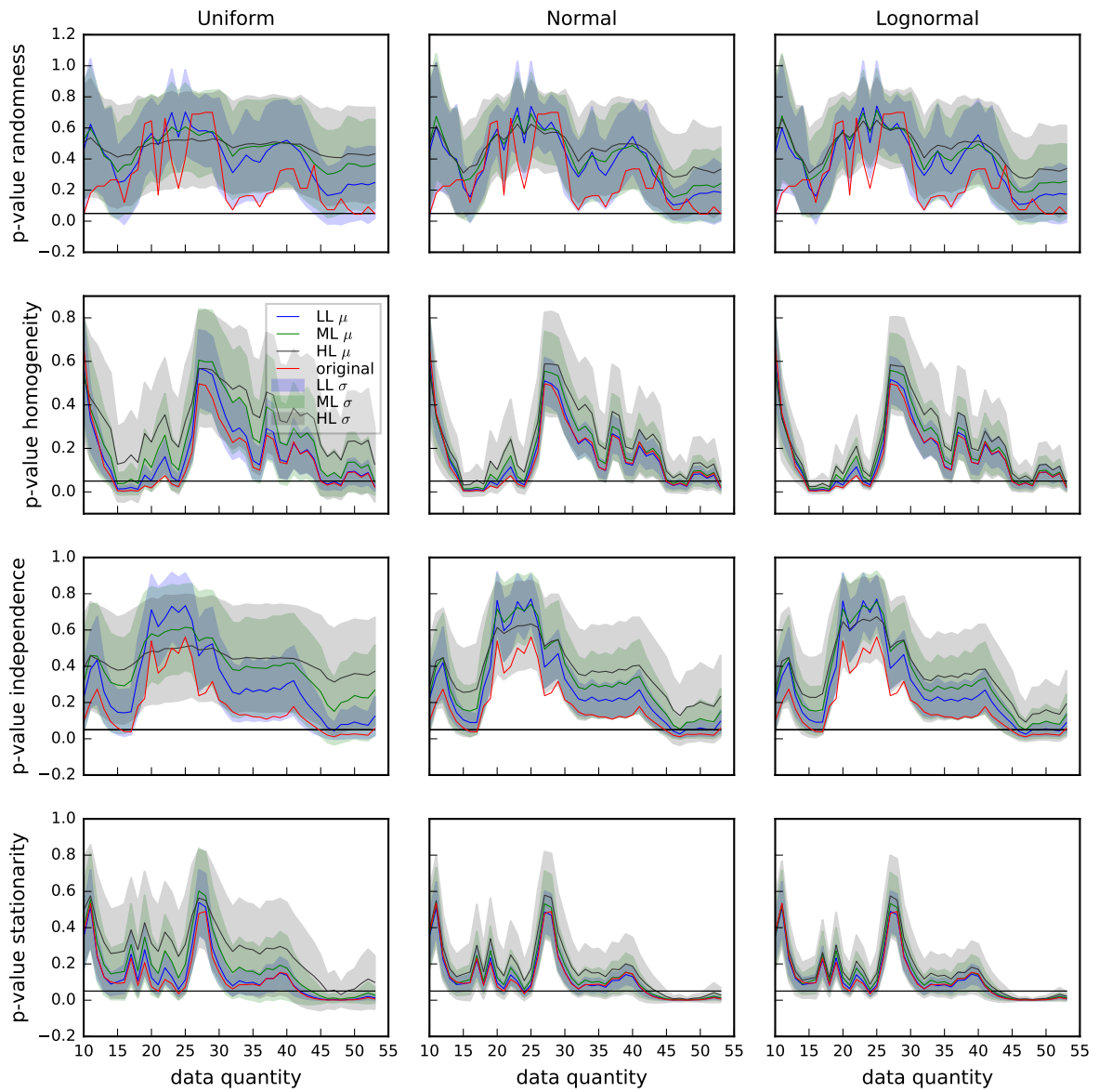
TP - IG5

Figure 158 – Evolution of RHIS p-values from TP concentration time series from IG5. Red line = p-value from OTS. Blue, green, gray lines = average p-value from STS in LL, ML and HL scenarios, respectively. Blue, green, gray bands = std of p-values from STS in LL, ML and HL scenarios, respectively. Black line = significance level (α = 0.05). Reject H_0 if p-value < 0.05
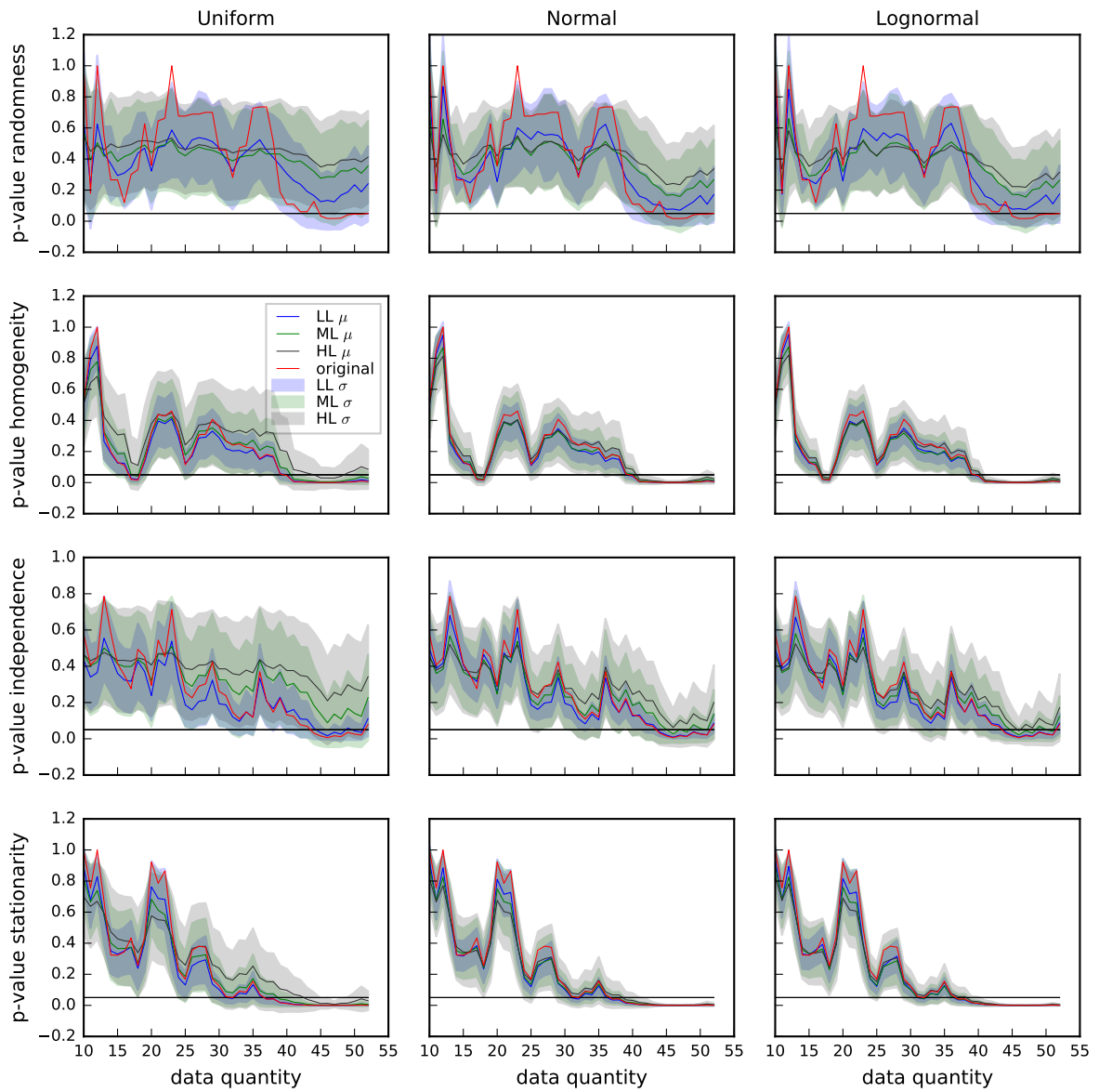
TP - IG6

Figure 159 – Evolution of RHIS p-values from TP concentration time series from IG6. Red line = p-value from OTS. Blue, green, gray lines = average p-value from STS in LL, ML and HL scenarios, respectively. Blue, green, gray bands = std of p-values from STS in LL, ML and HL scenarios, respectively. Black line = significance level ($\alpha = 0.05$). Reject H_0 if p-value < 0.05
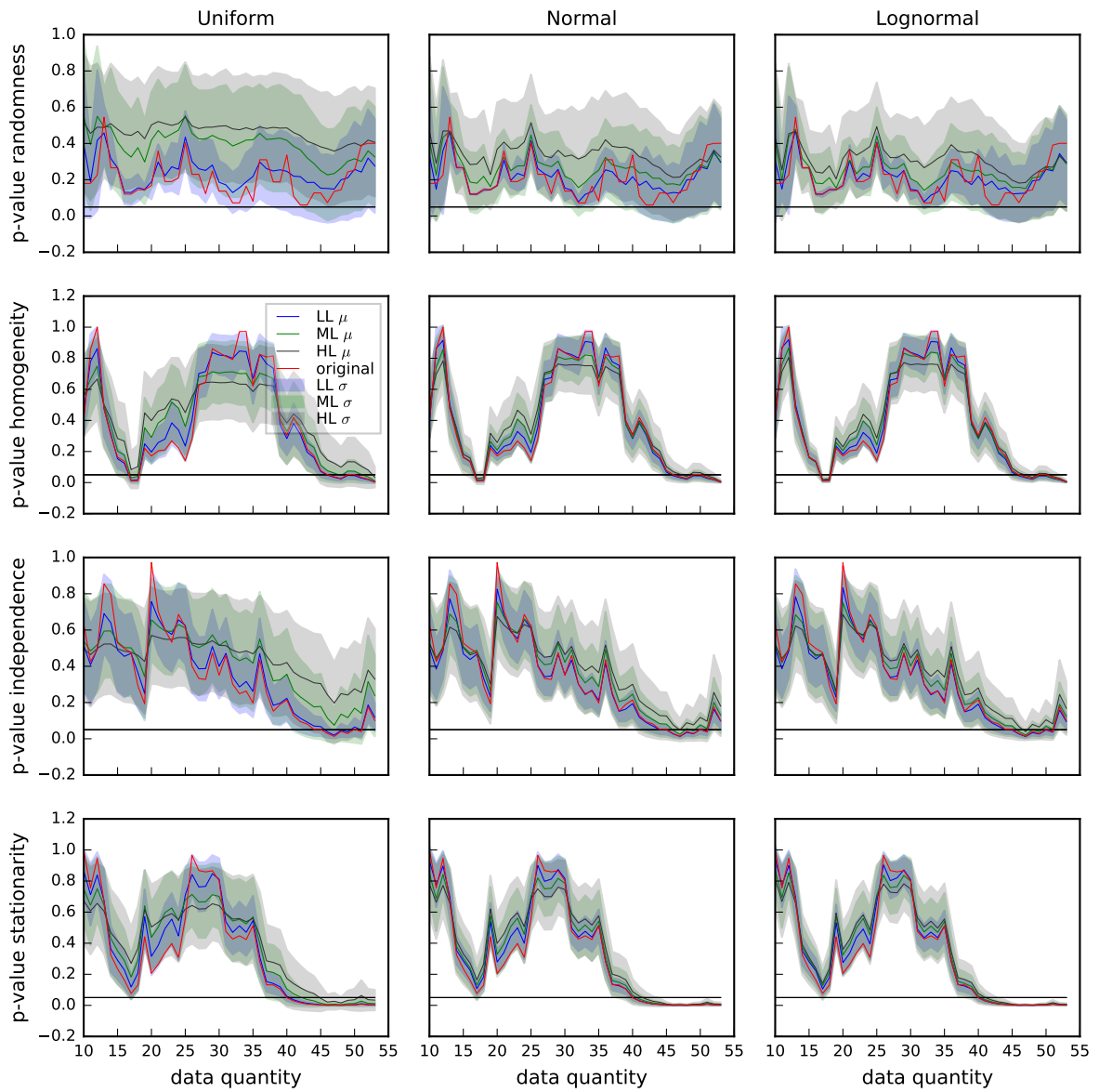
TP - IG7

Figure 160 – Evolution of RHIS p-values from TP concentration time series from IG7. Red line = p-value from OTS. Blue, green, gray lines = average p-value from STS in LL, ML and HL scenarios, respectively. Blue, green, gray bands = std of p-values from STS in LL, ML and HL scenarios, respectively. Black line = significance level (α = 0.05). Reject H_0 if p-value < 0.05
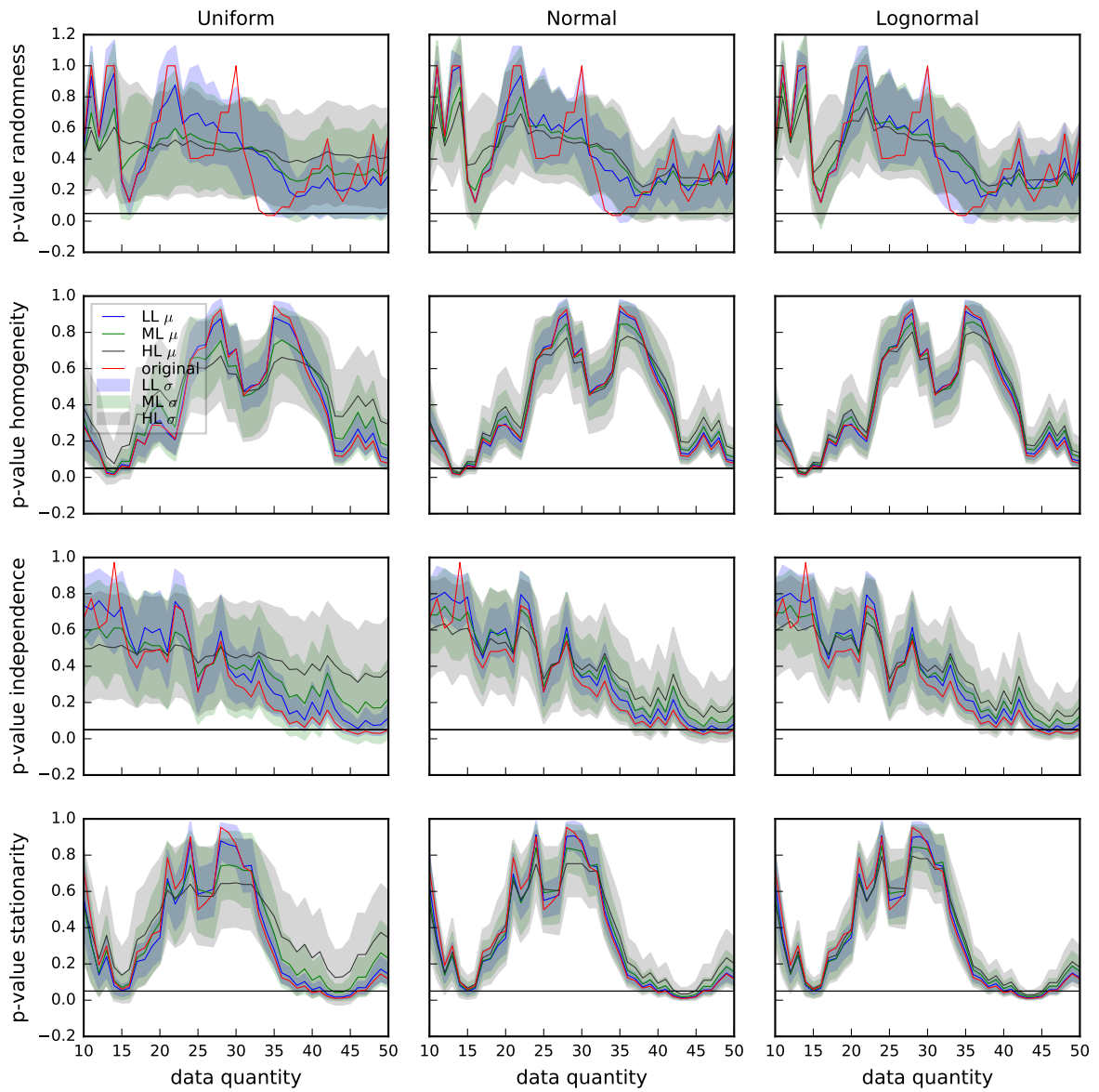
VDS - IG3

Figure 161 – Evolution of RHIS p-values from VDS concentration time series from IG3. Red line = p-value from OTS. Blue, green, gray lines = average p-value from STS in LL, ML and HL scenarios, respectively. Blue, green, gray bands = std of p-values from STS in LL, ML and HL scenarios, respectively. Black line = significance level ($\alpha = 0.05$). Reject H_0 if p-value < 0.05
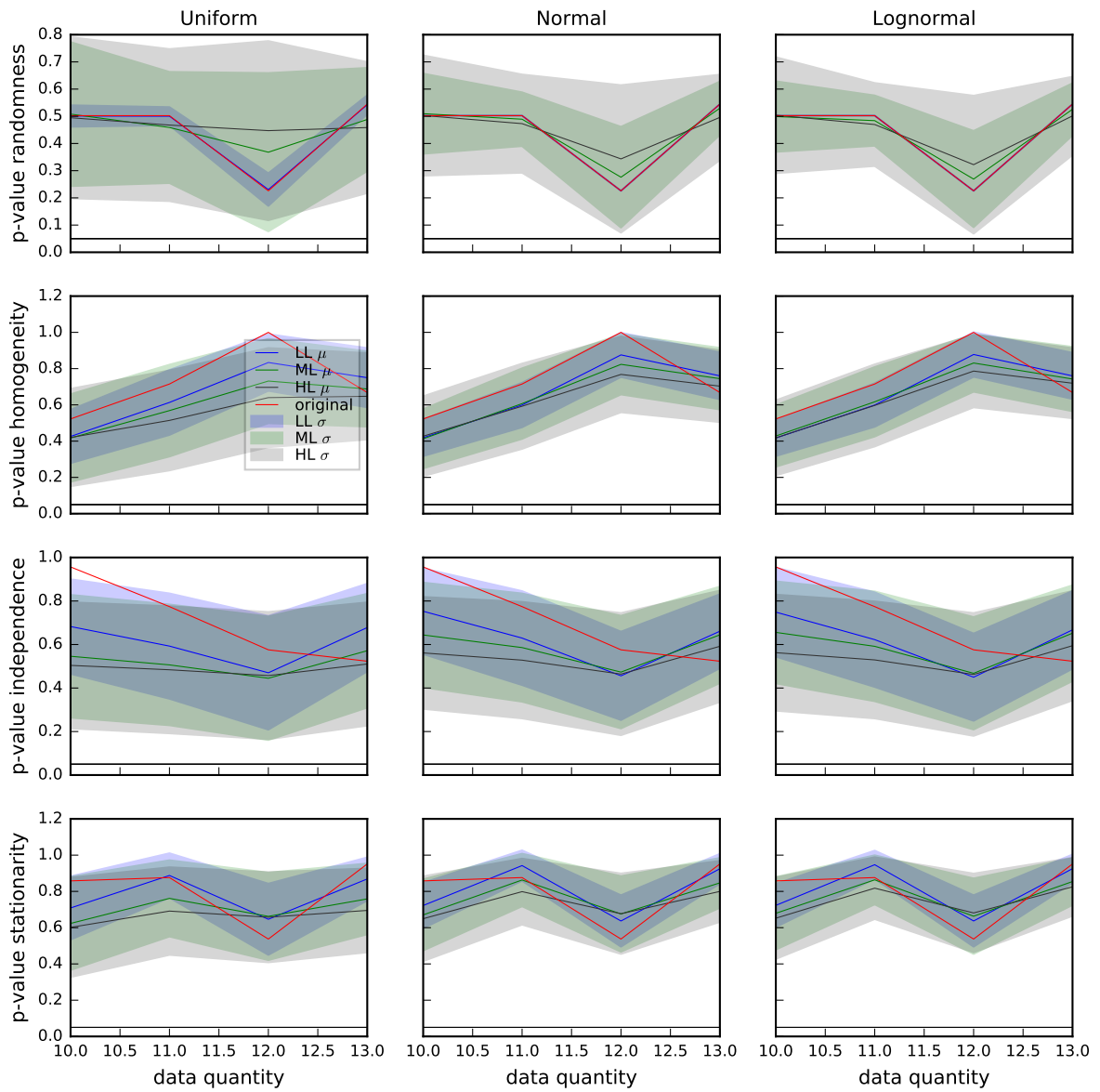
VDS - IG4

Figure 162 – Evolution of RHIS p-values from VDS concentration time series from IG4. Red line = p-value from OTS. Blue, green, gray lines = average p-value from STS in LL, ML and HL scenarios, respectively. Blue, green, gray bands = std of p-values from STS in LL, ML and HL scenarios, respectively. Black line = significance level ($\alpha = 0.05$). Reject H_0 if p-value < 0.05
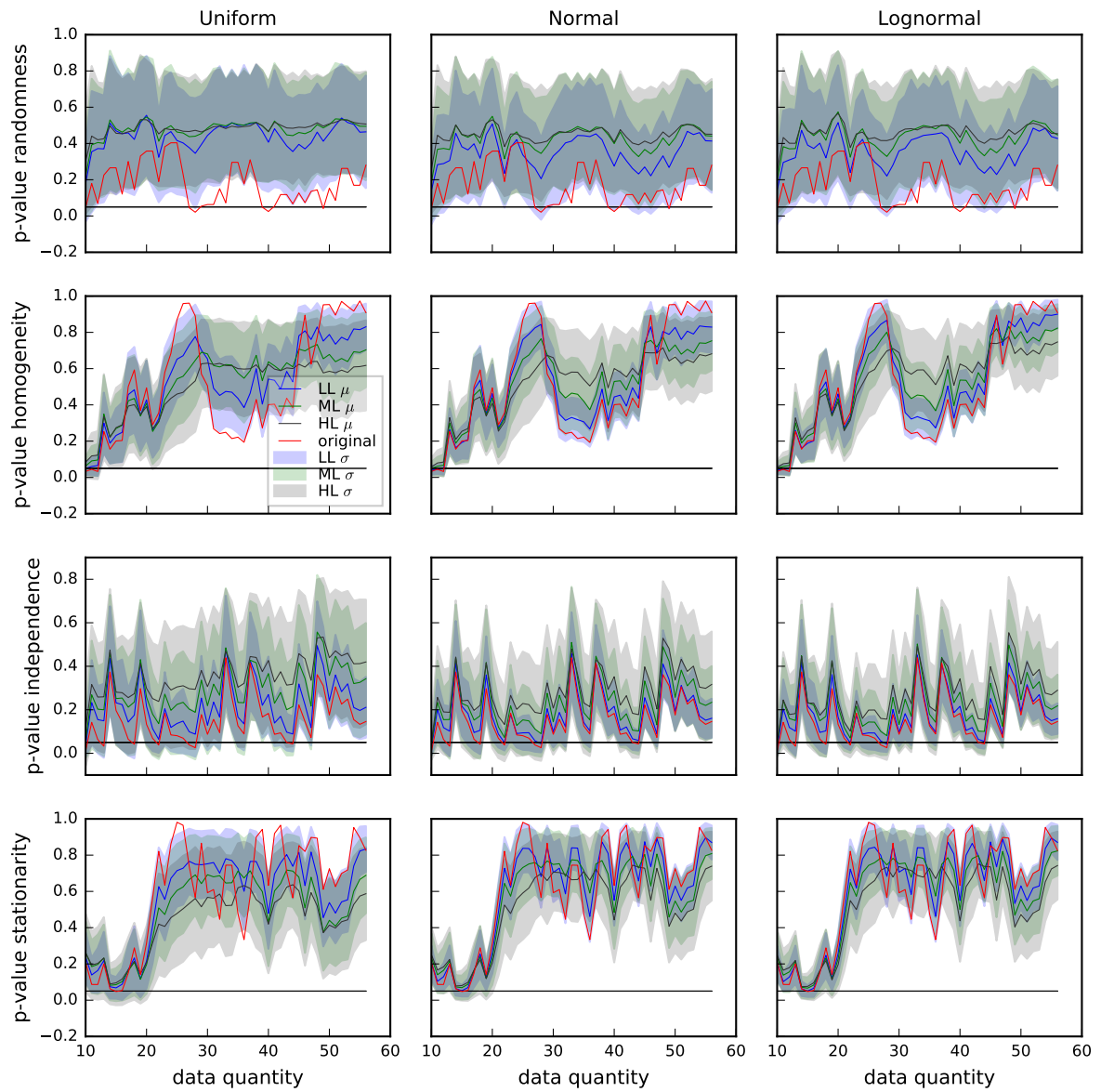
VDS - IG5

Figure 163 – Evolution of RHIS p-values from VDS concentration time series from IG5. Red line = p-value from OTS. Blue, green, gray lines = average p-value from STS in LL, ML and HL scenarios, respectively. Blue, green, gray bands = std of p-values from STS in LL, ML and HL scenarios, respectively. Black line = significance level (α = 0.05). Reject H_0 if p-value < 0.05
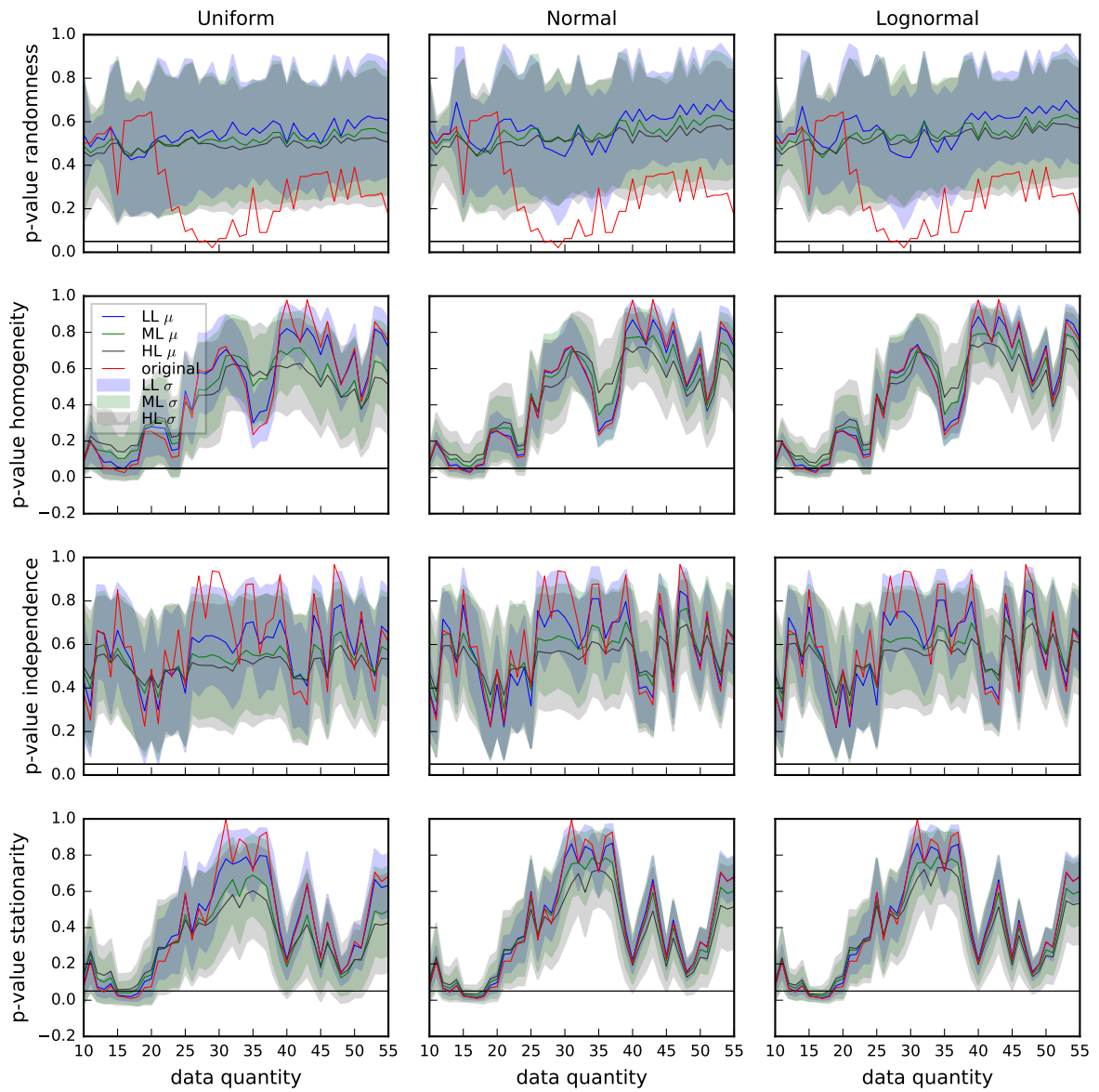
VDS - IG6

Figure 164 – Evolution of RHIS p-values from VDS concentration time series from IG6. Red line = p-value from OTS. Blue, green, gray lines = average p-value from STS in LL, ML and HL scenarios, respectively. Blue, green, gray bands = std of p-values from STS in LL, ML and HL scenarios, respectively. Black line = significance level (α = 0.05). Reject H_0 if p-value < 0.05

VDS - IG7

Figure 165 – Evolution of RHIS p-values from VDS concentration time series from IG7. Red line = p-value from OTS. Blue, green, gray lines = average p-value from STS in LL, ML and HL scenarios, respectively. Blue, green, gray bands = std of p-values from STS in LL, ML and HL scenarios, respectively. Black line = significance level ($\alpha = 0.05$). Reject H_0 if p-value < 0.05
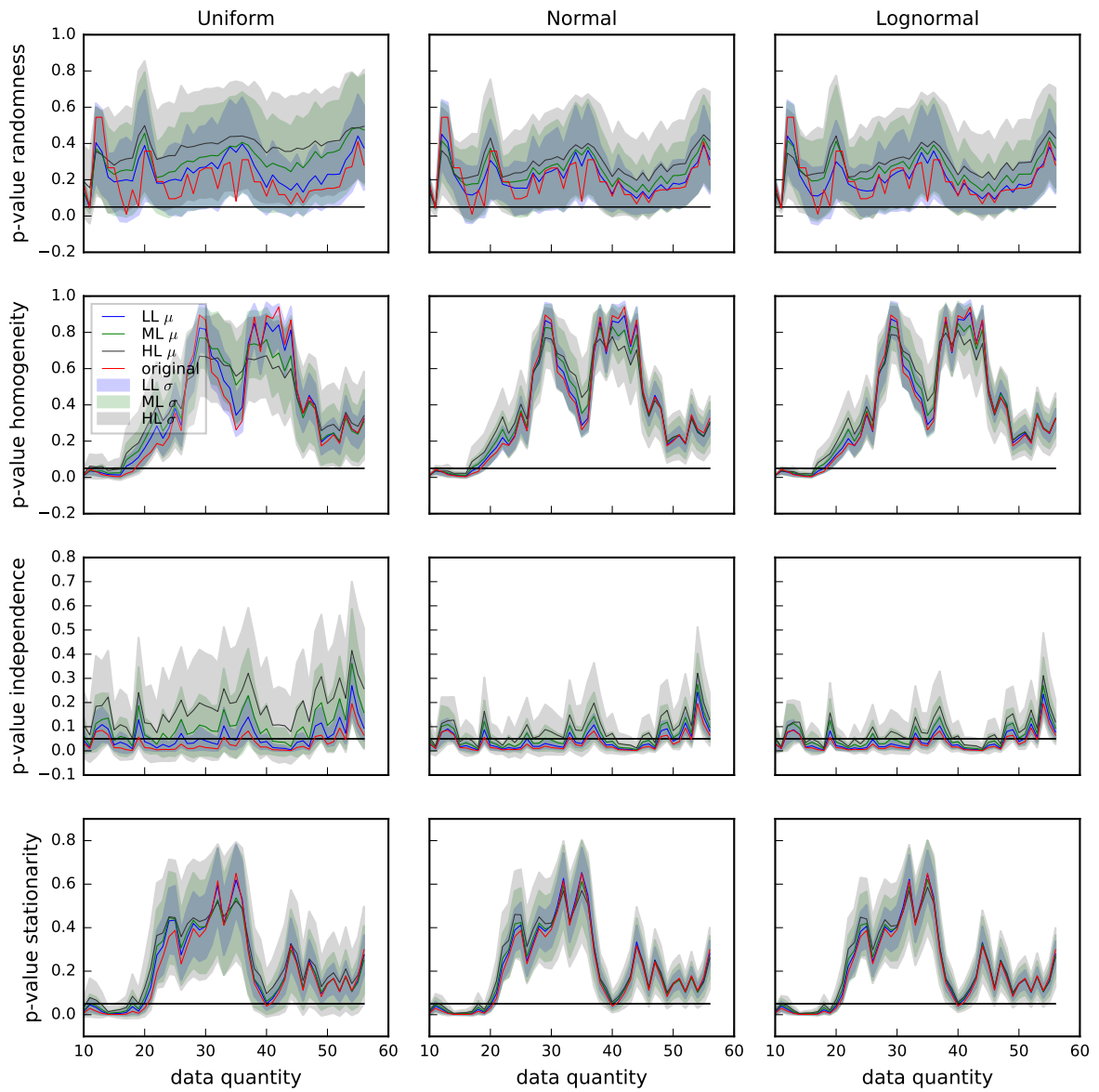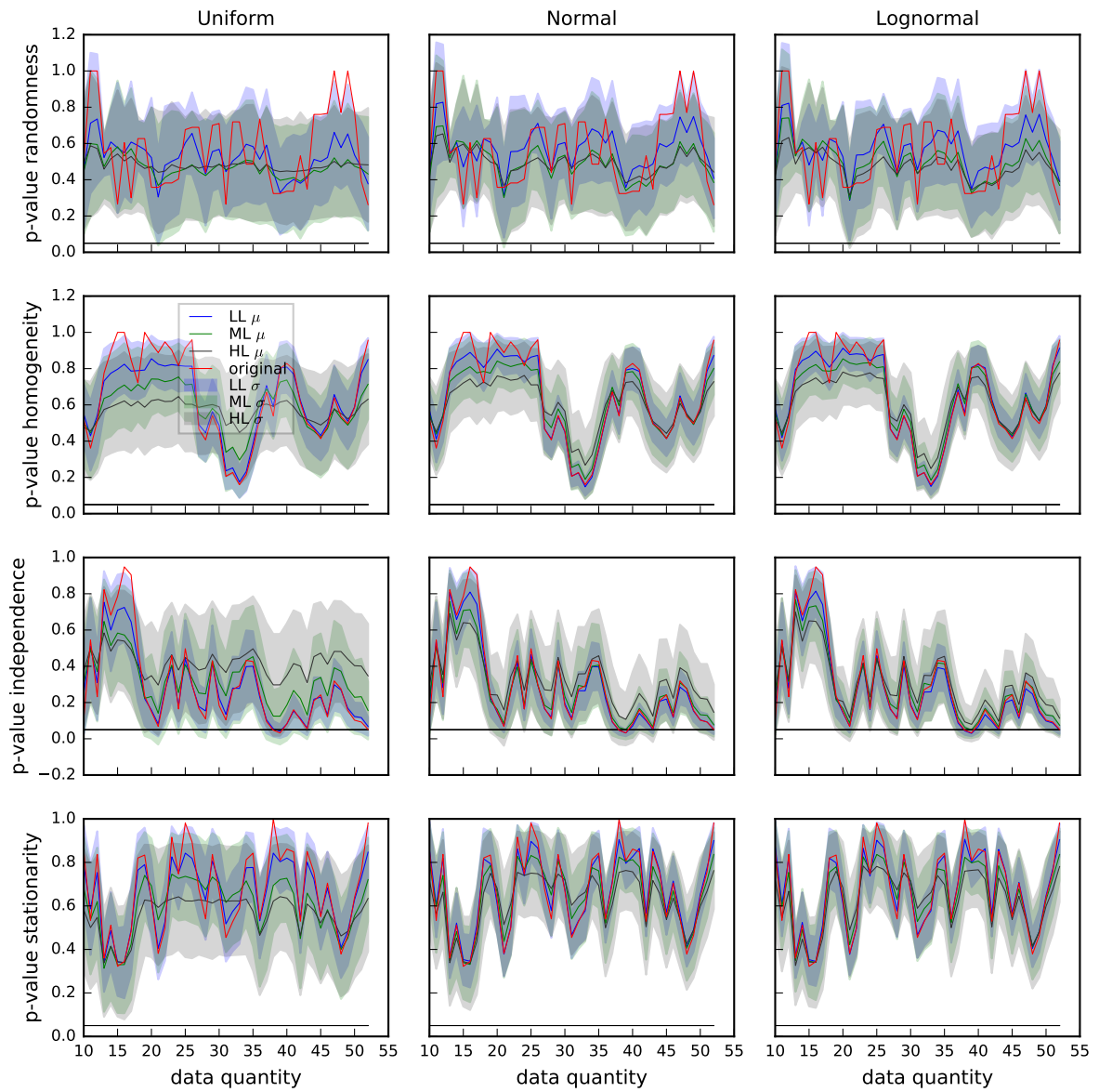
A.10   RHIS (ton/d)

BOD - IG3

Figure 166 – Evolution of RHIS p-values from BOD loads time series from IG3. Red line = p-value from OTS. Blue, green, gray lines = average p-value from STS in LL, ML and HL scenarios, respectively. Blue, green, gray bands = std of p-values from STS in LL, ML and HL scenarios, respectively. Black line = significance level (α = 0.05). Reject H_0 if p-value < 0.05
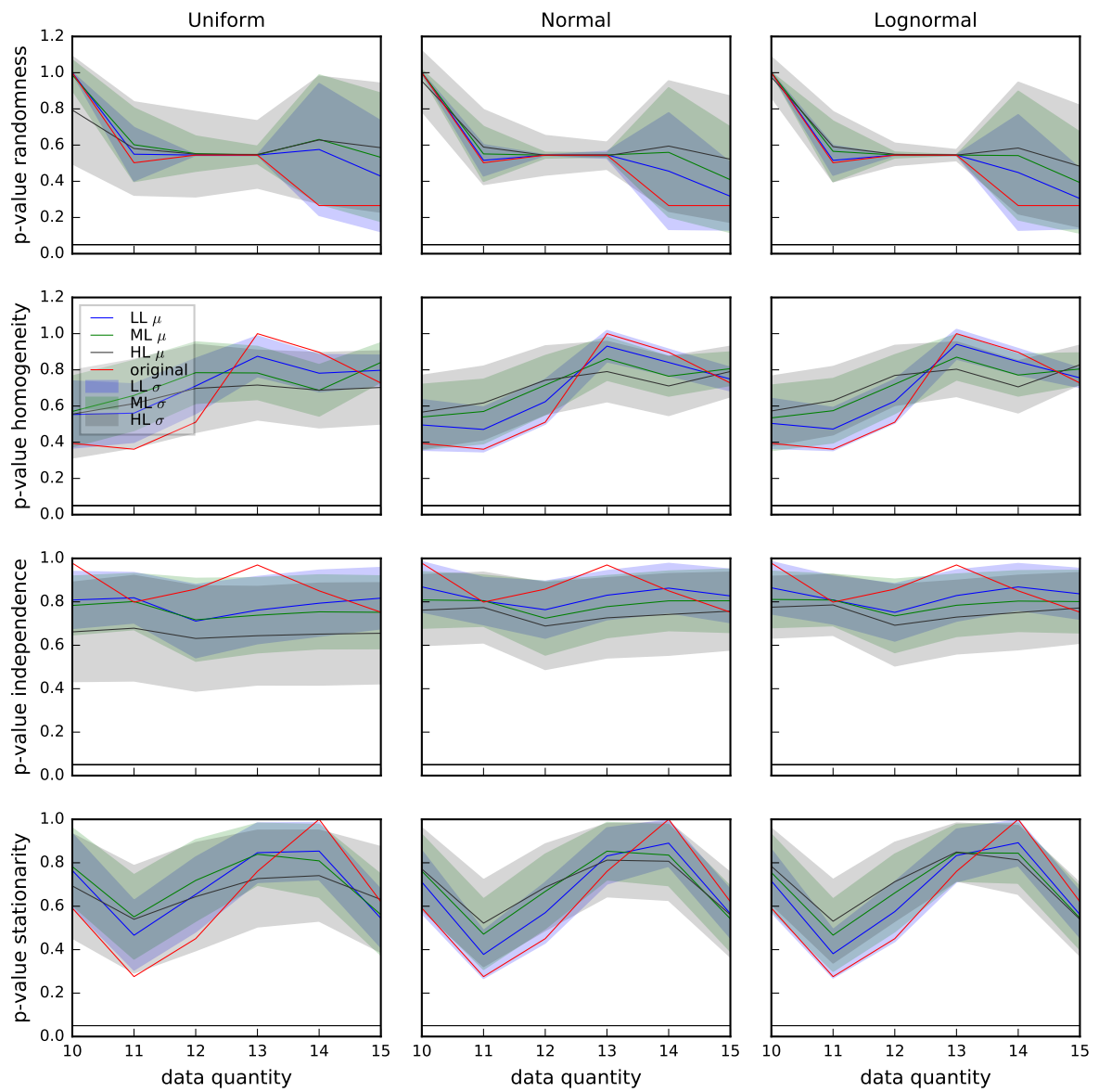
BOD - IG4

Figure 167 – Evolution of RHIS p-values from BOD loads time series from IG4. Red line = p-value from OTS. Blue, green, gray lines = average p-value from STS in LL, ML and HL scenarios, respectively. Blue, green, gray bands = std of p-values from STS in LL, ML and HL scenarios, respectively. Black line = significance level ($\alpha = 0.05$). Reject H_0 if p-value < 0.05
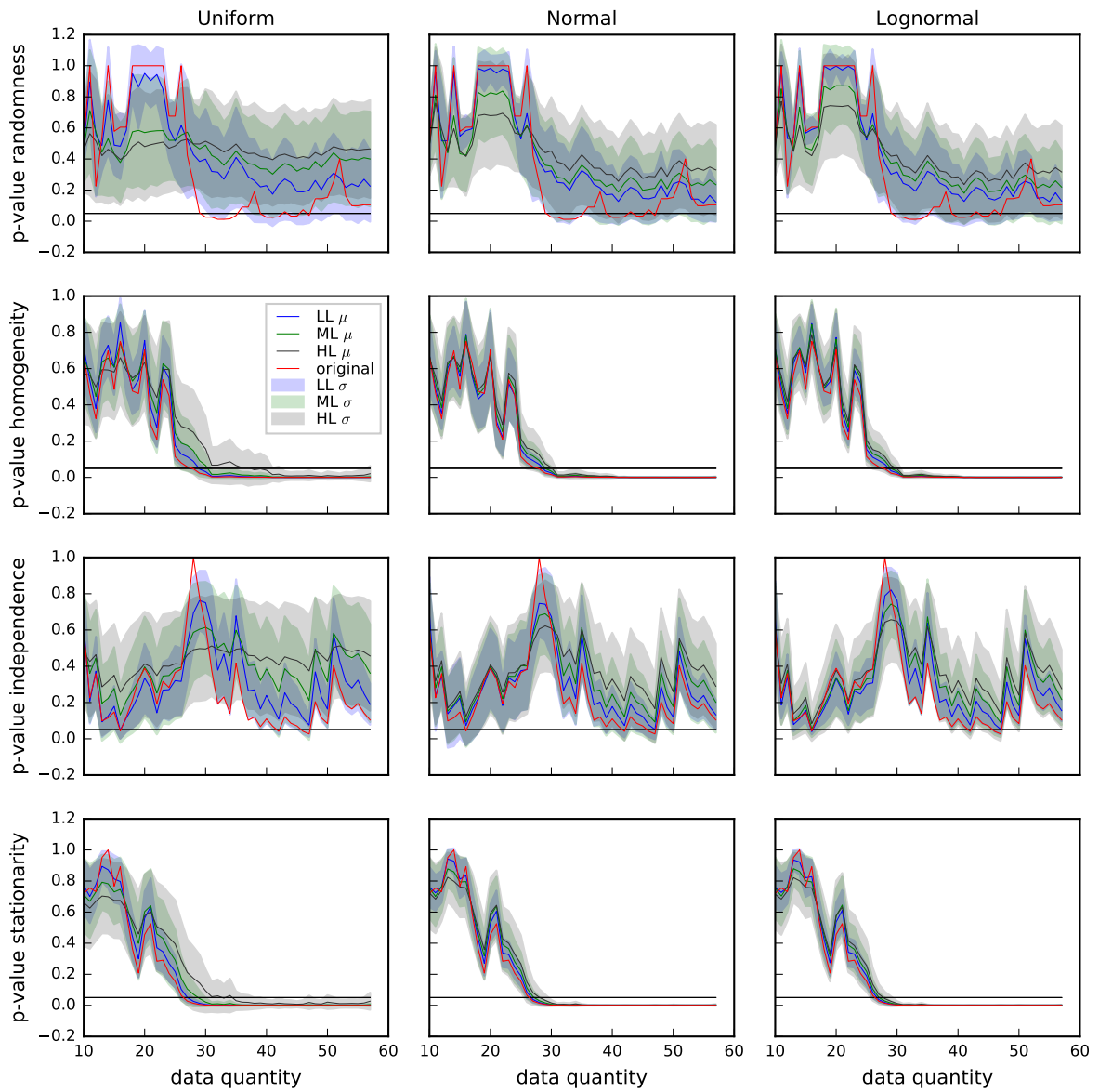
BOD - IG5

Figure 168 – Evolution of RHIS p-values from BOD loads time series from IG5. Red line = p-value from OTS. Blue, green, gray lines = average p-value from STS in LL, ML and HL scenarios, respectively. Blue, green, gray bands = std of p-values from STS in LL, ML and HL scenarios, respectively. Black line = significance level ($\alpha = 0.05$). Reject H_0 if p-value < 0.05

BOD - IG6

Figure 169 – Evolution of RHIS p-values from BOD loads time series from IG6. Red line = p-value from OTS. Blue, green, gray lines = average p-value from STS in LL, ML and HL scenarios, respectively. Blue, green, gray bands = std of p-values from STS in LL, ML and HL scenarios, respectively. Black line = significance level ($\alpha = 0.05$). Reject H_0 if p-value < 0.05
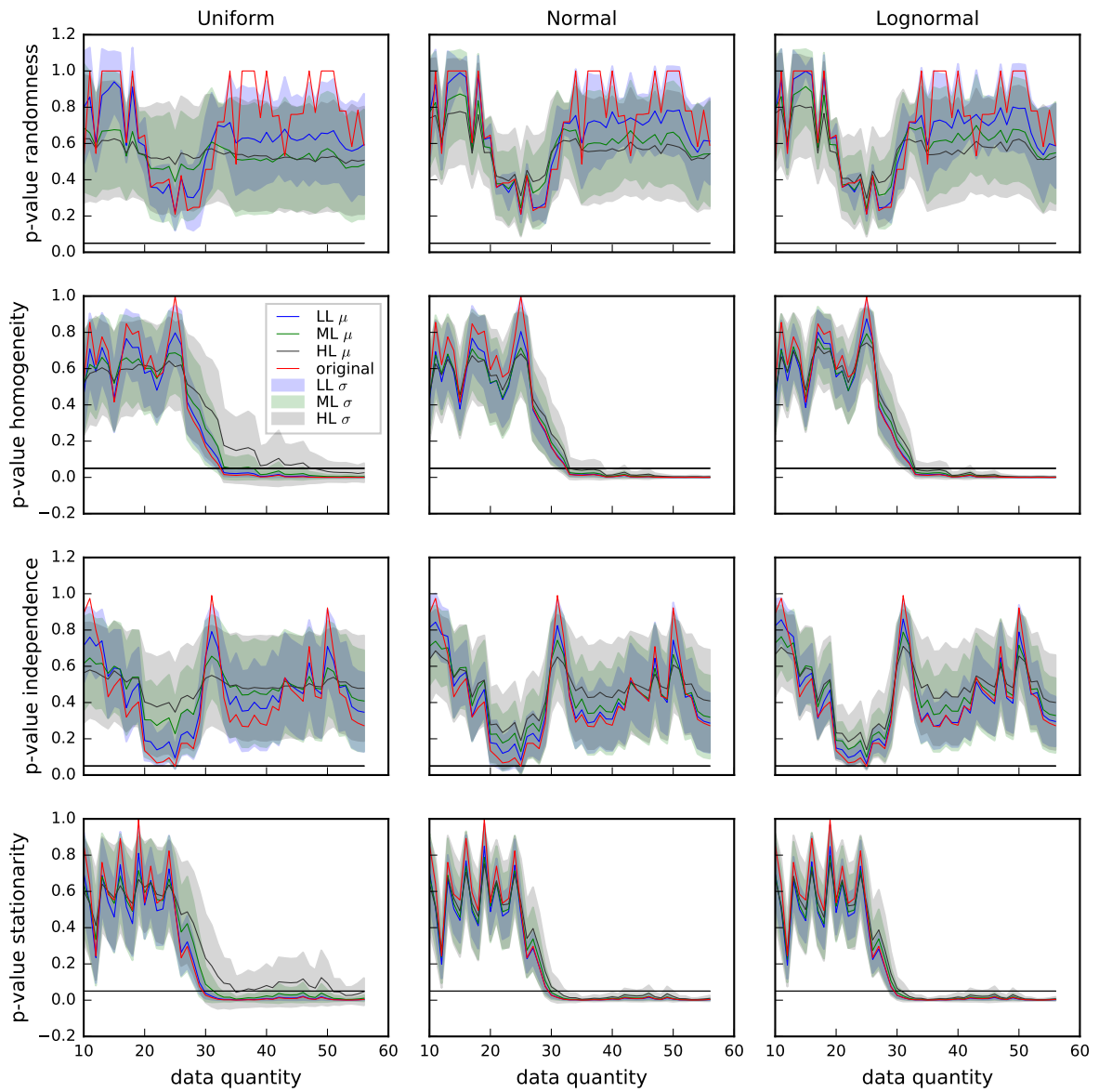
BOD - IG7

Figure 170 – Evolution of RHIS p-values from BOD loads time series from IG7. Red line = p-value from OTS. Blue, green, gray lines = average p-value from STS in LL, ML and HL scenarios, respectively. Blue, green, gray bands = std of p-values from STS in LL, ML and HL scenarios, respectively. Black line = significance level (α = 0.05). Reject H_0 if p-value < 0.05
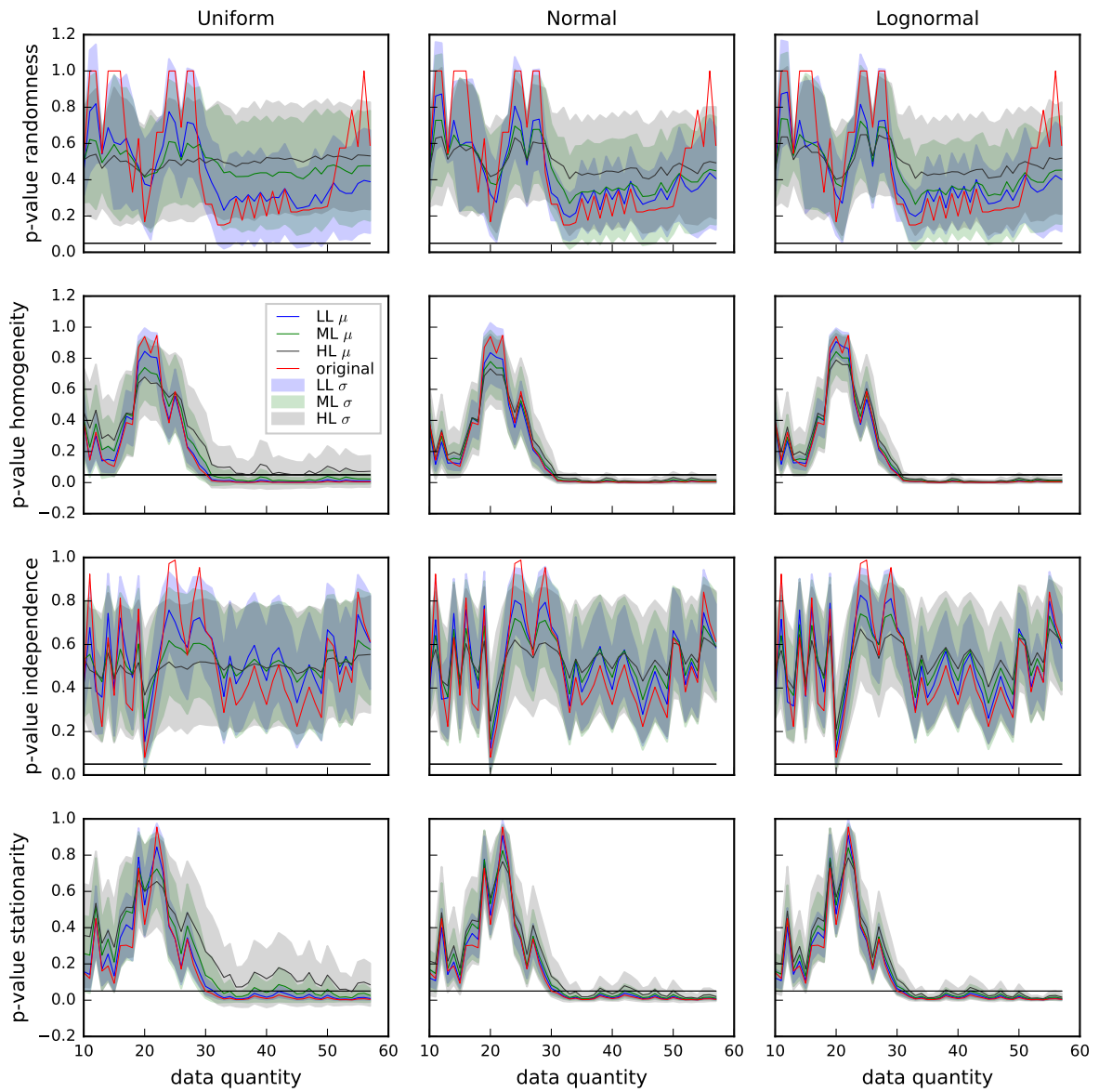
DO - IG3

Figure 171 – Evolution of RHIS p-values from DO loads time series from IG3. Red line = p-value from OTS. Blue, green, gray lines = average p-value from STS in LL, ML and HL scenarios, respectively. Blue, green, gray bands = std of p-values from STS in LL, ML and HL scenarios, respectively. Black line = significance level ($\alpha = 0.05$). Reject H_0 if p-value < 0.05
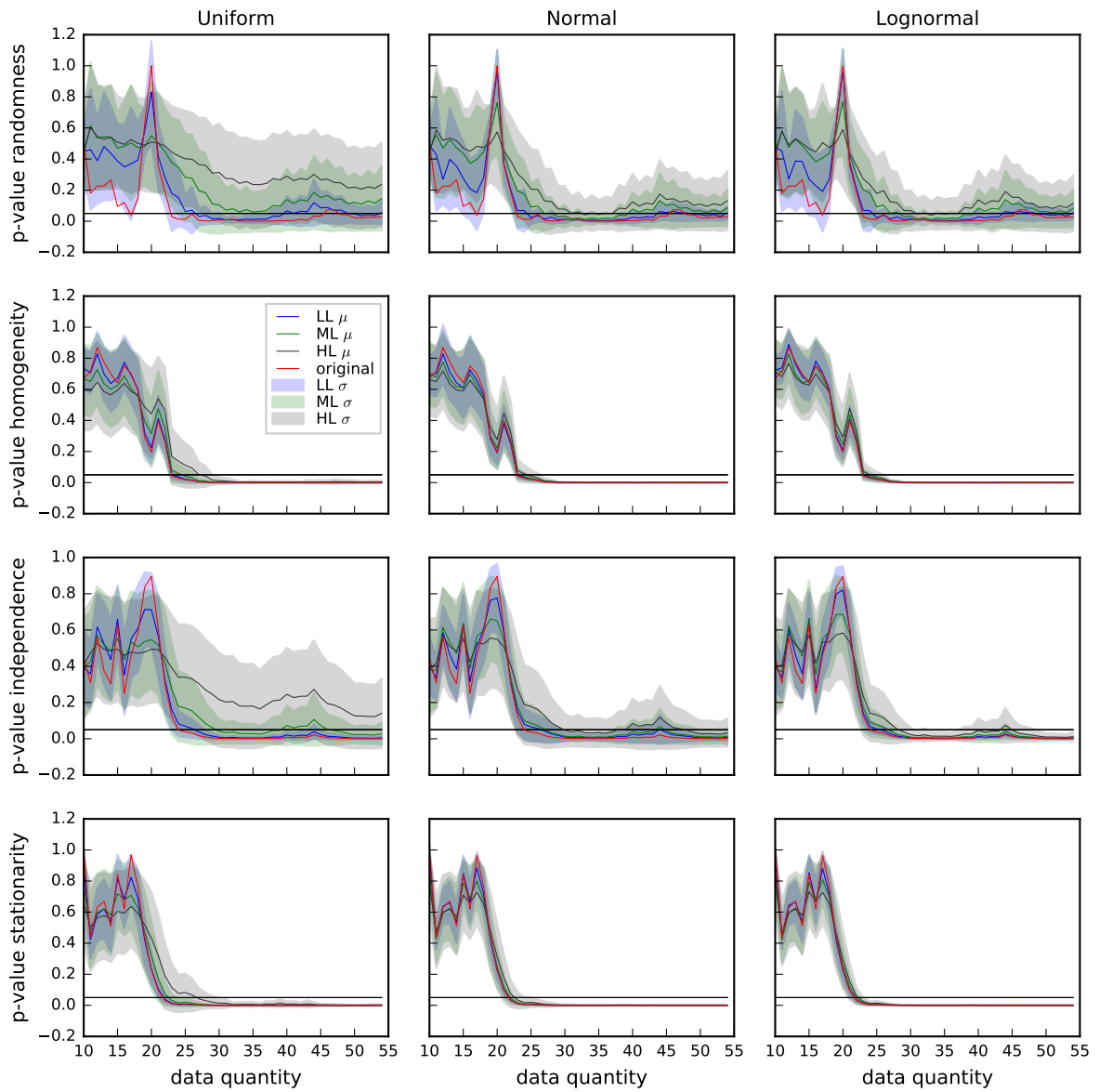
DO - IG4

Figure 172 – Evolution of RHIS p-values from DO loads time series from IG4. Red line = p-value from OTS. Blue, green, gray lines = average p-value from STS in LL, ML and HL scenarios, respectively. Blue, green, gray bands = std of p-values from STS in LL, ML and HL scenarios, respectively. Black line = significance level ($\alpha = 0.05$). Reject H_0 if p-value < 0.05
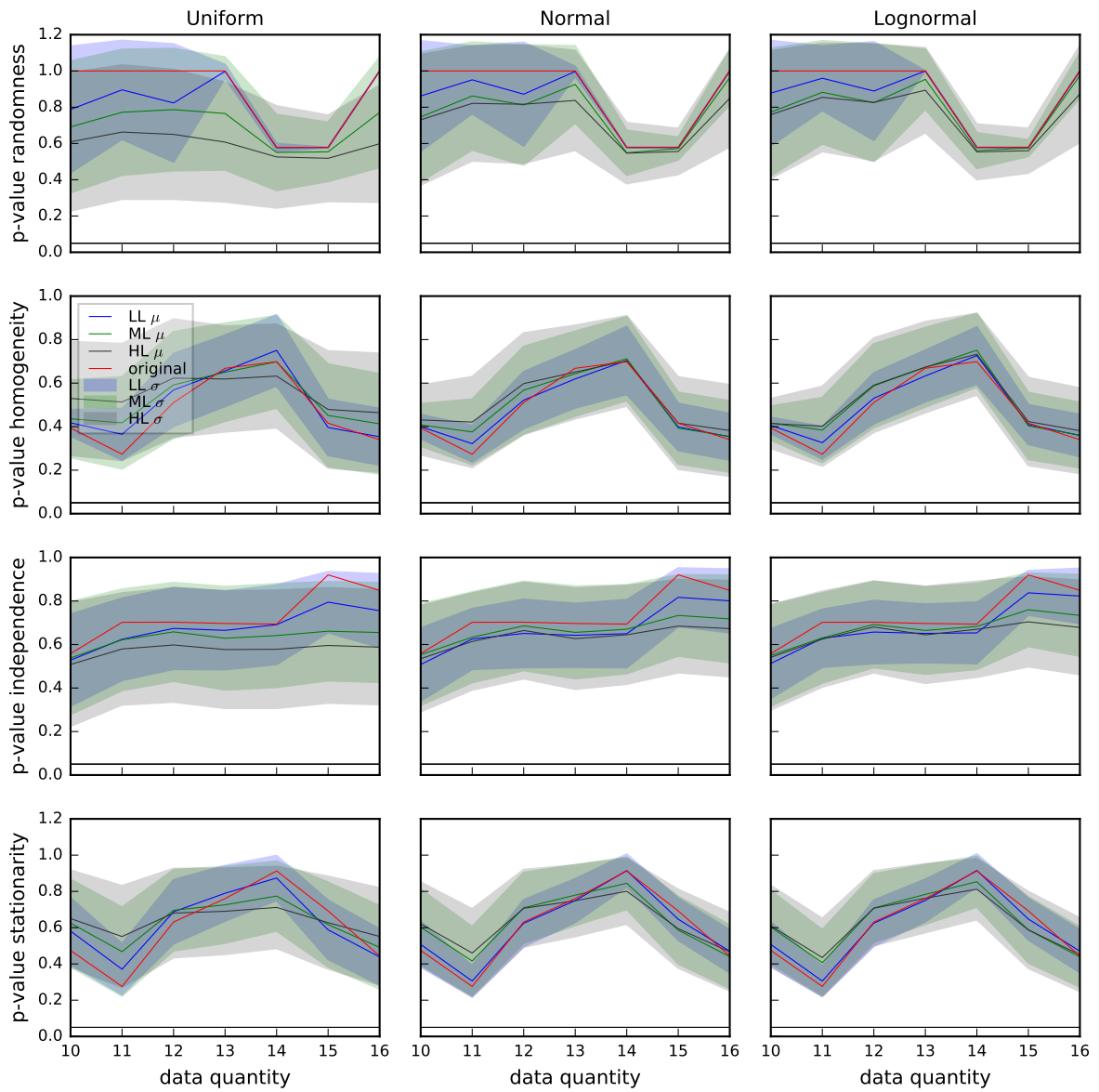
DO - IG5

Figure 173 – Evolution of RHIS p-values from DO loads time series from IG5. Red line = p-value from OTS. Blue, green, gray lines = average p-value from STS in LL, ML and HL scenarios, respectively. Blue, green, gray bands = std of p-values from STS in LL, ML and HL scenarios, respectively. Black line = significance level ($\alpha = 0.05$). Reject H_0 if p-value < 0.05
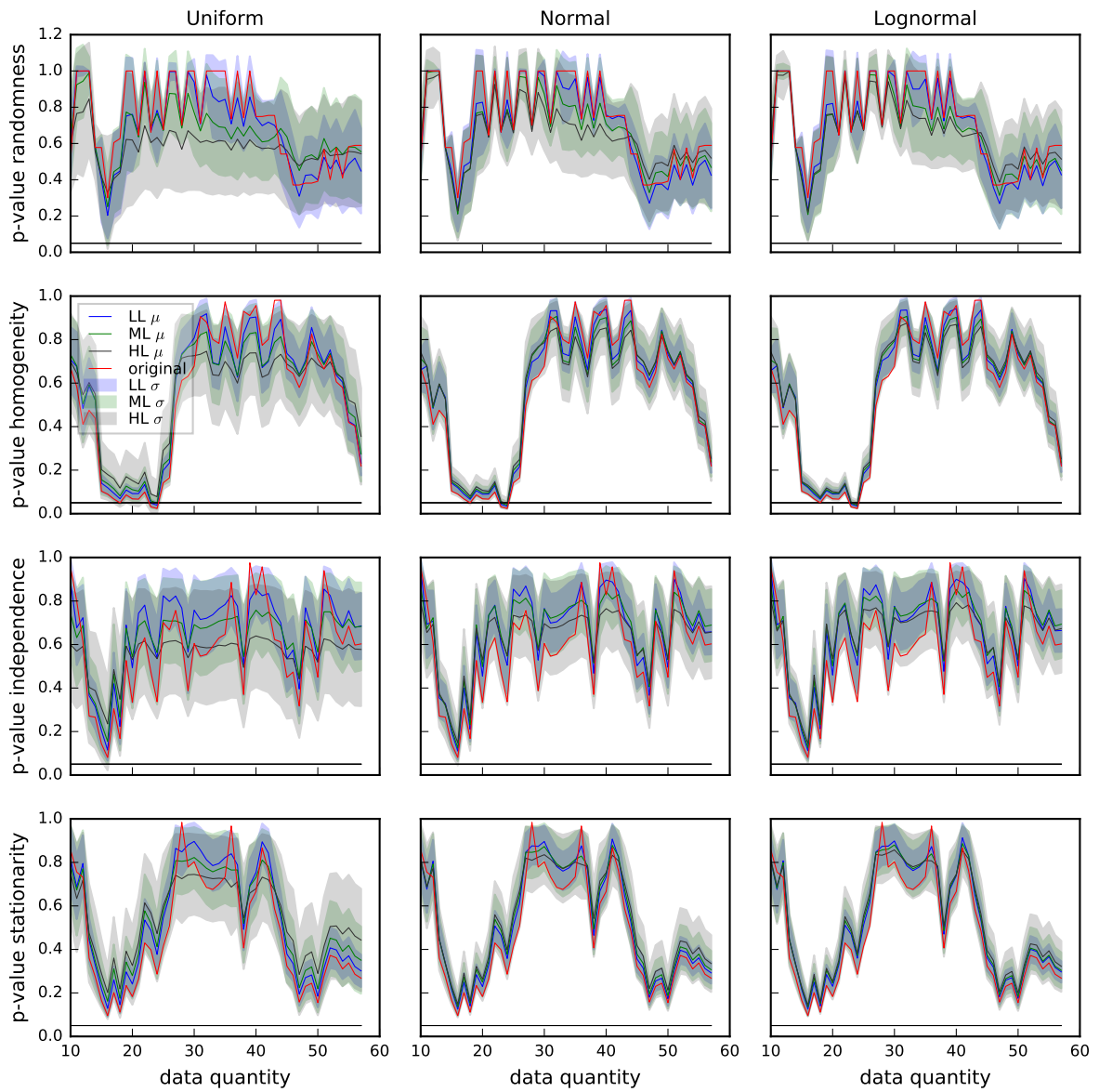
DO - IG6

Figure 174 – Evolution of RHIS p-values from DO loads time series from IG6. Red line = p-value from OTS. Blue, green, gray lines = average p-value from STS in LL, ML and HL scenarios, respectively. Blue, green, gray bands = std of p-values from STS in LL, ML and HL scenarios, respectively. Black line = significance level ($\alpha = 0.05$). Reject H_0 if p-value < 0.05
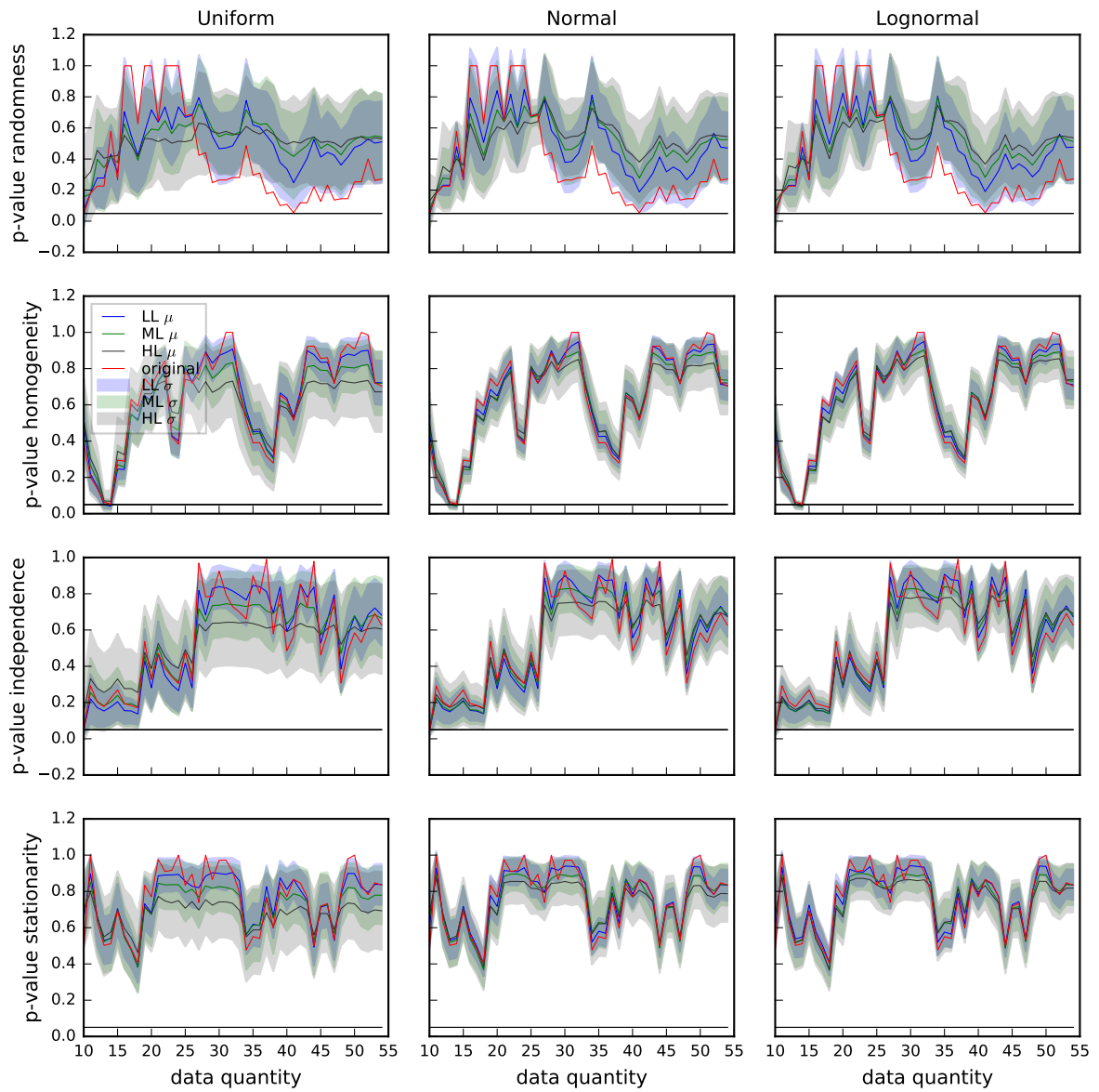
DO - IG7

Figure 175 – Evolution of RHIS p-values from DO loads time series from IG7. Red line = p-value from OTS. Blue, green, gray lines = average p-value from STS in LL, ML and HL scenarios, respectively. Blue, green, gray bands = std of p-values from STS in LL, ML and HL scenarios, respectively. Black line = significance level ($\alpha = 0.05$). Reject H_0 if p-value < 0.05
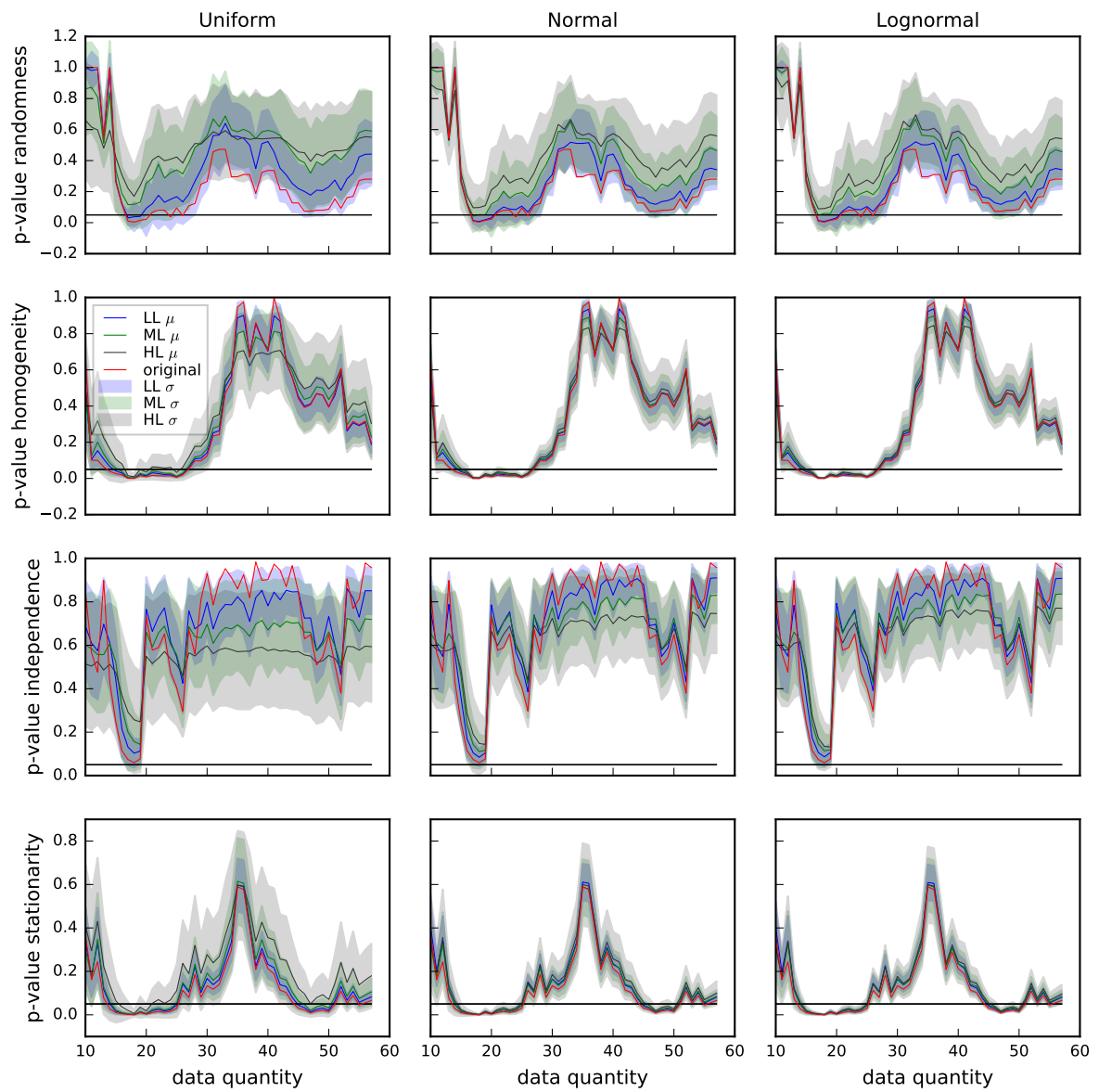
DOC - IG3

Figure 176 – Evolution of RHIS p-values from DOC loads time series from IG3. Red line = p-value from OTS. Blue, green, gray lines = average p-value from STS in LL, ML and HL scenarios, respectively. Blue, green, gray bands = std of p-values from STS in LL, ML and HL scenarios, respectively. Black line = significance level ($\alpha = 0.05$). Reject H_0 if p-value < 0.05

DOC - IG4

Figure 177 – Evolution of RHIS p-values from DOC loads time series from IG4. Red line = p-value from OTS. Blue, green, gray lines = average p-value from STS in LL, ML and HL scenarios, respectively. Blue, green, gray bands = std of p-values from STS in LL, ML and HL scenarios, respectively. Black line = significance level ($\alpha = 0.05$). Reject H$_0$ if p-value < 0.05
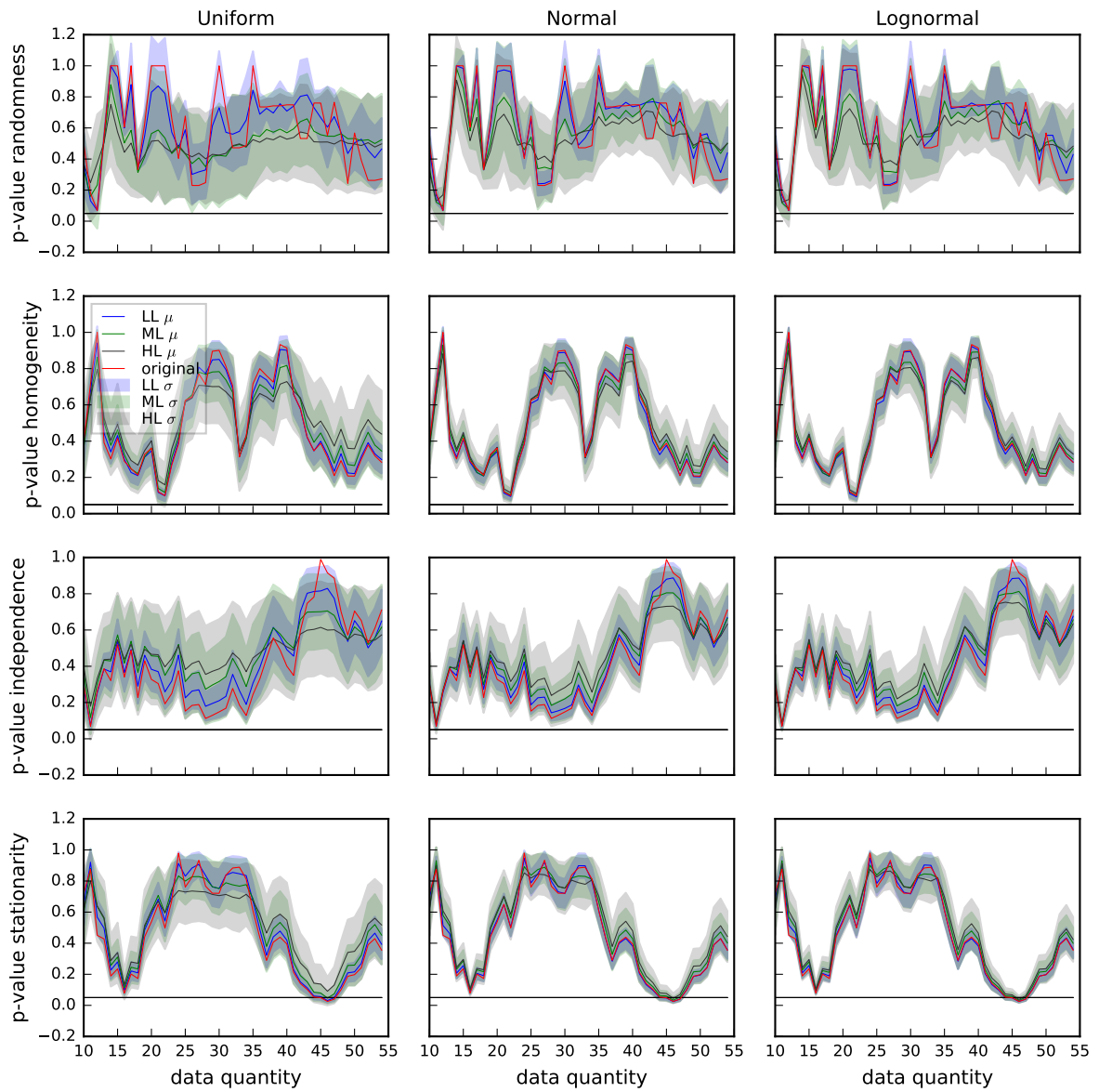
DOC - IG5

Figure 178 – Evolution of RHIS p-values from DOC loads time series from IG5. Red line = p-value from OTS. Blue, green, gray lines = average p-value from STS in LL, ML and HL scenarios, respectively. Blue, green, gray bands = std of p-values from STS in LL, ML and HL scenarios, respectively. Black line = significance level ($\alpha = 0.05$). Reject H_0 if p-value < 0.05
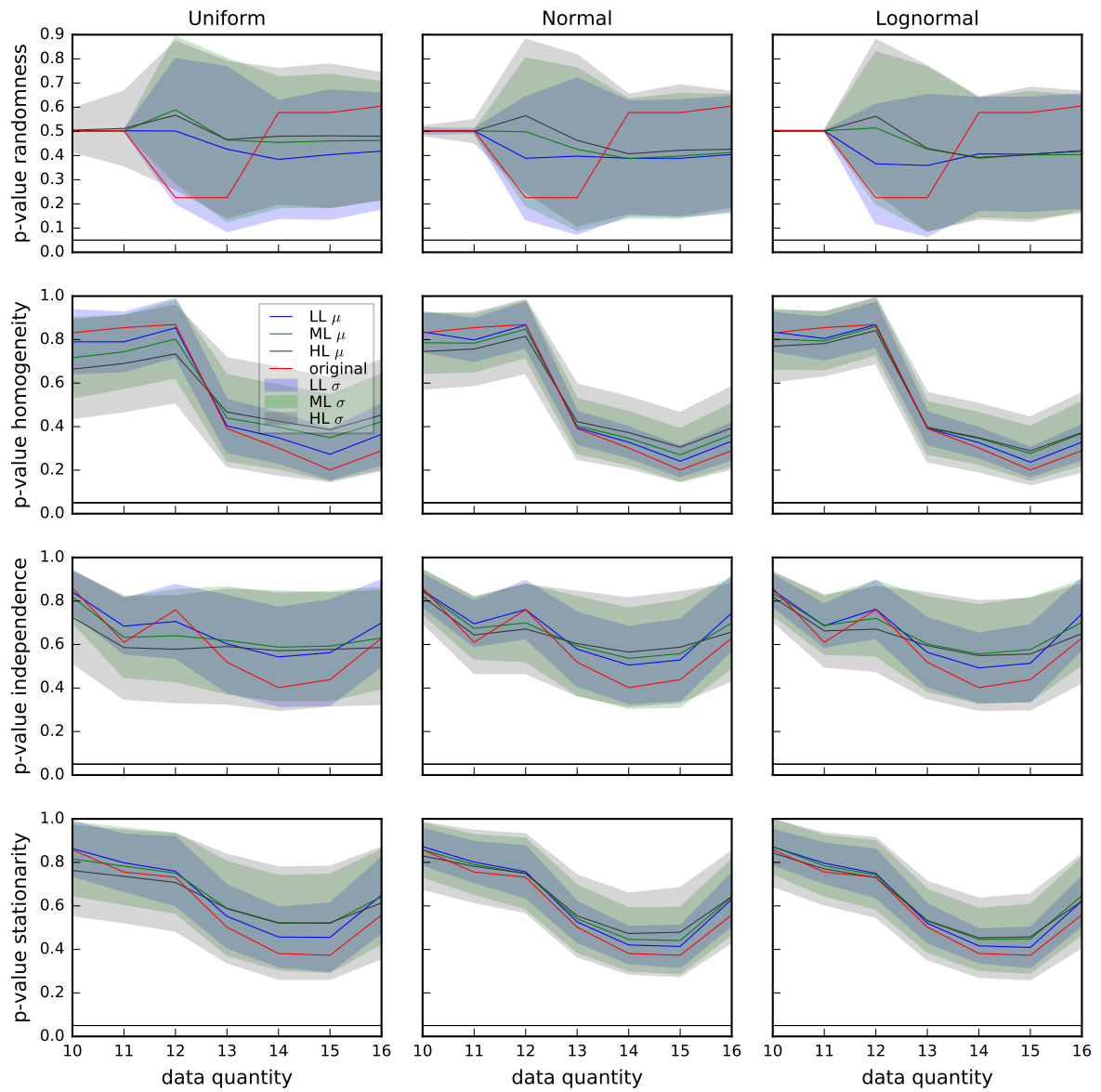
DOC - IG6

Figure 179 – Evolution of RHIS p-values from DOC loads time series from IG6. Red line = p-value from OTS. Blue, green, gray lines = average p-value from STS in LL, ML and HL scenarios, respectively. Blue, green, gray bands = std of p-values from STS in LL, ML and HL scenarios, respectively. Black line = significance level ($\alpha = 0.05$). Reject H_0 if p-value < 0.05

DOC - IG7

Figure 180 – Evolution of RHIS p-values from DOC loads time series from IG7. Red line = p-value from OTS. Blue, green, gray lines = average p-value from STS in LL, ML and HL scenarios, respectively. Blue, green, gray bands = std of p-values from STS in LL, ML and HL scenarios, respectively. Black line = significance level ($\alpha = 0.05$). Reject H_0 if p-value < 0.05

NH4 - IG3

Figure 181 – Evolution of RHIS p-values from NH4 loads time series from IG3. Red line = p-value from OTS. Blue, green, gray lines = average p-value from STS in LL, ML and HL scenarios, respectively. Blue, green, gray bands = std of p-values from STS in LL, ML and HL scenarios, respectively. Black line = significance level ($\alpha = 0.05$). Reject H_0 if p-value < 0.05

NH4 - IG4

Figure 182 – Evolution of RHIS p-values from NH4 loads time series from IG4. Red line = p-value from OTS. Blue, green, gray lines = average p-value from STS in LL, ML and HL scenarios, respectively. Blue, green, gray bands = std of p-values from STS in LL, ML and HL scenarios, respectively. Black line = significance level ($\alpha = 0.05$). Reject H_0 if p-value < 0.05

NH4 - IG5

Figure 183 – Evolution of RHIS p-values from NH4 loads time series from IG5. Red line = p-value from OTS. Blue, green, gray lines = average p-value from STS in LL, ML and HL scenarios, respectively. Blue, green, gray bands = std of p-values from STS in LL, ML and HL scenarios, respectively. Black line = significance level ($\alpha = 0.05$). Reject H_0 if p-value < 0.05

NH4 - IG6

Figure 184 – Evolution of RHIS p-values from NH4 loads time series from IG6. Red line = p-value from OTS. Blue, green, gray lines = average p-value from STS in LL, ML and HL scenarios, respectively. Blue, green, gray bands = std of p-values from STS in LL, ML and HL scenarios, respectively. Black line = significance level (α = 0.05). Reject H_0 if p-value < 0.05

NH4 - IG7

Figure 185 – Evolution of RHIS p-values from NH4 loads time series from IG7. Red line = p-value from OTS. Blue, green, gray lines = average p-value from STS in LL, ML and HL scenarios, respectively. Blue, green, gray bands = std of p-values from STS in LL, ML and HL scenarios, respectively. Black line = significance level (α = 0.05). Reject H_0 if p-value < 0.05

TP - IG3

Figure 186 – Evolution of RHIS p-values from TP loads time series from IG3. Red line = p-value from OTS. Blue, green, gray lines = average p-value from STS in LL, ML and HL scenarios, respectively. Blue, green, gray bands = std of p-values from STS in LL, ML and HL scenarios, respectively. Black line = significance level ($\alpha = 0.05$). Reject H_0 if p-value < 0.05

Figure 187 – Evolution of RHIS p-values from TP loads time series from IG4. Red line = p-value from OTS. Blue, green, gray lines = average p-value from STS in LL, ML and HL scenarios, respectively. Blue, green, gray bands = std of p-values from STS in LL, ML and HL scenarios, respectively. Black line = significance level ($\alpha = 0.05$). Reject H_0 if p-value < 0.05

TP - IG5

Figure 188 – Evolution of RHIS p-values from TP loads time series from IG5. Red line = p-value from OTS. Blue, green, gray lines = average p-value from STS in LL, ML and HL scenarios, respectively. Blue, green, gray bands = std of p-values from STS in LL, ML and HL scenarios, respectively. Black line = significance level ($\alpha = 0.05$). Reject H_0 if p-value < 0.05

TP - IG6

Figure 189 – Evolution of RHIS p-values from TP loads time series from IG6. Red line = p-value from OTS. Blue, green, gray lines = average p-value from STS in LL, ML and HL scenarios, respectively. Blue, green, gray bands = std of p-values from STS in LL, ML and HL scenarios, respectively. Black line = significance level (α = 0.05). Reject H_0 if p-value < 0.05

TP - IG7

Figure 190 – Evolution of RHIS p-values from TP loads time series from IG7. Red line = p-value from OTS. Blue, green, gray lines = average p-value from STS in LL, ML and HL scenarios, respectively. Blue, green, gray bands = std of p-values from STS in LL, ML and HL scenarios, respectively. Black line = significance level ($\alpha = 0.05$). Reject H_0 if p-value < 0.05

VDS - IG3

Figure 191 – Evolution of RHIS p-values from VDS loads time series from IG3. Red line = p-value from OTS. Blue, green, gray lines = average p-value from STS in LL, ML and HL scenarios, respectively. Blue, green, gray bands = std of p-values from STS in LL, ML and HL scenarios, respectively. Black line = significance level ($\alpha = 0.05$). Reject H_0 if p-value < 0.05

VDS - IG4

Figure 192 – Evolution of RHIS p-values from VDS loads time series from IG4. Red line = p-value from OTS. Blue, green, gray lines = average p-value from STS in LL, ML and HL scenarios, respectively. Blue, green, gray bands = std of p-values from STS in LL, ML and HL scenarios, respectively. Black line = significance level ($\alpha = 0.05$). Reject H_0 if p-value < 0.05

VDS - IG5

Figure 193 – Evolution of RHIS p-values from VDS loads time series from IG5. Red line = p-value from OTS. Blue, green, gray lines = average p-value from STS in LL, ML and HL scenarios, respectively. Blue, green, gray bands = std of p-values from STS in LL, ML and HL scenarios, respectively. Black line = significance level ($\alpha = 0.05$). Reject H_0 if p-value < 0.05

VDS - IG6

Figure 194 – Evolution of RHIS p-values from VDS loads time series from IG6. Red line = p-value from OTS. Blue, green, gray lines = average p-value from STS in LL, ML and HL scenarios, respectively. Blue, green, gray bands = std of p-values from STS in LL, ML and HL scenarios, respectively. Black line = significance level ($\alpha = 0.05$). Reject H$_0$ if p-value < 0.05

VDS - IG7

Figure 195 – Evolution of RHIS p-values from VDS loads time series from IG7. Red line = p-value from OTS. Blue, green, gray lines = average p-value from STS in LL, ML and HL scenarios, respectively. Blue, green, gray bands = std of p-values from STS in LL, ML and HL scenarios, respectively. Black line = significance level ($\alpha = 0.05$). Reject H_0 if p-value < 0.05

APPENDIX B – Data and results from photos and movies

B.1 Time series and boxplots

BOD - IG3
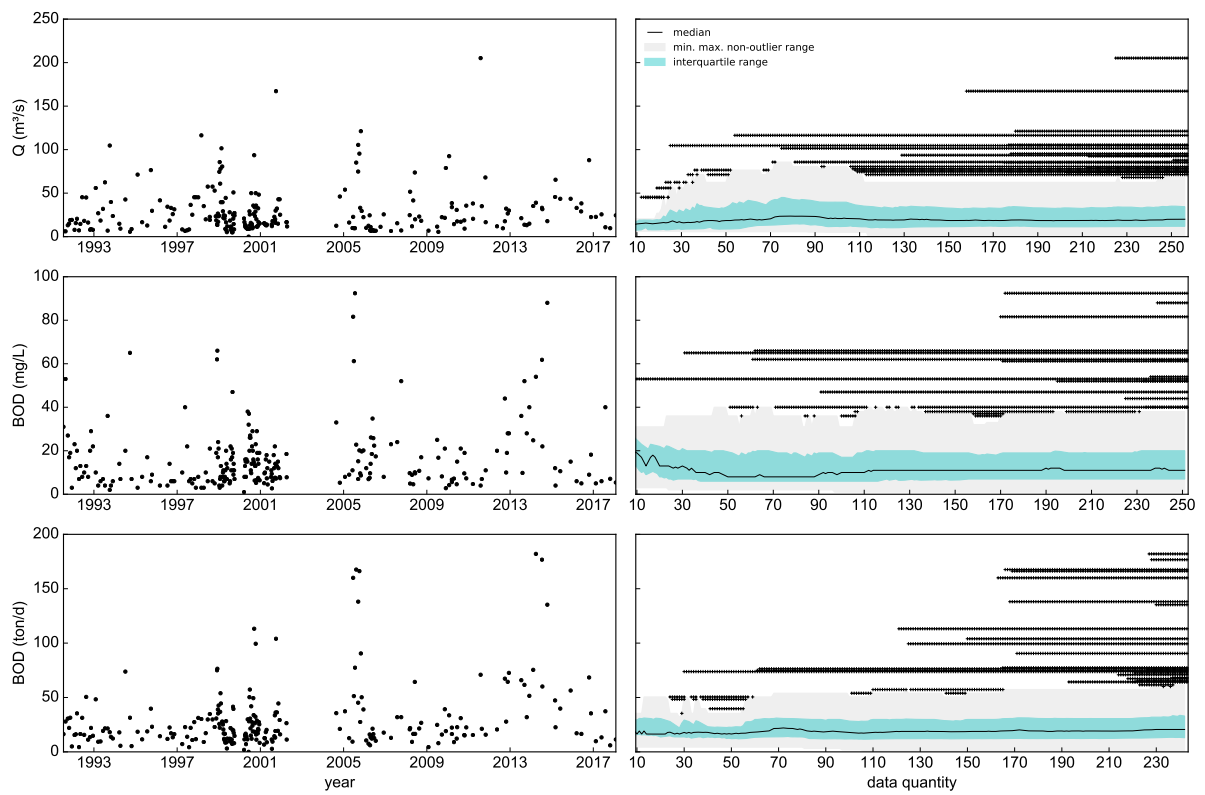
Figure 196 – Time series and boxplot evolution. Q, BOD concentrations and loads, station IG3. Updated boxplots at each data, starting with 10 elements and ending with all data. The min. max. non-outlier range is the range defined by the minimum and maximum non-outlier values. The outlier values are represented by black crosses.
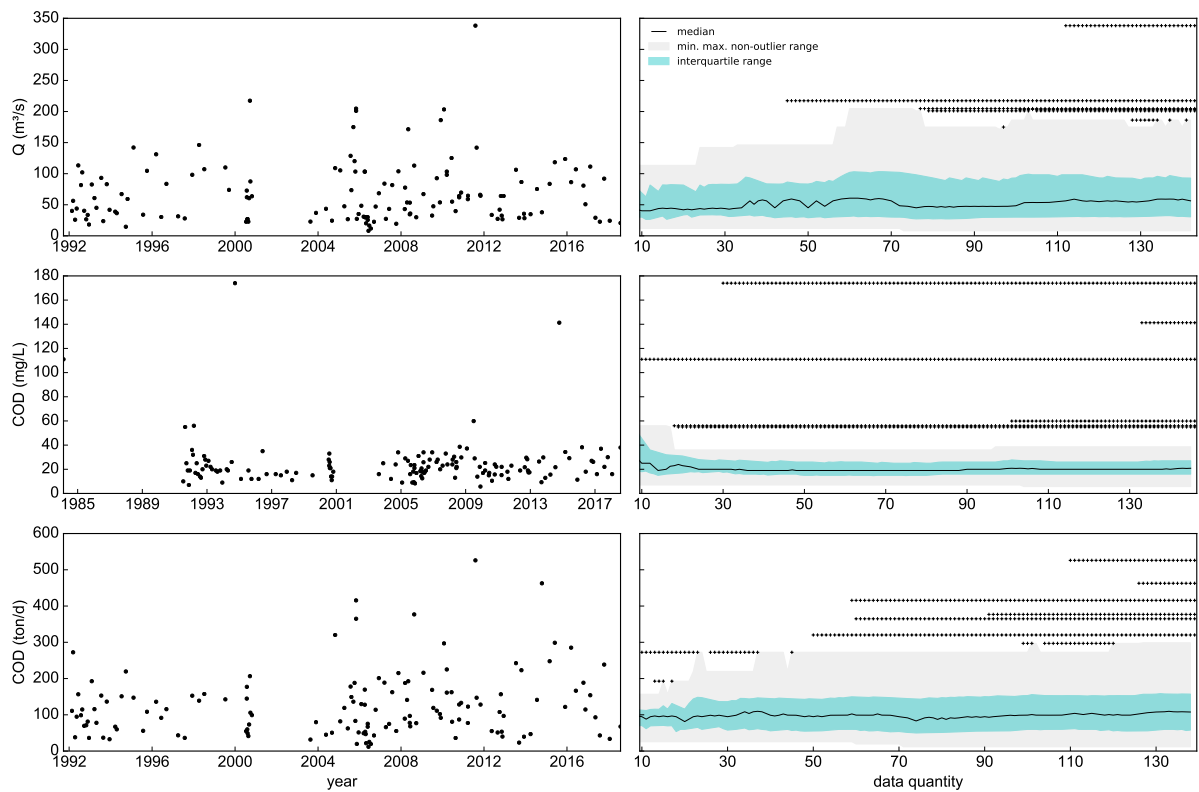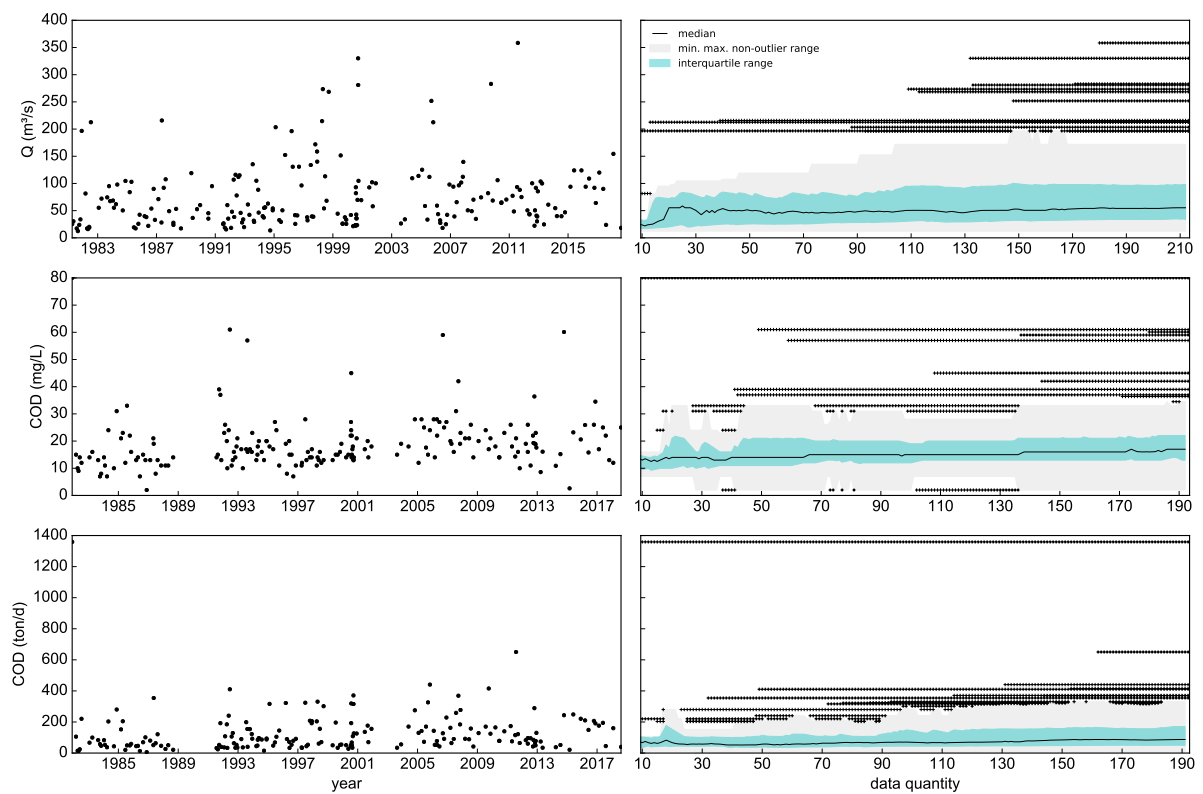
BOD - IG4
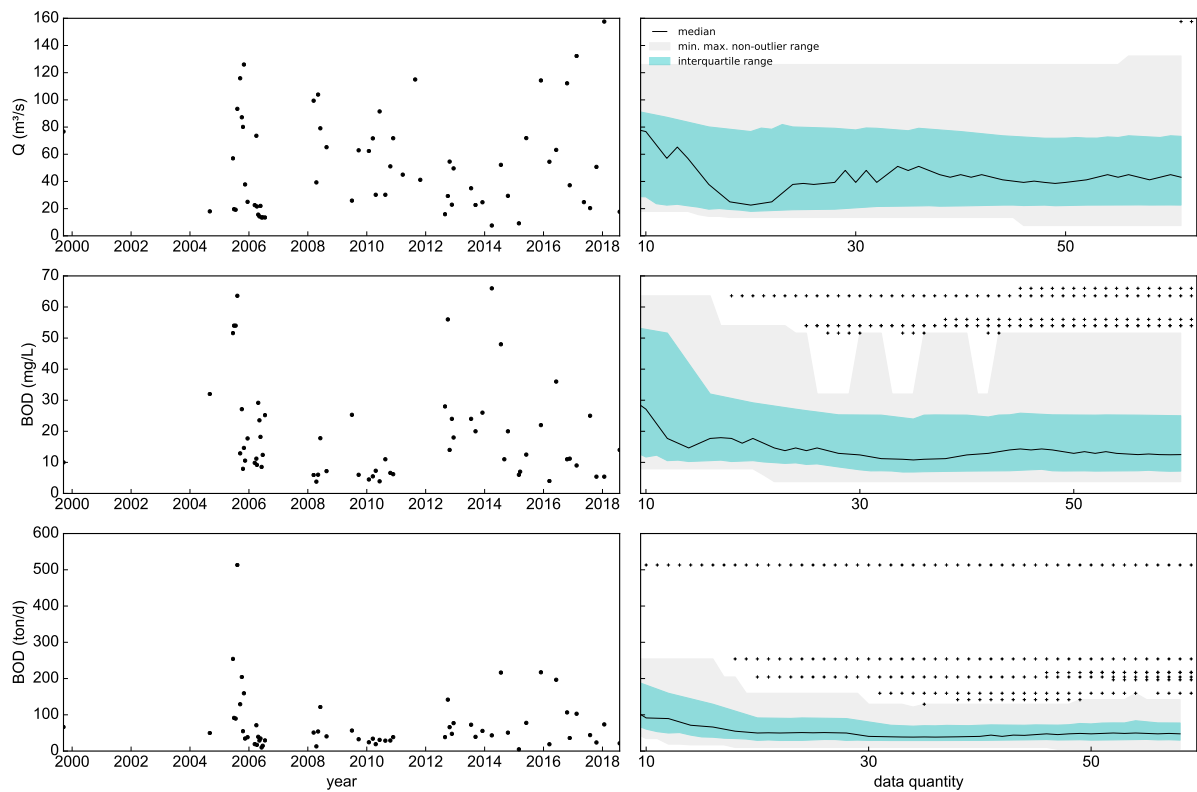
Figure 197 – Time series and boxplot evolution. Q, BOD concentrations and loads, station IG4. Updated boxplots at each data, starting with 10 elements and ending with all data. The min. max. non-outlier range is the range defined by the minimum and maximum non-outlier values. The outlier values are represented by black crosses.

BOD - IG5
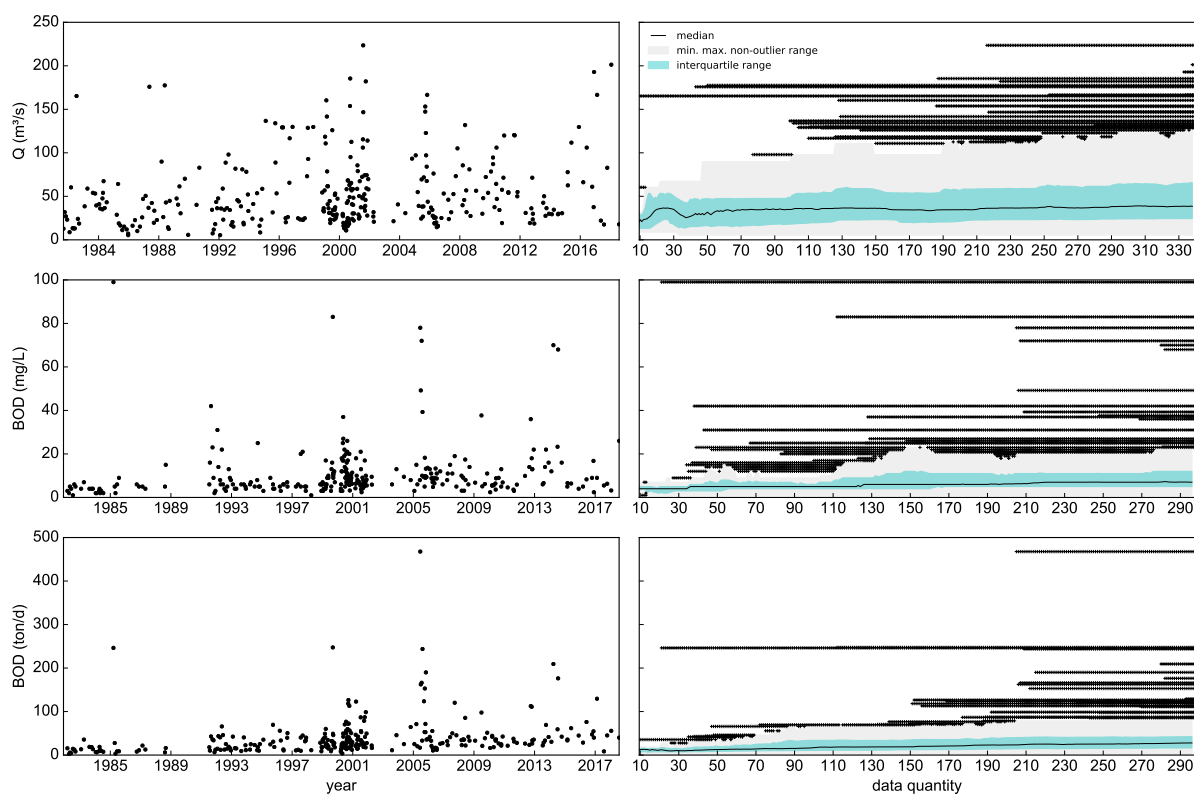
Figure 198 – Time series and boxplot evolution. Q, BOD concentrations and loads, station IG5. Updated boxplots at each data, starting with 10 elements and ending with all data. The min. max. non-outlier range is the range defined by the minimum and maximum non-outlier values. The outlier values are represented by black crosses.
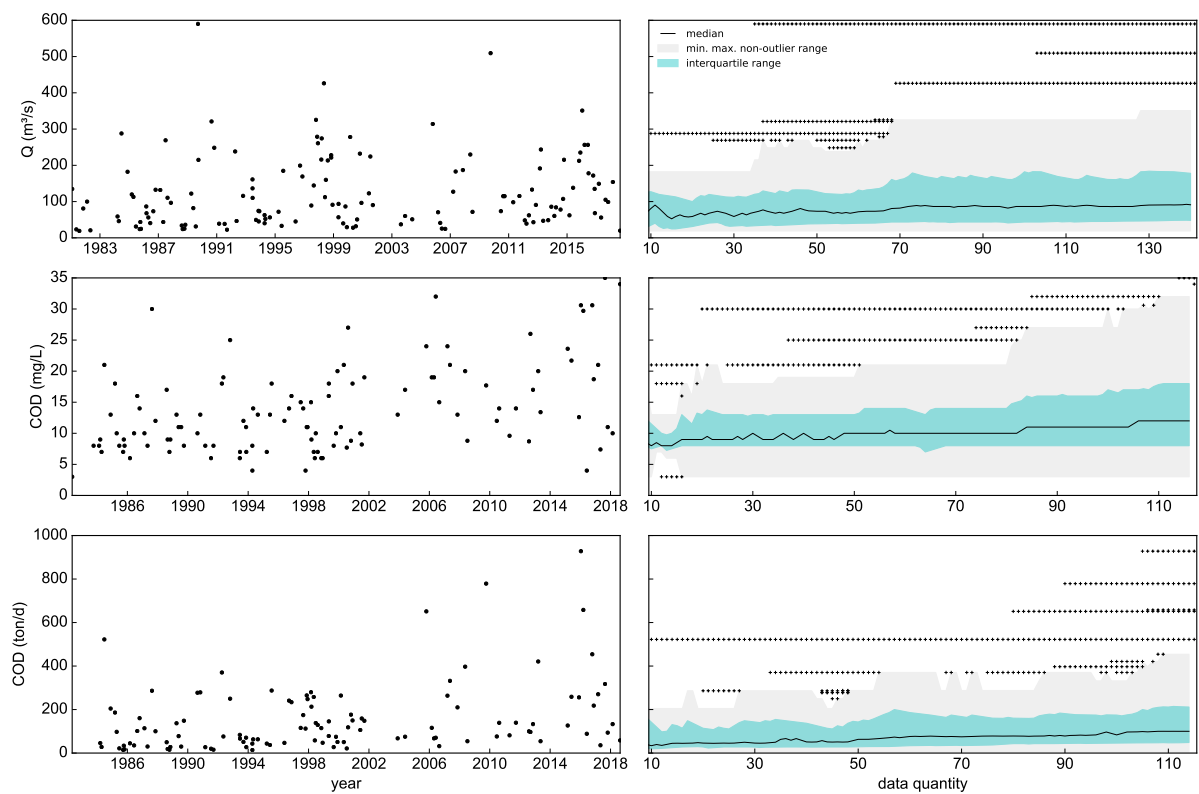
BOD - IG6
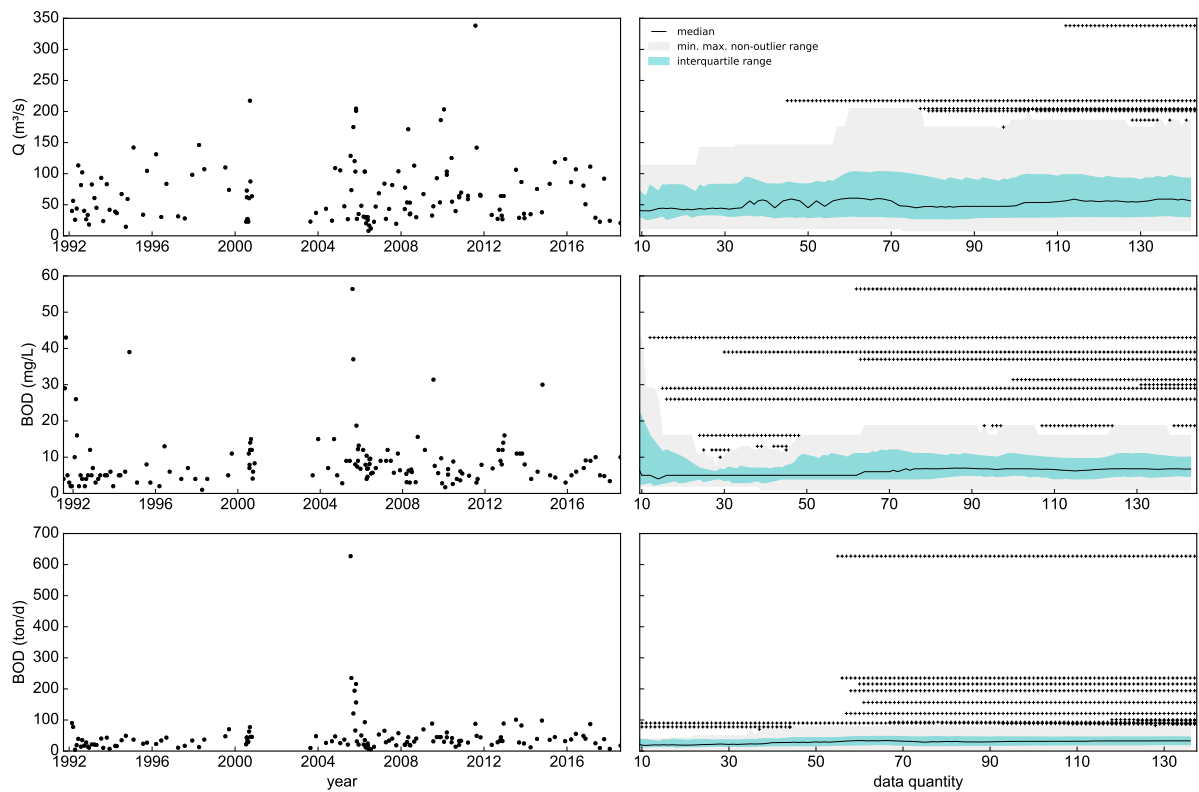
Figure 199 – Time series and boxplot evolution. Q, BOD concentrations and loads, station IG6. Updated boxplots at each data, starting with 10 elements and ending with all data. The min. max. non-outlier range is the range defined by the minimum and maximum non-outlier values. The outlier values are represented by black crosses.
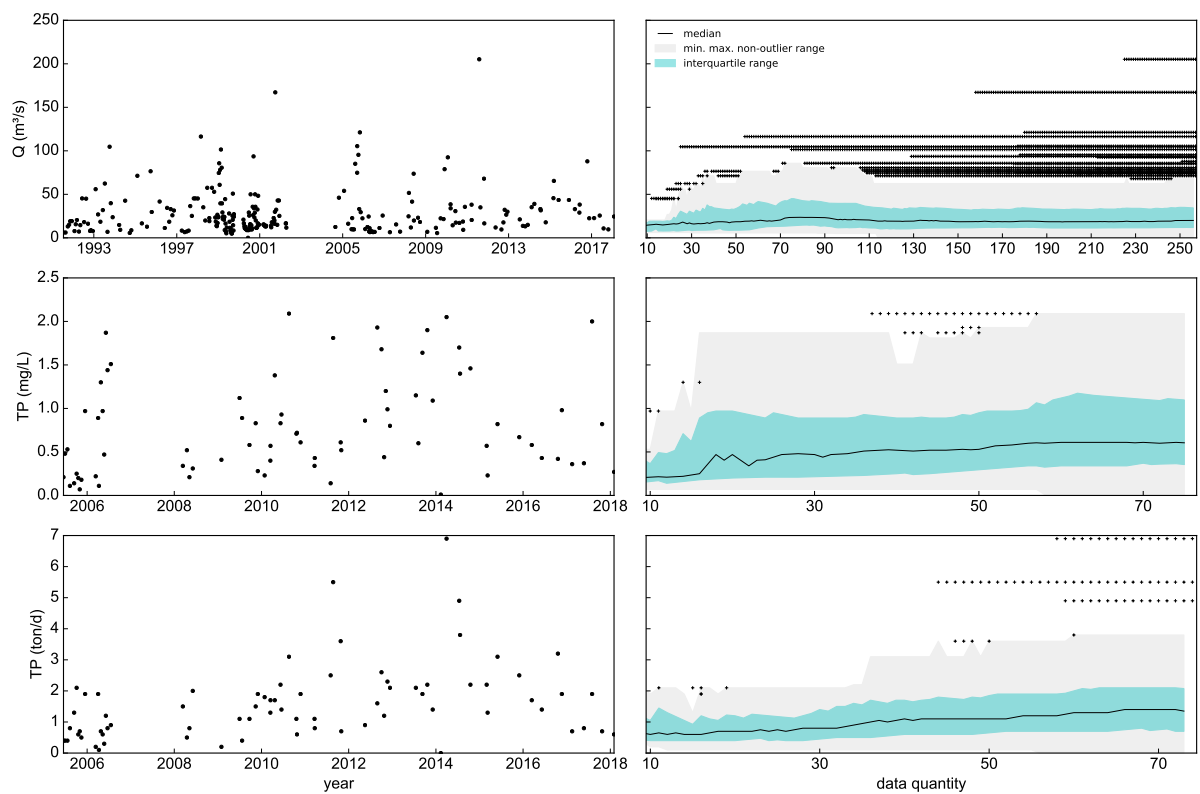
BOD - IG7
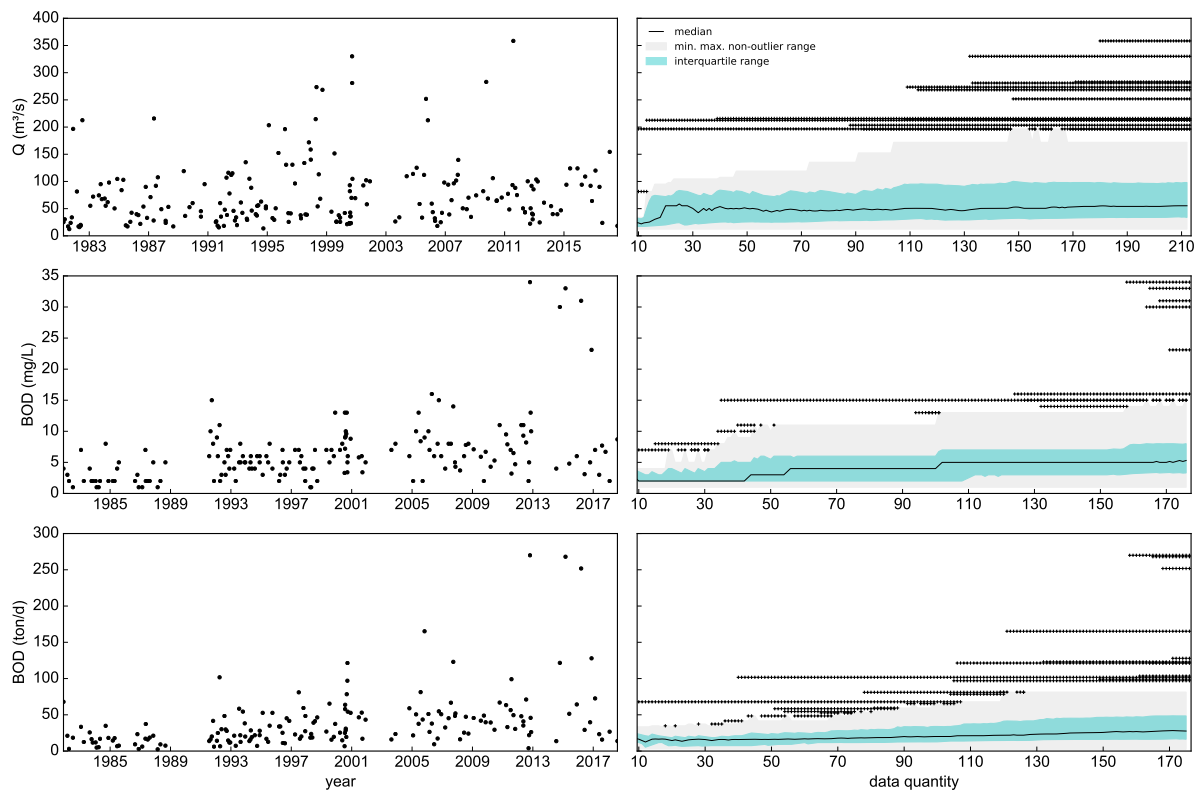
Figure 200 – Time series and boxplot evolution. Q, BOD concentrations and loads, station IG7. Updated boxplots at each data, starting with 10 elements and ending with all data. The min. max. non-outlier range is the range defined by the minimum and maximum non-outlier values. The outlier values are represented by black crosses.
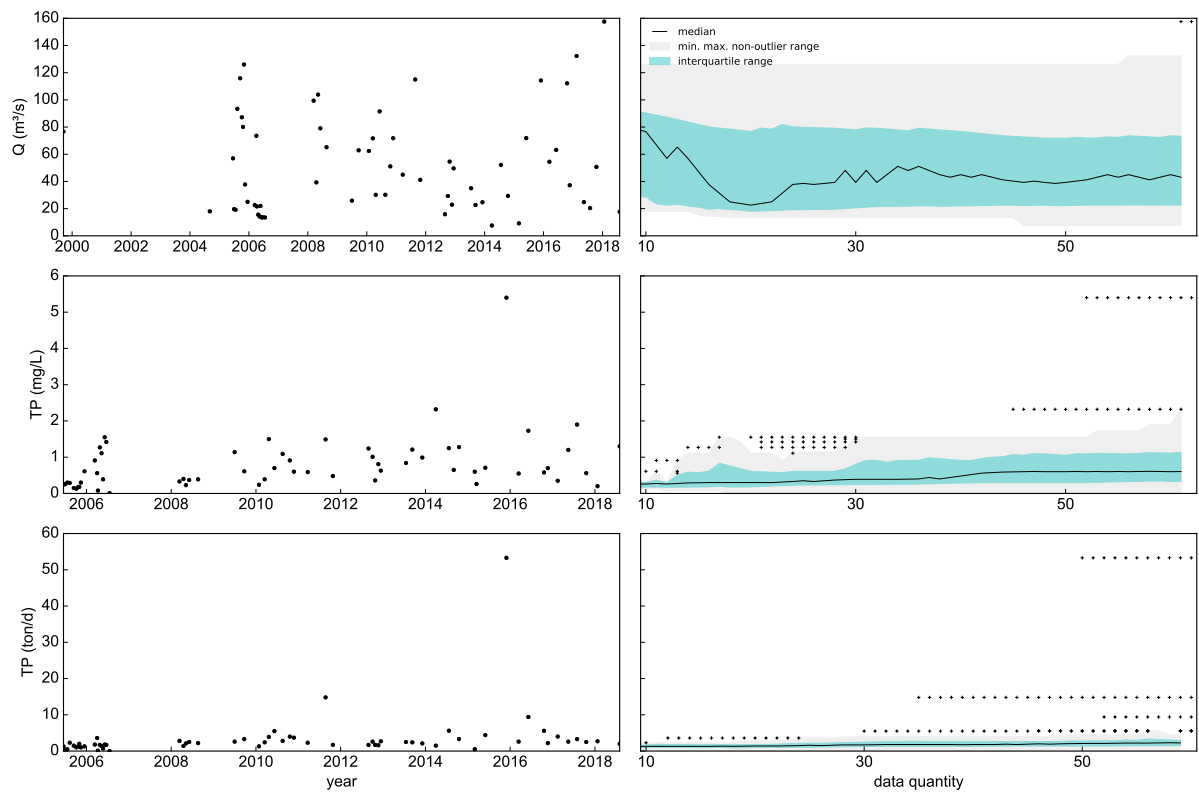
BOD - IG8
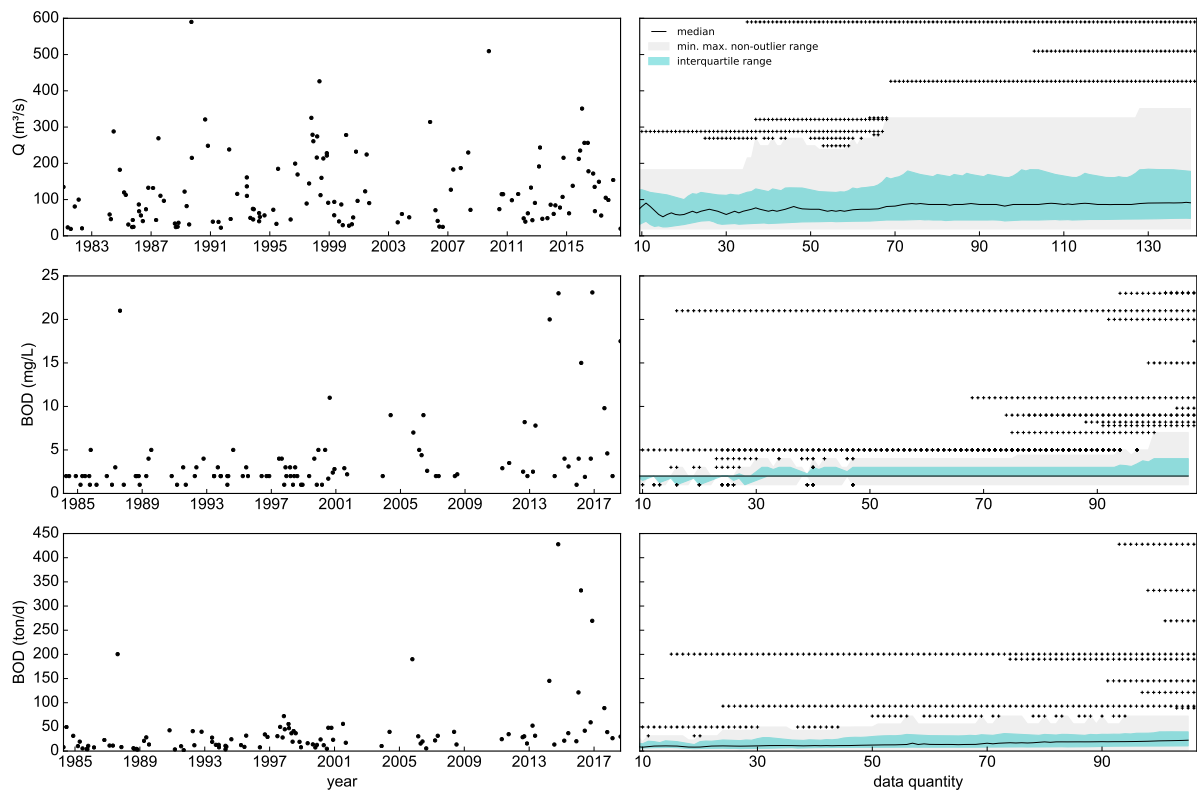
Figure 201 – Time series and boxplot evolution. Q, BOD concentrations and loads, station IG8. Updated boxplots at each data, starting with 10 elements and ending with all data. The min. max. non-outlier range is the range defined by the minimum and maximum non-outlier values. The outlier values are represented by black crosses.
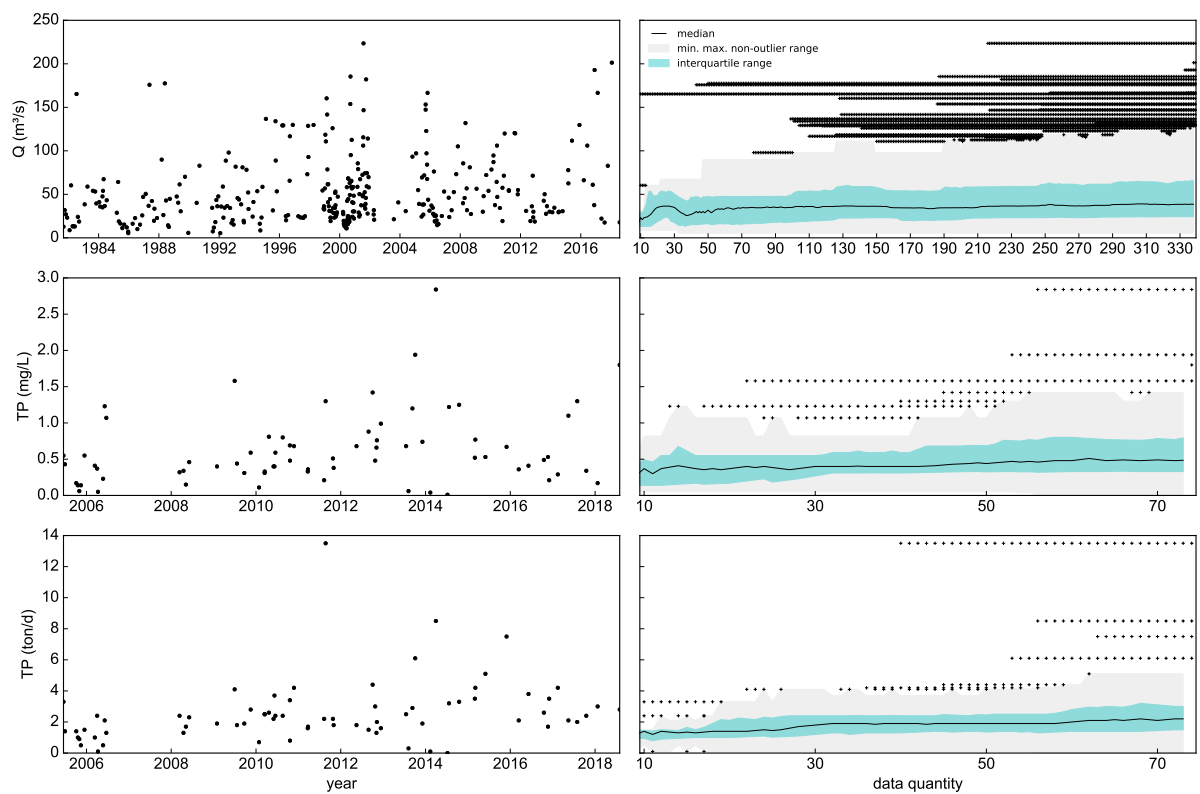
NH4 - IG3
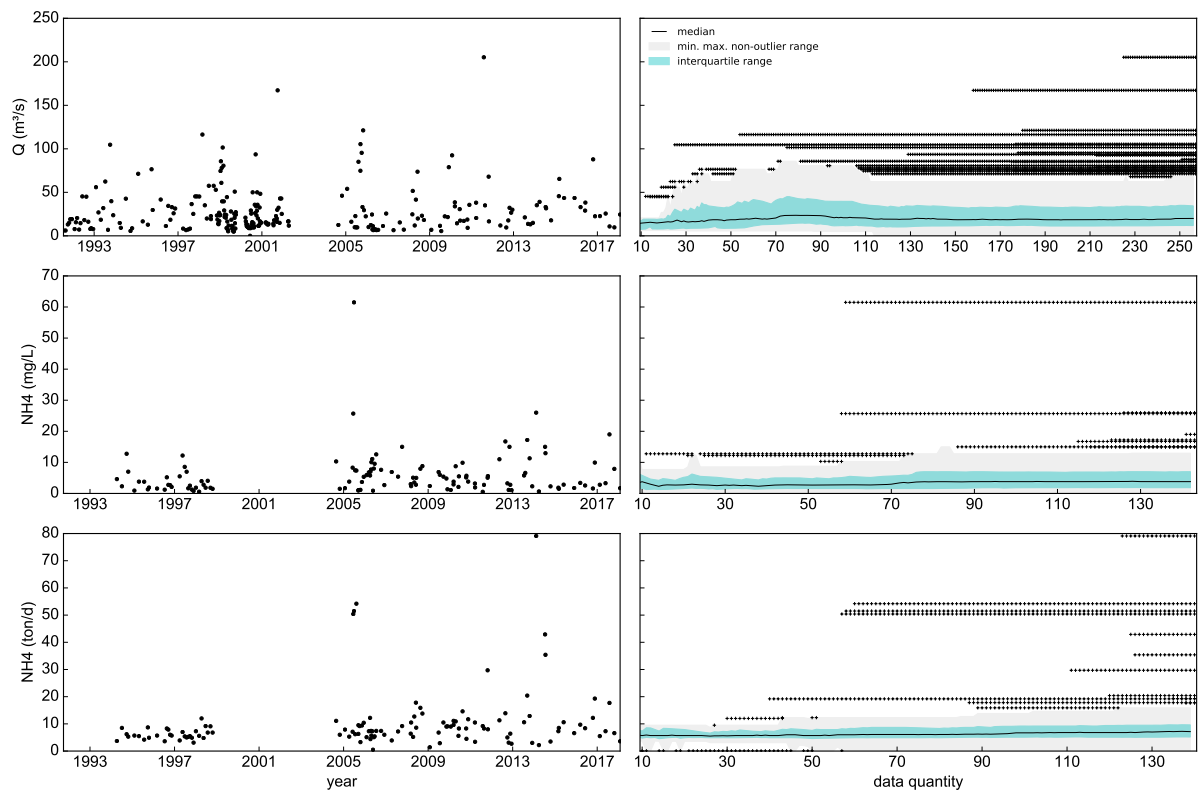
Figure 202 – Time series and boxplot evolution. Q, NH4 concentrations and loads, station IG3. Updated boxplots at each data, starting with 10 elements and ending with all data. The min. max. non-outlier range is the range defined by the minimum and maximum non-outlier values. The outlier values are represented by black crosses.
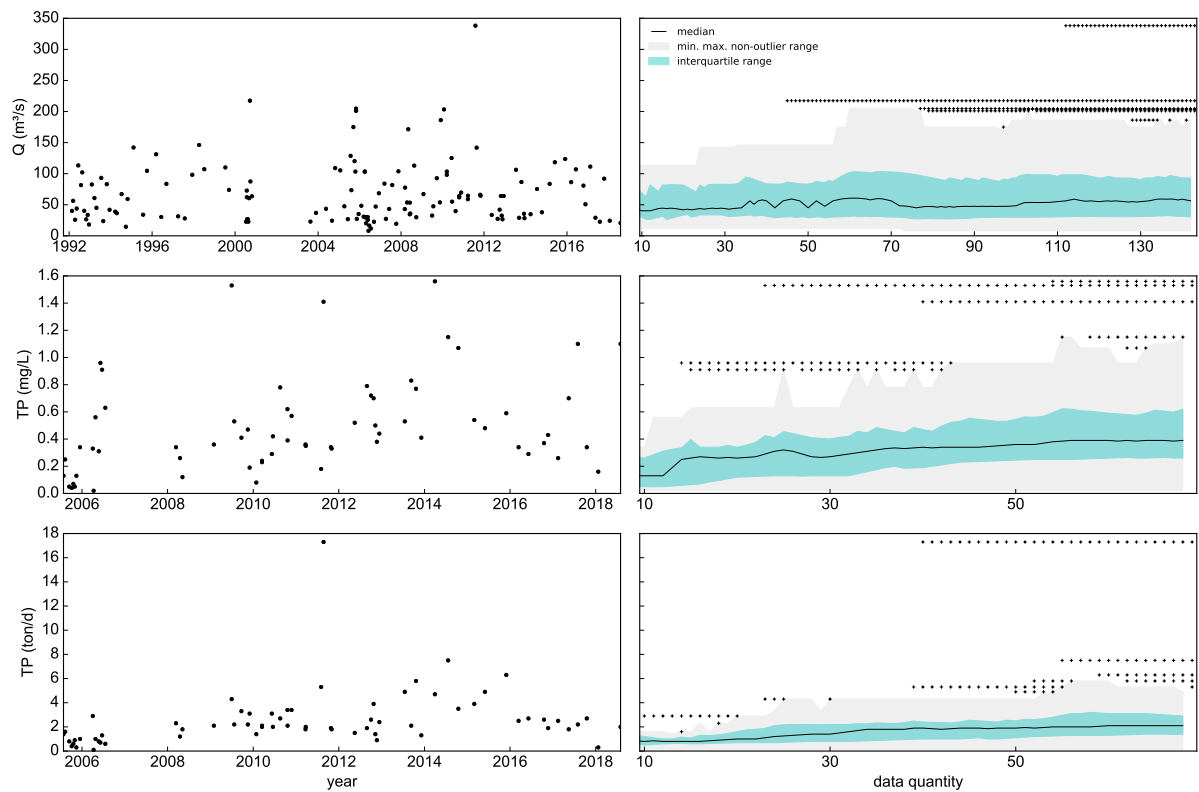
NH4 - IG4
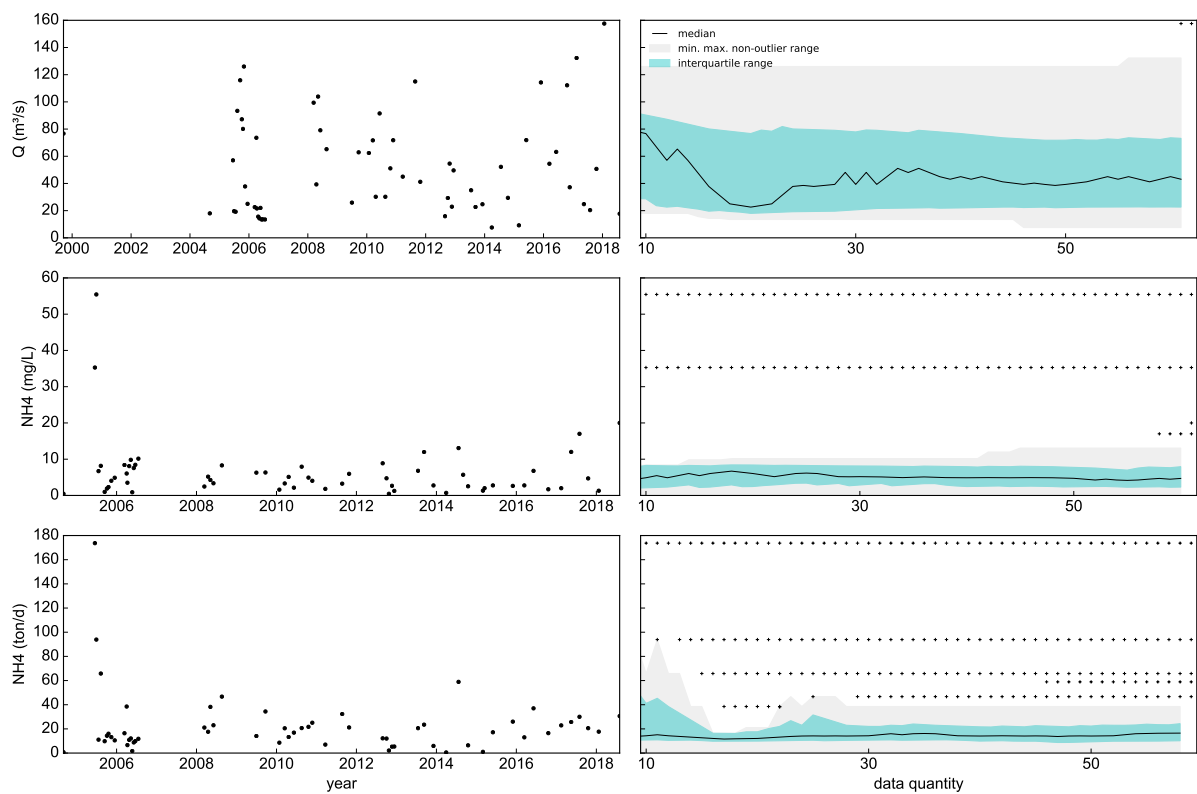
Figure 203 – Time series and boxplot evolution. Q, NH4 concentrations and loads, station IG4. Updated boxplots at each data, starting with 10 elements and ending with all data. The min. max. non-outlier range is the range defined by the minimum and maximum non-outlier values. The outlier values are represented by black crosses.

NH4 - IG5
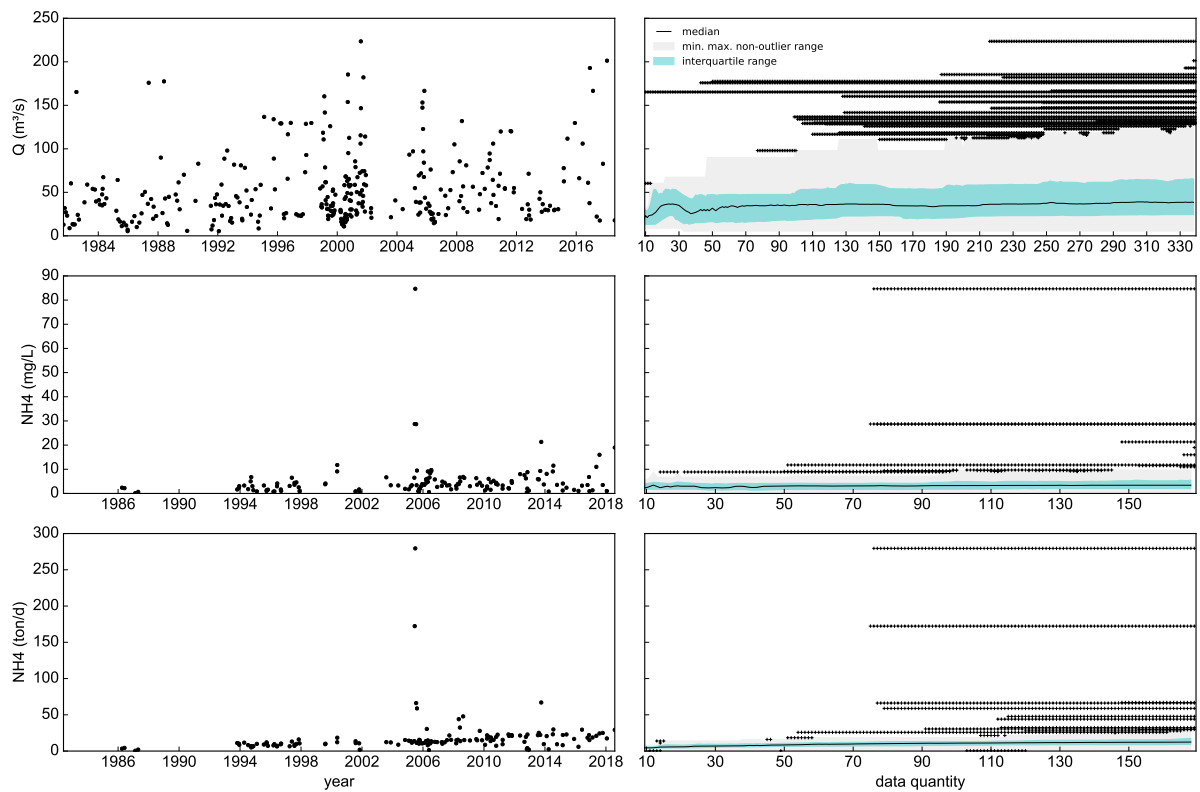
Figure 204 – Time series and boxplot evolution. Q, NH4 concentrations and loads, station IG5. Updated boxplots at each data, starting with 10 elements and ending with all data. The min. max. non-outlier range is the range defined by the minimum and maximum non-outlier values. The outlier values are represented by black crosses.
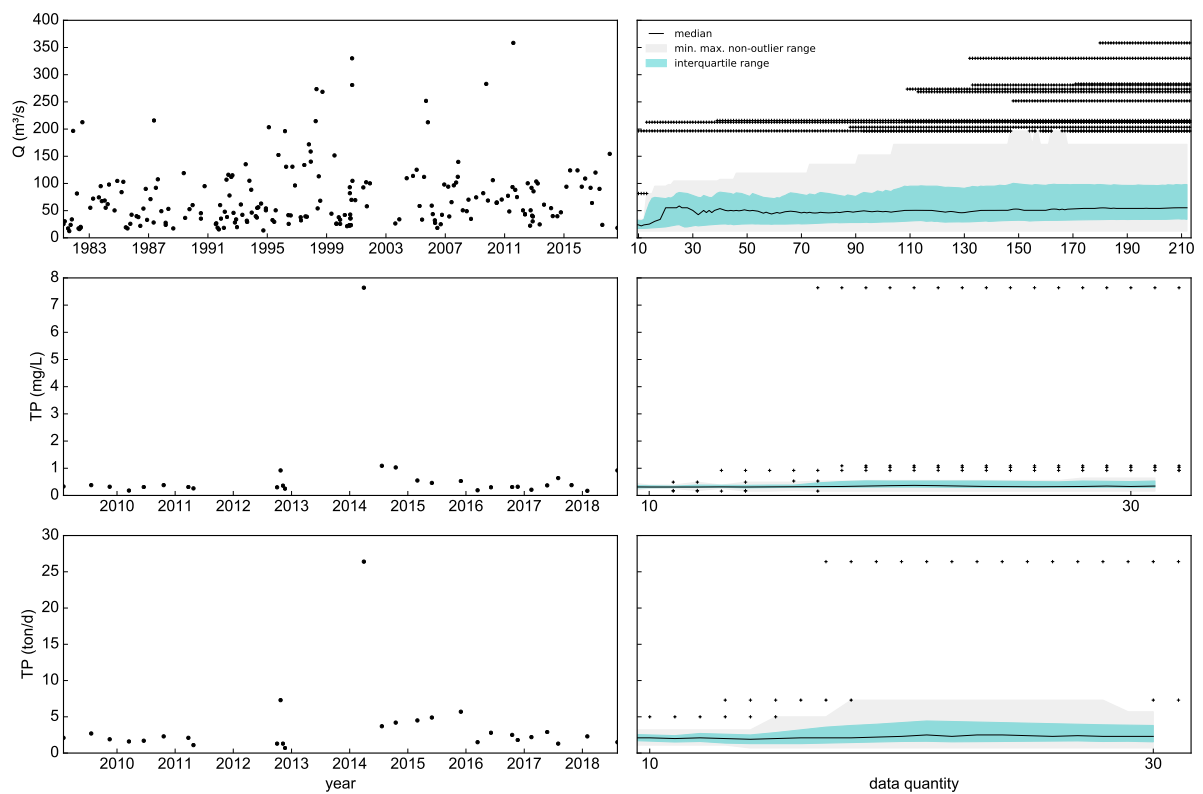
NH4 - IG6
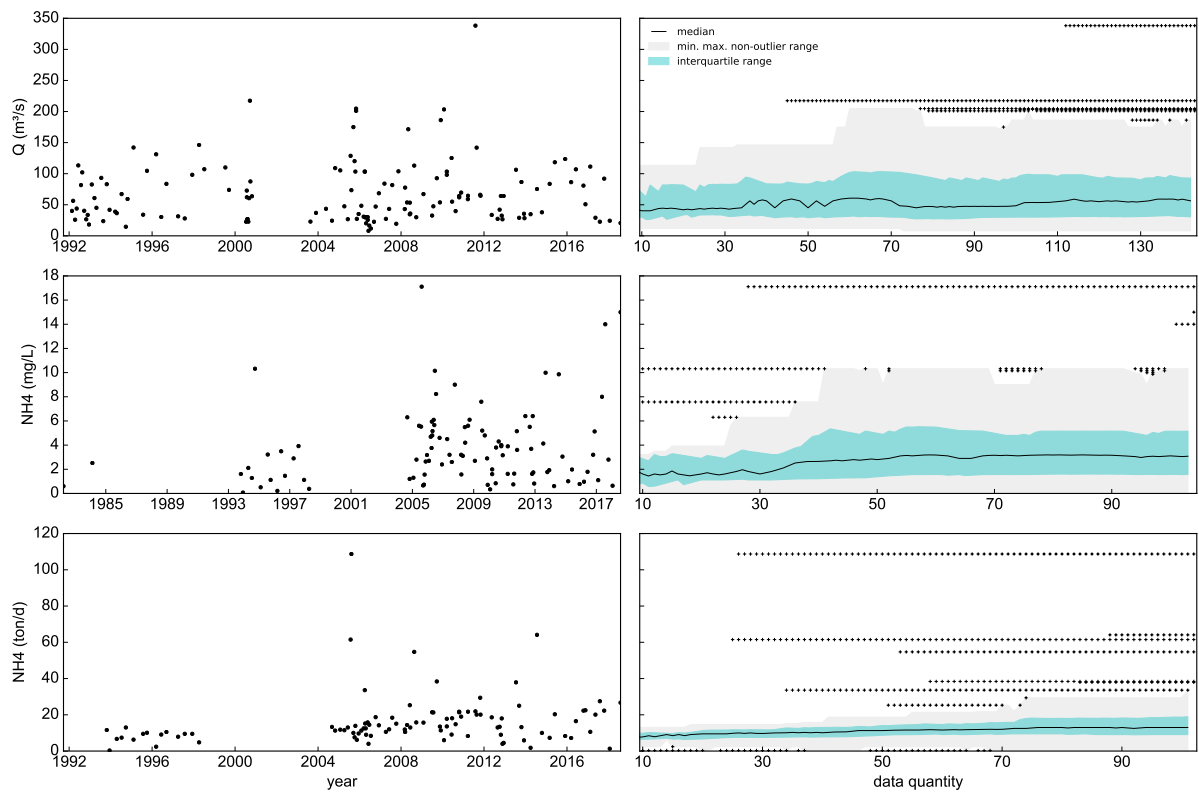
Figure 205 – Time series and boxplot evolution. Q, NH4 concentrations and loads, station IG6. Updated boxplots at each data, starting with 10 elements and ending with all data. The min. max. non-outlier range is the range defined by the minimum and maximum non-outlier values. The outlier values are represented by black crosses.
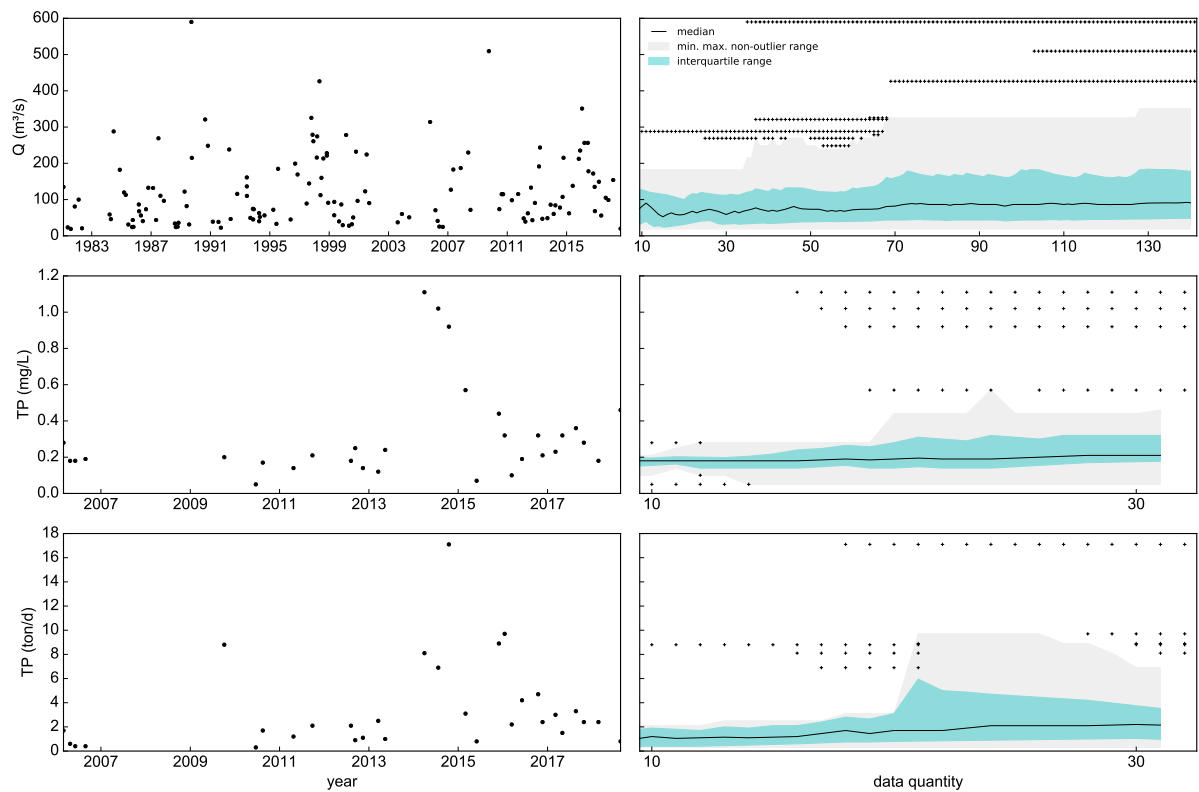
NH4 - IG7
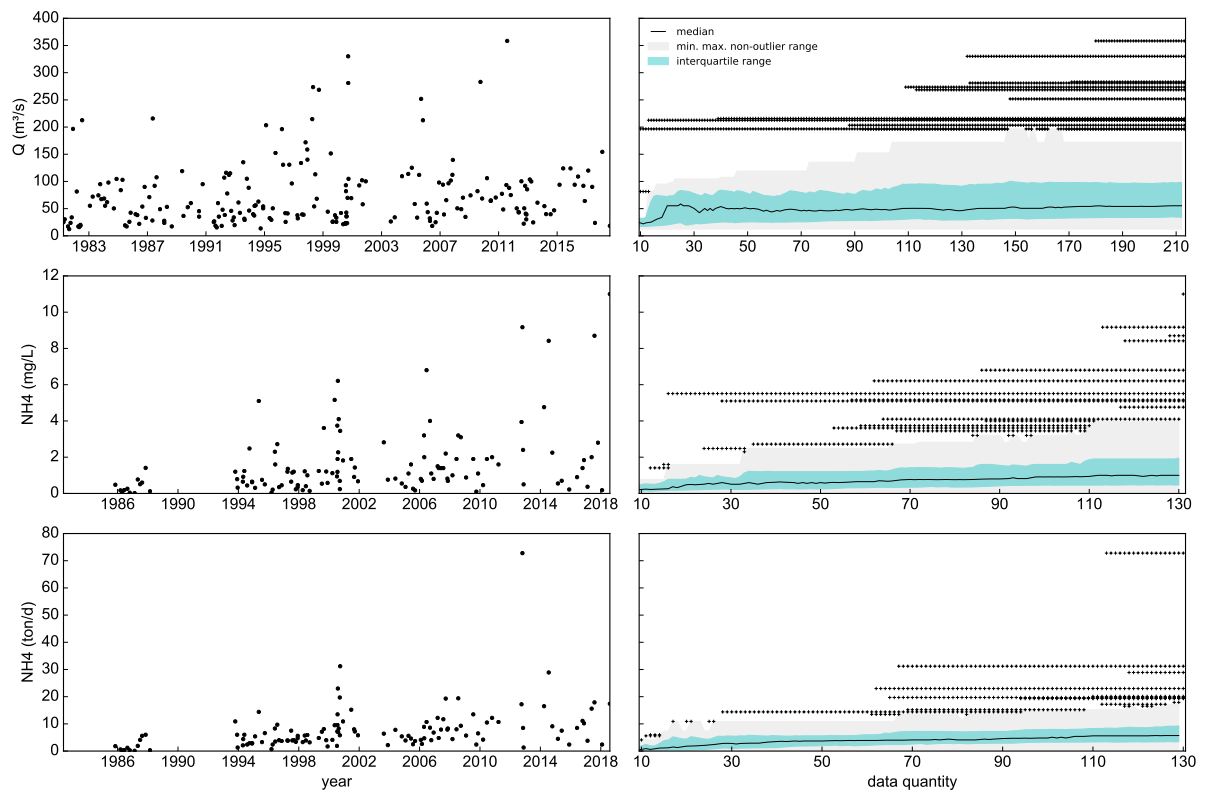
Figure 206 – Time series and boxplot evolution. Q, NH4 concentrations and loads, station IG7. Updated boxplots at each data, starting with 10 elements and ending with all data. The min. max. non-outlier range is the range defined by the minimum and maximum non-outlier values. The outlier values are represented by black crosses.
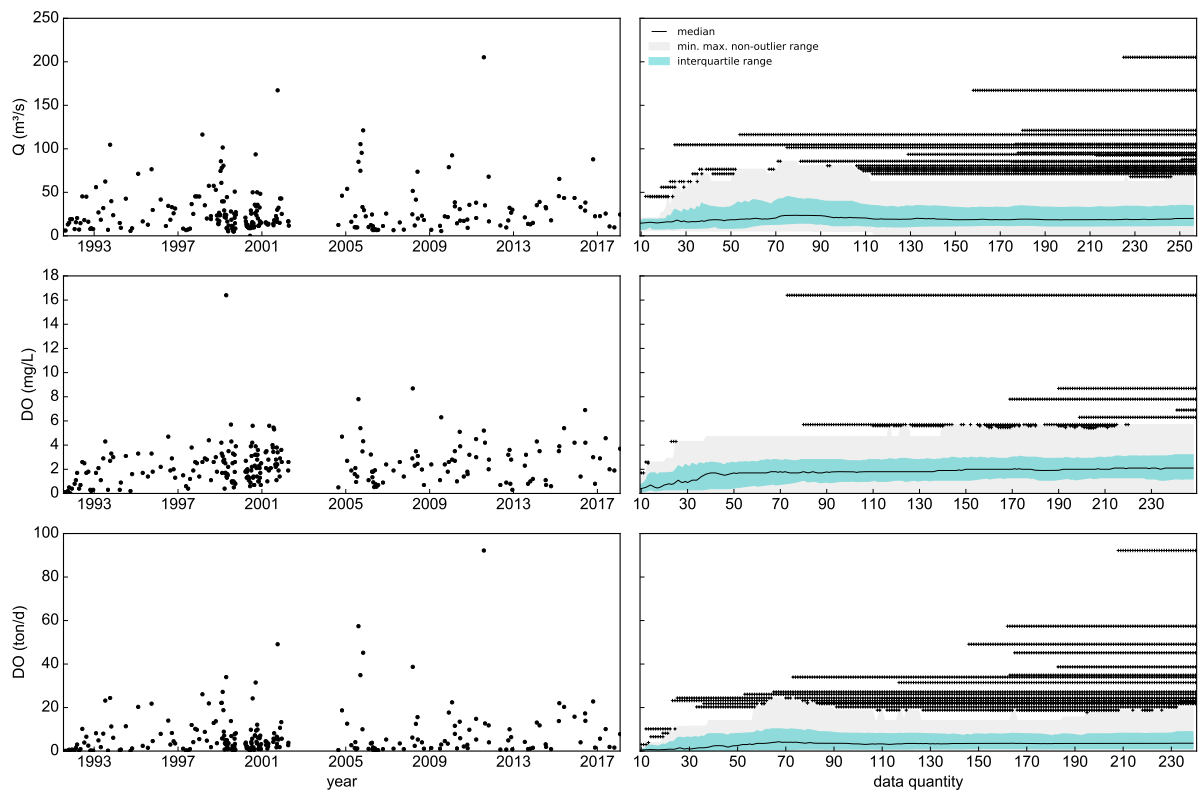
NH4 - IG8
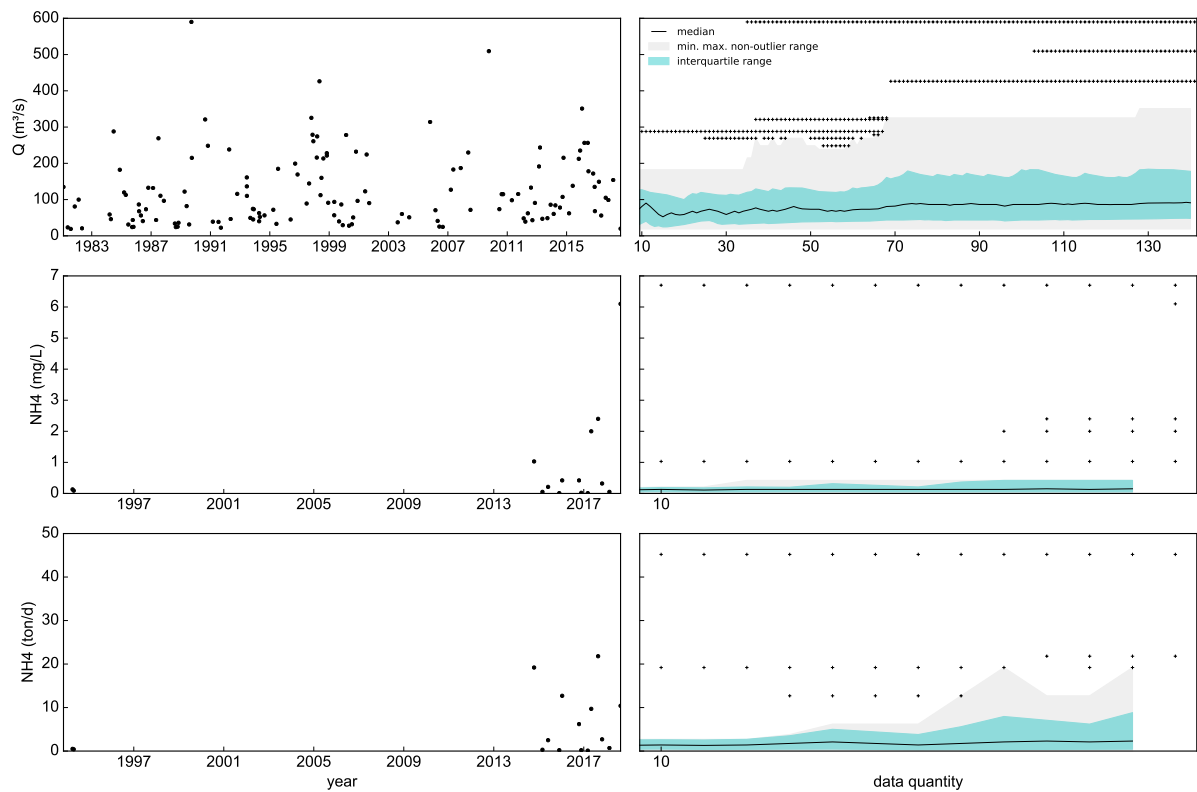
Figure 207 – Time series and boxplot evolution. Q, NH4 concentrations and loads, station IG8. Updated boxplots at each data, starting with 10 elements and ending with all data. The min. max. non-outlier range is the range defined by the minimum and maximum non-outlier values. The outlier values are represented by black crosses.
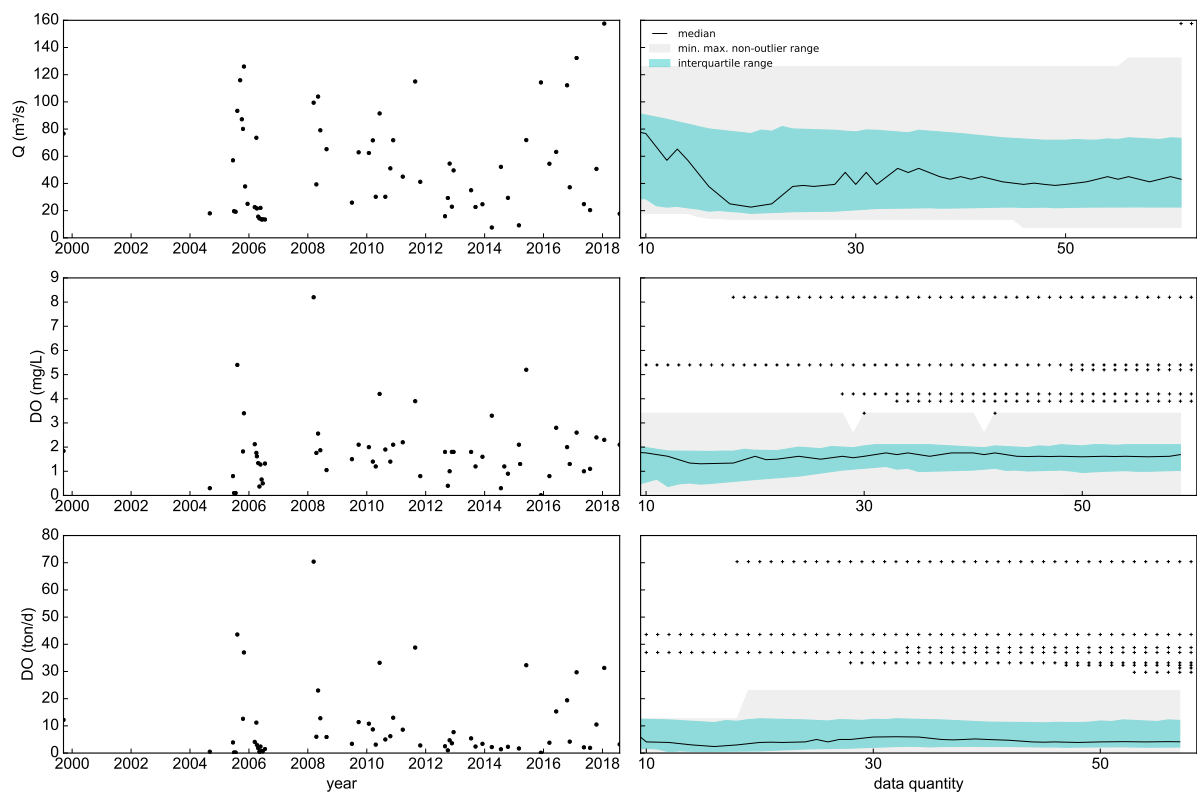
COD - IG3
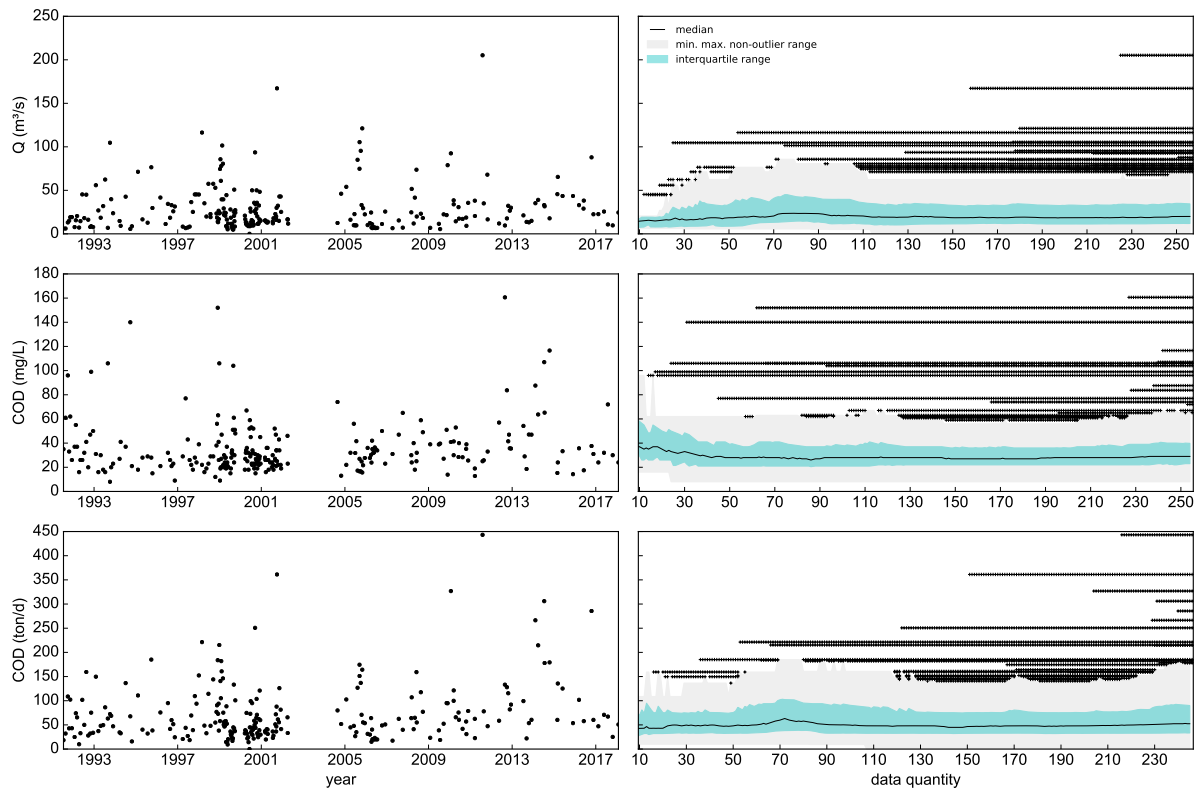
Figure 208 – Time series and boxplot evolution. Q, COD concentrations and loads, station IG3. Updated boxplots at each data, starting with 10 elements and ending with all data. The min. max. non-outlier range is the range defined by the minimum and maximum non-outlier values. The outlier values are represented by black crosses.
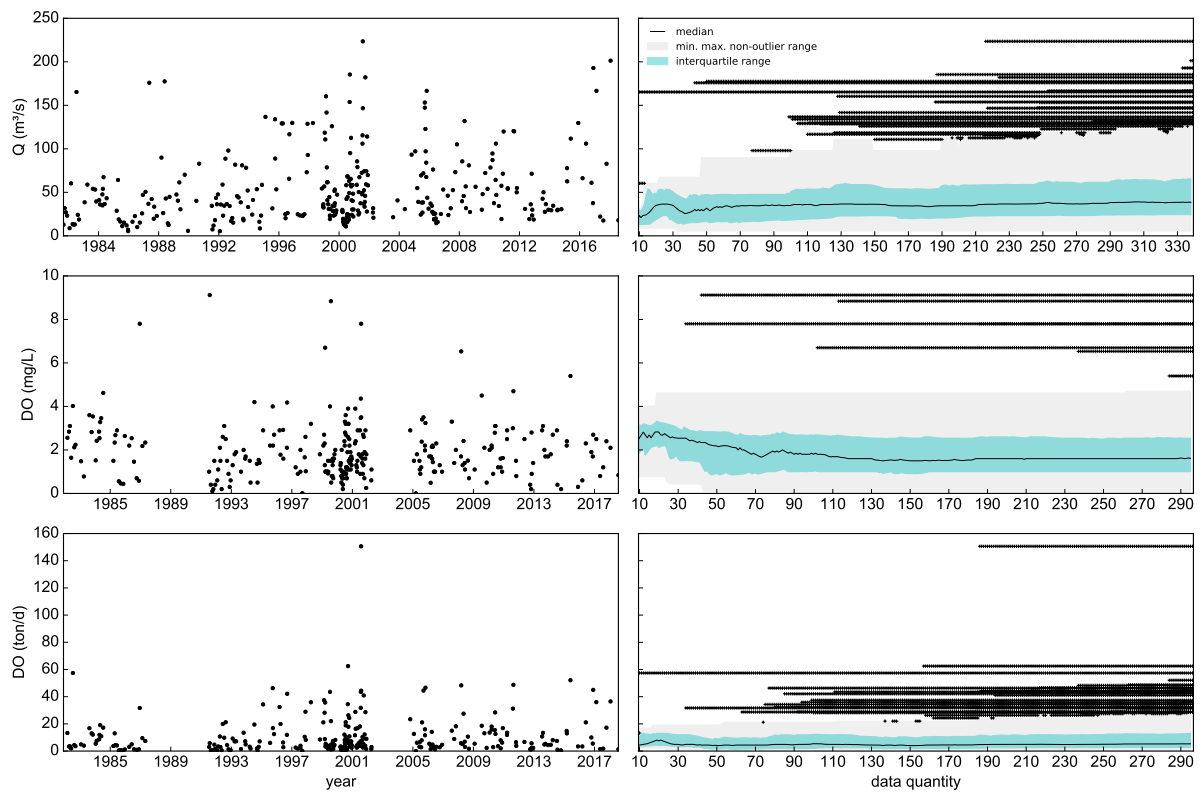
COD - IG4
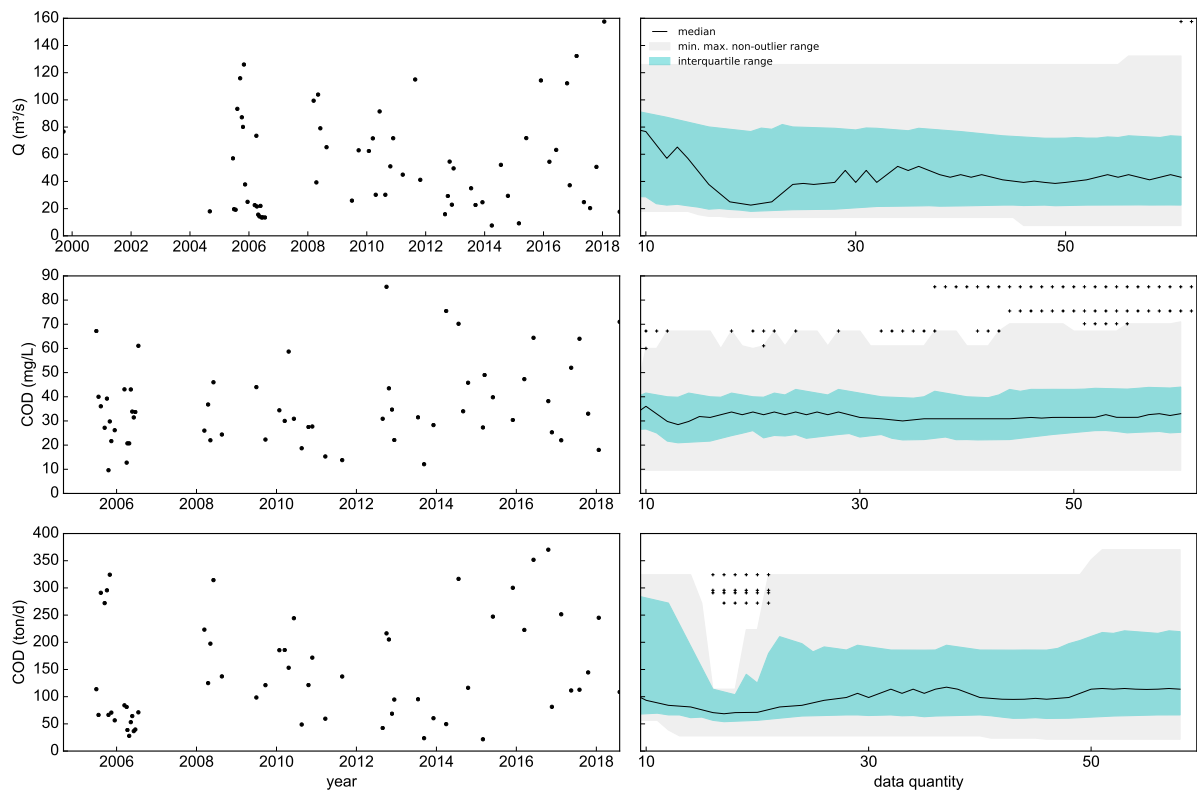
Figure 209 – Time series and boxplot evolution. Q, COD concentrations and loads, station IG4. Updated boxplots at each data, starting with 10 elements and ending with all data. The min. max. non-outlier range is the range defined by the minimum and maximum non-outlier values. The outlier values are represented by black crosses.

COD - IG5
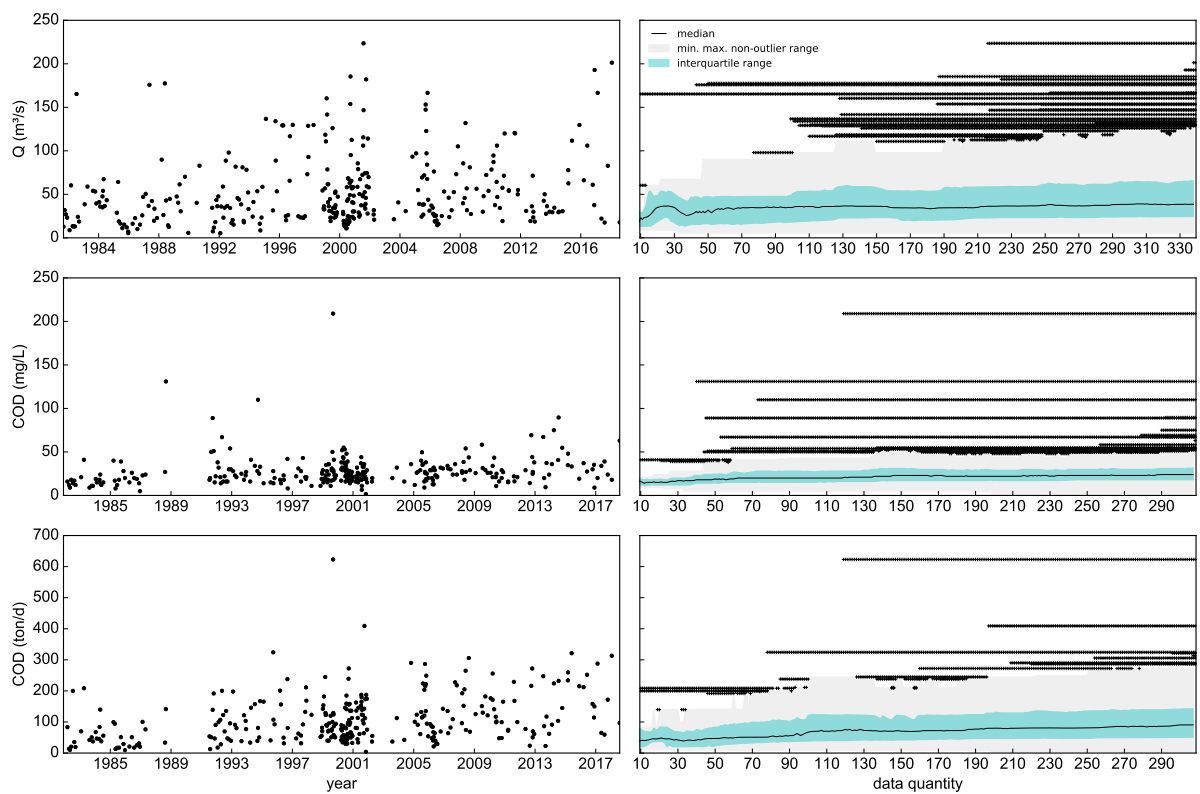
Figure 210 – Time series and boxplot evolution. Q, COD concentrations and loads, station IG5. Updated boxplots at each data, starting with 10 elements and ending with all data. The min. max. non-outlier range is the range defined by the minimum and maximum non-outlier values. The outlier values are represented by black crosses.
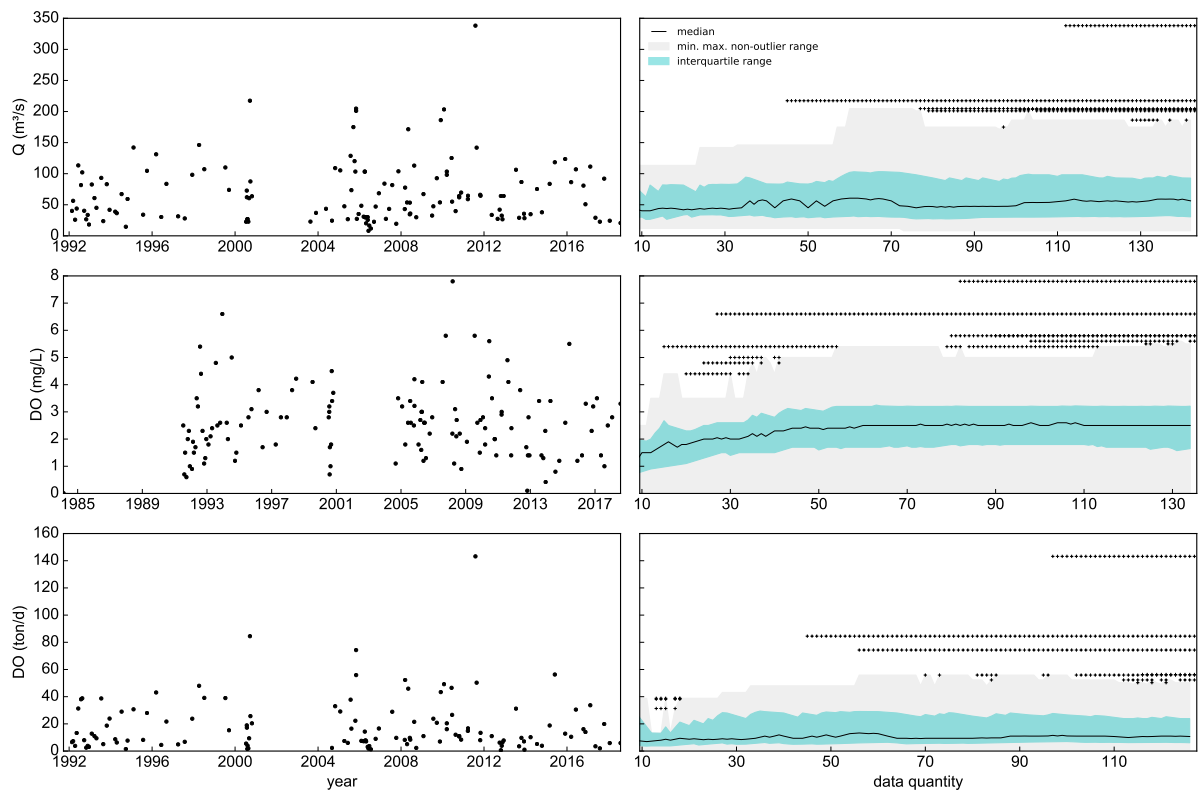
COD - IG6

Figure 211 – Time series and boxplot evolution. Q, COD concentrations and loads, station IG6. Updated boxplots at each data, starting with 10 elements and ending with all data. The min. max. non-outlier range is the range defined by the minimum and maximum non-outlier values. The outlier values are represented by black crosses.
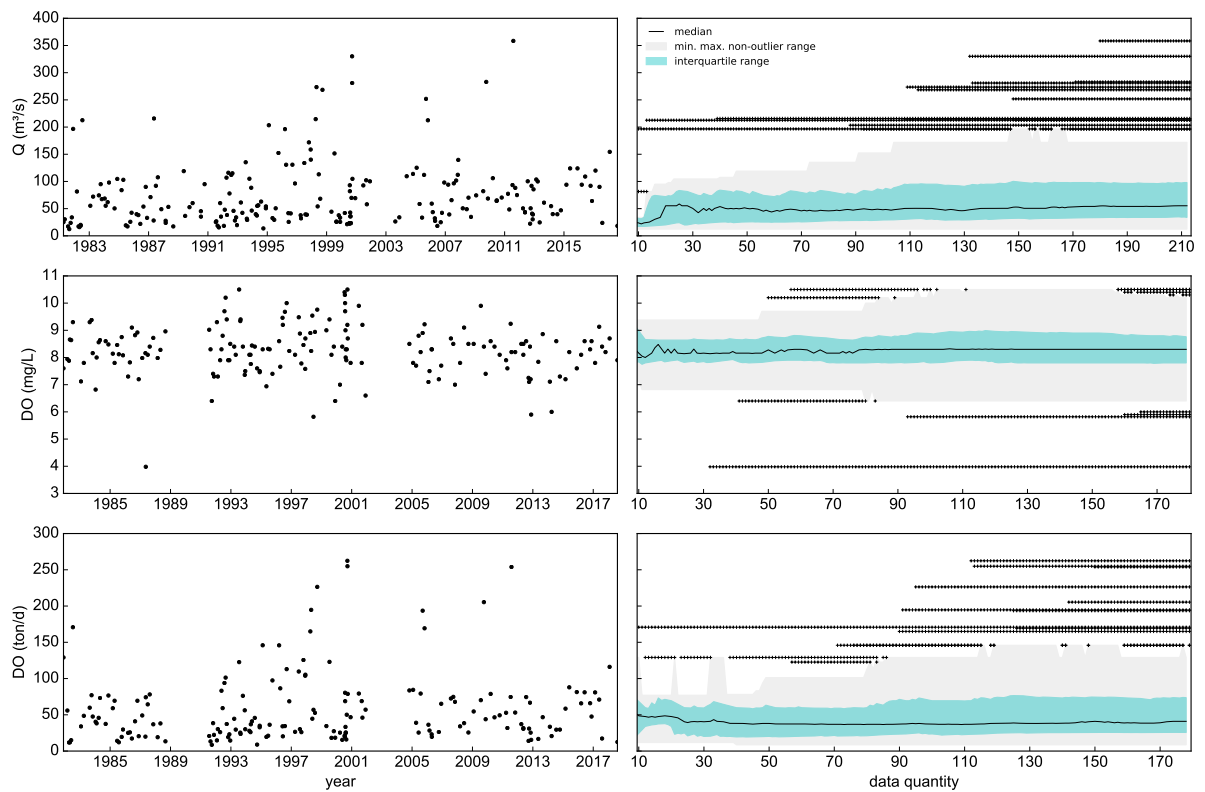
COD - IG7

Figure 212 – Time series and boxplot evolution. Q, COD concentrations and loads, station IG7. Updated boxplots at each data, starting with 10 elements and ending with all data. The min. max. non-outlier range is the range defined by the minimum and maximum non-outlier values. The outlier values are represented by black crosses.
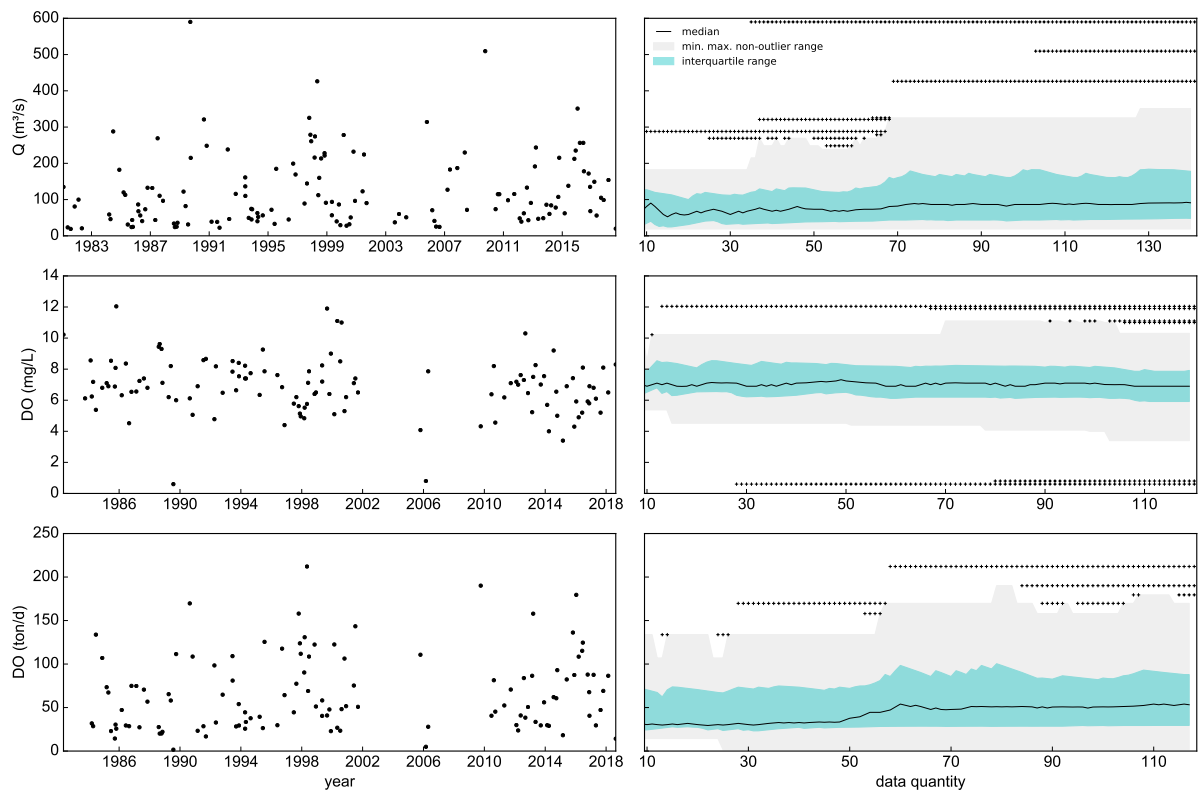
COD - IG8

Figure 213 – Time series and boxplot evolution. Q, COD concentrations and loads, station IG8. Updated boxplots at each data, starting with 10 elements and ending with all data. The min. max. non-outlier range is the range defined by the minimum and maximum non-outlier values. The outlier values are represented by black crosses.
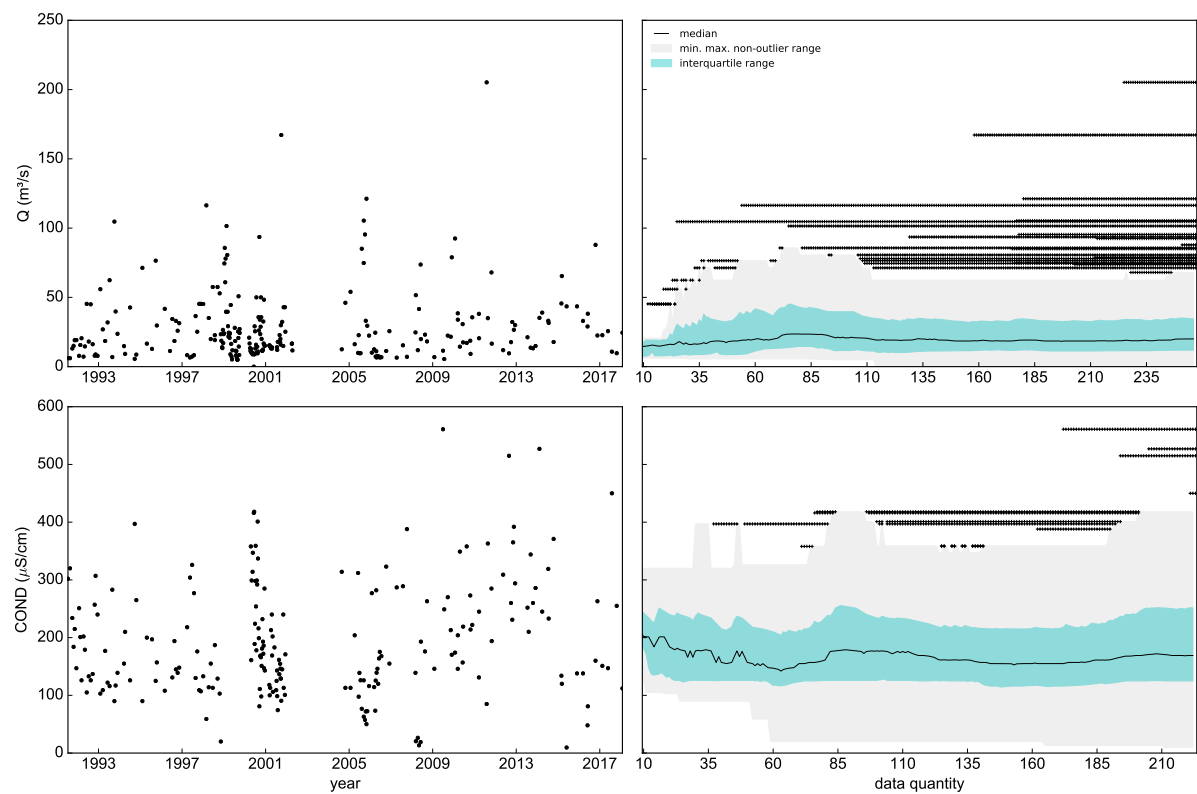
TP - IG3

Figure 214 – Time series and boxplot evolution. Q, TP concentrations and loads, station IG3. Updated boxplots at each data, starting with 10 elements and ending with all data. The min. max. non-outlier range is the range defined by the minimum and maximum non-outlier values. The outlier values are represented by black crosses.
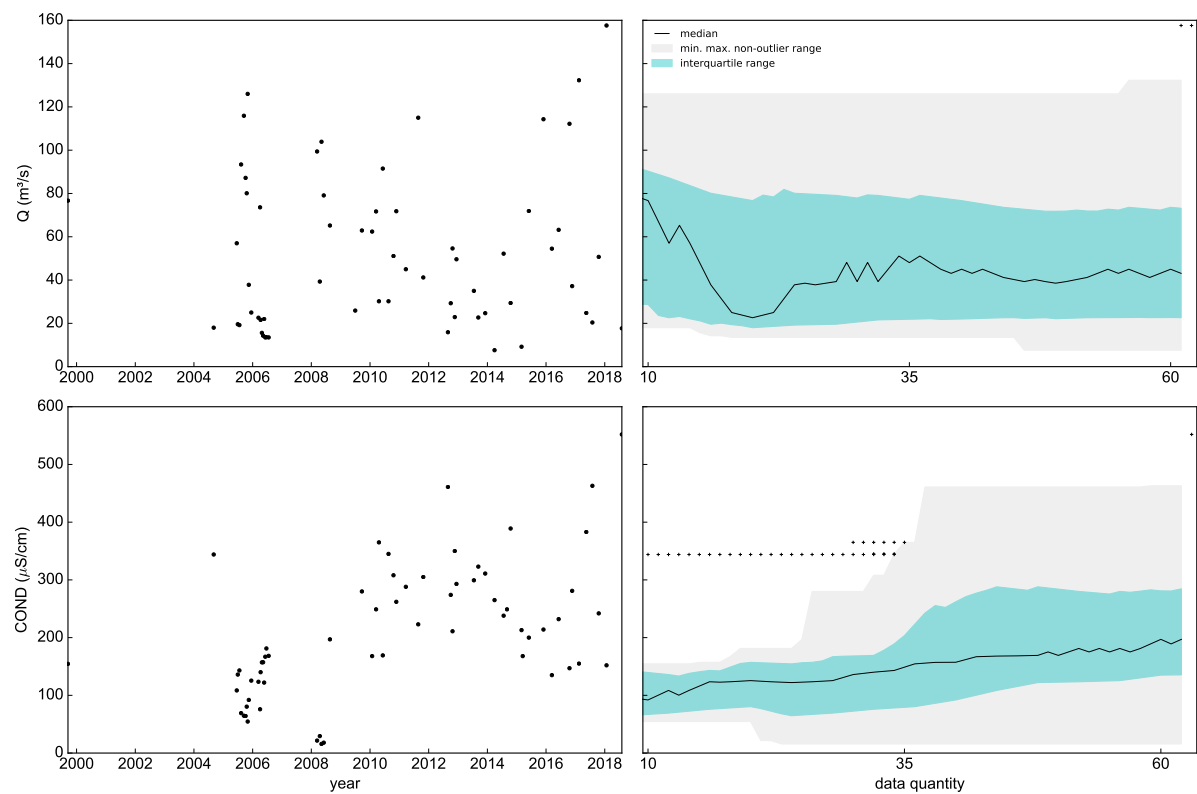
TP - IG4

Figure 215 – Time series and boxplot evolution. Q, TP concentrations and loads, station IG4. Updated boxplots at each data, starting with 10 elements and ending with all data. The min. max. non-outlier range is the range defined by the minimum and maximum non-outlier values. The outlier values are represented by black crosses.
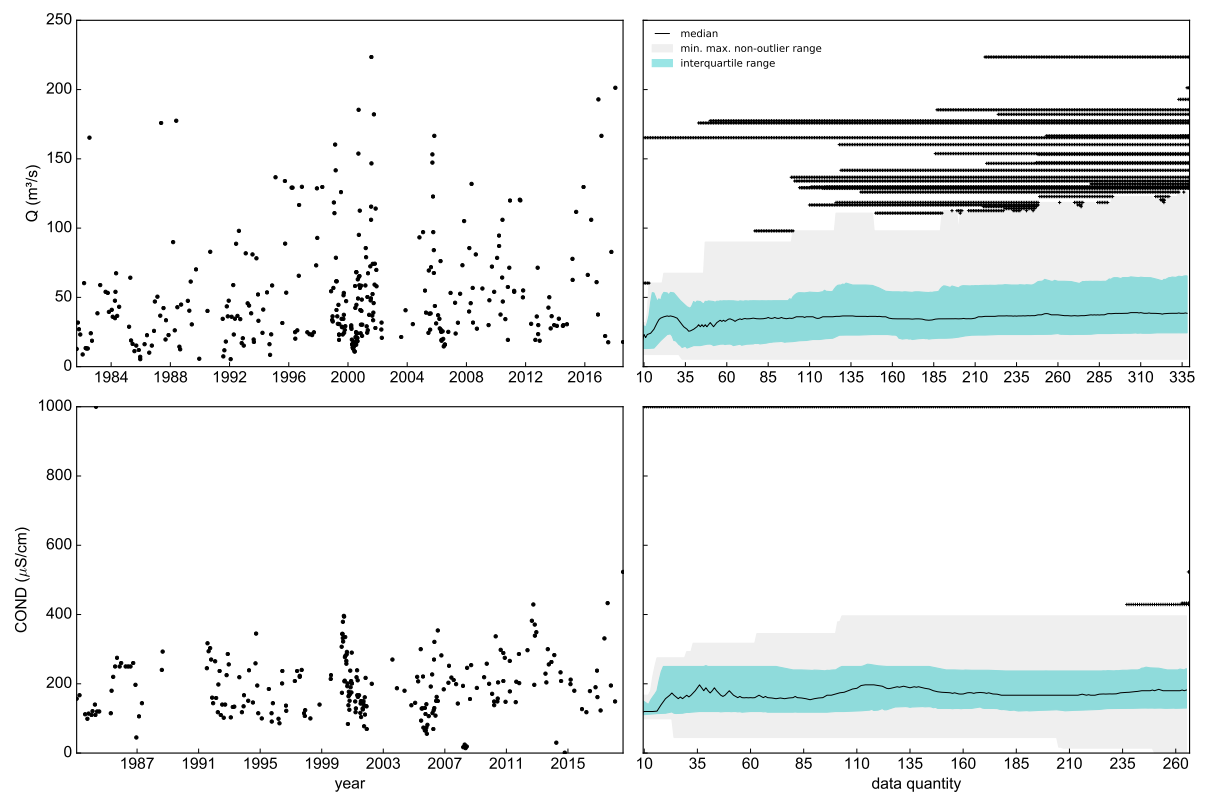
TP - IG5

Figure 216 – Time series and boxplot evolution. Q, TP concentrations and loads, station IG5. Updated boxplots at each data, starting with 10 elements and ending with all data. The min. max. non-outlier range is the range defined by the minimum and maximum non-outlier values. The outlier values are represented by black crosses.

TP - IG6

Figure 217 – Time series and boxplot evolution. Q, TP concentrations and loads, station IG6. Updated boxplots at each data, starting with 10 elements and ending with all data. The min. max. non-outlier range is the range defined by the minimum and maximum non-outlier values. The outlier values are represented by black crosses.
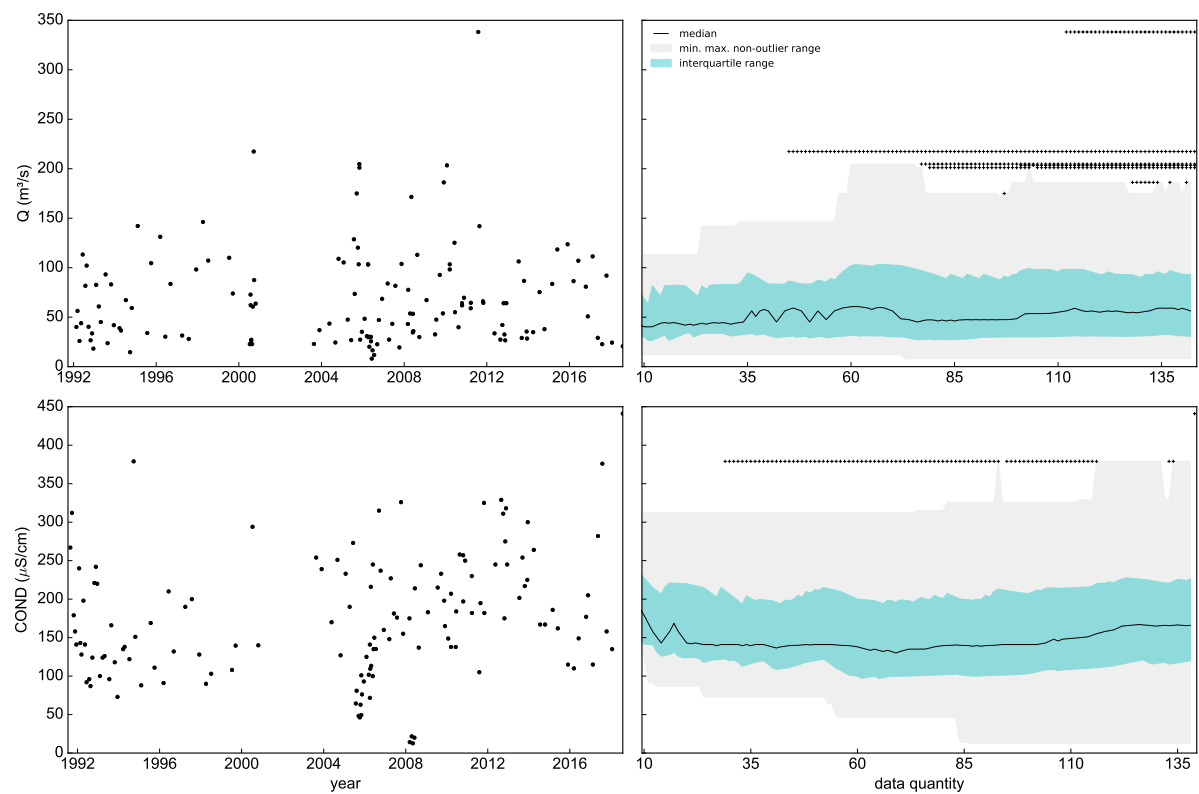
TP - IG7

Figure 218 – Time series and boxplot evolution. Q, TP concentrations and loads, station IG7. Updated boxplots at each data, starting with 10 elements and ending with all data. The min. max. non-outlier range is the range defined by the minimum and maximum non-outlier values. The outlier values are represented by black crosses.
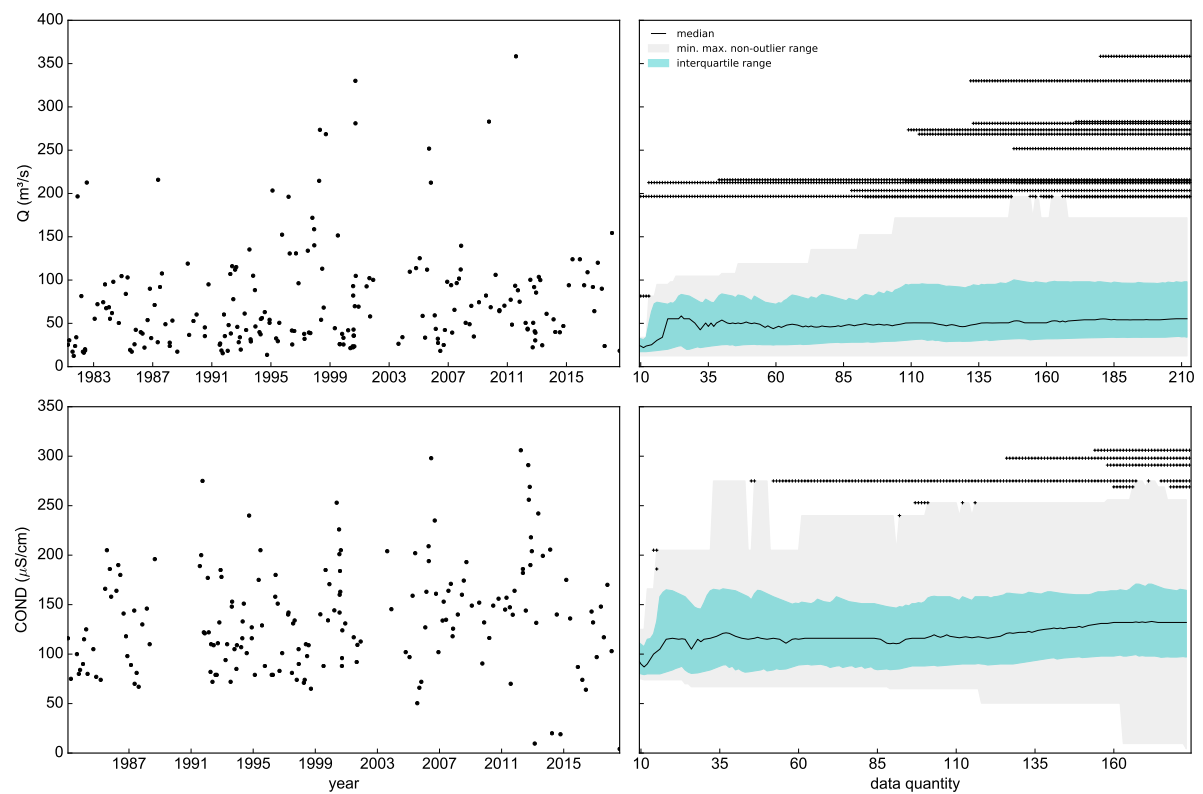
TP - IG8

Figure 219 – Time series and boxplot evolution. Q, TP concentrations and loads, station IG8. Updated boxplots at each data, starting with 10 elements and ending with all data. The min. max. non-outlier range is the range defined by the minimum and maximum non-outlier values. The outlier values are represented by black crosses.
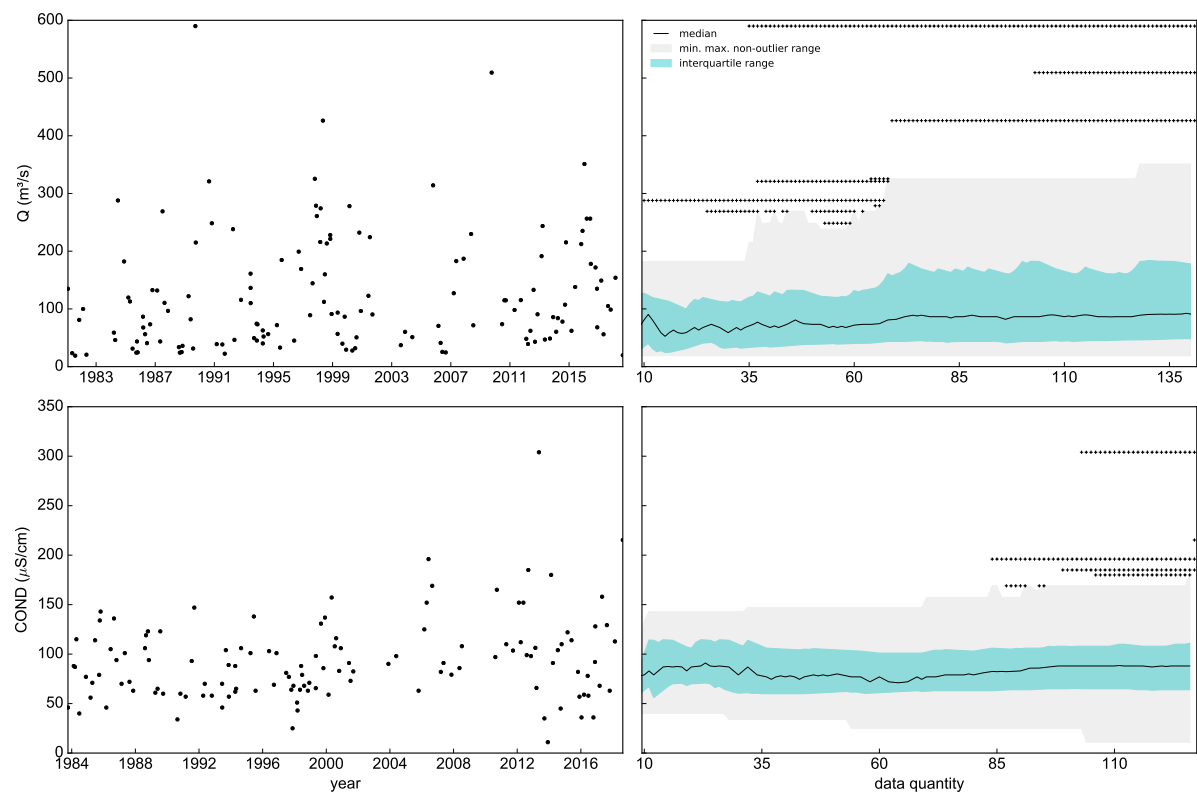
DO - IG3

Figure 220 – Time series and boxplot evolution. Q, DO concentrations and loads, station IG3. Updated boxplots at each data, starting with 10 elements and ending with all data. The min. max. non-outlier range is the range defined by the minimum and maximum non-outlier values. The outlier values are represented by black crosses.

DO - IG4

Figure 221 – Time series and boxplot evolution. Q, DO concentrations and loads, station IG4. Updated boxplots at each data, starting with 10 elements and ending with all data. The min. max. non-outlier range is the range defined by the minimum and maximum non-outlier values. The outlier values are represented by black crosses.

DO - IG5

Figure 222 – Time series and boxplot evolution. Q, DO concentrations and loads, station IG5. Updated boxplots at each data, starting with 10 elements and ending with all data. The min. max. non-outlier range is the range defined by the minimum and maximum non-outlier values. The outlier values are represented by black crosses.

DO - IG6

Figure 223 – Time series and boxplot evolution. Q, DO concentrations and loads, station IG6. Updated boxplots at each data, starting with 10 elements and ending with all data. The min. max. non-outlier range is the range defined by the minimum and maximum non-outlier values. The outlier values are represented by black crosses.

DO - IG7

Figure 224 – Time series and boxplot evolution. Q, DO concentrations and loads, station IG7. Updated boxplots at each data, starting with 10 elements and ending with all data. The min. max. non-outlier range is the range defined by the minimum and maximum non-outlier values. The outlier values are represented by black crosses.

DO - IG8

Figure 225 – Time series and boxplot evolution. Q, DO concentrations and loads, station IG8. Updated boxplots at each data, starting with 10 elements and ending with all data. The min. max. non-outlier range is the range defined by the minimum and maximum non-outlier values. The outlier values are represented by black crosses.

COND - IG3

Figure 226 – Time series and boxplot evolution. Q and COND, station IG3. Updated boxplots at each data, starting with 10 elements and ending with all data. The min. max. non-outlier range is the range defined by the minimum and maximum non-outlier values. The outlier values are represented by black crosses.

COND - IG4

Figure 227 – Time series and boxplot evolution. Q and COND, station IG4. Updated boxplots at each data, starting with 10 elements and ending with all data. The min. max. non-outlier range is the range defined by the minimum and maximum non-outlier values. The outlier values are represented by black crosses.

COND - IG5

Figure 228 – Time series and boxplot evolution. Q and COND, station IG5. Updated boxplots at each data, starting with 10 elements and ending with all data. The min. max. non-outlier range is the range defined by the minimum and maximum non-outlier values. The outlier values are represented by black crosses.

COND - IG6

Figure 229 – Time series and boxplot evolution. Q and COND, station IG6. Updated boxplots at each data, starting with 10 elements and ending with all data. The min. max. non-outlier range is the range defined by the minimum and maximum non-outlier values. The outlier values are represented by black crosses.

COND - IG7

Figure 230 – Time series and boxplot evolution. Q and COND, station IG7. Updated boxplots at each data, starting with 10 elements and ending with all data. The min. max. non-outlier range is the range defined by the minimum and maximum non-outlier values. The outlier values are represented by black crosses.

COND - IG8

Figure 231 – Time series and boxplot evolution. Q and COND, station IG8. Updated boxplots at each data, starting with 10 elements and ending with all data. The min. max. non-outlier range is the range defined by the minimum and maximum non-outlier values. The outlier values are represented by black crosses.

B.2 Regression results

B.2.1 Flows

Station to station
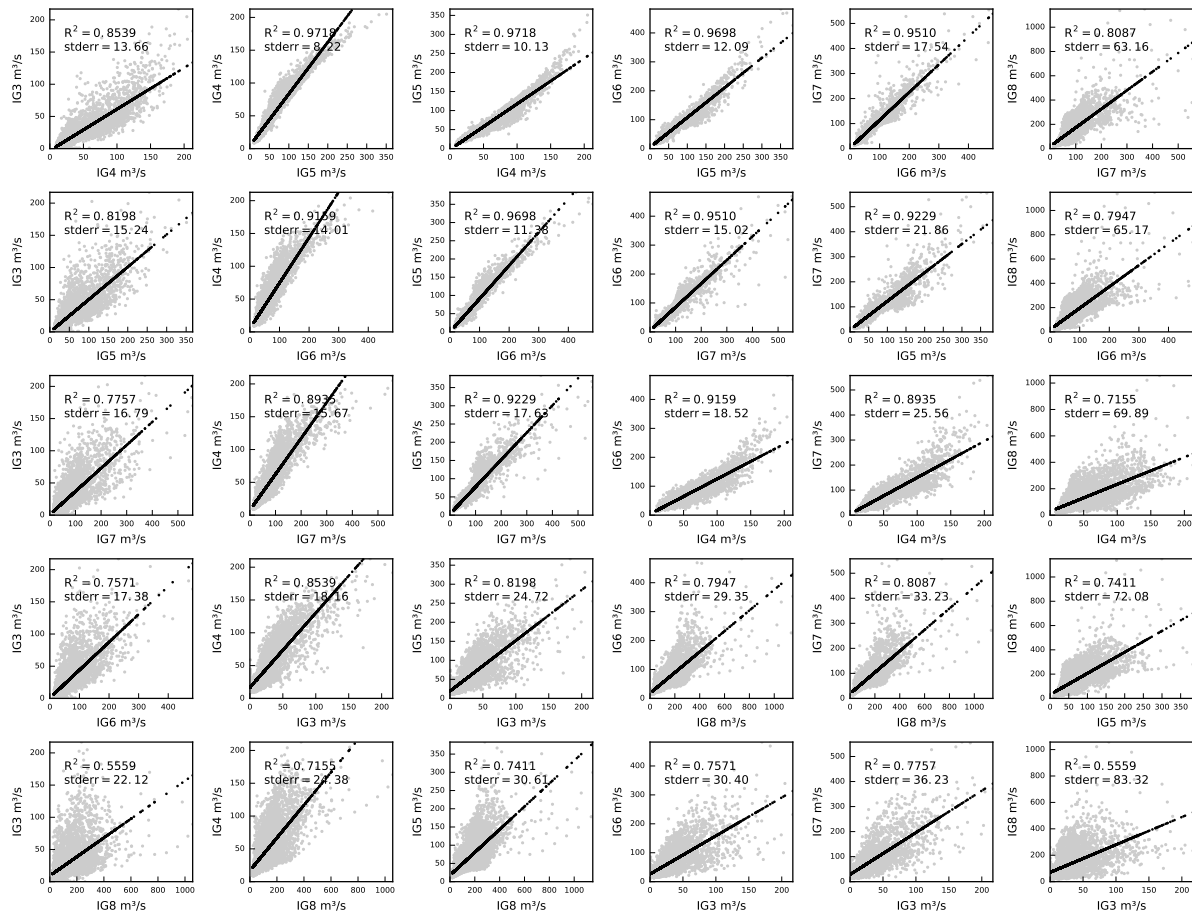
Figure 232 – Results from simple linear regression of each station to the others

B.2.2   Concentrations
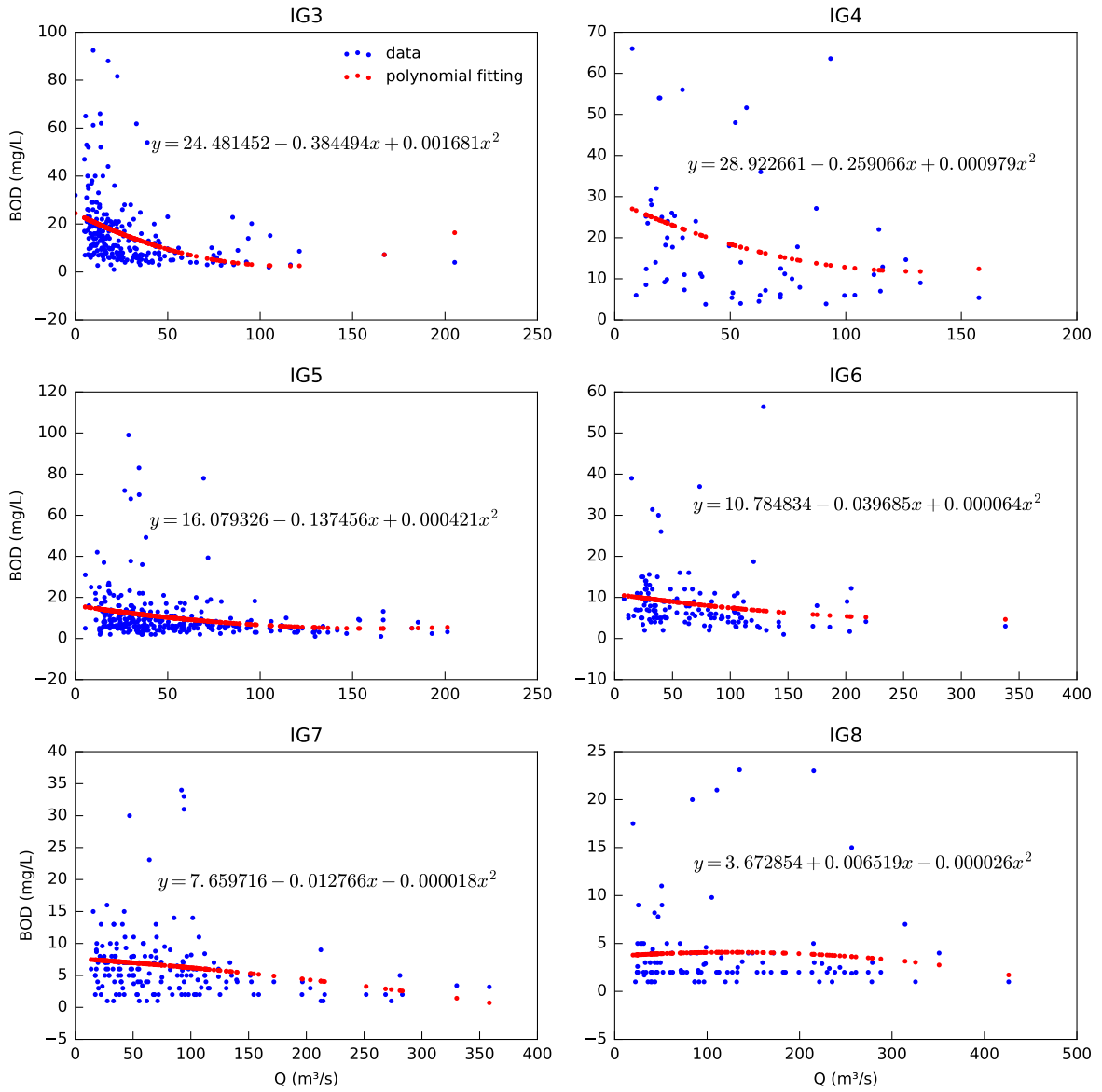
Figure 233 – Results from polynomial regression on flows and concentration photos for BOD

Regression model - DO
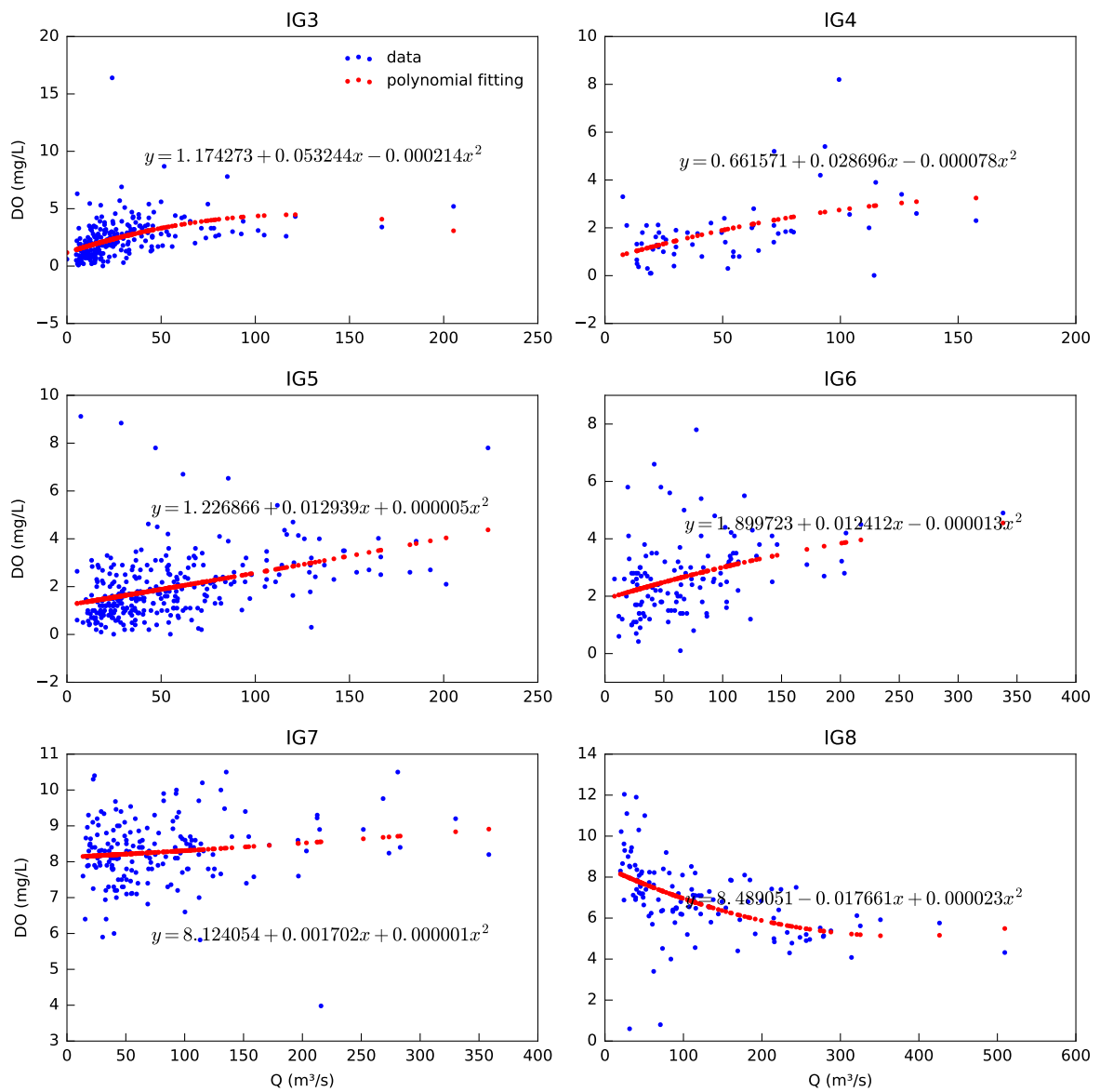
Figure 234 – Results from polynomial regression on flows and concentration photos for DO

Regression model - NH4
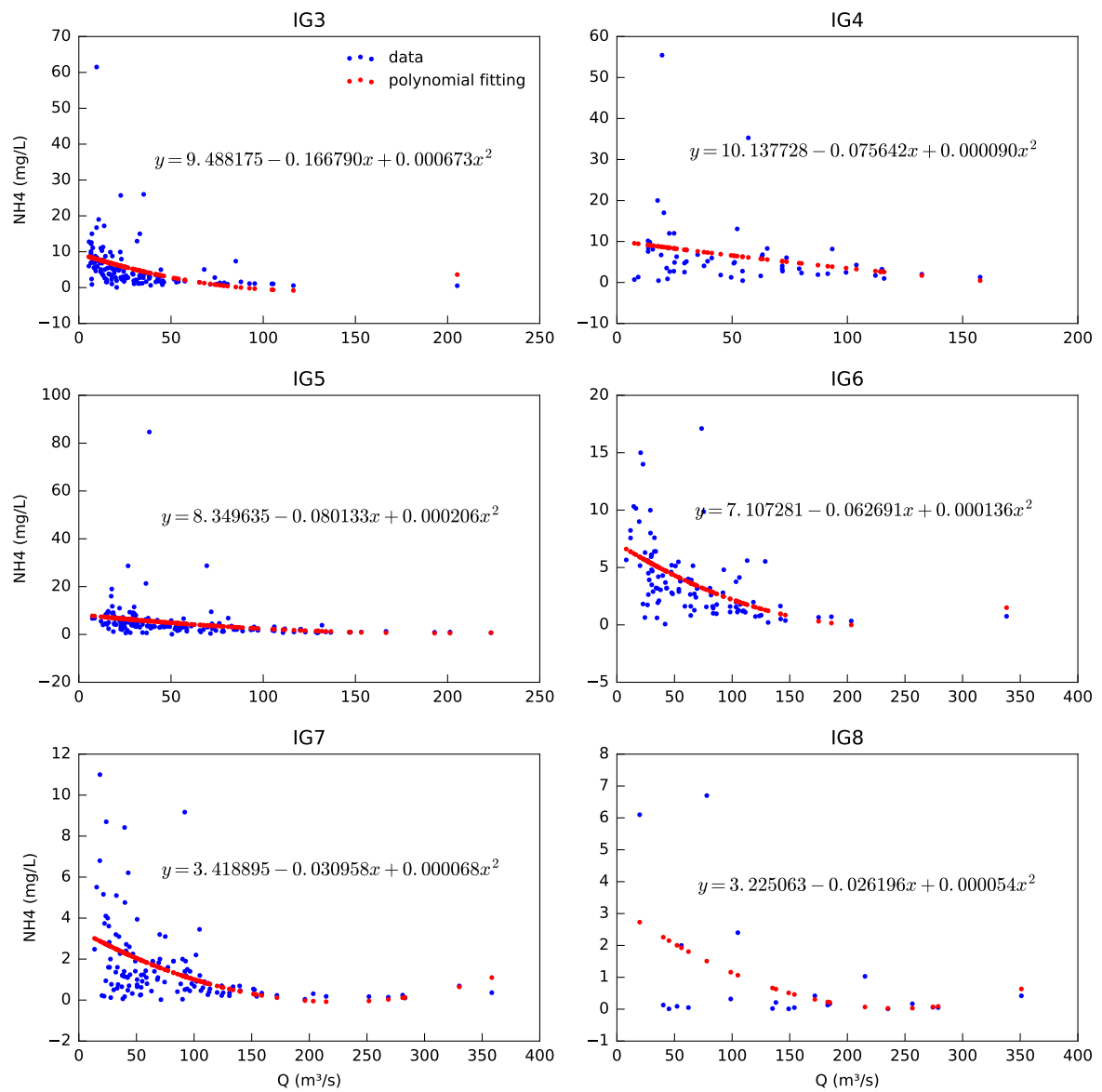
Figure 235 – Results from polynomial regression on flows and concentration photos for NH4

Regression model - TP
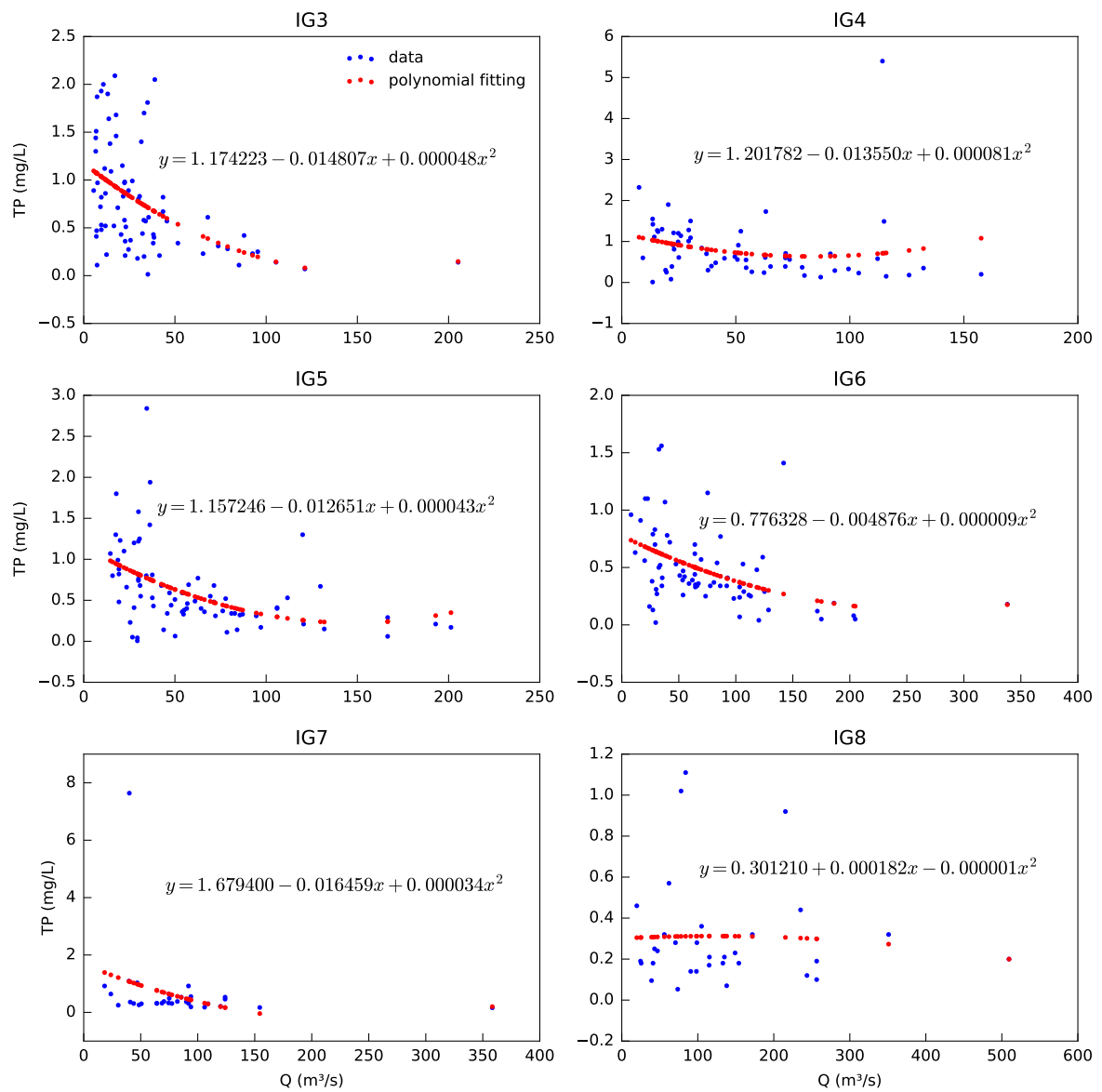
Figure 236 – Results from polynomial regression on flows and concentration photos for TP

Model error - BOD
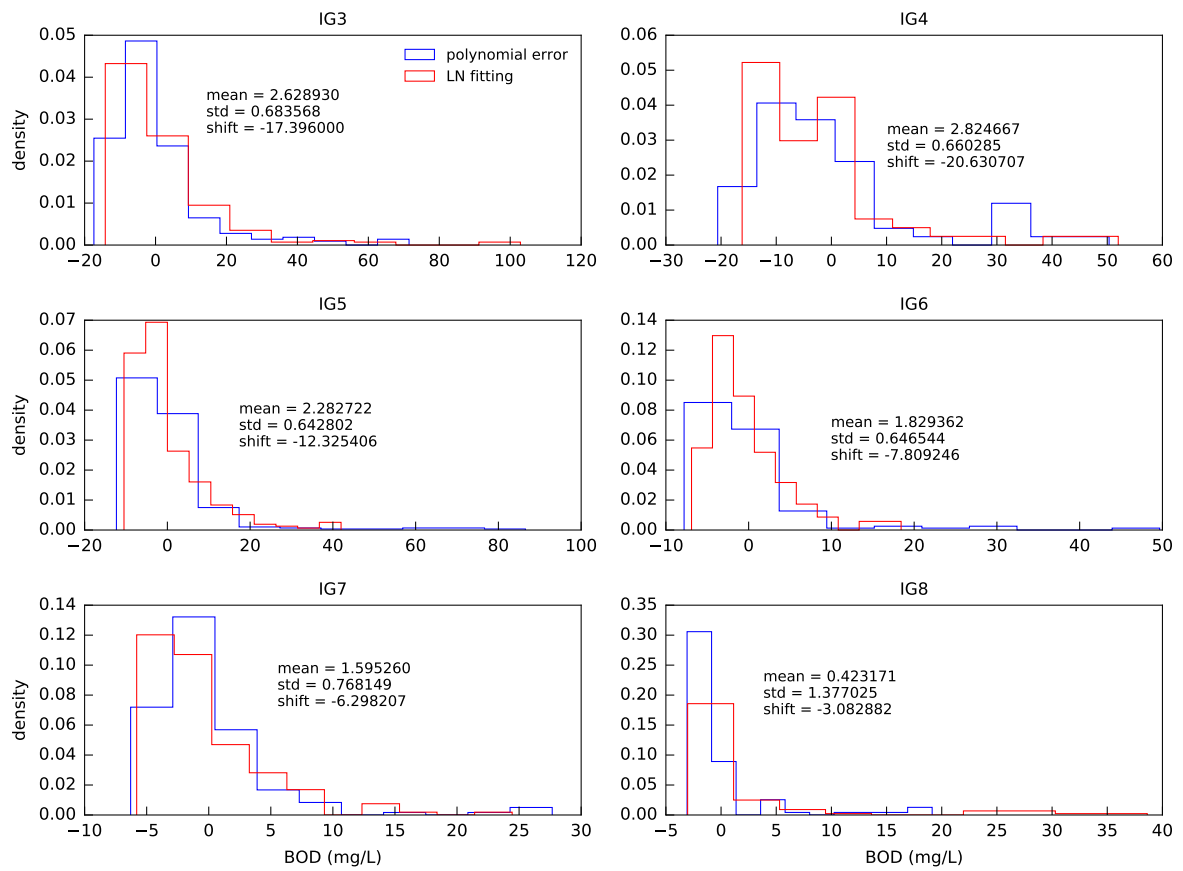
Figure 237 – Fitting of the 3 parameters-lognormal distribution to the errors of the polynomial regression model for BOD

Model error - DO
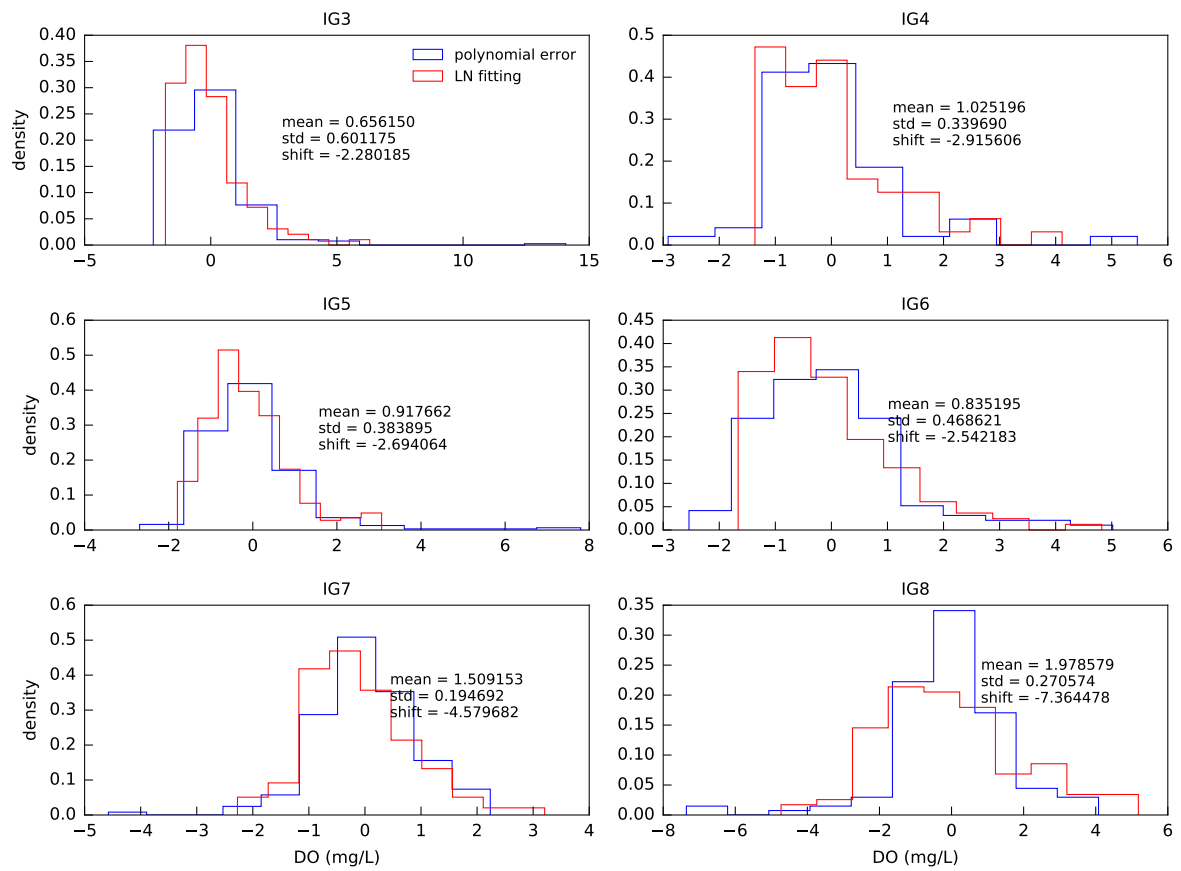
Figure 238 – Fitting of the 3 parameters-lognormal distribution to the errors of the polynomial regression model for DO

Model error - NH4
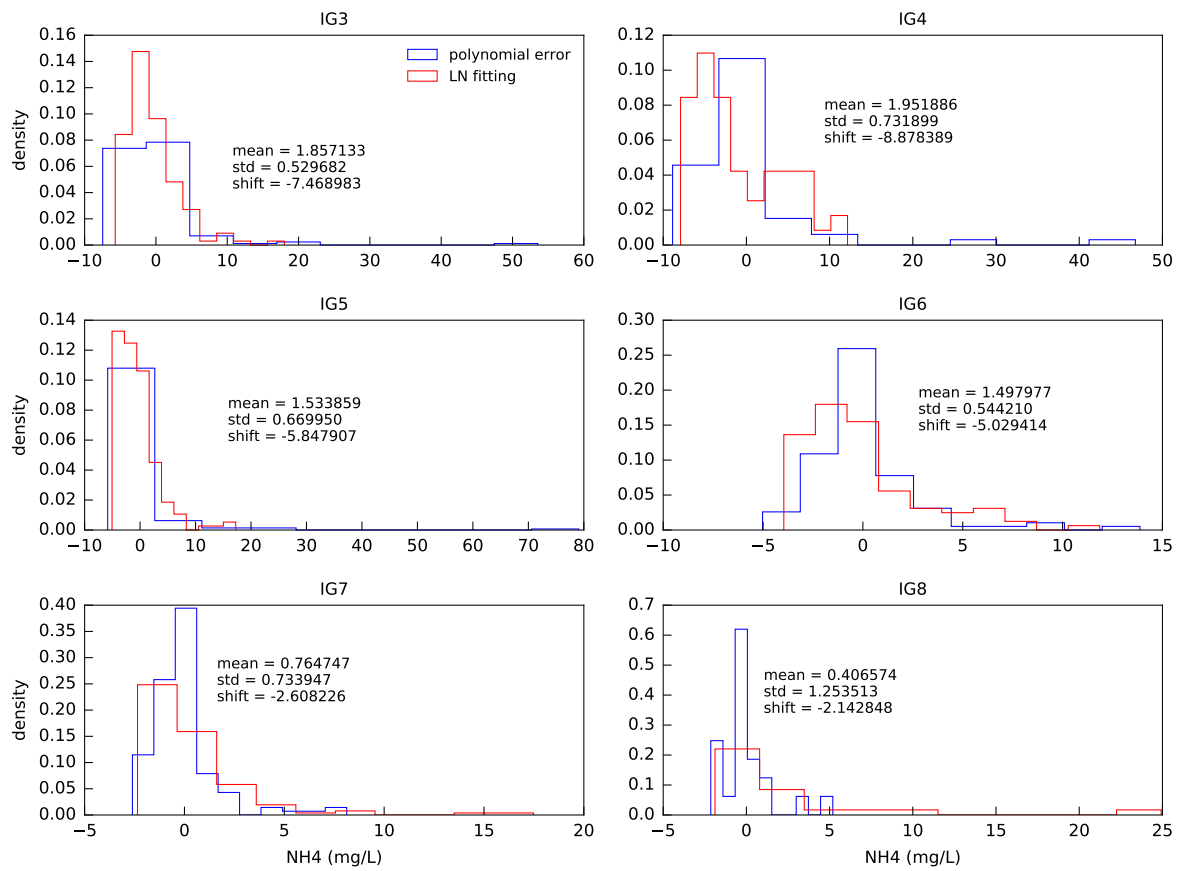
Figure 239 – Fitting of the 3 parameters-lognormal distribution to the errors of the polynomial regression model for NH4

Model error - TP
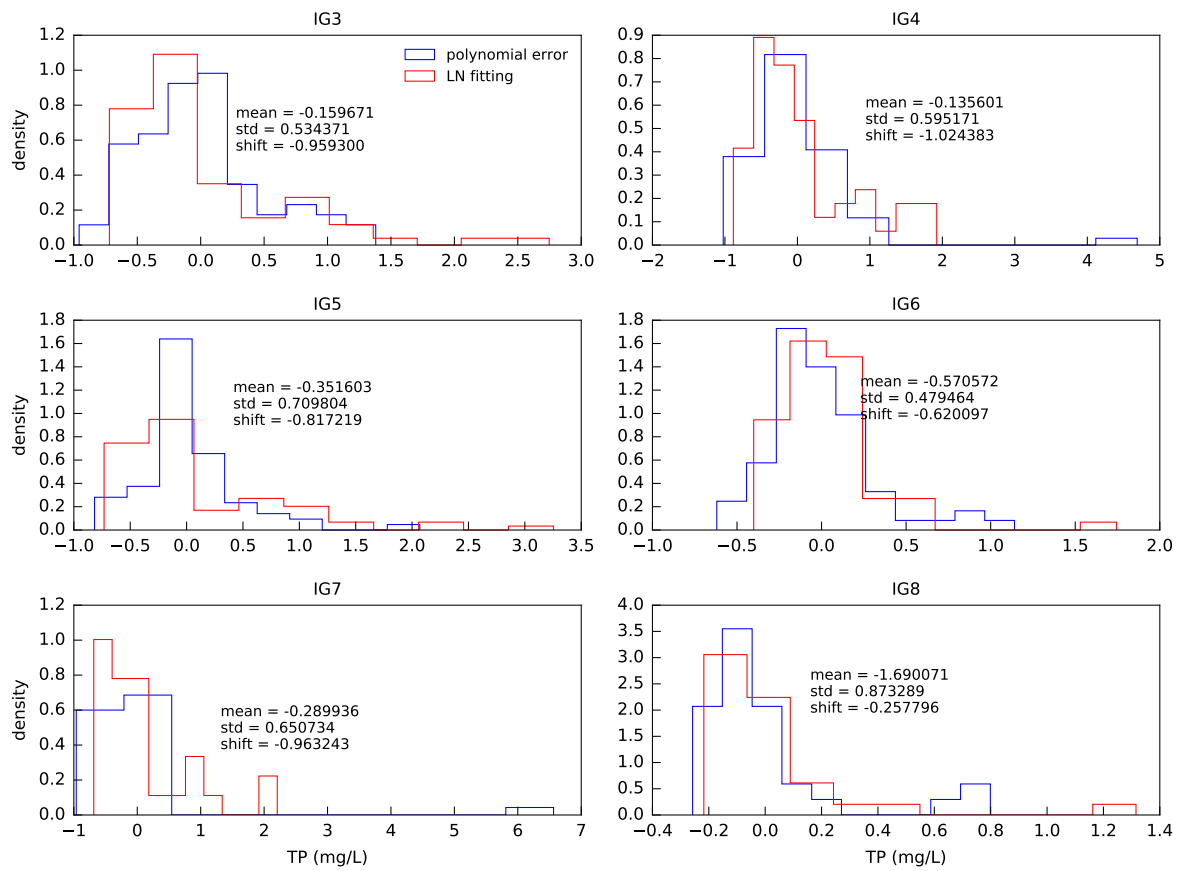
Figure 240 – Fitting of the 3 parameters-lognormal distribution to the errors of the polynomial regression model for TP

B.3   RHIS

BOD
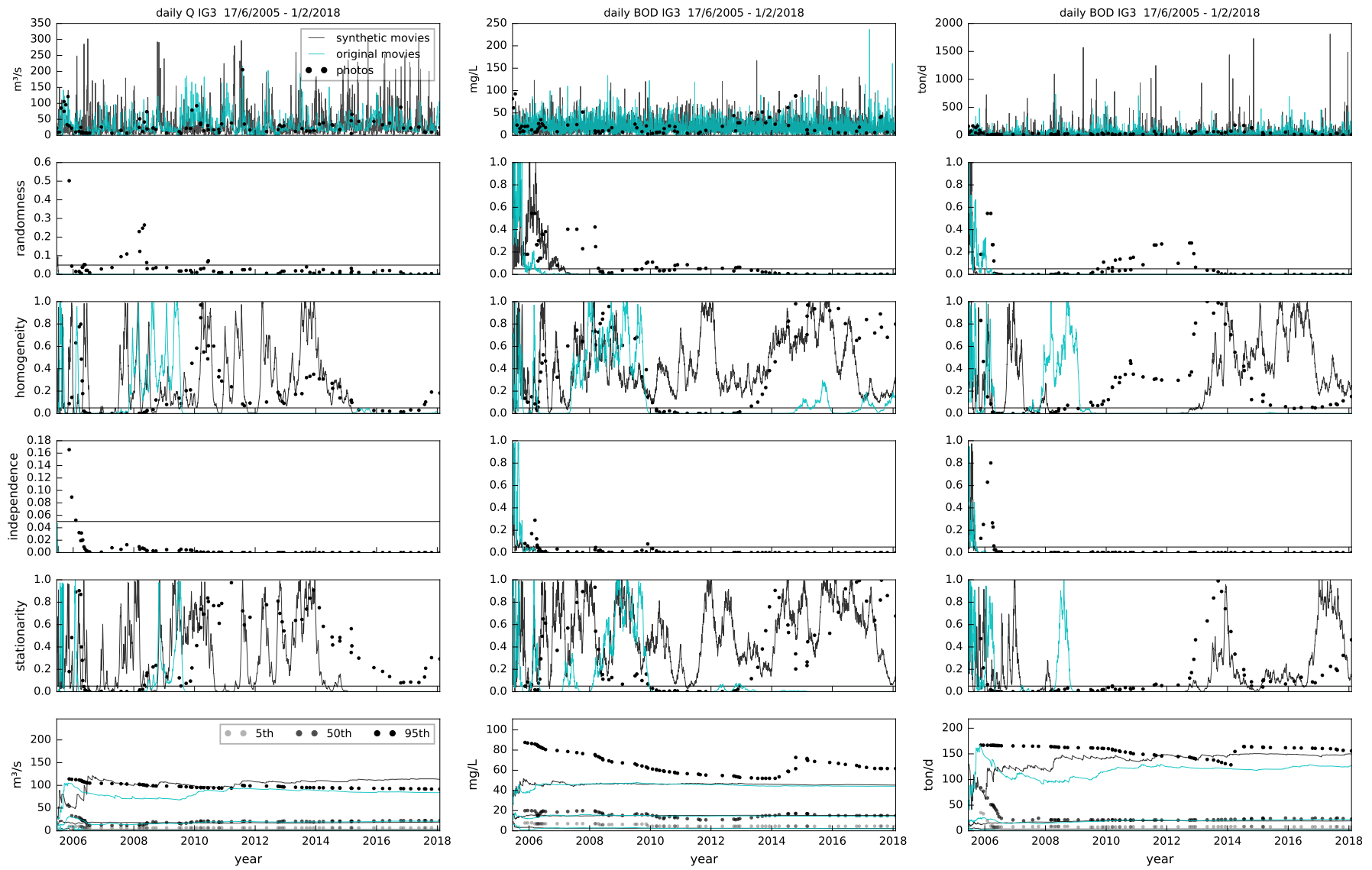
Figure 241 – Evolution of the RHIS p-values and percentiles of Q, C and W, BOD station IG3, photos and daily movies
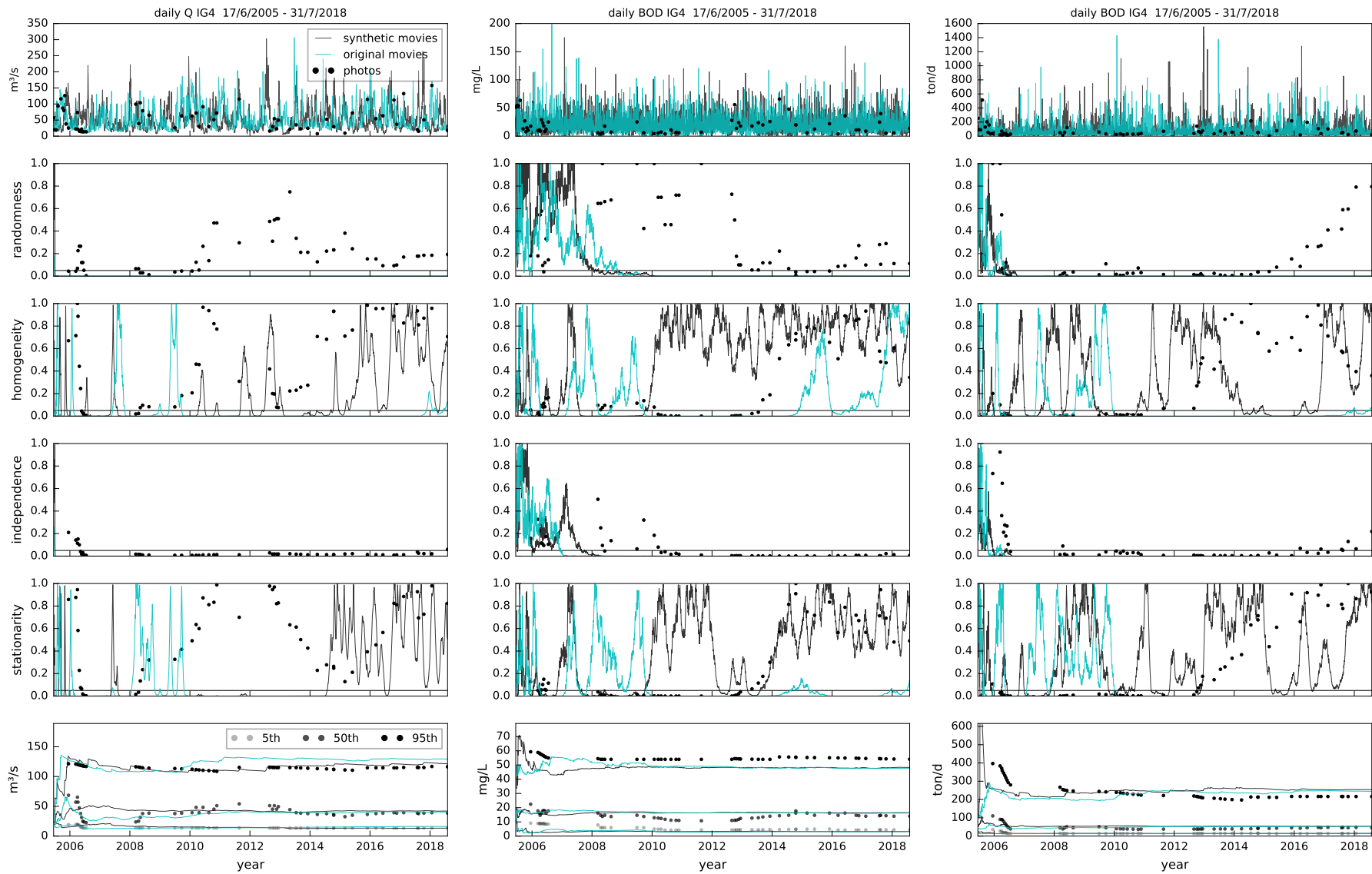
Figure 242 – Evolution of the RHIS p-values and percentiles of Q, C and W, BOD station IG4, photos and daily movies
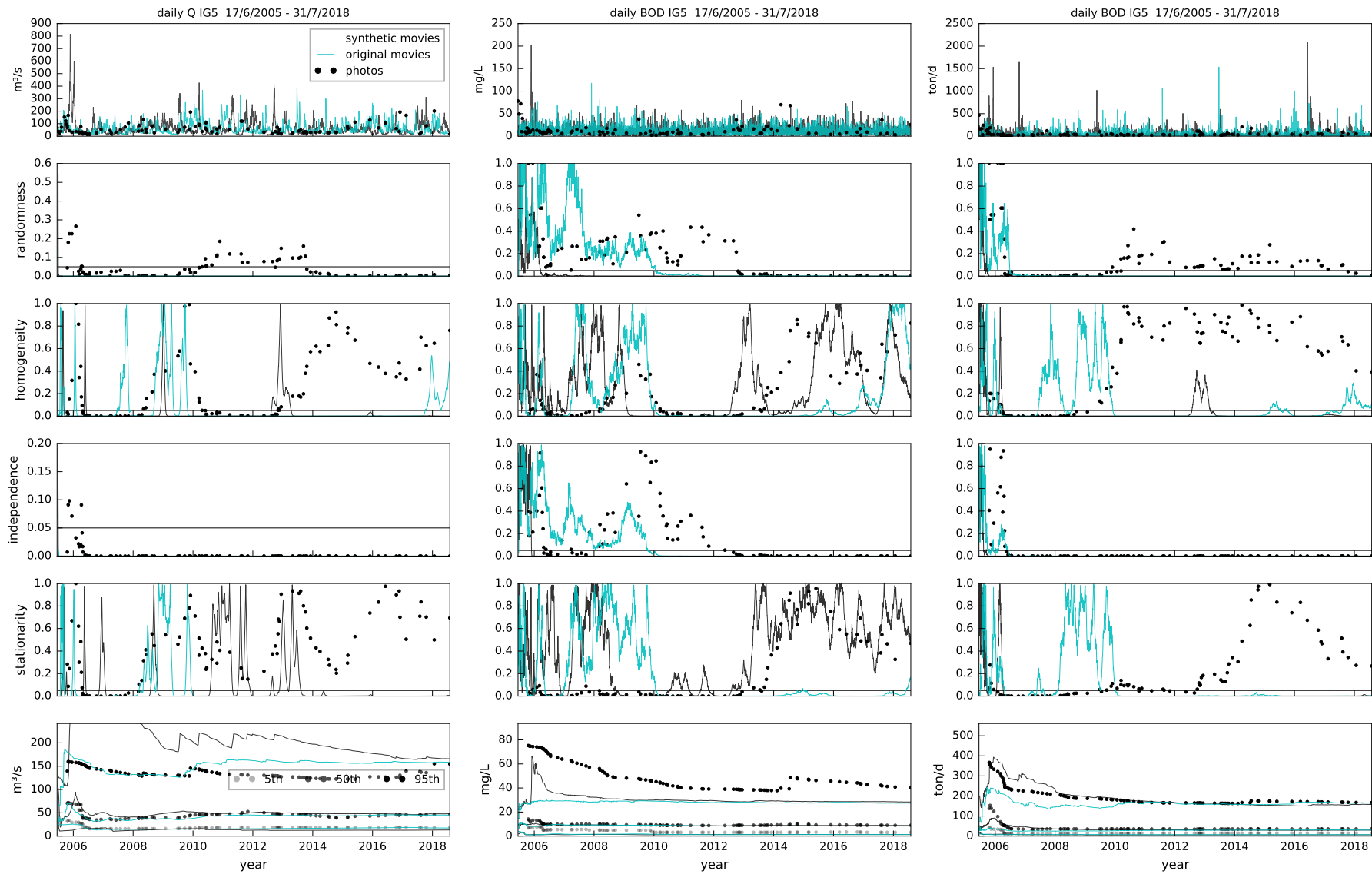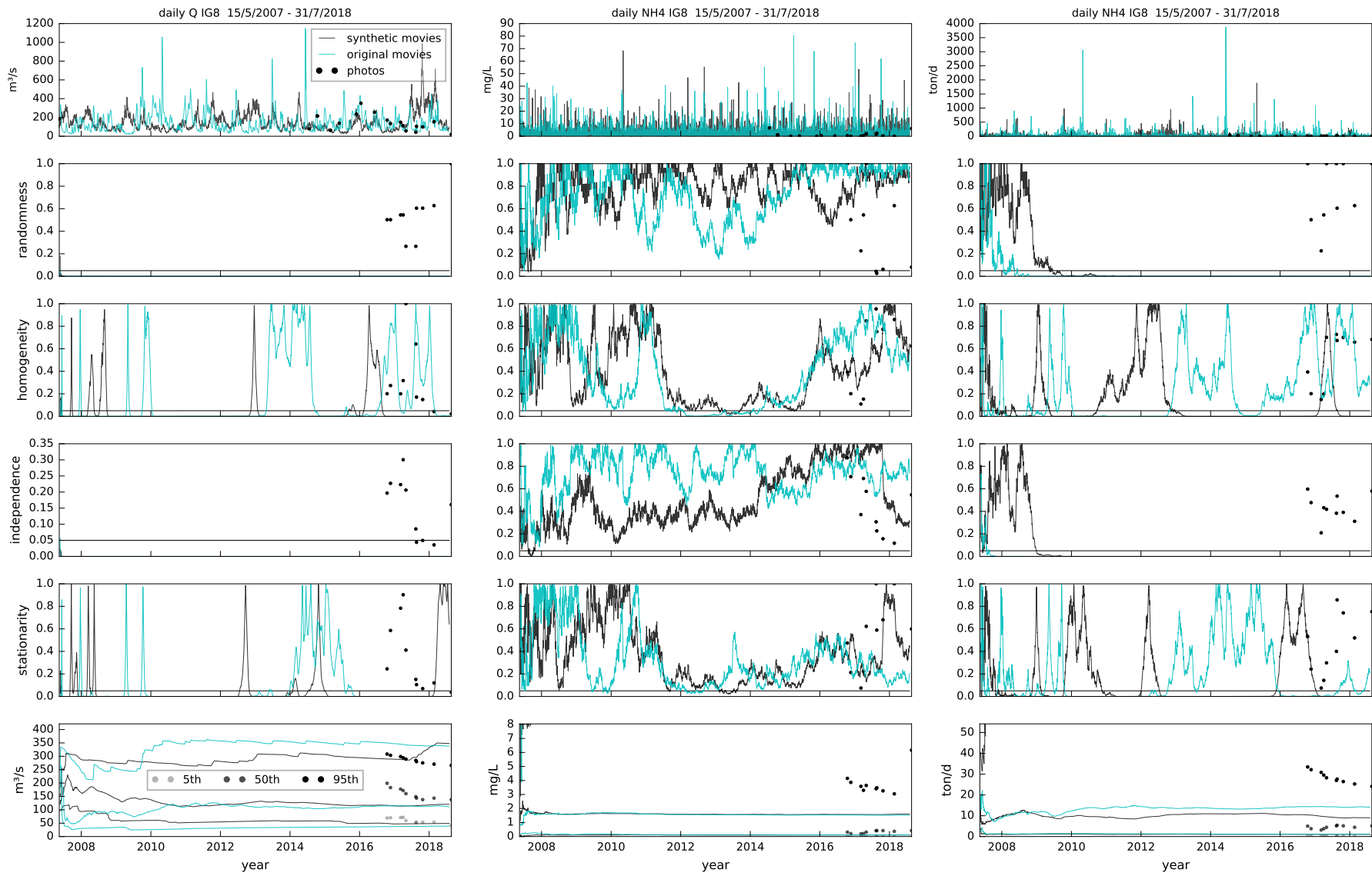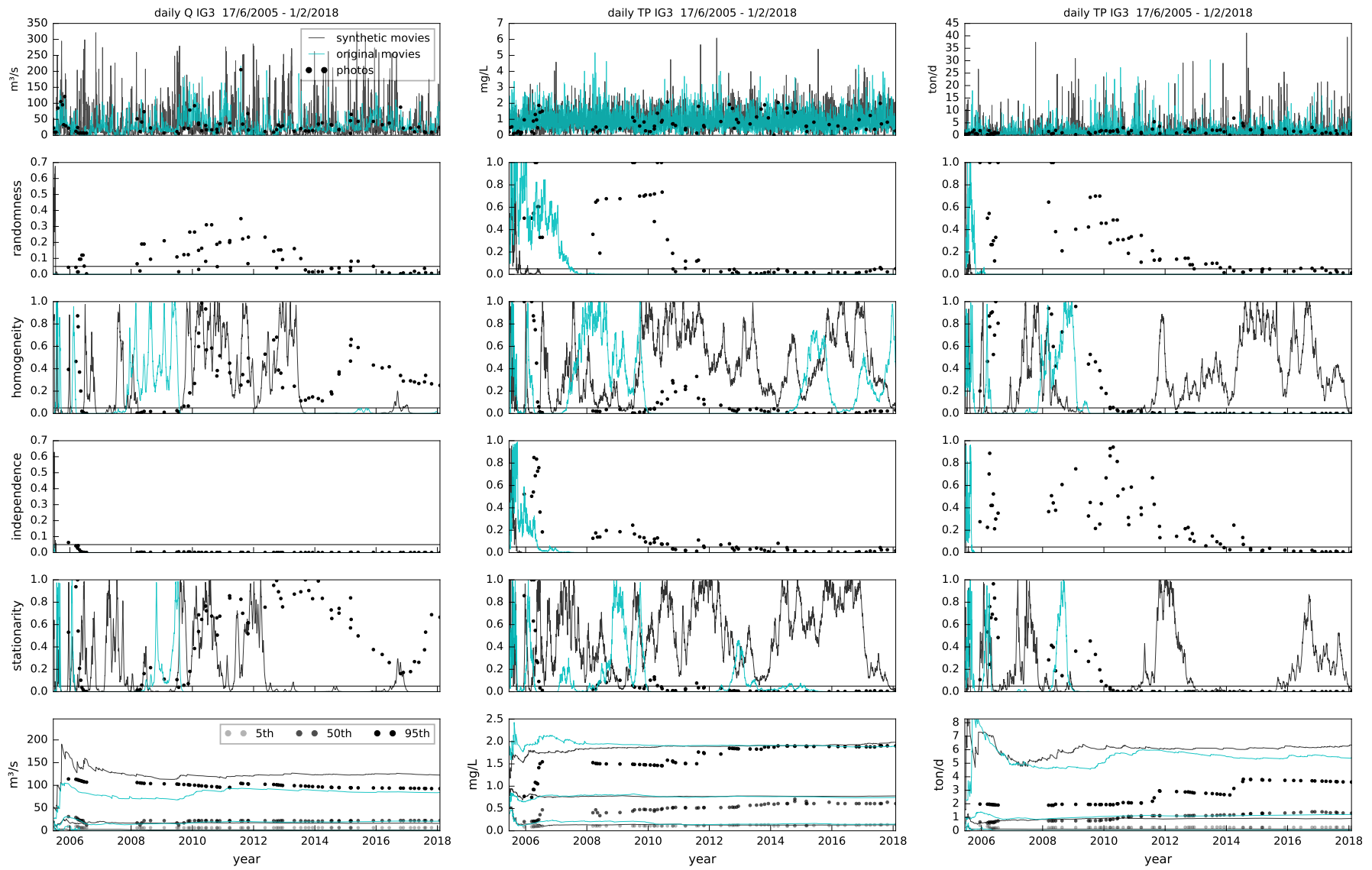
Figure 243 – Evolution of the RHIS p-values and percentiles of Q, C and W, BOD station IG5, photos and daily movies
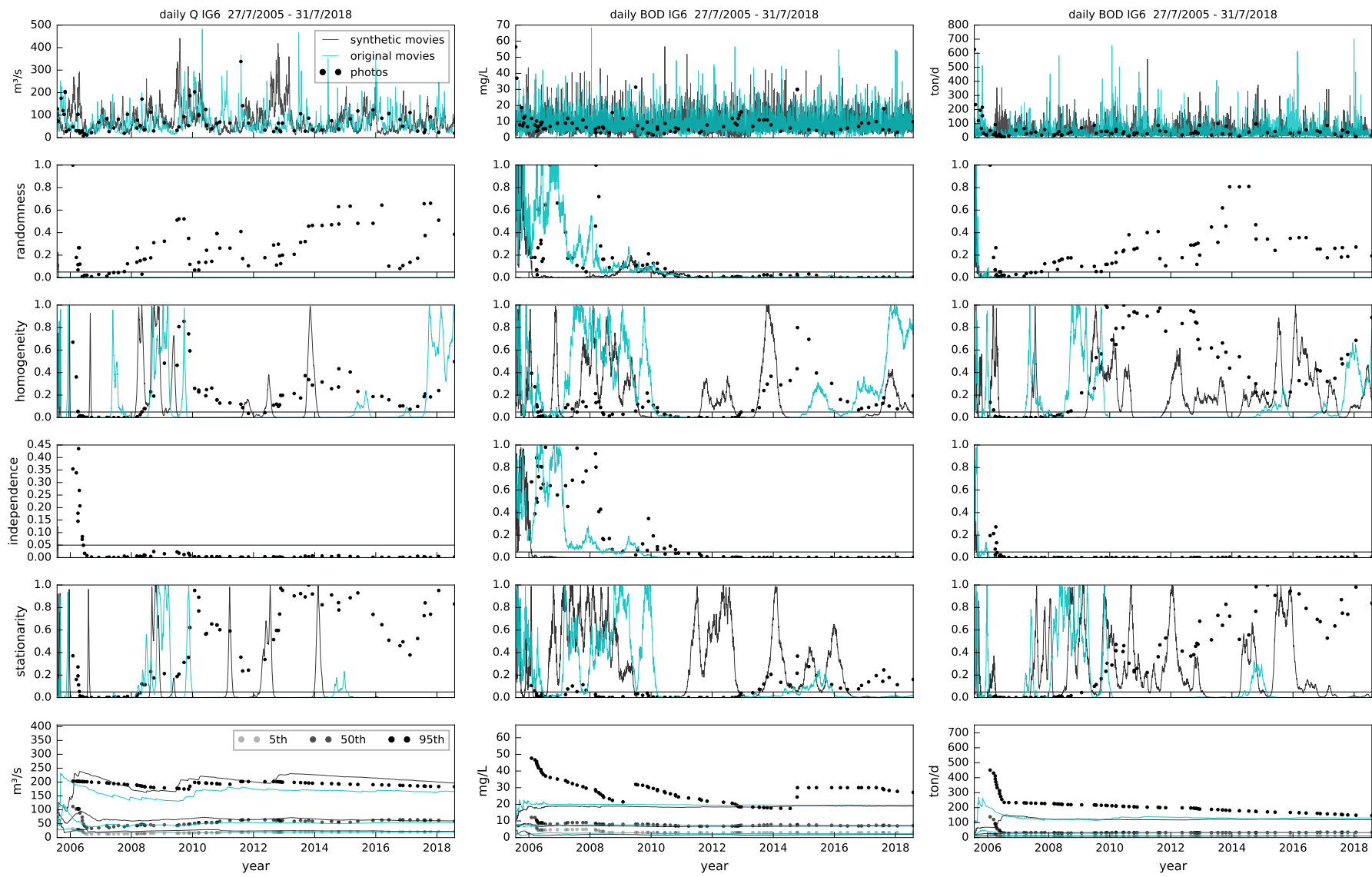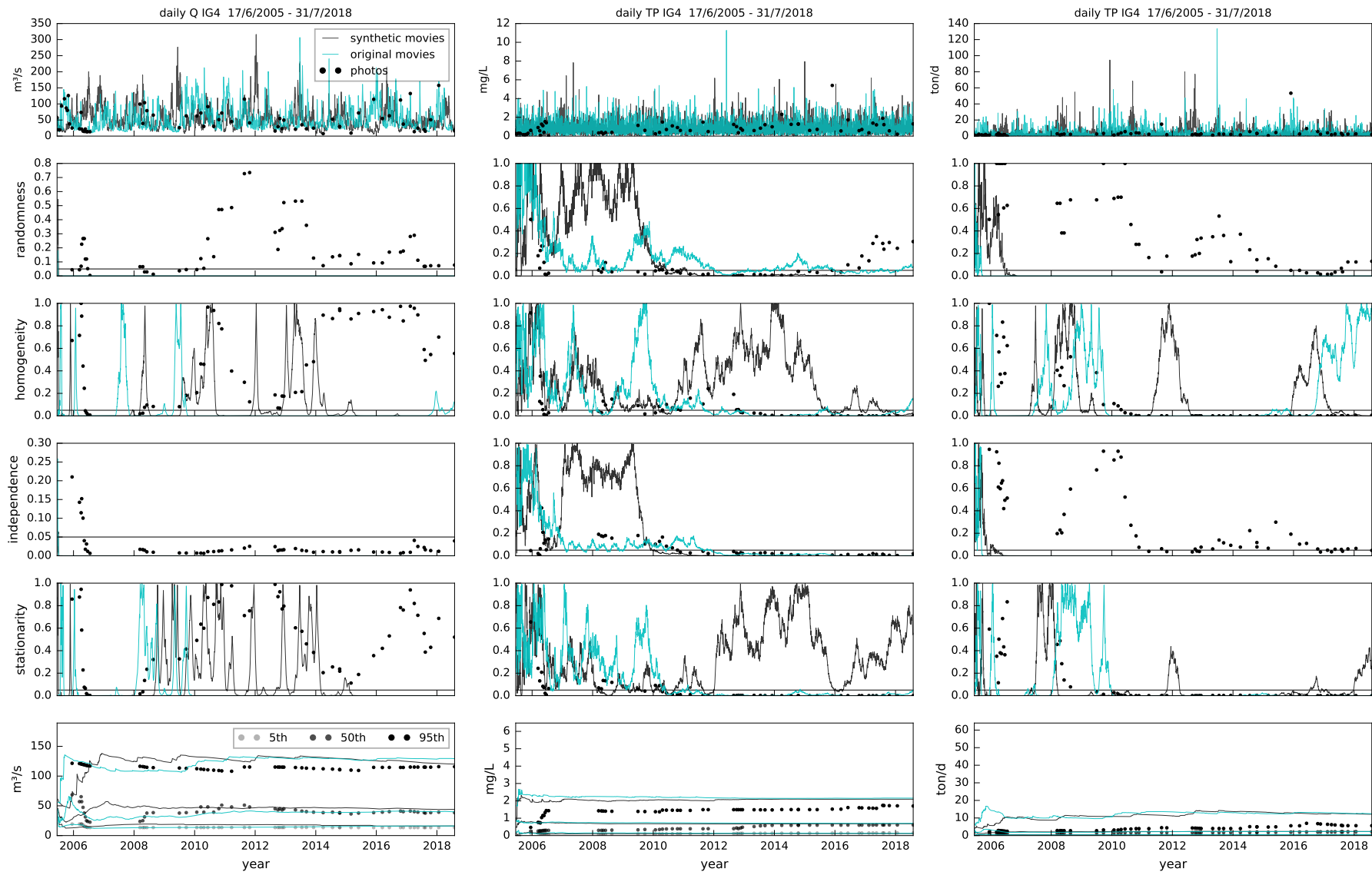
Figure 244 – Evolution of the RHIS p-values and percentiles of Q, C and W, BOD station IG6, photos and daily movies
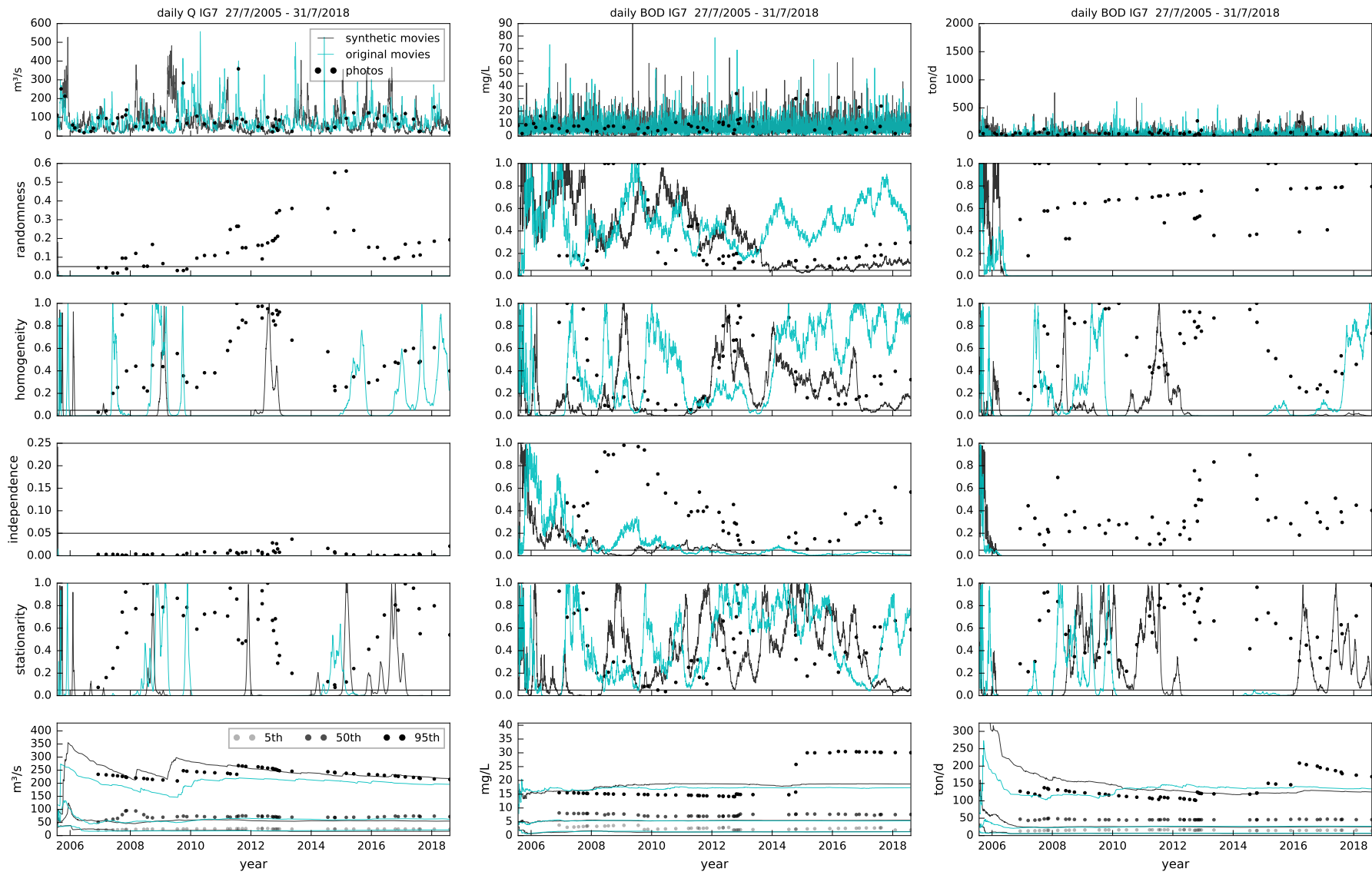
Figure 245 – Evolution of the RHIS p-values and percentiles of Q, C and W, BOD station IG7, photos and daily movies
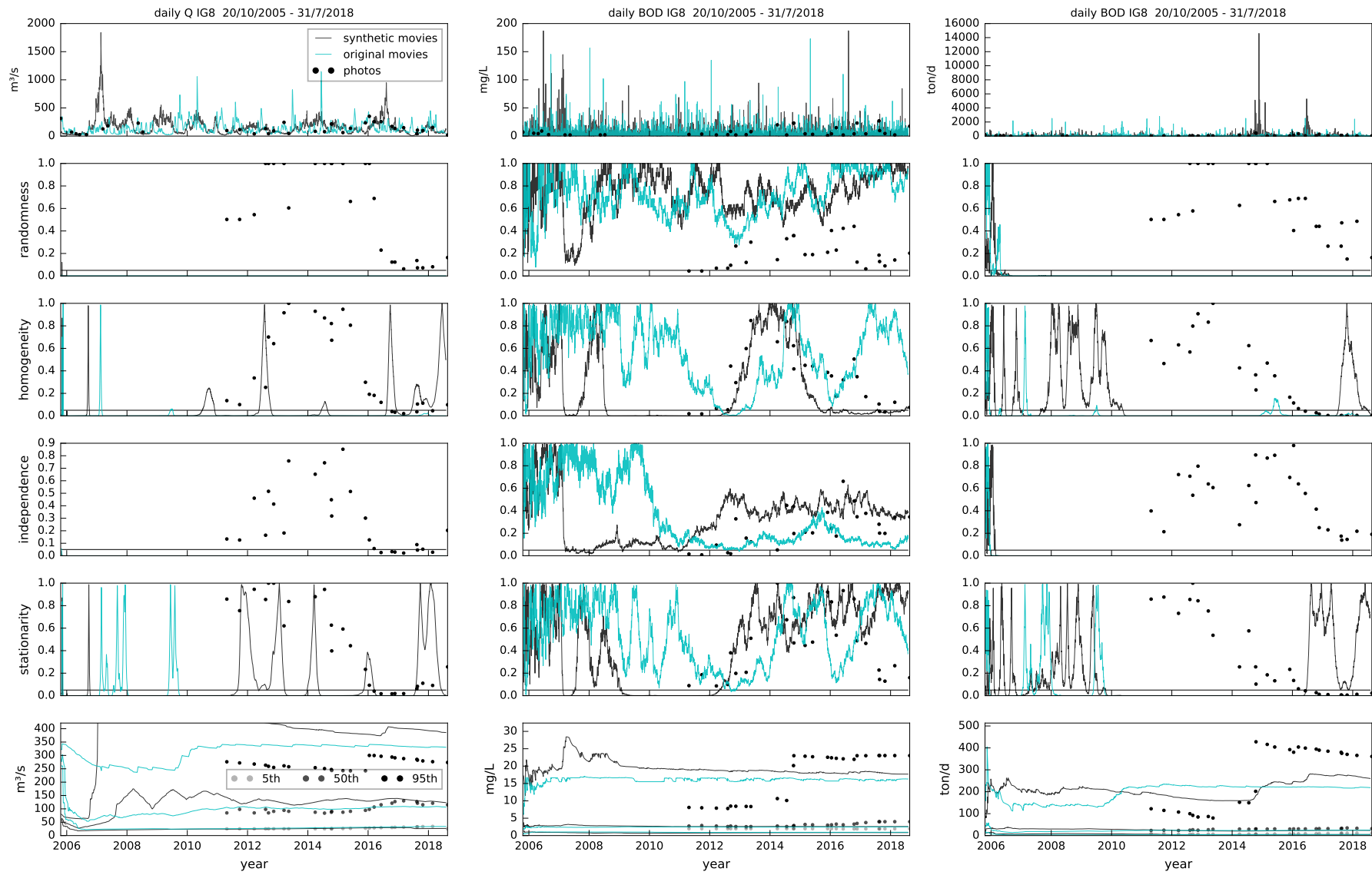
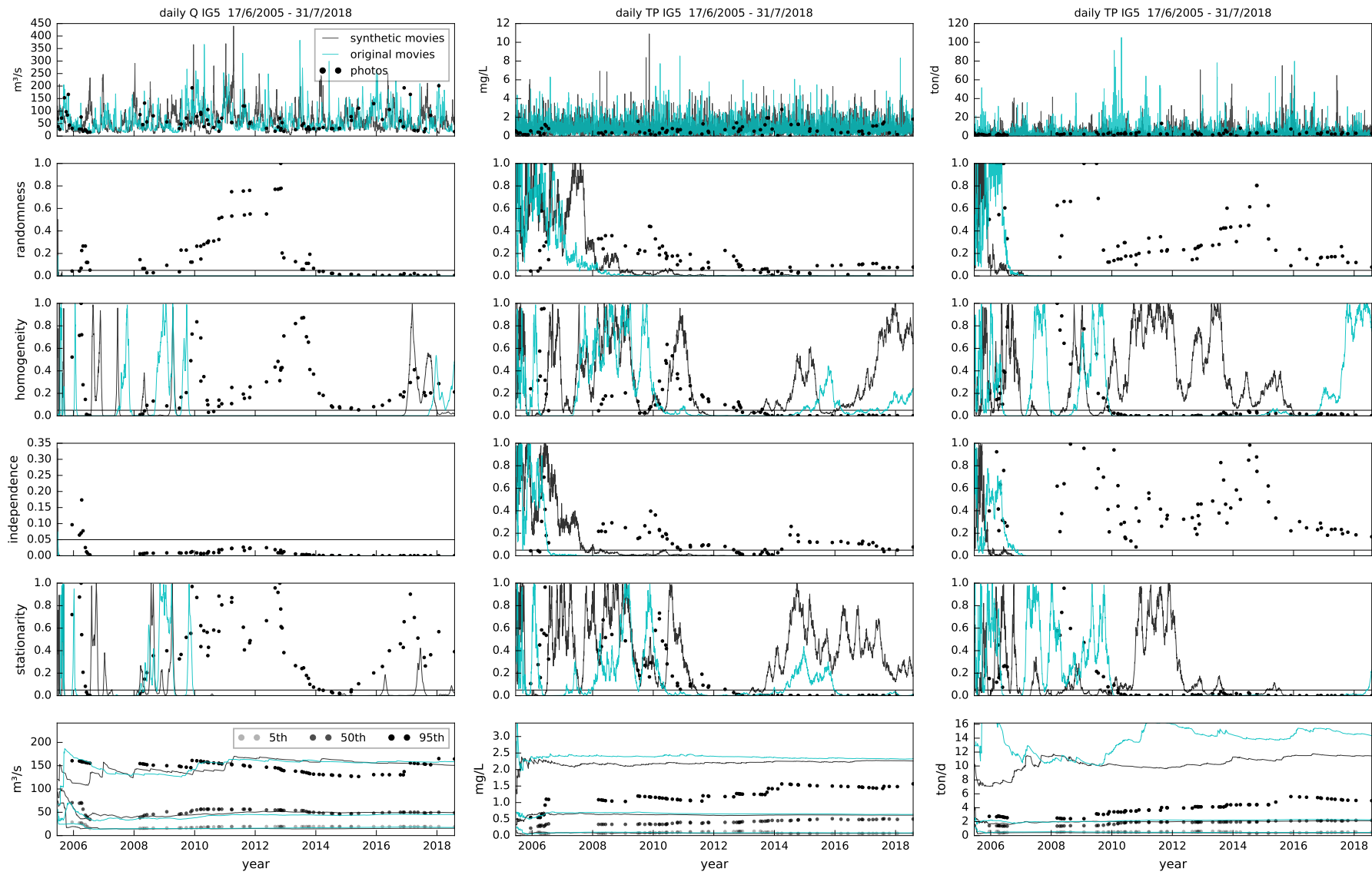Figure 246 – Evolution of the RHIS p-values and percentiles of Q, C and W, BOD station IG8, photos and daily movies

NH4
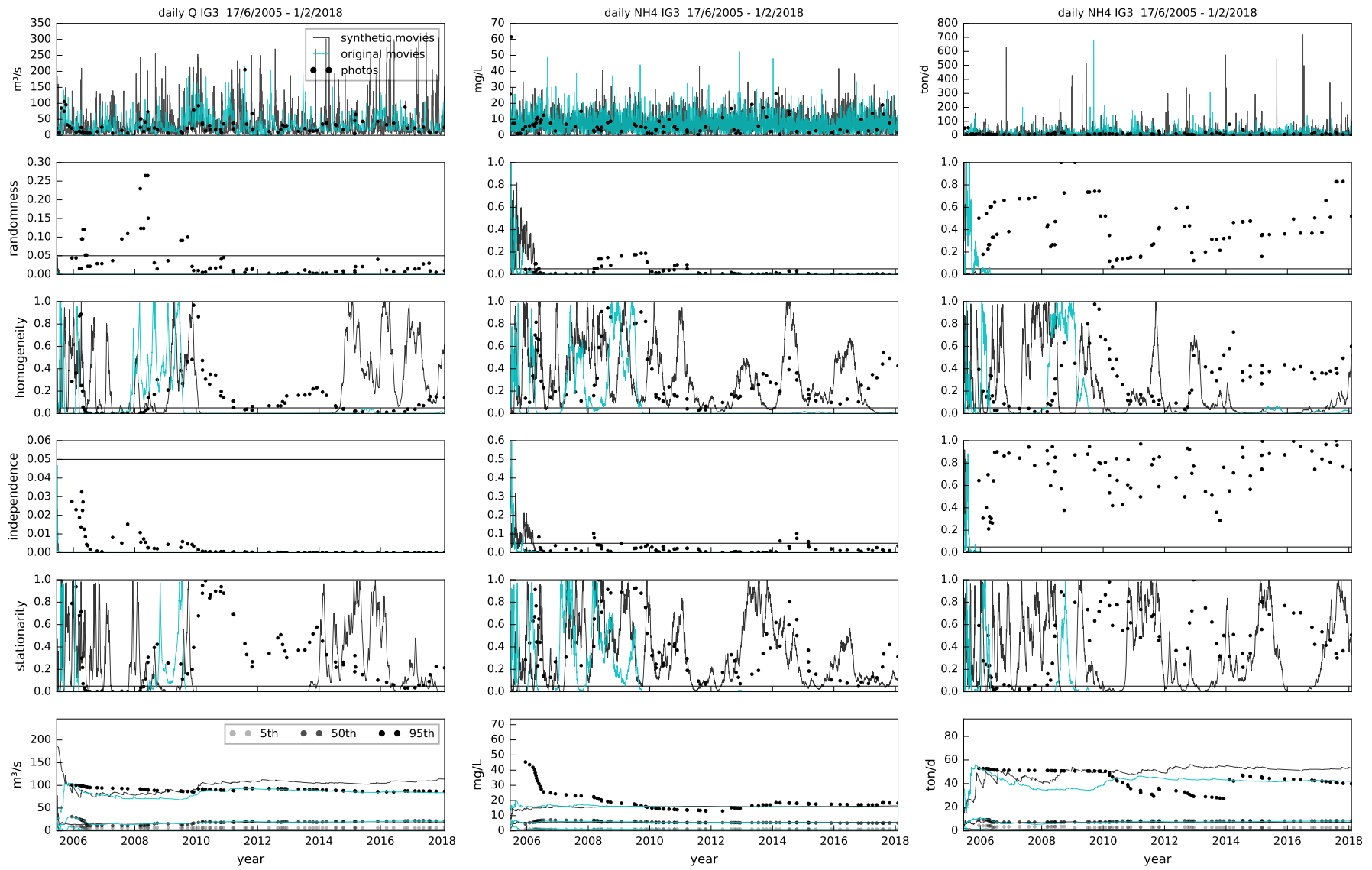
Figure 247 – Evolution of the RHIS p-values and percentiles of Q, C and W, NH4 station IG3, photos and daily movies
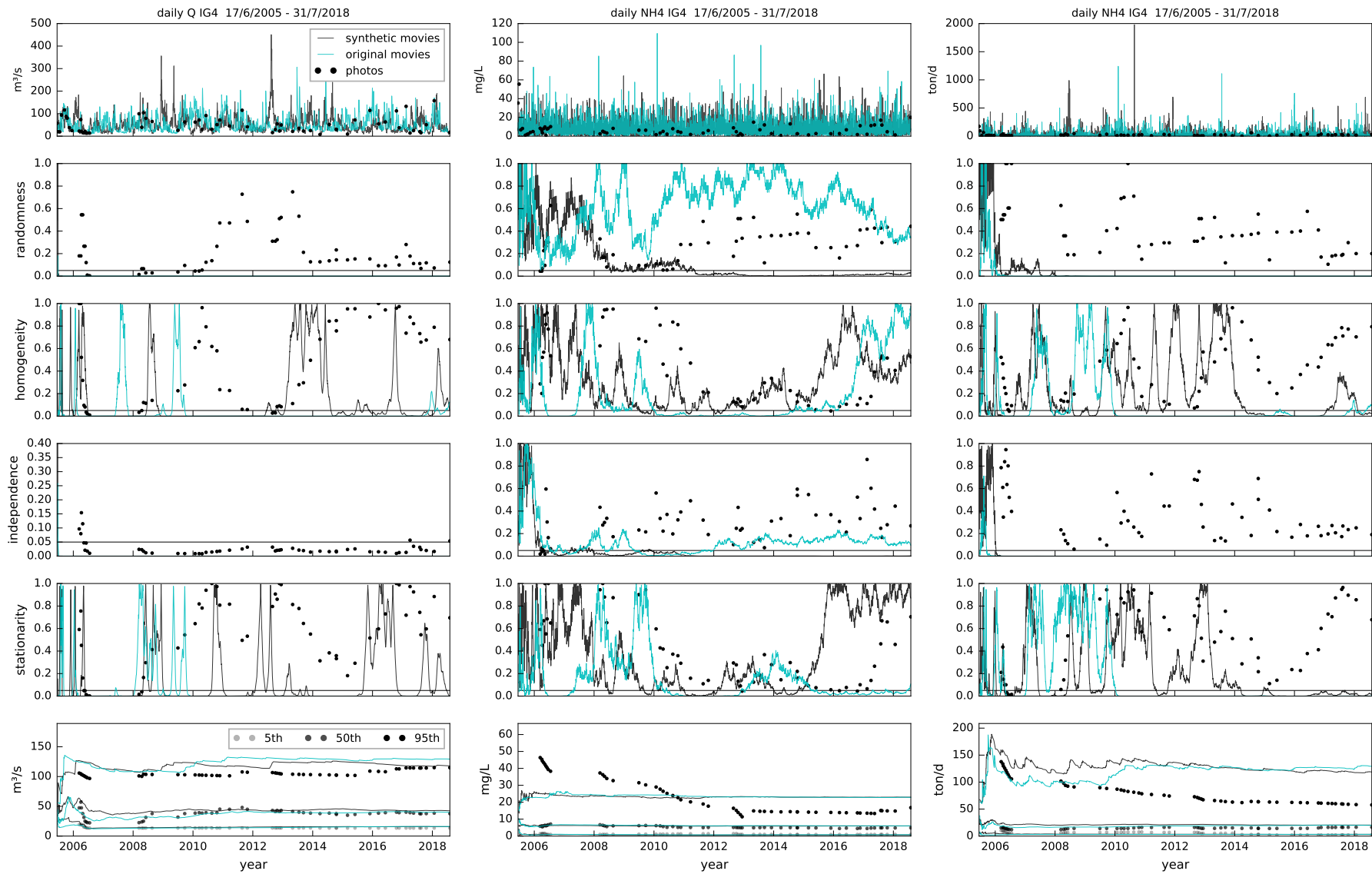
Figure 248 – Evolution of the RHIS p-values and percentiles of Q, C and W, NH4 station IG4, photos and daily movies
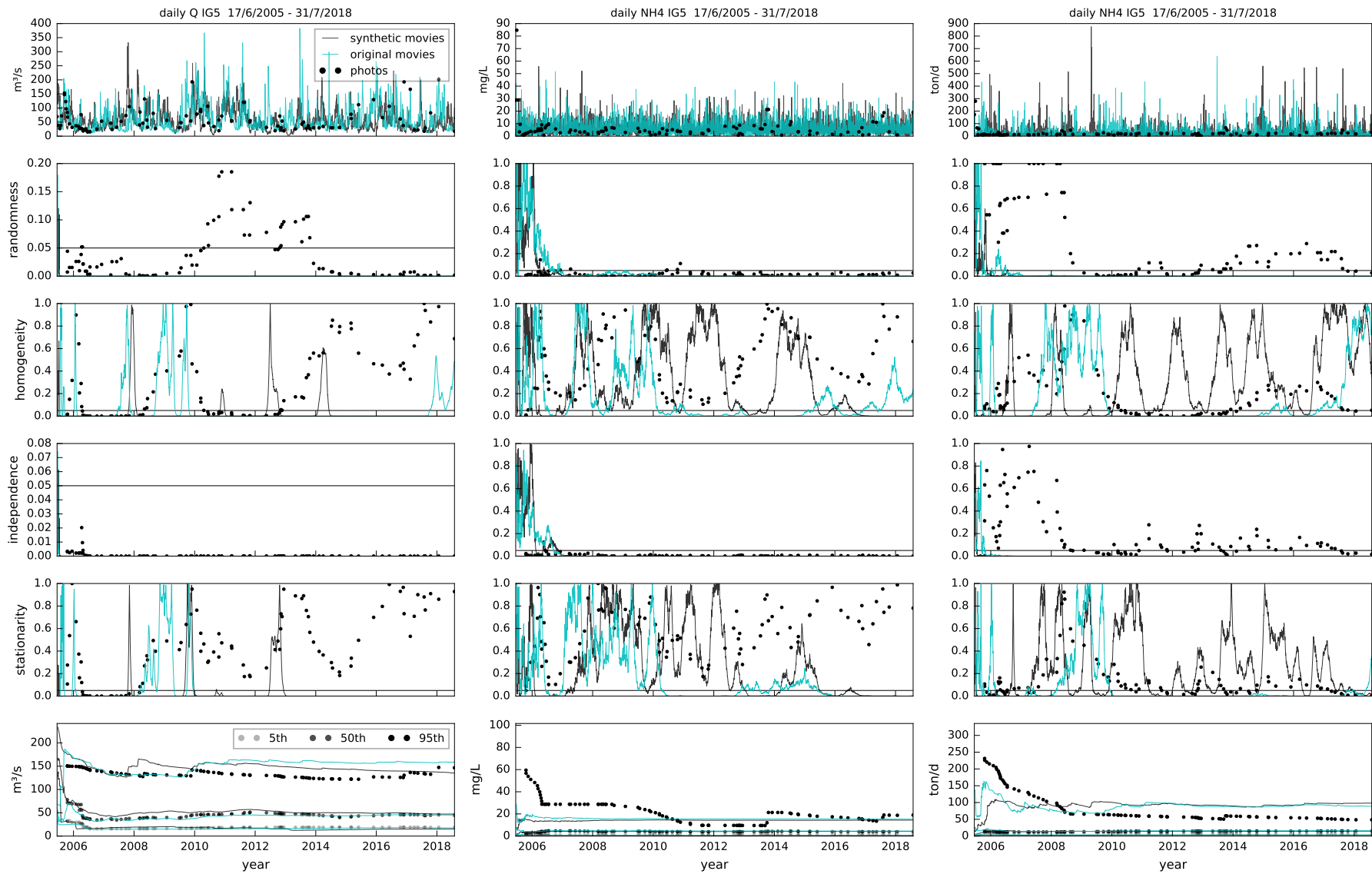
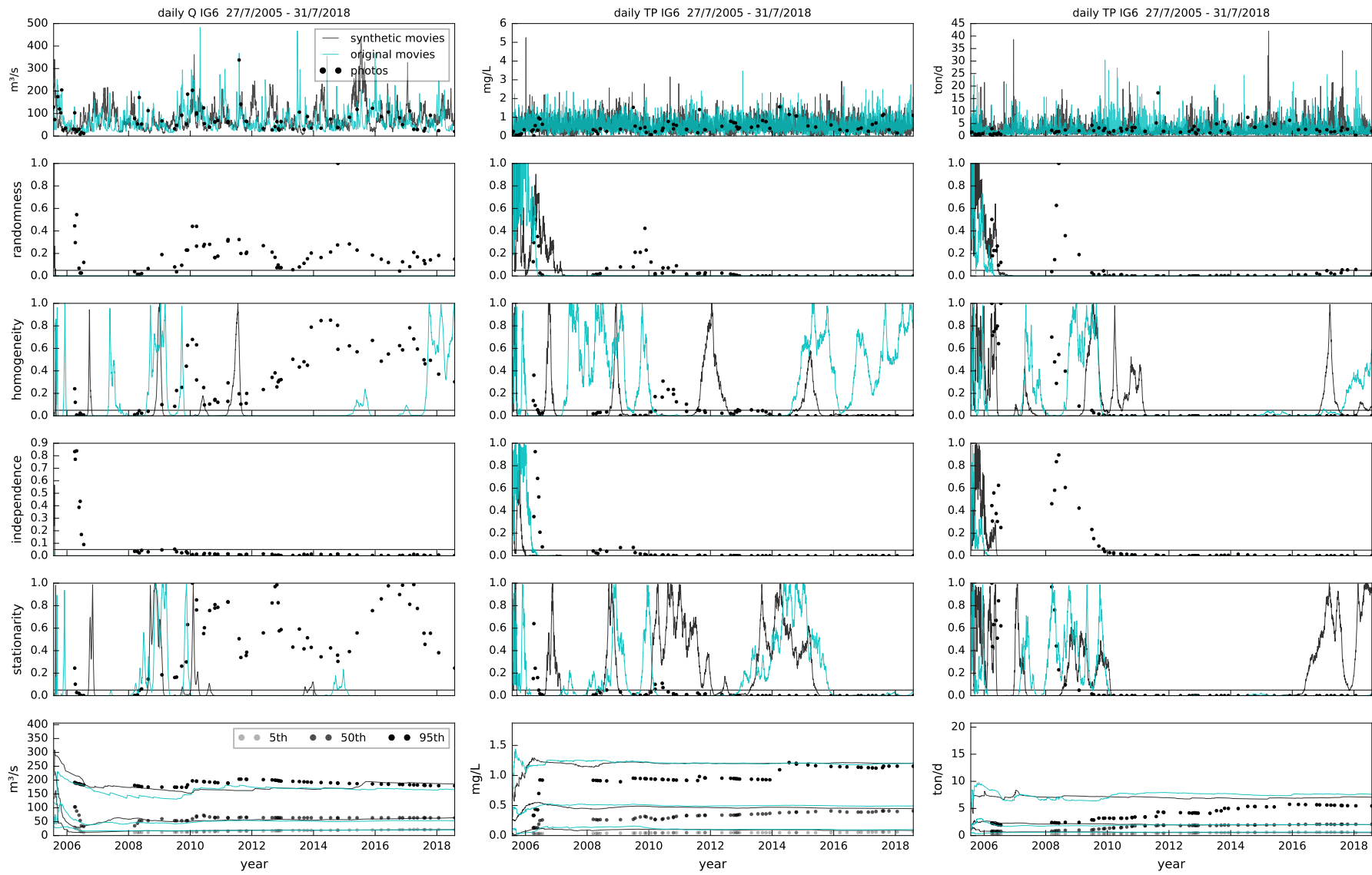Figure 249 – Evolution of the RHIS p-values and percentiles of Q, C and W, NH4 station IG5, photos and daily movies
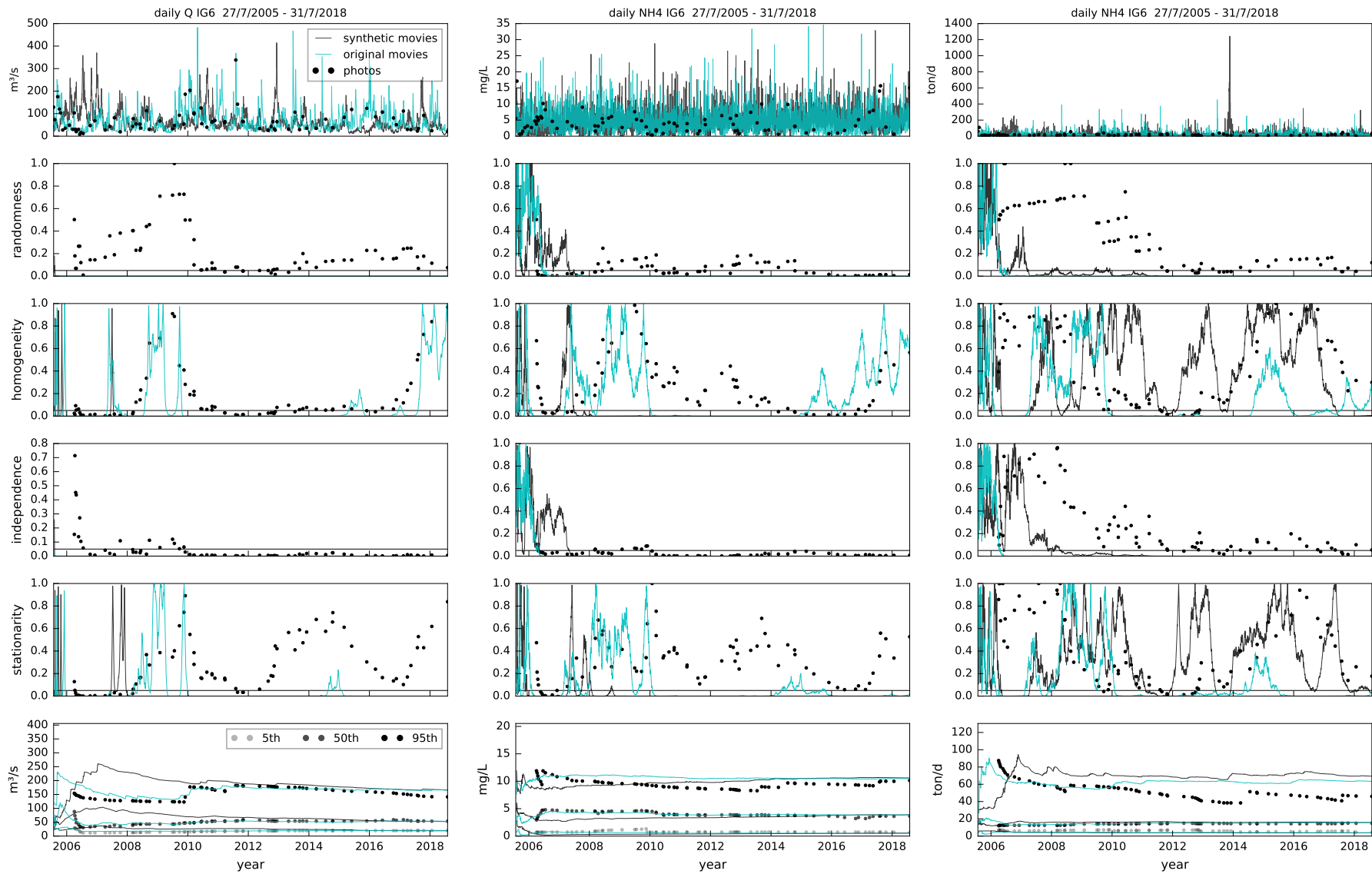
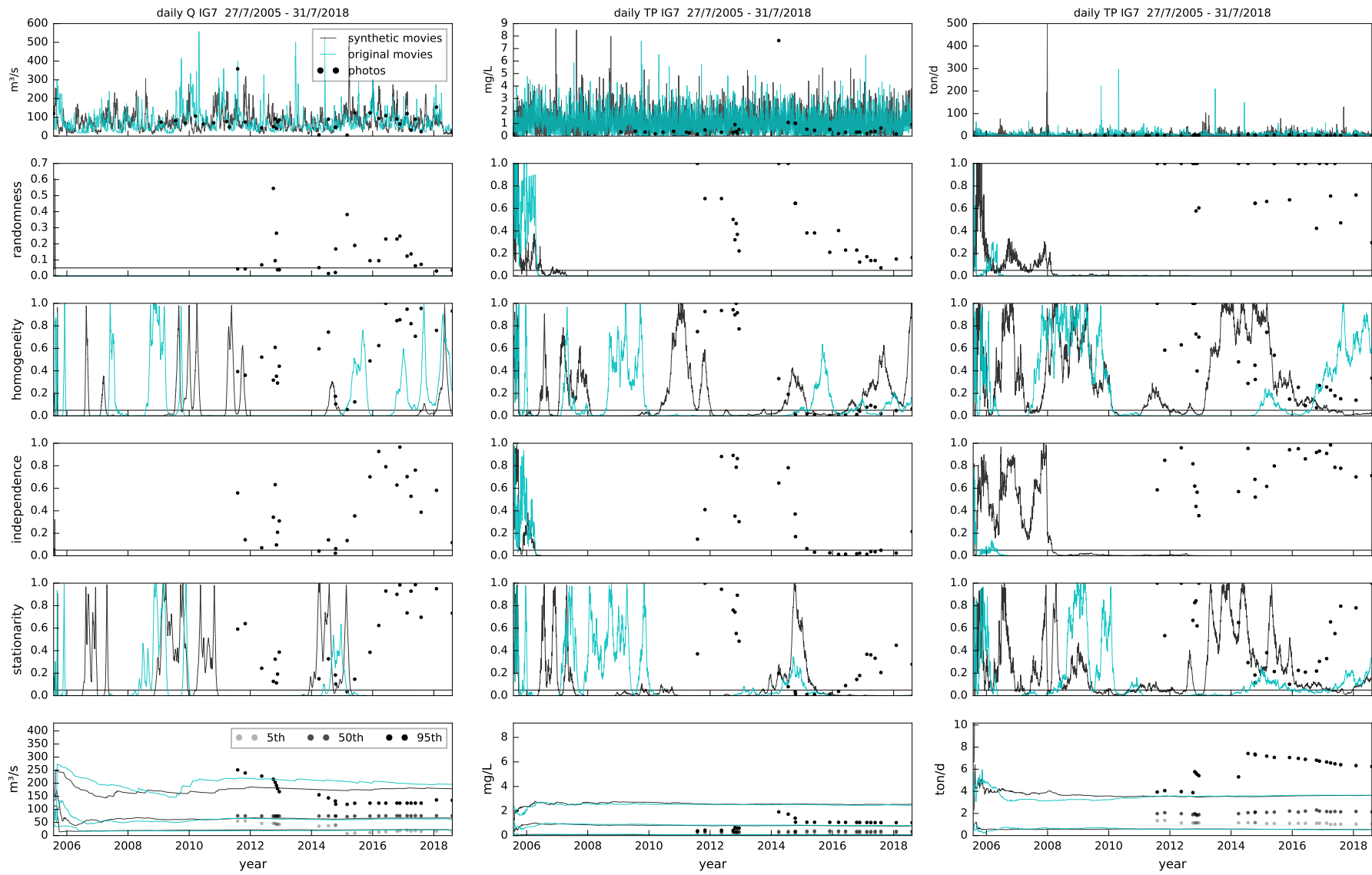Figure 250 – Evolution of the RHIS p-values and percentiles of Q, C and W, NH4 station IG6, photos and daily movies
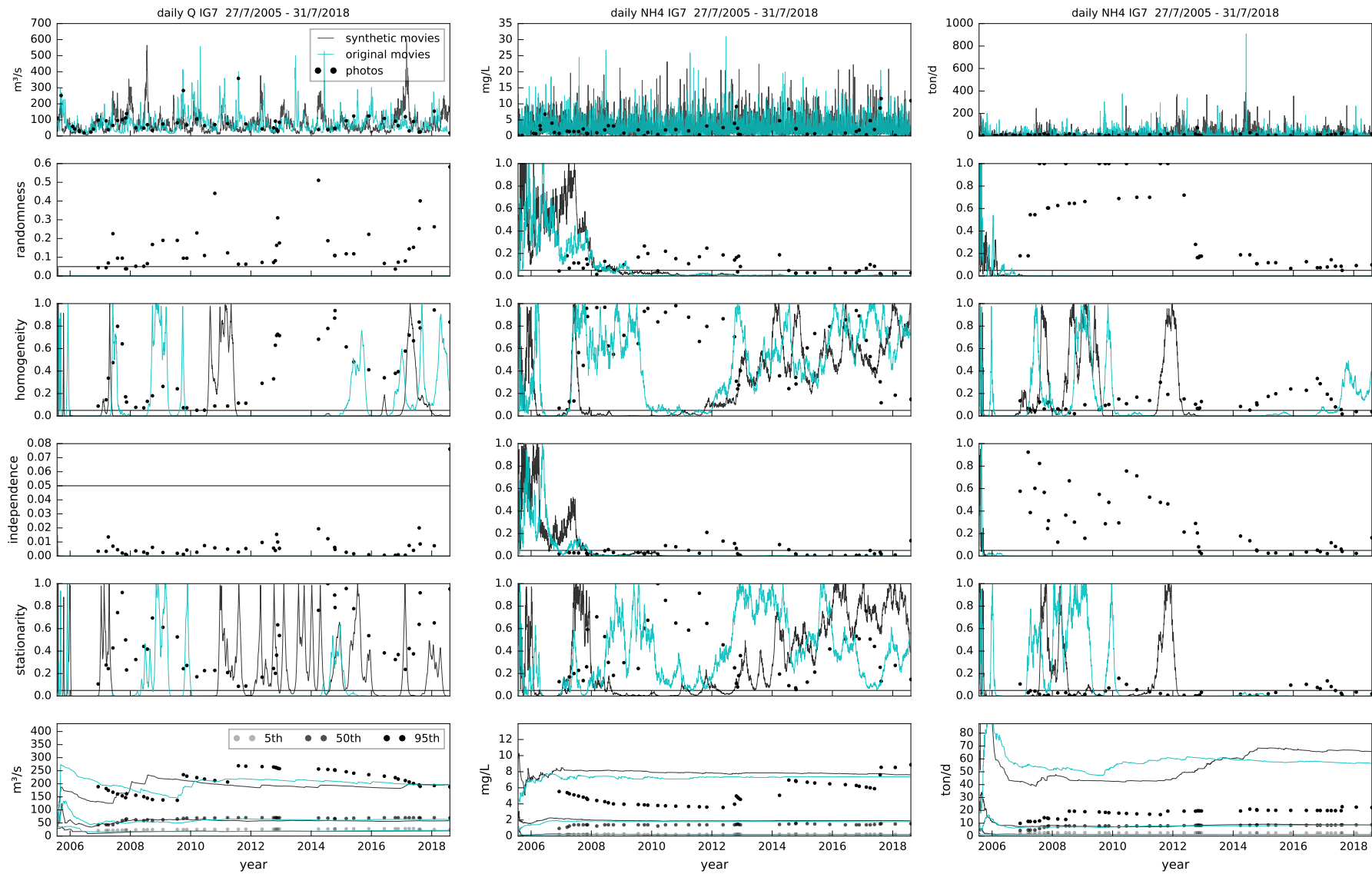
Figure 251 – Evolution of the RHIS p-values and percentiles of Q, C and W, NH4 station IG7, photos and daily movies
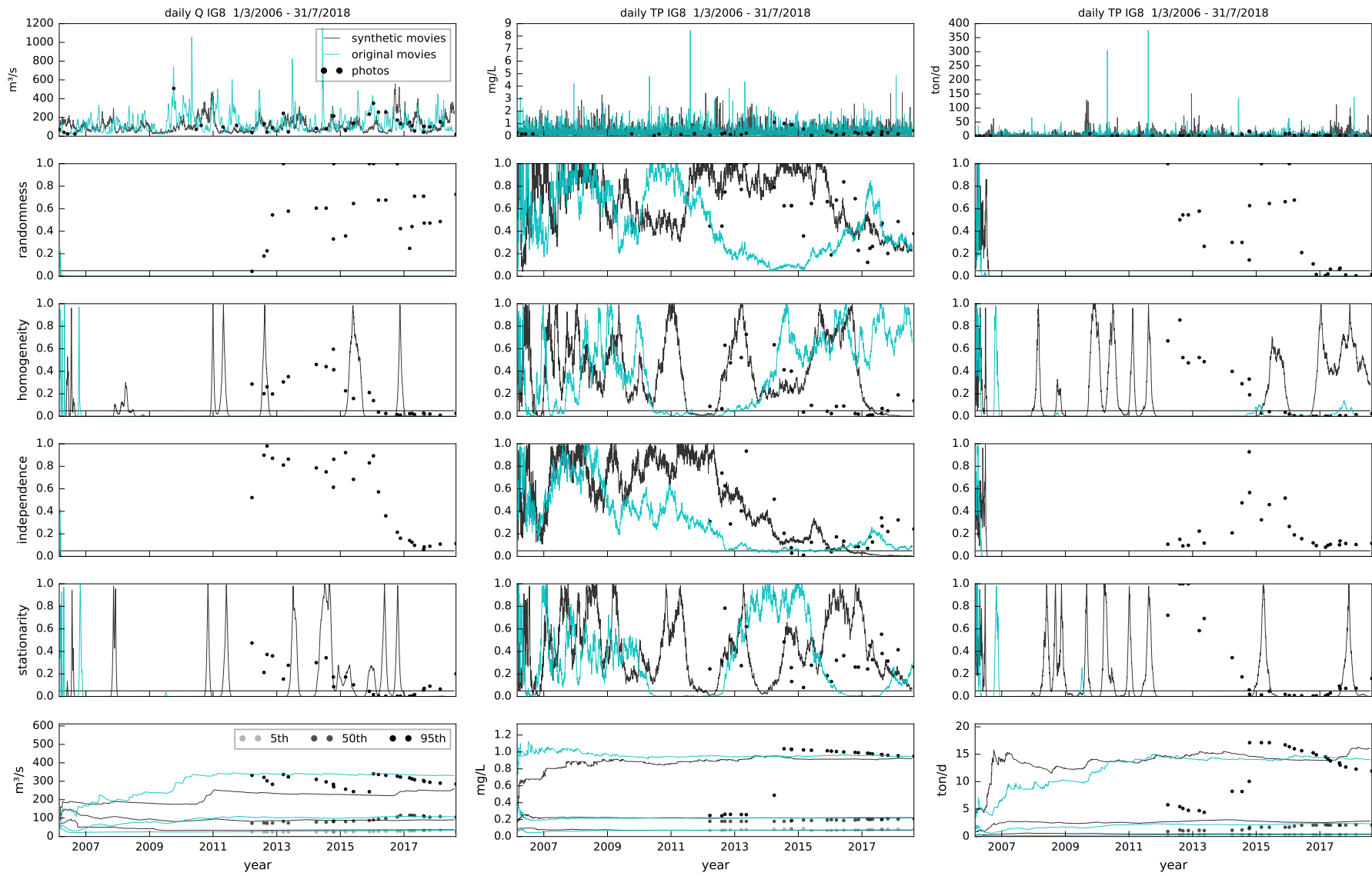
Figure 252 – Evolution of the RHIS p-values and percentiles of Q, C and W, NH4 station IG8, photos and daily movies

TP

Figure 253 – Evolution of the RHIS p-values and percentiles of Q, C and W, TP station IG3, photos and daily movies

Figure 254 – Evolution of the RHIS p-values and percentiles of Q, C and W, TP station IG4, photos and daily movies

Figure 255 – Evolution of the RHIS p-values and percentiles of Q, C and W, TP station IG5, photos and daily movies
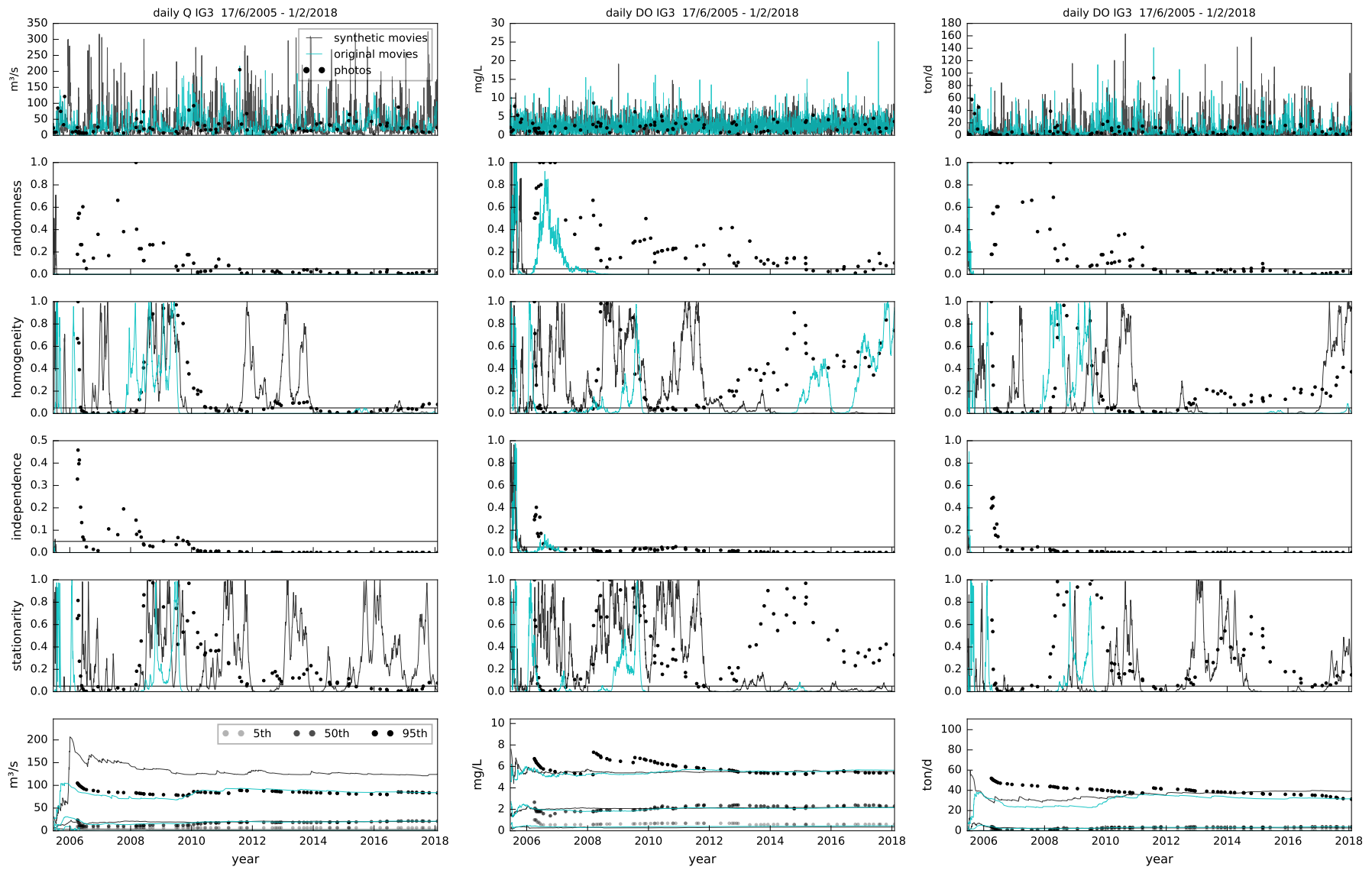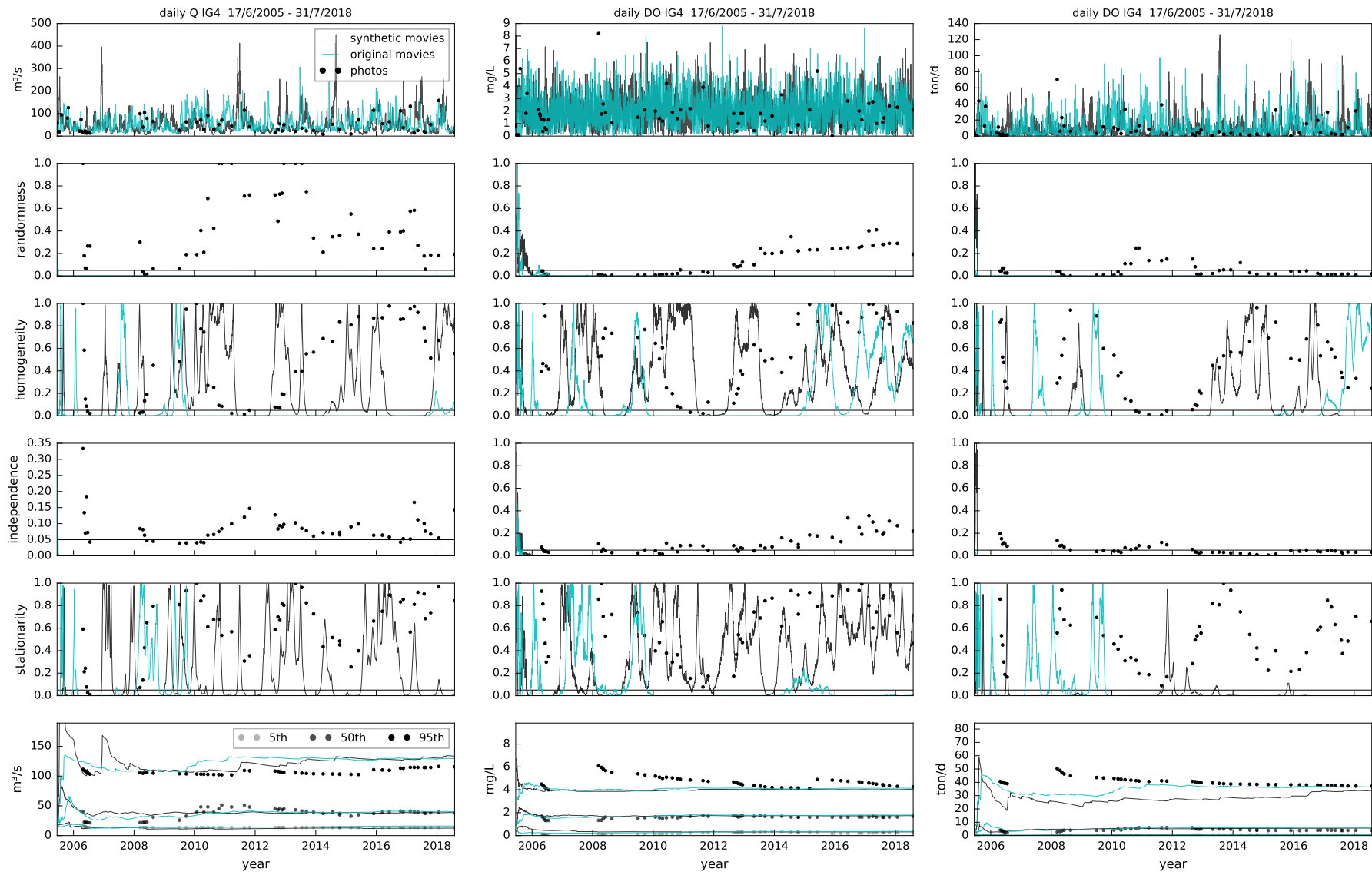
Figure 256 – Evolution of the RHIS p-values and percentiles of Q, C and W, TP station IG6, photos and daily movies

Figure 257 – Evolution of the RHIS p-values and percentiles of Q, C and W, TP station IG7, photos and daily movies

Figure 258 – Evolution of the RHIS p-values and percentiles of Q, C and W, TP station IG8, photos and daily movies
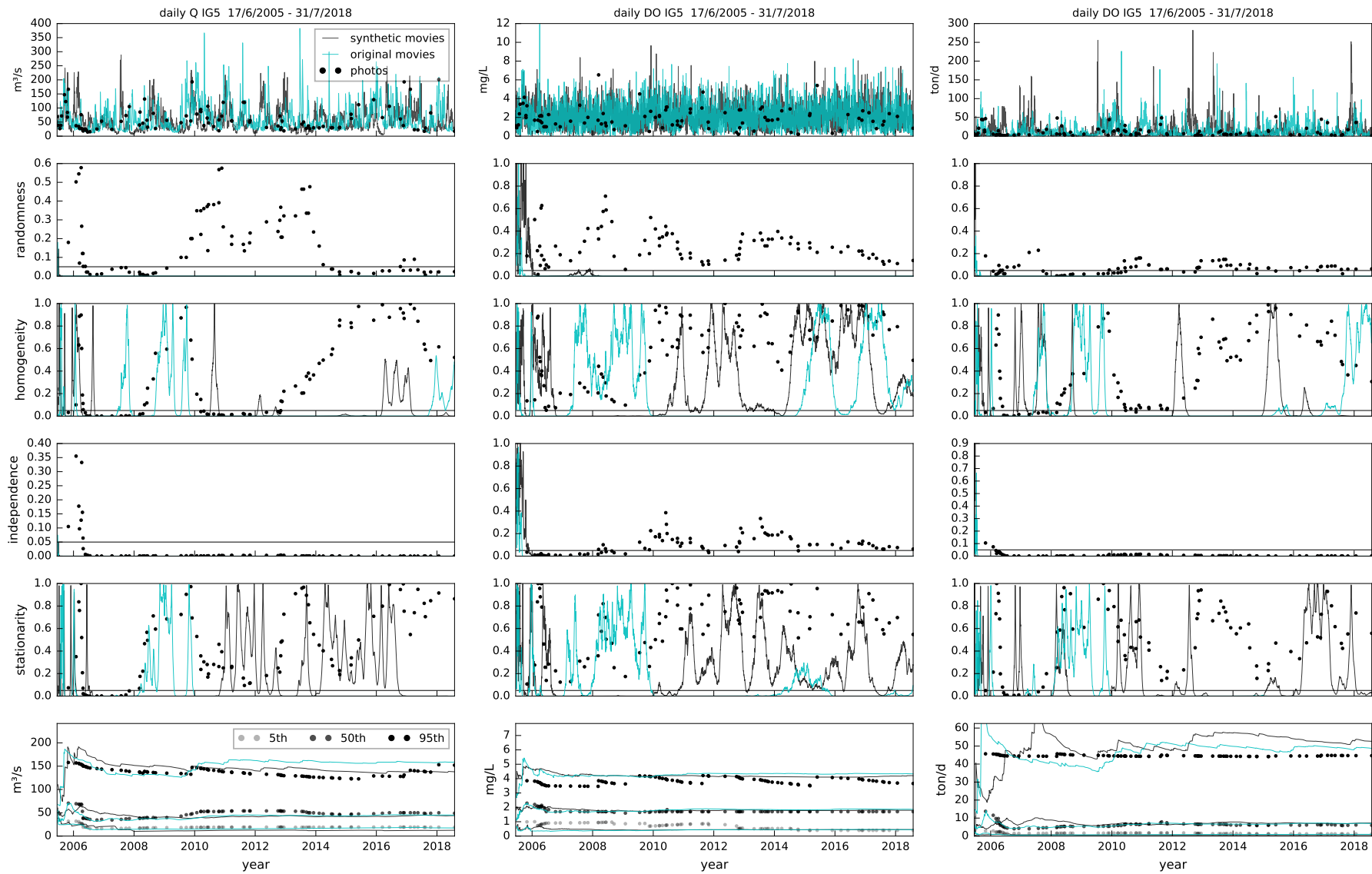
DO

Figure 259 – Evolution of the RHIS p-values and percentiles of Q, C and W, DO station IG3, photos and daily movies

Figure 260 – Evolution of the RHIS p-values and percentiles of Q, C and W, DO station IG4, photos and daily movies

Figure 261 – Evolution of the RHIS p-values and percentiles of Q, C and W, DO station IG5, photos and daily movies
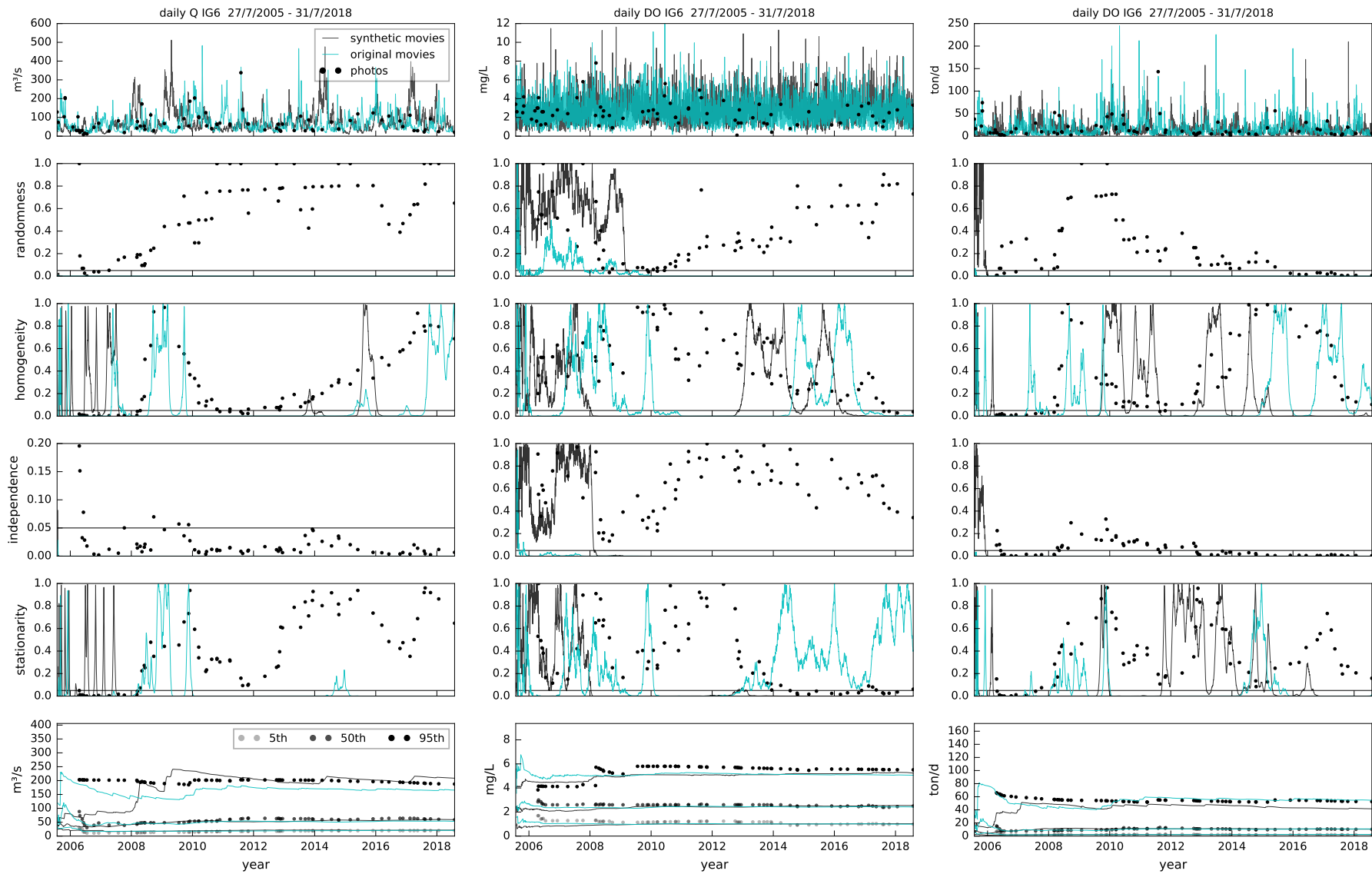
Figure 262 – Evolution of the RHIS p-values and percentiles of Q, C and W, DO station IG6, photos and daily movies
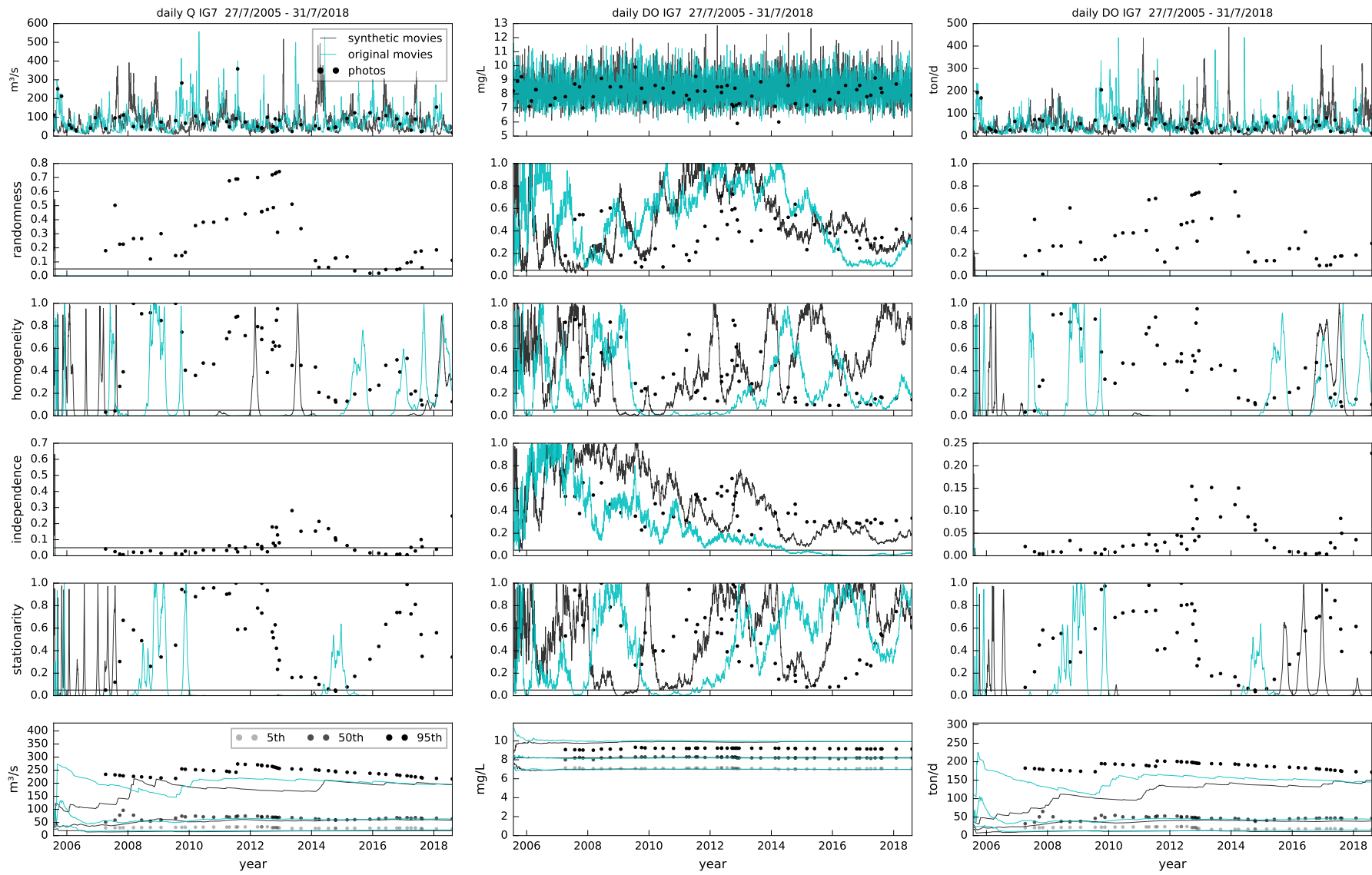
Figure 263 – Evolution of the RHIS p-values and percentiles of Q, C and W, DO station IG7, photos and daily movies
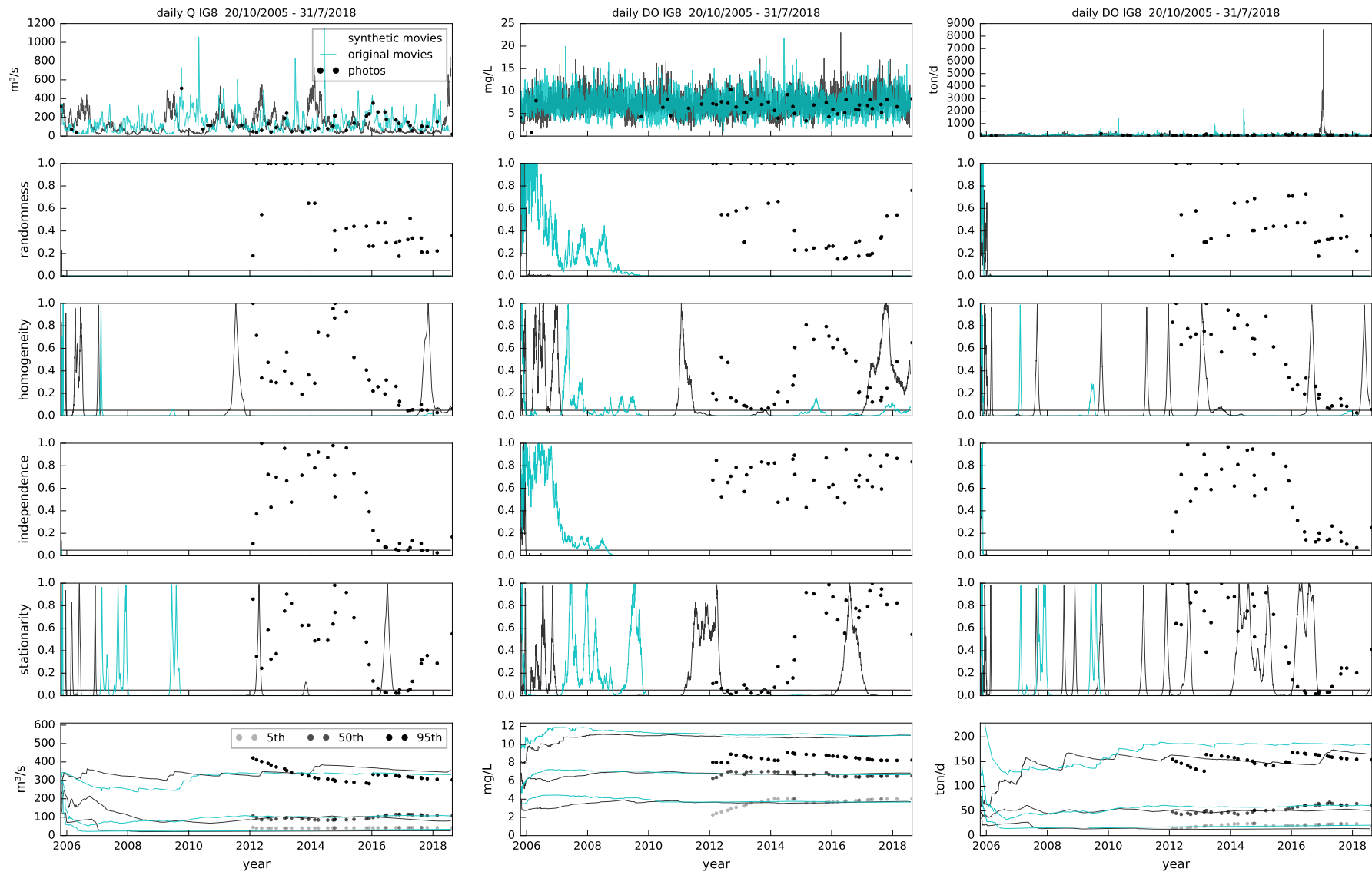
Figure 264 – Evolution of the RHIS p-values and percentiles of Q, C and W, DO station IG8, photos and daily movies